THE UNIVERSITY *of* EDINBURGH

Regulation and Function of AGR2 and p53 pathways

Magdalena Maria Maslon

Doctor of Philosophy

The University of Edinburgh

2011

“Every sentence I utter must be understood not as an affirmation, but as a question.”

Niels Henrik David Bohr (1885-1962)

TABLE OF CONTENTS

FIGURES AND TABLES

Acknowledgments

I would first like to thank my supervisor, Ted Hupp for his invaluable help, believing in me and my data at times when I questioned my work, for his enthusiasm and ability to find the positives in any kind of data and for his endless ideas. Many thanks are due to Euan for proof reading my thesis, for being the most approachable person you can ever meet, and for all his help and advice. Many thanks go to Jenny for providing me with the active p53 protein. Thanks also go to Terry, who suggested the library for writing-up, as it was a genious idea. I would like to thank everyone in the lab, for making my time here truly enjoyable. Many thanks go to Vivien for being a great friend and for her support.

I would like to thank my parents, Elzbieta and Franciszek Maslon, and my sisters, Agata and Ania, who have always provided me with the support and encouragement. Finally, I would like to thank Kuba, for being my best friend, for his patience over the past four years and for always believing in me.

Declaration

I hereby declare that I am the author of this thesis. The work herein is entirely my own unless otherwise clearly indicated and acknowledged. I can confirm that this thesis has been submitted for the degree of Doctor of philosophy and no part of this work has been submitted for any other degree or professional qualification.

Abbreviations

A	Alanine
Aa	Amino acid
AAA+	ATPases associated with various cellular activities
17-AAG	17-allylamino-17-demethoxygeldanamycin
ADP	Adenosine diphosphate
AGR2	Anterior Gradient-2
AGR3	Anterior Gradient-3
ALDH4A1	Aldehyde dehydrogenase 4 family member A1
ASCE	Additional Strand Conserved E Family
ATG	Autophagy-related genes
ATM	Ataxia-telangiectasia Mutated
ATP	Adenosine triphosphate
ATR	ATM and Rad-3 related
BAX	Bcl-2 associated protein X
Bcl-2	B-cell lymphoma-2
BSA	Bovine serum albumin
c	Control
C	Cysteine
CARP	Caspase 8/10-Associated RING Protein
CBP	CREB binding protein
cDNA	Complementary DNA
CDK	Cyclin dependent kinase
CDKN2AIP	CDKN2A-interacting protein
C/EBPß	CCAAT/enhancer-binding protein beta
CHIP	Carboxy terminus of Hsp70p-Interacting Protein
CHK1	Checkpoint kinase 1
CHK2	Checkpoint kinase 2
CIP1	CDK interacting protein 1
CCDC106	Coiled-coil domain-containing protein 106

COP1	Constitutively Photomorphogenic 1
CPM	Counts per minute
CREBB	CREB binding protein
CRM1	Karyopherin receptor 1
CRYAB	Alpha-crystallin B chain
CTD	C-terminal domain
D	Aspartic acid
DAPK	Death-associated protein kinase
DBD	DNA binding domain
DCTN2	Dynactin subunit 2
DD	Death domain
DLS	Dynamic Light Scattering
DMEM	Dulbecco's modified eagle's medium
DMSO	Dimethyl Sulfoxide
DNA	Deoxyribonucleic acid
DNMT3A	DNA (cytosine-5)-methyltransferase 3A
DRAM	Damage-regulated autophagy modulator
dsDNA	Double stranded DNA
DTT	Dithiolthretiol
DYNC1	Cytoplasmic dynein 1
E	Glutamic acid
EBNA-5	Epstein-Barr nuclear antigen leader protein
E. coli	Escherichia coli
ECL	Enhanced chemiluminescence
EDTA	Ethylene diamine tetra-acetic acid
EGFR	Epidermal growth factor receptor
ELISA	Enzyme linked immunosorbent assay
ELM	Eukaryotic Linear Motif
EM	Electron microscopy
EMT	Epithelial to mesenchymal transition
EP400	E1A-binding protein p400
ER	Endoplasmic reticulum/ Estrogen receptor

ERK1	Extracellular signal regulated kinase 1
ERK2	Extracellular signal regulated kinase 2
Erp18	Endoplasmic reticulum protein 18kDa
F	Phenylalanine
FBS	Foetal bovine serum
FGF	Fibroblast growth factor
G	Glycine
GF	Growth factor
GOF	Gain-of-function
GPX1	Glutathione peroxidase 1
GST	Glutathione S-transferase
Gy	Gray
h	Hydrophobic
H	Histidine
HA	Hemaglutinin
HABP4	Hyaluronan-binding protein 4
HAT	Histone acetyltransferase
HDAC	Histone deacetylase
HEPES	N-(2-Hydroxethyl)piperazine-N'-(2-ethanesulfonic acid)
Hint1	Histidine triad nucleotide-binding protein 1
HNRNPUL1	Heterogeneous nuclear ribonucleoprotein U-like protein 1
HR	Homologous recombination
HRP	Horse radish peroxidase
Hsp	Heat shock protein
I	Isoleucine
IC50	Concentration required to achieve 50 % inhibition
IFN	Interferon
IP	Immunoprecipitation
IPTG	Isopropyl-β-thio-galactoside
IR	Ionising radiation
K	Lysine
kDa	Kilodalton

L	Leucine
LB	Luria Bertani
LOF	Loss of function
M	Methionine
mA	Milli-amperes
mAb	Monoclonal antibody
MAPK	Mitogen-activated protein kinases
MDM2	Mouse double minute 2
$MgCl_2$	Magnesium chloride
miRNA	micro RNA
MPHOSPH6	M-phase phosphoprotein 6
MRN	Mre11/Nbs1/Rad50
MS	Mass spectrometry
MT	Metallothionein
mTOR	Mammalian target of rapamycin
N	Asparagine
NCL	Nucleolin
NES	Nuclear export signal
NF-κB	Nuclear factor κB
NIR	Novel INHAT Repressor
NLS	Nuclear localisation signal
NMD	Nonsense-mediated mRNA decay
NP	Purine nucleoside phosphorylase
NP40	Nonidet P40
NR4A1	Nuclear receptor subfamily 4 group A member 1
NTP	Nucleoside triphosphate
O.D	Optical density
OSC	Oxidosqualene cyclase
P	Proline
PAb	Polyclonal antibody
PAFAH1B3	platelet-activating factor acetylhydrolase, isoform Ib, subunit 3

PAGE	Polyacrylamide gel electrophoresis
PAI-1	Plasminogen activator inhibitor 1
PBS	Phosphate buffered saline
PBST	PBS-Tween 20 (0.01 % v/v)
PCNA	Proliferating cell nuclear antigen
PDI	Protein disulfide isomerase
PHB	Prohibitin
PI3-K	Phosphoinositide 3-kinase
PIKK	Phosphoinositide 3-kinase related kinase
Pirh2	p53-Induced protein with a RING-H2 domain
PML	Promyelocytic leukaemia
PMSF	Phenylmethanesulphonyl fluoride
Poly(I):poly(C)	Polyinosinic polycytidylic acid
PPI	Protein-protein interaction
PPID	Peptidyl-prolyl cis-trans isomerase D
PRD	Proline-rich domain
PRMT5	Protein arginine methyltransferase
PSMD11	p53 proteasome 26S subunit, non-ATPase, 11
PTC	Premature translation termination codon
PTM	Posttranslational modification
PUMA	P53 upregulated modulator of apoptosis
Q	Glutamate
R	Arginine
RLU	Relative light unit
RNA	Ribonucleic acid
RNP	Ribonucleoprotein
ROS	Reactive oxygen species
RPA	Replication factor A
rRNA	ribosomal RNA
S	Serine
SB	Sample Buffer

SDS	Sodium dodecyl sulphate
SDS-PAGE	Sodium dodecyl sulphate polyacrylamide gel electrophoresis
SENP1	SUMO-sentrin-specific protease 1
SEP	Squamous epithelial induced stress protein
Ser	Serine
SESN	Sestrin
siRNA	Small interfering RNA
SMAD	Mothers against DPP homolog 4
SNIP1	SMAD nuclear interacting protein (SNIP1)
snoRNP	Small nucleolar RNP
snRNA	small nuclear RNA
SOD2	Superoxide dismutase 2
SRH	Second region of homology
ssDNA	single stranded DNA
STIP1	Stress-induced-phosphoprotein 1
SUMO	Small Ubiquitin- like Modifier
SUSP1	SUMO1-specific proteases 1
SYVN1	Synoviolin
T	Threonine
TAD	Transactivation domain
TAF	Transcription-associated factors
TBP	TATA-binding protein
TERC	Telomerase RNA component
TERT	Telomerase reverse transcriptase
TET	Tetramerization domain
TGF- β	Transforming growth factor-β
Tris	Tris(hydroxymethyl)methylamine
TRRAP	Transformation/translation domain associated protein
Tween 20	Polyoxyethylene sorbitan monolaurate
Ub	Ubiquitin
Ubc	Ubiquitin-conjugating enzyme

UBE3A	Ubiquitin-protein ligase E3A
UPF	Up-frameshift
UV	Ultra violet light
v/v	Volume per volume
VEGF-A	Vascular endothelial growth factor A
VIM	Vimentin
W	Tryptophan
w/v	Weight per volume
WT	Wild Type
WT1	Wilms tumor protein
x	Any aa
XPO1	Exportin-1
Y	Tyrosine

Abstract

Inactivation of p53 by mutation occurs in half of human tumours. The majority of these mutations affect the DNA-binding core domain and hence impair DNA binding and hinder transcription of p53 target genes. A wealth of data indicates that even cancers carrying wild type p53 protein, evolve mechanisms to render the p53 pathway inactive. Thus, inactivation of the p53 response, either by mutation or the alternative mechanisms, allows unpurturbed tumour growth. Recent work identified Anterior Gradient-2 (AGR2) as a protein overexpressed in wild type p53 expressing tumours and it was subsequently shown that AGR2 inhibits p53 pathway. In this study I confirmed that AGR2 protein inhibits p53 and AGR2 depletion potentiates p53-dependent DNA damage response. As there were no physiological signals known that regulate the AGR2-p53 axis, here I set out to identify pathways that activate or inhibit AGR2. I found that transforming growth factor β (TGF-β) triggers AGR2 protein reduction and this is concomitant with the stabilisation and increased activity of p53 protein. TGF-β halts AGR2 transcription in a SMAD4-dependent manner and triggers AGR2 protein degradation involving an ATM kinase. I found that SMAD nuclear interacting protein (SNIP1) mediated the ATM-dependent AGR2 degradation. Interestingly, SNIP1 overexpression by itself promoted AGR2 protein degradation. I found that AGR2 protein degradation was proteasome independent and involed autophagy-lysosomal degradation pathway. As the mechanism of p53 inhibition by AGR2 is not known, I reasoned that identifying interactors of AGR2 may potentially further our understanding of the mechanism accounting for AGR2-mediated p53 inhibtion. I isolated the ATP binding protein Reptin in the yeast two-hybrid system and subsequently validated it as an AGR2 binding partner. Mutations of the two ATP binding motifs in Reptin resulted in altered oligomerization and thermostability of Reptin and affected the AGR2-Reptin complex stability. I also identified the Reptin docking site and it was mapped to a divergent octapeptide loop. I found that AGR2-Reptin complex co-immunoprecipitated with the p53 protein. Subsequently, I showed that Reptin protein can influence p53 activity, and depending on local concentration, either inhibit the

transcription of p53-genes or chaperone its DNA binding activity. Interestingly, I found that Reptin formed a stable complex, independent of AGR2, with p53 R175H, p53 F270A, p53 S269D and p53 S269A, which has implication for the Reptin function in cancers bearing mutant form of p53 protein.

CHAPTER 1: INTRODUCTION

1.1 Cancer and therapy

1.1.1 Cancer

The initiation and the maintenance of cancer requires both aberrant gene regulation and acquired epigenetic abnormalities [1]. The genetic alterations involve mutations in pro-oncogenes and tumour suppressors and chromosomal deviations. Mutations that produce oncogenes hold the respective gene products active under the circumstances in which pro-oncogenes are not. In contrast, tumour suppressor genes undergo changes that render them inactive or reduce their activity [2-5]. However, tumourigenesis is also driven by epigenetic changes. These are changes in genes expression that are not accompanied by alterations in primary DNA sequence [6, 7]. Epigenetic alterations involve abnormal DNA methylation [7-9] and histone modifications [10, 11] and provide additional mechanisms that addict cells to certain pathways and promote selection for genetic changes in these pathways [12].

1.1.2 Hallmarks of cancer

The hallmarks of cancer, first defined in 2000 by Hanahan and Weinberg [4] and subsequently expanded along with research advances, provided a major foundation for understanding of the complexity of this neoplastic disease (Figure 1.1). These traits that enable malignant growth include: (1) ability to chronically proliferate, (2) evasion of programs that limit cell growth and (3) induce cell death, (4) unrestricted replicative potential, (5) capability to switch on angiogenesis and (6) activate invasion and metastasis. The newest, and at the same time oldest hallmark, as first suggested by Warburg in 1953, is (7) reprogramming energy metabolism [13] and (8) circumventing the immune system.

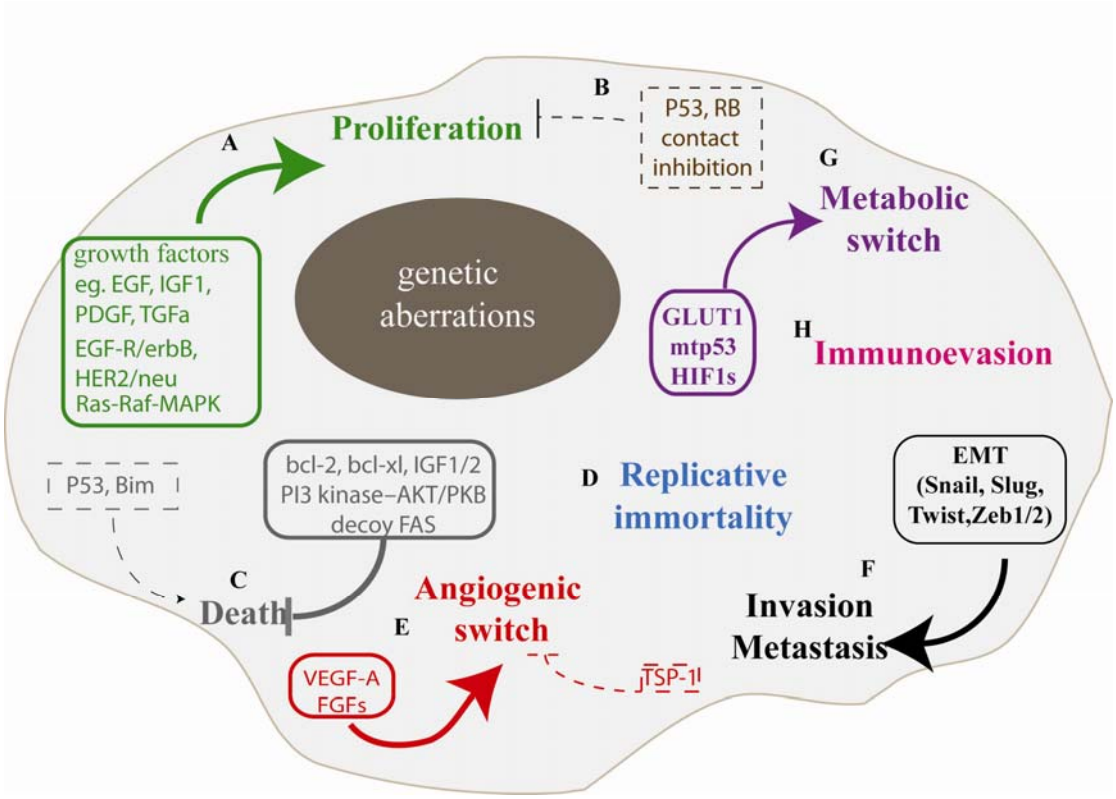

Figure 1.1 Illustration of the major hallmark capabilities of cancer. The hallmark capabilities of cancer include **(A)** sustaining proliferative signalling enabled by (a) autocrine and paracrine proliferative stimulation with growth factors (GF), (b) independent of GFs activation of GF signalling pathways, (c) activated GF receptors or (d) disruptions of negative feedback-loops; **(B)** evading negative growth regulators enabled by (a) GOF or LOF defect in tumour suppressors, (b) evasion from "contact inhibition" or (c) perturbed TGF-β-signalling; **(C)** resisting apoptosis enabled by (a) loss of p53, (b) increased expression of antiapoptotic proteins (Bcl-2, Bcl-xl) and prosurvival factors (Igf1/2), (c) decreased expression of proapoptotic factors (Bax, Bim, Puma) or (d) perturbed autophagy pathway; **(D)** acquiring replicative immortality enabled by (a) telomere maintenance; **(E)** activating angiogenesis enabled by (a) upregulation of angiogenesis inducers, such as vascular endothelial growth factor A (VEGF-A) and fibroblast growth factor (FGF) or (b) pericyte coverage; **(F)** capability for invasion and metastasis enabled by (a) epithelial to mesenchymal transition (EMT) orchestrated by Snail, Slug, Twist, Zeb ½, or (b) stromal cells; **(G)** reprogramming metabolism enabled by (a) upregulation of glucose transporter proteins (e.g. GLUT1) or (b) upregulation of enzymes of glycolytic pathway; **(H)** evading the immune system enabled by (a) mechanisms to avoid detection by the cells of immune system or (b) limiting the extent of immunological death (reviewed in [13])

1.1.3 Cancer therapy

The emergence of hallmarks of cancer and the mechanisms that govern each of them has been accompanied by the development of target-specific therapies. In addition, as the understanding of the genetics and biochemistry of human cancer progresses, so do the ideas and approaches towards effective cancer therapy. One of the most exploited strategies towards developing an effective drug has been to target a very specific factor or signalling pathway in the cancer cell that discriminates it from the normal counterpart.

1.1.3.1 Targeting "oncogenic addiction"

A great focus of drug discovery programmes has been put on targeting kinases, as inappropriate regulation of kinase function has emerged as one of the main mechanisms used by tumour cells to circumvent physiological programs that prevent excessive growth and survival [14]. Indeed, a significant proportion of tumours bear mutations in protein kinases [15]. Mutated kinases acquire transforming capacity and become indispensable for tumour cells survival due to the phenomenon reffered to as "oncogene addiction" [16]. Examples of such mutated kinases include Phosphatidylinositol 3-kinase subunit p110 alpha (PI3KCA) [17, 18], Abl [19], epidermal growth factor receptor (EGFR) [20], c-Kit [21] and B-RAF [22]. Most kinase inhibitors exploit the conserved ATP binding site with the conserved activation loop, and were developed to either mimic ATP in the ATP binding pocket or to form a covalent bond with the ATP binding site that can block subsequent ATP binding. In addition, the compounds that modulate kinase activity and bind outside the ATP binding pocket have been developed and the mechanism of their function involves allosteric modulation [14]. At the present, efforts to pharmacologically suppress mutationally activated kinases have been relatively successful. Drugs such as imatinib (Gleevec), gefitinib (Iressa) and trastuzumab (Herceptin), targeting BCR-Abl, EGFR and Her2 kinases, respectively, have been developed [23-25]. Unfortunately, for a number of drugs, acquired resistance has been reported, through mechanisms involving additional mutations of the targets [26] or upregulating of alternative pathways [27].

1.1.3.2 Targeting the metabolome

Tumour cells rewire metabolic pathways in order to survive and thus, these may be good targets for development of cancer therapeutics [28]. The specific alterations in the tumour include increased glucose uptake and elevated rate of glycolysis [29]. One of the therapeutic strategies that have been exploited so far was to target upstream modulators of metabolic signalling. For example PI3K-AKT pathway that regulates mammalian target of rapamycin (mTOR) is misregulated in sporadic and hereditary cancers [30]. Essentially, mTOR regulates ribosomal biogenesis and protein synthesis and regulates cellular response to stress conditions such as nutrient deprivation [31]. Inhibition of mTOR by temsirolimus and everolimus has proven relatively successful in renal cell carcinoma treatment [32, 33]. Substantial inhibition of tumour expansion has been noted using inhibtors of glucose transport [34] and direct inhibitors of hexokinase, the enzyme that controls the first step of glycolysis and is upregulated by HIF and Myc, are currently in the clinical trials [35, 36].

1.1.3.3 Emerging strategy: targeting protein-protein interactions (PPIs)

The most innovative ideas in the field of cancer drug discovery involve strategies to disrupt protein-protein interactions. These concepts are founded by the realization that the changes in the cell signalling are enabled by the dynamism of protein-protein interaction networks. Protein networks encompass all of the cellular proteins with their respective binding partners, and include hub proteins, that interact with hundreds of proteins and are at the centre of cellular signalling. These networks may be significantly altered in cancer cells. For example a mutant variant of a hub protein is likely to rewire the wild type protein's PPI landscape and this could contribute to its cancer-promoting activity. In addition the genes responsible and associated with the tumour development, the "disease genes", are often encoding hub proteins [37]. Therefore, efforts to modulate protein-protein interactions may have an enormous therapeutic potential. For example the p53 tumour suppressor protein is commonly mutated in human cancer [38] and the wild type p53 protein is involved in over 300 protein-protein interactions [39] making it one of the major hubs in the cell.

Apart from exploiting classic strategies to switch on p53 pathway and to reactivate mutant p53 protein that led to discovery of mutant p53 refolding PRIMA-1 [40], the p53 field realizes now that understanding and learning how to drug the interactome of mutant p53 may prove to be a more effective strategy (discussed in 1.2.2.2).

Molecular chaperones are proteins that assist the folding and unfolding or the assembly and disassembly of other proteins [41]. They are at the central position in protein-protein interaction systems, form dynamic, temporary interactions and enable network rearrangements, for example, in response to stress. Cancer cells are frequently exposed to proteotoxic stress that is manifested by the presence of unfolded or misfolded proteins, and as a result they become dependent on the chaperone pathways that promote protein folding and are overactivated in several cancers. Heat shock protein (Hsp) Hsp90 is a major hub activated in cancer [42] and it relies on its ATPase activity for chaperoning its client proteins. Accordingly, the inhibitors of Hsp90, namely geldanamycin and its derivative 17-allylamino-17-demethoxygeldanamycin (17-AAG), target the ATP binding pocket and have been shown to efficiently inhibit tumour cell growth [43-45].

1.2 Interactomic nodes in homeostasis and cancer

Protein networks have to be perfectly balanced to maintain homeostasis. Conversely if a protein or pathway are lost or gained, this can result in disease. The hierarchical character of the interactome, involving hubs and their interacting proteins, has its implications in the pathogenesis of disease. This means that in general networks are quite resistant to the loss of a random part of the network however the perturbance or removal of hubs has usually detrimental consequences [46, 47]. Indeed, the aberrant expression or mutations of hub proteins such as p53, Mouse double minute 2 (MDM2) or p300 commonly leads to human cancers [48-51].

1.2.1 p53

1.2.1.1 p53 function

I p53 in tumour suppression

Evolution has equipped mammalian cells with a variety of tumour suppressive mechanisms that are imperative to prevent rising of the autonomously dividing cells. There are two general mechanisms that enable the cell to constrain tumourigenesis, namely apoptosis and senescence, which are promptly initiated should cell division become abnormal. p53 tumour suppressor protein has emerged in the last few decades as a master inhibitor of tumour development. Indeed, over half of human cancers bear mutations in the p53 encoding gene and germline inheritance of mutant p53 allele is an underlying cause of Li-Fraumeni syndrome [52]. Apoptosis is one of the key programmes initiated by p53 to eliminate neoplastic cells. Transgenic mice harboring a p53 mutation, which disrupts p53 ability to initiate cell cycle arrest, but not apoptosis, did not develop spontaneous tumours [53]. In principle activation of both intrinsic and extrinsic cell death programmes by p53 involves transcriptional activation of expression of pro-apoptotic members of Bcl2 family, such as p53-upregulated modulator of apoptosis (PUMA) [54], NOXA [55],

BID [56] and BAX [57], as well as other components of the apoptotic pathway, including elements of death-receptor pathways and components of the apoptotic effector machinery [58-63] (Figure 1.2 A). p53 can, however, control apoptosis in a transcription independent manner [58] (Figure 1.2 I). Importantly, p53 can prevent tumour progression in the absence of apoptosis. This observation was made in a study of PUMA knockout mice. Interestingly, despite showing that PUMA is an essential mediator of the p53-mediated apoptotic response [64], the PUMA knockout mouse strain did not show an increased rate of cancer incidence [65], hinting that p53's antitumour functions involve other mechanisms than just cell death response. Indeed, another tumour suppressor function of p53 is linked to its ability to temporarily or irreversibly forestall aberrant cell proliferation and growth. Reversible cell cycle arrest is achieved by inducing genes such as the cyclin-dependent kinase (CDK) inhibitor p21, 14-3-3 sigma and GADD45 [66] (Figure 1.2 B). If the transient cell cycle block is insufficient, for example following p53 activation in response to telomere attrition or oncogene activation [67-69], the senescence pathway coupled to the induction of p21 [70] and plasminogen activator inhibitor 1 (PAI-1) [71] is triggered (Figure 1.2 C).

In addition to transcriptional regulation of genes encoding aforementioned proteins, p53 can regulate and modulate cell fate by controlling expression of micro RNAs (miRNAs), non-coding RNA molecules that by binding to specific mRNA inhibit protein translation and often enhance degradation of the respective protein. For example p53 targets promoters of miR-34a, miR-34b and miR-34c, miR-192, miR-215 and miRNAs are thought to be key effectors of p53 functions, such as apoptosis, cell cycle progression, senescence, DNA repair or regulation of angiogenesis and hence contribute to tumour suppressive activities of p53 [72-78]. Interestingly, some of the p53-responsive miRNA targets, such as cell fate regulators CDK4, cyclin E2, p21 and the antiapoptotic factor Bcl-2 as well as proto-oncogene mesenchymal-epithelial transition factor (MET), are also transcriptionally regulated by p53, exemplifying the intricacy of p53 fine-tuned signalling.

II Expanding on p53 tumour suppressive activities

As mentioned earlier anomalous energy metabolism is one of the hallmarks of cancer (Warburg effect). Tumour cells gain the ability to metabolise glucose under both normoxia and hypoxia and thus can produce macromolecules that fuel their growth despite adverse microenvironmental conditions [79]. These signals that favour a metabolic switch in cancer cells can also elicit a p53 response. Under normal conditions, p53 ensures the appropriate rate of glycolysis and regulates reactive oxygen species (ROS) formation (Figure 1.2 G). For example p53 poses an intricate response to ROS and induces either antioxidant genes, such as glutathione peroxidase 1 (GPX1), mitochondrial superoxide dismutase 2 (SOD2), aldehyde dehydrogenase 4 family member A1 (ALDH4A1) and sestrin 1 and sestrin 2 (SESN1 and SESN2), under conditions of physiological oxidative stress; or proapoptotic genes, including PUMA, Bax and Pig3, when the levels of ROS are abnormally high [80, 81]. Intriguingly, p53 curbs the Warburg Effect and impinges on glycolysis by inhibiting glucose uptake [82], inducing genes that suppress glycolysis [54] and enhancing mitochondrial respiration [83]. In addition, p53 can be activated by nutrient deprivation or other metabolic stress through activation of AMP-activated protein kinase (AMPK) and inhibition of p53 degradation promoting Akt kinase [84]. Activated p53 induces AMPK, TSC2, IGFBP3, PTEN, Sestrin1/2 and REDD1 that in turn inhibit mTOR protein [85-87]. mTOR protein senses glucose, amino acids, ATP/AMP and growth factors levels and is a major modulator of protein translation [87]. mTOR has also been implicated in the negative regulation of autophagy, a process promoting cell survival under stress conditions and contributing to genome stability. Accordingly, p53 protein promotes autophagy by negative regulation of mTOR, but also through transactivation of lysosomal proteins including damage-regulated autophagy modulator (DRAM), thus contributing to increased genome stability [88] (Figure 1.2 H and J). However, inhibition of p53 pathway can also induce autophagy [89]. This indicates that any aberrant signals, leading to either activation or inhibition of p53, may promote autophagy. To take this further, tumour cells containing wild type p53 may take advantage of this originally

tumour suppressive pathway, and use it as a prosurvival mechanism under the stress conditions posed by tumour microenvironment.

III p53 in development

In terms of evolution p53's tumour suppressive activity is not an early adaptation. The p53 gene family emerged in lower organisms which do not require the tumour suppressive signalling, as this is imperative only for specialised tissues homeostasis [90, 91]. In fact, p53 protein evolved to respond to stresses and to monitor normal development [92] . Several studies have shown p53 function in embryonic development. For example, it has been demonstrated using chicken and mouse models that both p53 mRNA and protein levels are differentially regulated during embryogenesis. Firstly, p53 mRNA appears to be present in most tissues, later however its expression becomes restricted to distinct tissues and its levels are almost negligible in terminally differentiated tissues. Interestingly, only the nervous system appears to exhibit high p53 activity even in late stages of embryogenesis or in newborn mice [93] [94-97].

The importance of the gradual loss of p53 during development has been shown in studies using Mdm2 and Mdm4 knockouts. These animals exhibit lethality during early embryogenesis. This is due to abnormally high levels of p53 and increased p53-dependent apoptosis and cell cycle arrest, instead of essential at this stage of development rapid cell divisions. Accordingly, Mdm2 and Mdm4 knockout mice which were p53-deficient were viable [98-100].

Further evidence of p53 developmental role came from the studies of the p53 knockdown mice. In addition to the predisposition to cancer development at early age [101], p53 null mice display high frequency of developmental abnormalities. For example, females of some backgrounds exhibit neural tube-closure defects called exencephaly [102, 103] and both females and males display lower fertility [104-106]. Moreover, other abnormalities occur at a higher incidence in p53 null mice, such as polydactily of the hind limbs or defects in upper incisor tooth formation [102].

The relatively moderate effect of p53 absence in mouse embryogenesis may be due to the fact, that p63 or p73, which are also expressed at early developmental stages in

mouse, can provide compensatory mechanism for the p53 loss. Indeed, p53 loss has more severe defects in animals, which do not express p63 or p73 during embryogenesis [107]. In the *Xenopus leavis* p53 engages the SMAD pathway in central embryonic germ layer specification [108] and its loss hinders mesoderm differentiation and consequently leads to severe developmental abnormalities [109]. Similarly to frog, studies in zebrafish have further confirmed p53 role in the early developmental stages [110, 111] and the p53 expression is also essential for salamander's limb regeneration [112].

In addition to clear role of p53 in embryonic development, it also participates in differentiation programs. For instance p53 has a critical role in neural differentiation. Apoptosis of the cells of the nervous system constitute the major mechanism for normal neural development [113]. Studies on neuronal precursors derived from p53 knockout mice revealed the importance of p53 antiproliferative signalling in neurons [114]. Furthermore, p53 has been implicated in osteogenic differentiation and bone formation and has either an inhibitory or activating role in osteogenic differentitation depending on the context [115-117]. Additionally, p53 protein has been reported to be upregulated during myogenic differentiation [118] and together with other members of the p53 family activate the pRb protein, which is essential for permanent cell cycle inhibition and induction of muscle-specific genes [119]. Another study demonstrated p53's function in the B-cell differentiation [120], differentiation of granulocytic or monocytic lineage [121] and its activation during megakaryocytic differentiation [122, 123]. Consistent with its role in differentiation and development, p53 has a function in keeping stem cell renewal in check [124, 125]. Furthermore by suppressing Nanog, p53 induces differentiation of mouse embryonic stem cells [126] and reducing p53 expression in human stem cells diminishes spontaneous apoptosis and differentiation [127]. Importantly, the excessive self-renewal of tissue stem cells has been linked to tumourigenesis as some cancers arise from tissue stem cells or from cells that re-differentiated into cells with stem cell properties [128]. Indeed, deletion of the p53 gene in mice has been shown to give a proliferative advantage to stem cells and these formed hyperplastic regions in the subventricular zone of brain [129]. Finally, the osteoblasts-restricted loss of p53 led to excessive proliferation of these cells and mice developed osteosarcomas [130].

IV p53 as a hub protein

The p53 protein has been shown to interconnect several signalling pathways and act as hub protein. This can explain p53's ability to regulate such an intricate set of diverse aspects of life. The current list of p53 binding partners exceeds three hundreds [39] and could be grouped into p53 activators, p53 inhibitors and effectors of p53 function.

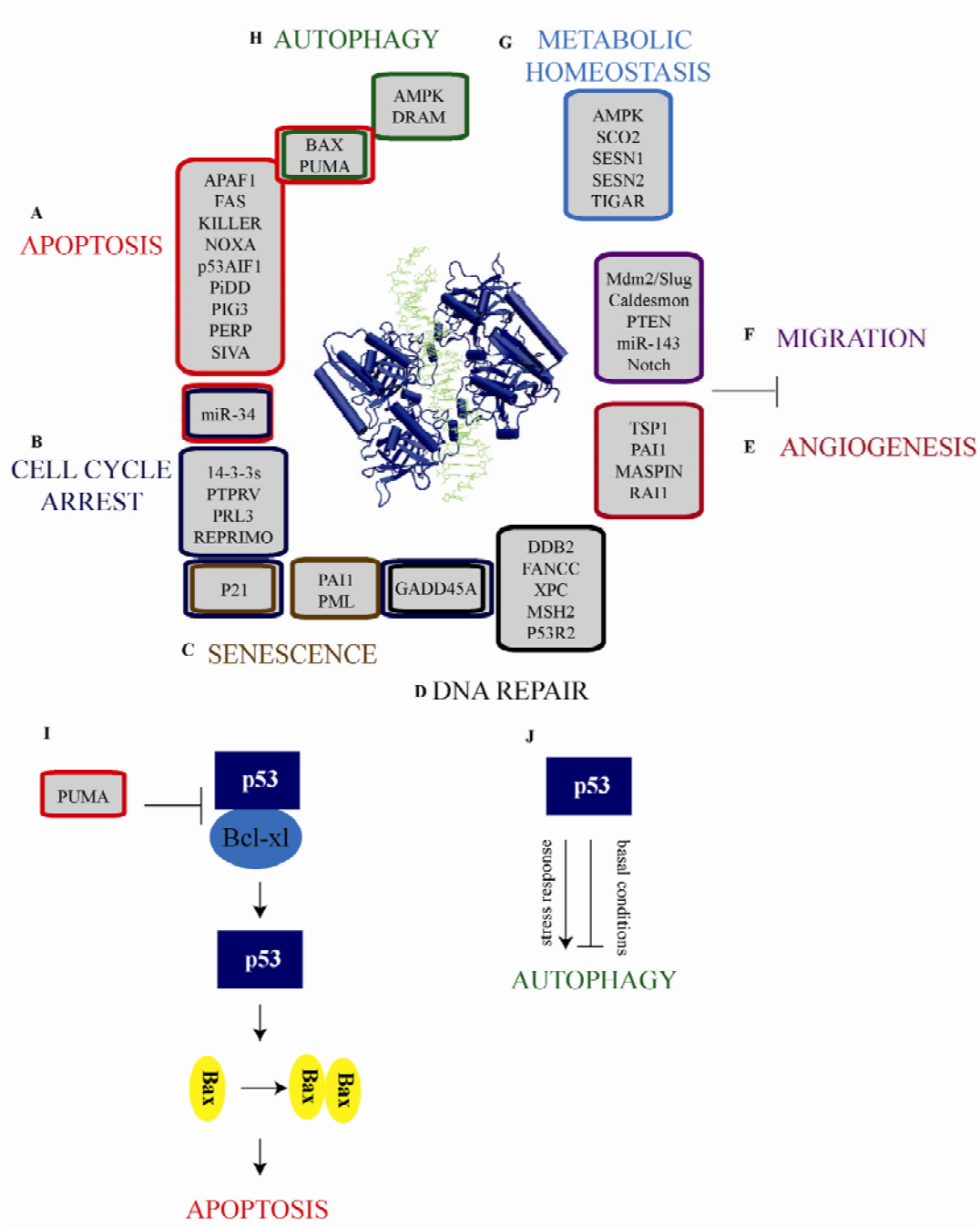

Figure 1.2 Overview of p53 functions. (A-I) Nuclear functions of p53. In response to different oncogenic signals, depending on the extent of damage, p53 activates genes involved in **(A)** apoptosis or **(C)** senescence or genes involved in **(B)** cell cycle arrest and **(D)** DNA repair. **(G)** p53 is also involved in preventing "Warburg effect" by regulating metabolism; it suppresses metastasis, by inhibiting **(E)** angiogenesis and **(F)** migration, and **(H)** activates autophagy. **(I-J) Cytoplasmic functions of p53.** In addition to activating/ repressing transcription of its target genes by nuclear p53, cytoplasmic p53 also regulates cell death and growth by regulating **(I)** apoptosis and **(J)** autophagy. The structure of p53 oligomer bound to a DNA is shown (pdb code:3q05 [131])

1.2.1.2 p53 and disorder

Several reports have shown that cellular hubs are enriched in intrinsically disordered proteins [132]. Natively unstructured proteins are characterized by low globularity, extended conformation and little secondary structure [133]. Disorder equips the protein with conformational plasticity that is required for adopting different structures depending on the cellular context. A disordered region can form flexible linkers between globular domains conferring their unrestricted movement [134] [135]. An unstructured region can itself provide a binding site. The hundreds of p53 interactions have been mapped in detail to the different regions of p53 protein, namely N-terminal domain, Proline rich domain, DNA binding domain, tetramerization domain and C-terminal negative regulatory domain [136, 137] (Figure 1.4 A). Interestingly, p53 protein has been found to be rich in intrinsically disordered regions (Figure 1.3 A). For example, structural studies of N-terminal portion of p53 revealed an absence of well defined secondary and tertiary structure and a high flexibility of the main chain [138-140]. This is consistent with the N-terminal sequence of p53 that is rich in acidic residues and has few hydrophobic amino acids, determinants typical for highly unstructured regions [133, 141]. The induction of secondary structures upon ligand binding is often observed for unfolded proteins. Specifically, peptide motifs can undergo the process of disorder to order transition upon protein binding [133, 141-144]. Indeed, a short segment of conserved hydrophobic residues in the transactivation domain of p53 becomes helical upon binding to MDM2 [145-147], Mdm4 [148], p300 [149], replication protein A [150] or yeast TFIIH [151] (Figure 1.5 A).

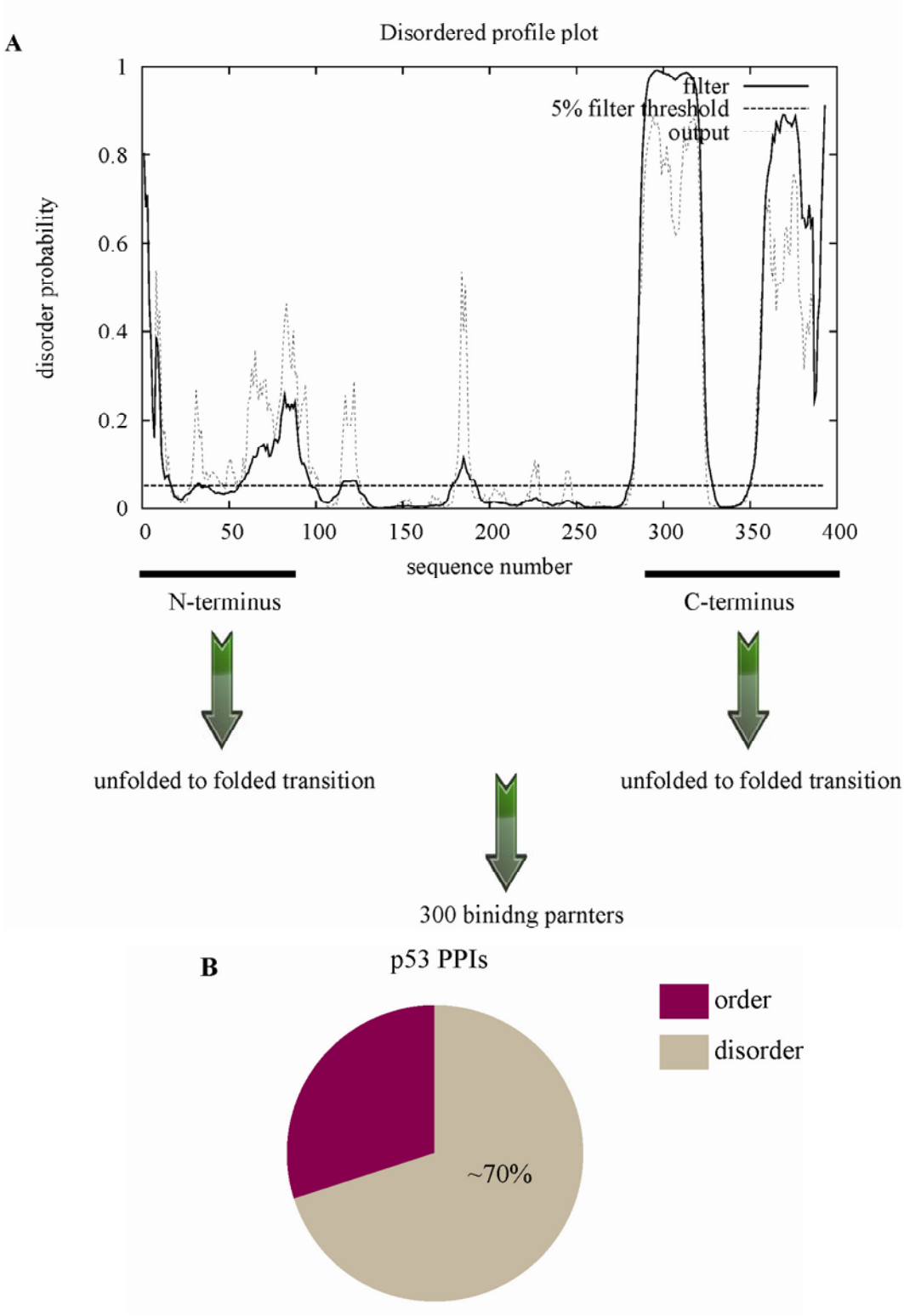

Figure 1.3 Predicted disordered regions in p53 protein. **(A)** Disordered regions in p53 protein as predicted using. p53 protein contains regions of disorder in N- and C-terminal portion of its sequence. Disorder provides p53 protein with great binding promiscuity, hence it has an enormous interactome. **(B)** A pie chart representing a percentage of p53's PPIs involving its disordered regions.

Further, the C-terminal regulatory domain is also unstructured [138] and undergoes folding transition as a consequence of binding to its vast range of binding partners (Figure 1.5 C). Interestingly, multiple secondary structures can be adopted depending on the ligand, which further emphasises the binding promiscuity and adaptability of p53 protein. Overall, it has been estimated that disordered regions of p53 confer approximately 70 % of p53 known interactions [152] (Figure 1.3 B). Interestingly, the DNA-binding domain of p53 binds to several proteins as well. The core domain is apparently folded, however significant differences in its structure have been observed depending on the bound partner [152]. This indicates that this domain is only transiently folded or in equilibrium between different conformations that allows it multiple specificities. Indeed, the core domain is relatively unstable at room temperature, and a peptide motif that precedes it can bind to and stabilise it [153].

1.2.1.3 p53: modules, linear motifs and multiple docking sites

a. Modules

Albeit structurally mostly disordered, functionally p53 can be divided into distinct domains (Figure 1.4 A). Briefly, the N-terminal domain, encompassing two transactivation domains, is involved in the interactions with the components of transcriptional machinery, such as p300 [154, 155], and forms a docking site for MDM2 [156]. In addition N-terminal domain is subjected to multiple post translational modifications (PTMs), mainly stress-induced phosphorylations that finely modulate p53 activity. The central (core) domain controls sequence-specific DNA binding and harbours most of the p53 inactivating mutations found in human cancers [157, 158]. It comprises four conserved regions, namely Box II, III, IV, V. Box V domain (270- 286) [159] is a multiprotein docking site and forms interactions with MDM2 [160] as well as with Chk1, Chk2 and DAPK-1 calcium kinase superfamily members [161]. Further, Box V functions as a primary ubiquitination signal for MDM2 [161, 162] and Box V unfolding in mutant p53 protein results in its hyperubiquitination [163]. Recent study has shown that Ser269 in this region can be targeted by phosphorylation and this inactivates p53 [164]. Box V is deleted in one

of the p53 isoforms, namely deltap53, that has been shown to transactivate only certain p53-dependent genes [165]. As such, by controlling modification of the p53 protein, allosteric regulation of p53 tetramer and its transcriptional activity, Box V provides multiple mechanisms to determine the p53 response upon stress. The DNA-binding domain is followed by the tetramerization domain (320-356) that allows formation of the transcriptionally active p53 tetramer [166-168]. The p53 tetramer is a dimer of dimers [167, 169]. Two monomers associate via their antiparallel β-sheets and helices into dimers. The dimers assemble via a hydrophobic core into a four-helix bundle arranged orthogonally into tetramers [170, 171]. The residues critical for the formation and stabilization of tetramer within the hydrophobic core are: F328, L330, I332, R337, F338, M340, F341, L344 and L348 [172-176]. In addition the tetramerization domain is involved in protein-protein interactions, either directly by forming a docking site, or indirectly in the instances when interactions are regulated by p53 oligomeric status. For example, tetramerization domain forms direct interaction with proteins including the casein kinase 2 [177], the Ca^{2+}-dependent protein kinase C [178, 179], the adenovirus E4orf6 protein [179], S100A4 and S100B [180], CUL7 [181], Pirh2 [182]. Lastly, the C-terminus encompasses a negative regulatory module that maintains p53 protein in a latent state for specific DNA binding. The six lysine residues present in this module (370, 372, 373, 381, 382, 386) can undergo various posttranslational modifications, including acetylation, methylation, ubiquitination, sumoylation and neddylation. Additionally, Serine and Threonine residues within this region can be subjected to phosphorylation. Both phosphorylation and acetylation stimulate core domain mediated DNA binding [183-185]. The C-terminal region of p53 forms a docking site for a variety of proteins, including S100B [186, 187], Sir2 [187], CDK2/ Cyclin A [188, 189] and CREB binding protein (CBP) [189].

A

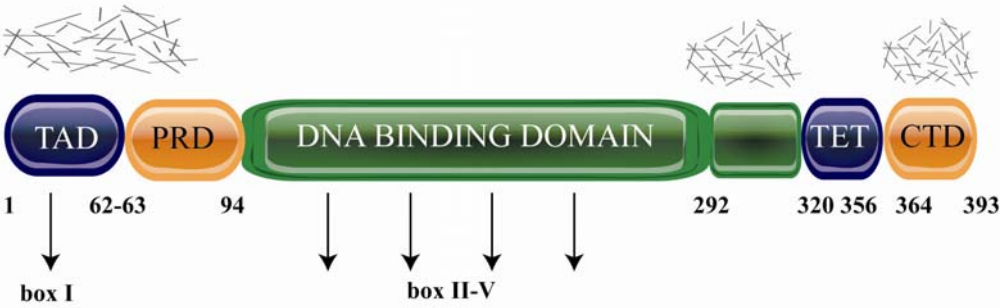

B

```
        10         20         30         40         50         60
MEEPQSDPSV EPPLSQETFS DLWKLLPENN VLSPLPSQAM DDLMLSPDDI EQWFTEDPGP

        70         80         90        100        110        120
DEAPRMPEAA PPVAPAPAAP TPAAPAPAPS WPLSSSVPSQ KTYQGSYGFR LGFLHSGTAK

       130        140        150        160        170        180
SVTCTYSPAL NKMFCQLAKT CPVQLWVDST PPPGTRVRAM AIYKQSQHMT EVVRRCPHHE

       190        200        210        220        230        240
RCSDSDGLAP PQHLIRVEGN LRVEYLDDRN TFRHSVVVPY EPPEVGSDCT TIHYNYMCNS

       250        260        270        280        290        300
SCMGGMNRRP ILTIITLEDS SGNLLGRNSF EVRVCACPGR DRRTEEENLR KKGEPHHELP

       310        320        330        340        350        360
PGSTKRALPN NTSSSPQPKK KPLDGEYFTL QIRGRERFEM FRELNEALEL KDAQAGKEPG

       370        380        390
GSRAHSSHLK SKKGQSTSRH KKLMFKTEGP DSD
```

Figure 1.4 p53 protein. (A) Schematic of p53 domain organisation. Transactivation domain (TAD), Proline-rich domain (PRD), DNA binding domain, Tetramerization domain (TET) and C-terminal domain (CTD) and conserved box regions are highlighted. Regions of disorder are depicted using "random hatching" symbol. **(B)** Sequence of human p53.

b. Linear motifs

The ability of the disordered region to bind such a diversity of proteins is conferred by short linear motifs that can adapt themselves to fit their binding partners (discussed in Chapter 4). As mentioned above, the same peptide motif from the C-terminal regulatory domain of p53 binds to different classes of proteins. A peptide region from this domain assumes a helical conformation upon S100B binding [186], a β-sheet in complex with Sir2 [187], an acetylated form of this peptide forms a β-turn-like structure in complex with the bromodomain of CBP [189], whereas lack of regular secondary structure is observed upon CDK2 binding [188] (Figure 1.5 C). It appears that the diversity of the assumed structures stems from the ability to "read" the same amino acids sequence differentially by the distinct interactors [152]. Further the PGGS motif in this domain binds to the deubiquitinase HAUSP/USP7 [190].

Similarly, the N-terminal domain of p53 is flexible and contains multiple docking sites. The Box I motif from the intrincically unstructured N-terminal region of p53 forms a high affinity binding site for the N-terminal hydrophobic pocket of MDM2 [191] and p300 [192]. Three amino acids in the transactivation domain of p53 (F19, W23, L26) are major contributors to the MDM2/4-p53 binding energy [145, 193-195] (Figure 1.5 A). Further, in addition to MDM2 interaction with its primary binding motif in the N-terminal domain of p53, MDM2 acidic domain binding to the second linear motif, namely Box V, in the conformationally flexible core domain in p53, within the S9-S10 loop/S10 β-sheet, is critical for p53 ubiquitination [160] (Figure 1.5 B). Interestingly, this region is highly flexible and forms a docking site for the protein kinases that phosphorylate p53 in its N-terminal domain [161, 196].

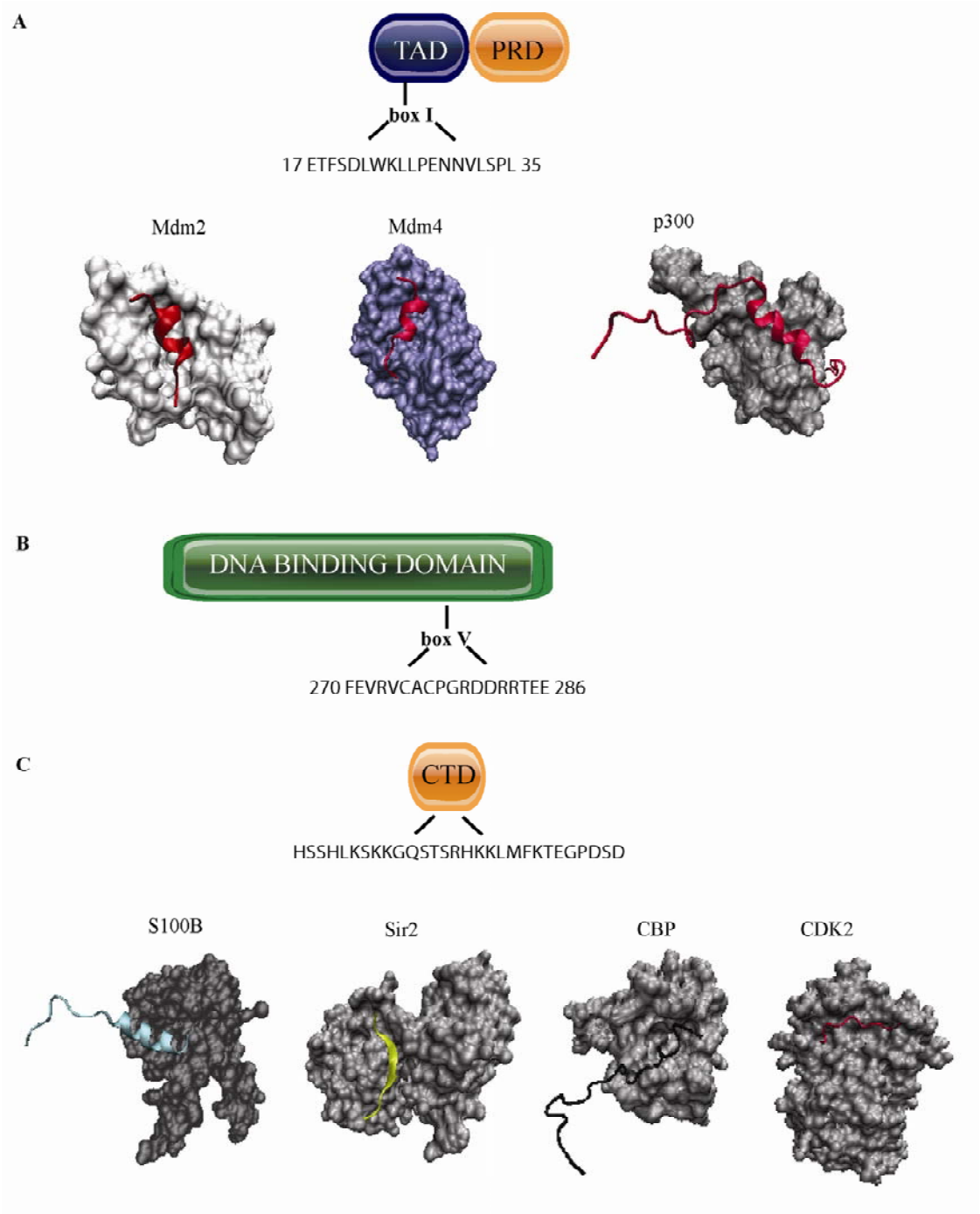

Figure 1.5 Linear motifs in p53 and disorder. (A) Box I region assumes helical conformation upond binding to MDM2 (PDB: 1ycq), Mdm4 (PDB: 3dac), p300 (PDB: 2k8f). **(B)** Box V sequence. **(C)** Schematic representing combinatorial diversity of the peptide motif in C-terminal region of p53. Peptide motifs adopt different conformations in complexes with S100b (PDB:1dt7), Sir2 (PDB:1ma3), CBP (PDB: 1jsp), CDK2 (PDB:1h26).

1.2.1.4 The p53 interactome: interactions with other cellular hubs

a. MDM2

The ring domain E3 ubiquitin ligase MDM2 (mouse double minute-2) has been the most studied p53-binding partner and rightly so as both these proteins appeared and evolved together [90]. Due to its ancient origins, the p53-MDM2 axis has had significant time to develop many layers of control, and it incorporates processes such as transcription, mRNA translation and protein degradation. The supremacy of MDM2 amongst other p53 binding partners is emphasised by the observation that the early lethality in mice with E3-ligase dead MDM2 can be rescued by knocking out the p53 gene [197]. Similarly to p53, MDM2 binds hundreds of proteins, and a significant subset of its binding partners overlaps with those of p53 protein (Figure 1.6 A). MDM2 is a multidomain protein, including the N-terminal hydrophobic pocket [145], the central acidic domain [198] and the C-terminal RING domain [199] (Figure 1.6 B). In addition, the presence of a flexible and unstructured pseudo-substrate motif in the N-terminus has been recently described, and named the lid, as it constantly moves around, being either over or outside the pocket [200]. MDM2 is best known for its role in the negative regulation of p53. MDM2 ubiquitinates p53 and targets it for proteasomal degradation [201-203]. This MDM2-mediated ubiquitination of p53 has been described by a dual-site mechanism [162]. Firstly, the Box I transactivation domain of p53 binds to the allosteric N-terminal hydrophobic pocket of MDM2, and the substrate binding results in conformational changes that stabilise the interaction of a flexible motif in the Box V domain of p53. In addition, for the initial binding of Box I to N-terminus of MDM2 to occur, the pseudo-substrate motif needs to dissociate from the hydrophobic groove and this is induced by lid phosphorylation [200] (Figure 1.6 C). Furthermore, MDM2 hinders p53 transcritional activity both directly by (1) binding p53's transactivating domain and (2) sterically occluding p53 association with transcription factors, through binding to interfaces overlapping with their binding interfaces [191, 204, 205]; and (3) indirectly, by sequestering p53 out of nucleus [206]. As MDM2's transcription is activated by p53 [207], these two proteins are engaged in the p53 autoregulatory feedback loop [204]. Interestingly, MDM2 can

positively regulate p53 activity and stability via interaction with p53 mRNA that stimulates p53 synthesis and blocks MDM2-dependent p53 ubiquitination [208].

In addition to MDM2, p53 binds to the closely related MDM4, which does not possess E3 ligase activity [209]. Similarly to MDM2, MDM4 binds to transactivation domain of p53 and blocks the recruitment of transcriptional machinery, resulting in the inhibition of p53-mediated transcription. In addition to MDM2, other E3 ligases bind to p53 and regulate its degradation and cytoplasmic localization. RING domain containing E3-ligases, such as Constitutively Photomorphogenic 1 (COP1), p53-Induced protein with a RING-H2 domain (Pirh2), Carboxy terminus of Hsp70p-Interacting Protein (CHIP), Caspase 8/10-Associated RING Proteins 1 and 2 (CARP1, CARP2), TRIM24 or Synoviolin or the HECT domain containing ARF-Binding Protein 1 (ARF-BP1), and Ubiquitin-conjugating enzyme 13 (UBC13) can catalyze p53 polyubiquitination and target it for degradation [210-215].

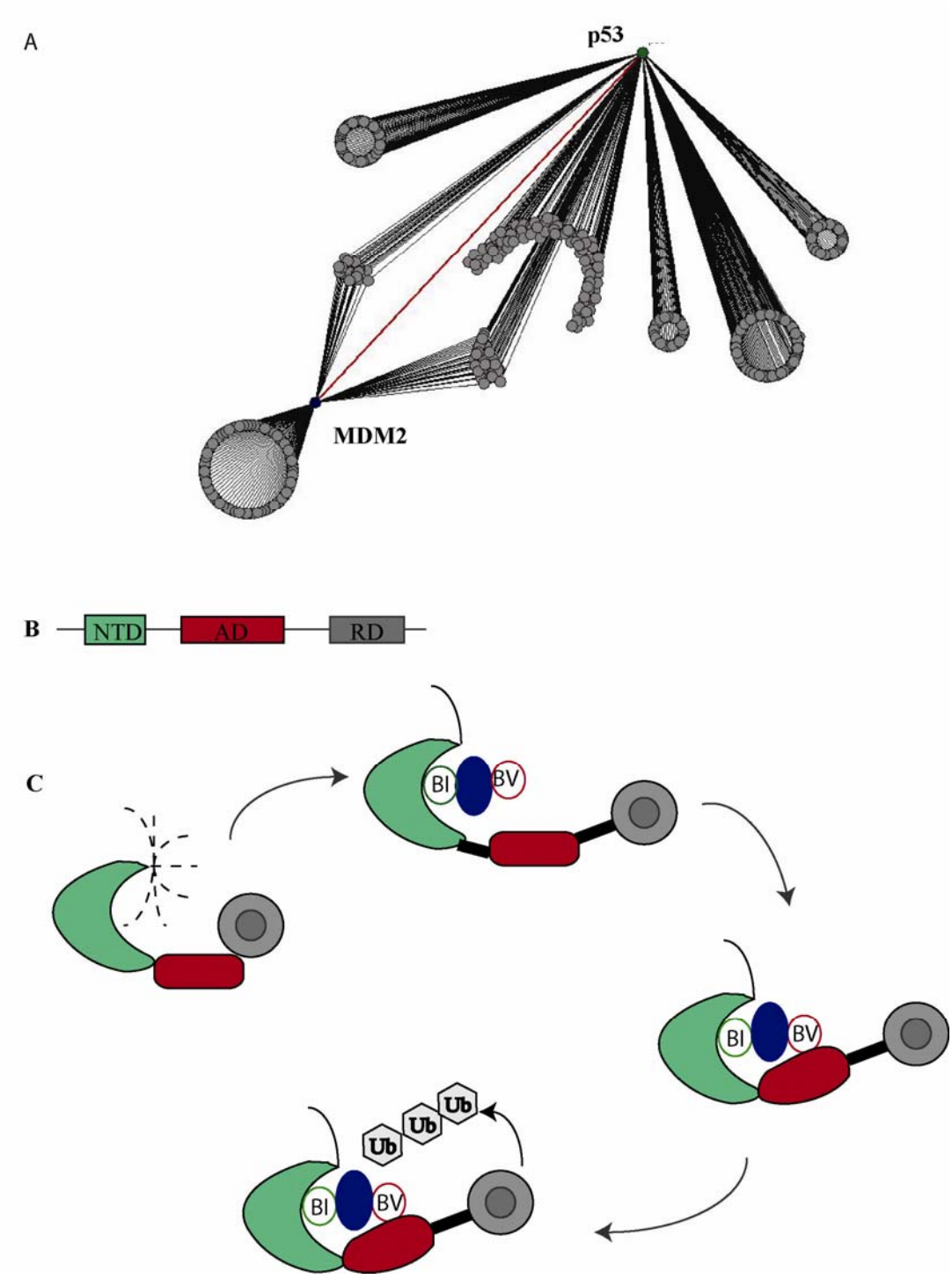

Figure 1.6 MDM2 and p53 interaction. (A) The interactomes of p53 and MDM2. Shared and non-overlapping interactions are highlighted (p53 binding partners and listed in the appendix). **(B)** Schematic of domain structure of MDM2, NTD-N-terminal domain, AD-Acidic domain, RD-Ring domain. **(C)** Dual site mechanism, BI- Box I, BV- Box V, Hydrophobic pocket: green, Acidic domain: red, Ring domain: greys, Lid-dashed and solid line.

b. p300

Similar to p53, the transcriptional coactivator p300 is a prime example of the disordered hub protein and it has approximately 400 interacting partners [192]. It is predicted that approximately half of this protein consists of intrinsically unstructured regions [216] and that these are connected by folded domains of p300. p300 possesses histone acetyltransferase activity and this confers its role in relaxing compact chromatin structure [192]. It also acetylates targets other than DNA, however, and indeed, it was found that p300 mediates acetylation of the C-terminal region of p53 [217]. The p300-binding region of p53 overlaps with residues that are involved in the tight biding to MDM2 [154, 218, 219]. p53 binds to several different p300 peptide-binding minidomains, including C/H1, C/H3, IBiD, IHD, SPC-1, SPC-2, KIX, and Bromodomain [220, 221]. p300 or its homolog, CREB-binding protein (CBP), binding to p53 stimulates its activity [154, 219, 222-224] catalyzing acetylation of the C-terminal lysines as well as K164 [225]. p53 acetylation is critical for the efficient recruitment of transcription-associated factors (TAFs) and subsequent activation of p53-responsive genes [137]. As MDM2 and p300 compete for the same binding site, p300 binding may inhibit MDM2-mediated ubiquitination of p53, whereas MDM2 binding prevents assembly of transcription complexes on the p53 protein. The choice of the binding partner depends on the posttranslational modifications of p53 (discussed in 1.2.1.6). Interestingly, in addition to preventing p53 binding to p300, MDM2 can also employ other mechanisms to decrease p53 acetylations. For example it recruits histone deacetylase 1 (HDAC1) complex or degreades another p53 acetyltransferase PCAF [226].

1.2.1.5 The p53 interactome: interactions with scaffolding proteins and chromatin modulating proteins

A number of co-factors regulate p53 association with acetyltransferases. For example, junction-mediating and regulatory protein (JMY) can bind to p53-p300 complex [227, 228]. Following DNA damage, JMY and another cofactor STRAP

accumulate in the nucleus, in which they associate with p300/CBP-p53 and promote p53-dependent transcription and apoptosis [227, 228]. Additionally, protein arginine methylatransferase (PRMT5) can be recruited by STRAP to the JMY-STRAP-p300-p53 complex, and subsequent arginine methylation of p53 stimulates transactivation of the p21 promoter which switches the p53 response from apoptosis to cell-cycle arrest [229]. In addition to p300 and CBP other factors are implicated in the activation of p53-dependent transcription. For example, other acetyltransferases are recruited by and acetylatate p53, including Tip60, hMof or PCAF [230-232].

1.2.1.6 The p53 interactome: PTMs modulate specificity of disordered region and the resulting PPI landscape

p53 protein is targeted by multiple post-translational modifications (Figure 1.7) and interestingly these sites are primarily located in the unstructured regions of this protein [152]. This provides additional mechanism for the fine adaptation of the p53 interactome to the cellular conditions and is characteristic for other intrinsically disordered hub proteins [233]. The linear motifs that are targeted for covalent modification can anchor the enzyme and allosterically activate it. Post-translational modifications regulate the specificity and the interactome of p53 protein. Firstly, several phosphorylation events at the N-terminal domain of p53 activate p53 and substantially rearrange its interactome. These phosphorylations involve PPIs with several kinases such as Mutated in Ataxia-Telangiectasia (ATM), A-T and Rad3-related (ATR), the checkpoint kinases 1 and 2 (Chk1 and Chk2), Jun JNK (NH2-terminal kinase), p38 and others. For example, ATM kinase catalyses p53 phosphorylation on multiple sites, the most common being S15, S20 and S33 [234-237], calcium-calmodulin family members Chk1 and Chk2 kinases phosphorylate T18 and S20 [238, 239]. CBP/p300 and MDM2 compete for the binding site and the modification sites on p53. Interestingly, S15 phosphorylation increases p53 binding to CBP [240], phosporylation at S20 and T18 stabilises p53 interaction with p300 [155, 241] and T18 phosphorylation decreases binding to MDM2 [241-244]. The sequence of the p300-p53 complex formation following

posttranslational modifications is well established. The binding of CHK2 and CHK1 to p53 stimulates p53 phosphorylation at T18 and S20 [245]. The phosphorylation of these residues stabilises p300 binding to the LXXLL motif in the N-terminal domain of p53 [241], and is followed by p300 anchoring to the phospho-LXXLL and PXXP motifs in the transactivation domain of p53 [155]. These phosphorylation and docking events lead to sequence-specific DNA binding by p53 that enforces structural changes in the p53 tetramers followed by PXXP-dependent acetylation of p53. The latter modification stabilises the p300-p53-DNA complex and this fact further reinforces the importance of PTMs in regulating PPIs [155]. Importantly, these events are essential for p53 stabilisation upon stress.

Interestingly, stress induced phosphorylation of the proline rich domain of p53, by kinases including Jun, p38, HIPK2 on S33, S46, T81 or S315 [246-248], induces binding of Pin1 [249, 250]. Pin1 catalyzes phosphorylation-dependent prolyl isomerisation [251]. Pin-1-mediated rearrangements at T81-P82 result in Chk2 binding and phosphorylation of S20 on p53 and consequently dissociation of MDM2 [250, 252] and p300 recruitment [241], whereas recognition of S46 leads to iASPP dissociation [253]. Further Pin1 favours p53 binding to chromatin and this promotes p300 binding to p53 and the subsequent acetylation [253]. By stimulating acetylation and iASPP dissociation, Pin1 leads to activation of p53 apoptotic function.

Another example of PTM being involved in the complex formation includes Lysine residues in the C-terminal domain of p53. Three sites, K370, K382 and K372 are methylated by Smyd2, Set8 and Set9, respectively [254-256]. Interestingly, demethylation of p53 by p53-interacting histone lysine-specific demethylase 1 (LSD1) [257] at K370 and K382 enhances the avidity of p53BP1 to p53 and enables recruitment of p53 to sites of DNA damage [258, 259]. Further tuning of this interaction was proposed to be achieved by acetylation of K381 and phosphorylation of S371 in CTD domain [258]. In addition p300 and MDM2 compete for the same binding site and phosphorylation of T18 in TAD region favours p300 over MDM2 binding [218, 241].

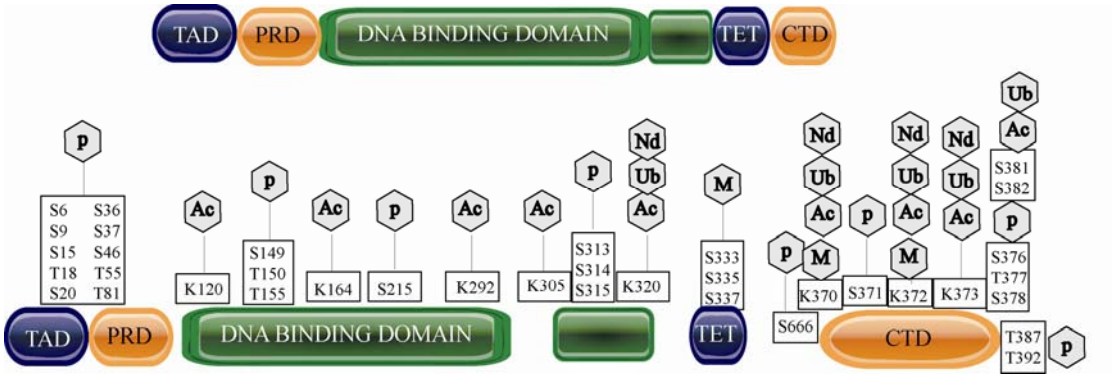

Figure 1.7 Posttranslational modifications on p53. P-phosphorylation, M-methylation, A-Acetylation, Ub-ubiquitination, N-neddylation.

1.2.1.7 The p53 interactome: chaperones

Molecular chaperones are proteins that assist the folding and unfolding or the assembly and disassembly of other proteins [41]. Heat-shock protein family members, Hsp70 and Hsp90 proteins, are the most studied molecular chaperones that in association with their cellular cofactors form the so called "cell chaperone network" [260]. Interestingly, recombinant wild type p53 protein was shown to interact with Hsp90 and Hsp70-Hsp40 chaperone systems [261]. For example, p53 has been reported to interact with molecular chaperone Hsp90 and this interaction maintained the folded state of p53 [262]. Subsequently, Hsp90 was found to be essential *in vivo* for wild type p53 binding to the target DNA sequence at physiological temperatures [263] and its overexpression stabilised p53 protein [264, 265] and stimulated the p21 expression [264]. Further Hsp70-40 chaperones were found to cooperate with Hsp90 to fold p53 under heat-shock conditions or after its prolonged incubation at 37ºC [263]. This latter observation supports the idea that the "structure" of non-native p53 may encompass different kinds of unfolded or misfolded species [266] that could be regulated by distinct types of chaperones. Interestingly, the process of Hsp90-mediated chaperoning of p53 requires the presence of ATP, which enables dissociation of partially unfolded p53 from Hsp90 and further folding to the active conformation [264]. Further, CHIP E3 ligase binds intrinsically disordered N-terminal domain of p53 and can restore DNA binding activity of heat-denatured p53 [267]. In addition MDM2 can chaperone p53 and could substitute for Hsp90 in stimulating p53 binding to its target DNA sequence [268].

1.2.2 Mutant p53 protein- hub

The absence of functional p53, either by silencing or mutating p53 gene, is the most common aberration in human cancers [52]. The main activity of p53, mediated by the core domain of this protein, is linked to its sequence specific DNA binding and regulation of transcription of several hundreds genes. Each residue in the

DNA-binding coding region was found to be mutated in human tumours. Additionally hot spot mutations that account for over 25 % of all the mutations found in human tumours are located in the core domain [269]. Various p53 mutations exert different effects on the structural properties of the resulting protein, an idea that was explored relatively early in the history of p53 biochemistry with the use of p53 monoclonal antibodies, namely PAb1620 and PAb240 that could discriminate folded and unfolded states of p53, respectively [270]. Consequently, the mutations in the p53 cancer mutants can be broadly divided in two distinct classes [136]. DNA-contact mutations, such as R273H or R248W, result in a mutant p53 protein that has reduced capability to bind DNA. Consequently, this mutant protein is essentially unable to regulate transcription of its target genes, which hampers its paradigmatic tumour suppressive activity [271]. As the DNA-binding domain of p53 is quite labile already in the wild type protein, some mutations in this region, so called structural mutations, such as V143A or R249S, can further reduce its thermodynamic stability and produce substantial conformational change or highly destabilised protein [136].

1.2.2.1 Prooncogenic functions of mutant p53 and mutant p53 interactome

p53 protein regulates expression of hundreds of genes and this function is commonly lost or altered by mutant p53 in human tumours. Classically, mutant p53 protein is regarded as a protein that cannot bind the p53 target promoters which in turn reduces expression of these genes [66, 272, 273]. However, p53 can in fact repress a subset of genes, and loss of wild type p53-dependent suppression of these targets leads to their increased expression. For example, p53 represses expression of the growth- and survival-promoting factor CD44 [274] (Figure 1.8). CD44 functions as a receptor for the extracellular matrix, regulates growth factor binding to their receptors and activates various pathways, such as RhoA GTPase pathway. In addition, CD44 is involved in stem cell renewal [275]. All these actions account for the oncogenic properties of CD44 [276] and emphasise the importance of loss of p53-mediated repression of this gene in tumours.

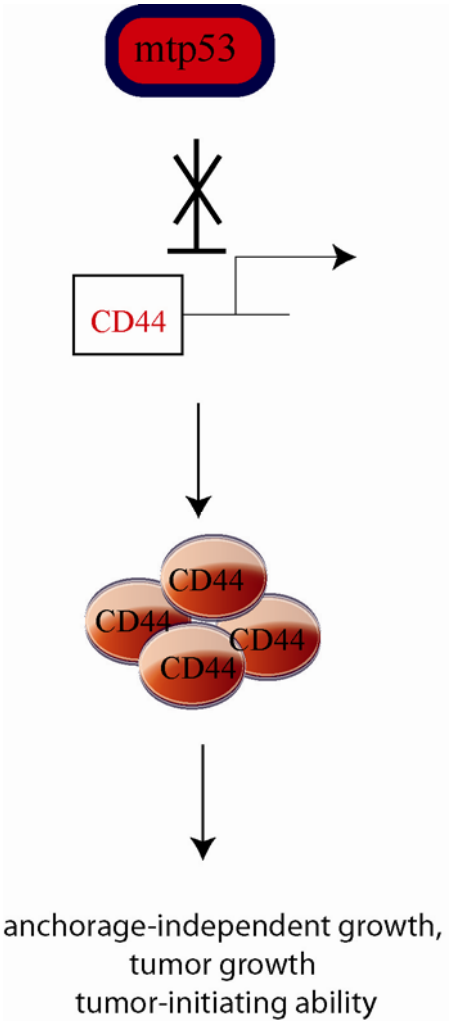

Figure 1.8 Example of the loss of function of p53.

The loss of DNA binding ability and consequently loss of tumour suppressive activity by mutant proteins is just a simplified view of the effect of the emergence of mutant p53 protein in the cell. The significant stabilisation of mutant p53 protein in cancer cells (discussed in 1.2.2.1 V) indicates that there are pro-oncogenic advantages of expressing mutant p53 protein. Indeed, in addition to dominant negative effect of p53 mutations, mutant p53 can acquire new, oncogenic activities. This concept of mutant p53 protein exerting gain-of-function properties is further supported by the observation made in transgenic models of mutant and knock-out p53, that mutant p53 expressing cells but not cells with the genetic loss of p53 have increased metastatic properties [277].

The loss-of-function to gain-of-function phenomena can be partially linked to two classes of mutations, as the structural outcome of mutations has been shown to correlate with the aggressiveness of cancer. The structural mutants are associated with more severe phenotypes and DNA-contact mutants are less aggressive in transformation assays [278]. However, the determinants that drive gain-of-function properties of mutant p53 protein are more complicated and cannot be always explained by this simple classification. For example, the R273H form of p53, traditionally perceived as a DNA contact mutant protein, exhibits conformational changes in some assays. Accordingly, in a study looking at the regulation of expression of Ras dependent inflammatory chemokines, cytokines, interleukins and extracellular matrix proteins, collectively named 'Cancer-related Gene Signature' (CGS) by mutant p53 [279, 280], conformational mutants had a similar to p53-null cells effect on Ras activity, suggesting loss of function, whereas DNA contact mutants further induced Ras activity, by GOF mechanism [281, 282].

The notion that the mutant protein has lost the ability to bind to the wild type p53 consensus site, raises the question of how this protein can "gain its functions" or otherwise actively stimulate transcription. The most obvious possibility is that it is through binding to a distinct set of proteins. Indeed, given the disorder and promiscuity of p53 protein and its large interactome, mutant variants of p53 are likely to rewire the wild type p53 landscape and as they gain and loose functions they can gain and loose their binding partners. Paradoxically, despite good comprehension of wild type p53 interactome, and the fact that mutant p53 has been studied for

longer than wild type protein, mutant p53 interactome is far from being fully understood. This can be partially explained by the fact that there is not a single mutant p53 protein, but a collection of distinct types of proteins that are likely to have a very specific set of interacting partners exists.
The changes in signalling in cells expressing mutant p53 can be explained in part by the protein interactions of mutant p53 and are discussed below and in Figure 1.9.

I Mutant p53 PPIs: NF-Y, HDAC1, p300

The mutant p53 interactions with the heterotrimeric transcription factor NF-Y, histone deacetylase and p300 are an interesting example of how mutant p53 can rewire the wild type p53 PPI landscape [283]. Similarly to the wild type protein, mutant p53 can bind to NF-Y on the promoters of NF-Y-regulated genes [283]. Following DNA damage however, instead of recruiting histone deacetylases (HDACs) and dissociating from histone acetyltransferases (HATs), as the wild type p53 does [284], mutant p53 protein does the opposite. Consequently, rather than repressing cell cycle control genes such as cyclin A, cyclin B2, cdk1, and cdc25C, mutant p53 transactivates them, which results in abnormal cell cycle regulation. Further, in unstressed cells, wild type p53 recruits p300 and activates the expression of NF-Y dependent genes, and mutant p53 represses them in a HDAC-1 dependent mechanism.

II Mutant p53 PPIs: p63 and p73

Interestingly some of the mutant p53 functions arise from its interactions with the p53 gene family members, namely p63 and p73. All three proteins are structurally related in terms of having three highly conserved domains: N-terminal transactivation domain, DNA-binding domain and oligomerization domain [285]. Further, full length p63 and p73 can activate transcription of some of the p53 responsive genes and consequently activate cell cycle arrest or apoptosis [286-290]. Interestingly, the oligomerization domains of p63 and p73 can form heterotetramers, however neither of them can hetero-oligomerize with the wild type p53 [291].

Despite this, a substantial number of mutant p53 proteins, including conformation and contact mutants, have acquired the ability to form a direct interaction with either p63 or p73 [292-298]. Interestingly, both mutant p53-p63 and mutant p53-p73 complexes are not mediated through tetramerization domain but via their respective DNA-binding domains [292, 293, 296]. An explanation as to why these interactions become possible in the mutant p53 background could be that it is due the structural changes that core domain undergoes upon mutation. Indeed, the PAb240 reactive mutant p53 proteins or PAb240 reactive purified wild type protein associate with either p63 or p73 [296]. Similarly, structural p53 mutants that associated with hsp70 were also found in complex with p73 [296, 299]. However, it was found that truncated versions of wild type p53 protein expressed in insect cells or some p53 contact mutants that do not show significant conformation changes retained ability to bind to p63/p73 [296] and it is possible that these variants of the protein can exhibit some structural changes that, given the promiscuity of p53 domains in respects to their PPIs, may be sufficient to form or expose a binding motif for these proteins. Importantly, the complex formation interferes with the p63/p73 capability to bind to their target promoters [292-294]. This leads to inactivation of transcriptional activity of p63 and p73 and their growth suppressive and apoptotic functions, thus conferring abnormal cell proliferation [292-294, 296-298]. There are a number of physiological consequences of this newly acquired PPI. Firstly, a correlation was found between human cell lines resistance to doxorubicin, taxol, cisplatin, etoposide and ability of mutant p53 to bind p73 [295, 298]. To take this further a study of murine equivalents of human p53 R175H and R273H mutants showed that these mice had a greater metastasis propensity compare to p53 knockout mice. Interestingly, these mutant proteins interacted with both p63 and p73 in cells derived from these mice and silencing either p63 or p73 stimulated the phenotype of p53-null cells, supporting the hypothesis that increased metastasis in mice bearing mutant p53 may be through inhibition of p63 and/or p73 [300, 301].

A recent study demonstrated the role of p63 in promoting metastasis in mutant p53 background [302]. p63 regulates expression of genes whose products are involved in executing adhesion programme, including laminin-binding integrins (α3β1, α6β1, α6β4) and integrin subunits (α5, β1) that bind to fibronectin in the extracellular

matrix [303]. Interestingly, Muller et al. demonstrated that enhanced integrin and EGFR recycling from endosomes to the cell membrane, correlating with the increased phosphorylation of Akt, could account for the ability of the mutant p53 to promote metastasis [302] (Figure 1.9 D). Further, in an intestinal tumour model driven by the loss of the wild type adenomatous polyposis coli (Apc) gene, expression of mutant p53 increases invasiveness by 75 % [272]. In this report, the effects of various p53 mutants on cell migration were monitored in response to treatment with epidermal growth factor (EGF). The invasive phenotype of mutant p53-expressing cells was found to be conferred by inhibition of p63 by mutant p53 protein, as overexpression of transactivation domain of p63 was sufficient to inhibit migration and invasion of the mutant p53 cells, whereas depletion of p63 in p53 null cells enhanced cell invasivness. It is worth stressing that in this system, p63 acted as tumour suppressor as it negatively regulated migration and invasion. In this study, mutant p53 could drive invasion in a TGF-β-independent manner, however a different study found that TGF-β signalling, in fact, co-operated with mutant p53 to promote metastasis [276].

III Mutant p53 PPIs: SMADs, p63

As discussed in chapter 3, TGF-β signalling cascade has both tumour suppressive and oncogenic properties depending on the cellular context [304]. Wild type p53 protein cross-talk to this pathway is well established and it has been recently shown that wild type p53 can confer TGF-β tumour suppressive activity, by its interaction with SMADs that leads to induction of p21 and growth suppression [305]. Interestingly, mutant p53 can also engage into interaction with SMAD protein and as a complex sequester p63 (Figure 1.9 E). This ternary complex disables p53 from binding to the promoters of its transcriptional targets. The co-operation of TGF-β signal and mutant p53 results in aberrant gene expression, for example in downregulation of Sharp-1 or Cyclin G2, and drives invasion and metastasis [306]. Interestingly, in another report it was found that mutant p53 attenuated TGF-β signalling pathway and suppressed expression of a range of TGF-β-dependent genes, including MMP2, MMP9, and TGFβRII, contributing to the suppression of

TGF-β-stimulated migration [307] (Figure 1.9 F). These apparently inconsistent findings are in line with the broad spectrum of mutations that p53 can acquire as well as with the importance of the cellular context in dissecting the pro-metastatic potential of mutant p53. In addition mutant p53's ability to either induce [302] or suppress [307] motility was observed in response to different stimuli and indeed different signalling pathways are likely to have a major implication for the PPIs of mutant p53.

IV Mutant p53 PPIs: ASPP2 and Bcl-Xl

The wide spectrum of possible consequences of p53 mutation is exemplified by the different effects distinct mutations have on the mutant p53's PPIs. For example, given that each residue in the core domain of p53 has been found to be mutated, it is not surprising that the heterogeneity in respects to mutant protein's structure, and consequently its PPI and function, is observed [308]. For instance, Bcl-Xl and p53BP2/ASPP2 bind to the DNA-binding domain of wild type p53, through different, albeit overlapping residues [309, 310]. The core domain of wild type p53 interacts with the C-terminal domain portion of ASPP2 (p53-binding protein 2-53BP2), and this is associated with the apoptotic function of p53, but not with the cell cycle arrest, as genes such as BAX and PIG3, but not p21 are transactivated (reviewed in [311], [309, 312]). Interestingly, DNA contact mutants, such as R273H, retain the 53BP2 binding ability, but have no transactivation activity. Other mutants, such as R175H, lose both DNA binding and ASPP2 binding ability. Interestingly, two p53 mutants R181E or G245S can no longer bind to 53BP2, however they retain their DNA-binding activity [313-315]. Wild type p53 interaction with Bcl-Xl promotes apoptosis in a transcription-independent way. Interestingly, some mutant p53 protein can no longer bind to Bcl-Xl and this prevents cytochrome c realease. This is an interesting example of how mutation in tumours is selected to concomitantly perturb the transcriptional and PPI-dependent p53-activated apoptosis [310]. In addition, these data suggest that different cancers present specific ways of disrupting p53-proapoptotic pathway, and these may have further implications in comprehensive approaches to targeting cancer with different mutant p53 signatures.

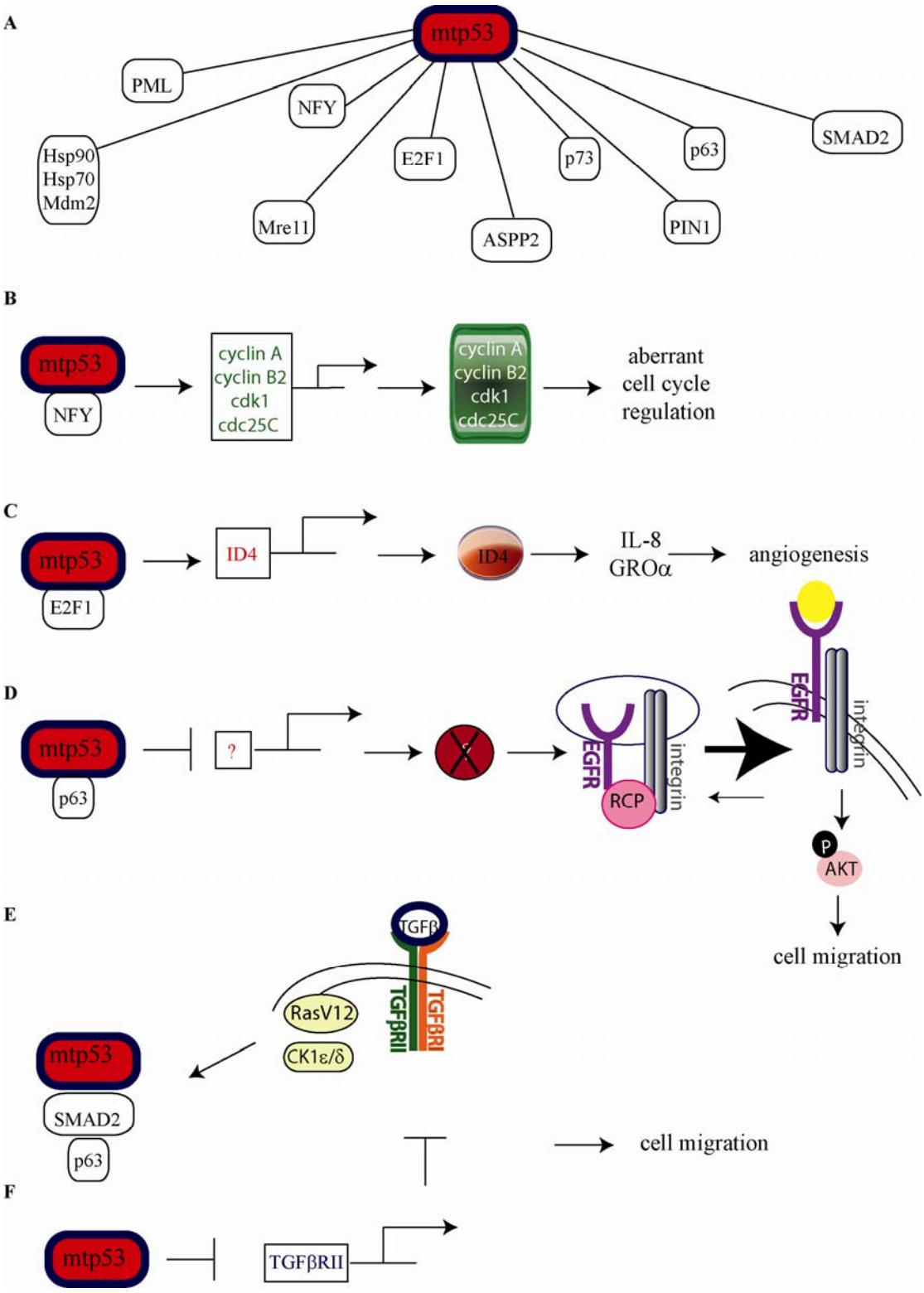

Figure 1.9 Mutant p53 interactome. (A) The schematic of the growing interactome of mutant p53. The mutant p53 protein binding partners include p63 and p73, SMAD2, E2F1 [316], PML [317], Mre11 [318, 319], Pin1, ASPP2, NFY, molecular chaperones and others. **(B-F)** Gain of function properties of mutant p53 through its PPIs. **(C)** Both mutant and wild type p53 protein [320] can form the interaction with the transcription factor E2F1. Mutant p53 protein binds to E2F1 and is recruited to the ID4 promoter. The production of ID4 leads to the expression of pro-angiogenic genes. The significance of interactions **(D-F)** is discussed in the main text.

V Mutant p53 PPIs: the proteasome/chaperone system

Mutant p53 protein accumulates in the nucleus of cancer cells [299, 321]. Several possibilities to explain the stabilization of p53 protein in tumours have been proposed. For example, it has been suggested that the lack of induction of MDM2 by mutant variants of p53 accounted for its accumulation. Alternative hypotheses included decreased sensitivity of conformationally changed mutant proteins to degradation, increased stability of mutant p53 mRNA or increased mutant p53 mRNA translation. However, the intricacy and complexity to the underlying mechanism was increased by the observation that in transgenic mice tumour cells express mutant p53 at much higher levels than normal cells [301, 322]. In fact, mutant p53 protein was extremely unstable in normal cells [301]. Indeed, the second binding site for MDM2 on p53, located in the core domain, is exposed in the mutant protein [323] and is hypersensitive to ubiquitination *in vitro* [160, 163], yet, the human mutant p53 protein is stabilised *in vivo* [324, 325]. The first interacting partners of p53 identified were members of the heat shock protein chaperone network, including Hsp70 and 90, and this binding events regulated the stability of p53 [326, 327]. Mutant p53 does not fold properly and forms complex with Hsp70 that targets it for CHIP-mediated degradation [328]. On the other hand, Hsp90 protects mutant p53 from MDM2-dependent ubiquitiniation and degradation [329-331]. Hsp90 mediates folding of p53 and can form a stable complex with the unfolded mutant proteins [328] and tumour cells are “addicted” to the activated heat shock system and require it for their survival [332]. Further it was hypothesised that Hsp90-mutant p53 interaction engages MDM2 and/or CHIP and “traps” them in an inactive state [332]. Therefore, the interaction of the proteins of proteasome/chaperone system with mutant p53 may differentially affect the balance between the degradation and stabilisation of p53 protein and shift it towards increased stability in cancer cells. The implication for these observations is that the different amounts of mutant p53 between cancer and normal cells are a direct reflection of the differences of chaperone/proteasome complexes between these cells.

1.2.2.2 p53- PPIs and drug discovery

The obvious implication of the pro-oncogenic function of mutant p53 protein is that targeting the mutant p53 protein pathway should give significant therapeutic benefits. The key approaches to develop therapeutics that target mutant p53 include: re-establishing wild type functions in mutant p53 protein, inducing degradation or inhibiting synthesis of mutant p53 and finally interfering with the oncogenic component of the mutant p53 PPI landscape. The latter strategy could be the most effective, as the complexity of protein PPI's has a major contribution to the gain-of-function properties of mutant p53 protein.

Targeting the p53-MDM2 interaction has been the most exploited approach to reactivate wild type p53. Nutlins were the first identified small molecules that could displace p53 from MDM2 [333, 334] and were subsequently shown to inhibit tumour growth [335, 336]. Further, a small molecule screen for the compounds that could reactivate wild type p53 activity led to identification of RITA (reactivation of p53 and induction of tumour cell apoptosis; 2,5-bis (5-hydroxymethyl-2-thienyl) furan, NSC-652287) [337-339]. The originally proposed mechanism for RITA-mediated p53 activation, was that it disrupts MDM2-p53 complex [339]. However, it was earlier found that RITA induces DNA damage [337, 338], hence a more complex mechanism may lead to the observed cellular outcome. Recently, it was found that RITA activates ATM/ATR DNA damage response pathway, and subsequently Chk1 kinase, the latter being dependent on the presence of p53. Moreover, RITA could prolong S phase and induce DNA damage only in p53 expressing cells [340]. Lastly, RITA could downregulate two p53 regulators, MDM2 and WIP1, potentiating p53-mediated cell death [341]. Importantly, since currently the mechanisms that switch MDM2 from being a p53 inhibitor to it being a stimulator are not fully understood, small molecules that bind MDM2 may actually induce metastasis, for example by interfering with MDM2 mediated degradation of Slug [342]. Furthermore, given that the substrate binding by the hydrophobic pocket can in fact enhance MDM2 mediated ubiquitination [162, 200], drugging this interface may not give the desired effect of the inhibition of p53 ubiquitination. The allosteric effect of MDM2-p53 interaction is not exclusive to the hydrophobic pocket. In fact all of the domains are involved in the dynamic allosteric interactions.

For example the RING domain regulates the conversion of the acidic domain between open and closed conformations [343]. As the phospho-mimetic MDM2 lid can stabilize interaction of the acid domain with the ubiquitination signal in p53, this second PPI interface may be a better target for developing small molecules that inhibit MDM2 ubiquitination of p53. In addition, MDM2 has a dual role in inhibiting p53, as it not only targets it for degradation, but also suppresses p53-mediated transactivation of its target genes. Therefore drug leads that are effective at inhibiting E3 ligase activity of MDM2 are likely to be different to these that release p53 from MDM2-mediated suppression of p53 transcription.

Targeting mutant p53 protein by small molecules is a great challenge. The diversity of mutations in combination with the cell type and microenvironment pose a requirement for different strategies. Indeed, the understanding of the selective pressures that drive the choice of the type of mutation that dominates in the given cancer tissue, may be essential for developing effective therapeutics. The data regarding the PPIs of mutant p53 have provided a number of potential drug targets. For example targeting factors that prevent degradation of mutant p53 protein could show therapeutic benefits. Indeed, in some tumour cells inhibition of HSP90 with geldanamycin or its derivatives induced chaperone-mediated degradation of mutant p53 [328]. Further, targeting the complex of mutant p53 with SMADs and p63 could be a potential option for inhibiting metastasis. Specifically, molecules disrupting mutant p53 and p63 complex could be effective.

An interesting strategy involves inhibitors of RAS-CK1 signalling, which is required for the stabilisation of mutant p53-SMAD2 complex, and these are currently undergoing clinical trials. However, for the successful mutant p53 drug development, the growing size of its PPIs network has to coincide with the understanding of the functions of a specific PPI or subset of PPIs. In addition, developing inhibitors of specific mutant p53 PPI has to coincide with designing assays that would enable the understanding as to how the function of the particular PPI is affected. An example of such an approach, has led to the identification of RETRA [344]. As p53 mutant proteins can form a complex with p63 and p73 and block their transcriptional activity [296], it was hypothesised that identifying small molecules that could stimulate p73 in the mutant p53 background, could provide a very specific drug that could strictly

suppresses cancer in the mutant p53-expressing cells [344]. A transcriptional reporter assay was established to screen for molecules that could reactivate the tumour suppressor pathway in mutant p53-bearing cells. The p53-responsive promoter was used in these cells in a high-throughput screening of a chemical library and several compounds that could transactivate the promoter were identified. Interestingly, RETRA compound was not active in the wild type p53-expressing cells or p53-null cells. When this compound was further tested, it was found that p73 had a significant contribution into the observed actions of RETRA, as p73 depletion led to decreased activity of the drug. Subsequently it was found that RETRA inhibited p53/p73 interaction, and release of p73 from suppressing mutant p53 resulted in the induction of p53/p73-regulated genes [344].

The allostery model of protein control describes how ligand binding by an unstable protein can stablise it and/or shift it to the active coformation. Wild type and even more so mutant p53 protein are unstructured and unstable. Therefore, reactivation of mutant p53 through small molecules appears to be an interesting therapeutic strategy. Recent advances and contributions from different fields led to identification of molecules that can interact with mutant p53 and shift equilibrium from the unfolded to folded conformation. For instance PRIMA-1 and its analogue APR-246 that can form stabilising covalent modification in the core domain of mutant p53 protein were identified [40, 345, 346]. These modifications restore DNA binding activity and trigger p53-dependent apoptosis. Interestingly, PRIMA-1 could also activate mutant p63 and p73 proteins [347]. This raises the question of the mechanism of PRIMA-1 mediated activation of p53 family members. For example, PRIMA-1 has been recently shown to enhance cell death in cell expressing truncated mutant p53, and raises the possibility of a more complicated than initially assumed mode of action [348]. In fact, PRIMA-1 may modulate many proteins in the cell and act as a pharmacological chaperone, an antioxidant, a concept supported by recent observation by Grinter and colleagues, that in addition to p53, PRIMA-1 can inhibit oxidosqualene cyclase (OSC), which is part of the cholesterol synthetic pathway [349]. Converesly, another OSC inhibitor, namely Ro 48-8071, decreased the viability of mutant p53 expressing cells.

Another approach is to use *in silico* modelling to identify molecules that will bind to cavities or grooves that form in the core domain of the mutant p53 protein. For example p53 Y220C is an example of such a mutant protein, where the Tyrosine to Cysteine substitution forms a cavity away from the functional surfaces of the p53 protein, but do not grossly affect the overall structure [278]. An *in silico* algorithm led to identification of the molecule PhiKan059 that could bind and stabilise p53 Y220C protein [350, 351]. The power of *in silico* modelling in efforts to isolate lead molecules that could stabilise active conformation, or shift equilibrium towards more stable conformation has been reinforced in a recent study aimed at identifying ligands that can allow recovery of mutant p53 proteins that have lost the ability to form the active tetramer [352].

1.2.3 Chaperone-like hub- Reptin

Reptin, also called Ruvbl2 and Tip48, and Pontin, also called Ruvbl1 or Tip49 are two highly conserved members of ATPases associated with various cellular activities (the AAA+) family of proteins. AAA+ proteins perform a myriad of functions, such as protein folding and degradation, aggregate disassembly, maintenance of organelle function, transcription, replication, recombination and cellular transport and are hence commonly referred to as a novel class of chaperones. Similar to other members of AAA+ family, these proteins contain highly conserved Walker A and B motifs, responsible for ATP binding and hydrolysis and are believed to form hexameric structures (discussed in detail in Chapter 5).

Reptin and Pontin are part of different protein and nucleoprotein complexes and are implicated in processes such as chromatin transcription regulation, DNA damage response, and ribonucleoprotein complex biogenesis. Below the functions and PPIs of Reptin protein are briefly discussed.

1.2.3.1 Reptin's PPIs and chromatin chaperoning

Given the compact structure of chromatin, its remodelling is critical for gene transcription in the cell. In principle, remodelling is facilitated by ATP-dependent chromatin remodelling through mobilizing nucleosomes and a set of enzymes that can covalently modify histones and allow access to underlying DNA [353, 354]. Interestingly, one of the most studied functions of Reptin involves its chromatin remodelling activity. This activity is essential for transcription and essentially involves energy dependent processes that facilitate access to DNA. Reptin is an integral subunit of yeast INO80 and SWR-C chromatin remodelling complexes as well as human INO80, SWR-C like SRCAP and the transformation/transcription domain-associated protein (TRRAP)-Tip60 histone acetyltransferase (HAT) complex.

I INO80

INO80 has a broad spectrum of functions ranging from regulation of transcription, chromatin remodelling to DNA repair and DNA replication [355]. Reptin was found to form a transient interaction with the components of the yeast INO80 complex and be critical for the chromatin remodelling activity of this assembly [356, 357]. Mechanistically, Reptin seems to be involved in the assembly of the INO80 complex. Indeed, Reptin appears to nucleate recruitment of actin-like Arp5p, one of the critical subunits of the INO80 complex. In addition Ino80 and Reptin regulate expression of a similar set of genes. Similarly, Reptin is incorporated in the human INO80 complex, however its role in this assembly has not been established yet [358].

II SWR1/SRCAP

SWR1 complex is involved in histone H2B-H2AZ substitution onto chromatin [359]. Both yeast SWR1 and mammalian SWR1 homolog- SRCAP engage Reptin protein, however it is unclear whether Reptin regulates assembly, ATPase activity of the complex or nucleosomal exchange.

III TIP60

Human TIP60 complex and its catalytic subunit Tip60 have a range of activities, including a well established role in transcription through binding and acetylation of various substrates such as histones [360], the Androgen Receptor (AR) [361] or p53 [230, 231]. The TIP60-p53 interaction has been shown to be critically important for cell cycle arrest and apoptosis programmes of p53. Interestingly, E2F can bind Tip60 at E2F target promoters, which triggers recruitment of other subunits of TIP60 complex including Reptin [362]. In addition, Myc-Maz complex interacts with Tip60 and recruits Reptin to Myc-dependent promoters, which results in the formation of a gene activating complex [363]. Surprisingly, despite the clear role of TIP60-Reptin in Myc transcription activation, Reptin was found to associate with a Myc-Miz1 repressor complexes, which leads to suppression of p21 and consequently to cell proliferation [364]. The mechanism of Reptin function in this complex has not been identified yet, but it is possible that Reptin acts here as an assembly factor, as it was found for the TIP60 or INO80 complexes. This hypothesis could be extended to other Reptin-containing repressor complexes, such as Polycomb, β-catenin, and nuclear factor (NF)-κB [365-367].

IV Transcription factors

The presence of Reptin in transcription activating or repressing complexes was found to be mediated through its direct interaction with transcription factors, such as TBP [368, 369], Myc [370], E2F1 [362], ATF2 [371] or transcription-associated protein β-catenin [365, 367]. Reptin also binds to the promoters of the genes targeted by these transcription factors [362, 363, 367] and, as it was mentioned above, these events often involve TIP60 complex. These interactions confer Reptin's role in transcription and could set a starting point for the discussion on the roles of Reptin overexpression in the pathogenesis of disease. For example Reptin potentiates c-Myc mediated repression of p21 gene, hence impedes cell cycle arrest. Further, Reptin represses β-catenin-dependent reporters. This may indirectly point to Reptin playing a role in cellular transformation, as deregulation of

β-catenin signalling, due to an activating mutation of β-catenin or its interacting partners, was observed in several cancers [372-374]. Furthermore, together with the co-repressor TLE1 and histone deacetylases HDAC1 and HDAC2, Reptin was found to localize to the promoters of two β-catenin targets *hesx1* and *pit1*. As these proteins are implicated in cell fate decisions, Reptin-mediated repression of the expression of these genes has a role in maintaining cell pluripotency [375]. Similarly, co-operation of Reptin and histone deacetylaes in gene repression was observed for the nuclear factor κB (NF-κB) driven expression of KAI1 [367]. Apparently, the formation of this PPI is dependent on the relative ratios of repressors to activators that can be differentially recruited to the KAI promoter. In non-metastatic cells, Tip60 coactivator is expressed at high levels. It recruits Pontin to the promoter region of KAI1, mediates acetylation of histones and subsequently induces KAI1 expression. In metastatic cells, the levels of nuclear β-catenin increase. Consequently, β-catenin-Reptin complex is preferentially recruited to KAI1 promoter and becasue Reptin is associated with histone deacetylase HDAC1, this leads to KAI1 suppression. Interestingly, Reptin-HDAC1 interaction is stimulated by SUMO-specific E2-conjugating enzyme (Ubc9), which catalyses sumoylation of Reptin. Contrary to that, Reptin interaction with HDAC1 is inhibited by the SUMO-processing enzymes SENP1 and SUSP1. Interestingly, levels of Ubc9 and sumoylated Reptin are increased in metastatic cells [376]. This is an interesting example of how PPIs can be modulated by post translational modification of the interacting protein and by the cellular context. As KAI1 increases cell adhesion and thereby inhibits metastasis, the implication for Reptin-mediated repression of this protein is that it may be involved in cellular transformation. Another Reptin-interacting protein that modulates Reptin-mediated repression is the Histidine triad nucleotide-binding protein 1 (Hint1) [377]. Interestingly, Hint1 disrupts formation of Reptin-Pontin complex, and can possibly disrupt Reptin's hexamerization. Hint1 is recruited with Reptin to β-catenin and enhances Reptin-mediated suppression of β-catenin. Collectively, it appears that Reptin in combination with β-catenin, recruits histone deacetylases to different promoters and converts the chromatin to a repressive state. Interestingly, Reptin binds two

endosomal proteins APPL1 and APPL2 and this interaction is likely to reduce Reptin-HDAC1 complex and relieve Reptin mediated repression of β-catenin [378].

V DNA repair

The important physiological function of Reptin in the chromatin remodelling complexes is linked to the DNA damage response. The DNA damage response checkpoints involve three members of the phosphatidylinositol 3-kinase-related protein kinase (PIKK) family: ATM, ATR, and DNA-dependent protein kinase catalytic subunit (DNA-PKcs) and clamp loader/polymerase clamp (RFC/PCNA)-related Rad17-RFC/9-1-1 complex [379]. Upon DNA damage ATM kinase autophosphorylates at Ser1981. This converts an inactive dimer into an active monomer that can bind to chromatin and phosphorylate its substrates [380]. Activated ATM phosphorylates histones to "mark" damaged sites and this triggers recruitment of amplifying or repairing proteins, like MDC1, MRN complex, 53BP1, and BRCA1 [379]. In addition, chromatin remodelling machines also have to be recruited to facilitate opening and repairing of the altered chromatin structure. Interestingly, the Reptin-containing chromatin remodelling complexes such as TIP60, yeast Ino80 and Swr1 as well as human INO80-YY1 complex are also recruited to DNA damage sites [381-384]. The loss of the functional yeast Ino80 and yeast Swr1 complexes as well as human YY1, Ino80 and Reptin results in hypersensitivity to DNA-damaging agents [356, 382, 384]. Tip60 is critical for ATM acetylation and this modification precedes ATM activation [385, 386]. Additionally, functional human TIP60 complex is required for the recruitment of Rad51, a protein catalysing homologous recombination in the repair of DNA, to the sites of DNA damage [387]. Furthermore, TIP60 is involved in histone H4 acetylation, which is important for the subsequent dephopshorylation of histone H2AX [388]. Interestingly, Reptin depletion leads to an increased amount of the phospho H2AX foci [389]. Collectively, given that Reptin is incorporated in these complexes and is believed to be essential for their assembly, these findings suggest that Reptin may be involved in DNA repair pathway due to the requirement for chromatin remodelling at the DNA damage sites. Intriguingly, Reptin interacts directly with the members of

PIKK family and its silencing resulted in attenuation of PIKK signalling following DNA damage [390].

1.2.3.2 Reptin's PPIs- chaperoning Ribonucleoproteins (RNPs) assembly

snoRNPs are RNA processing enzymes and were found to modify small nuclear RNA (snRNA), ribosomal RNA (rRNA), and tRNAs [391]. Reptin protein was found to associate with small nucleolar RNPs (snoRNPs) in different species [392-395] and be involved in their biogenesis and assembly in the process involving a chaperone multicomplex of Tah1 (Rpap3), Pih1 (Nop17), Pontin and Hsp90 [396].

In addition to snoRNP, Reptin is involved in the assembly of the telomerase complex [397]. Telomerase complex consists of the telomerase reverse transcriptase (TERT), telomerase RNA component (TERC) and the TERC-binding protein dyskerin [398]. Reptin together with Pontin interact with dyskerin and this is important for the assembly and stability of the TERC RNP. Moreover, both these proteins interact with TERT. Interestingly this PPI is regulated by the cell cycle and is increased in the S phase. The TERT-Reptin-Pontin complex displays reduced telomerase activity, and precedes formation of the active telomerase complex which coincides with Reptin/Ponitn dissociation [397]. In addition, the transiency of this interaction is consistent with the chaperoning activity of these proteins.

1.2.3.3 Reptin's PPIs- chaperoning mitosis

Reptin, together with Pontin associate with tubulin and localize to the mitotic spindles, spindle poles, midzone during telophase and to the midbody during cytokinesis [399, 400]. Interestingly, deletion of Pontin in cultured cells or in *Xenopus* extracts unveiled it role in organising and microtubule assembly, however Reptin appeared to potentiate Pontin's effect [401].

1.2.4 AGR2- a protein with an undefined interactome

AGR2 protein belongs to the family of the Anterior Gradient proteins comprising several proteins, including the founder member XAG-2. XAG-2 was ascribed a developmental role, and together with organiser-secreted factors, such as noggin, chordin, follistatin and cerberus, is incorporated in the pathway involved in ectodermal patterning in *Xenopus* embryos [402-406]. As XAG-2 transcription is activated by organizer-secreted factors, it converges with the BMP-4 antagonising pathway.

Following discovery of the frog's gene, the human homologoue, namely AGR2, known also in literature as AG2, GOB4, HAG-2, PDIA17, was identified in estrogen receptor (ER)-positive breast cancer cell lines [407]. Interestingly, as much as nine alternative transcripts of AGR2 gene were described and six of them give rise to proteins of 119 to 188 amino acids [408].

Generally, AGR2 is highly expressed in mucus-secreting cells and endocrine organs, such as lung, stomach, colon, prostate and small intestine, and to a lesser extent in pituitary gland, salivary gland, mammary gland, bladder, appendix, ovary, uterus, pancreas, kidney, testis and thyroid gland [407, 409, 410]. AGR2 is expressed in several cell types in small intestine crypts, including mature goblet, Paneth and enteroendocrine cells, as well as Musashi-1 (MSI1)-positive intestinal stem/early progenitor cells and proliferating secretory progenitors [411]. Its presence in the mucus-secreting organs appears to be evolutionarily conserved as XAG-2 expressing cement gland also secrets mucus. At present, the function of AGR2 in mammalian systems is not fully understood, mainly because there are no well-validated binding partners known for this protein. Below the known or predicted functions of AGR2 protein are briefly discussed.

1.2.4.1 AGR2- a molecular chaperone?

In addition to being a part of the AG family, human AGR2 is incorporated in the family of chaperone-like proteins, namely protein disulfide isomerase (PDI)

superfamily [412]. PDI and PDI-related proteins are microenvironmentally regulated proteins that can catalyse the formation, reduction or isomerization of disulphide bonds in their client proteins. These enzymatic reactions facilitate protein maturation into bioactive conformation in the endoplasmic reticulum (ER) [413]. These proteins contain the thioredoxin motif (CXXC or CXXS) [414-417]. In addition to the active motifs, most members of the PDI family contain H/KDEL ER retention signal. Interestingly, AGR2 possess both of the key determinant attributes of the PDIs family. Firstly, AGR2 possesses the CXXS motif instead of CXXC, which is present in other members of this family, such as TRX1, TRX2 or ERP18. CXXS exibits lower activity in terms of disulfide bond reorganization, however, it is believed that it may participate in the isomerization of already existing disulfide bridges and have alternative functions in the ER [418, 419]. AGR2 also has a C-terminal putative ER retrival sequence that can localise AGR2 to ER [420]. The putative role of the thioredoxin fold in the PDIs family is to form disulfide bonds with the substrate and facilitate their maturation and folding. If PDI substrates are not isomerised, the misfolded proteins may accumulate in the ER which could instigate ER stress and subsequently cell cycle arrest and apoptosis. As AGR2 embeddes itself in the PDIs family, it is possible that it is also involved in chaperoning ER proteins. Indeed, AGR2 was recently shown to form mixed disulfides with intestinal Mucin 2 (MUC2) and this reaction was essential for the correct pairing of cystine residues in the processing of this cysteine-rich glycoprotein [421]. AGR2 knock-out mice failed to produce mucus, had no morphologically normal goblet cells and were susceptible to experimentally induced colitis [421]. In addition, another study [422] found that even in the absence of damaging agents, loss of AGR2 resulted in the severe inflammation, abnormal expansion and localisation of Paneth cells. This was associated with the increased expression of WNT signalling feedback inhibitor, namely Sox9. Interestingly, AGR2 knock-down has affected two types of cells that are a major part of secretory pathway in the intestine, namely (1) goblet cells, which produce the major components of the mucus barrier and (2) the Paneth cells that produce a range of antimicrobial molecules. These cells exert high levels of baseline protein biosynthesis under normal conditions. However, environmental and inflammatory triggers further increase synthesis and secretion by these cells and

these inputs may disturb ER homeostasis and result in the increased ER stress, that subsequently leads to inflammation, caused by inappropriate folding. As in Zao et al. study, AGR2 knock-down elevated ER stress, we could speculate that AGR2 is indeed important for appropriate protein folding, at least for certain secreted proteins.

1.2.4.2 The AGR2 interactome

Early studies on AGR2 protein suggested its interaction with prometastatic factors C4.4A and alpha-dystroglycan (DAG-1). However, to date none of these interactions have been properly validated [423]. Interestingly, a peptide aptamer screen found AGR2 binding peptide PTTIYY, that can specifically interact with AGR2 *in vitro* and change its subcellular localisation as well as reactivate p53 *in vivo* [424, 425]. This finding could serve as a starting point to search for the cellular proteins that have this consensus motif (S/T)xIhh (where x is any amino acid and h is an amino acid with a hydrophobic side chain) and validate them as AGR2 binding partners [424].

1.2.4.3 AGR2 role in cancer and cancer related pathways

AGR2 protein is overexpressed in a wide range of cancers, including breast [409, 426-428], prostate [410, 429], fibrolamellar [430], pancreatic [410, 431, 432], colon [433], ovarian [434] cancer. AGR2 has also been proposed as a useful metastasis marker in breast, prostate and colorectal cancer [407, 423, 427, 435], and it is associated with poor survival of prostate and breast cancer patients [426, 429, 436]. AGR2 overexpression in cancer cells has several implications for the biology of the resulting tissue.

I AGR2 as a p53 inhibitor

AGR2 was found to attenuate p53 activity by suppressing p53-dependent response to DNA damage [437]. In detail, AGR2 was shown to decrease p53-dependent transcription to a similar extent as MDM2 did, and the AGR2-mediated inhibition of p53 was augmented by DNA damage. Interestingly, AGR2 ability to suppress p53 transcription was concomitant with a decrease in p53 phosphorylation at both Ser15 and Ser392 [437] and the nuclear exclusion of p53 protein [420]. Further, AGR2 depletion using siRNA promoted translocation of a fraction of cytoplasmic p53 to the nucleus and membrane/organelles. However, these studies were performed in a lung cancer cell line that normally does not express neither p53 nor AGR2 and as such, cell systems expressing endogenous proteins have to be studied to definitely assess AGR2 function in the p53 pathway. A recent study found that 2,3,7,8-Tetrachlorodibenzo-p-dioxin (TCDD), a toxin and human carcinogen [438] that attenuates the p53 response to DNA-damaging agents [439, 440], induces AGR2, further implicating AGR2 role in p53 inhibition [441].

II AGR2 in metastatis and transformation

Several studies in cell lines indicated that AGR2 may play a role in tumour growth, cell migration and metastasis. For example, transfection of AGR2 into a benign rodent mammary cell line promoted metastatic phenotype and it was suggested to be due to enhanced adhesive properties of AGR2-positive cells [427]. A subsequent study found that AGR2 knock-down in a non-small lung carcinoma cell line and in pancreatic cancer cells compromised anchorage independent growth *in vitro* and the growth of xenograft tumours *in vivo* [411, 442]. In addition AGR2-overexpressing stable human ovarian cancer cells up-regulated the expression of genes involved in cell proliferation, invasion, and angiogenesis and down-regulated expression of the negative regulators of these processes [434]. Moreover, AGR2 was found to act as a prosurvival factor as stable overexpression of AGR2 in H1299 cells enhanced colony formation [437]. Recently AGR2 protein was shown to be differentially expressed in metastatic gastric cancer cells, compared to a

non-metastatic counterpart [443], which further reinforces AGR2 role in metastasis. Finally, in stress conditions that resemble the tumour microenvironment, such as serum depletion, hypoxia, AGR2 was upregulated together with other prosurvival, angiogenic, and proinvasive genes, indicating that AGR2 may act as a prosurvival factor in these tumour growth-stimulating pathophysiological stress conditions [444].

III AGR2 in development

The functions of AGR2 protein in normal tissues are poorly understood. As mentioned before, the founder member of the Anterior Gradient protein, XAG-2 has been described as a critical factor in embryonic development and its expression was found to be confined to anterior regions that will differentiate into cement gland [402]. Furthermore, similarly to the organiser-secreted factors, such as noggin, chordin, follistatin and cerberus, XAG-2 has the capacity to activate ectodermal patterning in *Xenopus* embryos [402-406]. In fact, XAG-2 transcription is activated by organizer-secreted factors, and as such may act as a mediator of anterior/posterior axis specification downstream of the inhibitors of BMP-4 pathway present in axial mesoderm [402]. In addition, a model for XAG-2-dependent formation of cement gland has been put forth. It infers that a combination of both stimulatory and inhibitory signals restricts XAG-2 protein to the cement gland anlage [445] and once its expression is established at the extreme anterior of the embryo, secreted XAG-2 triggers the cement gland formation [402].

In addition, developmental role of Anterior Gradient protein was observed for newt anterior gradient (nAG) protein, which was found to be involved in newt limb regeneration [446]. nAG was detected in Schwann cells of the distal nerve sheath and later, at the early bud stage, it was expressed in gland cells of the wound epidermis and functioned as a growth factor. Furthermore, expression of nAG in denervated tissue that had lost the ability to regenerate could rescue it and support a regeneration of distal structures [446].

Studies using normal mice, germline and inducible AGR2 knockout mice as well as AGR2 knockdown in cell culture have helped to shed the light on the functions of AGR2 in normal tissue. Interestingly, AGR2 has been found to be

expressed in distinct cell types of the small intestine. The lining epithelium of the small intestine forms crypts with nutrient absorbing enterocytes being the major cell population within this organ. Other three major intestinal cells are goblet cells, Paneth cells and enteroendocrine cells, and all of these three cell types have a secretory function [447]. Interestingly, AGR2 is strongly expressed in differentiated goblet, Paneth and enteroendocrine cells, as well as in intestinal stem cells and progenitor cells [411]. Two recent studies using AGR2 knockout mice as well as cell culture where AGR2 was depleted using AGR2-specific siRNA, have shown that AGR2 has a role in maintaining intestinal homeostasis, in particular homeostasis of goblet and Paneth cells [421, 422]. Loss of AGR2 abolishes goblet cells ability to produce intestinal mucus [421] and changes goblet cells morphology [421, 422]. In addition, one study of AGR2 knockout mice revealed additional abnormalities in the small intestine such as drastic changes in intestinal Paneth cells as well as severe intestinal inflammation [422]. Specifically, AGR2 loss results in the abnormal localization of Paneth cells, as well as their expansion along the entire small intestine. This is followed by severe inflammation, which is consistent with Paneth cells role in the inflammatory response. Moreover, AGR2 loss causes disruption of enterocyte homeostasis, with decrease in proliferation, increase in apoptosis and blunting of villi [422]. Interestingly, it was found that the expression of Sox9, a feedback inhibitor of WNT signalling, is increased in the intestine of AGR2 knockout mice. The components of the WNT pathway, such as Frizzled 5, EphB3 and Apc, determine proper cell location along the crypt-villus axis [448-450]. The observation that loss of AGR2 causes mislocalization of Paneth cells and upregulation of Sox9, may indicate the cooperation of AGR2 and WNT pathway, at least in specifying appropriate architecture of the small intestine.

Furthermore, AGR2 loss elevates ER stress, in some of the intestine cell types, and it provides with the first evidence for AGR2 function in ER dependent protein folding. Interestingly, AGR2 knockout phenotype resembles human Crohn's disease and this is consistent with the finding that the AGR2 genetic variants that decreased AGR2 mRNA expression are associated with increased risk of both Crohn's disease and ulcerative colitis [451].

Interestingly, besides its clear involvement in maintaining small intestine homeostasis, AGR2 is involved in the regulation of maturation program of the intestine epithelial cells as they migrate along the crypt-villus axis, with AGR2 being a specific marker of the differentiated cells population [452].

In addition to intestinal expression of AGR2, recent studies have identified AGR2 in the fetal liver and its expression pattern is conserved in adult liver [430], with AGR2 being present in the tall columnar but not in cuboidal cells of the intrahepatic, hilar and extrahepatic biliary tree [453]. Interestingly, the differentiation program of the biliary epithelial cells lining bile ducts involves acquiring columnar and mucus-secretory phenotype [453]. These observations led to hypotheses that AGR2 could have a function in the differentiation of the biliary tree cells. Given that AGR2 has been shown to have a role in ER stress regulation in goblet cells and the secretion of mucin 2 and ascribed a chaperone role, it is possible that liver-expressed AGR2 supports secretory functions of mucin-producing differentiated cells, which could subsequently regulate organ physiology.

It is interesting that both p53 and AGR2 have a function in normal tissue development, affect differentiation programmes and are involved in limb regeneration. This indicates that despite its clear p53-inhibitory role in cancer cells, AGR2 and p53 could in fact cooperate *in vivo*.

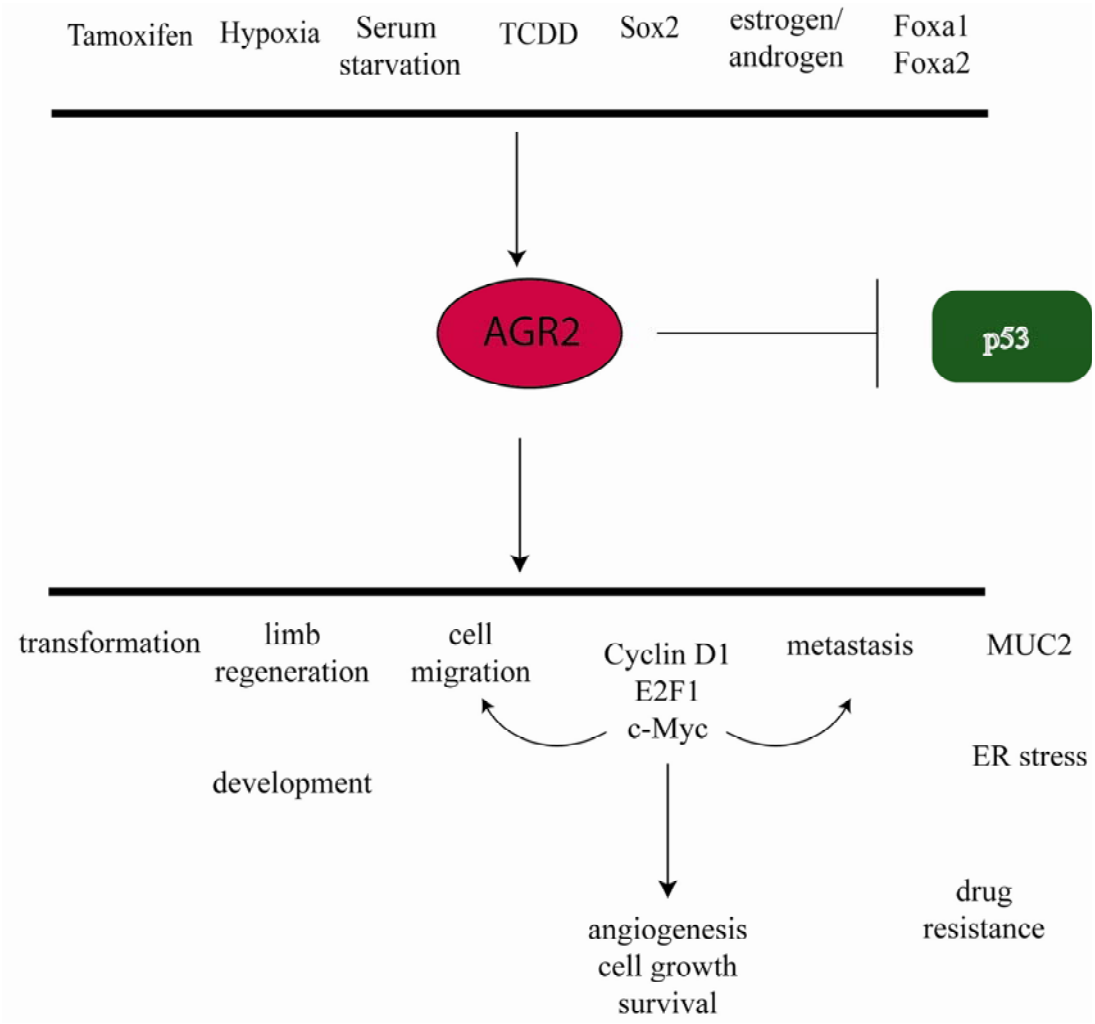

Figure 1.10 Schematic representation of the factors that regulate AGR2 and AGR2 functions.

1.3 Objectives

The p53 tumour suppressor protein has emerged in last decades as a key inhibitor of tumour development. Indeed over half of human cancers bear mutations in the p53 encoding gene. Interestingly, some tumours retain the wild type p53 gene, and these cancers develop other mechanisms to inhibit the tumour suppressive signalling by p53. Recently, AGR2 protein was identified as a p53 protein inhibitor, however, the molecular mechanism underlying this function is not known. The aim of this project was to identify physiological signals that regulate AGR2-p53 pathway. Finding such extracellular inputs, in particular tumour suppressor signals that antagonize the pro-oncogenic function of AGR2 can provide model systems to study AGR2 regulation and facilitate development of drugs aiming at reactivating wild type p53 in cancers. In addition, to further our understanding of the AGR2 functions, we focused on identifying novel AGR2 binding partners. We characterised the new interaction between AGR2 and Reptin protein and investigate the role of this interaction with respect to the p53 pathway.

CHAPTER 2: MATERIALS AND METHODS

2.1 Reagents, chemicals and plasmids

Chemical and reagents were purchased from Sigma, unless otherwise indicated. The human HA-tagged Reptin was a gift from Argyro Fourtouna; HA-tagged Reptin K456R and myc-tagged Pontin were a kind gift from Dr Marta Miaczynska; the mature wild type AGR2-pDEST 3.2 was from Dr Euan Murray; p53 S269D and p53 S269A were from Dr Jenny Fraser, HA-tagged SNIP1 was from Dr Neil Perkins. Phospho-specific antibodies to SNIP1 were developed by Moravian Biotechnology.

2.2 Equipment

A Fluroskan (Ascent FL) and Victor 3 (Perkin Elmer) were used to read 96-well plates. RNA and DNA concentrations were measured using a NanoDrop® spectrophotometer. X-ray irradiation treatment was performed using Faxitron® cabinet X-ray system, 43855D (Faxitron X-ray Corporation). SDS-PAGE was carried out using Biorad Protean II mini-gel system. Radioactivity-containing gels and plates were visualised with the use of Phosphoimager. X-ray films were developed using a Konica Medical Film Processor (Model SRX-101A). Sorvall RC-5C plus and Eppendorf 5415R were used for all centrifugations. PCR was performed using DNA Engine Dyad peltier thermal cycler (Bio Rad) and Real Time PCR using MJ Reseach PTC-200 peltier thermal cycler (Bio Rad).

2.3 Microbiological techniques

2.3.1 Growing bacterial cultures

Bacterial cultures were grown in Luria-Bertani (LB) media, at 37ºC, with shaking at 220 rpm, and in the presence of a selective antibiotic when required, at the following final concentrations: 100 μg/ml ampicilin, 50 μg/ml kanamycin and 30 μg/ml chloramphenicol. Cultures were inoculated from a single colony or from glycerol stocks, and grown in the sterile flasks with a capacity of at least four times the culture volume, to allow appropriate aeration.

LB media
1 % (w/v) bacto-tryptone,
0.5 % (w/v) bacto-yeast extract,
1 % (w/v) NaCl,
Dissolve in distilled water and autoclave at 121°C for 20 minutes.

LB agar plates were prepared using LB media containing 1.5 % (w/v) bacto-agar. LB agar was first melted by heating in the microwave oven and then cooled to about 45°C. Subsequently the appropriate antibiotic was added and LB agar was poured into 90 mm petri dishes (Sterilin), and allowed to cool. The culture plates were stored at 4°C for no longer than one month and were warmed to 37°C for 1 hour prior to use.

2.3.2 Glycerol stocks

Glycerol stocks were prepared to allow the long term storage of bacteria. 800 μl of an overnight bacterial culture was mixed with 200 μl of 80 % sterile glycerol in a cryotube (Nunc), snap frozen in liquid nitrogen and stored at -80°C.

2.3.3 Preparation of competent cells

Bacterial cells were inoculated into 5 ml of LB and incubated overnight at 37^{o}C with shaking at 220 rpm. The overnight culture was diluted 1:200 in 100 ml LB and incubated at 37^{o}C until the $O.D_{600nm}$ reached 0.6. Following centrifugation (20 minutes, at 4^{o}C, 4000 rcf), cell pellets were resuspended in 15 ml of ice cold buffer 1 and incubated on ice for 1 hour. Cells were then centrifuged as above; the pellet was resuspended in 4 ml of ice cold buffer 2 and incubated on ice for 15 minutes. Subsequently, the cells were aliquotted (100 µl) into pre-chilled sterile microcentrifuge tubes, snap frozen in liquid nitrogen and stored at -80^{o}C.

Buffer 1
100 mM RbCl
79 mM $MnCl_2$
30 mM CH_3COOK pH 7.5
13.5 mM $CaCl_2$
15 % (v/v) Glycerol
Adjust to pH 5.8 and filter sterilise.

Buffer 2
10 mM MOPS pH 6.8
10 mM RbCl
13.5 mM $CaCl_2$
15 % (v/v) Glycerol
Adjust to pH 6.8 and filter sterilise.

2.3.4 Transformation of bacterial cells

100 ng of plasmid DNA was added to 50 µl of freshly thawed competent cells and incubated on ice for 30 minutes. Next, cells were heat shocked at 42ºC for 1 minute, and placed in ice to cool. Subsequently, 500 µl of LB broth was added and

the mixture was incubated at 37ºC, for 60 minutes, with shaking. 100 µl was then plated onto LB-agar plate containing the appropriate antibiotic and incubated overnight at 37ºC.

2.4 Molecular Biology Techniques

2.4.1 Amplification, purification and quantification of plasmid DNA

A single bacterial colony was picked from a LB-agar plate and inoculated into 5 ml of LB broth containing a selective antibiotic when required, and grown for several hours, at 37ºC, with shaking at 220 rpm. Following incubation, the starter culture was diluted into 500 ml of LB broth containing selective antibiotic (if required) and grown overnight, at 37ºC, with shaking at 220 rpm. The next day, bacterial culture was centrifuged at 4ºC, for 10 minutes, with shaking at 6000 rcf and plasmid DNA extracted using plasmid DNA Maxi kit (Qiagen) according to manufacturer's instructions. If lower yield of plasmid DNA was required, plasmid DNA was purified directly from the starter culture using plasmid DNA Mini kit (Qiagen). Plasmid DNA was eluted in nuclease-free water and stored at -20ºC. The concentration of obtained DNA was measured using a NanoDrop ND-1000.

2.4.2 Agarose gel electrophoresis of DNA

Agarose gel electrophoresis was used to separate and analyse DNA. Agarose gels were prepared by adding electrophoresis-grade agarose (Invitrogen) to 1x TAE buffer to a final concentration of 1 % and melted by heating in a microwave oven. The agarose was then cooled to about 60ºC and ethidium bromide was added to a final concentration of 0.5 µg/ml. The solution was then poured into a casting tank and allowed to set at the room temperature. The gel was then submerged in 1x TAE buffer. DNA samples were mixed with the 6x DNA loading buffer at a 5 to 1 ratio of

DNA to loading buffer. Upon loading DNA samples, the agarose gel was run for approximately 60 minutes at 100 V. Subsequently, the bands were visualised under UV transilluminator using Syngene (Genesnap).

1x TAE buffer
40 mM Tris
1 mM EDTA
Adjust pH to 8.0

6x DNA loading buffer
0.25 % bromophenol blue
0.25 % xylene cyanol FF
15 % Ficoll

2.4.3 DNA sequencing

DNA sequencing was carried out using the Big Dye Terminator V3.1 Cycle Sequencing Kit (Applied Biosystems). In details, a sequencing reaction was performed as follows:

PCR
2 μL of 5X Sequencing Buffer Big Dye Terminator V1.1, V3.1
1 μL of Big Dye Terminator V3.1 Cycle Sequencing Kit
300 ng of DNA template
1 μl of sequencing primer (10 μM)
Adjust to a final volume of 10 μl with Nuclease-free water

Thermal cycling conditions were:

1. 96ºC for 1 minute
2. 96ºC for 10 seconds
3. 50ºC for 5 seconds
4. 60ºC for 4 minutes
5. Repeat steps 4-6 for 25 cycles
6. Hold at 4ºC

Ethanol/EDTA precipitation

Following PCR, 2.5 μL of 125 mM EDTA and 30 μL of 100 % ethanol were added to the sequencing reaction. The mix was vortexed and incubated for 15 minutes at room temperature. Samples were then centrifuged for 20 minutes at maximum speed and the supernatant was removed. The samples were briefly spun again to remove any residual ethanol. The DNA pellet was then washed with 70 % ethanol and centrifuged for 5 minutes, at 4ºC, at maximum speed. The supernatant was removed, samples briefly spun again and all remaining ethanol discarded. Finally, the pellet was air dried in a fume hood and the sequences were analyzed by Geneservice DNA Sequencing Service at Cambridge.

2.4.4 Cloning

2.4.4.1 Gateway cloning

In order to clone the sequence of interest using the Gateway system (Invitrogen) manufacturer's protocol was followed. Firstly, insert flanked by attB recombination sites was generated (refer to section I). This was followed by generation of an entry clone in BP reaction (refer to section II) and finally destination clone was created in LR reaction (described in III).

I Producing attB-PCR products

Primer design

To generate PCR products suitable for Gateway's BP reaction, primers were designed such that they incorporated attB recombination sites into PCR product (see below) and contained 18-25 bases corresponding to the N-terminal and C-terminal portion of the protein to be cloned. Specifically, the primers were designed to allow expression of Reptin protein with N-terminal fusion GST tag. In addition a Prescission cleavage site was incorporated in the forward primer to allow removal of the GST tag, when required.

Primers' sequences were as follows:

Forward primer (5'-3'):
GGGGACAAGTTTGTACAAAAAAGCAGGCTTCCTGGAAGTTCTGTTCCAG
GGGCCCATGGCAACCGTTACAGCCACAACC
Reverse primer (5'-3'):
GGGGACCACTTTGTACAAGAAAGCTGGGTCTCAGGAGGTGTCCATGGTCT
CG
Red = polyG required for recombination of attB;
Green = attB (1 or 2) site;
Purple = nucleotide insert to maintain correct reading frame;
Pink = protease cleavage site;
Black = gene sequence

PCR

HA-tagged Reptin plasmid DNA was used as a template DNA. The PCR reaction was set up as follows:

12.5 µl 2X Pfu Master Mix (Vhbio)
2.5 µl Band Doctor (supplied with Pfu Master Mix)
50 ng Template DNA
1.3 µl Forward Primer (10 µM stock)

1.3 µl Reverse Primer (10 µM stock)
Nuclease-free water to 25 µl

Thermal cycling conditions were:
1. 95°C for 2 minutes
2. 95°C for 30 seconds
3. 58°C for 1 minute
4. 72°C for 2 minutes
5. Repeat steps 2-4 for 30 cycles
6. 72°C for 5 minutes
7. Hold at 4°C

Following PCR, the amplified DNA was cleaned using the Qiagen PCR Clean-up Kit, and eluted into 30 µl of nuclease-free water. 5 µl of the purifed PCR product was loaded onto a 1 % agarose gel to confirm success of amplification.

II Creating an entry clone

To generate an entry clone a BP reaction was performed using attB-flanked PCR product and attP-containing donor (pDONR-221).

The reaction was set up as follows:
150 ng PCR product
150 ng pDONR-221
2 µl BP clonase mix
Adjust to 10 µl with TE Buffer (pH 8)

Reaction was incubated at 25°C, overnight. The following day, 1 µl of Proteinase K solution (Invitrogen) was added and incubated at 37°C for 10 minutes. Subsequently, 5 µl of the BP recombination reaction was transformed into DH5α and plated out onto LB-agar plates containing kanamycin. Next, a single colony was picked from

the plate, 5ml cultures grown, which was followed by plasmid DNA extraction using plasmid DNA Mini kit (Qiagen).

III Creating an expression clone

To obtain an expression clone a LR reaction was performed between an entry clone and a destination vector of choice (pDEST 15). The reaction was set up as follows:
150 ng entry clone
150 ng pDEST15
2 µl LR clonase mix
Adjust with TE Buffer (pH 8) to 10 µl

Reaction was incubated at 25°C, overnight. The following day, 1 µl of Proteinase K solution (Invitrogen) was added and incubated at 37°C for 10 minutes. Subsequently, 5 µl of the LR recombination reaction was transformed into DH5α and plated out onto LB-agar plates containing ampicilin. Next, a single colony was picked from the plate, 5ml cultures grown, which was followed by plasmid DNA extraction using plasmid DNA Mini kit (Qiagen). Insertion of the desired sequence in frame and absence of any mutations were verified by sequencing.

2.4.4.2 Conventional cloning using restriction enzymes

In order to clone the sequence of interest into the required vector, the desired sequence was first amplified by PCR using primers flanked by appropriate restriction sites (refer to section I). This was followed by restriction enzyme digestion of both insert and vector (described in II) and subsequent ligation of double-digested vector and insert (described in III).

I PCR amplification

Primer design

Primers were designed such that they contained 18- 25 bases corresponding to the N-terminal and C-terminal portion of the sequence to be cloned and the appropriate restriction sites chosen according to the Multiple Cloning Site (MCS) of the vector to be inserted in. A number of nucleotide bases were incorporated adjacent to restriction sites to ensure efficient annealing of the primers. Additional bases were inserted when necessary to ensure that the sequence of interest was in frame relative to downstream sequences. Lastly, sequences of primers were modified to obtain an acceptable GC content (40-60 %) and melting temperature (60-80º C). A list of primers used is given in Table 2.1 and a list of the recognition sequences of the restriction enzymes (RE) used is given in Table 2.2.

Vector	**Target**	**Primer sequence (5'- 3')**
pGL3-basic (Promega)	AGR2 promoter (-1584 to +96)	GGGGTACCCCTAATACATATGACTGTG TCCTTATAA
pGL3-basic (Promega)	AGR2 promoter (-1584 to +96)	TTACCCCGGGGTTAGAA ACTGAGGCTCTGCTGA

Table 2.1 Primers used for AGR2 promoter cloning. Green is a restriction enzyme recognition sequence, Red is a linker sequence.

Restriction enzyme	**Recognition sequence (5'-3')**
KpnI	GGTACC
XmaI	CCCGGG

Table 2.2 Recognition sequences of the restriction enzymes used in this study

PCR

Genomic DNA obtained from MCF7 cells was used as a template DNA. The PCR reaction was set up as follows:

12.5 µl 2X Pfu Master Mix
2.5 µl Band Doctor (supplied with Pfu Master Mix)
50 ng Template DNA
1.25 µl Forward Primer (10 µM stock)
1.25 µl Reverse Primer (10 µM stock)
Adjust to 25 µl with nuclease-free water

Thermal cycling conditions were:
1. 95°C for 2 minutes
2. 95°C for 20 seconds
3. 58°C for 40 seconds
4. 72°C for 2-5 minutes (1 minute/ 2 kb)
5. Repeat steps 2-4 for 25-35 cycles
6. 72°C for 5 min
7. Hold at 4°C

Following PCR the amplified DNA was cleaned up using the Qiagen PCR Clean-up Kit, and eluted in 30 µl of nuclease-free water. 5 µl of the purifed PCR product was loaded on a 1% agarose gel to verify the appropriate quantity and quality of the PCR product.

II Restriction digest

Restriction digests for the vector and insert were performed using restriction enzymes and buffers (as required) supplied by New England Biolabs. Double digest reactions were set up as described below

Double digestion of vector

1 µg of DNA

5 µl NEB Buffer

5 µl BSA (if required)

1 unit RE 1

1 unit RE 2

Adjust to 50 µl with nuclease-free water

Double digestion of insert

30 µl of PCR product

5 µl NEB Buffer

5 µl BSA (if required)

1 unit RE 1

1 unit RE 2

Adjust to 50 µl with nuclease-free water

In addition single digest reactions were set up to ensure that each of the enzymes was active under the conditions of reaction used. The digests were incubated for 2 hours at 37ºC in a water bath. Following the incubation, the entire reaction volume was loaded onto a 1% agarose gel. The bands were visualised under the UV lamp and the single bands corresponding to double-digested insert and double-digested vector were excised and purified using gel extraction kit (Qiagen) according to manufacturer's protocol. DNA was eluted in nuclease-free water and quantified using NanoDrop-2000.

III Ligation

Ligation reactions of double-digested insert and vector DNA were carried out using T4 Ligase (Promega) following the manufacturer's guidelines. 100 ng of double-digested vector was used and the amount of insert to be added was estimated using the formula below:

((ng vector) x (kb size of insert) / (kb size of vector) x molar ratio (insert/vector) = ng insert

In most experiments 1:1 molar ratio of insert to vector was used.

The reaction was set up as follows:

1 µl of T4 buffer

X ng insert

100 ng of vector

1 µl of T4 ligase

Adjust to 10 µl with nuclease-free water

As a control, double-digested vector without an insert was used to check for re-ligation. The mixtures were incubated overnight at 4ºC. The entire reaction volume was then transformed into DH5α cells and plated out onto LB-agar plates containing an appropriate selective antibiotic. Next, 3 single colonies were picked from the plates, 5 ml cultures grown, which was followed by plasmid DNA extraction using plasmid DNA Mini kit (Qiagen). Insertion of the desired sequence in frame and absence of any mutations was verified by sequencing.

2.4.4.3 Site-directed mutagenesis

In order to create a specific mutation in the sequence of interest the desired sequence was first amplified by PCR using primers such that they contain the desired base/bases change (Table 2.3).

Mutation	**Primer sequence (5'-3')**
AGR2	Forward: TGGCAGAGCAGGCTGTCCTCCTC
F104A	Reverse: GAGGAGGACAGCCTGCTCTGCCA
AGR2	Forward: CCTCAATCTGGTTGCTGAAACAACTGAC
Y111A	Reverse: GTCAGTTGTTTCAGCAACCAGATTGAGG

Reptin	Forward: AGCACGGGGGCGACGGCCATCG
K83A	Reverse: CGATGGCCGTCGCCCCCGTGC
Reptin	Forward: GAGTGCTGTTCATCAACGAGGTCCACATGC
D299N	Reverse: GCATGTGGACCTCGTTGATGAACAGCACTC
SNIP1	Forward: GACGGGATCGAGACGCTCAGAACCTGCAG
T169A	Reverse: CTGCAGGTTCTGAGCGTCTCGATCCCGTC
SNIP1	Forward: GACGGGATCGAGACGATCAGAACCTGCAG
T169D	Reverse: CTGCAGGTTCTGATCGTCTCGATCCCGTC
SNIP1	Forward:
S202A	TTGGTGGTGGCGGCAGTGAGGCTCAGGAGTTGG
	Reverse:CCAACTCCTGAGCCTCACTGCCGCCACCACCAA
SNIP1	Forward: GTGGCGGCAGTGAGGATCAGGAGTTGGTTC
S202D	Reverse: GAACCAACTCCTGATCCTCACTGCCGCCAC
P53 I332V	Forward: ACCCTTCAGGTCCGTGGGC
	Reverse: GCCCACGGACCTGAAGGGT
P53 R333A	Forward: CTTCAGATCGCTGGGCGTGAGC
	Reverse: GCTCACGCCCAGCGATCTGAAG
P53 R335A	Forward: AGATCCGTGGGGCTGAGCGCTTCG
	Reverse: CGAAGCGCTCAGCCCCACGGATCT
P53 R337A	Forward: GCGTGAGGCCTTCGAGATGTTCC
	Reverse: GGAACATCTCGAAGGCCTCACGC
P53 F338A	Forward: GCGTGAGCGCGCCGAGATGTTCC
	Reverse: GGAACATCTCGGCGCGCTCACGC
P53 E339A	Forward: AGCGCTTCGCGATGTTCCGAGAGC
	Reverse: GCTCTCGGAACATCGCGAAGCGCT

Table 2. 3 Site-directed mutagenesis primers. Red are mutated nucleotides.

The PCR reaction was assembled as follows:

12.5 µl 2x Pfu Master Mix

2.5 µl of 5x Band Doctor (supplied with Pfu Master Mix)

50 ng template DNA

1.25 µl forward primer (10 µM)

1.25 µl reverse primer (10 µM)

Adjust to 25 µl with nuclease-free water

Thermal cycling conditions were:

1. 95°C for 1 minute
2. 95°C for 50 seconds
3. 55°C for 90 seconds
4. 68°C for 10 minutes
5. Repeat steps 2-4 for 19 cycles
6. 68°C for 14 minutes
7. Hold at 4°C

Following PCR, 1 µl of DpnI restriction enzyme (5 U/µL, Invitrogen) was added to PCR product and incubated for 2 hours, at 37ºC in water bath. DpnI was heat inactived by incubation for 10 minutes at 65ºC. 2 µl of the DpnI treated product was then transformed into DH5α cells and plated out onto LB-agar plates containing an appropriate selective antibiotic. Next, 3 single colonies were picked from the LB-agar plates, 5 ml cultures grown, followed by plasmid DNA extraction using plasmid DNA Mini kit (Qiagen). Presence of required mutations was verified by sequencing.

2.5 Biochemical Techniques

2.5.1 Separation of protein by SDS-PAGE

SDS-polyacrylamide gels were prepared according to the formula below as described by Laemmli [235] using the Mini-Protean kit (Bio-Rad). First, the separating gel was cast and overlaid with water to ensure an even surface of the gel. Following the polymerisation of the separating gel, water was removed and the stacking gel was poured and the 15-well comb added. Prior to loading the combs were removed and the wells rinsed with the Running buffer. Samples were mixed with 2x or 4x sample buffer to obtain the final concentration of sample buffer of 1x. Sample were then heated for 5 minutes at 95ºC and loaded onto the gel. In addition, the pre-stained protein standards (Fermentas) were loaded as size markers. Proteins were separated by electrophoresis at 150 V in 1X running buffer, until the Bromophenol Blue dye reached the bottom of the gel.

	Separating gel 10%	**Separating gel 12%**	**Stacking gel**
Reagent	Final concentration		
30% acrylamide mix	10%	12%	5%
1.5 M Tris (pH 8.8)	0.39 M	0.39 M	NA
1 M Tris (pH 6.8)	NA	NA	0.13 M
10% (w/v) SDS	0.1%	0.1%	0.1%
10% (w/v) APS	0.1%	0.1%	0.1%
TEMED (v/v)	0.04%	0.04%	0.1%
Water	As required		

1x Running buffer

192 mM Glycine

25 mM Tris

0.1% (w/v) SDS

Sample Buffer 4x

4% (w/v) SDS

200 mM Tris-HCl pH.6.8

20% Glycerol

10 mM EDTA pH 8.0

Bromophenol blue

Sample Buffer 2x

5 % (w/v) SDS

125 mM Tris-HCl pH.6.8

25 % Glycerol

Bromophenol blue

2.5.2 Coomassie staining

Following SDS-PAGE, proteins were visualised by Coomassie blue staining. This was achieved by 30 minutes incubation of the gel with the Coomassie stain. Gel was destained by overnight incubation with Destain solution, followed by wash step in water. Finally, gel was dried onto a chromatography paper using a heated vacuum gel dryer (Gel Master Model 1426, Welch Rietschle Thomas).

Coomassie stain

5 % Coomassie blue R-450 (Sigma)

50 % (v/v) methanol

10 % (v/v) acetic acid

Destain

7.5 % (v/v) Methanol

10 % (v/v) Acetic acid

2.5.3 Western blotting

Following separation by SDS-PAGE, proteins were transferred onto 0.2 μm Hybond-C nitrocellulose membranes (GE Healthcare) in transfer buffer with an ice pack at 130 V for 60 minutes. The membranes were then ink stained to confirm even protein transfer and loading. Subsequently, non-specific binding sites were blocked using 5 % milk-PBST [5 % (w/v) dried skimmed milk (Marvel) in PBST] for 1 hour at room temperature with gentle agitation. Membranes were then incubated with the appropriate primary antibodies solution in 5 % milk-PBST overnight at 4ºC or for 1 hour at room temperature. After three washes using PBST, membranes were incubated with horse radish peroxidase (HRP) conjugated secondary antibodies (Dako) for 1 hour at room temperature. Following another set of washes, a bound antibody signal was detected using enhanced chemiluminescence (ECL) reagent. In brief, membranes were treated with the 1:1 mixture of ECL solution I and ECL solution II for 1 minute, exposed to X-ray film and then developed using a Konica Medical Film Processor (Model SRX-101A). All the antibodies that were used are listed in

Table 2.4

1x Transfer buffer

0.192 M glycine

25 mM Tris

20 % (v/v) methanol

ECL solution I

100 mM Tris (pH 8.5)

2.5 mM Luminol

0.4 mM p-Coumaric acid

ECL solution II

100 mM Tris (pH 8.5)

0.02 % (v/v) H_2O_2

Target	kDa	Clonality	Supplier	Dilution
AGR2(K47)	19	Rabbit polyclonal	Moravian Biotechnology	1:2000
AGR2	19	Mouse monoclonal	Novagen	1:1000
β-actin	42	Mouse monoclonal	Sigma	1:5000
GST	35	Mouse monoclonal	Sigma	1:2000
HA	1	Mouse monoclonal	Sigma	1:1000
His	1	Mouse monoclonal	Novagen	1:1000
Myc	1.2	Rabbit polyclonal	Sigma	1:1000
p21	21	Mouse monoclonal	Oncogene	1:500
p53 (DO1)	53	Mouse monoclonal	Moravian Biotechnology	1:5000
p53 (CM1)	53	Rabbit polyclonal	Moravian Biotechnology	1:1000
Reptin	51	Rabbit polyclonal	Abcam	1:1000

Table 2.4 Primary Antibodies

2.6 Cell culture

2.6.1 Cell lines and media

All cell lines were incubated at 37ºC and 5 % CO_2 in a humidified incubator (Hera). Media (Gibco) were supplemented with 10 % (v/v) FBS and 1 % (v/v) penicillin/ streptomycin (Invitrogen). Table 2.5 lists the cell lines used in this study, their source, culture media and AGR2 status.

Cell line	Source	Medium	AGR2 status
A549	Human carcinomic alveolar basal epithelial cells	DMEM	Positive
H1299	Human non-small cell lung carcinoma cells	RPMI	Negative
MCF7	Human breast adenocarcinoma cells	DMEM	Positive

Table 2.5 Cell lines and culture media, Dulbecco's modified eagle's medium (DMEM) and Roswell Park Memorial Institute (RPMI)

2.6.2 Subculturing of cells

Cells were maintained in sterile 10 cm diameter culture dishes and cultured to 100 % confluence. When cells were confluent, culture medium was removed and cell monolayer washed in 10 ml of sterile PBS. Subsequently, 2 ml of Trypsin-EDTA was added and the cells were incubated at 37^{o}C until they became rounded and started to detach from the plastic surface of the plate. Next, 8 ml of fresh medium was added and the suspension of the cells was collected into a 15 ml falcon tube. After appropriate dilution, cells were seeded into new cell culture plates, as required.

2.6.3 Freezing and recovery of cells

When cells were 80-100 % confluent, culture medium was removed and cell were trypsinised as described in 2.6.2. Once cells were detached, fresh medium was added and cells were transferred to a 15 ml falcon tube. Cells were then centrifuged at 200 rcf for 5 minutes, supernatant removed and the cells pellet resuspended in 5 ml of freezing media. Cells were then aliquoted into cryotubes (Nunc) and stored in Nalgene^{TM} Cryo 1ºC freezing container at -80^{o}C overnight before permanent storage in liquid nitrogen.

In order to thaw and recover the cells from liquid nitrogen, a cryovial containing cells was rapidly thawed at 37ºC in a water bath. Subsequently, the cells were transferred to a 10 cm diameter culture dish containing 10 ml of fresh medium. The next day, the medium was changed and the cells were allowed to grow until they reached confluence.

2.6.4 Transient transfection of DNA

For transfection of DNA cell were cultured to 70-90 % confluence. The transfections were carried out using Attractene (Qiagen). The amounts of DNA transfected were normalised using appropriate empty vector DNA. In detail, for each well in a 6-well transfection, the appropriate quantity of DNA (as indicated in the figure legend) and attractene (3 times the amount of DNA [µg]) was added to 100 µl of serum-free and antibiotic free medium and incubated at room temperature for 10 minutes. In the meantime 2000 µl of fresh medium was added to each well. Following incubation, 100 µl of transfection reaction was added to the cells and the cells were incubated for 24 hours or 48 hours and then harvested or treated as indicated in figure legends.

2.6.5 Transient transfection of siRNA

I Transient transfection of siRNA (Dharmacon)

For transfection of siRNA cells were seeded into 6-well plates and cultured to 30-50 % confluence. AGR2 siRNA, p53 siRNA, ATM siRNA or negative control siRNA were used at the final concentration of 50 nM. In detail, for each well 5 µl of a 20 µM stock of appropriate siRNA was diluted into 195 µl of serum free and antibiotic free medium and 4 µl of DharmaFECT reagent was diluted into 196 µl of serum free and antibiotic free medium. Following 5 minutes incubation at room temperature, the diluted siRNA and DharmaFECT were mixed and incubated for 20

minutes at room temperature. In the meantime, 1600 µl of the fresh medium was added to each well. Following incubation, 400 µl of transfection reaction was added to the cells and the cells were incubated for 24 hours or 48 hours and then harvested or treated as indicated in figure legends.

II Transient trasfection of siRNA (Qiagen)

For transfection of siRNA cells were seeded into 6-well plates and cultured to 30-50 % confluence. SMAD2 siRNA, SMAD3 siRNA, SMAD4 siRNA, SMAD7 siRNA, SNIP1 siRNA, ATG5 siRNA, ATG10 siRNA, ATG12 siRNA or negative control siRNA were used at the final concentration of 5 nM. In detail, for each well 1.15 µl of a 10 µM stock of appropriate siRNA and 12 µl of HiPerFect reagent were diluted into 100 µl of serum free and antibiotic free medium, mixed gently, and incubated for 10 minutes at room temperature. In the meantime, 2000 µl of fresh medium was added to each well. Following incubation, 100 µl of transfection reaction was added to the cells and the cells were incubated for 24 hours or 48 hours and then harvested or treated as indicated in figure legends.

2.6.6 Cell irradiation

Cells were irradiated in culture medium using a Faxitron cabinet X-ray system, 43855D (Faxitron X-ray Corporation), at a central dose rate of 2 Gy/min.

2.6.7 Drug treatment

For the experiments described in Results, cells were treated with drugs or chemicals prior to harvesting and lysis. Following drugs were used (Table 2.6)

Drug	From	Concentration	Time
Chloroquine	Sigma	100 μM	15-36h
Cycloheximide	Supelco	30 μg/ml	20'-4h
DNA-PKi	Merck	10 μM	24-48h
E64D	Sigma	10 μg/ml	24-48h
KU-55933	Merck	10 μM	24-48h
MAPKi	Merck	1 μM	24-48h
3-methyladenine	Sigma	10 μM	15-36h
MG132	Calbiochem	10 μM	4-6h
Monensin	Sigma	10 μM	24-48h
Pepstatin	Sigma	10 μg/ml	24-48h
TGF-β	R&D Biosystems	1-2.5 ng/ml	1-48h

Table 2. 6 Drugs and details of treatment

2.6.8 Harvesting cells

Cells were placed on ice and the cell culture medium was discarded. The cell monolayer was then washed with ice-cold PBS (2ml for a 6-well plate and 10 ml for a 10 cm dish), following this cells were scraped into ice-cold PBS (0.5 ml for a 6-well plate and 1 ml for a 10cm dish) using a cell scraper, transferred to microfuge tube and centrifuged for 5 minutes at 5000 rpm, at 4°C. The supernatant was discarded, and the cell pellets snap frozen and stored at -80°C. In some cases (as indicated below), cells were scraped directly into lysis buffer.

2.6.9 Cell lysis

Approximately two volumes (with respect to the size of the cell pellet) of fresh UREA lysis buffer (unless indicated otherwise) was added to partially thawed cell pellet and pipetted up and down 6-10 times. Samples were incubated for 30 minutes on ice and then centrifuged for 12 minutes, at 4°C, at maximal speed. The supernatant was transferred to a fresh tube and protein concentration assessed in a Bradford assay.

UREA lysis buffer
6.24 M Urea
0.1 M DTT
0.05 % Triton X-100
25 mM NaCl
20 mM HEPES-KOH, pH 7.6
1 tablet of protease inhibitor coctail (Roche)

2.7 Protein expression and purification from *E.coli*

2.7.1 Protein expression from *E.coli*

Wild type or mutant AGR2 or Reptin protein expression vectors were transformed into BL21-AI cells. A single colony was then picked from the LB-agar plate, inoculated into 50 ml LB containing the appropriate antibiotic, and incubated overnight, at 37ºC, with shaking at 220 rpm. The starter culture was added to 1000 ml of LB containing the appropriate antibiotic, and incubated at 37ºC, with shaking at 220 rpm until the OD_{600nm} reached 0.6. The protein expression was then induced with 0.2 % of arabinose. Following 3 hours incubation, at room temperature, with shaking at 220 rpm, cells were centrifuged for 15 minutes, at 4ºC, at 6000 rcf, and the resulting pellets were snap frozen and stored at -80ºC.

2.7.2 Purification of His-tagged AGR2

The cell pellet was resuspended in 10 ml of the lysis buffer and incubated on ice for 30 minutes. Cells were then sonicated 3 times for 15 seconds, at amplitude 7.5 microns with 10 seconds incubations on ice between each burst. Next, the lysate was centrifuged for 15 minutes, at 4ºC, at maximum speed and the supernatant was transferred to 1ml of Ni^{2+}-NTA agarose beads (Qiagen) (washed with 5 ml of Wash buffer I) and incubated for 1 hour, at 4ºC, on a rotary shaker. The mixture was then transferred to the disposable column and allowed to flow through by gravity. Next, column was washed twice with Wash buffer I and three times with Wash buffer II. Following washes, 7 ml of the Elution buffer was added and 500 ml fractions were collected and stored at -80ºC.

Lysis buffer/ Wash buffer I
20 mM Tris.HCl pH 8.0
150 mM NaCl
10 mM $MgCl_2$
0.05 % Tween 20
10 % glycerol (optional if not freezing)
20 mM imidazole pH 8.0

Wash buffer II
Lysis buffer
40 mM imidazole
Elution buffer
Lysis buffer
150 mM imidazole

2.7.3 Purification of GST-tagged Reptin

The cell pellet was resuspended in 10 ml of the lysis buffer and incubated on ice for 30 minutes. Cells were then sonicated 3 times for 15 seconds, at amplitude of 7.5 microns with 10 seconds incubations on ice between each burst. Next, the lysate was centrifuged for 15 minutes, 4ºC, at maximum speed and the supernatant was transferred to the tube containing 500 µl of glutathione-sepharose 4B beads (Amersham GE) (washed 4 times in PBS), and incubated for 1.5 hours at 4°C on a rotating table. Next, the beads were washed twice in 5 ml of High Salt Wash buffer and twice in 5 ml of the Low Salt Wash buffer. Next, 5 ml of Elution buffer was added to the beads and incubated for 30 minutes, at 4°C, on the rotating table. Eluted protein was collected and stored at -80°C.

Lysis buffer
10 % Sucrose
50 mM Tris pH 8.0
0.4 M NaCl
0.5 mg/ml Lysosyme
0.5 % Triton X- 100
1 mM DTT
1 mM benzamidine
1 x PI tablet

High salt Wash buffer
20 mM Hepes pH 7.5
1 M NaCl
1 mM DTT
1 mM benzamidine

Low salt Wash Buffer
20 mM Hepes pH 7.5
0.05 M NaCl

1 mM DTT
1 mM benzamidine

Elution buffer
100 mM Tris (pH 8)
120 mM NaCl
40 mM reduced glutathione

2.7.4 Removal of GST tag using Prescission Protease

For the removal of GST tag, following the Low salt wash, beads were washed with the Prescission buffer and resuspended in 1 ml of Prescission buffer. Next, 30 µl of Prescission protease (GE Healthcare) was added to the beads and incubated for 1.5 hours, at 4ºC, on a rotating table. The mix was then centrifuged for 2 minutes, at 4ºC, at 2000 rpm and the supernatant containing cleaved protein was transferred to a fresh tube and stored at -80ºC.

Precission buffer
50 mM Tris HcL (pH 8)
1 mM EDTA
120 mM NaCl
1 mM DTT

2.8 Assays

2.8.1 *In vivo* peptide binding assay.

H1299 cells were grown in 10 cm dishes as required and then lysed in 400 µl of the 0.1 % Triton Lysis buffer (as described in 2.6.9). Next, 40 µg/ml avidin was added to the lysates, and the mixture was incubated for 30 minutes on ice. After centrifuging the samples (5 minutes, 4ºC, at maximum speed), the pellet was discarded and the lysates were pre-cleared using 100 µl of streptavidin Agarose beads (Millipore or Sigma) (prewashed 3 times in Wash Buffer) for 1 hour, at 4ºC, on a rotating table. Subsequently, beads were centrifuged, the lysate was collected, and the protein concentration was measured using Bradford reagent. In the meantime, 0.4 µl of the appropriate peptide (Mimotopes) was added to 20 µl of Streptavidin-Agarose beads (Sigma) (prewashed 3 times in Wash Buffer) in 200 µl of Buffer W, incubated for 1 hour, at room temperature, on a rotator. Next, the beads were washed three times with 300 µl of Buffer W. Subsequently, the lysate containing 200 µg of total protein was added to the peptides coupled to beads and incubated for 1 hour at room temperature on a rotating table. This was followed by 1 wash with buffer W, 4 washes with PBS+0.2 % Triton, and again 1 wash with buffer W. The bound fraction was eluted of the beads with 40 µl of 4x Sample buffer by boiling 3 times for 5 minutes, at 95ºC. Finally, the beads were centrifuged, and the supernatant collected.

0.1 % Triton Lysis Buffer
50 mM HEPES
0.1 mM EDTA
150 mM NaCl
10 mM NaF
2 mM DTT
0.1 % Tritonx100
1 tablet of protease inhibitor coctail

Buffer W

100 mM Tris pH8

150 mM NaCl

1 mM EDTA

2.8.2 *In vitro* peptide binding assay

Streptavidin (1 μg per well in 50 μl of PBS) was coated onto a 96-well microtitre plate overnight at 37ºC. The following day wells were washed 4 times with 200 μl of PBS containing 0.1 % (v/v) Tween-20 (PBS-T). Next, 0.5 μg of biotinylated peptide per well in 50 μl of water was added and incubated for 1 hour at room temperature with shaking. Following 6 washes with 200 μl of PBS-T, the non-reactive sites were blocked with 200 μl of 3 % BSA in PBS-T for 1 hour at room temperature with shaking. Subsequently, the protein of interest (as indicated in figure legends) was added in 50 μl of 3 % BSA in PBS-T and incubated for 1 hour at room temperature with shaking. Next, the wells were washed 6 times as above and 1 in 1000 dilution of the appropriate primary antibody in 50 μl of 3 % BSA-PBS-T was added and incubated for 1 hour at room temperature with gentle agitation. The wells were again washed 6 times as above and then incubated with HRP-conjugated secondary antibody (1 in 1000 dilution in 50 μl of 3 % BSA-PBS-T) and incubated for 1 hour at room temperature with shaking. After the final set of 6 washes, ECL was added and the extent of binding was measured using a luminometer (Fluoroskan Ascent FL equipment, Labsystems).

2.8.3 ELISA

A 96-well microtitre plate was coated with 100 ng of the protein (as described in figure legend) in 50 μl of 0.1 M $NaHCO_3$ buffer (pH 8.6) at 4°C overnight. The following day wells were washed 6 times in 200 μl of PBS-T and non-reactive sites were blocked using 200 μl of 3 % BSA in PBS-T for 1 hour at room temperature

with gentle agitation. Next, a titration of the protein (in 50 μl per well) in 3 % BSA-PBS-T was added and incubated for 1 hour at room temperature with shaking. After 6 washes, an appropriate primary antibody was added (1 in 1000 dilution in 50 μl of 3 % BSA in PBS-T) and incubated for 1 hour at room temperature with gentle agitation. This was followed by another round of 6 washes and then 1 in 1000 dilution of HRP-conjugated secondary antibody was added, and incubated for 1 hour at room temperature with shaking. After the final round of 6 washes, ECL was added and the extent of binding was measured using a luminometer (Fluoroskan Ascent FL equipment, Labsystems).

2.8.4 ATPase assay

The reactions were set up in a total volume of 20 μl of buffer T. Reactions were initiated by adding 20 pmol of the wild type or mutant Reptin protein. In addition, double- or single-stranded DNA was added and the mixtures were incubated for various times at different temperatures as indicated in figure legends. Aliquots (1 μl) of the reaction mix were spotted onto polyethyleneimine-cellulose TLC plates, which were allowed to dry for 5 minutes. TLC plates were developed in 1 M formic acid and 0.5 M LiCl. Plates were then dried and exposed to Phosphoimager screen overnight. The following day plates were visualised and the amount of the released phosphate quantified with the use of Phosphoimager.

Buffer T
20 mM Tris-HCl, pH 7.5
70 mM KCl
1 mM $MgCl_2$
1.5 mM dithiothreitol
0.1 mM ATP (Merck)
0.96 μCi of [γ-^{32}P] ATP (Perkin Elmer)

2.8.5 ATP filter binding assay

Reptin was incubated with 0.57 μCi [γ-^{35}S] ATP (Perkin Elmer) for 15 minutes at 4°C in 20 μl of ATP binding assay buffer, in the presence or absence of ATP, as indicated in the figure legends. Samples were passed through nitrocellulose membranes (Millipore HA, 0.45 μm) and washed 4 times with 400 μl of ice-cold ATP binding assay buffer. The radioactivity remaining on the filter was monitored with a liquid scintillation counter.

ATP binding assay buffer
20 mM Tris-HCl pH 7.5
1 mM $MgCl_2$
70 mM KCl

2.8.6 ATP binding by ELISA

Streptavidin (1 μg per well in 50 μl of PBS) was coated onto a 96-well microtitre plate overnight at 37ºC. The following day wells were washed 4 times with 200 μl of PBS containing 0.1 % (v/v) Tween-20 (PBS-T). Next, 1.5 mM N6-(6-Amino) hexyl-adenosine-5'-triphosphate-Biotin, 8-[(6-Amino)hexyl]-amino-adenosine-5'-triphosphate-Biotin, 2'/3'-O-(2-Aminoethyl-carbamoyl)-adenosine-5'-triphosphate-Biotin, γ-[6-Aminohexyl]-adenosine-5'-triphosphate-Biotin (Jena Bioscience); Biotin-11-adenosine-5'-triphosphate (Perkin Elmer), Biotin-17-adenosine-5'-triphosphate (Enzo) (called N6-, 8-, EDA, γ-, 11-, 17-ATP thereafter) in 50 μl of water were added and incubated for 1 hour at room temperature with shaking. Following 6 washes with 200 μl of PBS-T, the non-reactive sites were blocked with 200 μl of 3 % BSA in PBS-T for 1 hour at room temperature with shaking. Subsequently, Reptin preincubated or not with ATP or ADP (as indicated in figure legends) was added in 50 μl of 3 % BSA in PBS-T and incubated for 1 hour at room temperature with shaking. Next, the wells were washed 6 times as above and 1 in 1000 dilution of the appropriate primary antibody in 50 μl

of 3 % BSA-PBS-T was added and incubated for 1 hour at room temperature with gentle agitation. The wells were again washed 6 times as above and then incubated with HRP-conjugated secondary antibody (1 in 1000 dilution in 50 µl of 3 % BSA-PBS-T) and incubated for 1 hour at room temperature with shaking. After the final set of 6 washes, ECL was added and the extent of binding was measured using a luminometer (Fluoroskan Ascent FL equipment, Labsystems).

2.8.7 Crosslinking of the protein using glutaraldehyde

Recombinant wild type or mutant reptin protein (1 µg), with or without 1 mM ATP, were mixed with serial two fold dilutions of glutaraldehyde (from 0.2 to 0 % in PBS), in a total volume of 20 µl and incubated for 1 hour at room temperature. Reaction was stopped by addition of 10 µl of 1 M Tris pH 8.0. Next, sample buffer was added, the samples were boiled and run on a Tris- Glycine precast gels (Invitrogen).

2.8.8 Thermal denaturation assay

The extent of protein unfolding was measured using fluorescent SYPRO Orange dye (Invitrogen). The purified wild type or mutant Reptin protein was diluted to 5 µM final concentration in buffer containing 50 mM Tris HcL (pH 8), 1 mM EDTA, 120 mM NaCl, 1 mM DTT and aliquoted into a 96-well PCR plate. Next, SYPRO Orange dye (5000x stock) was diluted to 50 x and added to the samples. The plate was then sealed with optical-quality sealing film (Bio-Rad). The samples were heated from 20°C to 90°C at 1°C increments with a 30-seconds incubation at each increment and the rate of protein unfolding was measured using an iCycler iQ Real-Time PCR system (Bio-Rad). Fluorescence intensity was measured using excitation/emission wavelengths of 485 nm/575 nm in relative fluorscent units (RFU) and thermal denaturation graphs were plotted as a function of the gradient of protein unfolding against the temperature gradient [d(RFU)/dT].

2.8.9 Dynamic light scattering (DLS)

Prior to size analysis Reptin protein was passed through a 0.22 μM filter (Ultrafree-MC, Millipore, UK) centrifuged at 4°C, at 12000 rcf. Analysis was carried out on 50 μM Reptin in 50 mM Tris HCl (pH 8), 1 mM EDTA, 120 mM NaCl, 1 mM DTT at 10°C with Zetasizer APS (Malvern instruments, UK) equipped with a 50 mW laser light source of wavelength 830 nm. Scattering data was collected at a scattering angle of 90°C for 10 seconds, repeated at least twelve times and averaged. The experiments were repeated in triplicate. Autocorrelation data was fit to a model of a multiple exponential form suitable for polydisperse solutions, using the protein specific software supplied with the instrument. This generated a distribution of particles by size. DLS is very sensitive to aggregation as scattering is a function of R_h to the sixth power. In addition, to monitor temperature induced unfolding of the protein, the temperature of the sample cell was increased from 4°C to 90°C at 2°C intervals. A rapid increase of scattering intensity is indicative of protein unfolding and subsequently aggregation to form much larger particles. Unfolding was also monitored by a single exponential or cummulants fit of the scattering data to give the Z-average (ISO13321). The Z-average is global descriptor of the particles in solution weighted by scattering intensity. It represents a hypothetical sphere that has the same scattering function as the distribution of particles in solution.

2.8.10 Immunoprecipitation (IP)

H1299 cells, A549 cells or MCF7 cells were transfected with AGR2, wild type or mutant Reptin, wild type or mutant p53 protein, as indicated in figure legend. The following day cells were scraped into 500 μl of one of the IP lysis buffers (1-6) as indicated in the figure legend and in the text. The lysates were pre-cleared by incubation with 100 μl Sepharose CL 4B (Sigma-Aldrich; washed 4 times in PBS) for 40 minutes, at 4°C with rotation. Pre-cleared lysate was collected and concentration of total protein quantified by Bradford method. Subsequently, 1 μg of appropriate primary antibody was incubated with 600 μg of total protein in the

pre-cleared lysate, in a final volume of 200 µl for 2 hours at 4°C with gentle rotation. Next, 15 µl of protein protein G-Sepharose™ 4 FastFlow (GE Healthcare; washed 4 times in PBS) was added to the above samples and incubated for 1 hour at 4°C with gentle rotation. Supernatant (flow-through) was collected, to establish amount of the unbound protein, and the beads were washed four times with 500 µl of IP buffer. Samples were then eluted by adding 50 µl of 4x SDS sample buffer containing 0.2 M dithiothreitol and incubating at 95°C for 5 min. The eluate was then collected and analyzed by Western blotting.

IP buffer 1
0.15 M NaCl,
0.5 % Tween- 20
50 mM HEPES pH 7.6

IP buffer 2
0.15 M NaCl
1 % Triton X-100
50 mM Hepes pH 7.6

IP buffer 3
0.15 M NaCl
1 % NP40
50 mM Hepes pH 7.6

IP buffer 4
0.3 M NaCl
0.5 % Tween-20
50 mM Hepes pH 7.6

IP buffer 5
0.3 M NaCl
1 % Triton X- 100

50 mM Hepes pH 7.6

IP buffer 6

0.4 M KCl

25 mM Tris pH 7.2

1 % NP-40

1mM DTT

1× protease inhibitor mixture

2.8.11 *In vivo* ubiquitination assay

H1299 cells were seeded onto a 6-well plate following which they were transfected with His-tagged Ubiquitin, SUMO-1, NEDD-1, Reptin, p53, AGR2 as indicated in the figure legend. The next day, cells were treated with MG132 for 4 hours. Cells were then harvested into 1 ml of ice cold PBS, and the cells suspension was divided into 2 aliquots: 200 µl aliquot for direct lysis and 800 µl for analysis by His-pull down. Both aliquots were centrifuged at 4ºC, for 5 minutes at 2500 rcf. The supernatant was discarded and the cell pellets snap-frozen or lysed. The pellet from 800 µl aliquot was lysed in 1 ml ice cold lysis buffer by pippeting up and down and passing it through a needle and syringe 10-15 times. Subsequently, the lysate was transferred to a 15 ml falcon tube containing a further 4 ml lysis buffer. Next, 75 µl Ni^{2+}-NTA agarose beads (Qiagen) was added to the lysate and incubated on a rotating table, at 4^{o}C for 4 hours or overnight. Following incubation, the beads were collected by centrifugation at 4ºC, for 5 min, at 500 rcf. The beads were then resuspended in 750 µl of buffer A, transferred to microfuge tube and incubated on a rotating table, at room temperature, for 15 minutes. Similarly, the beads were washed in buffers B-E. Following the final wash, 75 µl of elution buffer was added to the beads, and incubated on a rotating table, at room temperature for 30 minutes. The beads were collected by centrifugation at 4^{o}C, for 5 minutes, at 500 rcf. The eluate was then transferred to a fresh tube and mixed with an equal volume of 2x sample buffer. The samples were boiled at 95^{o}C, for 5 minutes and 50 µl of each sample was

loaded onto a 4-12 % NuPAGE gel (Invitrogen) and run at 200 V for 60 minutes in 1x MOPS buffer (Invitrogen). The resolved proteins were transferred to nitrocellulose and the extent of ubiquitination, sumoylation or neddylation was monitored by immunoblotting using anti-p53 or anti-Reptin antibodies.

The pellet from 200 µl aliquot was lysed in 10 µl of 1 % NP-40 Lysis buffer. The lysate was mixed with an equal volume of 2x sample buffer. The samples were boiled at 95^{o}C, for 5 minutes and 5 µl of each sample was loaded onto a 10 % SDS-polacrylamide gel and run at 150 V for 60 minutes in 1x running buffer. The resolved proteins were transferred to nitrocellulose and the extent of ubiquitination, sumoylation or neddylation was monitored by immunoblotting using anti-p53 or anti- Reptin antibodies.

Lysis buffer
Buffer A + 5 mM Imidazole

Buffer A
6 M Guanidinium-HCl
95 mM Na2HPO4
5.3 mM NaH_2PO_4
10 mM Tris-HCl, pH 8.0
0.01 M β-mercaptoethanol
Adjust to pH 8.0

Buffer B
8 M Urea
95 mM Na_2HPO_4
5.3 mM NaH_2PO_4
10 mM Tris-HCl, pH 8.0
0.01 M β-mercaptoethanol
Adjust to pH 8.0

Buffer C

8 M Urea

22.5 mM Na2HPO4

77.5 mM NaH2PO4

10 mM Tris-HCl, pH 6.3

0.01 M β-mercaptoethanol

Adjust to pH 6.3 and make up to 200 ml with water.

Buffer D

Buffer C + 0.2 % Triton X-100

Buffer E

Buffer C + 0.1 % Triton X-100

Elution buffer

0.2 M Imidazole

5 % SDS

150 mM Tris-HCl (pH 6.8)

10 % glycerol

0.72 M β-mercaptoethanol

NP-40 Lysis buffer

25 mM HEPES (pH 7.5)

1 % (v/v) NP40

150 mM KCl

50 mM NaF

5 mM DTT

1X protease inhibitor mix

2.8.12 Dual Luciferase reporter assay

H1299 cells were seeded onto 24-well plates and transfected with pCMV-Renilla luc (30 ng per well) together with 70 ng of either p21-Firefly luc or MDM2-Firefly luc and with wild type p53, a titration of wild type Reptin, wild type AGR2 protein, wild type MDM2 (see figure legend). Alternatively, A549 cells were seeded onto 24-well plates and transfected with pCMV-Renilla luc (125 ng per well) together with a titration of AGR2 promoter-Firefly luc and treated with the titration of TGF-β (see figure legend). Twenty four hours post transfection and treatment luciferase assays were performed using the Dual Luciferase Reporter Assay System (Promega) according to the technical manual with some modifications. In brief, the cells were washed once in 0.5 ml of ice-cold PBS and lysed in 100 µl of 1 x Passive Lysis Buffer (supplied in the kit) for 10 minutes, at room temperature with shaking. Afterwards, the cell lysate was mixed by pipetting and transferred to microfuge tubes. Next, 5 µl of the lysate was aliquoted onto a 96-well microtitre plate and then 20 µl of luciferase assay reagent was added (LAR; supplied in the kit). Firefly luciferase luminescense was then measured using a Fluroskan Ascent F1 luminometer (Labsystems). Subsequently, 20 µl of Stop and Glo reagent (supplied in the kit) was added to each well and the Renilla luciferase signal was measured. Signals were normalised using the internal control (renilla luciferase signal) and expressed as a ratio of firefly:renilla luciferase. Results are represented as mean of at least two independent experiments ± SD.

2.8.13 Electrophoretic mobility shift assay (EMSA)

DNA binding activity of p53 under different condition was measured by EMSA. First, specific complementary oligonucleotides containing p53 consensus site from the p21 promoter were labelled using γ-^{32}P ATP.

In order to do this, following reaction was assembled:
2.5 µl of p21 Forward Primer (stock: 1 mg/ml)

2.5 µl of p21 Reverse Primer (stock: 1 mg/ml)

1 µl of T4 DNA kinase buffer

0.4 µl of T4 DNA kinase

4 µl of 10 mCi/ml γ-^{32}P ATP

p21 Forward Primer:
TGCCAGAGCTCAACATGTTGGGACATGTTCCTGATGGCCA
p21 Reverse Primer:
TGGCCATCAGGAACATGTCCCAACATGTTGAGCTCTGGCA

The mixture was then incubated for 2 hours at 37ºC, following which 15.5 µl of TE buffer and 4.5 µl of 1 M KCl was added. After 2 minutes incubation at 95ºC, the mixture was allowed to slowly cool down and then purified by centrifugation through 1.5 ml micro-Biospin 30 column into an eppendorf tube.
Next, 5 % native polyacrylamide gel mixture was prepared according to the formula below:

	Separating gel 5 %
Reagent	Final concentration
30 % acrylamide mix	5 %
5x TBE	1x
10 % (w/v) APS	0.1 %
10 % (v/v) Triton- X100	0.1 %
Water: 44.2 ml	
Volume for one gel: 70 ml	

TEMED (3 %) was added to 2 ml of the gel mix and poured immediately into bottom of the gel to form a plug. TEMED (0.1 %) was then added to the rest of the mixture and casted and the 25-well comb added. Before loading the samples, the gels were pre-run at 35 mA, for 30 minutes, at 4 ºC.

The reaction was prepared as follow:

2 µl of 6x reaction buffer

p53 (from Sf9 cells)

Reptin (as indicated in the figure legend)

ATP or ADP (as indicated in the figure legend)

Adjust to 12 µl with water

6x reaction buffer

120 mM HEPES pH 7.5

300 mM KCl

30 % Glycerol

2.4 mM DTT

0.6 mg/ml BSA

3 % TritonX-100

The mixture was then incubated for 30 minutes at 20-37ºC (as indicated in the figure legend) and 0.2 µl of ten-fold dilution of the p53-specific probe was added. Following 30 minutes incubation on ice, 2.5 µl of DNA loading dye was added and the samples were loaded onto a gel and run at 35 mA for 150 minutes at 4 ºC. Subsequently, the gel was dried in a vacuum gel dryer and exposed to Phosphoimager screen overnight. The following day the plate was visualised and the amount of the free probe and DNA-bound p53 quantified with the use of Phosphoimager.

2.8.14 RNA extraction and RT PCR

Cell were seeded in the 6-well plate and treated as indicated in the figure legend. After treatment cell were harvested as usual and RNA was isolated using the RNeasy Mini kit (Qiagen), according to the manufacturer's instruction. RNA was then used to synthesize cDNA using the Omniscript RT kit (Qiagen) as described below.

2.8.14.1 Reverse transcription

RNA (0.5 µg) was diluted in 7 µl of water and heated at 65ºC for 5 minutes. RNA was cooled on ice and mixed with 13 µl of RT Master Mix.

RT Master Mix
2 µl of 10X RT Buffer
2 µl of 5 mM dNTP
0.2 µl 0.5 mg/ml oligo dT primer
0.2 µl 40 U/µl RNase inhibitor
2 µl 100 mM DTT
1 µl Omniscript RT
5.6 µl Nuclease-free water
The mixture was incubated for 1 hour at 37ºC and subsequently used for PCR with the appropriate gene-specific primers.

2.8.14.2 PCR

PCR was performed using cDNA template obtained as described in 2.8.13.1. In detail, PCR reactions were assembled as follows:

5 µl 2X PCR (Taq) Master Mix
1 µl cDNA template
0.7 µl Forward primer (10 µM)
0.7 µl Reverse primer (10 µM)
Nuclease-free water 2.6 µl

Thermal cycling conditions were:
1. 94°C for 15 minutes
2. 94°C for 30 seconds
3. 55°C for 30 seconds

4. 72°C for 30 seconds
5. Repeat steps 2-4 for 25 cycles
6. 72°C for 10 min
7. Hold at 4°C forever

Primer sequences are listed in Table 2.7

Target	**Primer sequence (5'-3')**	**Size of the product**
AGR2	Forward GCTCCTTGTGGCCCTCTCCTACAC	354 bp
	Reverse ATCCTGGGGACATACTGGCCATCAG	
GAPDH	Forward GTCAGTGGTGGACCTGACCT	123 bp
	Reverse ACCTGGTGCTCAGTGTAGCC	

Table 2.7 RT-PCR primers

Following PCR, 6x DNA loading buffer was added to each reaction and the entire volume was loaded and resolved on 1.5 % agarose gel in 1x Tris borate-EDTA buffer. The bands were visualized under a UV transilluminator, photographed in a gel 1000 ultraviolet documentation system (*BioRad*).

CHAPTER 3: ATM and TGF-β pathway converge to activate p53 signalling pathway.

3.1 Introduction

3.1.1 Cancer models

Classically, the development of tumour can be explained as a process involving mutations that either activate growth-promoting genes or inactivate proteins that inhibit growth or induce cell death [2-5]. The most commonly used clinical models that have been put forth to elucidate the genetics of oncogenesis at different stages of disease progression are sporadic colorectal cancer [454] and esophageal adencoarcinoma cancer [455]. For example, in colorectal cancerogenesis a sequence of genetic alterations starts with an inactivating mutation of FAP/APC gene in hyperproliferative epithelium, which is followed by genomic DNA hypomethylation and an activating mutation of the K-RAS oncogene in adenoma and in the expanding tumour. In metastasizing tumours a number of additional genetic changes occur, including mutations in p53 tumour suppressor encoding locus [454, 456, 457]. Similarly to colorectal cancer, esophageal adenocarcinoma cancer also proceeds through a stepwise acquisition of genetic alterations, including mutation of the p53 gene [458], p16 promoter methylation and p15 deletion [459], or EGFR amplification and overexpression [460]. Subsequently, these lead to histopathological changes of epithelium, from premalignant stage of metaplasia and dysplasia (collectively termed Barrett's esophagus or Barrett's epithelium) to carcinoma *in situ* and finally invasive carcinoma [460].

3.1.2 p53 pathway alterations in cancer

In normal tissue p53 controls a broad range of cellular processes and maintains tissue integrity (as discussed in 1.2.1.1). It is kept under tight control and once activated it induces either cell cycle arrest or programmed cell death, depending on the cell type and cellular environment. Loss of p53 function contributes to genetic instability, perturbed growth arresting pathway and results in the survival of cells with an increased tumourogenic capacity [458]. In different cancers distinct changes are observed with respect to p53 pathway. For instance, p53 mutations are found in both colorectal and eoseophegal cancer, however the loss of p53 function is observed relatively late or quite early in the disease progression, respectively. In addition, the nucleotide substitutions that occur in the p53 sequence can be cancer specific [458]. On the other hand, not all human cancers have p53 gene mutations and in such instances mutations in the activators of p53 or overexpression of p53 inhibitory proteins can account for attenuation of the p53 response. The most common examples of such mechanism include inactivation of p53 kinases Chk2 or ATM [461] or overexpression of E3 ligases that promote p53 degradation, such as MDM2, PirH2, COP-1, and CHIP [39]. Further, cancer is a tissue-specific disease and as such it is not surprising that tissue-specific p53-inhibitory pathways have been identified. For instance, in the search for the mechanisms that can drive survival of Barrett's epithelium cells containing the wild type p53 protein, stress responsive SEP70, SEP53 and glutamine-glutamyl transferase were identified [462, 463]. Additionally, the presence of the oncogenic signals that could inhibit wild type p53 pathway in Barrett's have been suggested, and indeed, AGR2 protein was found to be overproduced in this tissue and was shown to inhibit DNA damage-induced activation of p53 pathway [437]. Additionally, AGR2 has been found to be overexpressed in other cancers, such as breast [407], pancreatic [431, 432], prostate [410] cancers. Its role in carcinogenesis has been further reinforced by demonstrating that its overexpression enhances rate of adhesion, results in greater propensity to form metastases [427, 442] and supports anchorage-independent growth [411]. Given that Barett's epithelium cells are constantly exposed to different stress stimuli and AGR2 protein is elevated in this tissue, it is plausible that AGR2 could be

responsive to a variety of pathophysiological stress within the tumour microenvironment and serve as a survival factor. Indeed, AGR2 expression could be induced by hypoxia or serum depletion conditions often observed in cancer tissue [444]. However, it is currently unclear what the pathways that control AGR2-p53 axis are. Interestingly and similarly to AGR2, Transforming Growth Factor-β (TGF-β) has been shown to impact the adhesion processes and was also found to cooperate with p53. Based on this data, I formulated a working hypothesis that the TGF-β may act as an extracellular signal that regulates the AGR2-p53 pathway.

3.1.3 TGF-β

TGF-β is the prototypical member of a larger superfamily of more than 30 cytokines which includes TGF-βs, activins, bone morphogenetic proteins (BMPs), and growth and differentiation factors (GDFs) [464]. In mammals TGF-β exists in three variants: TGF-β1, TGF-β2, and TGF-β3 and the formation of bioactive molecule requires homo- or hetero-dimerization. In order to propagate the signal to the nucleus, TGF-β binds to dimeric complex of type I and type II receptors (TGFβRI and II respectively). Upon ligand binding, TGFβRII recruits and phosphorylates TGFβRI [465, 466]. Subsequently, TGFβRI propagates signalling inside the cell by recruitment and phosphorylation of SMAD2 and SMAD3. The activated SMAD proteins can then heteromerize with the common mediator of this pathway, SMAD4, and subsequently translocate to the nucleus [465, 467-469]. SMAD proteins can bind to DNA with low affinity and in order to achieve high affinity and selectivity, association with other DNA-binding factors is required [470]. A variety of transcription factor families have been shown to cooperate with SMAD-DNA complexes, including the forkhead, homeobox, zinc-finger, bHLH, ETS and AP1 families [471, 472]. In addition to transcription factors, SMADs cooperate with several coactivators and corepressors, which fine tune the magnitude of the TGF-β response. For instance, they recruit activators like p300/CBP, MSG1 or SKIP [473-479] or corepressors such as: c-Ski, SnoN or SNIP1 [480-483]. Depending on the combination of SMAD2/3-SMAD4 and transcription factor,

different set of genes are activated or repressed (reviewed in [484]). SMADs are central players in most TGF-β triggered cellular events and are involved in so called canonical pathway of TGF-β signal transduction. However, an alternative SMAD-independent mechanism of TGF-β signaling exists and it incorporates Mitogen-activated protein kinases (MAPKs) pathway. For instance the TRAF6–TAK1–p38/JNK pathway [485, 486] or the Erk-MAP kinase signalling [487] can be activated downstream of TGF-β receptors.

TGF-β plays a regulatory role in processes such as cellular proliferation, differentiation, survival, adhesion and maintenance of the cellular microenvironment [488]. In normal tissue, TGF-β enforces homeostasis and exerts tumour suppressive effects. However, cancer cells evade the tumour suppressive effects of TGF-β and adapt the TGF-β pathway to their advantage, and use it as a pro-invasive and pro-metastatic factor [464]. Interestingly, the convergence of the p53 and TGF-β pathway has been recently unveiled. p53 protein has been shown to associate directly with SMAD2 and SMAD3, act as a cofactor in a promoter-specific manner in *Xenopus* embryos and by this regulate TGF-β-dependent expression of mesendodermal genes [109, 489]. This is mediated by phosphorylation of p53 at Ser 6 and Ser 9 by the Ras/ CK1 signalling pathway, which facilitates p53 binding to SMAD2 and SMAD3 [305]. Similarly, p53, SMAD2 and SMAD4, SnoN, mSin3A protein were found to form a repressive complex at the alphafetoprotein (AFP) promoter and silence its expression [490, 491]. Further, TGF-β induces p21, plasminogen inhibitor activator (PAI-1) and metalloproteinase 2 (MMP2) and expression of p53 is required for this effect [109, 489].

Given the extensive links between the p53 and TGF-β signalling pathways, and the role of AGR2 in regulating cell migration, we reasoned that TGF-β signalling might affect AGR2 protein pathway responses. In this chapter we establish the link between TGF-β and AGR2-p53 axis, we report on TGF-β-mediated downregulation of AGR2 protein and demonstrate evidence for ATM dependent lysosomal degradation of AGR2.

3.2 Results

3.2.1 Exploring physiological signals regulating AGR2- p53 axis.

Previous reports on the ability of AGR2 to suppress the p53 pathway were based on studies performed in H1299 lung tumour cells that do not contain endogenous AGR2 or p53. Therefore, we sought to define the physiological signals that regulate the AGR2-p53 axis in the cells expressing both proteins endogenously. A549 are the lung tumour cells that, contrary to H1299 cells, contain a wild-type p53 pathway. In addition, these cells have a well-characterised response to genotoxic and non-genotoxic stress, that leads to p53 induction as defined by its increased phosphorylation and acetylation [492]. A549 cells have been reported to undergo epithelial to mesenchymal transition upon TGF-β treatment. Intriguingly, the search for the physiological inputs that activate p53 identified TGF-β and since then there have been a number of reports showing the p53-TGF-β interplay [109, 305, 489]. In addition, A549 cells also express AGR2 protein. Interestingly, its expression appears not to be estrogen driven, as it is in other cell models, since serum withdrawal leads to increase, rather than decreased levels of AGR2 protein (Figure 3.1). Similarly, AGR2 mRNA was found to be increased in response to depletion of serum in another cell line [444].

In order to evaluate how diverse signalling pathways control AGR2-dependent inhibition of p53 activity, we set out to look at DNA damage response or TGF-β pathway in A549 cells in more detail. In order to confirm that applying genotoxic stress or TGF-β treatment results in p53 activation in A549 cells, A549 cells were treated with either X-rays or TGF-β. As expected, ionizing radiation triggered p53 protein stabilisation in the absence or presence of TGF-β (Figure 3.2 B, lanes 2 and 4). However, there was relatively little increase in the p53-inducible p21 protein, except under combined treatment of cells with both radiation and TGF-β (Figure 3.2 C, lanes 1-3 vs. 4). As A549 cells contain high levels of AGR2 (Figure 3.2 A, lane 1), we were interested to test whether AGR2 depletion would increase p53 steady-state levels or stimulate its transcriptional activity, as measured

by evaluating p21 protein levels. To this end A549 cells were treated with AGR2 siRNA. AGR2 knock-down resulted in an increase in the levels of p53 protein in untreated and treated cells which indicates the AGR2 indeed negatively regulates p53 protein (Figure 3.2 B, lanes 5-8). Additionally, AGR2 depletion potentiated p21 induction upon treatment, relative to that observed for cells treated with scrambled siRNA (Figure 3.2 C, lanes 5-8 vs. 1-4). This latter data is consistent with previous observation, that AGR2- dependent inhibition and nuclear exclusion of p53 are more pronounced in DNA damaged cells [420, 437]. Moreover, since using the cells expressing endogenous AGR2 and p53 we were able to replicate observations made previously in cells with ectopically expressed AGR2 and p53, we can conclude that p53 inhibitory function of AGR2 is physiologically relevant.

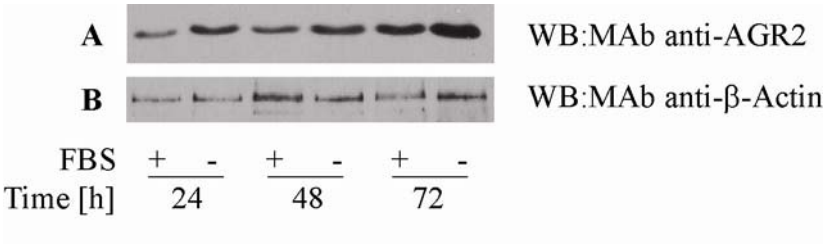

Figure 3.1 Serum withdrawal induces AGR2 protein. A549 cells were grown in DMEM + 10 % FBS or in serum free medium for the times as indicated. The cells were then lysed and the steady-state levels of **(A)** AGR2 (19kDa) and **(B)** β-Actin were measured by immunoblotting using AGR2 specific monoclonal antibodies against respective proteins.

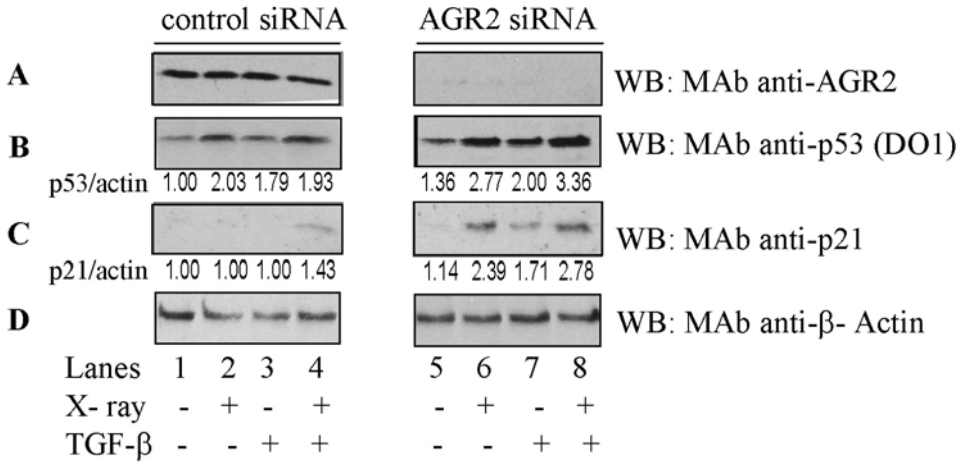

Figure 3.2 AGR2 depletion using siRNA induces p53/p21 pathway in X-ray-irradiated or TGF-β-treated cells. A549 were transfected with 50 nM AGR2 siRNA or with control siRNA and 48 hours post transfection were treated for 30 minutes with 2.5 ng/ml TGF-β, or carrier prior to irradiation with 5 Gy. After 2 hours the cells were lysed and the steady-state levels of **(A)** AGR2, **(B)** p53, **(C)** p21, **(D)** β-Actin proteins were measured by immunoblotting and quantified with ImageJ. The fold change in p53 and p21 protein levels was established and normalized against β-Actin.

In order to examine p53 activation in response to TGF-β treatment or radiation, we performed a more refined time course and monitored correlation between AGR2, p53 and p21 protein levels. First, A549 cells were treated with the increasing amounts of TGF-β for 24 to 72 hours in the presence or absence of serum. TGF-β increased p53 protein levels, with the maximal induction at 48 hours time point (Figure 3.3 D). Surprisingly, TGF-β treatment resulted in attenuation of AGR2 protein levels and by 48 hours or 72 hours we observed a complete suppression of AGR2 protein (Figure 3.3 A-C, lanes 2-3 vs. 5-6). Interestingly, serum withdrawal appeared to rescue TGF-β dependent decrease in AGR2 protein, at least at 24 hours time point (Figure 3.3 A, lane 1 and 4 vs. 2-3 and 5-6). This is in agreement with the earlier observed stabilisation of AGR2 protein in serum free medium (Figure 3.1). To further investigate the TGF-β-dependent reduction in AGR2 protein, cells were treated with a titration of the cytokine for 1 hour to 24 hours. At times from 1 hour to 12 hours there was no noticeable change in AGR2 protein levels. However, we observed a dose dependent decrease in AGR2 levels, starting between 12 hours to 18 hours post- treatment (Figure 3.3 E). Accordingly, the increase in p21 levels occurred (Figure 3.3 G). In addition, a dose-dependent correlation was observed between the AGR2 levels and the changes in the p53/p21 pathway. Specifically, we found that the initial suppression of AGR2 at about 12 hours to 18 hours post treatment coincided with an increase in p21 levels. These data are consistent with the experiment described above, wherein depletion of AGR2 using siRNA resulted in more pronounced TGF-β induced increase in p21 protein levels (Figure 3.2).

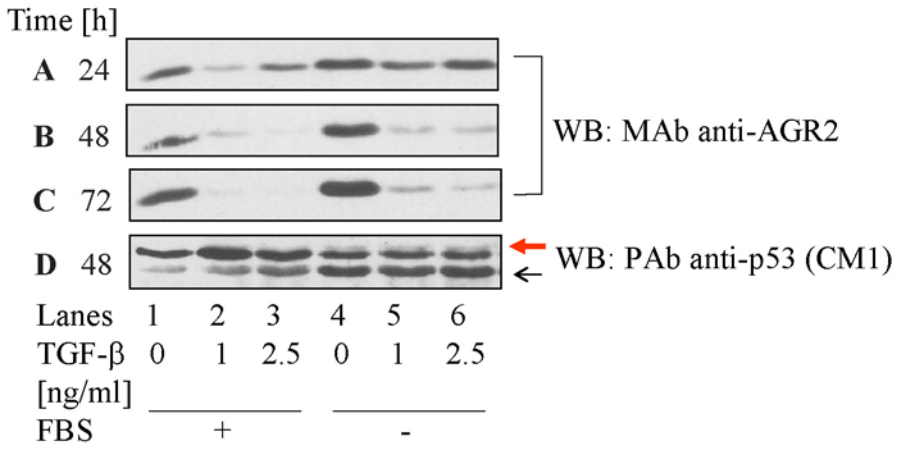
Time [h]
A 24
B 48
C 72
D 48
WB: MAb anti-AGR2
WB: PAb anti-p53 (CM1)
Lanes 1 2 3 4 5 6
TGF-β [ng/ml] 0 1 2.5 0 1 2.5
FBS + -

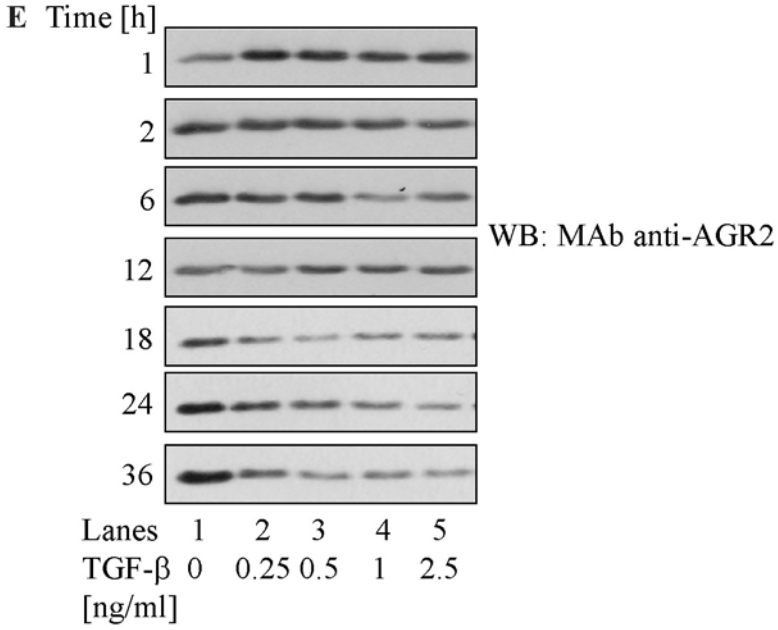
E Time [h]
1
2
6
12
18
24
36
WB: MAb anti-AGR2
Lanes 1 2 3 4 5
TGF-β [ng/ml] 0 0.25 0.5 1 2.5

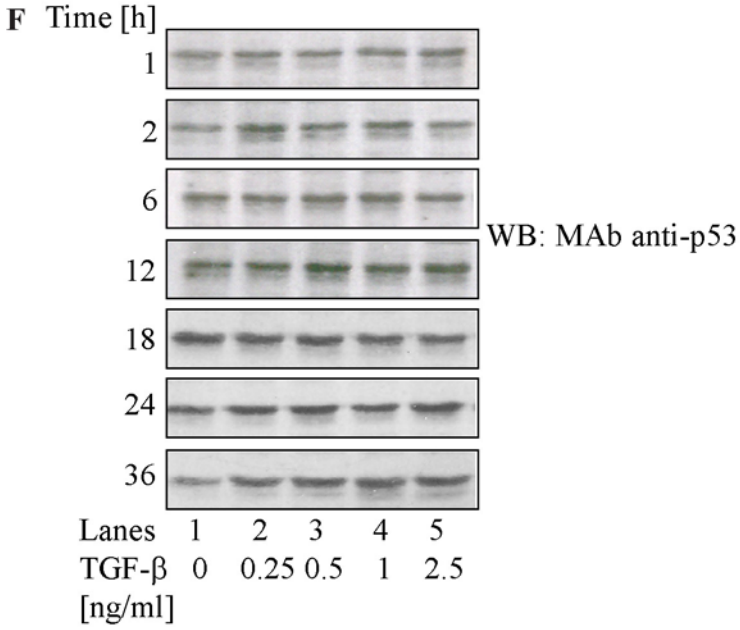
F Time [h]
1
2
6
12
18
24
36
WB: MAb anti-p53
Lanes 1 2 3 4 5
TGF-β [ng/ml] 0 0.25 0.5 1 2.5

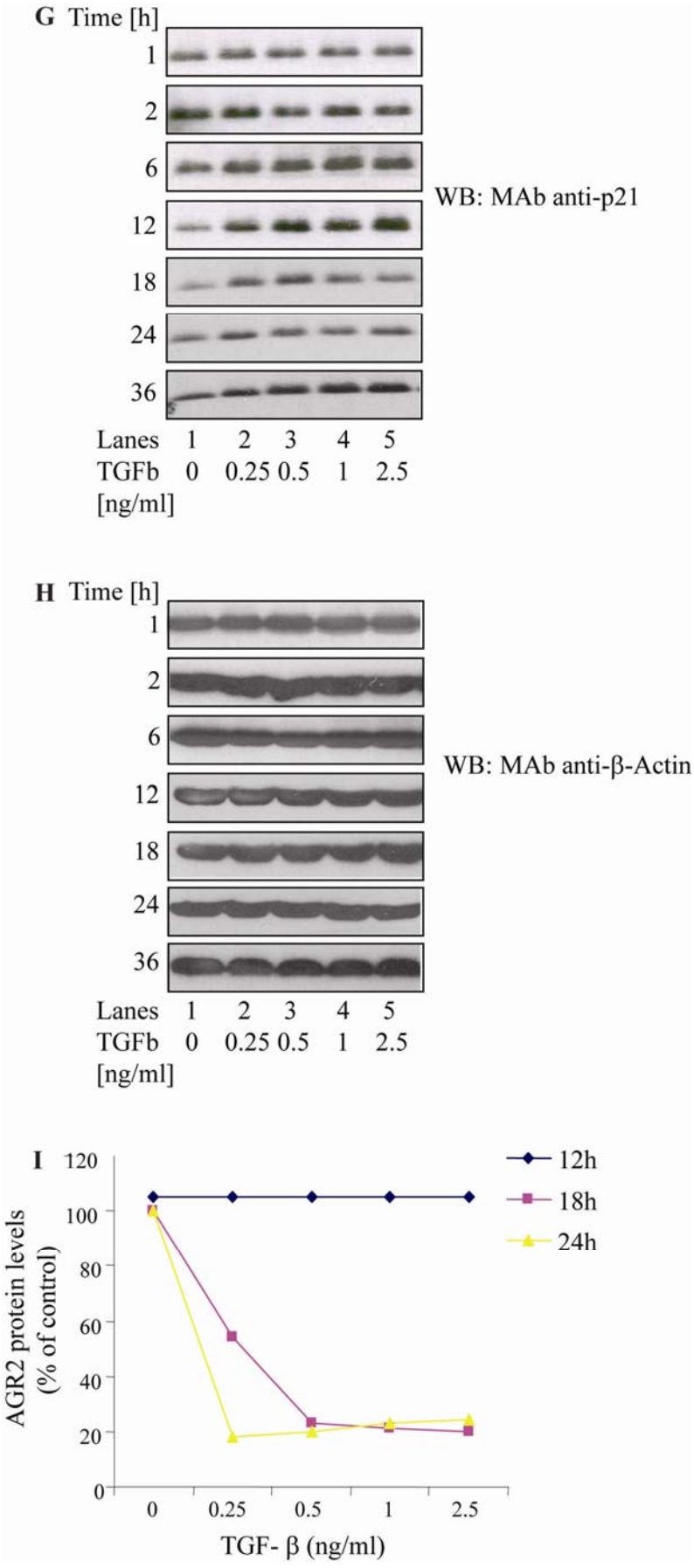
G Time [h]
1
2
6
12
18
24
36
WB: MAb anti-p21
Lanes 1 2 3 4 5
TGFb 0 0.25 0.5 1 2.5
[ng/ml]
H Time [h]
1
2
6
12
18
24
36
WB: MAb anti-β-Actin
Lanes 1 2 3 4 5
TGFb 0 0.25 0.5 1 2.5
[ng/ml]
I
AGR2 protein levels (% of control)
120
100
80
60
40
20
0
0
0.25
0.5
1
2.5
TGF- β (ng/ml)
12h
18h
24h

Figure 3.3 TGF-β triggers AGR2 protein reduction. (A-D) Time course of TGF-β suppression of AGR2 protein. A549 cells were grown for **(A)** 24 hours **(B and D)** 48 hours, or **(C)** 72 hours without the addition of cytokine (lane 1) or with the addition of the indicated levels of TGF-β. The cells were lysed and the steady-state levels of **(A-C)** AGR2 and, **(D)** p53 were measured by immunoblotting using specific antibodies against indicated proteins. The red arrow marks the migration of full-length p53 and the black arrow marks the migration of the alternative translation initiation gene product named p47. **(E-I)** TGF-β downregulates AGR2 protein in a time- and dose-dependent manner. A549 cells were stimulated with different concentrations of TGF-β for the periods as indicated from 2 hours to 24 hours. The cells were lysed and the steady-state levels of **(E)** AGR2, **(F)** p53, **(G)** p21, **(H)** β-Actin proteins were measured by immunoblotting using specific antibodies against respective proteins and quantified usinig Image J. **(I)** Summary of the change in the levels of AGR2 at selected time points.

As we observed a direct correlation between AGR2 and p21 protein levels, we next determined whether the apparent p21 induction was indeed p53 dependent. To this effect p53 protein was depleted using siRNA and the cells were treated with TGF-β. p53 knock-down prevented the induction of p21 protein (Figure 3.4 C-D, lanes 1-3 vs. 4-6), which was consistent with previous reports showing that p53 is required for TGF-β-dependent elevation of p21 [109]. In addition, we were keen to establish if p53 pathway was required for TGF-β mediated suppression of AGR2. To this effect, AGR2 protein levels were measured in the same set of samples. We found that AGR2 could be attenuated to the same extent in the presence or in the absence of p53 protein (Figure 3.4 G-H, lanes 2-3 vs. 5-6), indicating that TGF-β mediated suppression of AGR2 is in fact p53-independent.

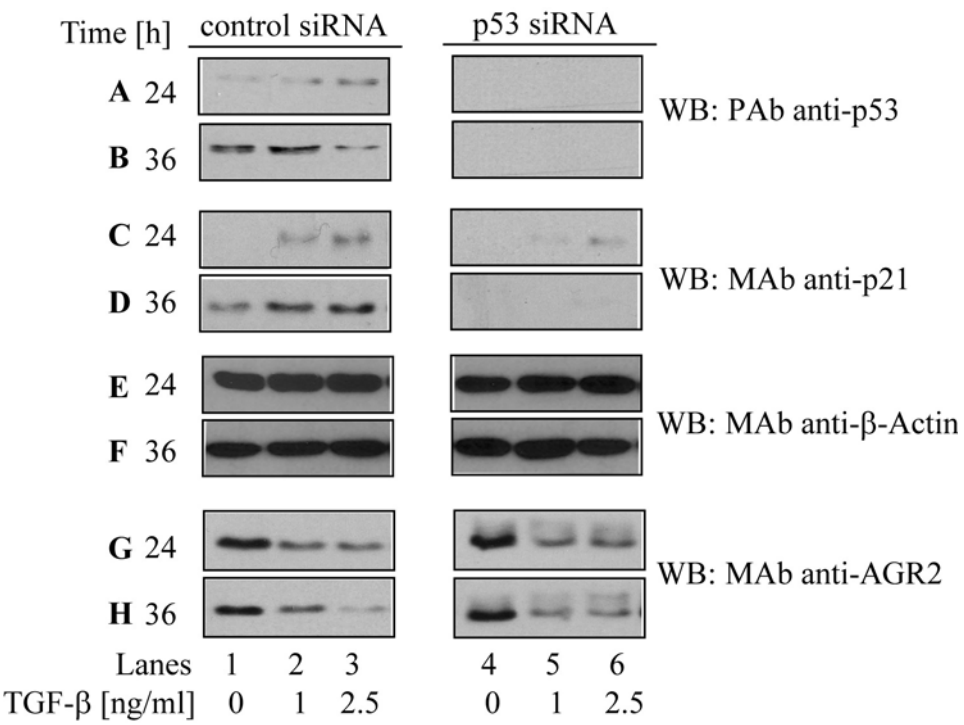

Figure 3.4 TGF-β induction of p21 is p53-dependent, but TGF-β suppression of AGR2 is not. A549 cells were transfected with 50 nM p53 siRNA or control siRNA and 48 hours post transfections the cells were treated with different concentrations of TGF-β for the times as indicated. Cells were then lysed and the steady-state levels of **(A)** p53, **(B)** p21, **(C) β-**Actin, **(D)** AGR2 proteins were measured by immunoblotting using specific antibodies against respective proteins.

3.2.2 Mechanism of TGF-β-mediated suppression of AGR2

In order to determine whether TGF-β-mediated depletion of AGR2 is due to its increased degradation, we evaluated a time course of AGR2 protein reduction in the presence and absence of MG132, a proteasome inhibitor. As before, AGR2 reduction was found to occur 12 hour to 15 hours after treatment (Figure 3.5 A, lane 1 vs. 2-3). The addition of MG132 did not prevent TGF-β-induced suppression of AGR2 protein, suggesting a proteasome independent mechanism of AGR2 protein loss (Figure 3.5 A, lanes 2-3 vs. 5-6, E). As a control, p53 and p21 protein levels were monitored upon MG132 treatment. As expected, basal levels of both proteins increased under these conditions (Figure 3.5 B-C, E). This result indicated that TGF-β mediated loss of AGR2 protein is proteasome independent.

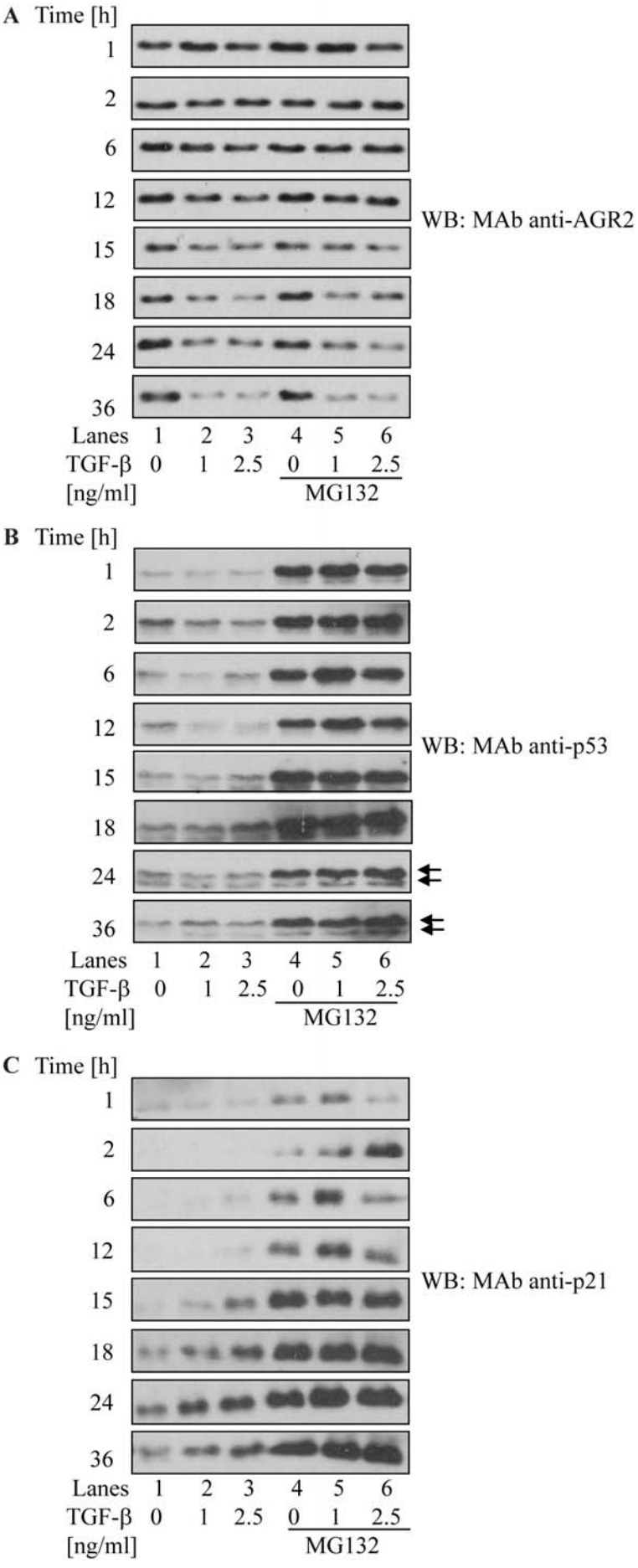
A Time [h]
1
2
6
12
15
18
24
36
WB: MAb anti-AGR2
Lanes 1 2 3 4 5 6
TGF-β 0 1 2.5 0 1 2.5
[ng/ml]
MG132
B Time [h]
1
2
6
12
15
18
24
36
WB: MAb anti-p53
Lanes 1 2 3 4 5 6
TGF-β 0 1 2.5 0 1 2.5
[ng/ml]
MG132
C Time [h]
1
2
6
12
15
18
24
36
WB: MAb anti-p21
Lanes 1 2 3 4 5 6
TGF-β 0 1 2.5 0 1 2.5
[ng/ml]
MG132

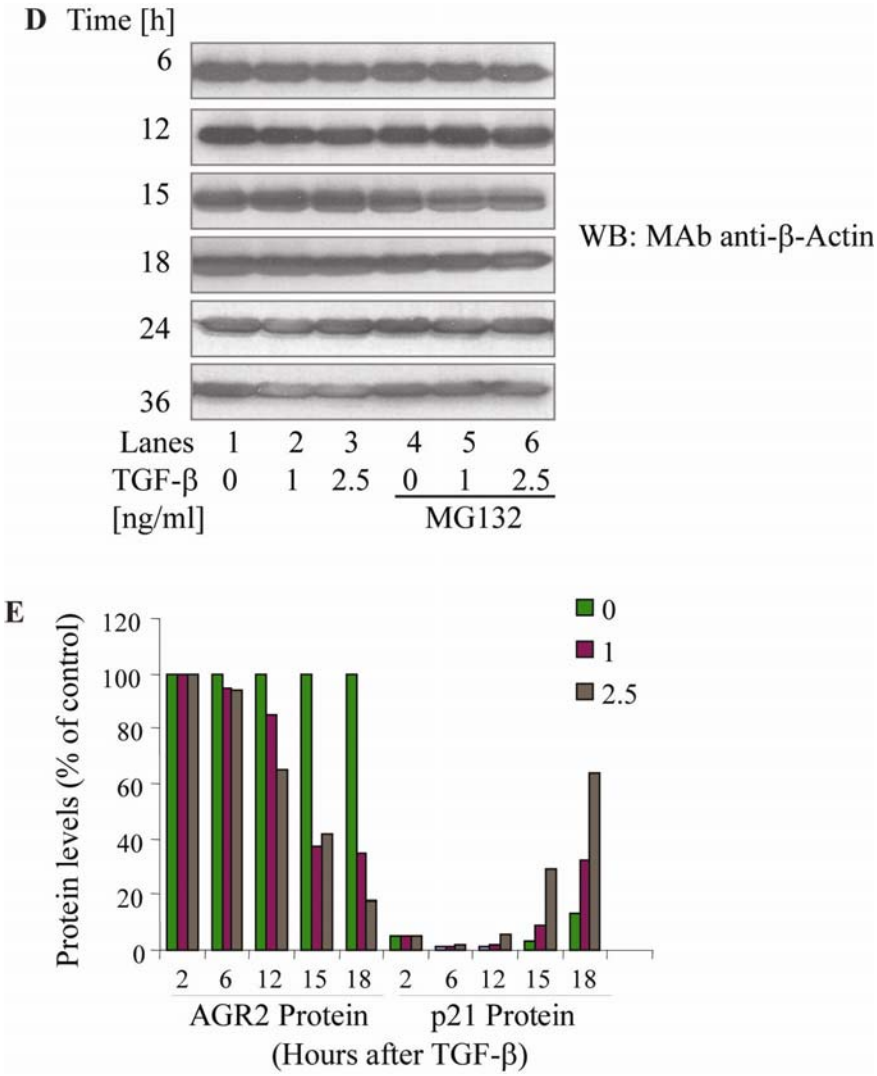

Figure 3.5 AGR2 downregulation in response to TGF-β is proteasome-independent. A549 cells were treated with or without TGF-β for the times as indicated. Cells were then incubated with the proteasomal inhibitor 10 μM MG132 or DMSO as indicated and subsequently lysed and the steady-state levels of **(A)** AGR2, **(B)** p53, **(C)** p21, **(D)** β-Actin proteins were measured by immunoblotting. **(E)**. Quantitation of the changes in AGR2 and p21 protein levels is plotted as a function of time after TGF-β treatment.

As such, we next examined whether transcription, protein synthesis or posttranslational events could explain AGR2 protein depletion by TGF-β. To this effect, mRNA was isolated at different time points from TGF-β-treated and untreated cells; and the amount of AGR2 mRNA was quantified using RT-PCR. Interestingly, the complete loss of AGR2 mRNA was observed at the 36 hours time point, which correlated with the full suppression of AGR2 protein and the maximal activation of the p53 pathway (Figure 3.6 A, lane 1 vs. 2-3). As AGR2 mRNA can be induced by withdrawal of serum [444] and as we also observed increased levels of AGR2 protein in cells cultured in serum free media (Figure 3.1), we examined TGF-β inhibition of AGR2 expression in serum-starved cells. Surprisingly, we observed a similar suppression after TGF-β treatment (Figure 3.6 A, lanes 2-3 vs. 5-6). These results indicate that AGR2 protein is negatively regulated at the level of gene expression by TGF-β. However, loss of AGR2 mRNA could also be a result of mRNA degradation. To rule out this possibility, we sought to establish whether TGF-β reduces AGR2 promoter activity. Specifically, a gene reporter assay was performed using the minimal AGR2 promoter (-1584- +96) fused to firefly luciferase (Figure 3.6 B). When A549 cells were transfected with the pGL3-basic-AGR2 reporter or pGL3-luc plasmid control, it was found that the basal reporter activity could be suppressed by the treatment of cells with TGF-β (Figure 3.6 C). Additionally, when A549 were cells transiently transfected with the pGL3-basic-AGR2 reporter or pGL3-luc plasmid control and treated with increasing amounts of the TGF-β, a dose-dependent decrease in the basal activity of the reporter was observed (Figure 3.6 D). Together, these results suggest that AGR2 promoter activity can be suppressed by the TGF-β signalling pathway.

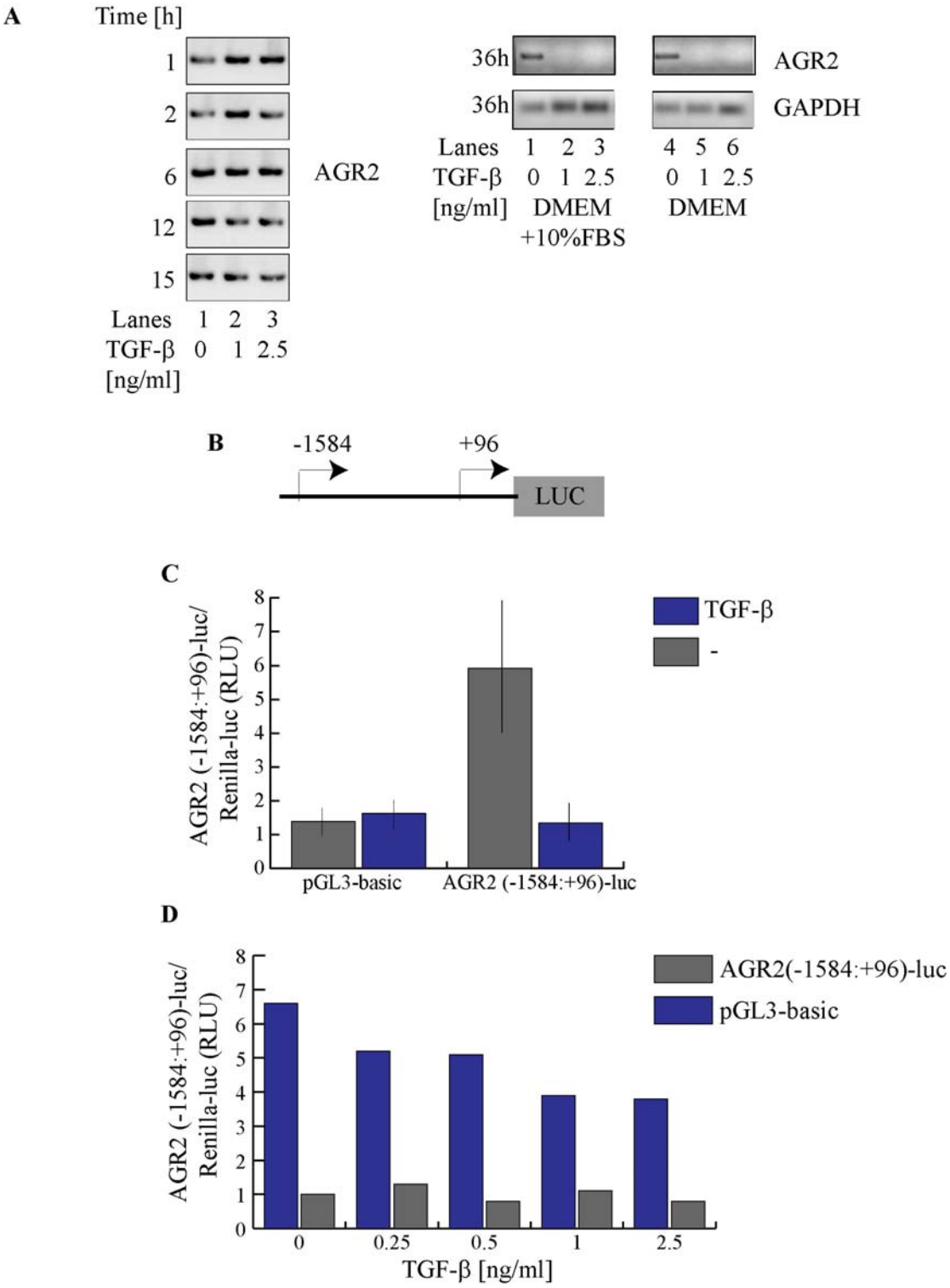

Figure 3.6 TGF-β represses the AGR2 promoter activity. (A) Effects of TGF-β on AGR2 mRNA levels. A549 cells were treated with or without TGF-β (2.5 ng/ml) for 36 hours followed by determination of AGR2 mRNA levels by RT-PCR using AGR2 specific primers. **(B) Summary of AGR2 promoter construct cloned for examining TGF-β responses.** A DNA construct containing AGR2 gene sequence, -1584 to +94, was cloned upstream of the firefly luciferase gene. **(C and D) Effects of TGF-β on AGR2-luc promoter activity. (C)** A549 cells were co-transfected with 140 ng of pGL3 basic-AGR2 and 150 ng of a separate construct that contained the promoter driving transcription from a Renilla luciferase gene. The cells were subsequently treated with 2.5 ng/ml of

TGF-β, and the activity of the AGR2 promoter was determined by luciferase assay. As a control, promoter activity of a Renilla promoter construct was also measured. Results are plotted as the normalized firefly luciferase activity over the value of Renilla luciferase and represent the mean of three independent experiments. The graph represents mean ± S.D. from three independent experiments. **(D)** A549 cells were co-transfected with 140 ng of pGL3 basic-AGR2 and 150 ng of a separate construct that contained the promoter driving transcription from a Renilla luciferase gene. The cells were subsequently treated with increasing amounts of TGF-β, and the activity of the AGR2 promoter was determined by luciferase assay. As a control, promoter activity of a Renilla promoter construct was also measured. Results are plotted as the normalized firefly luciferase activity over the value of Renilla luciferase.

Next, we were interested to determine which components of the TGF-β signalling pathway are involved in the apparent loss of AGR2 protein. TGF-β pathway has been extensively characterised and it is know that it propagates the signal through binding to the dimeric complex of TGFβRI and TGFβRII. The activated receptor recruits and phosphorylates SMAD2 and SMAD3. Subsequently, SMAD2/3 proteins heteromerize with SMAD4 and translocate as a complex to the nucleus [465, 467-469]. In the nucleus this complex is further built up by binding to co-repressors or co-activators, to form transcription complexes that regulate expression of a wide variety of target genes [484]. We decided to evaluate whether the canonical pathway could account for the observe suppression of AGR2 protein. As such, A549 cells were treated with siRNA to SMAD2, SMAD3, SMAD4, and SMAD7 and treated with TGF-β or left untreated. Depletion of none of the SMAD proteins led to changes in the p53 protein levels in TGF-β-untreated cells (Figure 3.7 B, lanes 1-5). Interestingly, it was found that cells treated with siRNA to SMAD4 and SMAD7 had reduced levels of AGR2 protein in the absence of TGF-β (Figure 3.7 A, lanes 4-5 vs. 1-3). Further, upon addition of TGF-β, AGR2 suppression was observed, as expected, however, the treatment of cells with siRNA to SMAD4 had the most striking influence on attenuating AGR2 protein suppression (Figure 3.7 A, lane 6 vs. 9, Figure 3.7 D, lane 1 vs. 3). As a control, the efficiency of siRNA-mediated depletion of SMAD4 protein was evaluated and indeed it was selectively depleted in cells transfected with SMAD4 but not SMAD2, SMAD3 or SMAD7 (Figure 3.7 E). Steady-state levels of p53 protein were also examined upon addition of TGF-β. It was found that TGF-β-mediated induction of p53 was independent of SMAD4 (Figure 3.7 B). In fact, it appeared that p53 protein levels were increased in cells treated with siRNA to SMAD4 compare to control or cells treated with siRNA to other SMAD proteins (Figure 3.7 B, lane 9 vs. 6-8 and 10). This data indicate a dominant role of SMAD4 in TGF-β-mediated suppression of AGR2.

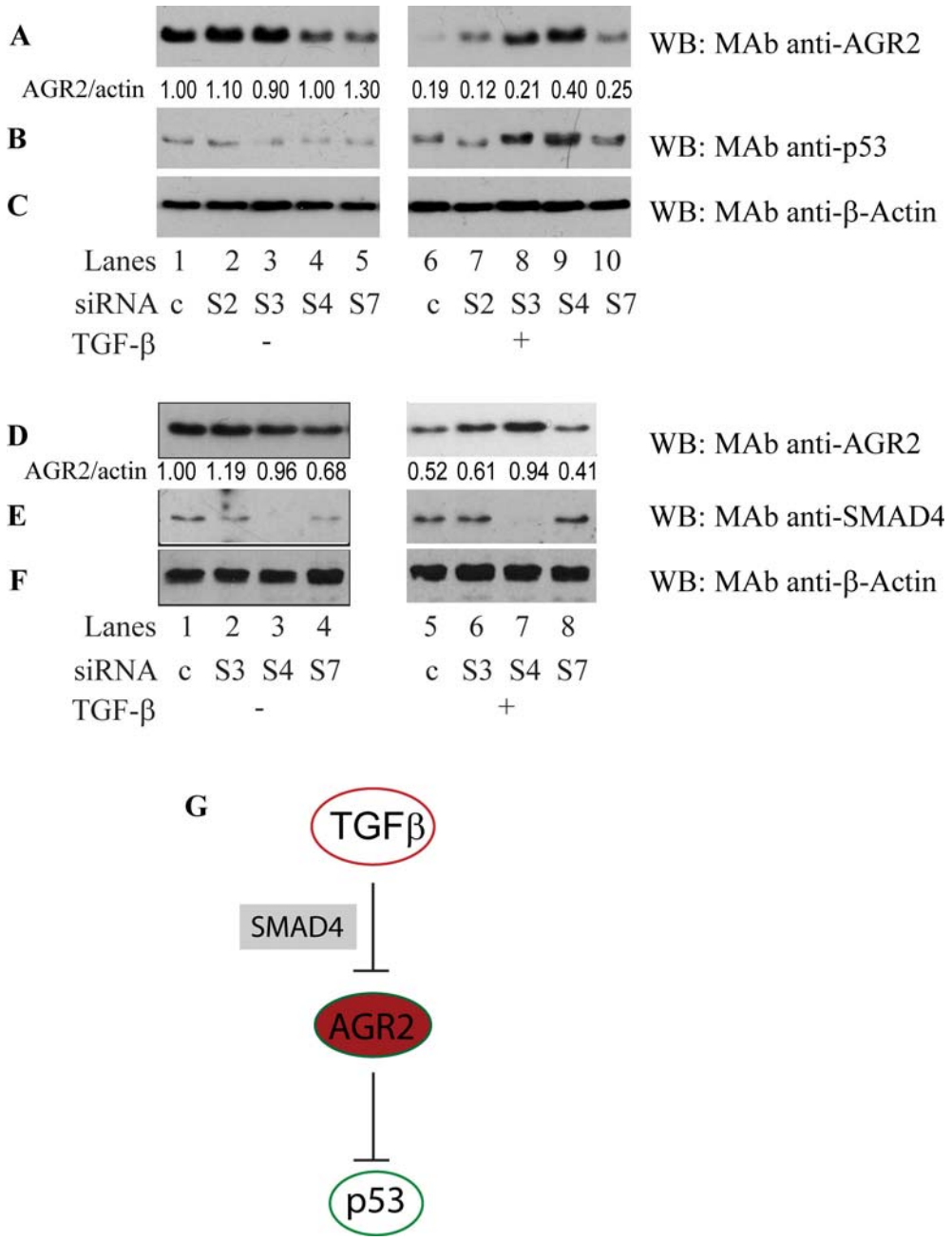

Figure 3.7 Reduction of SMAD4 using siRNA prevents AGR2 downregulation in TGF-β-treated cells. **(A-B)** A549 were transfected with 5 nM SMAD2 (S2), SMAD3 (S3), SMAD4 (S4), SMAD7 (S7) siRNA or with control siRNA and 48 hours post transfection cells were treated with 2.5 ng/ml TGF-β or carrier. After 48 hours, the cells were harvested and **(A)** AGR2, **(B)** p53 protein levels were examined by immunoblotting using specific monoclonal antibodies. **(C)** Cell lysates were immunoblotted using anti-β-Actin antibody as a loading control. **(D-F)** A549 were transfected with 5 nM S2, S3, S4, S7 siRNA or with control siRNA and 48 hours post transfection cells were treated with 2.5 ng/ml TGF-β or carrier, and harvested at different time points. **(D)** AGR2, **(E)** SMAD4 protein levels were examined by immunoblotting using specific monoclonal antibodies. **(F)** Cell lysates were immunoblotted using anti-β-Actin antibody as a loading control. **(G)** Schematic of TGF-β-mediated activation of p53 pathway through SMAD4-dependent inhibtion of AGR2 protein.

3.2.3 AGR2 protein degradation in response to TGF-β treatment.

The data above demonstrated that TGF-β canonical signalling pathway accounts, at least in part, for the observed loss of AGR2 protein upon TGF-β treatment. However, we were also interested to find the mechanism of AGR2 protein degradation, under the conditions when its gene expression was repressed. As mentioned above, this appeared to be independent of the proteasome, as addition of MG132 did not prevent degradation of AGR2 protein in cells treated with TGF-β (Figure 3.5 A). To further elaborate on the possibility that TGF-β could also downregulate AGR2 levels in post-transcriptional manner, we performed a half-life analysis. Specifically, A549 cells were treated with cycloheximide for various times in the presence and in the absence of TGF-β. It was found that AGR2 protein was a long-lived protein, as the addition of cycloheximide did not decrease its levels in the absence of TGF-β (Figure 3.8 A, lane 1 vs. 4). Additionally, *de novo* protein synthesis is not required for TGF-β signalling, as the AGR2 protein suppression occurred regardless of the presence of cycloheximide (Figure 3.8 A, lane 2-3 vs. 5-6). Interestingly, 2 hours post cycloheximide treatment; TGF-β-induced reduction of AGR2 protein was enhanced (Figure 3.8 A, lane 2-3 vs. 5-6). The increase in the turnover of AGR2 indicates that there must be a mechanism of degradation that could explain the loss of AGR2 protein.

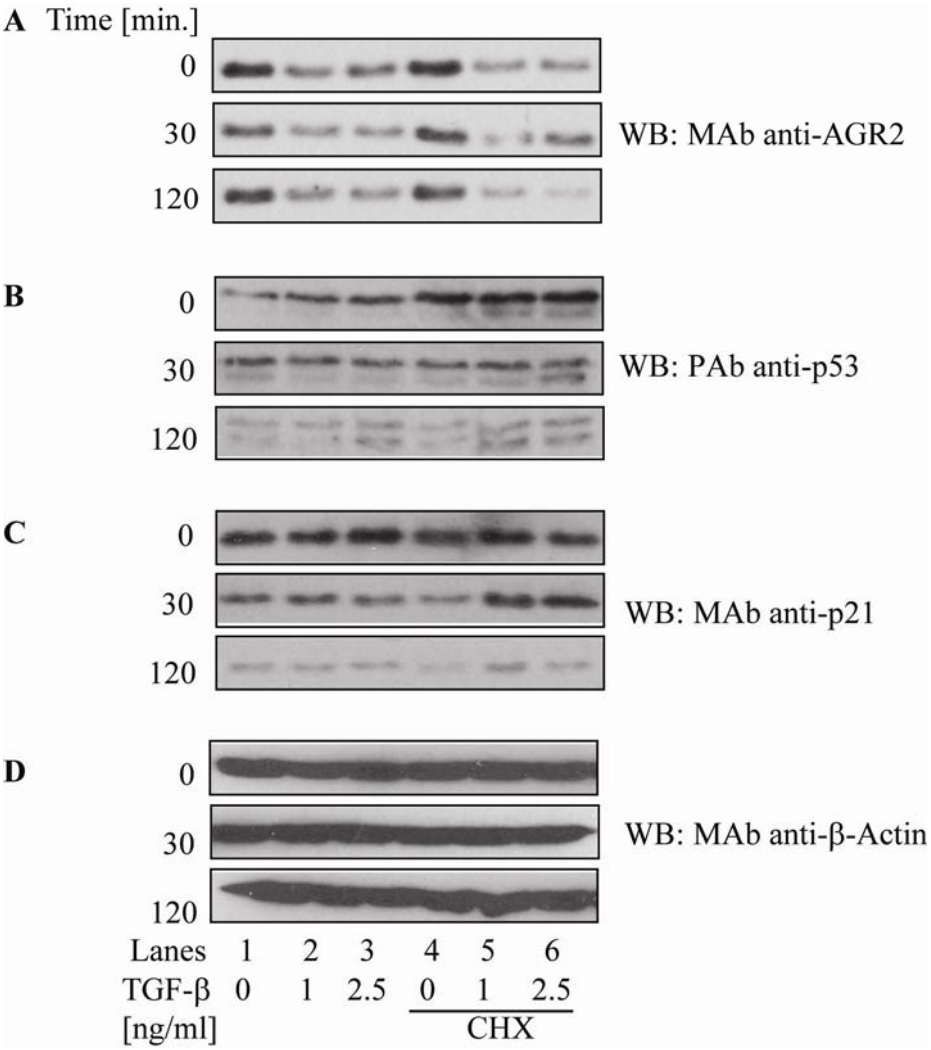

Figure 3.8 TGF-β does not require *de novo* protein synthesis to downregulate AGR2 protein. A549 cells were stimulated with different concentrations of TGF-β for 24 hours and then treated with 30 μg/ml cycloheximide (CHX) or water for the time indicated. **(A)** AGR2, **(B)** p53, **(C)** p21 protein and **(D)** β-actin levels were examined by immunoblotting using specific monoclonal antibodies.

In order to help us to define the degradation pathway for AGR2 protein upon TGF-β treatment, we decided to screen a range of protein kinase inhibitors. In detail, ATM kinase inhibitor KU55933, DNA-PK inhibitor NU7441 and MAPK inhibitor UO126 were used. Interestingly, inhibition of ATM kinase and to a lesser extent of DNA-PK kinase, but not MAPK kinase led to stabilization of AGR2 protein (Figure 3.9 A, lane 5 vs. 6-7). These data suggested that ATM kinase activity could be involved in the TGF-β-dependent degradation of AGR2. To rule out the possibility that the inhibition of ATM kinase was linked to AGR2 gene expression, AGR2 mRNA levels were measured in cells treated with TGF-β in the presence or absence of KU55933. It was found, that AGR2 mRNA levels remained low in TGF-β treated cells that were preincubated with ATM kinase inhibitor (Figure 3.9 E, lane 3 vs. 4). We concluded that ATM kinase pathway accounts for the degradation of AGR2 protein upon TGF-β treatment. In addition, ATM kinase seems not to be involved in SMAD4-dependent inhibition of AGR2 gene transcription.

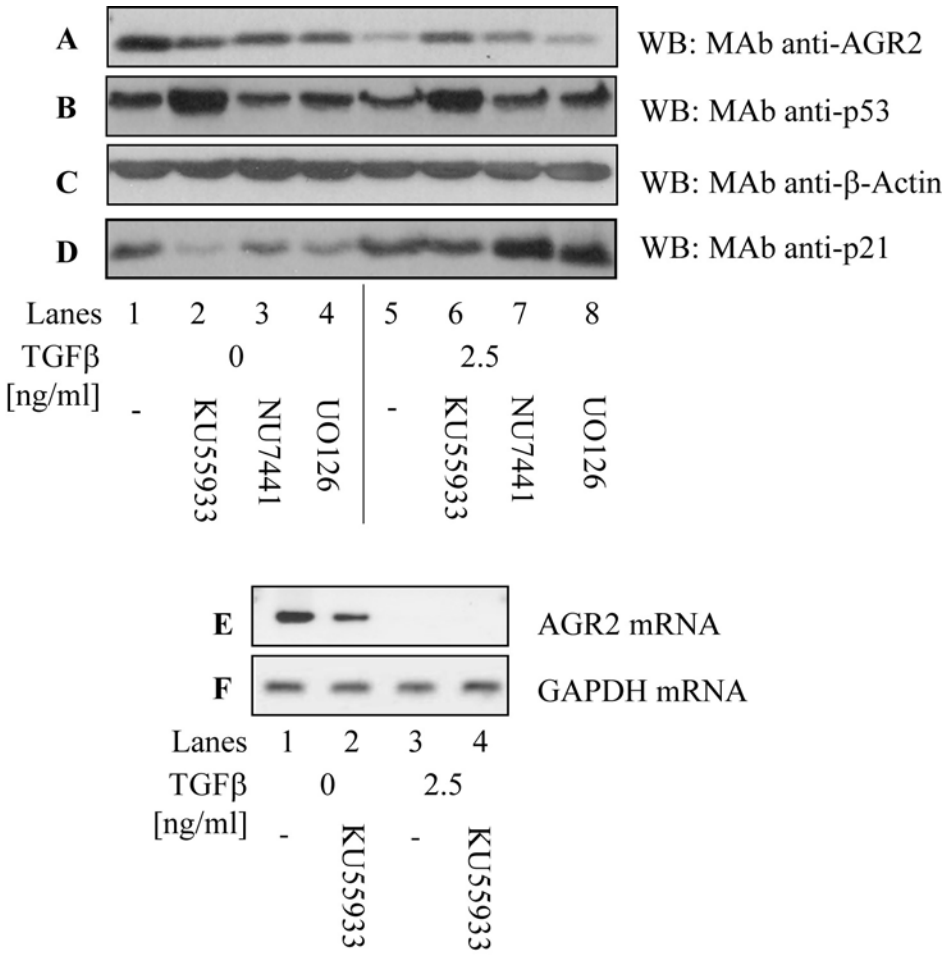

Figure 3.9 ATM-dependent TGF-β-triggered AGR2 degradation. A549 cells were pre-treated for 30 minutes with either: 10 μM ATM kinase inhibitor (KU55933), 1 μM DNA-PK kinase inhibitor (NU-7441), 10 μM MAPK kinase inhibitor UO126 or DMSO and then stimulated with 2.5 ng/ml of TGF-β for 24 hours. **(A)** AGR2, **(B)** p53, **(C)** p21, **(D)** β-actin protein levels were examined by immunoblotting using specific antibodies. **(E and F) ATM is not involved in TGF-β-dependent AGR2 gene suppression.** A549 cells were treated for 30 minutes with either 10 μM ATM kinase inhibitor (KU55933) or DMSO and then stimulated with or without TGF-β (2.5 ng/ml) for 36 hours followed by determination of **(E)** AGR2 mRNA and **(F)** GAPDH levels by RT-PCR using gene specific primers.

3.2.4 SNIP1 protein induces AGR2 protein degradation

In the light of the finding that AGR2 protein degradation is regulated by ATM kinase pathway, we were eager to investigate this mechanism in more detail. This appeared to be a daunting task, as a recent mass spectrometry screen identified about 900 targets of ATM and ATR kinases [493]. The functional importance of most of these phosphorylation events is not yet understood, and just a fraction of these had a well characterised role in assembly of protein complexes that are implicated in DNA damage response. Interestingly, when we analysed this catalogue of ATM/ATR substrates in detail, we found a few proteins that were linked to the TGF-β pathway. Therefore, we decided to look into these genes, reasoning that one of them could be an ATM target mediating degradation of AGR2 protein in response to TGF-β. The substrates found were IRS1, IRS2 and SNIP1 (Figure 3.10 A). In order to establish whether any of these genes was implicated in TGF-β-mediated degradation of AGR2, first A549 cells were transfected with siRNA to IRS1, IRS2 and SNIP1 and SMADs and treated with TGF-β, and the levels of AGR2 protein were monitored. Interestingly, only depletion of SNIP1 could increase AGR2 levels, indicating that this protein may be a downstream of ATM effector of AGR2 degradation (Figure 3.10B). In order to further characterise this ATM substrate, determine whether it is indeed involved in the regulation of AGR2 protein and confirm that these sites could be phoshorylated *in vivo*, we generated phospho-specific antibodies to the sites in SNIP1 that were found to be regulated by ATM, T169 and S202. Specifically, phospho-specific antibodies were generated to the peptides DRD[phospho]T_{169}QNL and GSE[phospho]S_{202}QEL using the protocol described before [494]. Indeed, we were able to confirm that at least one of the sites, T169, was targeted for phosphorylation *in vivo* (Figure 3.10 C and D). In addition, this modification was ATM-dependent, as cells treated with ATM inhibitor in the presence or absence of TGF-β had reduced levels of phospho-SNIP1 (Figure 3.10 C and D, lane 1 vs. 2 and 3 vs. 4). It is worth stressing, that we observed basal SNIP1 phosphorylation in untreated cells and this was not increased by TGF-β stimulation (Figure 3.10 C and D, lane 1). This indicates that ATM pathway for SNIP1

phosphorylation is DNA damage-independent and is presumably constitutively on to maintain steady-state levels of AGR2 protein.

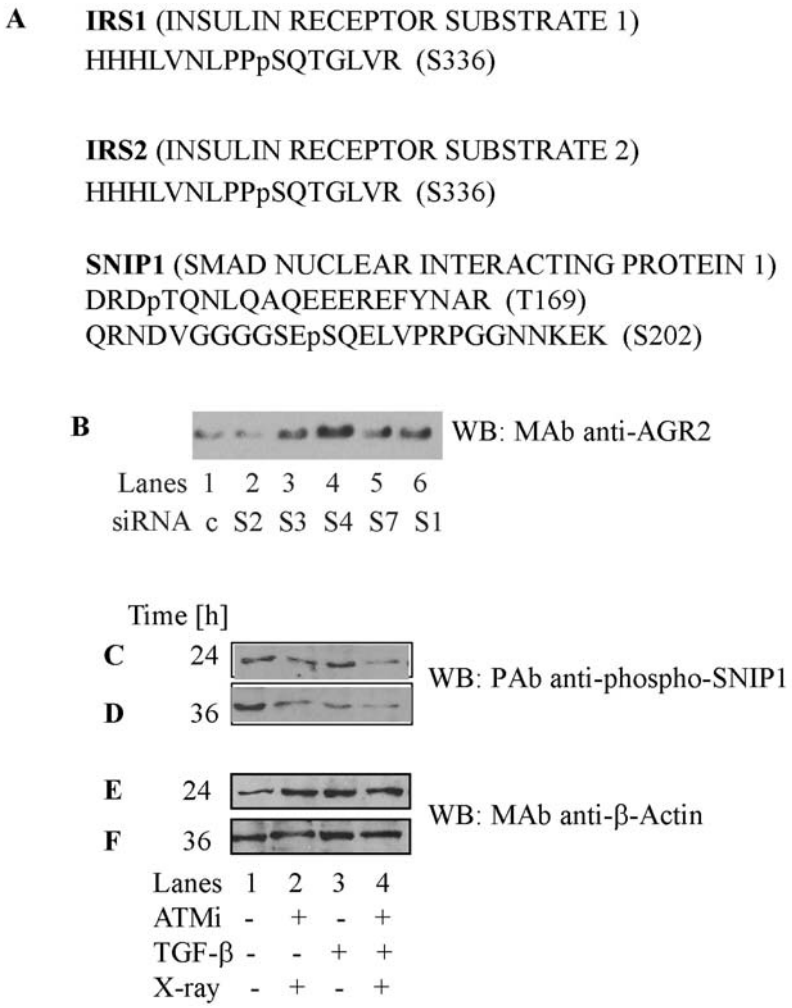

Figure 3.10 SNIP1 is phosphoryalted at Thr169 by ATM kinase *in vivo.* (A) The peptide sequence surrounding the previously identified ATM/R phosphorylation site in the SMAD interacting protein SNIP1. **(B)** A549 were transfected with 5 nM SMAD2 (S2), SMAD3 (S3), SMAD4 (S4), SMAD7 (S7), SNIP1 (S1) siRNA or with control siRNA and 48 hours post transfection cells were treated with 2.5 ng/ml TGF-β. After 48 hours, the cells were harvested and AGR2 protein levels were examined by immunoblotting using specific monoclonal antibodies. **(C-F)** A549 cells were pre-treated for 30 minutes with 10 μM KU55933 (ATMi) or DMSO and with or without 2.5 ng/ml of TGF-β prior to irradiation with 5Gy. After 24 hours the cells were lysed and the steady-state levels of **(C and D)** SNIP1 phospho-T169 protein levels were examined using phospho-specific antibodies generated to the peptide DRD[phospho]T169QNL. **(E and F)** β-actin protein levels were examined by immunoblotting using specific antibodies.

Next, we were interested to see if the transfection of SNIP1 was alone sufficient to stimulate the otherwise TGF-β-dependent AGR2 degradation and if yes, whether or not this was an ATM-dependent process. To this effect, increasing amounts of HA-tagged SNIP1 DNA were transfected into A549 cells. Interestingly, SNIP1 protein overexpression (Figure 3.11 A) resulted in a dose-dependent decrease in AGR2 steady-state levels (Figure 3.11 B). The decrease in AGR2 protein coincided with the stimulation of p53 and p21 protein levels (Figure 3.11 C and D). The activation of p53 pathway is also consistent with another report showing that SNIP1 can act as the activator of p53 protein [495]. In order to establish if SNIP1-triggered degradation of AGR2 protein was indeed dependent on ATM kinase we overproduced SNIP1 protein in cells pre-treated with ATM kinase inhibitor (Figure 3.11 F). We no longer observed AGR2 protein reduction upon inhibition of ATM kinase, revealing that ATM-dependence to SNIP1-induced degradation of AGR2 protein (Figure 3.11 G). Having shown the role of ATM-SNIP1 pathway in AGR2 protein reduction, we wanted to evaluate the effects of mutation of T169 on AGR2 steady-state levels. To this effect, SNIP1 T169D and T169A mutants were created, with the former acting as a phosphomimetic, and the latter representing the unphosphorylated form of SNIP1. In addition, SNIP1 S202D and T202A mutants were also generated, because despite the fact that we failed to produce phospho-specific antibodies against this site, we could not rule out the possibility that modification of these residues was involved in ATM-dependent regulation of AGR2. It was found that SNIP1 T169D retained the ability to promote AGR2 protein degradation. Surprisingly, SNIP1 T169A not only could not induce loss of AGR2 protein, but acted as a dominant negative protein by increasing steady-state levels of AGR2 (Figure 3.11 I). The basal levels of SNIP1 T169D and T169A were compared, to establish whether differential expression could account for the apparent difference in the activities of these mutants. Despite the fact that the basal levels of SNIP1 T169D were lower than these of SNIP1 T169A, only the former could efficiently induce reduction of AGR2 protein (Figure 3.11 J). Surprisingly, SNIP1 S202D caused increase in levels of AGR2 protein compare to SNIP1 S202A, indicating that phosphorylation of this site may actually be involved in the positive regulation of AGR2 protein (Figure 3.11 I). Collectively, these results show that the

overexpression of SNIP1 alone and SNIP1 T169D can reconstitute the ATM and TGF-β induced degradation of AGR2 protein in A549 cells.

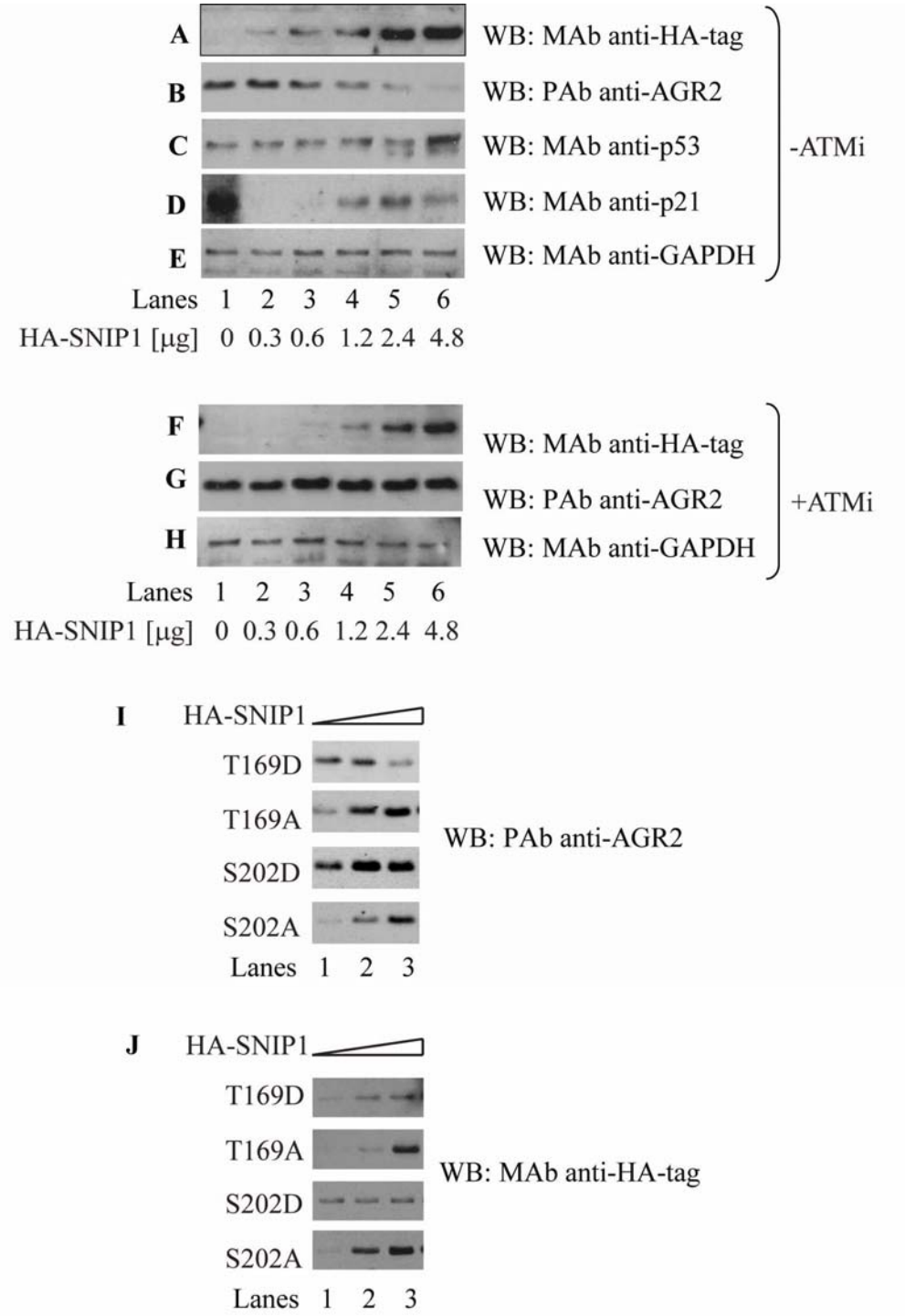

Figure 3.11 Effects of SNIP1 transfection on AGR2 protein levels. (A-H) SNIP1 gene transfection de-stabilizes AGR2 protein in an ATM-dependent manner. A549 cells were transfected with increasing amount of wild type HA-tagged SNIP1 expression plasmid in **(A-E)** the absence of 10 µM KU55933 (ATMi) **(F-H)** or in the presence of the 10 µM ATMi. After 24 hours, the cells were harvested and **(A and F)** HA-tagged SNIP1, **(B and G)** AGR2, **(C)** p53, **(D)** p21 and **(E and H)** GAPDH protein levels were examined by immunoblotting using specific antibodies. **(I and J) Mutation of ATM phospho sites in SNIP1 protein affect AGR2 protein levels.** A549 cells were transfected with increasing amount of phospho-mimetic mutants HA-tagged SNIP1-T169D or HA-tagged SNIP1-S202D, or unphosphorylated counterparts (HA-tagged SNIP1-T169A or HA-tagged SNIP1-S202A). After 24 hours, the cells were harvested and **(I)** AGR2 and **(J)** HA-tagged SNIP1 protein levels were examined by immunoblotting using specific antibodies.

3.2.5 AGR2 protein is degraded via lysosomal pathway.

Despite the fact that TGF-β-induced loss of AGR2 protein is proteasome-independent, we reasoned that there has to be some other mechanism that could provide the efficient removal of this protein. As the cellular pathways for protein degradation involve not only the ubiquitin-linked proteasomal degradation, but also autophagic-lysozomal pathway (reviewed in [496-498]), we set out to determine whether the latter played a role in TGF-β induced degradation of AGR2 protein. To this effect, we evaluated a time course of AGR2 protein reduction in the presence or absence of chloroquine or the autophagy inhibitor 3-methyladenine (3-MA), upon TGF-β treatment. There was no significant difference in the AGR2 protein levels between drug-treated and untreated cells at the time points between 1 hour to 18 hours (data not shown). Interestingly, incubation of cells with chloroquine for 24 hours to 36 hours prevented degradation of AGR2 protein in the cells treated with TGF-β, whereas only minimal protection was observed in the cells treated with 3-MA (Figure 3.12 A). In addition, chloroquine treatment resulted in the stabilisation of p53 protein, which was in agreement with previous reports (Figure 3.12 B). A chloroquine-dependent increase in AGR2 protein levels indicated that AGR2 is degraded via lysosomal pathway. To further examine the lysosomal pathway of AGR2 protein degradation more specific inhibitors of lysosomal functions were used. Specifically, cells were treated with general lysozomal hydrolase inhibitors, including pepstatin A and E64D, and Na+/H+ ionophore monensin A, which increases lysosomal pH preventing activation of the lysosomal enzymes. As a control, cells were also treated with the ATM inhibitor or chloroquine. However, only chloroquine and ATM inhibitor, but not pepstatin A, E64D or monensin A increased AGR2 protein in the cells treated with TGF-β (Figure 3.12 E). Interestingly, the basal levels of AGR2 protein increased upon treatment with pepstatin A and E64D, indicating that in unstressed cells the slow turn-over of AGR2 protein is provided via the lysosomal degradation pathway (Figure 3.12 D).

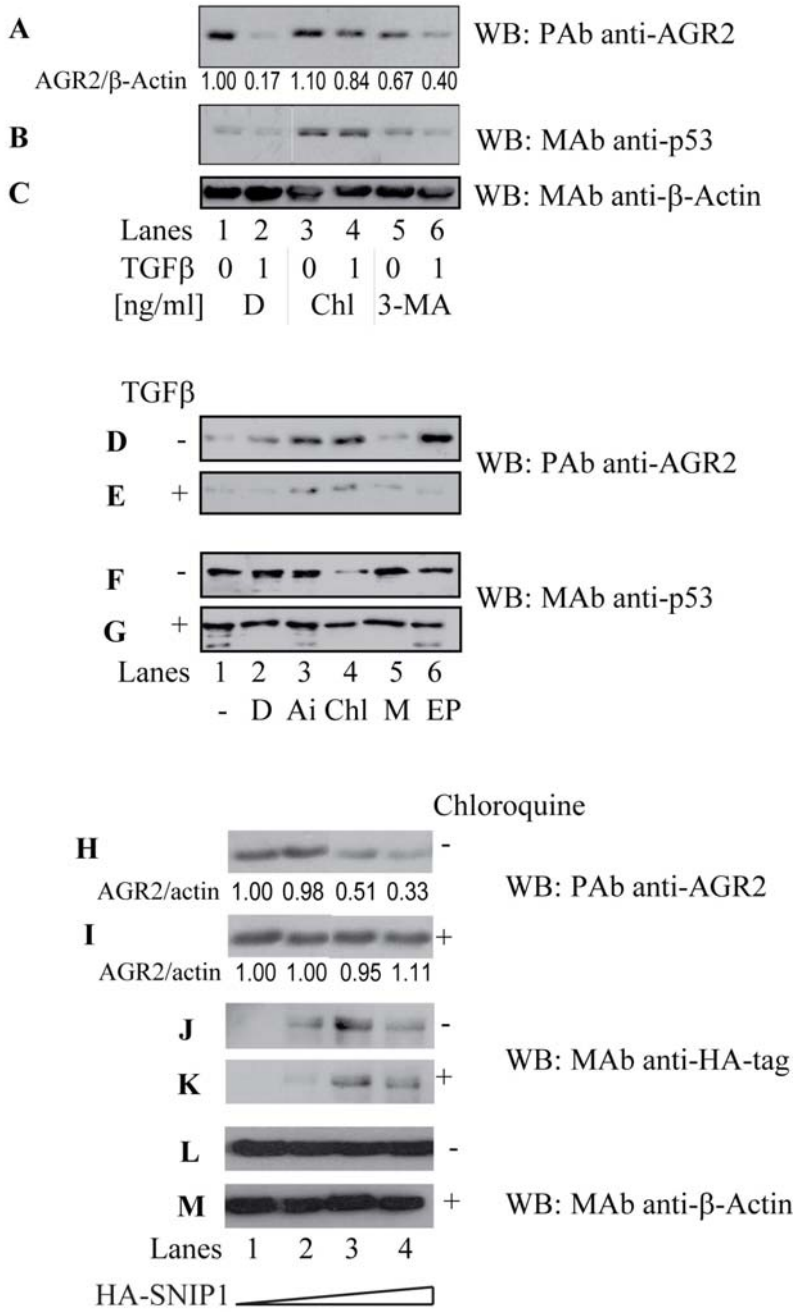

Figure 3.12 AGR2 protein is degraded via lysosomal pathway. (A-C) A549 were treated with the lysozomal inhibitor chloroquine (Chl) or the autophagy inhibitor 3-methyladenine (3-MA) or DMSO control **(D)** in (lanes 2, 4 and 6) the presence or (lanes 1, 3 and 5) absence of 1 ng/ml of TGF-β. After 36 hours cells were harvested and **(A)** AGR2, **(B)** p53 and **(C)** β-actin protein levels were examined by immunoblotting using specific antibodies. **(D-G)** A549 were treated with the lysozomal inhibitors Chloroquine (Chl), Pepstatin D and E64D (EP), Monensin A (M) or the ATMi, or DMSO control **(D)** in **(E and G)** the presence or **(D and F)** absence of 1 ng/ml of TGF-β. After 36 hours cells were harvested and **(D and E)** AGR2 and **(F and G)** p53 protein levels were examined by immunoblotting using specific antibodies. **(H-M)** A549 cells were transfected with increasing amount of wild type HA-tagged SNIP1 and treated without **(H, J, L)** or with 100 μM chloroquine **(I, K, M)**. After 36 hours cells were harvested and **(H and I)** AGR2 and **(J and K)** HA-tagged SNIP1, and **(L and M)** β-actin protein levels were examined by immunoblotting using specific antibodies. The data are representative of three independent experiments and changes in the levels of AGR2 as a ratio of protein/β-actin were quantified using Image J software.

As the overexpression of SNIP1 alone could reconstitute the ATM and TGF-β induced degradation of AGR2 protein in A549 cells, we were interested to see whether this was due to enhanced AGR2 lysosomal degradation. Hence, cells were transfected with increasing amounts of SNIP1 and treated with or without chloroquine. As it was seen before, SNIP1 overexpression resulted in depletion of AGR2 protein (Figure 3.12 H). Interestingly, chloroquine treatment could prevent AGR2 degradation (Figure 3.12 I) and this was not through decreased levels of SNIP1 protein (Figure 3.12 J and K). This data indicates that indeed SNIP1 protein triggers the lysosomal degradation pathway for AGR2.

Subsequently, we sought to determine whether AGR2 protein localised to lysosomes upon TGF-β treatment. To this end, we analysed AGR2 cellular distribution using AGR2-specific antibody in cells treated with or without TGF-β. We found that AGR2 protein localised mainly to ER-compartment and to nucleus, and the decreased levels of AGR2 protein were observed upon addition of TGF-β. Chloroquine treatment intensified staining for AGR2 protein, confirming that this drug interfered with the loss of AGR2 protein. In addition, AGR2 localised to punctuate foci that were adjacent to vesicles positive for LAMP-1, a known marker for lysosomes and late endosomes (Figure 3.13 A).

Furthermore, autophagy-related genes (ATG) proteins have been shown to be involved in the formation of the autophagosome- compartment that delivers a cargo to the lysosome. As such we decided to investigate whether or not depletion of ATG5, ATG10 or ATG12 using specific siRNA could prevent AGR2 degradation. Indeed, increased levels of AGR2 protein were observed when ATG specific siRNAs were used. Furthermore, the stabilisation of AGR2 protein was observed in both TGF-β treated and un-treated cells, which indicates that basal AGR2 turnover occurs in these cells (Figure 3.13 B).

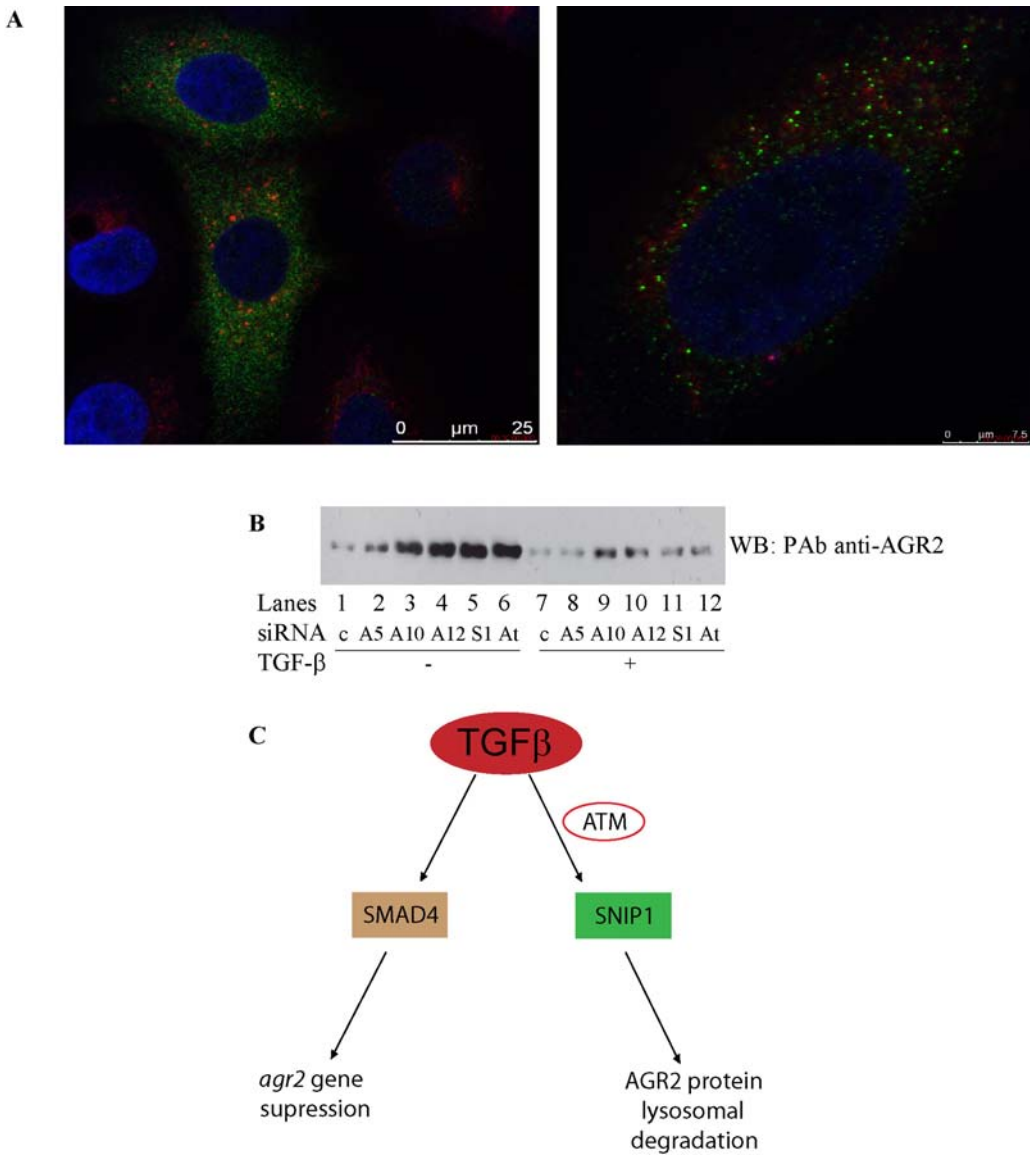

Figure 3.13 (A) A549 were treated with 2.5 ng/ml TGF- β and 24 hours later stained with AGR2 polyclonal Antibody (Green) and LAMP-1 specific antibody (Red) (Data courtesy of Dr Nicky MacLaine) **(B)** A549 were transfected with 5 nM ATG5 (A5), ATG10 (A10), ATG12 (A12), SNIP1 (S1) and ATM (At) siRNA or with control siRNA (c) and 48 hours post transfection cells were treated with 2.5 ng/ml TGF-β or carrier. After 48 hours, the cells were harvested and AGR2 levels were examined by immunoblotting using specific monoclonal antibodies. **(C)** Model of TGF-β suppression of AGR2 protein. Data in this study highlight two distinct pathways that play a role in the AGR2 suppression by TGF-β. First, TGF-β-mediated suppression of AGR2 protein occurs by suppression of AGR2 gene expression leading to AGR2 protein depletion which is SMAD4-dependent and p53-independent. Second, TGF-β triggers a ATM/SNIP1-dependent AGR2 protein lysosomal degradation.

3.3 Discussion

The p53 protein is a transcription factor that has a well established role in tumour suppression [499]. In cells containing functional p53, it is activated in response to a variety of stresses including DNA damage [500-502], hypoxia [503], inappropriate cell proliferation, telomere erosion [504], type-I interferons [505], viral infection [505, 506], metabolic stress [507, 508] and others. Once activated, p53 readily modulates the expression of number of target genes, whose products regulate diverse processes such as cell cycle arrest, senescence, apoptosis and others [509]. Thus, p53 activation contributes to tumour suppression, whereas attenuation of its activity favours selection of cell variants with increased tumourogenic potential. Accordingly, large proportion of human cancers bears mutations in the p53 gene. Common p53 mutations give rise to proteins that are inactive as transcription factors for genes that normally are induced by wild type p53 to maintain homeostasis. In addition, variants of mutant p53 can emerge that possess new activities, so called gain-of-function properties that can further contribute to tumourigenesis. Nevertheless, there are a number of wild type p53 protein carrying tumours, which developed indirect mechanisms to disrupt p53 pathway, mainly by promoting p53 protein degradation, blocking p53-activating kinases or triggering enzymes that block p53-dependent transcription. In these tumours, strategies to reactivate wild type p53 may have therapeutic benefits. For example, it was shown that disruption of p53-MDM2 complex using small molecules could restore p53 functions and induce apoptosis [335]. Discovering and characterising novel inhibitors of p53 in the wild type p53 context may increase chances of finding compounds with significant antitumour effects [510]. For example, recently performed proteomic screen revealed a novel p53-inhibitory pathway involving AGR2 protein [437]. However, the signalling inputs that coordinate AGR2- p53 pathway have not been studied yet and in this study we sought to establish the effects of different physiological factors on AGR2 and p53 protein.

In search for regulators of AGR2, we found that TGF-β acted as a potent inhibitor of AGR2. We showed that TGF-β signalling suppressed AGR2

transcription in SMAD4-dependent manner and triggered protein degradation by engaging ATM- SNIP1 autophagic-lysosomal degradation pathway.

This and other studies reported that AGR2 protein could inhibit p53 pathway. Firstly, it was observed that ectopically expressed AGR2 could inhibit DNA damage-triggered activation of p53 [437]. Additionally, AGR2 overexpression resulted in the increased shuffling of p53 protein out of the nucleus after UV irradiation [420] and targeting AGR2 protein with AGR2-specifc aptamer [424] could further stimulate it [425]. In keeping with p53-inhibitory role of AGR2 protein, we observed that AGR2 depletion using siRNA enhanced the stimulatory effect of TGF-β or radiation treatment on p53 (Figure 3.2). Moreover, TGF-β-dependent loss of AGR2 protein resulted in the stabilization of p53 protein and its target gene p21. As AGR2 depletion potentiated p53 response to irradiation and/or TGF-β and given that AGR2 appears to inhibit p53 to a greater extent in DNA damaged cells, we could speculate that AGR2-positive, wild type p53-containing tumours could be resistant to otherwise effective p53-activating DNA damaging agents.

The loss of AGR2 protein in response to TGF-β highlights the tumour suppressive function of this cytokine. Here, we found that transcriptional inhibition is likely to be mediated by SMAD pathway, as SMAD4 depletion prevented TGF-β-mediated downregulation of AGR2 (Figure 3.7). SMAD proteins have been shown to interact with a range of repressors; however these interactions are not usually implicated in the active repression of TGF-β genes, but are thought to repress SMAD-mediated transactivation [511]. Further, there is relatively little known about the mechanisms of TGF-β-SMAD-dependent gene repression. For instance, there is some evidence for the association of histone deacetylases with SMADs [512, 513]. Unfortunately, at the moment we do not know what factors, other than SMAD4, are involved in AGR2 gene suppression. Additional studies, for example using HDAC inhibitors as well as chromatin immunoprecipitation (CHIP) on AGR2 promoter will be required to define factors that are involved in TGF-β-mediated inhibition of AGR2 transcription.

AGR2 protein was shown to be induced by estrogens and its promoter contains four putative estrogen responsive elements [407, 514]. Unexpectedly, we observed higher levels of AGR2 protein in A549 lung cancer cells upon serum starvation (Figure 3.1). These data indicated that AGR2 expression can be provided

by a hormone-independent pathway. In other cell lines, for example the MCF7 breast cancer cell line, AGR2 expression is dependent upon estrogen [436]. These data clearly highlight distinct pro-oncogenic signalling pathways that regulate AGR2 production. The question that arises is whether TGF-β could integrate into both estrogen-dependent and estrogen-independent AGR2-regulatory pathways. Interestingly, links between TGF-β and ER signalling have been observed before. Specifically, these studies shown that SMAD4 was implicated in TGF-β-mediated transrepression of ERα activity [515, 516], SMAD3 acted as its coactivator [517], whereas SMAD4/3 complex had an inhibitory effect [515]. This implies that TGF-β can potentially regulate AGR2 expression in other cell systems. Further, as TGF-β has been shown to regulate ERα activity in either a positive or negative manner, it is plausible that TGF-β could switch from a repressor to an activator of AGR2 protein depending on the cellular context. Interestingly, SMAD4 mutations are observed at high frequency in human tumours [518-520]. Particularly, mutations of it were observed in breast carcinoma [521, 522] and it was found that SMAD4 protein was reduced in Barrett's [523]. It is likely that deficiency of functional SMAD4 could explain high levels of AGR2 protein in these tissues. Surprisingly, in this study SMAD4 depletion downregulated AGR2 in the absence of TGF-β signal. One possible explanation is that SMAD4 may recruit different kind of cofactors, histone acetylases or histone deacetylases, depending on the TGF-β signalling status. Indeed, SMAD4 was shown to activate expression of c-myc oncogene in the absence of TGF-β signalling, whereas it cooperated with Smad3 to reduce expression of c-myc in response to TGF-β [524].

The physiological outcome of TGF-β mediated suppression of AGR2 is, as yet, unknown. TGF-β signalling plays a pivotal role in the control of tumour initiation, progression and metastasis, cell growth and proliferation, apoptosis, differentiation and migration; as well as in a broad range of both cancer cell-cancer cell and host-tumour interactions. Another layer of complexity comes from the fact that TGF-β has a biphasic role in cancer progression, with tumour suppressive effects in early stages and oncogenic outcomes in later phases of cancerogenesis [525]. In some studies it was found that the Barrett's-derived esophageal adenocarcinoma cells exhibit

reduced responsiveness to TGF-β [526] and downregulation and alterations in SMAD4 protein could potentially account for the loss of antiproliferative response to TGF-β in this tissue [523]. However, it remains unclear whether or not AGR2 overexpression in Barrett's is indeed due to decreased responsiveness to TGF-β. In fact some studies reported on the overexpression rather than downregulation of TGF-β signalling in this tissue [527]. Given that TGF-β can exert both tumour-suppressive and tumour-promoting activities, we can hypothesise that in TGF-β-responsive AGR2-overexpressing Barrett's, TGF-β acts as an autocrine activator of oncogenic pathways that maintain high levels of AGR2. Future research of the Barrett's model might explore the relationship between AGR2 and TGF-β pathways in more detail. Further, the TGF-β-AGR2 pathway should be studied in relation to the p53 status in oesophageal disease. However one would expect the physiological outcomes of TGF-β-SMAD pathway to be tissue and disease-specific.

One well established outcome of TGF-β signalling is epithelial to mesenchymal transition (EMT) (reviewed in [528]). EMT process leads to major changes in cellular phenotype. Specifically, during EMT cells acquire mesenchymal morphology, lose cell-cell junction proteins and can migrate and invade through extracellular matrix (ECM) [529]. EMT has a critical role in the embryonic development and in response to tissue injury; however, the significance of EMT in cancer progression and fibrosis has also been highlighted. As epithelial cancer cells undergo EMT, they become more invasive and begin dissemination from the primary location to distant organ sites. One of the main hallmarks of epithelial to mesenchymal transition is loss of E-cadherin [530]. Considering that TGF-β treatment was shown to downregulate E-cadherin and induce EMT in A549 cells [531], it would be interesting to evaluate whether AGR2 loss is accompanied by EMT-associated changes. If TGF-β indeed triggers EMT, it would be the first evidence that AGR2 repression is required or correlates with EMT. At first, this may appear contradictory to the previously found role of AGR2 in metastasis [427]. However, the new concepts on cancer progression have been recently emerging that could explain AGR2 disappearance during EMT. Apparently, EMT is critical only in the initial phases of cancer when ability of individual cells to migrate is essential [532]. However, having reached their destination, migratory cells have to be able to

proliferate and form epithelial growths in these distal loci. It has been proposed that this process requires re-differentiation, namely mesenchymal to epithelial transition (MET) [528, 533] and was supported by observations that many metastatic carcinomas follow this route [534, 535]. In keeping with this, re-expression of E-cadherin was observed in some prostate cancer metastases to the liver [535]. Similarly, considering that AGR2 is regarded as a growth-promoting factor and as it stimulates attachment, it is plausible that its repression by TGF-β could be relieved once distant sites are populated.

In search of the mechanism that could account for the loss of AGR2 protein upon TGF-β treatment, we found that its turnover was regulated by lysosomal pathway, as we were able to prevent TGF-β mediated degradation using chloroquine. Further, the general lysosomal hydrolase inhibitors, namely Pepstatin A and E64D increased basal levels of AGR2 protein. Interestingly, TGF-β induced lysosomal degradation is not restricted to AGR2 protein as it was also reported for E-cadherin [536]. Janda and colleagues showed that TGF-β/MAPK pathway could induce E-cadherin localization to LAMP-1 positive structures, a marker for lysosomes. When we investigated AGR2 localization upon TGF-β treatment, we found that AGR2 protein colocalized to endoplasmic reticulum punctuate foci adjacent to lysosomal vesicles. AGR2-containting foci did not appear to overlap with LAMP-1 foci, however, localization "next to" lysosomes suggests that AGR2 is indeed degraded in these vesicles or in the compartments in close association with lysosomes. Similar localization was observed for cIAP1-TRAF2 complex [537] and was regarded as evidence for lysosomal degradation. Furthermore, a subunit of the T-cell antigen receptor that is targeted by this pathway could be localised to foci near lysosomal compartments [538]. The lysosomal degradation of intracellular proteins is often linked to macroautophagy (autophagy), a process that involves ATG proteins-dependent formation of autophagosomes. These vesicles deliver cargo to be degraded to lysosomes. The autophagic pathway is thought to play a pivotal role in the degradation of long-lived proteins as well as organelles [539]. A recent study has also highlighted that TGF-β can induce autophagy in cancer cell lines mainly due to the increased expression of some ATG proteins [540, 541]. Although 3-MA can inhibit autophagy [542], in our current study this inhibitor was not able to suppress

AGR2 protein degradation after TGF-β treatment to the same extent as chloroquine did (Figure 3.12). However, as depletion of the components of autophagic pathway, namely ATG5, ATG10 and ATG12 could induce levels of AGR2 protein, it is likely that lysosomal degradation of AGR2 in A549 cells follows the ATG5/7/DAPK autophagic pathway activation. Alternatively, as AGR2 resides in endoplasmic reticulum and it has an N-terminal leader sequence it is also possible that TGF-β induces AGR2 secretion. Further studies, including establishing the levels of AGR2 in the media from TGF-β treated cells, will be required to determine whether or not AGR2 is indeed secreted.

As mentioned, loss of E-cadherin has been associated with development of epithelial-derived tumour types [543] and with epithelial to mesenchymal transition in mammalian cell systems [530]. Interestingly a distinct set of enzymes is activated downstream of TGF-β and accounts for the degradation of E-cadherin and AGR2 proteins. Specifically, Rab 5/7 GTPases are involved in degradation of E-cadherin, whereas ATM kinase triggers degradation of AGR2, as defined by using KU55933 or ATM depletion by ATM specific siRNA. The activation of a variety of kinases by TGF-β signalling is not surprising since besides the canonical SMAD pathway, TGF-β has been shown to propagate signalling and converge with other pathways. For example, MAPKs [544], including ERKs, p38 and JNKs; NF-kB, Phosphoinositide 3 (PI3)-kinase and AKT kinase pathways can contribute to TGF-β response [305, 545]. TGF-β induces activation of Ras, RhoB and RhoA, TAK1 and protein phosphatase 2A, which generally results in the activation of the MAPK pathway and the suppression of S6 kinase [546]. In addition, ATM activation in response to genotoxic stress has been shown to be perturbed by loss of TGF-β signalling as it decreased ATM's autophosphorylation and compromised phosphorylation of p53 [547]. Our results reveal that ATM kinase is indeed activated upon TGF-β treatment and enhances p53 activation by switching on lysosomal degradation of AGR2 protein. The ATM kinase has been implicated in the autophagic pathway before. The most recent study showed that ATM kinase inhibitor, combined with DNA-damaging agent treatment, diminished autophagy [548]. The opposite was observed, however, when ATM was depleted using ATM specific siRNA [548]. In another study it was found that ATM represses the kinase

mTOR in the mTOR complex 1 (mTORC1) and induces autophagy in response to reactive oxygen species. Furthermore ATM knockout prevented the induction of autophagy in response to this stress [549].

It is somewhat contradtictory that chloroquine treatment results in increase in both AGR2 and p53 levels. p53 induction upon chloroquine treatment has been seen before and was reported to be ATM-dependent [380, 550]. One study has shown that chloroquine activates ATM and p53-dependent pathways in Myc-dependent B-cell models and impairs Myc-induced lymphogenesis in a transgenic mouse model of human Burkitt lymphoma [551-553]. We observed that chloroquine could inhibit the ability of SNIP1 to stimulate AGR2 protein degradation which indicates that this drug can act downstream of ATM function.

We found that ATM targets SNIP1 protein and SNIP1 overexpression could trigger ATM-dependent degradation of AGR2 protein in the absence of TGF-β signal. As SNIP1 T169D overexpression by itself could recapitulate the effects of TGF-β, we concluded that this protein mediates TGF-β induced lysosomal degradation of AGR2. SNIP1 is a 396 amino acid protein and was isolated in search for SMAD-binding partners. It contains a nuclear localisation sequence (NLS), coiled coil motif and a forkhead-associated (FHA) domain [480]. It was originally termed a transcriptional suppressor of TGF-β signalling and was shown to interact with SMAD4 protein and compete with SMAD4 for p300/CBP binding [480]. Later, SNIP1-inhibitory activity was confirmed for NF-κB-dependent transcription, also through a mechanism involving competition with RelA/p65 subunit for binding to CBP/p300 [554]. In this study we showed that SNIP1 downregulates AGR2 protein and it is dependent upon ATM kinase activity, because the addition of the specific chemical inhibitor of ATM, could rescue AGR2 protein levels in SNIP1-transfected cells. SNIP1 phosphorylation is not a new concept, and was previously suggested by Roche and colleagues [495]. It was speculated that the combination of SNIP1's modification and its cellular context could determine the nature of SNIP1 mediated response. Later, the presence of two different ATM phosphorylation sites was revealed by a proteomic screen [493]. Here, we established that SNIP1 phosphorylation of T169 is ATM-dependent and could account for AGR2 degradation. Interestingly, SNIP1 S202D actually increased levels of AGR2,

suggesting that SNIP1 could have multiple effects on AGR2 pathway. The signalling events that determine which sites on SNIP1 are phosphorylated are currently unclear and are likely to be intricately modulated by different cellular and extracellular signals. Accordingly, we observed some discrepancies in the effects of wild type SNIP1 overexpression on AGR2 protein levels and only "fixing" the phosphorylation status of SNIP1, by site directed mutagenesis, resulted in a reproducible outcome with respect to AGR2 protein levels. As SNIP1-mediated repression relies on competition for binding to p300/CBP, it is plausible that the phospho status of SNIP1 determines its affinity for CBP/p300. Indeed, a role for post-translational modifications of SNIP1 was suggested as the cellular environment seemed to affect SNIP1-p300 complex formation and it appeared to readily form in NMuMg cells, but not in U-2 OS cells [555].

Interestingly, patterns of expression of SNIP1 during embryogenesis are highly regulated [480, 554] and its levels significantly increase as the cells differentiate. Interestingly, we observed that culturing A549 cells results in the decrease and subsequent loss of AGR2 protein. Further, TGF-β mediated AGR2 loss is potentially associated with EMT differentiation pathway. The inverse correlation between AGR2 and SNIP1 proteins levels further supports the model of SNIP1 dependent regulation of AGR2. It would be interesting to establish the levels of SNIP1 protein, particularly phospho status of SNIP1, in differentiating A549 cells. *Xenopus* XAG-2, a homologue of human AGR2 protein, is required to determine an anterior fate, [402]. Interestingly, injection of SNIP1 protein was found to result in truncation of anterior structures [554] and it could be due to decrease in XAG-2 levels, if the role of SNIP1 in AGR2 downregulation is conserved across species. Additionally, XAG-2 is expressed only in the extreme anterior of dorsal ectoderm and SNIP1 may function as a regulatory element that restricts XAG-2 expression to this region. Further studies are required however to establish, whether the SNIP1 function in *Xenopus* embryos indeed involved XAG-2 protein.

It is worth noting, that similarly to AGR2, SNIP1 expression has been linked to positive regulation of cell proliferation and cell cycle, via induction of genes such as Cyclin D1 or c-Jun, or binding to and activating c-Myc [555-557]. This is not necessarily contradictory data. For example, it is likely, that SNIP1 effects as well as

AGR2 activity are regulated during the cell cycle. Interestingly, this was observed for SNIP1 and another oncogenic protein Skp2 with regards to c-Myc expression and was explained by differential expression of these proteins during cell cycle [556].

In addition, discrepancies between experiments may be partially explained by the fact that our model is based on transfections into an asynchronous cell population.

As SNIP1 is proving to be a multifunctional protein, a number of transcription-independent functions of SNIP1 proteins have also been described. For example, SNIP1 regulates ATR checkpoint kinase function and mediates induction of p53 activity following UV treatment [495]. This is in keeping with our data showing that SNIP1 overexpression leads to increase in p53 and p21 levels. However, at present, it is unknown whether transcription-dependent or transcription-independent, or both functions of SNIP1 account for the AGR2 downregulation by this protein. We believe that one possible way of answering this question can be by studying mutant SNIP1 protein, where its NLS domain is disrupted. As expected, the NLS mutation resulted in an increased cytoplasmic localisation of SNIP1, but there was no consistent effect of perturbed nuclear localisation of SNIP1 on AGR2 protein level (data not shown). It is possible that post-translational modifications of SNIP1, such as phosphorylation could still occur in this mutant. Presumably combination of different mutations that affect both phosphorylation and localisation of SNIP1 will have to be performed to gain a deeper understanding of this pathway.

In summary, in this chapter we evaluated effects of serum and growth factor on regulation of AGR2 protein in cancer cells with a wild type p53 pathway. We found that TGF-β signalling suppresses AGR2 gene transcription in a SMAD4-dependent manner and triggers AGR2's autophagic/lysosomal degradation that involves ATM-SNIP1-dependent pathway. Thus, we identified tumour suppressive signals that antagonize the pro-oncogenic function of AGR2 and stimulate p53 activity. This knowledge could potentially be used to identify novel ways of reactivating wild type p53 pathway in cancer cells.

CHAPTER 4: A divergent substrate-binding loop within the pro-oncogenic protein Anterior Gradient-2 forms a docking site for Reptin.

4.1 Introduction

4.1.1 Protein- protein networks

The human and other organisms' genome sequence projects have provided an immense amount of information that predicts the existence of tens of thousands of gene products. For example, the human proteome itself is believed to consist of over 25000 unique proteins in their unique functional states, with different post-tranlational modifications, etc. [558]. Despite the vast amount of data, the current understanding of the human organism is somewhat limited and the functions of thousands of the human proteins are simply not known. The key to acquiring a comprehensive picture of the functions of any given protein is building the protein's interaction systems- the logic of that being that most proteins are incorporated into complexes of other proteins to perform their specific function. Therefore, if the function of the complex or of any of the interacting partner within the complex is known, the function of the studied protein can be predicted [559, 560]. Apart from understanding the function of the signalling protein, the potential application of characterising the system within which it operates, is that it might enable understanding of developmental and disease processes. Additionally it may help to design novel drugs that would target a specific protein interaction and therefore a specific function, rather than entire spectrum of functions [561].

Currently, there are two main technical approaches used for identifying novel binding partners. They are the yeast two-hybrid system and co-immunoprecipitation combined with mass spectrometry (MS), which enable the identification of potential binary or complex interactions, respectively. In the yeast two hybrid screen the DNA binding domain of the transcription factor (bacterial lexA or yeast Gal4) is fused to

protein A (the bait) and the activation domain is fused to protein B (the prey) [562]. When bait and prey are co-expressed in the nucleus, protein A and protein B interaction reconstitutes the transcription factor, which can then activate a reporter gene. The two hybrid assay has been successively applied to map protein-protein interactions in a number of model organisms. For example, the first comprehensive two-hybrid studies in *Saccharomyces cerevisiae* revealed about 1000 interactions involving 1004 proteins [563]. Interestingly, the study that followed, detected four times more interactions [564], but the overlap between the two analyses was rather small. Subsequently, large-scale two-hybrid-based protein interaction studies were performed for *Helicobacter pylori*, *Escherichia coli*, hepatitis C, vaccinia virus and *Caenorhabditis elegans* [565] as well as for the *Drosophila melanogaster* [566]. In addition, this system was used to study human protein interactions, to describe proteome-wide interaction networks [567] as well as to characterise individual protein's interactomes. For example, ERK1 and ERK2 were shown to bind to DAPK DD, and this finding helped to unravel the proapoptotic function of the latter [568].
A technique complementary to yeast-two hybrid screens that is used to identify interactions among several proteins involves immunoprecipitation of the protein of interest followed by identification of other proteins that were "pulled down" with it by mass spectrometry. The advantage of this approach over yeast two-hybrid assay is that it identifies the complexes that form in the cellular context. However, the purification method can be a limitation and lead to either loss of an interaction or to false positives.

4.1.2 Short linear motifs

Traditionally, the behaviour of native protein was described by the protein's ordered structure that, in turn, would determine its ability to interact with its binding partners. Indeed, many proteins are modular and form domains, which are folded into distinct structures and can perform their function in isolation [569]. Accordingly, numerous protein-protein interactions were shown to be mediated through domain-domain interaction. Recently the field of systems biology has started to acknowledge that several functional proteins contain large disordered segments and

that protein-protein interactions can often be mediated by these unstructured stretches, namely short linear motifs (SLiMs). The first example of such functional short motif was the KDEL sequence, that targeted the protein to ER retention detective 2 (ERD2), a receptor, which is required for retention of luminal ER proteins [570]. Linear motifs are usually 3 to 10 amino acids in length with usually only 2 or 3 residues being crucial for their function [571]. In contrast to domains, these sequences are usually not evolutionarily conserved. Quite the contrary, the single mutation in the polypeptide's sequence may be sufficient to either create a functional motif from the inert peptide or cause an inactivation of the existing motif. The complexes that are mediated by these motifs are usually transient and their binding affinities are much lower that those of domains. For example, the affinity of the Cyclin-binding motif and 14-3-3 binding motif have been measured as 0.19 μM and 0.15 μM, respectively [572, 573]. This type of interaction is ideal for cellular signalling or response to stimulus, in which dynamics and flexibility are essential. The interactions mediated by short linear motifs can be studied using libraries of peptides. These have been successfully used to discover novel complexes between DAPK and MAP1B and DAPK and TSC2 [574, 575].

4.1.3 AGR2 network

Despite numerous reports describing AGR2's role in various biological pathways, its involvement in cancer progression and drug resistance and inhibition of p53 tumour suppressor activity; its function and regulation are poorly characterised. The ambiguity of the mechanism of function of AGR2 is in part due to the fact that there are surprisingly few interactions validated for this protein.

Different approaches have been taken to try to dissect the interactome of AGR2. For example, combinatorial phage-peptide library was used to search for a high-affinity peptide ligand for AGR2 [424]. Interestingly, AGR2 protein was shown to have a peptide binding activity for two peptide aptamers identified, that could bind AGR2 in Western blot or ELISA format. Specifically, AGR2 could bind to the following peptide motif: (S/T)xIhh (where x indicates any amino acid and h is an amino acid with a hydrophobic side chain). This data indicates that AGR2 could potentially

interact with the proteins containing these motifs in an *in vivo* context. Supporting this is the fact that it was found that this motif could modulate AGR2 activity in cells. When the (S/T)xIhh peptide was tagged to penetratin or fused to GFP, it increased AGR2 protein levels and induced p53 activity [420, 425].

Indeed, several proteins bearing the consensus sequence were retrieved using Prosite and a group of them have already been tested for the direct binding in an ELISA (Table 4.1)

Protein	**Motif's sequence**	**Role**
HERC2	LTTEFG	E3 ligase
SMG-7	LPTLIYY	Nonsense-mediated mRNA decay factor
	TIYY	
TMEM67 /Meckelin	PTPIFY	Transmembrane protein : Involved in cilia formation
TMEM63B	PTIVYY	Transmembrane protein
HECTD1	STIFY	E3 ligase

Table 4.1 Summary of AGR2 potential interactors

Another method that has been used to identify AGR2 binding partners was pulling out AGR2 from the cells that had been treated with a crosslinking agent and then identifying proteins present in the AGR2 complex by mass spectrometry. Despite the fact that AGR2 appeared to form high-molecular weight complexes, only AGR2 was identified in this experiment and it was later confirmed that indeed it can form homo-dimers both *in vivo* and *in vitro* [576].

Lastly, yeast two-hybrid screens identified proteins such as C4.4 and DYS1, but none of these interactions have been validated *in vivo* as yet. Therefore, the current challenges with respect to AGR2 protein is to (1) develop new techniques to study its interactome or (2) try to validate existing list of potential binding proteins and (3) establish the pathways this protein is embedded in.

4.2 Results

4.2.1 Performing a Yeast Two-Hybrid Assay in order to identify novel AGR2 binding partners.

As it was mentioned above several methods have been employed to identify AGR2 interacting proteins, however most of these interactions are poorly characterised or have not been validated as yet. In our search for the interactome of the AGR2 protein, a yeast two-hybrid was carried out (Hybrygenics, France). AGR2 protein was fused with LexA and used as bait against a cDNA library derived from breast cancer cells. Upon sequencing analysis a number of potential novel AGR2 binding proteins were identified. Table 4.2 lists names and the accession numbers of the most significant hits as well as their functions.

Name	Accession number	Function
C4.4A	AF082889	Metastasis linked activity, previously published, unvalidated AGR2-Y2H interactor
CKAP2	AAH10901	Regulates cyclin- kinase functions
DAG1	L19711	Metastasis linked activity, previously published, unvalidated AGR2-Y2H interactor
HECTD1	AAW65983	HECT-homology domain containing Ubiquitin ligase superfamily
LGN	AAN01266	Modulation of G protein activation
Reptin	CAG38538	Interacts with Tip60 and Myc transcription factors, contains intrinsic ATPase and helicase functions
Rip140	NP_003480	Nuclear de-acetylase that interacts with hormone receptor activation domains
TMEM123	AL050161	Cell-membrane mediated cell death

Table 4.2 Summary of AGR2 yeast two-hybrid Interactors

For example DAG1 and C4.4A were found. Both of these proteins have been previously shown to bind to AGR2 in the yeast two hybrid system using placenta-derived prey library and a library derived from a pool of four breast cancer cell lines [423]. The consistency of the yeast two-hybrid data regarding these two proteins is encouraging; however, these interactions have not been validated as yet. Another protein that was identified in the screen was HECTD1, which contains an aptamer ligand sequence with homology to PTTIYY that has been demonstrated to bind to AGR2 with high affinity [424]. However, AGR2 interaction with HECTD1 has not been fully investigated yet. When the identified proteins were grouped by their localisation, a number of potential binding proteins were found to be localised to nucleus. Previously, it was shown that a mature isoform of AGR2 is present in the nucleus [420]. Moreover, the AGR2 binding aptamer, when added to the cells, shifts AGR2 from the nucleus to cytoplasm [420, 425]. These data suggest that the nuclear pool of AGR2 protein may have a distinct role in cellular pathways from functions of the cytoplasmic pool of AGR2. Therefore, we decided to validate interactions between AGR2 and the nuclear proteins found in the yeast two hybrid system, that could potentially help us to better understand the function of the nuclear AGR2. One of the nuclear proteins that was identified as a potential binding partner was a member of AAA+ superfamily named Reptin. Similarly to AGR2, Reptin protein was shown to mediate oncogenic signalling mainly by its interactions with proteins such as Myc or Tip60. In addition, it was shown to be overexpressed in some cancers, such as gastrointestinal cancer or hepatocellular carcinoma (see references in 1.2.3 and 5.1). In order to validate AGR2 and Reptin interaction we first decided to compare AGR2 and Reptin protein levels in samples from breast cancer biopsies and adjacent normal tissue derived from the same cancer patients. We found that AGR2 protein was elevated in the majority of the analysed tumour tissues, relative to their matched normal samples (Figure 4.1 A). Interestingly, Reptin was overexpressed in all of the analysed cancer specimens (Figure 4.1 B). Therefore, we reasoned that the combined overexpression of both AGR2 and Reptin in the primary cancers, made interaction between these two proteins plausible enough to warrant further investigation.

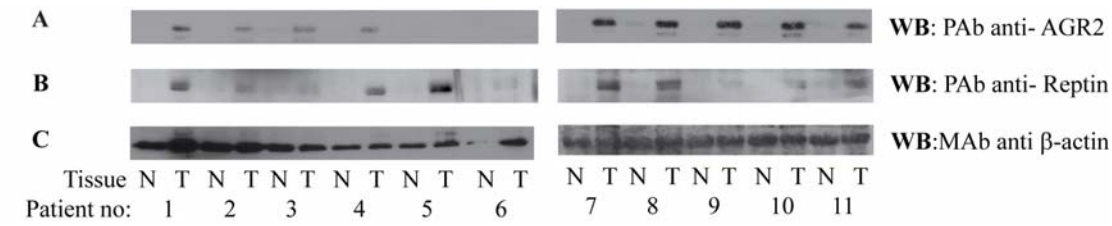

Figure 4.1 AGR2 and Reptin are overexpressed in breast cancer tissue compared to normal adjacent tissue. Sample biopsies from tumour (T) and normal (N) tissue from the same patient were lysed as described in [436]. Proteins were loaded onto 12 % SDS-PAGE gel and **(A)** AGR2, **(B)** Reptin, **(C)** β-actin were examined by immunoblotting using specific monoclonal antibodies.

4.2.2 Validation of Reptin binding to AGR2

In order to validate the direct binding of a Reptin protein to AGR2, we sought to develop an optimised protocol for capturing endogenously and exogenously expressed AGR2 protein from mammalian cell lysate. To this end, we wanted to establish the best lysis buffer that could be used to study the AGR2 interactome. Ideally, the lysis buffer would enable the release of sufficient amounts of proteins, maintain the complexes between the proteins of interest and give the lowest background. Therefore, six different lysis buffers were utilised, with variables such as salt concentration (that ranged from 150 mM to 400 mM) or type of the detergent (NP-40, Triton X-100, Tween-20). Interestingly, HA-tagged Reptin was present in anti-AGR2 immunoprecipitates from lysates of MCF7 cells regardless of the buffer used (Figure 4.2 A). However, only buffer 1 and buffer 6 (see 2.8.10) produced low to no background binding to the "beads" and "beads+lysate" controls when compared to the IP lane. For this reason, we decided to use lysis buffer 6 for the subsequent analysis of the AGR2-Reptin complex.

To further confirm the association between Reptin and AGR2 and to show it could occur in other cell types, we performed co-immunoprecipitation experiments using lysates of H1299 cells transiently expressing HA-tagged Reptin and AGR2 and of A549 transfected with HA-tagged Reptin only. We were able to detect both transfected and endogenous Reptin in the anti-AGR2 immunoprecipitate (Figure 4.2 B and C). Furthermore, endogenous Reptin was also present in anti-AGR2 immunoprecipitates from lysates of untransfected A549 cells, proving AGR2-Reptin interaction to be physiologically relevant (Figure 4.2 D).

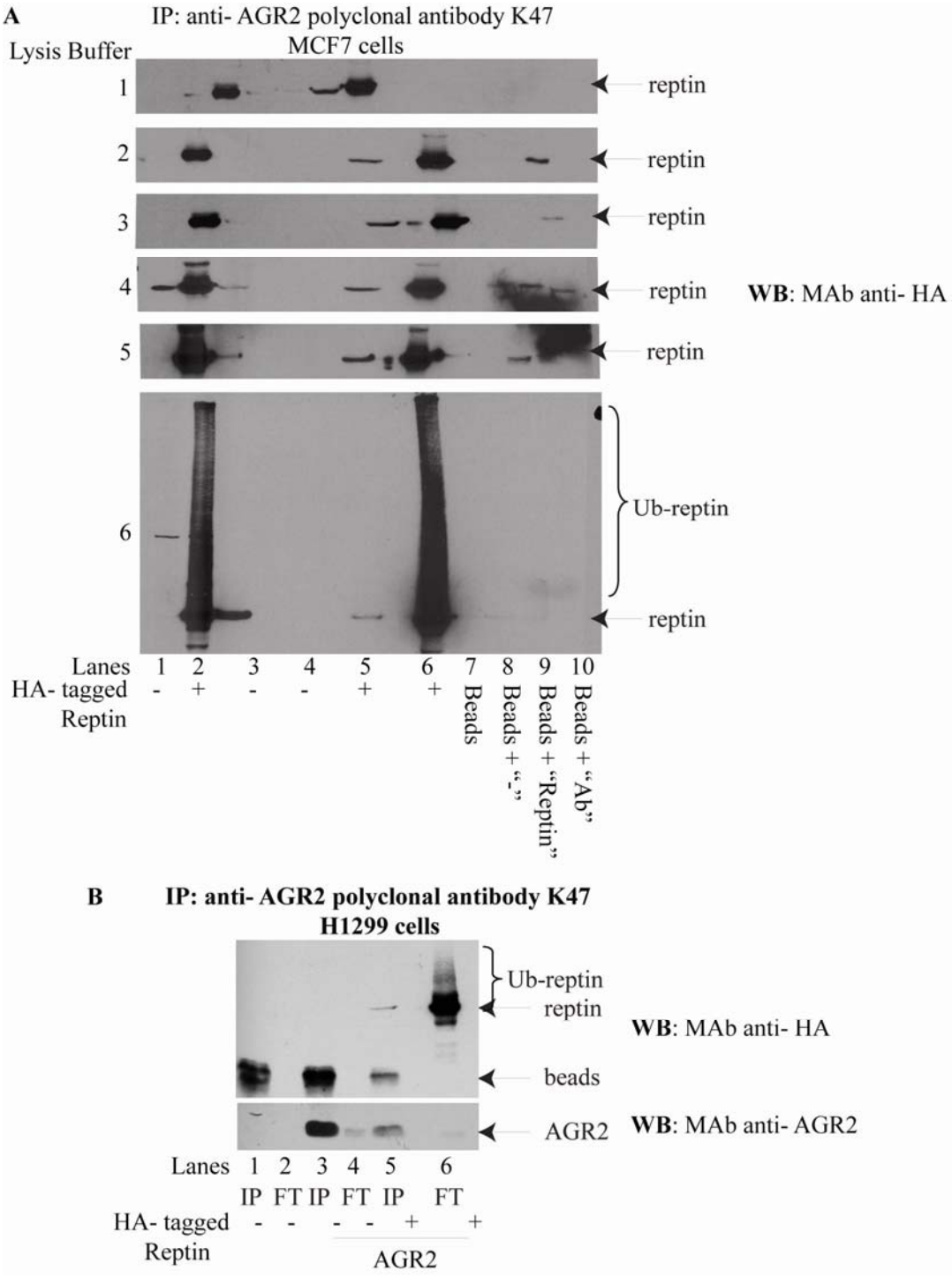
A
IP: anti- AGR2 polyclonal antibody K47
MCF7 cells
Lysis Buffer
1
2
3
4
5
6
reptin
reptin
reptin
reptin
reptin
Ub-reptin
reptin
WB: MAb anti- HA
Lanes 1 2 3 4 5 6 7 8 9 10
HA- tagged Reptin - + - - + + Beads Beads + "-" Beads + "Reptin" Beads + "Ab"
B
IP: anti- AGR2 polyclonal antibody K47
H1299 cells
Ub-reptin
reptin
beads
AGR2
WB: MAb anti- HA
WB: MAb anti- AGR2
Lanes 1 2 3 4 5 6
IP FT IP FT IP FT
HA- tagged Reptin - - - - + +
AGR2

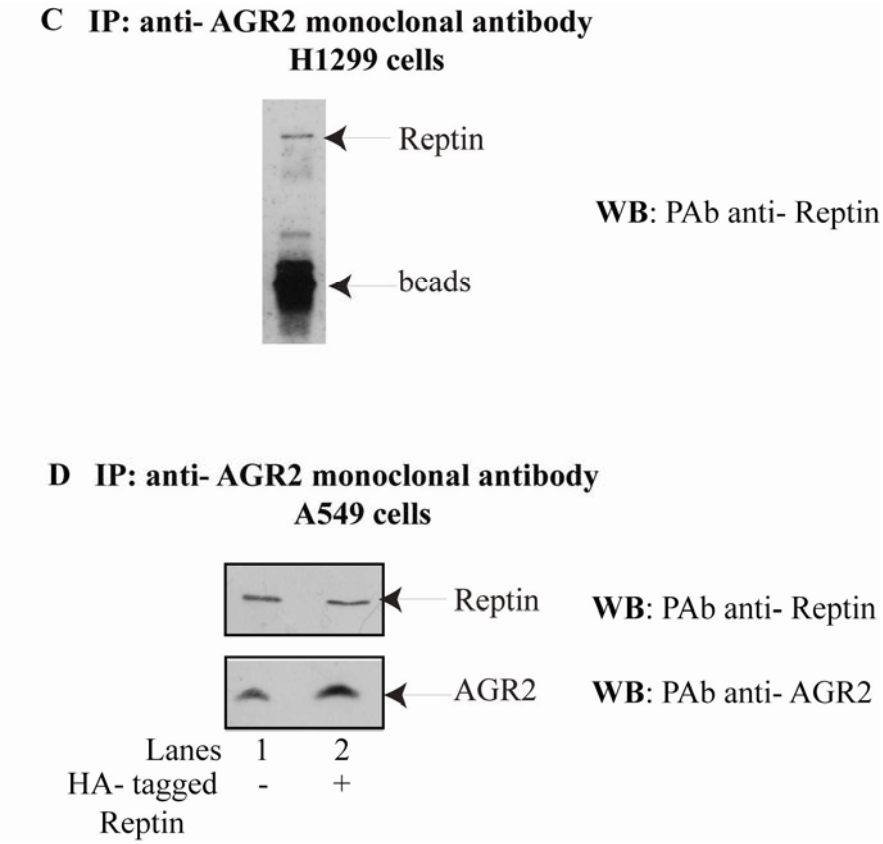

Figure 4.2 Human Reptin and AGR2 co-immunoprecipitate in human cancer cells. (A) MCF7 cells transfected with vector control (lanes 1, 3, 4, 8) or with HA-tagged Reptin (2, 5, 6, 9) were subjected to lysis in buffers 1-6 as described in 2.8.10. Lysates were incubated with anti-AGR2 polyclonal antibody and protein G beads. Beads alone, beads without antibody with the lysate or beads with the antibody without the lysate were used as a control. The load (lysate, lanes 1 and 2), the AGR2 immune precipitate (lanes 3, and 5), the unbound fraction (lanes 4 and 6) and the controls (lanes 7-10) were loaded onto a 12 % SDS-PAGE gel and analysed by immunoblotting using antibodies to HA-tag. Reptin and Ubiquitinated Reptin are highlighted. **(B)** Cell lysates from H1299 cells transfected with vector control (lanes 1 and 2) or with AGR2 (lanes 3 and 4) or with both AGR2 and HA- tagged Reptin (lanes 5 and 6) were incubated with anti- AGR2 polyclonal antibody and protein G beads. The AGR2 immune precipitate (IP; lanes 1, 3 and 5) and the unbound fraction (FT, lanes 2, 4 and 6) were loaded onto a 12 % SDS-PAGE gel and analysed by immunoblotting using antibodies to HA-tag and AGR2. Protein G beads, Reptin, Ubiquitinated Reptin and AGR2 are highlighted. **(C and D)** Cell lysates from **(C)** untransfected H1299 cells or **(D)** A549 cells transfected with vector control (lane 1) or with HA-tagged Reptin (lane 2) were incubated with anti- AGR2 monoclonal antibody and protein G beads. The AGR2 immune precipitate was loaded onto a 12 % SDS-PAGE gel and analysed by immunoblotting using antibodies to Reptin and AGR2. Reptin, beads and AGR2 are highlighted.

Interestingly, combination of high salt concentration (400 mM) and NP-40 in the lysis buffer 6 resulted in a pool of Reptin protein, in the unbound fraction, that was composed of the Ubiquitin-like ladder (Figure 4.2 A). In order to ascertain whether the high molecular mass adducts were indeed composed of either Ubiquitin or Ubiquitin-like proteins, the His-tagged versions of Ubiquitin, NEDD-8 and SUMO-1 were cotransfected into H1299 cells together with HA-tagged Reptin. Following purification of the *in vivo* His-tagged proteins, we could show that ubiquitination, but not neddylation or sumoylation was the prevailing modification of Reptin (Figure 4.3 A). As an additional control, we could detect basal ubiquitination and sumoylation of p53, whereas MDM2 enhanced ubiquitination or neddylation of p53 (Figure 4.3 C and D). These latter data indicate that the low level of neddylation or sumoylation of Reptin is not due to inadequate integrity of the His-tagged NEDD8 and SUMO-1 genes and highlights the specificity of ubiquitination of Reptin in this cell line.

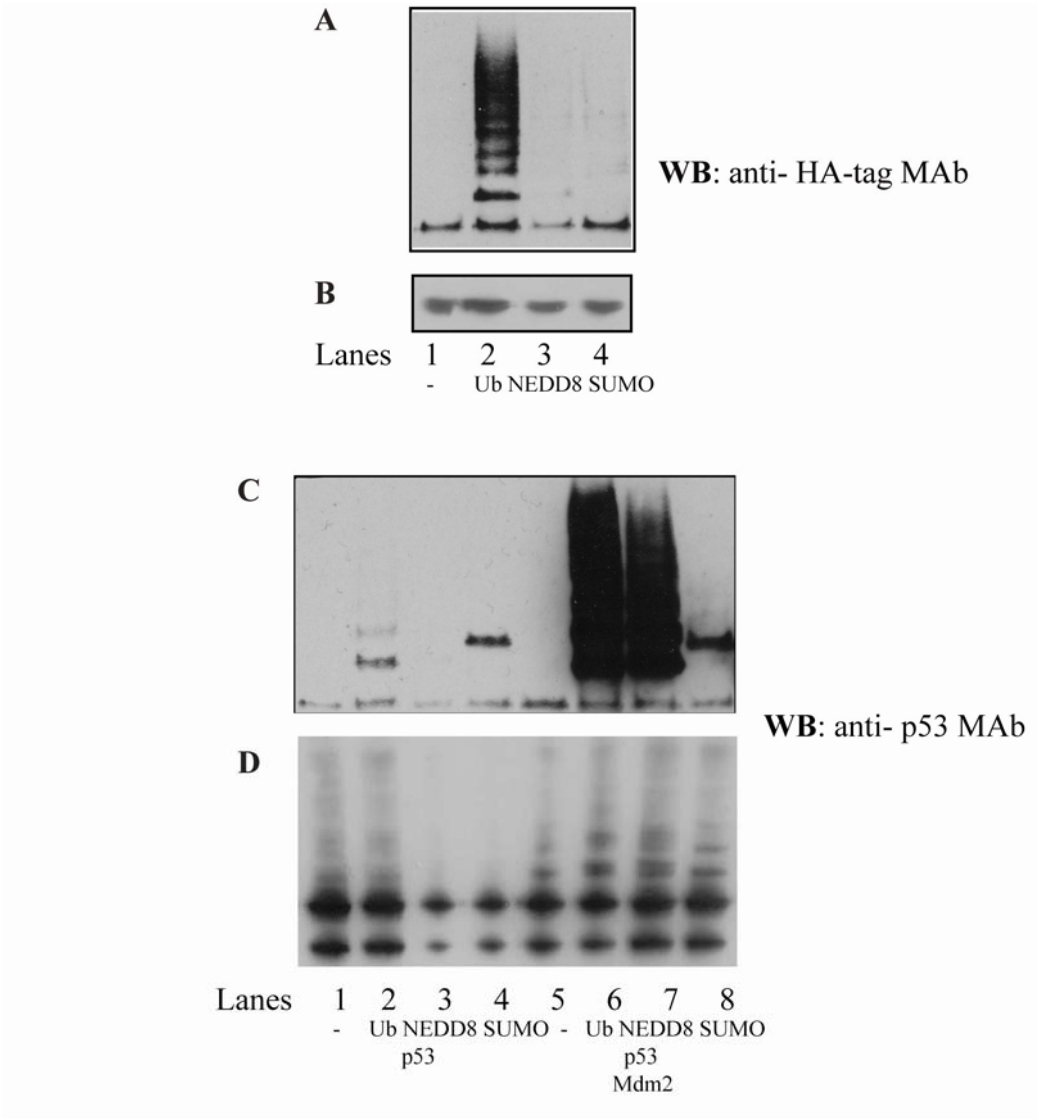

Figure 4.3 Reptin is ubiquitinated in cells. (A and B) H1299 cells were transfected with the HA-tagged Reptin and with either His-Ubiquitin (lane 2) or His-NEDD8 (lane 3) or His-SUMO-1 (lane 4). Post transfection cells were treated with 10 mM MG132 for 4 hours, **(A)** His-conjugates were isolated and the expressed Reptin was examined for changes in the amount of post translational modification by immunoblotting with an anti-HA-tag antibody. **(B)** The total amount of Reptin. **(C and D)** Evaluation of p53 UBL modification in cells. A vector expressing wild type p53 was co-transfeted with vectors expressing His-Ubiquitin, His-NEDD8, and His-SUMO-1 without (lanes 1-4) or with the co-transfection of MDM2 (lanes 5-8). **(C)** The expressed p53 was examined for changes in the amount of post-translational modification by immunoblotting with an anti-p53 antibody after the nickel affinity chromatography stage. **(D)** The total amount of p53.

Reptin has been previously shown to assemble with Pontin into high molecular complexes that have a role in chromatin remodelling, transcription, telomerase function (see 1.2.3). Therefore, we sought to test whether Pontin could also associate with AGR2. Interestingly, we could not detect Pontin in anti-AGR2 immunoprecipates from MCF7 lysates ectopically expressing myc-tagged Pontin (Figure 4.4 A), suggesting that the function of AGR2 and Reptin complex may be independent of Pontin.

To establish if Reptin could bind directly to AGR2, we set out to purify both Reptin and AGR2 from *E.coli*. To this end, the Reptin sequence was cloned into a GST-tagged expression plasmid. A prescission cleavage site was incorporated, in order to enable the removal of GST tag when necessary. We purified sufficient amounts of GST-tagged Reptin as detected by Coomassie staining (Figure 4.5 A) and Western Blotting (Figure 4.5 B). Interestingly, two bands of similar size were consistently detected, which may reflect some modification of Reptin protein. In addition AGR2 protein was purified using His-tagged expression plasmid as is evident from Coomassie blue stained gel and immunoblot (Figure 4.5 C and D).

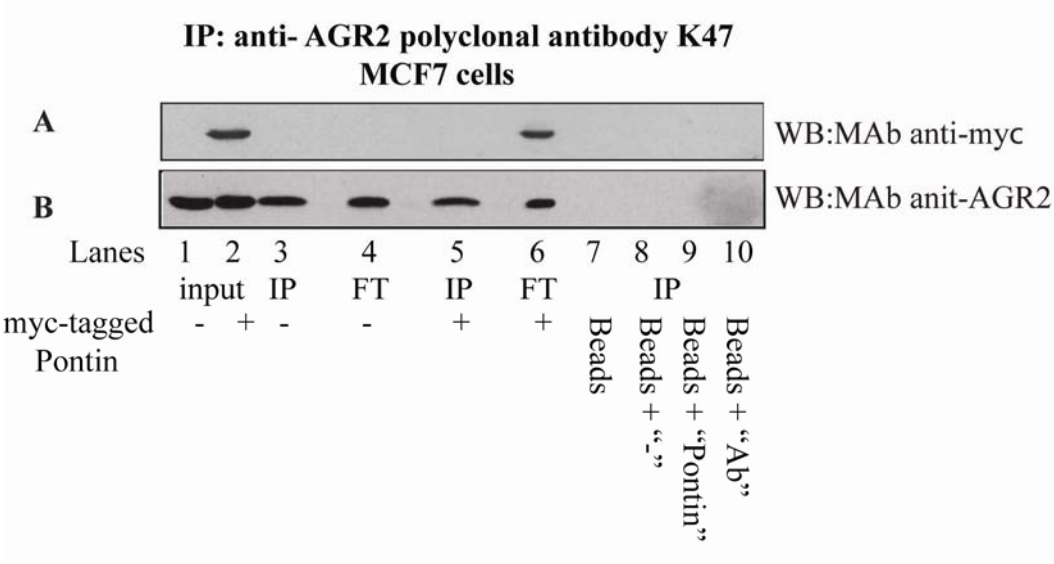

Figure 4.4 Human Pontin does not bind to AGR2 in human cancer cells. MCF7 cells transfected with vector control (lanes 1, 3, 4, 8) or with myc-tagged Ponin (2, 5, 6, 9) were subjected to lysis in buffers 6 as described in Materials and Methods. Lysates were incubated with anti-AGR2 polyclonal antibody and protein G beads. Beads alone, beads without antibody with the lysate or beads with the antbody without the lysate were used as a control. The load (lysate, lanes 1 and 2), the AGR2 immune precipitate (lanes 3, and 5), the unbound fraction (lanes 4 and 6) and the controls (lanes 7-10) were loaded onto a 12 % SDS-PAGE gel and analysed by immunoblotting using antibodies to **(A)** myc-tag and to **(B)** AGR2 protien.

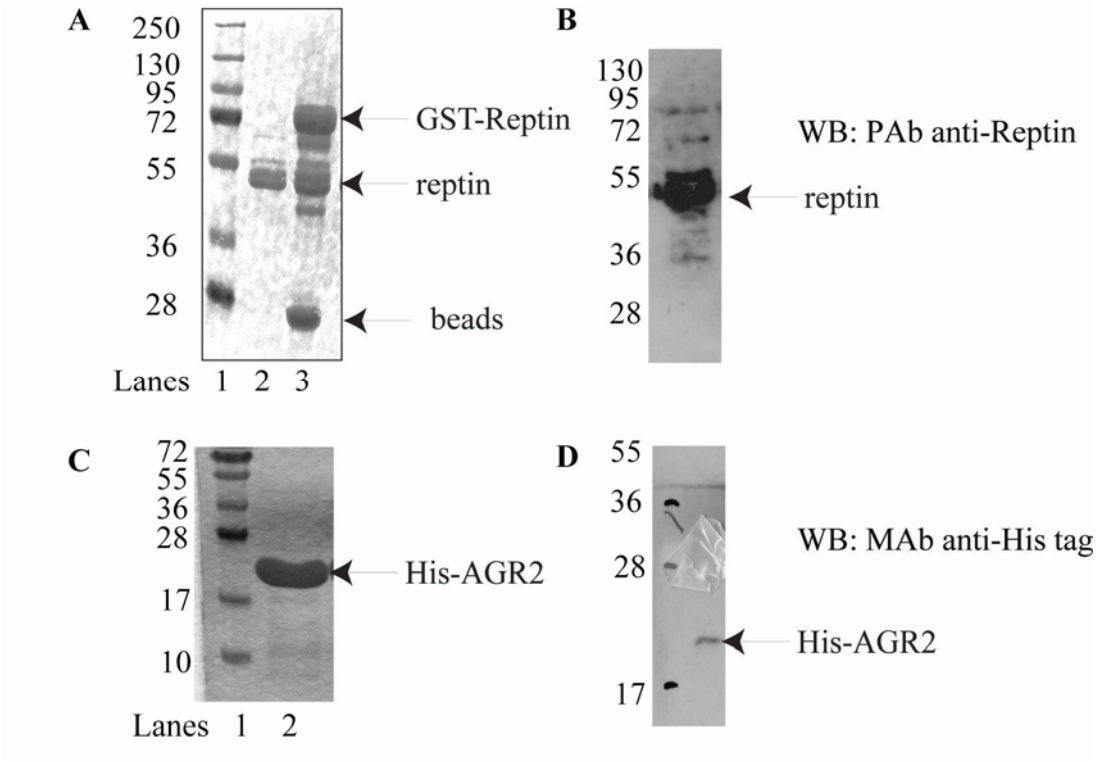

Figure 4.5 Purification of Reptin and AGR2 proteins. (A and B) Purification of recombinant Reptin. Reptin was cloned into a vector producing protein fused to GST. In addition a precision protease cleavage site was incorporated. GST-Reptin was captured onto the glutathione beads and either GST-Reptin was eluted off the beads with the use of reduced gluthatione or Reptin was cleaved off the beads through incubation with the prescission enzyme. **(A)** Coomassie stained gel: Lane 1: markers; Lane 2, full-length untagged Reptin; Lane 3, GST-tagged Reptin. **(B)** Immunoblot of purified untagged Reptin. **(C and D) Purification of recombinant AGR2.** AGR2 protein was purified with the use of the nickel affinity chromatography **(C)** Coomassie stained gel: Lane 1: markers; Lane 2: His-tagged AGR2 **(D)** Immunoblot of purified His-tagged AGR2.

Following successful purification, we performed an ELISA assay to establish whether Reptin could bind directly to AGR2. AGR2 protein was first immobilised onto a microtitre plate and incubated with a titration of GST-tagged Reptin protein or GST only. GST-tagged Reptin bound specifically to His-tagged AGR2 protein (Figure 4.6 A). Similarly, when GST-tagged Reptin was immobilised onto a microtitre plate and incubated with His-AGR2 in mobile phase, it was found that His-AGR2 could bind to GST-Reptin protein (Figure 4.6 B).

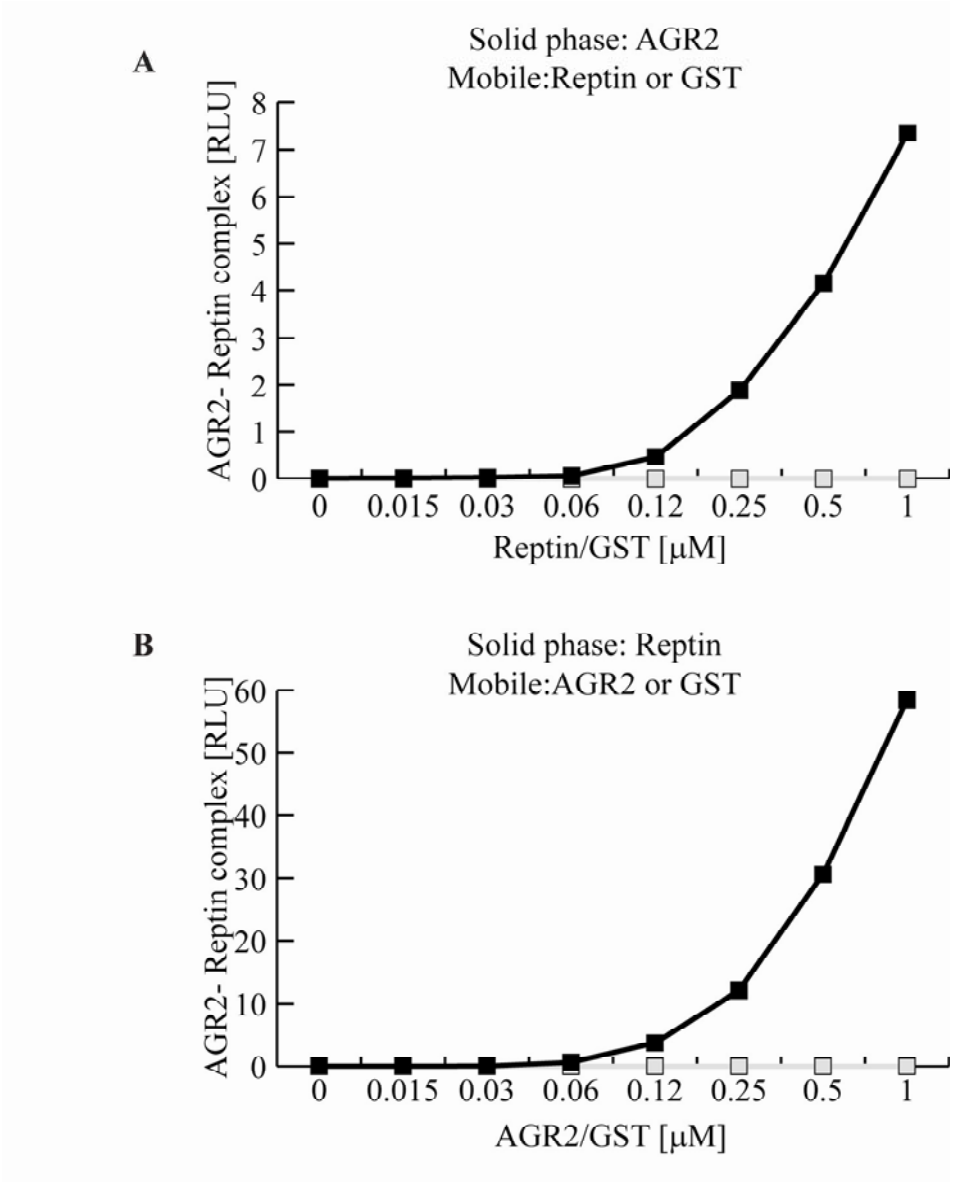

Figure 4.6 AGR2 binds directly to Reptin. Either AGR2 **(A)** or Reptin **(B)** was immobilized on the solid phase and a titration of either Reptin **(A)** or AGR2 **(B)** was added in the mobile phase. The amount of Reptin or AGR2 bound was quantified with antibodies specific for either protein using chemiluminescence. The data are plotted as the extent of protein-protein complex formation (in RLU) as a function of the amount of protein in the mobile phase [μM].

4.2.3 Reptin binds specifically to the short linear motif in AGR2 protein.

Having proved that Reptin and AGR2 interact *in vivo* and *in vitro* we sought to determine Reptin and AGR2 binding interface. There is an increasing number of studies showing that the native state of a protein is not necessarily a highly rigid globular structure. Many proteins contain disordered regions that in fact allow respective proteins to interact with specific binding partners. Therefore, we were interested to find out whether the AGR2 and Reptin interaction could be mediated by such an amino-acid stretch on the AGR2 protein. For this purpose a series of 16 AGR2 peptides (Figure 4.7 A) composed of 15 amino acids with 5 amino acids overlaps and N-terminal biotin tag was used in the peptide pull down assay developed in the lab (see 2.8.1 and [577]). In detail, streptavidin agarose beads were coated with AGR2 peptides and incubated with cell lysate. We found that one peptide, namely peptide 10 (AEQFVLLNLVYETTD), was able to specifically pull down ectopically expressed Reptin protein from H1299 cells lysate (data not shown) as well as endogenous protein (Figure 4.7 B). Similarly, endogenous Reptin from MCF-7 cells was pulled down with the same peptide (data not shown). To further dissect AGR2-Reptin binding interface we created a peptide library that contained deletion variants of peptide 10 and derivatives of peptide 10 in which each amino acid was consecutively replaced with Alanine (Figure 4.7 C). Subsequently, we used the library in to find the peptides that had a reduced or enhanced binding to cellular Reptin. We found that mutating amino acids 104-111 to Alanine could reduce peptide 10-Reptin binding. Mutation of F104 and Y111 entirely abolished the interaction (Figure 4.7 D, lanes 4-7 and 9-11). Interestingly, when Asparagine 108 was changed into Alanine the binding was in fact enhanced (Figure 4.7 D, lane 8). In addition deletion of residues A101 to Q103 or E112 to D115 did not affect peptide 10-Reptin binding (Figure 4.7 D, lanes 1-3 and 12-15). However, the truncation of F104 or Y111 abolished Reptin binding (Figure 4.7 D, lanes 26-39 and 20-22). This data led us to identify a distinct linear motif in the loop region of AGR2 that is required for the interaction with Reptin protein. This minimal region sequence is 8 amino acids long and its sequence is as follows: 104-FVLLNLVY-111. AGR2

belongs to AGR2 gene family that is composed of Erp18 and AGR2 paralog AGR3. Since these three proteins have high sequence similarities, we could model the AGR2 sequence into the crystal structure of Erp18 [578] (Figure 4.7 E). Interestingly, we found that peptide 10 maps to the previously discovered loop insertion present in the AGR2 gene family and proposed to be important for substrate interactions [578, 579]. Therefore, it was plausible, that this 8 amino acids stretch from AGR2 may define specificity in AGR2 interactions with its potential binding partners. Hence, we sought to determine if the AGR3 peptide that locates to this loop insertion could bind to Reptin. Interestingly, it appeared that peptide 10-Reptin interaction was very specific for AGR2, since the corresponding peptide from AGR3 did not bind to Reptin (Figure 4.7 D, lane 37). We then compared sequence of the AGR3 loop peptide (QNKFIMLNLMHETTD) to that of AGR2 (AEQFVLLNLVYETTD) (Figure 4.7 E, ii) and mutated amino acids outside and in the minimal region sequence of the AGR3 peptide to investigate if any of the introduced changes could restore AGR3 peptide binding to Reptin. When Lysine residue (outside 8 amino-acid motif) in AGR3 peptide was mutated to the corresponding AGR2 Glutamate residue, it still could not bind to Reptin (Figure 4.7 D, lane 38). However, introducing the Histidine to Tyrosine mutation (inside 8 amino acids motif) in AGR3 peptide restored its binding to Reptin (Figure 4.7 D, lane 39).

A

1. llvalsytlardttv
2. rdttvkpgakkdtkd
3. kdtkdsrpklpqtls
4. pqtlsrgwgdqliwt
5. qliwtqtyeealyks
6. alyksktsnkplmii
7. plmiihhldecphsq
8. cphsqalkkvfaenk
9. faenkeiqklaeqfv
10. aeqfvllnlvyettd
11. yettdkhlspdgqyv
12. dgqyvprimfvdpsl
13. vdpsltvraditgry
14. itgrysnrlyayepa
15. ayepadtallldnmk
16. ldnmkkalkllktel

B

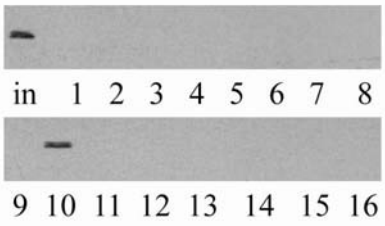

WB: PAb anti- Reptin

C

1. AEQFVLLNLVYETTD
2. AAQFVLLNLVYETTD
3. AEAFVLLNLVYETTD
4. AEQAVLLNLVYETTD
5. AEQFALLNLVYETTD
6. AEQFVALNLVYETTD
7. AEQFVLANLVYETTD
8. AEQFVLLALVYETTD
9. AEQFVLLNAVYETTD
10. AEQFVLLNLAYETTD
11. AEQFVLLNLVAETTD
12. AEQFVLLNLVYATTD
13. AEQFVLLNLVYEATD
14. AEQFVLLNLVYETAD
15. AEQFVLLNLVYETTA
16. AEQFVLLNLVYETT
17. AEQFVLLNLVYET
18. AEQFVLLNLVYE
19. AEQFVLLNLVY
20. AEQFVLLNLV
21. AEQFVLLNL
22. AEQFVLLN
23. EQFVLLNLVYETTD
24. QFVLLNLVYETTD
25. FVLLNLVYETTD
26. VLLNLVYETTD
27. LLNLVYETTD
28. LNLVYETTD
29. NLVYETTD
30. EQFVLLNLVYETT
31. QFVLLNLVYETT
32. FVLLNLVYETT
33. FVLLNLVYE
34. FVLLNLVY
35. FVLLNLVA
36. AVLLNLVY
37. QNKFIMLNLMHETTD
38. QNQFIMLNLMHETTD
39. QNKFIMLNLMYETTD
40. QNQFIMLNLMYETTD

D

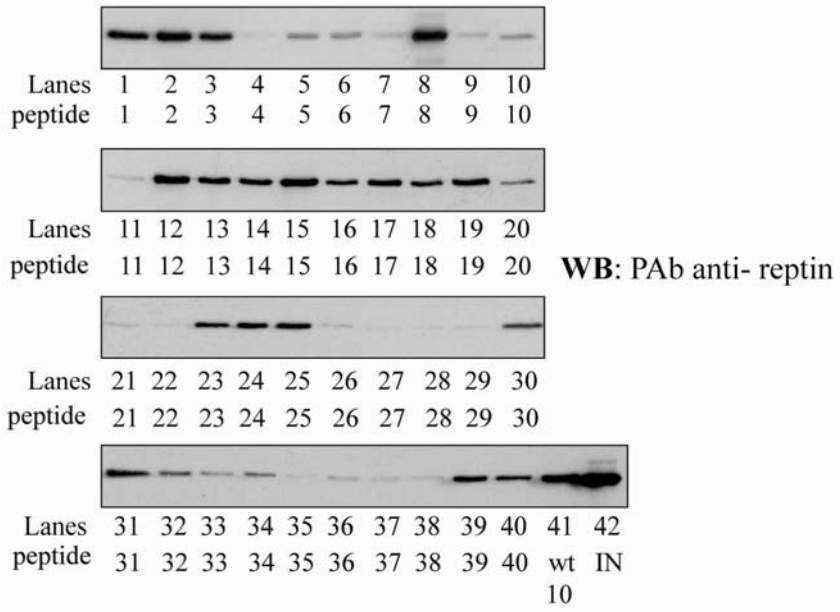

E i.

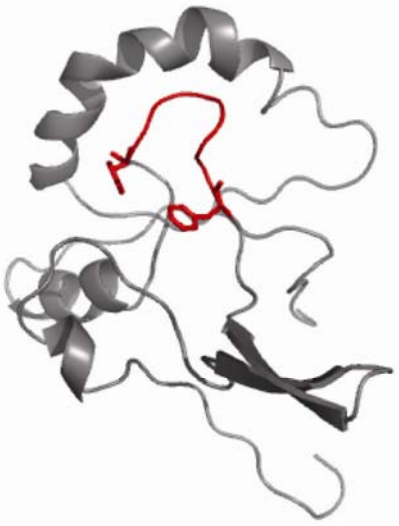

```
-MEKIPVSAFLLLVALSYTLARDTTVKPGAKKDTKDSRPKLPQTLSRGWGDQLIWTQTYE 59
MMLHSALGLCLLLVTVSSNLA--IAIK-------KEKRP--PQTLSRGWGDDITWVQTYE 49
-METRPRLGATCLLGFSFLLLVISSDG--------------HNGLGKGFGDHIHWR-TLE 44
 *   .      *: .*  *    :                 : *.:*:**.: *  * *

EALYKSKTSNKPLMIIHHLDECPHSQALKKVFAENKEIQKLAE-QFVLLNLVYET--TDK 116
EGLFYAQKSKKPLMVIHHLEDCQYSQALKKVFAQNEEIQEMAQNKFIMLNLMHET--TDK 107
DGKKEAAASGLPLMVIIHKSWCGACKALKPKFAESTEISELSH-NFVMVNLEDEEEPKDE 103
:.   :  *  ***:* * . *  .:***  **:. **.::::. :*:::**  *   .*:

HLSPDGQYVPRIMFVDPSLTVRADITGRYSNRLYAYEPADTALLLDNMKKALKLLKTEL- 175
NLSPDGQYVPRIMFVDPSLTVRADIAGRYSNRLYTYEPRDLPLLIENMKKALRLIQSEL- 166
DFSPDGGYIPRILFLDPSGKVHPEIINENGNPSYKYFYVSAEQVVQGMKEAQERLTGDAF 163
.:**** *:***:*:*** .*:.:* .. .*  * *   .   :::.**:* . :  :

---------
---------
RKKHLEDEL 172
```

Figure 4.7 Reptin protein binds specifically to a short linear motif within AGR2 protein sequence. (A) A list of AGR2 overlapping peptides, **(B)** Biotinylated peptides (as in **A**) were coupled to streptavidin beads and incubated with human cell lysate expressing Reptin. The amount of Reptin bound was evaluated by immunoblotting using Reptin-specific antibody; [IN] is an input fraction and the numbers 1-16 represent the peptides sequences in part A. **(C and D) Identification of key residues that stabilize the AGR2 peptide-Reptin complex. (C)** Peptides 1-36 represent modifications in "peptide 10", peptides 37-40 represent the divergent loop in the AGR2 orthologue AGR3 (peptide 37 is the AGR3 sequence and 38-40 mutations in this sequence), **(D)** Biotinylated peptides (as in **C**) were coupled to streptavidin beads and incubated with human cell lysate expressing Reptin. The amount of Reptin bound was evaluated by immunoblotting using Reptin-specific antibody; [IN] is an input fraction and the numbers 1-40 represent the peptides sequences in part **C**. The amount of Reptin bound was evaluated by immunoblotting using Reptin-specific antibody; the bound fractions (lanes 1-41), [IN] input fraction (lane 42); **(E)** [i] Homology model of the position of the divergent peptide loop from AGR2 that has the Reptin binding site based on the structure of the AGR2 orthologue Erp18; PDB code: 2K8V. [ii] Sequences in the divergent loop between AGR2, AGR3, and ERP18 proteins highlighted in red.

Subsequently, we wanted to establish the ability of purified GST-tagged Reptin to bind to AGR2 peptides in an ELISA. Unfortunately, we observed a relatively high background values in the ELISA. In addition, peptide 10 binding to Reptin was almost negligible (Figure 4.8 A). Surprisingly, we found that Reptin bound to peptide 4 the strongest in this set up (Figure 4.8 A). Recently, there has been a report showing that yeast Rvb1/Rvb2 purified proteins that contain a Histidine tag, can form different structures compare to untagged constructs [580]. Therefore, we decided to compare GST-Reptin and AGR2 peptides binding to this of untagged protein expressed in *E.coli* or Sf9 insect cells. Interestingly we found that only eukaryotically expressed protein could specifically bind to peptide 10 as well as peptide 11, the latter shares part of the sequence with peptide 10 (Figure 4.8 B). This shows, that Reptin protein has a dynamic nature, and different pools of Reptin, for example with respect to their oligomeric stage, or post translational modifications, show different binding affinity to AGR2 peptide.

Next, we set out to investigate if any of the AGR2 peptides that bind to Reptin could disrupt the AGR2-Reptin complex. To this end His-tagged AGR2 was immobilised on the plate and a fixed amount of GST-tagged Reptin protein preincubated with a titration of AGR2 peptides was added. Intriguingly, peptide 10 diminished formation of the AGR2-Reptin complex, with the Kd of about 60 μM, despite the fact that GST-Reptin could not bind to this peptide in an ELISA format. Surprisingly, peptide 4 induced AGR2-Reptin binding, indicating that this region on AGR2 may allosterically modulate Reptin protein. None of the other peptides or DMSO caused any significant changes in the AGR2-Reptin binding (Figure 4.8 C). Therefore, we concluded that Reptin specifically binds to peptide 10 and peptide 4.

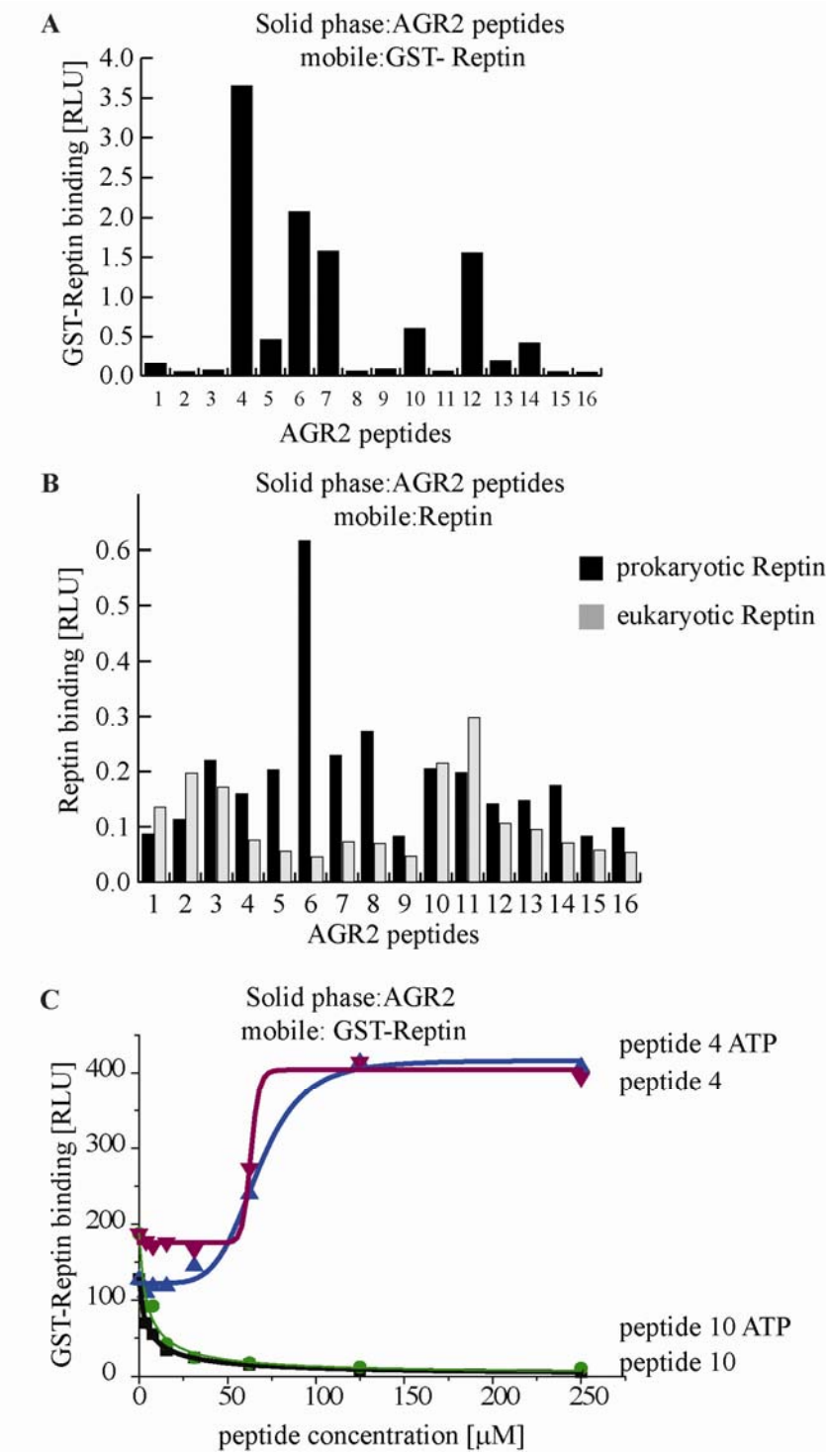

Figure 4.8 Differential binding of recombinant Reptin protein to AGR2 overlapping peptides. (A and B) A fixed amount of the indicated biotinylated peptides (as in **4.7 A**) was added to a microtitre plate coated with streptavidin and incubated with recombinant **(A)** GST-tagged Reptin, **(B)** untagged Reptin expressed in either prokaryptic or eukaryotic cells. The amount of Reptin bound was quantified with antibodies specific for Reptin using chemiluminescence. The data are plotted as the extent of protein-peptide complex formation [RLU] **(C)** Reptin protein was preincubated with a titration of peptide 4 and peptide 10, and added to immobilised AGR2 protein. The amount of Reptin bound to the full length AGR2 was quantified with antibodies specific for Reptin using chemiluminescence. The data are plotted as the extent of protein-protein complex formation [RLU].

Having defined the critical residues for the AGR2-Reptin interaction, namely F104 and Y111, we generated mutant proteins where respective residues were replaced by Alanine. Subsequently, we performed an ELISA assay to establish how replacing these two residues would affect full length protein binding. Initially, we wanted to establish whether the wild type and mutant AGR2 protein were recognised by the AGR2-specific antibody to the same extent. Specifically, it was important to rule out the possibility that the apparent differences in the affinity of wild type and mutant AGR2 protein to Reptin were caused by alterations in epitopes recognised by antibodies used in this assay. To this end, anti-His or anti-AGR2 monoclonal antibodies, or anti-AGR2 polyclonal antibodies were immobilised on the plate and incubated with the titration of either wild type His-tagged AGR2 or His-tagged AGR2 F104A, or His-tagged AGR2 Y111A proteins. This was followed by the incubation with the anti-AGR2 polyclonal antibody or anti-His monoclonal antibody. Interestingly, only when the AGR2 proteins were bound to monoclonal antibodies on the plate, we observed the comparable signal to noise ratio for the corresponding amounts of the His- tagged AGR2 proteins used (Figure 4.9 A and C). Therefore, we decided to use monoclonal antibodies for the subsequent experiments.

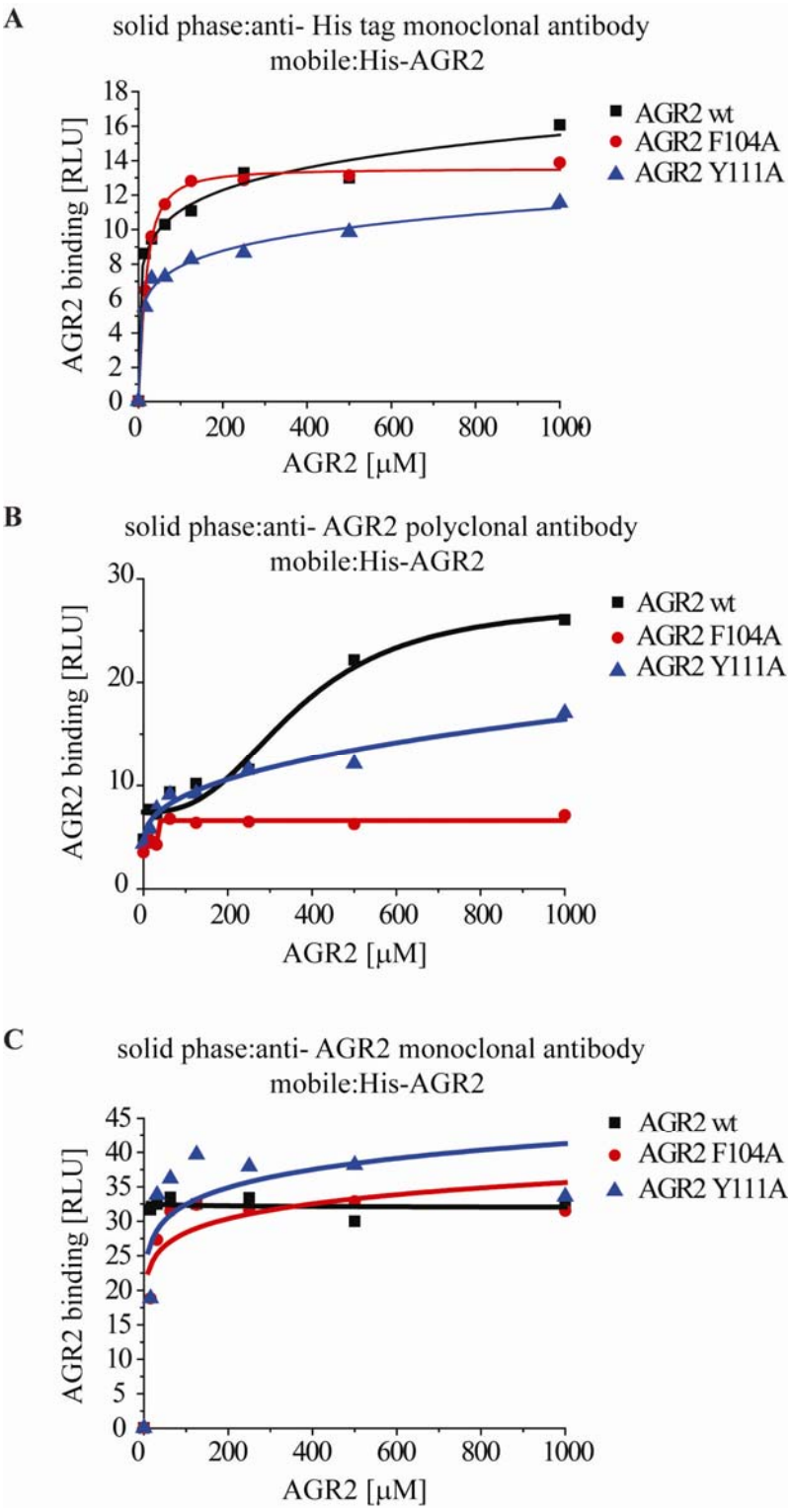

Figure 4.9 Quantification of AGR2 loop mutant proteins and wild type AGR2 protein. Monoclonal antibodies against **(A)** His tag, **(C)** AGR2 or **(B)** polyclonal antibody against AGR2 were coated onto a microtitre plate and incubated with a titration of wild type AGR2, AGR2 Y111A and AGR2 F104A mutant proteins. The amount of AGR2 protein captured was quantified with polyclonal **(A and C)** antibody against AGR2 or **(B)** monoclonal antibody against His tag. The data are plotted as the amount of AGR2 protein detected with the respective antibodies [RLU] as a function of the amount of the protein in the mobile phase [µM].

Firstly, sandwich ELISA was performed, wherein anti-Reptin antibody was immobilised on the plate and then incubated with the Reptin protein, followed by the incubation with wild type or mutant His-tagged AGR2 proteins (Figure 4.10 A). Both mutations affected the extent of binding to Reptin protein. Specifically, mutation in Y111A residue caused reduced binding to Reptin, whereas F104A mutation completely abolished AGR2-Reptin interaction. Surprisingly, when we performed an ELISA, wherein Reptin protein was immobilised directly onto a microtitre well, we found that the AGR2 F104A showed only slightly reduced binding, whereas Reptin Y111A showed almost complete loss of binding to Reptin protein (Figure 4.10 B). It may be that depending on the approach used to immobilise Reptin protein onto the plate, its conformation changes and this has an impact on its tolerance towards changes in the loop region of AGR2 protein. This hypothesis was further supported by the observation made, when wild type or mutant His-tagged AGR2 proteins were immobilised on the plate and Reptin titrated in the mobile phase (Figure 4.10 C). Specifically, Reptin could not bind to His-tagged AGR2 F104A, however when variants of AGR2 proteins were captured by the monoclonal antibody, both AGR2 F104A and AGR2 Y111A could bind to Reptin protein with to a similar extent as the wild type AGR2 (Figure 4.10 D).

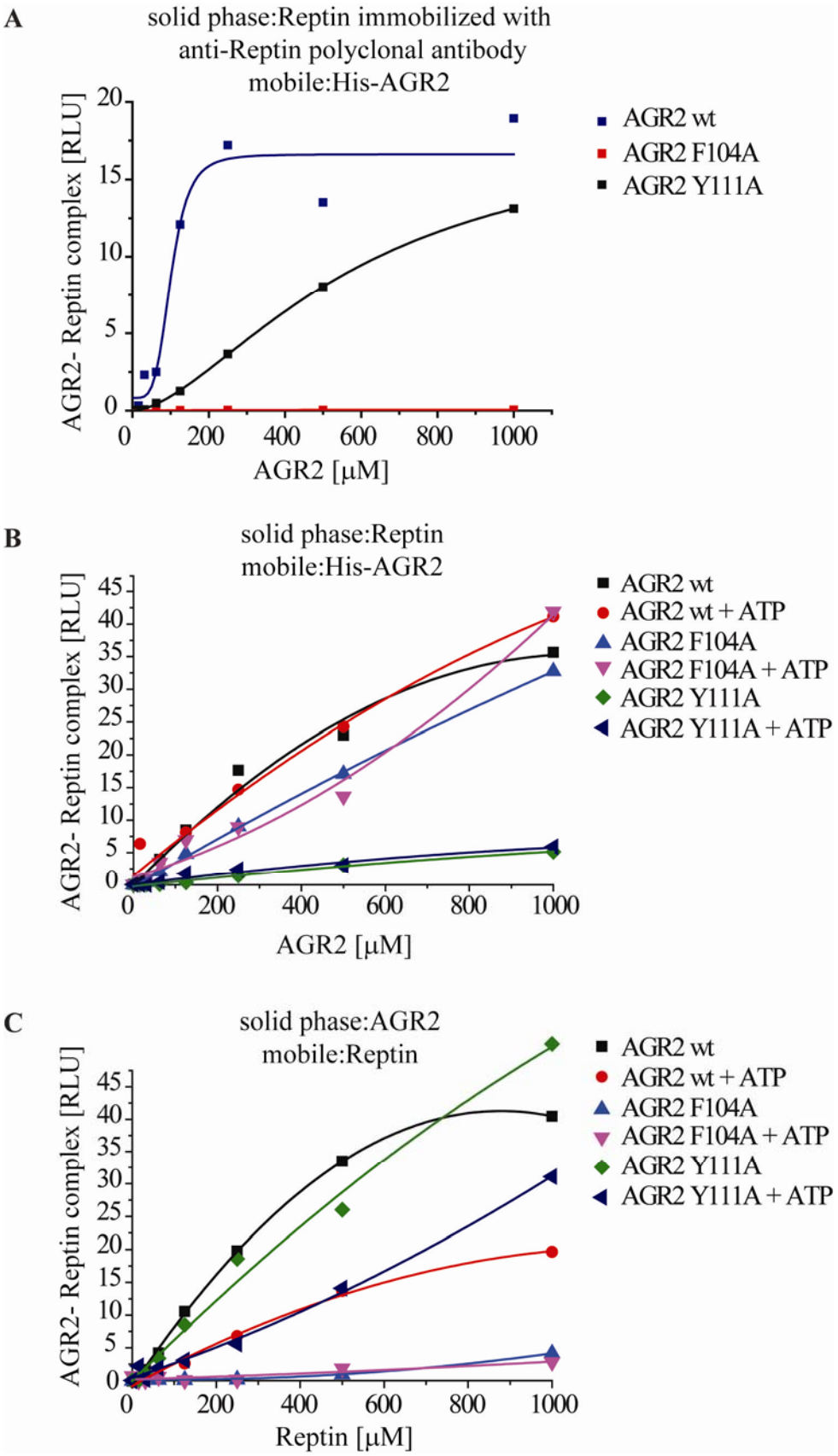
A
solid phase:Reptin immobilized with
anti-Reptin polyclonal antibody
mobile:His-AGR2
AGR2- Reptin complex [RLU]
AGR2 [μM]
AGR2 wt
AGR2 F104A
AGR2 Y111A
B
solid phase:Reptin
mobile:His-AGR2
AGR2- Reptin complex [RLU]
AGR2 [μM]
AGR2 wt
AGR2 wt + ATP
AGR2 F104A
AGR2 F104A + ATP
AGR2 Y111A
AGR2 Y111A + ATP
C
solid phase:AGR2
mobile:Reptin
AGR2- Reptin complex [RLU]
Reptin [μM]
AGR2 wt
AGR2 wt + ATP
AGR2 F104A
AGR2 F104A + ATP
AGR2 Y111A
AGR2 Y111A + ATP

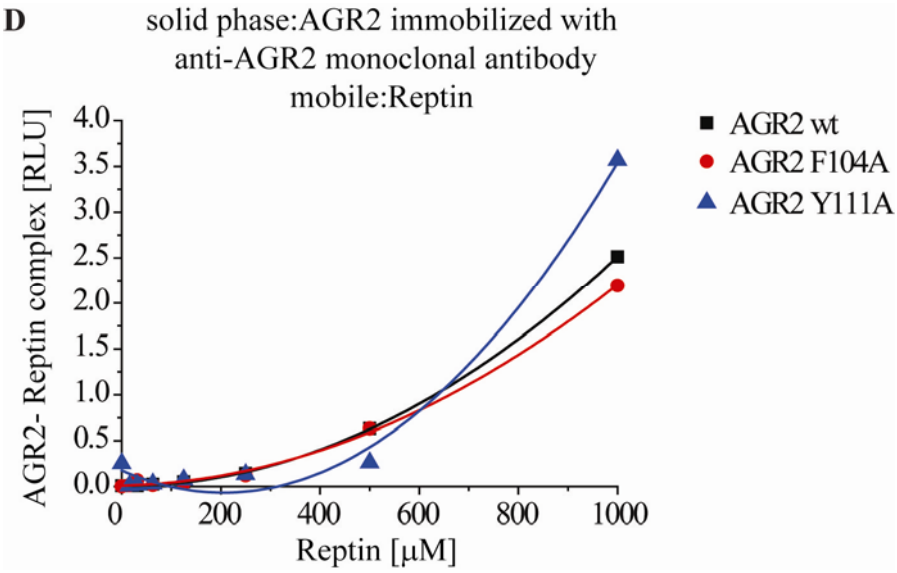

Figure 4.10 Mutations in the AGR2 loop destabilise the Reptin-AGR2 complex. (A and D) Polyclonal antibodies against **(A)** Reptin protein or monoclonal antibodies **(D)** against AGR2 protein were coated onto a microtitre plate and incubated with a titration of wild type AGR2, AGR2 Y111A, AGR2 F104A mutant proteins or Reptin protein, respectively. The amount of **(A)** wild type or mutant AGR2 or **(D)** Reptin bound was quantified with antibodies specific for either protein using chemiluminescence. The data are plotted as the extent of protein-protein complex formation [RLU] as a function of the amount of the protein in the mobile phase [μM]. **(B and C) (B)** Reptin protein or **(C)** wild type or mutant AGR2 protein were immobilised onto a microtitre plate and incubated with a titration of wild type AGR2, AGR2 Y111A, AGR2 F104A mutant proteins or Reptin protein, respectively. The amount of **(B)** wild type or mutant AGR2 or **(C)** Reptin bound was quantified with antibodies specific for either protein using chemiluminescence. The data are plotted as the extent of protein-protein complex formation [RLU] as a function of the amount of the protein in the mobile phase [μM].

4.2.4 Mutations in ATP binding motifs of Reptin alters its AGR2-binding activity.

Having shown a direct binding between AGR2 and Reptin proteins, we attempted to establish whether or not the presence of ATP has any effect on this interaction. We did this, because Reptin is a member of AAA+ proteins superfamily and has two conserved regions, namely Walker A and B, involved in ATP binding and hydrolysis. To test the effect of ATP addition on AGR2-Reptin complex formation, AGR2 was first captured onto a microtitre well and the titration of GST-Reptin protein that had been pre-incubated with ATP and $MgCl_2$ was added. Interestingly, inclusion of ATP could increase the stability of AGR2-Reptin complex by up to threefold (Figure 4.11 A). Next, we immobilised Reptin protein and added increasing amount of AGR2 protein in the presence or absence of ATP. Again, we observed an increase in the extent of AGR2-Reptin complex formation in the presence of ATP (Figure 4.11 B). However, the change was less pronounced. This indicates that in the presence of the ligand, Reptin undergoes some conformational changes that can be either compromised or are not possible when it is adsorbed onto the polystyrene plate. In addition, conformation of both AGR2 and Reptin proteins may be affected by adsorption onto the solid phase.

As mentioned before, the characteristics of AGR2-Reptin and AGR2 peptides-Reptin interaction can alter depending on the presence of tag or source of the protein. Therefore, we decided to determine whether or not these variables could also affect the impact the presence of ATP exerts on AGR2-Reptin complex. Surprisingly, when AGR2 was captured onto a microtitre well and the titration of untagged prokaryotic Reptin protein or eukaryotic Reptin protein that had been pre-incubated with ATP and $MgCl_2$ was added, we could observe a decrease rather than the increase in the stability of AGR2-Reptin complex (Figure 4.11 C and D). In addition, we immobilised AGR2 peptides and monitored Reptin's binding in the presence or absence of ATP. As before, in the absence of nucleotide, prokaryotically expressed Reptin showed unspecific peptide binding activity in an ELISA assay (Figure 4.11 E). However, addition of ATP could decrease the extent of the interaction, as it did in case of full length proteins binding. Contrary to that, we observed increased binding

of eukaryotic Reptin to AGR2 peptides upon inclusion of ATP. Importantly, Reptin (1) can hydrolyse ATP to ADP (chapter 5), (2) binds ADP (chapter 5) and (3) the crystal structures of Pontin and Reptin complex were solved in the presence of ADP [581]. As such, we monitored Reptin's binding to AGR2 peptides in the presence of ADP. Interestingly, increased binding of eukaryotically expressed Reptin to AGR2 peptides was observed in the presence of ADP compare to the presence of ATP (Figure 4.11 F).

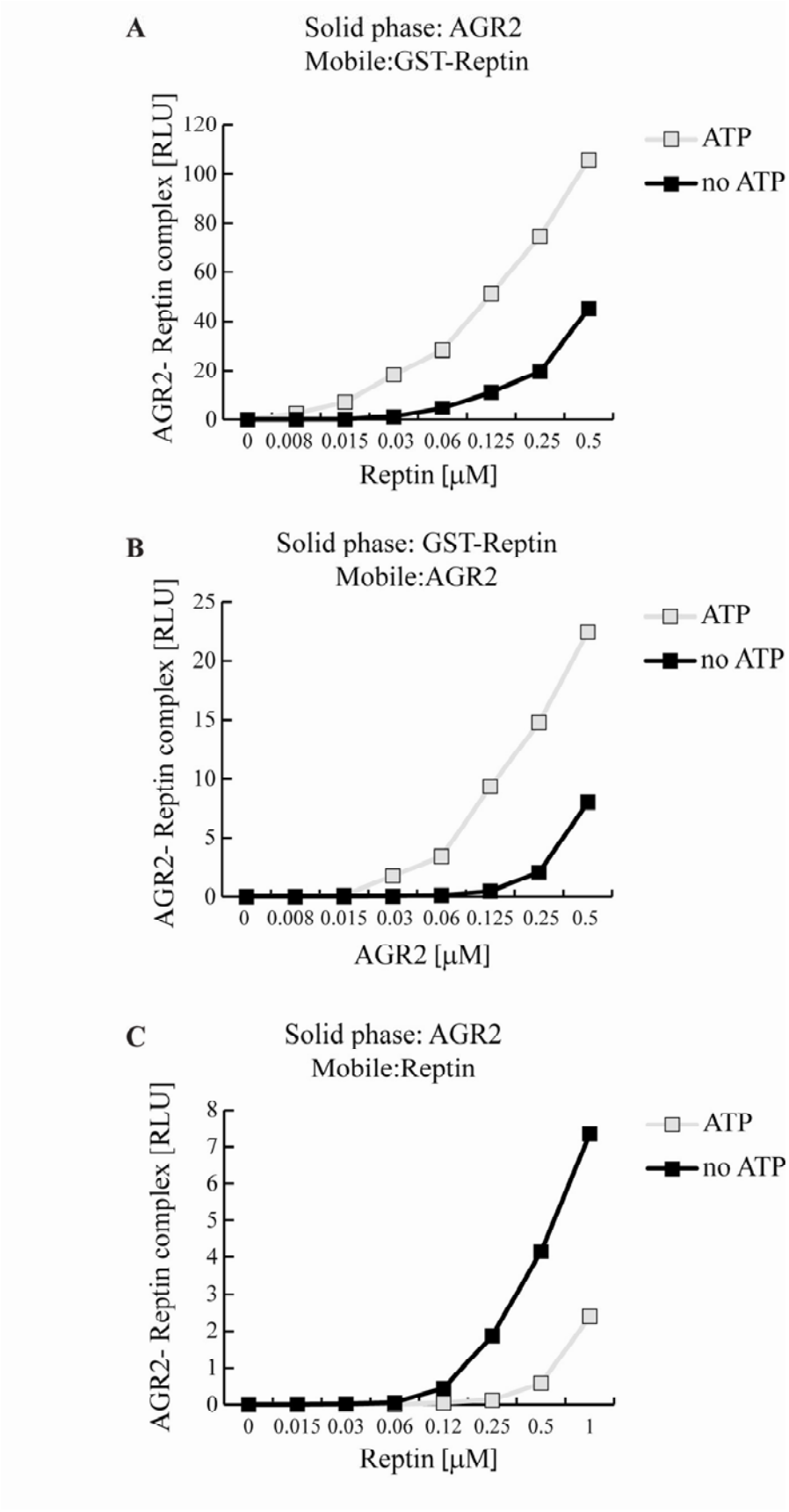
A
Solid phase: AGR2
Mobile:GST-Reptin
AGR2- Reptin complex [RLU]
120
100
80
60
40
20
0
0 0.008 0.015 0.03 0.06 0.125 0.25 0.5
Reptin [μM]
ATP
no ATP
B
Solid phase: GST-Reptin
Mobile:AGR2
AGR2- Reptin complex [RLU]
25
20
15
10
5
0
0 0.008 0.015 0.03 0.06 0.125 0.25 0.5
AGR2 [μM]
ATP
no ATP
C
Solid phase: AGR2
Mobile:Reptin
AGR2- Reptin complex [RLU]
8
7
6
5
4
3
2
1
0
0 0.015 0.03 0.06 0.12 0.25 0.5 1
Reptin [μM]
ATP
no ATP

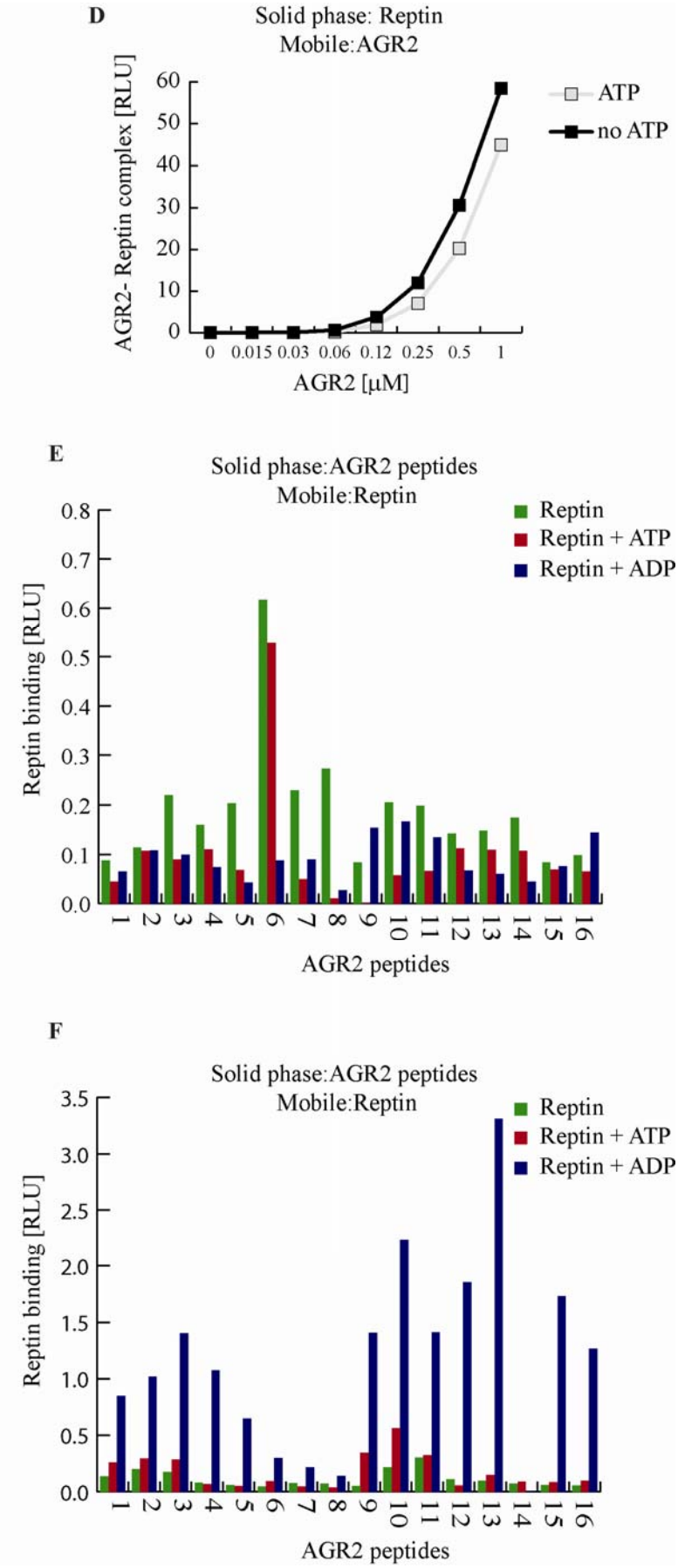
D
Solid phase: Reptin
Mobile:AGR2
AGR2- Reptin complex [RLU]
60
50
40
30
20
10
0
0 0.015 0.03 0.06 0.12 0.25 0.5 1
AGR2 [μM]
ATP
no ATP
E
Solid phase:AGR2 peptides
Mobile:Reptin
Reptin binding [RLU]
0.8
0.7
0.6
0.5
0.4
0.3
0.2
0.1
0.0
1 2 3 4 5 6 7 8 9 10 11 12 13 14 15 16
AGR2 peptides
Reptin
Reptin + ATP
Reptin + ADP
F
Solid phase:AGR2 peptides
Mobile:Reptin
Reptin binding [RLU]
3.5
3.0
2.5
2.0
1.5
1.0
0.5
0.0
1 2 3 4 5 6 7 8 9 10 11 12 13 14 15 16
AGR2 peptides
Reptin
Reptin + ATP
Reptin + ADP

Figure 4.11 ATP modulates AGR2-Reptin complex formation. Either **(A and C)** AGR2 or **(B)** bacterially expressed GST-Reptin or **(D)** untagged bacterially expressed Reptin were immobilized on the solid phase and a titration of either **(A)** bacterially expressed GST-Reptin or **(C)** untagged bacterially expressed Reptin or **(B and D)** AGR2 pre-incubated with or without ATP and $MgCl_2$ was added in the mobile phase. The amount of Reptin or AGR2 bound was quantified with antibodies specific for either protein using chemiluminescence. The data are plotted as the extent of protein-protein complex formation [RLU] as a function of the amount of protein in the mobile phase [μM]. **(E and F)** A fixed amount of the indicated biotinylated peptides (as in **4.7 A**) was added to a microtitre plate coated with streptavidin and incubated with recombinant untagged Reptin expressed in **(E)** *E.coli* or **(F)** insect cells. The amount of Reptin bound was quantified with antibodies specific for Reptin using chemiluminescence. The data are plotted as the extent of protein-peptide complex formation [RLU].

The apparent significance of ATP in the stability of AGR2-Reptin binding led us to investigate the importance of Reptin's nucleotide binding sites in the formation of AGR2-Reptin complex. Therefore, we focused on characterising its two highly conserved AAA domains, namely Walker A and Walker B (Figure 4.12 A). Walker A, also known as the P-loop NTP-binding motif and Walker B (the DEAD motif) are important for nucleotide binding and hydrolysis, respectively. Firstly, we introduced single point mutation in the Walker A and B motifs of Reptin, K83A and D299N. Subsequently, we compared the stability of the complex formation between AGR2 protein and wild type Reptin or Reptin ATP binding site mutants. When AGR2 protein was captured onto the microtitre plate and incubated with the titration of wild type Reptin or Reptin K83A mutant, in the presence or absence of ATP, the latter showed greatly reduced binding to AGR2 (Figure 4.12 B). Interestingly, Walker B mutant had similar to wild type Reptin (possibly enhanced) activity with respect to the AGR2 binding (Figure 4.12 C). We further examined the importance of Walker A and B sites by generating a double mutant, Reptin K83A D299N. Surprisingly, the double mutant showed significant decrease in the ability to bind to AGR2 when compared to the Walker B only mutant activity (Figure 4.12 C). This indicates that the K83A mutation is dominant over the D299N mutation, with respect to AGR2 binding.

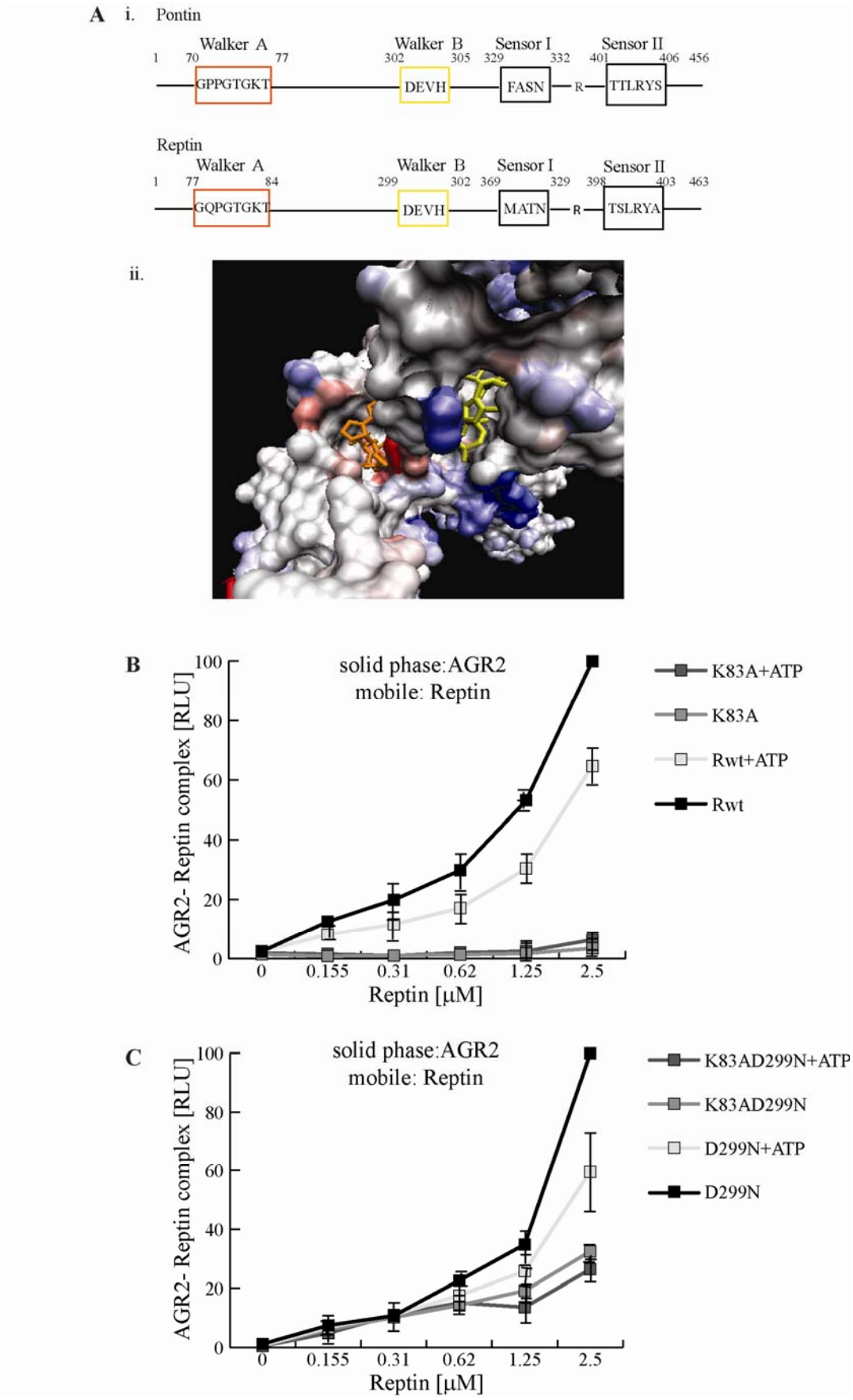
A
i.
Pontin
Walker A
Walker B
Sensor I
Sensor II
1
70
77
302
305
329
332
401
406
456
GPPGTGKT
DEVH
FASN
R
TTLRYS
Reptin
Walker A
Walker B
Sensor I
Sensor II
1
77
84
299
302
369
329
398
403
463
GQPGTGKT
DEVH
MATN
R
TSLRYA
ii.
B
solid phase:AGR2
mobile: Reptin
AGR2- Reptin complex [RLU]
Reptin [μM]
K83A+ATP
K83A
Rwt+ATP
Rwt
C
solid phase:AGR2
mobile: Reptin
AGR2- Reptin complex [RLU]
Reptin [μM]
K83AD299N+ATP
K83AD299N
D299N+ATP
D299N

Figure 4.12 Mutations in ATP-binding site in Reptin affect AGR2-Reptin complex formation (A) (i) The key functional domains of Reptin and its orthologue Pontin are shown including the Walker A and Walker B ATP-binding motifs and the "Sensor" motifs. (ii) Diagram of the structure of human Pontin with the Walker A and B ATP-binding sites highlighted in blue and red; PDB code: Pontin: 2C9O. **(B) The effects of the Walker A site mutation on the formation of Reptin-AGR2 protein complex.** AGR2 protein was immobilised onto the microtitre plate and a titration of either wild type or Reptin K83A proteins pre-incubated with or without ATP and $MgCl_2$ were added. The amount of AGR2 bound was quantified with antibodies specific for either protein using chemiluminescence. The data are plotted as the extent of protein-protein complex formation [RLU] as a function of the amount of protein in the mobile phase [μM]. **(C) The effects of the Walker B site mutation and WalkerA/B double mutation on the formation of Reptin-AGR2 protein complex.** AGR2 protein was immobilised onto the microtitre plate and a titration of either Reptin D299N or Reptin K83A D299N proteins pre-incubated with or without ATP and $MgCl_2$ was added. The amount of AGR2 bound was quantified with antibodies specific for either protein using chemiluminescence. The data are plotted as the extent of protein-protein complex formation [RLU] as a function of the amount of protein in the mobile phase [μM].

4.3 Discussion

Despite the growing amount of data regarding AGR2, we are currently not able to embed it in any particular pathway. Moreover, the mechanism of regulation of this protein is vaguely understood. We reasoned that, expanding on the AGR2 interactome and placing "AGR2 node" in the intricate network of cellular interactions could help to unravel its functions in normal and tumour tissues. There are several experimental approaches to identify novel interacting partners. One of the conventional methods used to identify binary interactions is yeast two-hybrid system. It is worth noting, that there are many limitations of this system that result in a number of existing interactions not being detected. For example, proteins of the secretory compartments or integral membrane proteins often do not interact in the environment of the yeast nucleus. In addition, detecting the binding events that are dependent on post-translational modifications not available in yeast may not be possible [582]. However, the two-hybrid system enables identification of weak or transient protein-protein interactions and since the assay is performed *in vivo*, it is more likely to reveal genuine interactions. As such, we decided to employ this method to investigate the interactome of AGR2. Interestingly, we found that some of the identified proteins have been previously detected in other screens, which had aimed to find AGR2 binding partners. For example, C4.4A and DAG1 were previously identified as potential binding partners for both AGR2 and AGR3 [423]. However, these interactions have not been validated and would require an extracellular localization of AGR2, the latter being controversial, since we could not detect a secreted or transmembrane form of AGR2. In addition E3 ubiquitin- protein ligase HECTD1 was identified in the screen, but we have not investigated this interaction yet neither in human cell systems nor *in vitro*. We decided to examine the interaction between AGR2 and Reptin in more detail for a number of reasons. Firstly, similar to AGR2, Reptin is overexpressed in various cancers. For example, it was shown to be overproduced in hepatocellular carcinoma [583-587]. Moreover data mining using Oncomine, a cancer microarray database, revealed an increased expression of Reptin in gastric [588], bladder [589, 590] and other somatic cancers as well as in Burkitt lymphoma [591]. Secondly, we were encouraged to validate Reptin

and AGR2 interaction, as both these proteins can localise to the nucleus. Specifically, Reptin has a number of nuclear functions, such as DNA repair, replication or transcriptional regulation and we have published the results showing that AGR2 can also localize to nucleus [420]. It is worth noting, that localization of both proteins can be shifted to different compartments of the cell. For example, an aptamer that can interact with AGR2 with high affinity can cause AGR2 to re-localise from the nucleus to the cytoplasmic fraction. Xie et al. showed that Reptin shifted from the nucleus to cytoplasm during the differentiation of 3T3-L1 cells to adipocytes [592]. Therefore, we decided to investigate the AGR2 and Reptin interaction in more detail and indeed using a combination of an *in vitro* experiments and cell-based assays, we were able to validate Reptin as an AGR2 protein binding partner (Figure 4.2, Figure 4.4, Figure 4.6, Figure 4.7). Interestingly, despite the fact that Reptin and Pontin are often found together in large molecular complexes, involved in chromatin remodelling and transcription, and form mixed oligomers, we did not detect Pontin in AGR2 immune complex under the conditions used in this study (Figure 4.4). One of the more recent realizations in the field of protein science is that only a fraction of the protein sequence information is associated with a globular conformation. The remaining parts of the protein sequence remain functional despite being completely disordered or containing long unstructured segments [141]. Often these non-globular regions contain short peptide sequences, namely short linear motifs that are involved in mediating protein-protein interactions, cell compartmentalization or post-translational modifications. As mentioned above, these sites are short, generally up to 10 residues in length and this allows a great evolutionary plasticity [571]. One of the key differences between linear motifs and globular domains is the binding affinity. Contrary to domains, which tend to form high affinity interactions, mini-motifs bind with much lower affinities [593]. Such a property is ideal for signalling networks and other transient interactions. For example linear motifs play an important role in hub proteins, where transiency and flexibility are essential. The p53 protein provides a good example of the hub protein that contains numerous short linear motifs that interact with different proteins. For example only three amino acids of p53 sequence, F19, W23, L26 are essential for the p53-MDM2 interaction and are inserted into a hydrophobic pocket of MDM2 [145]. Short linear motifs are difficult to identify just

by applying the sequence comparison procedures that have been successfully used in the past to discover domains [571]. However, there are resources available that can predict presence of a known motif in a protein of interest. For example, one of the expanding bioinformatic resources for finding peptide motifs is ELM [594]. When used for predicting presence of short linear motifs in AGR2, ELM retrieved several motifs, such as ER retention signal peptide: KTEL. Interestingly, when we used a library of AGR2 overlapping peptides to test whether there are any linear segments that can mediate AGR2-Reptin interaction, we found that peptide 10 could specifically bind to Reptin protein (Figure 4.7). A linear domain was localised by mutagenesis to residues 104-111 of AGR2. Surprisingly, ANCHOR, a server that combines prediction of disorder and binding regions [595], predicted that residues within this region could form protein binding sites. Interestingly, the solution of the structure of ERp18, a member of the ERp18/AGR2/AGR3 family of proteins, revealed a loop insertion, that is only present in ERp18, AGR2 and AGR3 and makes these proteins quite unique amongst other members of the thioredoxin fold proteins [578]. Notably, amino acids 104-111 are present in this divergent loop. The fact that the insert loop is unique for the ERp18/AGR2/AGR3 family led to speculations that this motif could be involved in direct interaction with substrates and mediating substrate specificity [579]. Indeed, insert loop from AGR3 could not bind to Reptin, but following H111 to Y111 mutation, this peptide acquired Reptin binding potential.

In addition peptide 4 from the AGR2 sequence was found to bind to Reptin protein and it could stimulate interaction between the full length proteins (Figure 4.8). It is worth noting, that contrary to the insert loop region; this region is identical in both AGR2 and AGR3. It appears that this region alone is sufficient for AGR2 and Reptin binding at least in an *in vitro* experiment. However, if this is true, it would be interesting to investigate whether or not AGR3 can bind to Reptin *in vivo*. It is possible that even if peptide 4 region is sufficient for binding, the AGR3 cellular localization may eliminate a possibility of the interaction with Reptin. Indeed, we observed differences in subcellular localization of AGR2 and AGR3, the latter being more mitochondrial and in the plasma membrane [420].

Interestingly, the aforementioned ELM search for the presence of the known motifs in the AGR2 sequence revealed that residues 98-112 contain a Leucine-rich nuclear

export signal (NES) binding to Karyopherin receptor 1 (CRM1)/exportin protein. As the name indicates, this motif regulates export of the protein out of the nucleus via nuclear pores [596-598]. The coexistence of overlapping linear motifs within the same region is not unusual. For example the C-terminal portion of p53 is predicted to contain multiple minimotifs that can be specifically bound by different proteins (see 1.2.1.3). As these motifs overlap, the interactions they mediate are exclusive, which allows p53 to switch its interactome depending on the cellular context. We could speculate that when Reptin binds to this region on AGR2 it prevents its interaction with CRM1 and subsequently its nuclear export. Additionally, we have previously reported that AGR2 can inhibit p53 transcriptional activity [437] and possibly via interaction with Reptin, AGR2 escapes cellular nucleus to cytoplasm shuttle system and therefore is able to modulate p53 activity in the nucleus.

Another important implication for the AGR2 and Reptin interaction comes from a study performed by us, in which an aptamer sequence specifically binding to AGR2 was described. The search for the proteins that contain this motif and could potentially interact with AGR2 revealed SMG-7 protein and the interaction was validated *in vitro* (unpublished data). SMG proteins function in the nonsense-mediated mRNA decay (NMD) pathway. NMD pathway recognises and ensures degradation of mRNA that contains premature translation-termination codons and evolved to ensure that only error-free mRNAs are translated [599]. This mechanism involves formation of the multi protein surveillance complex composed of the up-frameshift (UPF) 1-3 proteins and NMD effectors, namely SMG1, SMG5-7. In this complex, SMG1 phosphorylates UPF1, which leads to recruitment of SMG5-7 and results in the decay of bound mRNA. In addition, SMG5-7 mediate dephosphorylation of UPF1, which facilitates recycling of NMD effectors. Interestingly, recently Reptin and Pontin protein were found to associate with SMG1 protein and NMD transacting factors, and siRNA-mediated knock-down of these proteins impaired UPF1 phoshporylation and NMD [390]. The AGR2-SMG7 function in NMD has not been studied yet. We could speculate that AGR2 and Reptin complex have a role in the NMD pathway. As SMG1-mediated phosphorylation precedes SMG-7 binding to the surveillance complex, it is possible that Reptin protein bound to SMG-1 brings AGR2 to the complex. The presence of

AGR2 in this complex may poison Reptin in an inactive conformation or alternatively AGR2 may be required for the Reptin/Pontin mediated formation of the NMD assembly.

In this report we also found, that AGR2 binding to Reptin is modulated by ATP and mutations in ATP binding motifs of Reptin affected the interaction between these proteins. Interestingly, there are other examples of ATP binding proteins with interactome changes as a result of alterations in their functional motifs. For example, substitutions of crucial amino acids in the Walker B motif of Rad51, impairs the formation of Rad51D-XRCC2 and Rad51D-Rad51C complexes [600]. Contrary to AGR2-Reptin complex, Rad51D protein complexes do not require an intact Walker A motif. The crystal structure of Reptin protein has not been solved yet and there is no information about conformational dynamics and structure-function properties of Reptin. As such, it is difficult to establish whether the loss of binding observed as a consequence of Walker A mutation is caused by the mutation-induced changes in conformation, oligomerization or peptide 10/4-binding pocket of Reptin.

Interestingly, Reptin protein is required in the human TIP60 complex. TIP60 has a well-described role in transcription through acetylation of histones, but also other proteins such as the androgen receptor or p53 [230, 231, 360, 361]. Acetylation of K120 of p53 directs it to the promoters of proapoptotic target genes [230, 231]. In addition TIP60 binds to methylated p53 and this is required for subsequent acetylation of p53 and p53-induced cell cycle arrest in response to DNA damage [601]. Given AGR2 inhibitory role in p53-dependent response to DNA damage, it would be interesting to investigate whether AGR2-p53 and TIP60 pathways converge by the Reptin-AGR2 interaction. Intriguingly, TIP60 was found in complex with Pontin and induced expression of anti-metastatic KAI-1 [602]. In this context Reptin antagonised TIP60 function and together with β-catenin acted as a repressor of KAI-1 [367]. It would be interesting to explore whether prometastatic AGR2 uses its substrate-binding loop to differentially chaperone, or inhibit, Reptin transcriptional activity depending on the cellular context of the interaction. Interestingly, there are examples of Reptin interacting proteins that were found to modulate its activity. Tumour suppressor Hint1 was reported to enhance Reptin-induced repression [377]. Contrary to that, endosomal proteins APPL1 and APPL2

could reduce the association between Reptin and HDACs and between Reptin and β-catenin, and thus relieve Reptin-mediated repression [378]. Reptin protein was found to be sumoylated on lysine 456 and sumoylation was found to precede its transport to nucleus and be essential for KAI1 repression. Interestingly, SUMO-modified Reptin appeared not to interact with AGR2 protein. Additionally, two SUMO-processing enzymes: SUMO-sentrin-specific protease 1 (SENP1) and SUMO1-specific proteases 1 (SUSP1) were found to interact with Reptin [376]. Interestingly, we found that Reptin protein was predominantly ubiquitinated rather than sumoylated. It might reflect a cell-specific difference in the type of ubiquitin-like modification that is catalyzed on Reptin.

We have yet to unravel whether AGR2 protein has a role in Reptin-mediated transcriptional events and whether, for instance, it switches Reptin into inactive or activated transcriptional states. Further, we would like to explore whether the allosteric ATP binding motifs of Reptin regulate AGR2 function as a prometastatic factor in cancer. The sets of AGR2 and Reptin mutants that were generated will be useful for such cellular/*in vivo* assays. In addition, as both Reptin and AGR2 can be thought of as potential anticancer drug targets due to their prometastatic functions, biochemical screening assays that utilize the substrate-binding loop of AGR2 or ATP binding motifs of Reptin might be useful in the development of small molecules that regulate this protein-protein complex *in vivo*.

In summary, we report on the first well-validated protein–protein interaction for the pro-oncogenic protein AGR2. Reptin was identified as an AGR2 binding protein in a yeast two-hybrid screen and validated as an AGR2 binding protein in human cells. In the next chapter, detailed biochemical characterization of Reptin is described. We report on Reptin's ATP binding acitivity, ATPase activity and its oligomerization. We compare the wild type Reptin and Walker A and Walker B mutant Reptin proteins and speculate on the role of the Reptin's functional motifs in AGR2-Reptin protein complex formation as well as in modulating other Reptin- related processes.

CHAPTER 5 Biochemical characterisation of Reptin protein

5.1 Introduction

5.1.1 The AAA+ superfamily

A wide diversity of cellular events depends on the presence of complex assemblies of various proteins. Activity of these so called molecular machines depends on the coordinated work of the single components that enables their efficient assembly as well as the enzymatic and modulatory functions. A broad range of these supramolecular complexes comprises proteins belonging to the family of ATPases associated with various cellular activities (the AAA+ family). As the name indicates, this family of proteins performs a myriad of functions and is often referred to as a novel class of chaperones, as it assists in processes such as protein folding and degradation, aggregate disassembly, maintenance of organelle function, transcription, replication, recombination and cellular transport.

The AAA+ superfamily belongs to a large family of P-loop-type nucleoside triphosphate (NTP)-binding proteins [603]. Members of this family bind nucleoside triphosphates, catalyse hydrolysis of the β-γ phosphate bond and use the energy of this reaction to drive different cellular processes. Phylogentic analyses of P-loop NTPases revealed presence of two conserved sequence motifs, commonly called Walker A and B motifs, which bind phosphate moieties of the NTP and a Mg^{+2} cation [603-605]. One of the divisions of the P-loop NTPases, additional strand conserved E family (ASCE), is characterised by an additional β-strand in the core sheet and located between Walker A and Walker B motifs; and the presence of additional conserved catalytic Glutamate in the Walker B motif [606]. The AAA+ superfamily is confined to ASCE division, and in addition to the common sequence and structural arrangements of the ASCE group, it contains a number of unique characteristics [607, 608].

5.1.2 Structural elements of the AAA+ family

All the members of AAA+ superfamily are characterised by the presence of single or multiple regions of 200-250 amino acids, named "AAA+ module". On the basis of the available crystal structures, the module is believed to be made up of two domains: N-terminal α/β Rossman fold and nucleotide binding pocket and a C-terminal α-helical domain [609]. The N-terminal fold consists of the β5-1-5-3-2 sheet flanked on one side by two and on the other side by 3 helices.

The Walker A motif forms a highly conserved loop (the P-loop) between strand β1 and helix α2 and typically assumes the following sequence: GX2GXGK[S/T] (where X is any amino acid). Typically the first two Glycines of the Walker A motif are preceded by a Proline residue [603]. The conserved Lysine forms ionic interaction with the β and γ phosphate oxygens of ATP, whereas the conserved Threonine provides a metal ligand. The Lysine residue within the motif's sequence is crucial as its mutation usually abolishes nucleotide binding [610, 611].

The Walker B motif localises to strand β3 and typically assumes the form hhhhDE (where h represents a hydrophobic amino acid) with the acidic residues being important for ATP hydrolysis and metal coordination [605, 612]. Specifically, the carboxylate side chains of Aspartate and Glutamate project into the active site and are involved in the magnesium coordination sphere and form the catalytic base, respectively [609]. Mutation of the conserved glutamate blocks ATP hydrolysis and traps the substrate in the protein [610, 613]. In addition to Walker A and Walker B motifs, AAA+ superfamily contains additional insertions which are significant for their function. There is also the second region of homology (SRH) comprising Sensor 1/motif C and Arginine fingers in the C-terminal position of where Walker B motif is [607]. Sensor-1 is contained within strand 5 and is characterised by the presence of a conserved polar residue, Asparagine, Serine, Threonine or Histidine. Spatially, it is located between the Walker A and Walker B motifs, and forms polar contacts with the γ-phosphate of bound ATP and elements of the Walker B motif. It is proposed to have a role in ATP hydrolysis via either sensing the bound nucleotide or helping to orientate a water molecule for a nucleophilic attack of the bound nucleotide [614, 615]. The Arginine fingers are located at the loop between

α5 and β5. Typically members of AAA+ family form hexameric rings. This unique arrangement positions Arginine fingers close to the nucleotide bound to the neighbouring protomer and, together with other structural components discussed above, constitute an essential part of the ATP binding pocket. The Arginine fingers are proposed to translate an ATP hydrolysis event into the conformation changes in the adjacent subunit of the oligomer [615]. A conserved Arginine lying in the third helix of the C domain is referred to as a Sensor-2 and is likely to mediate the movement of the C-domain relative to N-domain during nucleotide hydrolysis [608, 609, 616]. Lastly AAA+ superfamily members have Box motifs, such as Box II, which is believed to have role in adenine recognition or Box VII that is involved in nucleotide interaction and intersubunit communication.

5.1.3 ATP hydrolysis

AAA+ proteins use the energy released by ATP hydrolysis to perform their diverse functions. There are two possible mechanisms of ATP hydrolysis. Classically, an associative mechanism is assumed and it requires elements of the ATP-binding pocket discussed above. It is believed to involve the nucleophilic attack of an activated water molecule at the γ-phosphorus of the ATP. This leads to the formation of a negatively charged transition-state, which is stabilised by the magnesium ion and by neighbouring positively charged groups, and hydrogen bond donors. However, the alternative mechanism, namely dissociative mechanism, is possible [617]. In this case, the catalytic base does not activate an attacking water molecule; however the presence of a Glutamate residue in the Walker B motif is required to orientate this water molecule into the appropriate position.

A number of models exist for the nucleotide binding and ATP hydrolysis by hexameric AAA+ ATPases are referred to as concerted or synchronised, and nonconcerted, the latter comprising rotational model and its derivative, sequential model [609]. In the concerted model, all subunits can bind and hydrolyze ATP and release the product simultaneously, and hence the symmetry is preserved. In the nonconcerted model not all the subunits are active; at least not all at the same time. The rotational model proposes that only three subunits are active and are always at

some stage of the reaction cycle. The sequential model predicts the all the subunits are active, but bind and hydrolyze ATP at different times [609].

The evolutionary classification of AAA+ ATPases by Iyer et al. led to formal definition of 26 AAA+ proteins families, amongst them TIP49 family [607]. The unique structural features of this family are the presence of a small N-terminal module and a new domain insertion, which separates Walker A and B motifs by about 170 amino acids [618]. This family comprises Reptin and Pontin in Eukaryotes and has the Archeal representative, namely RuvB, which is involved in branch migration in Holiday junctions [619-621].

5.1.4 Reptin and Pontin- ATP binding and ATPase activity

Despite the fact that for the several members of the AAA+ family the nature of ATP binding, as well as the mechanism of the ATP hydrolysis, are well described, the data available on the enzymatic activity of Reptin and Pontin are somewhat vague and often contradictory.

Some studies were not able to detect an intrinsic ATPase activity for these proteins. For example, Pontin expressed in baculovirus system by Qiu et al. did not catalyze ATP hydrolysis even in the presence of the DNA substrate [622]. Similarly, His-tagged Pontin purified using bacterial expression system had a very low ATPase activity that was not stimulated by addition of nucleic acids [623]. On the other hand, ATP hydrolysis by zebrafish Flag-tagged Reptin produced in insect Sf9 cells depended entirely on the presence of double stranded DNA [624]. Furthermore, rat His-tagged Pontin expressed in *E.coli* had a weak ATPase activity that could be strongly stimulated in the presence of single stranded DNA [625]. In addition, the same group described human Reptin protein as a single stranded DNA-stimulated ATPase [368]. Both reports ruled out stimulation by double stranded DNA. In another study both human and yeast Reptin were found to have an intrinsic ATPase activity [626]. The enzymatic activity was stimulated by single stranded DNA, and it was dependent on the length of the DNA. Interestingly, in this study hexameric fraction of Reptin appeared to be inactive for ATP hydrolysis. Another study of yeast Reptin and Pontin, established that whether alone or in complex, both proteins were

enzymatically active, with the complex displaying the highest activity [627]. Additionally, some reports suggested an absolute requirement for the formation of a stoichiometric complex of Reptin and Pontin to allow efficient ATP hydrolysis. For example, it was found that human TIP60 complex possesses ATPase activity derived from the presence of both Pontin and Reptin, but recombinant Pontin and Reptin on their own had no or very weak ATPase activity, respectively [360]. Similar has been noted for the human small and big H2A.Z-interacting complexes, the former possessing most components of the SRCAP chromatin remodelling and TIP60 HAT complexes, and the latter containing only a subset of SRCAP and TIP60 subunits. Interestingly, contrary to Reptin and Pontin that showed no detectable ATPase activity, small H2A.Z-interacting complex, with Reptin and Pontin being the only ATPases present, had a strong enzymatic activity [628]. Another study showed that the intact functional domains, namely Walker motifs, of both human Reptin and human Pontin are required for the ATPase activity of their dodecameric complex and that the individual proteins do not or weakly hydrolyze ATP [629].

In addition, AAA+ domain mutants were used to manipulate activity of Reptin and Pontin in order to further understand their ATPase activity-related functions. For instance, Walker A and/or Walker B in yeast Reptin and Pontin were individually indispensable for yeast growth and viability [357, 392, 630]. Furthermore, Walker A mutation was found to cause defect in snoRNA acculumulation in yeast [392]. Walker B motif mutations in Drosophila homologs of Reptin and Pontin led to loss in maintenance of Hox gene expression [366]. Similarly, human Reptin and Pontin proteins bearing mutations in Walker B could no longer regulate the abundance of PIKKs [390]. Finally, Walker B mutation in Pontin abolished its ability to maintain wild type levels of TERC [397] and inhibited transformation by Myc [370]. At the same time, many functions of both Reptin and Pontin with these mutations are retained. Overexpression of both wild type and mutant Reptin or Pontin in *Xenopus laevis* embryo led to increased cell division and bent phenotype [364]. Furthermore, intact Walker B in human Reptin was not required for its interference with the influenza virus polymerase activity and virus growth [631] or for the inhibition of basal and inducible transcriptional activities of ATF2 [371].

Members of AAA+ family usually self assemble into oligomers, predominantly hexamers, and this appears to be required for the biological activity [632]. Similarly to other members of AAA+ family, the oligomerization of Reptin and Pontin was observed. Several observations supporting oligomeric, mostly hexameric or dodecameric, nature of both Reptin and Pontin came from sedimentation equilibrium analysis of purified proteins. For instance, the wild type zebrafish Reptin was found to exist as a homotypic hexamer (310 kDa) or dimer (105 kDa) [624]. Pontin co-sedimented with TBP in fractions corresponding to molecular weight of 800 kDa [633] and similar was later observed by Kikuchi et al. and Gohshi et al. [634, 635]. Similarly, human Reptin and Pontin were present in complexes of 800-600kDa [368, 636] or even larger, >2000–500-kDa fractions [368]. In line with these findings, both Reptin and Pontin show 6:1 stoichiometry in comparison to other components of the chromatin remodelling complex INO80.

The low resolution structures of the human or yeast Reptin and Pontin assembly, solved by transmission electron microscopy, concluded the oligomeric nature of these proteins [627, 629, 637]. Specifically, the equimolar mixture of human or yeast Reptin and Pontin proteins, expressed in bacteria or in insect cells, respectively, formed a structure composed of two stacked hexameric rings. Because of the clear asymmetry of this assembly, it was suggested that either each ring is formed exclusively by one of the proteins or that each ring has identical composition but assumed different conformation [629, 637]. Contrary to that, yeast proteins expressed in bacteria were found to form a single hexameric ring [627]. Furthermore, individual proteins existed as monomers at 5 μM, and hexamerized at higher concentration (50 μM) [627]. Moreover, it was found that upon addition of nucleotide and metal cofactor Reptin eluted in a peak corresponding to a molecular mass of about 400 kDa, however Pontin was always monomeric regardless of the conditions used [629]. Opposite to this a recent study found that even in the absence of cofactor fraction of both Reptin and Pontin could form dimers, trimers and hexamers [638]. Discrepancies in these observations arise from the fact, that they are based on the limited resolution of electron microscopy. The differentiation of Reptin and Pontin in their assemblies requires solving the crystal structure of this complex. At this time, only the crystallopgraphic structure of Pontin is available [623]. The X-

ray analysis revelaled that Pontin forms a hexamer, complexed with ADP and each monomer folds into three distinct domains: DI, II and III, where DI and DIII form a typical AAA+ module.

5.2 Results

As mentioned above, there have been many conflicting reports about the properties of Reptin protein with regard to its ATPase activity, ATP binding potential and oligomeric state. In addition mutation in the Walker A and B in Reptin's sequence affected AGR2-Reptin complex formation (as described in chapter 4). To further understand function of Reptin protein, we decided to investigate the biochemical characteristics of Reptin protein in more detail. We reasoned that this knowledge could potentially help us: (1) identifying the roles of Walker A and Walker B with regard to ATP cycle and oligomerization (2) defining factors that may regulate the Reptin and AGR2 complex formation, and (3) subsequently, with the use of cellular systems, understand the physiological role of Reptin on its own or when complexed with AGR2.

5.2.1 ATPase activity of Reptin protein

Previous reports regarding human Reptin protein questioned its intrinsic ATPase activity and implied that only a complex of both Reptin and Pontin was able to hydrolyze ATP efficiently. However, Reptin protein is often found to function independent of Pontin *in vivo* and in these instances it should retain its catalytic activity. We hypothesised that the negligible hydrolytic activity of Reptin reported by different studies could be caused by the inactivation of protein during its preparation and we were interested to see whether or not our method of purification of Reptin protein retained its activity. Accordingly, we sought out to determine the ATPase activity of Reptin protein. To this end, we set up an assay that utilises radioactively labelled ATP and measures the amount of free phosphate released upon incubation of the protein with the nucleotide. A previous report showed that bacterial

RuvB has a high affinity for double stranded DNA. Moreover, some groups suggested that human Reptin could be stimulated by addition of single stranded DNA (see 5.1). Therefore, we also set out to investigate whether or not single stranded DNA modulated ATPase activity of Reptin. To this end, prokaryotically expressed Reptin protein was incubated with γ-^{32}PATP and with or without single stranded short DNA fragment or single stranded, circular DNA from M13 phage. Interestingly, Reptin had a relatively low intrinsic ATPase activity (Figure 5.1 B and D and lane 1 in A and C). However, its activity increased in the presence of single stranded DNA, both linear (Figure 5.1 A and B) and circular (Figure 5.1 C and D). This is in agreement with the original study of Reptin protein that indicated that it has a DNA-stimulated ATPase activity. In the current study, as little as 0.5 pmol of short oligonucleotide sequence or 4 fmol of M13 DNA induced ATPase activity of Reptin by eight-fold (Figure 5.1).

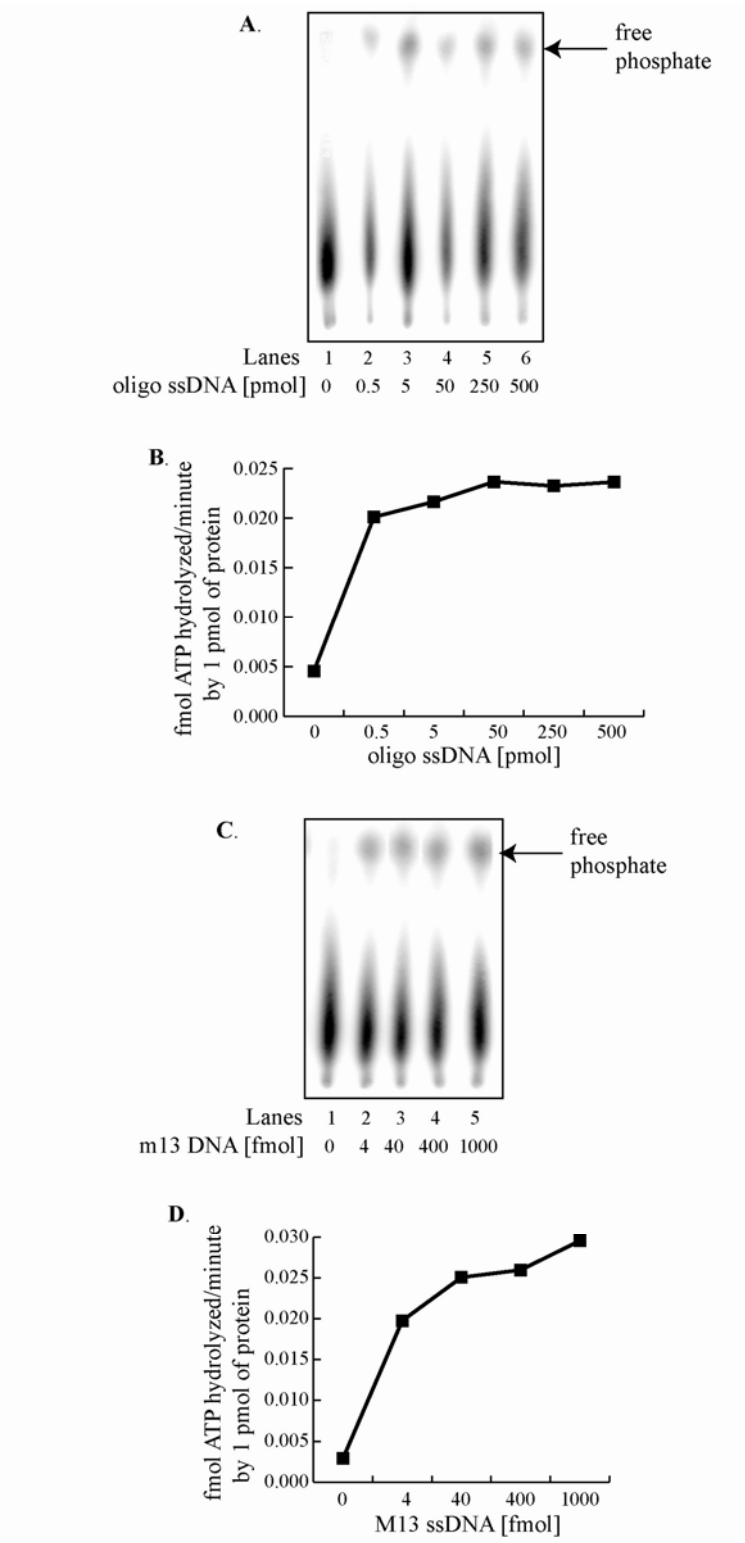

Figure 5.1 ATPase activity of Reptin is stimulated by DNA. ATPase activity was carried out in the buffer containing 0.15 μM γ^{32}P-ATP and 0.1mM non-radioactive ATP. Reptin protein was added in the presence or absence of the titration of DNA substrates: **(A and B)** single-stranded oligonucleotide or **(C and D)** single stranded DNA from M13 phage and incubated for 90 minutes at 37ºC. Reaction products were separated by TLC, exposed to phosphoimager screen and quantified using Phospoimager. **(B and D)** The data are plotted as fmol of ATP hydrolysed per 1 minute by 1 pmol of Reptin protein.

Next, we examined the effects that changes in the temperature exert on ATP hydrolysis by Reptin protein. To this end, Reptin protein was incubated with γ-^{32}PATP and with or without single stranded or double stranded DNA, at temperatures ranging from 0ºC to 42ºC (Figure 5.2 A and B). The ATPase activity of Reptin protein at 0ºC and 20ºC was not detectable. We found that the maximal enzymatic activity of Reptin protein could be reached at the physiological temperature (37ºC) and increasing the temperature further to 42ºC did not enhance it. Interestingly, at 30ºC double stranded DNA caused a more pronounced stimulation of ATP hydrolysis by Reptin protein compare to that induced by single stranded DNA. However, at higher temperatures, there was no significant difference between single and double stranded DNA-mediated increase in Reptin's ATPase activity.

Next, we determined the time course of ATP hydrolysis. Again, Reptin protein was incubated with γ^{32}P-ATP and with or without single stranded DNA and the amount of hydrolyzed ATP was measured at the different time points, ranging from 10 to 90 minutes (Figure 5.2 C and D). We found that incubation for up to 20 minutes resulted in a very low amount of the free phosphate released and it could not be stimulated by the addition of single stranded DNA. However, increasing time of incubation further to 45 or 90 minutes resulted in reaching a steady-state rate of Reptin's ATPase activity.

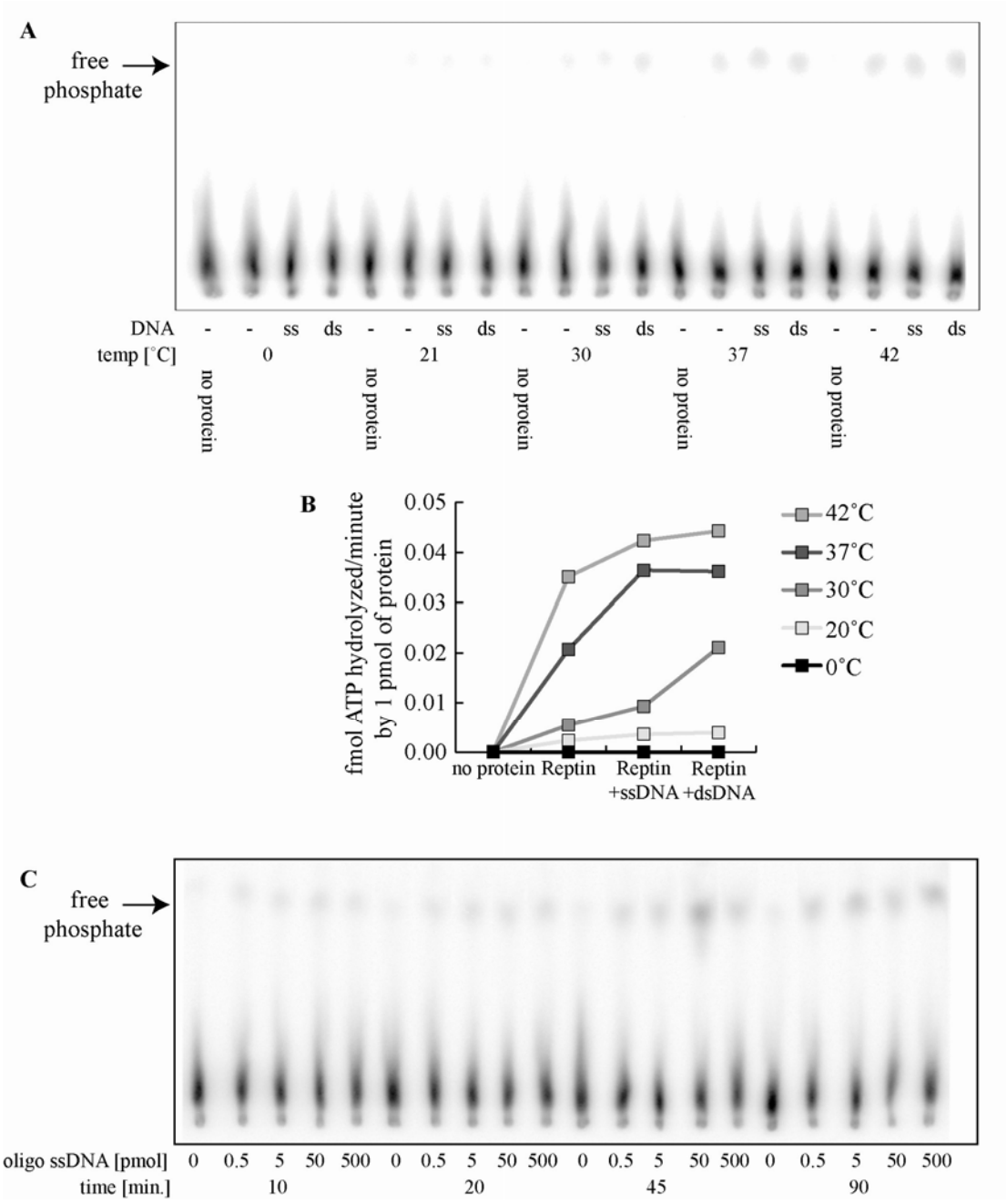
A
free
phosphate
DNA - - ss ds - - ss ds - - ss ds - - ss ds - - ss ds
temp [°C] 0 21 30 37 42
no protein
no protein
no protein
no protein
no protein
B
fmol ATP hydrolyzed/minute
by 1 pmol of protein
0.05
0.04
0.03
0.02
0.01
0.00
no protein
Reptin
Reptin +ssDNA
Reptin +dsDNA
42°C
37°C
30°C
20°C
0°C
C
free
phosphate
oligo ssDNA [pmol] 0 0.5 5 50 500 0 0.5 5 50 500 0 0.5 5 50 500 0 0.5 5 50 500
time [min.] 10 20 45 90

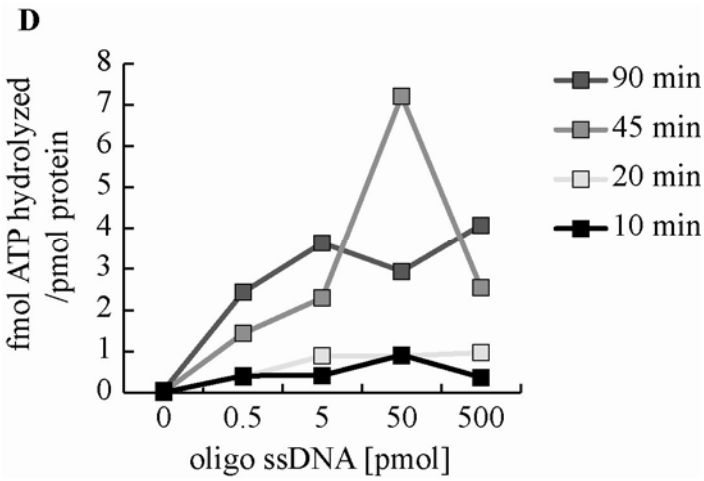

Figure 5.2 Time-dependence and temperature-dependence of ATPase hydrolysis by Reptin. ATPase activity was carried out in the buffer containing 0.15 μM γ^{32}P-ATP and 0.1 mM non-radioactive ATP. Reptin protein was added in the presence or absence of the DNA substrates and either **(A and B)** incubated for 90 minutes at 0ºC to 52ºC or **(C and D)** incubated at 37ºC for 10 to 90 minutes. Reaction products were separated by TLC, exposed to phosphoimager screen and quantified using Phospoimager. The data are plotted as **(B)** fmol of ATP hydrolysed per 1 minute by 1 pmol of Reptin protein or **(D)** fmol of ATP hydrolysed per 1 minute by 1 pmol of Reptin protein.

As mentioned before, Walker A and Walker B motifs play an important role with regard to AGR2 binding. Previous reports on the members of AAA+ ATPases indicated that the hydrolysis of the nucleotide required the intact Walker A and B motifs. Therefore, we were interested to determine whether single point mutation in the Walker A and B motifs of Reptin, affected its enzymatic activity. To this effect, we incubated wild type or mutant Reptin proteins in the presence of radioactive ATP and with or without single stranded DNA and monitored the amount of hydrolyzed ATP (Figure 5.3). Surprisingly, both Reptin K83A and Reptin D299N mutants were active in this assay. In fact, they appeared to have enhanced enzymatic activity compare to wild type protein. Interestingly, it was not further stimulated by the incubation with either linear (Figure 5.3) or circular single stranded DNA (data not shown). In fact, the addition of DNA seemed to decrease the amount of hydrolyzed ATP.

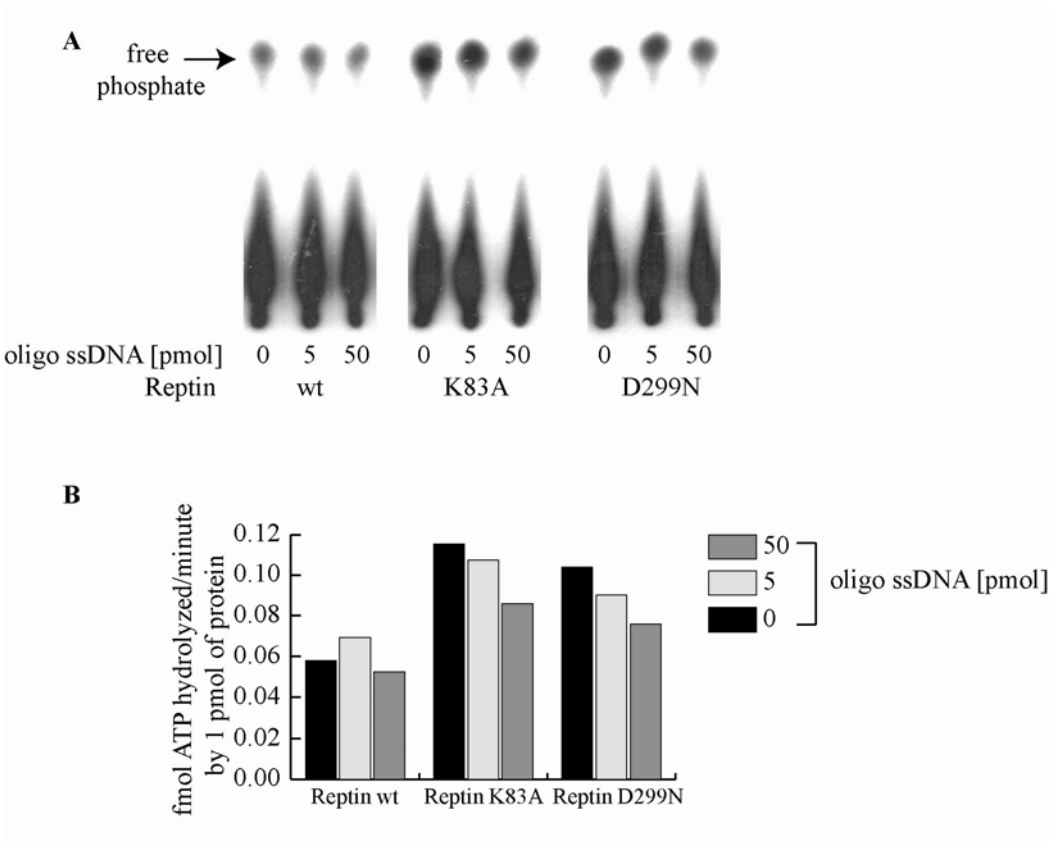

Figure 5.3 Reptin protein retains ATPase activity despite the presence of single point mutations in its functional motifs. (A) ATPase activity was carried out in the buffer containing 0.15 μM γ^{32}P-ATP and 0.1 mM non-radioactive ATP. Wild type Reptin, Reptin K83A or Reptin D299N proteins were added in the presence or absence of the DNA substrates and incubated for 90 minutes at 37ºC. Reaction products were separated by TLC, exposed to phosphoimager screen and quantified using Phospoimager. **(B)** The data are plotted as fmol of ATP hydrolysed per 1 minute by 1 pmol of Reptin protein.

5.2.2 ATP binding activity of Reptin

Having established that ATP regulates AGR2 and Reptin interaction and that Reptin's functional domains could regulate AGR2-Reptin binding, we sought out to study Reptin's ATP binding activity in more detail. In addition, we reasoned that characterisation and quantification of Reptin-nucleotide interaction could be crucial for understanding ligand-induced conformational and/or functional changes in Reptin protein. Moreover, if AGR2-Reptin complex has an oncogenic function that is modulated in the presence of nucleotide, understanding the kinetics of the ligand binding could be essential for any subsequent drug discovery attempts.

5.2.2.1 ATP binding by thermal shift assay.

Firstly, we analyzed Reptin's ATP binding potential using thermal shift assay. This method allows the evaluation of protein-ligand interactions, by monitoring changes in the melting temperature of the respective protein in the presence or absence of a ligand. Specifically, SYPRO Orange can be used, that fluoresces upon binding to the exposed hydrophobic regions or unfolded regions of proteins. For example, ligand binding can change the stability of a target protein, which would be reflected as a change in the rate of unfolding as a function of increasing temperature. Interestingly, we detected a high basal fluorescence of Reptin at room temperature, in the absence of ATP, which gradually reduced as the temperature increased (Figure 5.4 A). In fact, under ligand-free conditions, Reptin did not undergo a classic unfolding transition. This result indicates that the ATP binding regions on Reptin protein are hydrophobic and are exposed or not occupied in the absence of ATP. SYPRO Orange can therefore bind and this results in high fluorescence readings. When the temperatures increases, in the absence of ATP, hydrophobic regions of Reptin become concealed and a gradual drop in fluorescence is observed. In support of this hypothesis, we observed that when ATP was added to Reptin protein and ATP binding pockets were occupied, the fluorescence at the room temperature was greatly reduced compare to that observed in the absence of ATP. Upon increasing temperature in the presence of ATP, the increase in SYPRO Orange

was observed (Figure 5.4 A). When the negative first derivatives of the fluorescence intensity versus temperature were plotted, the minimum of the resulting curve corresponded to the melting temperature of 51ºC (Figure 5.4 B). It is worth stressing, that the apparent changes in the melting profile of Reptin protein in the presence versus absence of the ligand clearly indicate that the recombinant Reptin protein can indeed interact with ATP.

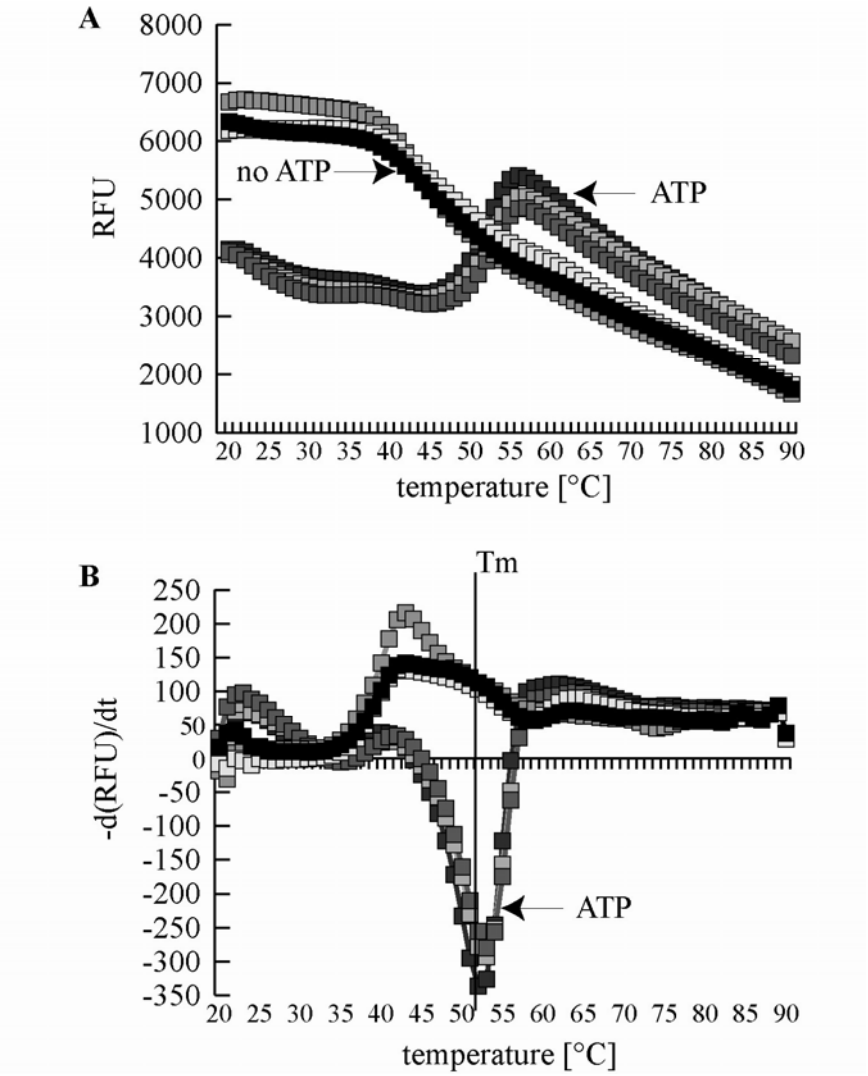

Figure 5.4 Reptin undergoes classic ligand-induced unfolding transition. Reptin protein (5 μM) was heated from 20°C to 90°C, in the absence or presence of ATP and Sypro Orange fluorescence was measured. Experiments were carried out in triplicate. **(A)** The raw data and **(B)** the gradient of protein unfolding was plotted against the temperature gradient to obtain the mid point temperature of transition (Tm) in the absence and presence of ATP.

5.2.2.2 ATP binding activity by nitrocellulose filter binding assay

Having established that Reptin protein was enzymatically active and melted upon addition of ATP, we sought to further characterise its ATP binding activity. To this end we used previously described nitrocellulose filter-based ATP binding assay [639]. In this method, the protein is incubated with radioactively labelled ATP and then the entire reaction volume is transferred to nitrocellulose filter. Next, the unbound ATP is washed away and liquid scintillator used to measure the amount of radioactivity retained on the filter. The latter reflects the amount of ATP bound to the protein of interest. The assay can be used to establish the stoichiometry of a protein-ligand complex. The specificity of the protein-ligand binding can be monitored by the addition of unlabelled ligand, which should compete with the radiolabelled molecule for the binding to the respective protein.

To determine ATP binding potential of Reptin protein, first increasing amounts of Reptin protein were incubated with α^{32}P-labeled ATP. It was found that Reptin protein could indeed bind ATP and this was proportional to the amount of protein (Figure 5.5 A). We established that approximately 0.5 mol of ATP can be bound per 1 mol of Reptin. Interestingly, when we used the nonhydrolyzable ATP analogue, namely γ-S-labelled ATP, only 0.18 mol of ATP could bind per 1 mole of Reptin protein. The decreased affinity for nonhydrolyzable analogue of ATP suggests that a hydrolysis process is required for efficient ligand binding. It is also possible that this analogue does not functionally mimic ATP. Other nonhydrolyzable analogues of ATP, such as PNP-AMP, could be used to test these hypotheses.

Next, Reptin protein was incubated with a constant amount of α^{32}P-ATP in the presence of increasing amounts of nonradioactive ATP ranging from 10 μM to 1 mM (Figure 5.5 B). The amount of unlabelled ATP added appeared to reach saturating levels, since we observed that almost all the radioactively-labelled ATP was found in the unbound fraction. Therefore, we were interested to see how the addition of lower amounts of unlabelled ATP would affect Reptin's ATP binding. Interestingly, the inclusion of unlabelled ATP in concentrations ranging from 1 μM to 1 mM revealed biphasic concentration dependence (Figure 5.5 C). Specifically, the binding of labelled ATP decreased gradually upon addition of 1 to 5 μM or 20 to 1000 μM ATP

but increased at 10 to 20 μM. This indicates that Reptin possesses at least two ATP binding sites, one with high and the other with relatively low ATP binding activity. It is worth stressing, that if Reptin protein does have two binding pockets for ATP, the measured stoichiometry should be 2 moles of ATP per 1 mole of Reptin. As the measured stoichiometry was just 0.5 moles per 1 mole of Reptin, we could speculate on a negative cooperativity between the two ATP binding pockets on the protein. Alternatively, the method used to assess ATP binding somewhat understates Reptin's ATP binding potential. In addition, although we consistently observed these two phases; the range of concentrations of the cold ATP where these occurred varied between experiments. This could be due to the fact that different preparations of the Reptin protein were used.

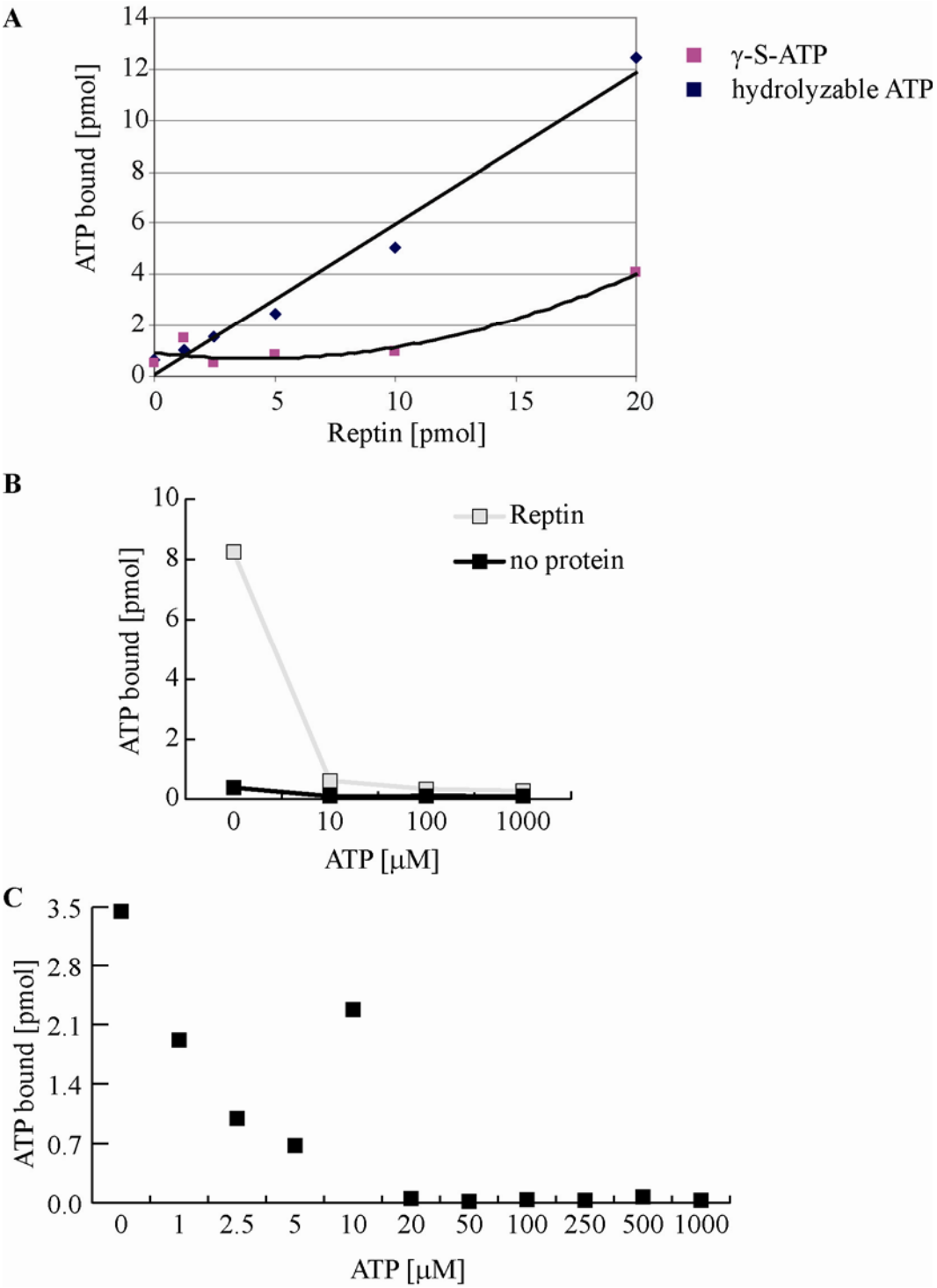

Figure 5.5 ATP binding activity of Reptin protein. (A) A titration of Reptin protein was incubated in the presence of 1 μM ATP and either radioactive α^{32}P-ATP or γ^{35}S-ATP. The amount of radioactive ATP bound to a nitrocellulose filter was measured with the use of scintillation counter. The data are plotted as pmol of ATP bound as a function of Reptin protein levels (pmol). **(B and C)** Reptin protein was incubated in the presence of α^{32}P-ATP and the titration of unlabelled ATP. The amount of radioactive ATP bound to a nitrocellulose filter was measured with the use of scintillation counter. The data are plotted as pmol of ATP bound as a function of the concentration of nonradioactive ATP added (μM).

Having established the stoichiometry of ATP binding to wild type Reptin protein, we were interested to characterise the ATP binding activity of the Walker A and Walker B mutants. This was especially intriguing, considering that we found that both mutants could effectively hydrolyze ATP. Firstly, wild type or mutant Reptin proteins were incubated with a constant amount of γ^{35}S-labeled ATP in the presence of a titration of hydrolysable ATP ranging from 10 μM to 1 mM and the amount of bound radiolabeled ATP was measured as described above. As expected, the wild type Reptin protein could bind to ATP and this was inhibited by the addition of an excess of unlabelled ATP (Figure 5.6 A). Interestingly, we found that mutating the conserved Lysine 83 residue to Alanine within the Walker A motif completely abolished ATP binding. Surprisingly, replacement of the Glutamate 299 residue within the Walker B motif not only retained ATP binding activity, but it increased it compare to that of wild type Reptin. In order to further analyse the effects of mutation on the ATP binding a titration of these proteins was incubated with nonhydrolyzable ATP analogue γ^{35}S-ATP in the presence of 1 μM of non-radioactive ATP (Figure 5.6 B). Again, the Walker A mutant exhibited a reduced binding affinity, whereas the Walker B mutant had greatly enhanced affinity for ATP compare to the wild type Reptin. The similar was observed when the proteins were incubated with radioactive γS-ATP in the presence of nonradioactive nonhydrolyzable ATP (Figure 5.6 C). The data obtained for the Walker A mutant, indicates that this mutation attenuates ATP binding by the remaining Walker B site. On the other hand the increased binding affinity observed for the Walker B mutant, suggests that this motif may exert inhibitory effect on Reptin's ATP binding potential. As Walker B mutant exhibited increased nucleotide binding, we wanted to evaluate whether introducing this mutation had changed thermostability of this protein. To this effect, the thermal shift assay was performed. Surprisingly, contrary to the wild type protein, Reptin D299N could undergo unfolding transition in the absence of the ligand. Addition of ATP resulted in stabilisation of the mutant protein, as indicated by 15ºC increase in the melting temperature (Figure 5.6 D).

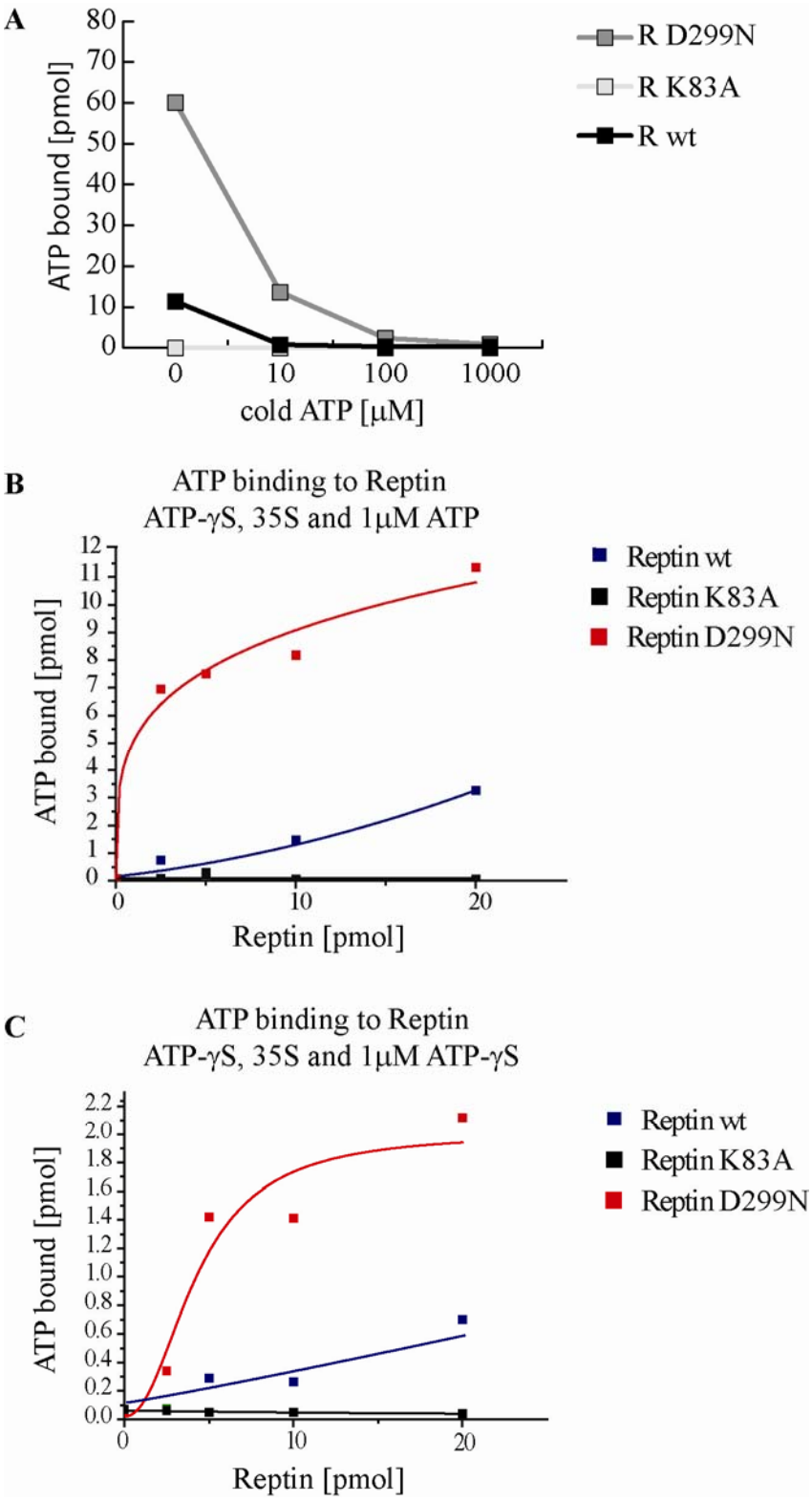
A
ATP bound [pmol]
cold ATP [µM]
R D299N
R K83A
R wt
B
ATP binding to Reptin
ATP-γS, 35S and 1µM ATP
ATP bound [pmol]
Reptin [pmol]
Reptin wt
Reptin K83A
Reptin D299N
C
ATP binding to Reptin
ATP-γS, 35S and 1µM ATP-γS
ATP bound [pmol]
Reptin [pmol]
Reptin wt
Reptin K83A
Reptin D299N

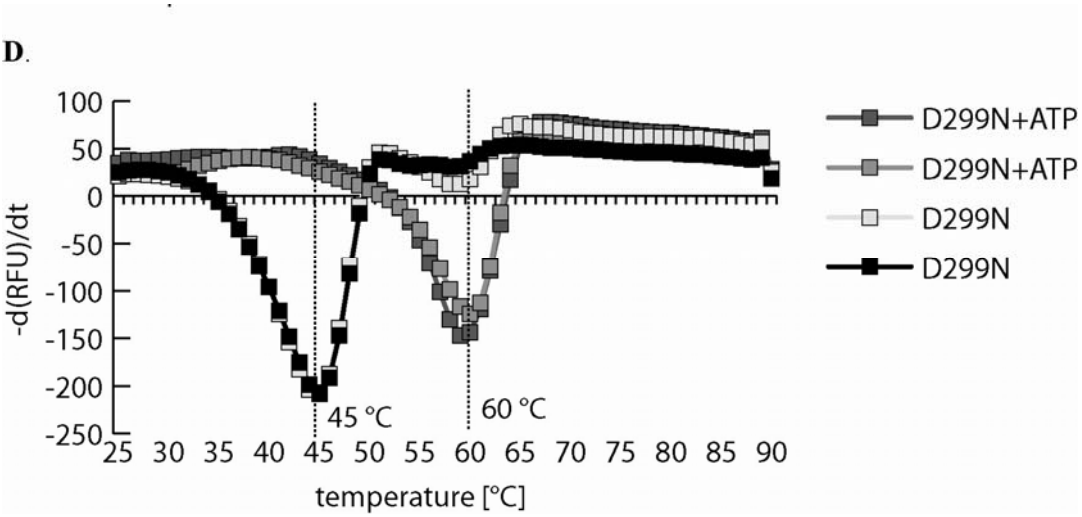

Figure 5.6 The effects of Reptin Walker A and B motifs mutation on ATP binding activity. (A) Wild type Reptin, Reptin K83A or Reptin D299N proteins were incubated in the presence of γ^{35}S-ATP and the titration of unlabelled ATP. The amount of radioactive ATP bound to a nitrocellulose filter was measured with the use of scintillation counter. The data are plotted as pmol of ATP bound as a function of the concentration of nonradioactive ATP added (μM). **(B and C)** A titration of wild type Reptin, Reptin K83A or Reptin D299N proteins was incubated with γ^{35}S-ATP in the presence of either 1 μM **(B)** ATP or **(C)** ATP-γS. The amount of radioactive ATP bound to a nitrocellulose filter was measured with the use of scintillation counter. The data are plotted as pmol of ATP bound as a function of Reptin protein levels (pmol) **(D)** Reptin D299N protein (5 μM) was heated from 20°C to 90°C, in the absence or presence of ATP. Sypro-orange fluorescence was measured. Experiments were carried out in triplicate. The gradient of protein unfolding was plotted against the temperature gradient to obtain the mid point temperature of transition (Tm) in the absence and presence of ATP.

5.2.2.3 ATP binding activity by ELISA

At the moment the function of Reptin-AGR2 assembly is not known, however, both proteins can individually, or as a complex, be thought of as potential anticancer drug targets. In the previous chapter we thoroughly validated Reptin as AGR2 binding partner and showed the importance of ATP interacting sites in Reptin for complex formation. In addition, we reported that addition of nucleotide modulated stability of the complex, albeit the effect altered depending on the method of purification of Reptin protein. We hypothesised that these differences may represent the actual plasticity of the Reptin protein. As such, it would be valuable to develop small molecules that could specifically target ATP binding pockets. These compounds could serve as a useful tool to study biochemistry of Reptin protein as well as to modulate AGR2-Reptin complex, and subsequently establish the function of this complex *in vivo*. Therefore, we decided to develop a high throughput screening method that would allow an efficient testing of a large number of molecules in the future. As we were particularly interested in creating molecules that would target the ATP binding pockets in Reptin, an ELISA method was developed which will allow monitoring of the effect a drug X has on Reptin-ATP interaction. In addition this was another assay that could confirm Reptin's ATP binding ability. To this effect, a range of biotinylated ATPs were used, that differed in the way that biotin side groups were attached. Namely, N6-(6-Amino)hexyl-adenosine-5'-triphosphate-Biotin, 8-[(6-Amino)hexyl]-amino-adenosine-5'-triphosphate-Biotin, 2'/3'-O-(2-Aminoethyl-carbamoyl)-adenosine-5'-triphosphate-Biotin, γ-[6-Aminohexyl]-adenosine-5'-triphosphate-Biotin, Biotin-11-adenosine-5'-triphosphate, Biotin-17-adenosine-5'-triphosphate (called N6-, 8-, EDA, γ-, 11-, 17-ATP thereafter) were utilised (Figure 5.7 A). Firstly, we wanted to establish wheter Reptin could bind any of the six biotinylated ATPs. To this effect, a range of biotinylated ATPs was immobilized onto a 96-well plate and incubated with the Reptin protein. We found that Reptin protein could bind all the ATPs, albeit to a different extent depending on the type of biotinylated ATP used (Figure 5.7 B). Next, the specificity of the Reptin-biotin ATP binding was confirmed in a competition assay. To this effect a titration of Reptin protein was preincubated with a titration of

the ATP and then added to biotinylated N6-ATP immobilised on the ELISA plate. We found that the incubation with ATP could decrease Reptin's binding to biotinylated ATP (Figure 5.7 C) and confirmed the specifity of Reptin-ATP binding in this assay.

Having confirmed that Reptin protein can bind ATP, we went on characterising the oligomerization status of Reptin protein in the presence and absence of the nucleotide ligand.

A

N6-ATP

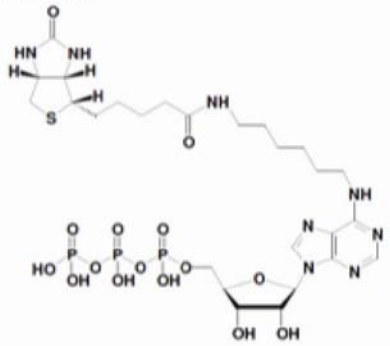

8-ATP

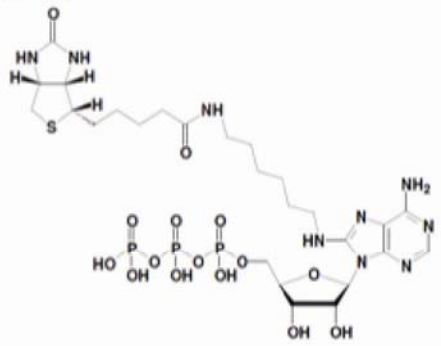

EDA-ATP

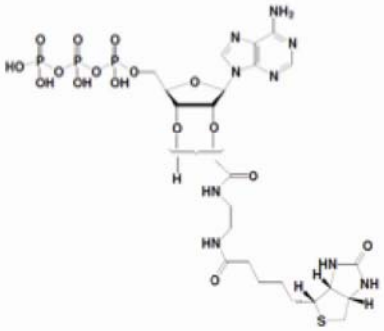

γ-ATP

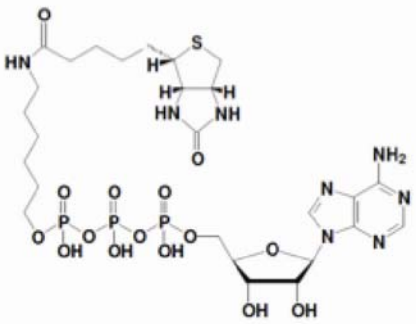

11-ATP

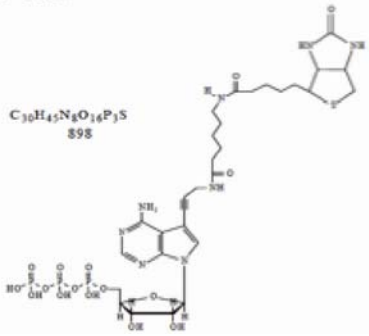

17-ATP

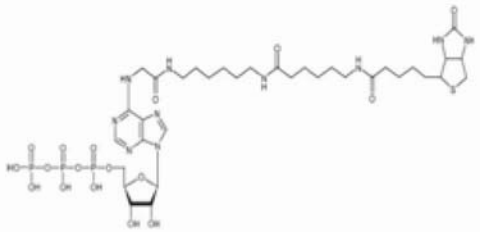

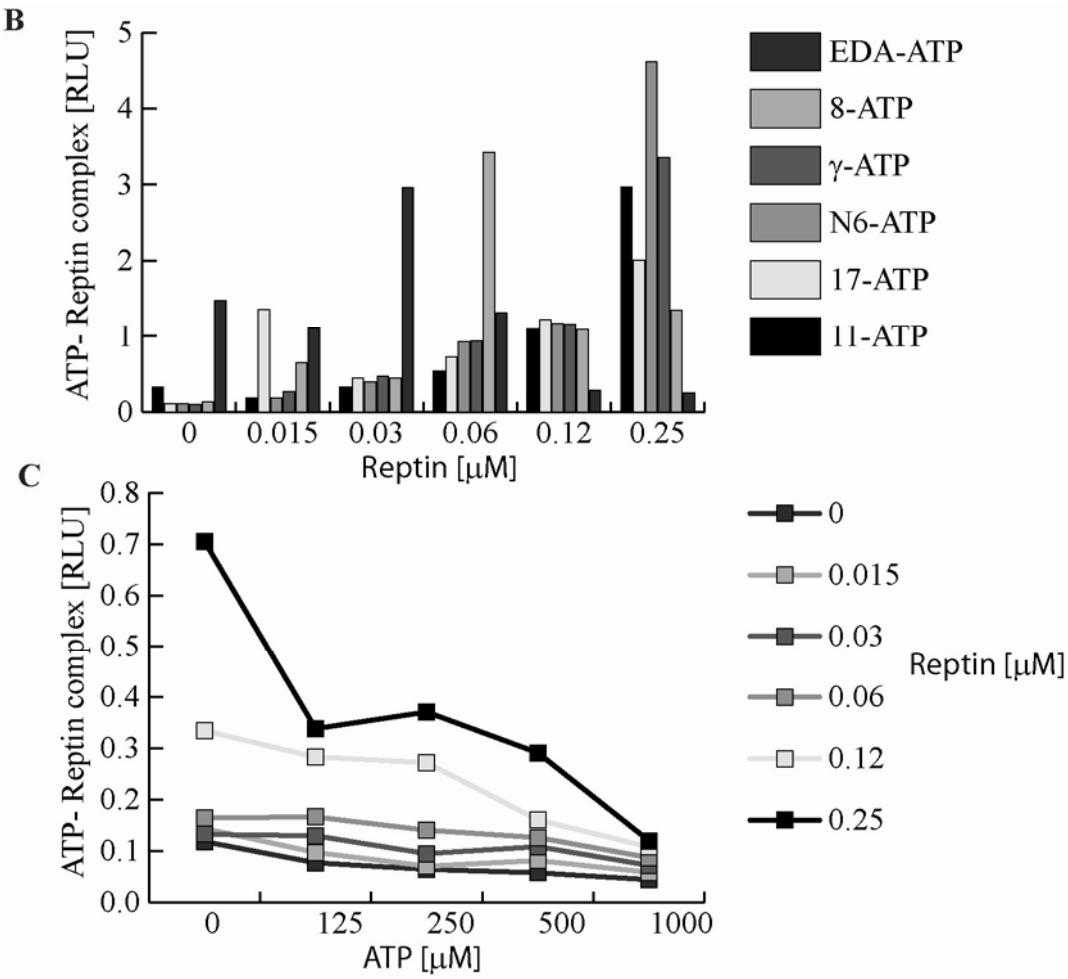

Figure 5.7 Developping non-radioactive ATP binding assay. (A) Schematic of biotinylated ATPs. **(B and C) Reptin protein interacts with biotinylated ATP.** A fixed amount of the indicated biotinylated ATPs (as in **4.7 A**) was added to a microtitre plate coated with streptavidin and incubated with **(B)** a titration of Reptin protein or **(C)** a titration of Reptin protein preincubated with a titration of ATP. The amount of Reptin bound was quantified with antibodies specific for Reptin using chemiluminescence. The data are plotted as the extent of protein-ATP complex formation [RLU]

5.2.2.4 Oligomerization of wild type and mutant Reptin

To assess Reptin oligomerization, we first used Dynamic Light Scattering (DLS) method. This technique determines the hydrodynamic size of the molecule of interest in solution and is routinely applied as a quick way to assess whether the buffer conditions used render the protein monodisperse, non-aggregated; or to determine its oligomeric state. Firstly, measurement of the hydrodynamic diameter of untagged Reptin protein with the use of DLS revealed that our preparation of Reptin did not form aggregates. In addition it had a relatively homogenous nature and consisted of a mixture of monomers, dimers, trimers and hexamers (Figure 5.8 A). Interestingly, upon addition of ATP, the apparent mass was shifted towards the higher values. This indicated that ligand binding results in changes in oligomerization of Reptin protein (Figure 5.8 B).

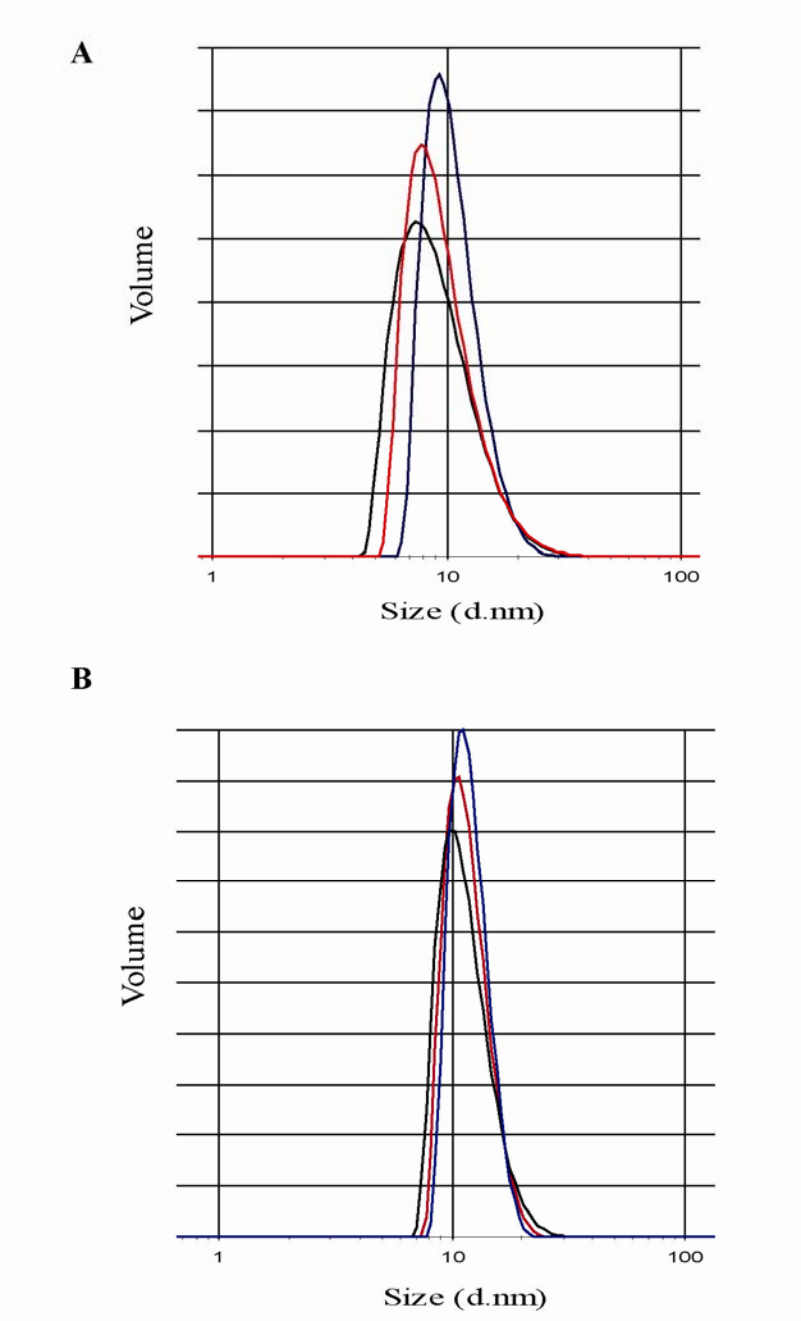

Figure 5.8 Oligomeric state of Reptin protein as defined by DLS. Reptin protein (50 μM) was subjected to analysis by light scattering in **(A)** the absence and **(B)** presence of ligand ATP, as indicated in the Methods.

Next, we sought to set up an assay that could complement the DLS method and allow us to easily determine the oligomeric state of Reptin protein under different conditions. We decided to try chemical cross-linking, as we reasoned that this method could be especially useful given that it enables one to observe both stable and transient events. Glutaraldehyde, homobifunctional amine cross-linker was used as a cross-linking chemical. Firstly, a titration of the cross-linker was incubated with wild type Reptin in the presence or absence of ATP, and compared to non-cross-linked protein (Figure 5.9 A, lanes 1-5 vs. 6). Interestingly, increasing addition of the cross-linker yielded an oligomeric ladder (Figure 5.9 A, lanes 1-5). A pool of Reptin protein showed to be resistant to cross-linking even at the highest concentration, which was reflected by the presence of the band corresponding to the monomeric protein. The inclusion of ATP did not result in a significant change in the oligomerization of Reptin (Figure 5.9 A, lanes 7-11). This was not surprising, since when using DLS we did not observe separate peaks that would indicate exclusive oligomeric states, but only a shift in the mass. We then went onto characterising Reptin Walker A and B mutants in the cross-linking assay. Interestingly, the respective mutant proteins exhibited striking and opposing behaviour to each other and to wild type Reptin (Figure 5.9 D and E). Specifically, in the absence of ATP, Walker B mutant protein was very sensitive to loss of monomeric subunit as a function of increasing concentration of cross-linker (Figure 5.9 C, lanes 1-5), but was resistant to cross-linking in the presence of the ligand (Figure 5.9 C, lanes 7-11). Contrary to Reptin D299N, Reptin K83A demonstrated similar to the wild type protein behaviour in the absence of ATP (Figure 5.9 B, lanes 1-5) but exhibited a very efficient loss of the monomeric state in the presence of ATP (Figure 5.9 B, lanes 7-11). These latter data was unexpected, since in the nitrocellulose filter ATP binding assay, Walker A mutant appeared not to bind ATP. The differential response to the cross-linker in the presence versus absence of the ligand indicates that this protein can in fact bind ATP. These results suggest that the mutation in either of the ATP motifs leads to conformationally different proteins, in respects to both oligomerization and ATP binding. Interestingly, in the case of wild type Reptin protein, where two motifs are intact, the contribution from both of them results in the oscillating response to the ligand.

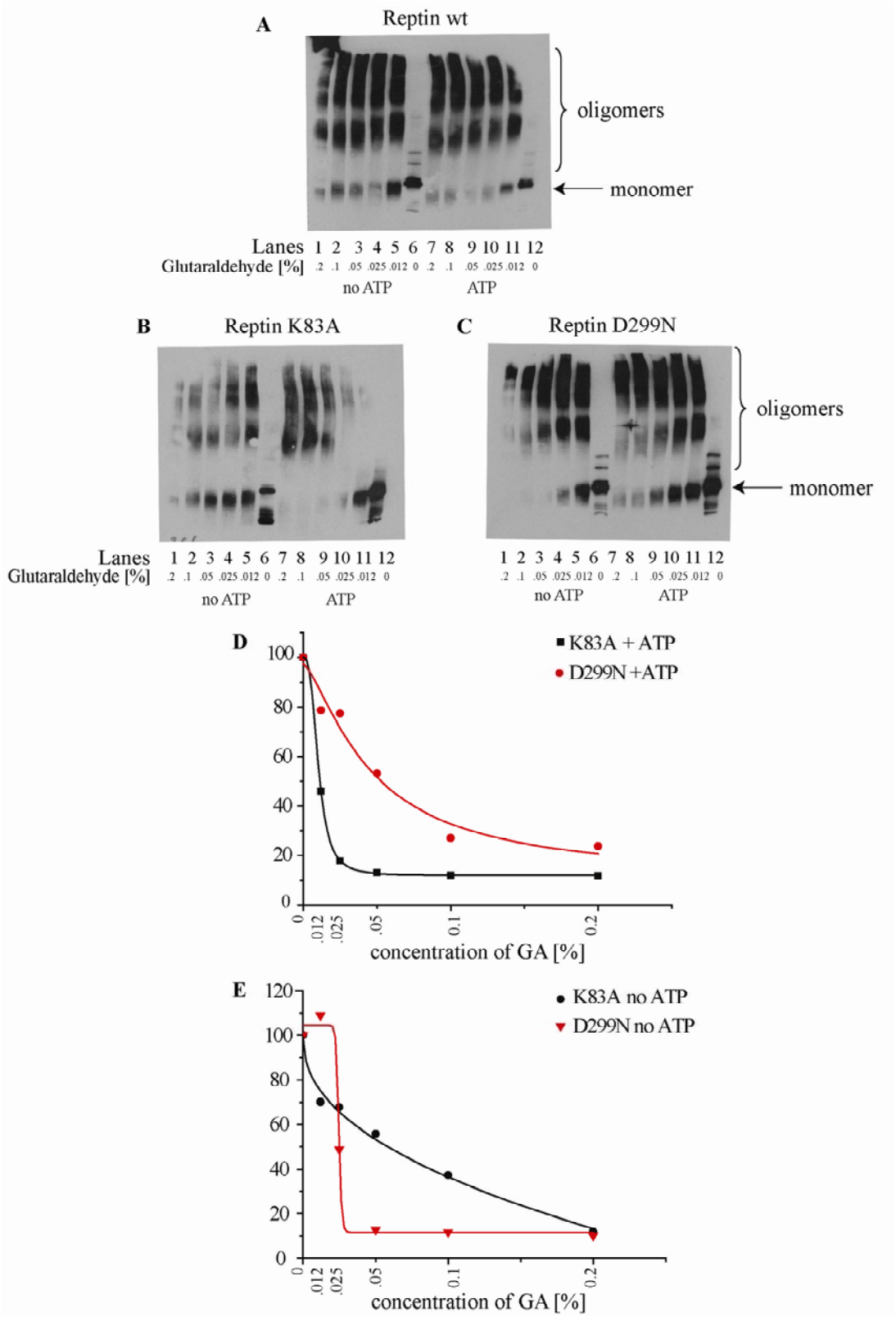

Figure 5.9 The effects of Reptin Walker A and B motifs mutation on their ATP-dependent oligomerization as defined using a cross-linking assay. (A) Wild type **(B)** Reptin K83A or **(C)** Reptin D299N proteins were incubated in PBS containing a titration of glutaraldehyde (from 0.012 % to 0.2 %) in the absence or presence of ATP. The extent of changes in oligomerization of Reptin from the monomeric state (arrow) was assessed by immunoblotting and **(D and E)** quantitated using ImageJ.

The apparent dynamic equilibrium between monomeric and oligomeric states was observed at room temperature. As the ATPase activity is induced upon increasing temperature, we were keen to see whether or not the oligomeric nature of Reptin can also be influenced by changes in temperature. To this end, we monitored the oligomerization of Reptin at 4°C and 37°C and compared it to this at room temperature. We found that changes in temperature did not result in a significant change in the oligomerization of wild type Reptin (data not shown), however, major differences between Walker A and Walker B mutants were observed. Firstly, we observed existence of different oligomeric ladders at 4°C for Walker A and B mutants. Essentially, Walker A mutant formed three distinct species of oligomers (Figure 5.10 A), whereas Walker B existed as a mixture of at least six different states (Figure 5.10 B). Strikingly, at physiological temperature (37°C) Walker B mutant was sensitive to loss of monomeric and lower order oligomeric forms and formed only high molecular weight oligomers, corresponding to the size of a hexamer (Figure 5.10 D). On the other hand, the oligomeric ladder obtained for Walker A mutant did not differ much from the one found at 4°C, however, it appeared that this protein was less stable under these conditions, as a lower amount of the protein was detected, compare to that at the lower temperatures (Figure 5.10 C). It is also possible, that under these conditions the antibody's epitope was masked in this mutant protein.

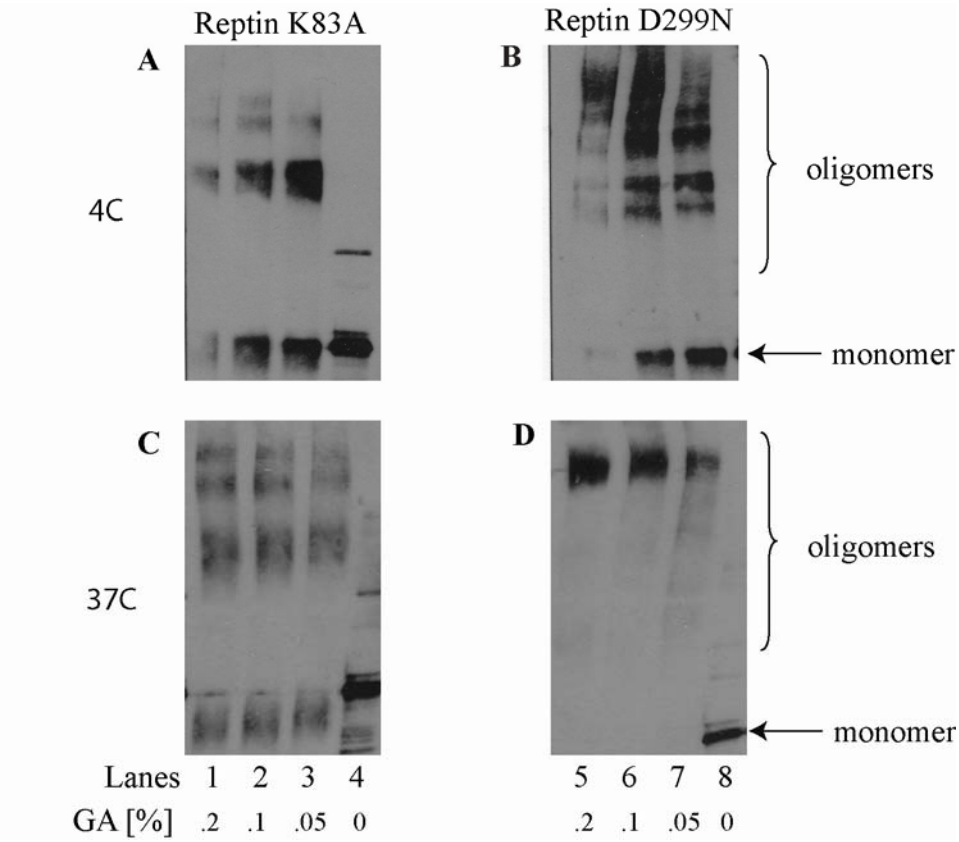

Figure 5.10 The effects of low and physiological temperature on Walker A and B mutant proteins oligomerization as defined using a cross-linking assay. (A and C) Reptin K83A or **(B and D)** Reptin D299N proteins were incubated in PBS containing a titration of glutaraldehyde **(A and B)** at 4°C or **(C and D)** at 37°C. The extent of changes in oligomerization of Reptin from the monomeric state (arrow) was assessed by immunoblotting using anti-Reptin polyclonal antibody.

5.3 Discussion

AAA+ ATPases couple ATP binding and energy released upon ATP hydrolysis to a diverse cellular activities including protein folding and unfolding events, DNA replication, organelle biogenesis and complex formation [640, 641]. Several types of models have been proposed to account for nucleotide binding and exchange for the different members of AAA+ family of ATPases. In a concerted model of action, all the subunits bind, hydrolyse and release the nucleotides simultaneously, whereas in a nonconcerted model, different subunits perform their function at distinct times [609]. These mechanisms require an allostery-based communication, which enables different subunits to regulate other subunits in the oligomer. In addition, a nonpatterned model has been proposed, whereby ATP is bound and hydrolysed in a noncyclical manner [642]. The nature of ATP binding and the mechanism of the ATP hydrolysis are well described for several members of the AAA+ family; however, the data available regarding the enzymatic activity of Reptin and Pontin are somewhat vague and often contradictory. In chapter 4 it was found that inclusion of nucleotide and mutations in ATP binding motifs of Reptin protein could affect AGR2-Reptin complex formation. Therefore, we were keen to explore a structure-function of Reptin protein in more detail. To this end, we were interested to test the ATP binding as well as ATPase activity of Reptin protein and identify the roles of Walker A and B sites. In addition, we wanted to characterize Reptin's structural integrity by oligomerization and unfolding studies.

Firstly, using a combination of radioactive and non-radioactive assays we established the stoichiometry of ATP binding and ATPase activity of Reptin. Initially, by performing heat denaturation of Reptin in the presence and absence of the nucleotide we confirmed that Reptin protein indeed binds ATP (Figure 5.4). Interestingly, the classic unfolding transition was observed upon addition of nucleotide. This is in keeping with the model of stabilisation of protein upon ligand binding. For example, in the absence of nucleotide the melting curve of Hsp90 consists of two transitions and addition of ATP-Mg increases the denaturation temperature by 2.6°C [643]. Surprisingly, Reptin alone does not undergo melting transition upon increasing temperature. The absence of a classic transition in the case

of Reptin could imply that it is unfolded in the absence of ligand. However, as a high flourescence was observed at room temperature it is possible that the ATP binding pockets of Reptin are hydrophobic and exposed in the absence of ATP. Accordingly, it is likely that the hydrophobic nucleotide binding sites become concealed rather than exposed upon heating. This would explain binding of Sypro-Orange and the high fluorescence readings at room temperature and the low fluorescence at higher temperatures.

In the current report we established the stoichiometry of Reptin-ATP interaction using hydrolysable as well as non-hydrolysable analogues of ATP. Previous report suggested that Reptin contains at least one putative ATP-binding site, namely the Walker A motif. If it was functional, we could expect a molar ratio of at least 1 to 1 ATP bound per Reptin monomer. However, we found that the stoichiometry of ATP binding to Reptin protein using a hydrolysable form of ATP was approximately 0.5-0.6 moles of nucleotide per 1 mole of protein (Figure 5.5 A). Considering the ring-like hexameric structure of Reptin's homolog Pontin and other AAA+ family members, we could assume a hexameric structure for Reptin protein as well. This would indicate that according to this data only three to four of the six subunits in the homo-hexameric complex are occupied. In other words, only 3 to 4 sites are capable of ATP binding at any given time. If this model is true and not all subunits of Reptin hexamer are occupied, the allosteric mechanism of nucleotide binding can be assumed, where ATP occupancy of one site, depends on the nucleotide state of the neighbouring subunits. Alternatively, it is theoretically possible that different populations of Reptin hexamers are present, comprised entirely of wholly nucleotide occupied or unoccupied monomers. The last model could be that at any give time, a mixture of different oligomers and monomers exists, and is able to bind to ATP. Indeed, dynamic light scatterring data revealed the presence of population of different oligomers and addition of ATP increased fraction of high molecular complexes. The substoichiometric binding of ATP is not unusual and was reported for others members of AAA+ family. For example, it was found that only four nucleotide molecules bound per PAN hexamer at saturating conditions [644, 645]. Further, ClpX was shown to bind 3 to 4 molecules of ATP per hexamer [646]. It was previously suggested for other helicases or translocases that

substoichiometric ligand binding by nucleotide-binding proteins may be important for their function [647, 648]. In addition, it has been shown for several AAA+ hexameric enzymes that only some subunits have a catalytic role [649, 650]. For example, the amount of subunits in the ATP-bound state may affect functions such as binding of other ligands. For instance, in ClpX hexamer three or more ATP-bound subunits must cooperate to allow tight ssrA peptide binding [646]. Therefore, it is possible that the subunits of Reptin that do not bind ATP have a regulatory or structural role.

Interestingly, the competition assay (using the titration of unlabeled nucleotide in the presence of radioactive ATP) revealed that the ATP binding curve was biphasic (Figure 5.5 B and C). This data implied that Reptin exhibits different classes of nucleotide-binding sites, one type with high and one with low affinity. If Reptin protein indeed hexamerises under these conditions, we could speculate that ATP binding to a high affinity site in some subunits alters the conformation of other subunits and creates subunits with low affinity. In addition, as the substoichiometric binding was detected, we could speculate, that in the Reptin hexamer there are at least three different conformations that the individual subunits can assume, one that binds ATP with high affinity, one that binds ATP with low affinity, and a nucleotide-free conformation. The existence of distinct classes of sites in the multisubunit enzymes that hydrolyze ATP appears to be a general feature of these assemblies. Various hexameric helicases have been shown to possess high and low affinity ATP binding sites [651-653], and there are often three rather than two high-affinity sites. Interestingly, bacterial ancestor of Reptin, namely RuvB hexamer, has been shown to possess non-equivalent active sites, which are ATP-bound, ADP-bound or nucleotide free [648, 654-656]. Similarly, subunits of PAN hexamer were reported to assume three different types of conformation. In addition, in PAN hexamer, although the binding curves for ATP showed typical saturation kinetics, binding to nonhydrolyzable analogue of ATP was multiphasic [645]. Hersh et al. showed that ClpX has different classes of ATP binding sites [646]. Interestingly, they used a different approach to us to establish equivalency of nucleotide binding sites. Instead of titrating competitor- unlabelled nucleotide in a filter binding assay, an excess of the nucleotide was added, and the dissociation kinetics were measured. As such,

ClpX nucleotide binding sites were described as “fast” and “slow” sites, depending on the time scale of nucleotide dissociation. It would be interesting to see whether or not we could observe the same differences in the release time in the case of Reptin.

Interestingly, addition of non-hydrolysable analogue of ATP reduces the stoichiometry to 0.18 moles of nucleotide per 1 mole of Reptin protein. Using nonhydrolyzable analogues of ATP should, in theory, freeze the protein of interest in the active, ATP-bound state. As we observed reduced stoichiometry using non-hydrolysable ATP-γ-S, we can conclude that the nucleotide exchange is essential for effective nucleotide binding by Reptin and the ATP hydrolytic cycle does not inhibit nucleotide binding. Additionally, as the curve of binding is not linear, as it is in the case of ATP, we could speculate that only low affinity sites/slow sites are active in these hexamers. This result also indicates that concerted or stochastic models for nucleotide binding and exchange can not be applied to Reptin, as this would require all the subunits to bind, hydrolyse and release the nucleotides simultaneously. However, here only some of the six subunits in Reptin hexamer could bind ATP-γ-S. Surprisingly, we found that the Walker B mutant displayed increased stoichiometry of ATP-γ-S binding compare to the wild type protein. This indicates that intact Walker B site negatively regulates ATP binding.

Interestingly, when the ATP binding was monitored by examining the effect of the concentration of the protein on nucleotide binding, the binding of nucleotides to wild type or Walker B mutant protein could be described by different curves. This is interesting as it may indirectly indicate whether stability of the hexamer is retained as the amount of protein changes and whether the concentration of protein required to adopt “nucleotide-binding permissive” conformation differs between wild type and mutant proteins. Here, as the linear increase in binding to ATP was observed with increasing concentration of wild type Reptin, one could speculate that the oligomeric status of wild type protein or the quality of ATP binding sites do not change in this range of concentrations. On the other hand, Reptin Walker B mutant protein binds ATP with high affinity at low concentrations of protein and it does not bind more at higher concentrations, indicating that at low concentration this mutant is already able to bind ATP with its full capacity. Interestingly, the shape of the curve of D299N Reptin binding to ATP suggests that the cooperative manner of ATP binding in case

of this mutant, as at the low concentrations of Reptin a non-linear increase in binding was observed. However, it is somewhat unclear whether ATP binding to wild type Reptin is cooperative. On one hand the presence of low-affinity and high-affinity binding sites was revealed. This would imply cooperative coupling and that Reptin had a single structural ATP-binding site that can assume two different binding affinities. On the other hand, it is possible that Reptin pre-exists in an asymmetrical conformation in the six protomers with some having their ATP binding site in a high-affinity conformation and the other having it in a low-affinity conformation. More kinetic studies, such as establishing velocities of ATP hydrolysis at different ATP concentrations could help us determine whether Reptin exhibits a cooperative effect in ATP binding and hydrolysis.

The apparent difference in ATP binding ability between wild type and Walker B mutant were further reflected by elevated intrinsic thermostability. Surprisingly, Walker B mutant could undergo thermal transition even in the absence of nucleotide. This indicates that the ATP binding pockets, which are presumably hydrophobic and exposed in wild type Reptin, are concealed in the mutant protein.

As Aspartate and Glutamate in the Walker B motif were shown to be essential to form hydrogen bonds with Walker A motif and with a bound water molecule, and to facilitate hydrolysis, the mutation of one of these critical sites should in theory result in the protein inactive as an ATPase. If this is true, the increased stoichiometry of ATP binding by Reptin D299N compared to wild type protein would suggest that ATP hydrolysis inhibits ATP binding in wild type protein. However we found that D299N mutation did not inhibit ATPase activity of Reptin. There could be several reasons for this. It is possible that D to N mutation was not sufficient to disrupt Walker B function in the hydrolytic cycle. For example, some studies described conserved Glutamate rather than Asparagine as the catalytic base for ATP hydrolysis [657]. In addition, it possible that ATP hydrolysis by Reptin is sensitive to its oligomeric status and less to its primary sequence.

The filter binding assay showed that the Walker A mutant was completely defective in ATP binding, which is inconsistent with the fact that this mutant protein was responsive to ATP in oligomerization using the chemical cross-linking assay and was active in the ATPase assay. However, filter assays have been found to

underestimate stoichiometry of binding before. For instance, 1.2 ATPs per ClpX hexamer was initially observed by filter binding assay, but isothermal titration calorimetry gave 3.4 ATPs bound per hexamer [646]. It was reasoned, that ligand dissociates too fast to be captured by this method [646]. It is also possible that the conformation of Reptin Walker A mutant protein is "more labile" than the conformation of wild type protein and undergoes denaturation when it is adsorbed onto the nitrocellulose filter. The ATP filter binding assay involves exploiting the difference between the hydrophobic interactions of ATP and target protein with the nitrocellulose filter and as such is very sensitive to temperature. Other studies, such as the protein binding assays, thermal shifts, and the oligomerization assay, were evaluated in solution at room temperature or higher. Thus, the lower temperatures required for wash buffer in filter binding assay might alter the affinity of ATP for the Walker A mutant protein. Interestingly, temperature was found to affect the stoichiometry of the ATP binding for other AAA proteins. For example a decrease in ADP binding activity with increasing temperature was observed for SecA [658]. In this study the washes were performed at different temperatures, however, we found that increasing the temperature greatly increased the background readings.

Reptin protein structure has not been solved yet, however X-ray structure of Pontin was reported [623] and it was found that Pontin oligomerizes as a hexameric ring, which is typical for AAA+ proteins [608]. There are various models for the Reptin/ Pontin oligomeric state, and different studies have described them as both single and double hexamers. In this report, we found that wild type Reptin increases in apparent mass in the presence of ATP as defined using light scattering, however, even in the absence of nucleotide a mixture of different oligomeric species was observed. Similar has been recently shown in another study in which analytical ultracentrifugation was used to identify the oligomeric nature of Reptin. It was found that Reptin protein was predominantly monomeric in the absence of ATP, however it also formed dimers, trimers and hexamers, and the hexamer species became predominant upon addition of nucleotide [638]. Importantly, earlier studies used tagged Reptin protein to establish oligomerization and the most recent report demonstrated that the His-tag induced the formation of double hexameric ring Reptin/Pontin complexes, whereas untagged proteins formed a single ring [580].

These changes in the oligomerization status of Reptin upon fusion with the tag, could explain the differences we observed with respect to Reptin-AGR2 or Reptin-p53 binding, when GST-tagged and untagged-Reptin were compared (Chapter 4 and 6).

We studied oligomerization characteristics of wild type and mutant Reptin proteins by glutaraldehyde cross-linking. Given that typically the nucleotide binding sites in AAA+ proteins are located at the interfaces between protomers in an oligomeric assembly [609], introducing mutations at these interfaces was likely to affect the oligomerization process. In this report, cross-linking experiments of wild type and mutant proteins resulted in mixtures of monomeric and oligomeric species. Interestingly, important differences in the properties of Walker A and B mutants were revealed. Surprisingly, Reptin K83A mutant protein was more responsive in ATP-mediated oligomerization than wild type Reptin. Contrary to that, Walker B mutant Reptin protein was sensitive to loss of monomeric subunit in the absence of nucleotide, but was similar to wild type Reptin in the presence of ATP. The importance of Walker A and B domains in oligomeriation was reported for other members of AAA+ proteins. For example, the mutation of Walker A in ClpB protein in the first AAA module abolished hexamer formation, whereas corresponding substitution in the second nucleotide binding site had no influence on ClpB hexamerization [659].

It is worth noting that glutaraldehyde cross-links protein by forming covalent bonds between lysine residues that are in close proximity to each other. The potential pitfall of this method with respect to studying effects of mutations in Walker A oligomerization is that in order to obtain this mutant the conserved Lysine was replaced. Therefore, it could be interesting to use different cross linking agents, to assess how mutations of the conserved residues in Reptin affect its oligomerization. On the other hand, as Walker B and wild type Reptin appeared to be less sensitive to loss of monomeric subunit in the presence of the nucleotide, it is possible that the Lysine 83 involved in the ATP-binding and intact in these proteins is exposed and may serve as a cross-link site.

Moreover, we found that the oligomerization of Reptin was dependent on temperature, especially at high temperatures. Interestingly, wild type and Walker A mutant form mixtures of oligomers, whereas Walker B mutant existed predominantly

as a hexamer at physiological temperature. As the ATPase activity of Reptin protein appeared to be stimulated at higher temperatures, it appears that this may be linked to the oligomerization process. This would be consistent with the observations made for other AAA+ proteins, for which hexamerization was shown to be essential for the enzymatic activity. However, as Reptin appears to exist as the mixture of different oligomers it is plausible that all of them have some physiological activity and it is not necessarily restricted to the hexameric-ring structure.

Further, as the chemical cross-linking can be used as an initial way to determine the organization of multisubunit assemblies, it would be interesting to use a more direct method of defining the oligomeric state of Reptin. For example, to determine an absolute measurement of the molecular weight of Reptin oligomers in solution, sedimentation equilibrium method could be applied.

Currently, there is no consensus as to the roles of ATP binding and hydrolysis in the Reptin functions. Gaining insight into Reptin's ability to self assemble could provide the basis for the *in vivo* studies of the Reptin's oligomerization and function within the cell. Here, we performed a detailed analysis of the effects of nucleotide and nucleotide binding sites on Reptin protein. We established that Reptin could bind and hydrolyze ATP and form oligomers, and that Walker A and B motifs were important for these activities.

CHAPTER 6 Regulation of p53 protein by the molecular chaperone Reptin

6.1 Introduction

The p53 tumour suppressor protein, aptly named the "guardian of a genome", has a central role in sensing and responding to a myriad of cellular stresses, including DNA damage [660]. Its tumour suppressive role is primarily linked to sequence-specific DNA binding and subsequent activation of genes [271, 661] that are components of apoptotic and growth arrest pathways [662]. Examples of such gene products are the p21WAF1/CIP1 growth inhibitor [66, 661] or proapoptotic Bax [663] that are frequently used as the read-out for the p53 transcriptional activation.

Common genetic alterations in cancer involve inactivation of wild type p53 or p53 gene mutation [38]. The majority of these changes is found in the DNA binding domain of p53 [664] and this is linked to the key function of p53 protein as a transcription factor. These mutations fall into two separate classes, namely DNA contact and conformation mutations [136]. DNA contact p53 mutants, such as p53 R248 or R273, bear mutations at the sites that form a direct interaction with DNA. Structural p53 mutants, including R175, G245, R249 or R282, are characterised by destabilised the local (core) or overall structure [136, 157]. In addition to the core domain, some p53 mutations were found in the teramerization domain. Interestingly, the frequency of germ line p53 mutations in the oligomerization domain is similar to that observed for the core domain [665].

p53 function is regulated by the network of proteins that ensures that the p53 pathway is downregulated in unstressed cells but can be rapidly activated upon stress stimuli [666]. These proteins control p53 stability, activity and localization. The p53 turn-over by ubiquitin degradation pathway is primarily mediated by E3 ligase MDM2 [201-203]. p53 ubiquitination by MDM2 was described by a dual-site mechanism, whereby p53 binds to the N-terminal hydrophobic pocket of MDM2, which triggers conformation change that stabilises the interaction between the acidic domain of MDM2 and the ubiquitination signal in the core domain of p53 [162]. The stress input in the cell results in the suppression of the p53 degradation pathways,

activation of collection of p53 modifying enzymes and consequently rapid activation of p53 network.

p53 protein can be considered as a major cellular signalling hub and so far it has been shown to bind to over 300 proteins [39]. The complexity of the p53 interactome and signalling and its rapid turnover are dependent on the intrinsic plasticity of the p53 protein. This is achieved by a combined action of its folded and disordered domains and p53's thermodynamical and kinetical instability [138, 667]. For example, p53 core domain has a half life of 9 minutes at 37ºC [668, 669] and it unfolds and aggregates at high rate [266, 670]. Further, p53 protein exists in the equilibrium between folded and unfolded states. However, the stable conformation is essential for the p53's physiological activity and a number of mechanisms exist that stabilises the conformation of wild type p53. p53 protein can be activated for sequence-specific DNA binding for example by modification events of its negative regulatory domain or by binding of the monoclonal antibody PAb421 which preserves a p53 tetramer [184, 671, 672]. Additionally, p53 can associate with molecular chaperones, and indeed heat shock proteins have been shown to bind to, stabilise and activate both wild type and mutant p53.

The interactome of p53 protein is growing and currently exceeds 300 proteins, including proteins involved in its degradation, folding and activation. Interestingly, mutant p53 protein can establish complexes with the components of wild type p53 network and rewire it to gain oncogenic activity. Understanding the interactome of wild type and mutant p53, may help to understand the mechanisms behind the increased stability of p53 mutant and effectively facilitate drug discovery.

6.2 Results

6.2.1 AGR2, Reptin and p53 form a trimeric complex.

As mentioned in the Introduction, AGR2 protein was identified in a proteomic screen aimed at identifying proteins that are overexpressed in Barrett's epithelium and can function to perturb the p53 pathway [437]. Subsequently, it was

demonstrated that cells overexpressing AGR2 decrease DNA-damage induced p53 phosphorylation at both Ser15 and Ser392. However, no evidence was found that AGR2 binds to p53 protein. In Chapter 4 we explored the AGR2 interactome and validated Reptin as AGR2 protein binding partner. We also speculated on the possible functions of this complex. One hypothesis was that it could be implicated in AGR2 mediated inhibition of the p53 pathway. Interestingly, other reports have already showed some link between p53 and Reptin proteins. For example, Reptin participates in p400 complex that regulates senescence and knocking down Reptin or Pontin, or p400 leads to p53-dependent replicative senescence [673]. In addition Reptin protein is implicated in regulation of transcription and chromatin remodelling and could have a function in p53-mediated transcriptional events. Therefore we decided to investigate whether or not AGR2 and Reptin interaction provide a signalling mechanism for the p53-specific AGR2-dependent oncogenic pathway. First, we decided to establish whether p53 protein is present in the AGR2-Reptin complex. To this end, we performed co-immunoprecipitation experiments using lysates of H1299 cells transiently expressing AGR2 only and/or HA-tagged Reptin and/or p53 as indicated in the figure legends. To our surprise, we were able to detect p53 protein in the anti-AGR2 immunoprecipitate from the cells transfected with p53 protein, but not in the p53-negative cells (Figure 6.1 A, lanes 3 and 5 vs. 7). As in the cellular context additional factors may be required for the complex formation, we set out to investigate, whether p53 indeed binds to either AGR2 or Reptin protein *in vitro*. To this effect, p53 protein was immobilised onto a microtitre plate and incubated with a titration of His-tagged AGR2 protein, GST-tagged Reptin protein or GST only. It was found, that GST-tagged Reptin but not His-tagged AGR2 or GST only bound specifically to p53 protein (Figure 6.1 B). Similarly, when GST-tagged Reptin was immobilised onto a microtitre plate and incubated with p53 protein in mobile phase, it was found that p53 could bind to GST-Reptin protein (Figure 6.1 C). Therefore, we concluded that AGR2, Reptin and p53 form a trimeric complex in cells and Reptin can directly associate with p53 *in vitro*.

As mentioned above, AGR2 protein was shown to prevent activation of p53 pathway in response to DNA damage. Since we found that p53 and AGR2 had a common interaction protein, namely Reptin, we were keen to determine if AGR2-

Reptin and Reptin-p53 pathways communicate with each other. In detail, we were interested to (1) confirm AGR2-mediated suppression of p53, (2) establish Reptin's function with respect to p53 activity. We reasoned that there are three possible functions for AGR2-Reptin complex in regulation of the p53 pathway. Firstly, AGR2 and Reptin may cooperate to inhibit p53 (Figure 6.1 D, i), secondly Reptin may act as an activator of p53 and AGR2 may interfere with this function of Reptin (Figure 6.1 D, ii), and lastly, Reptin may exert inhibitory effect on AGR2 protein and thus activate p53 (Figure 6.1 D, iii).

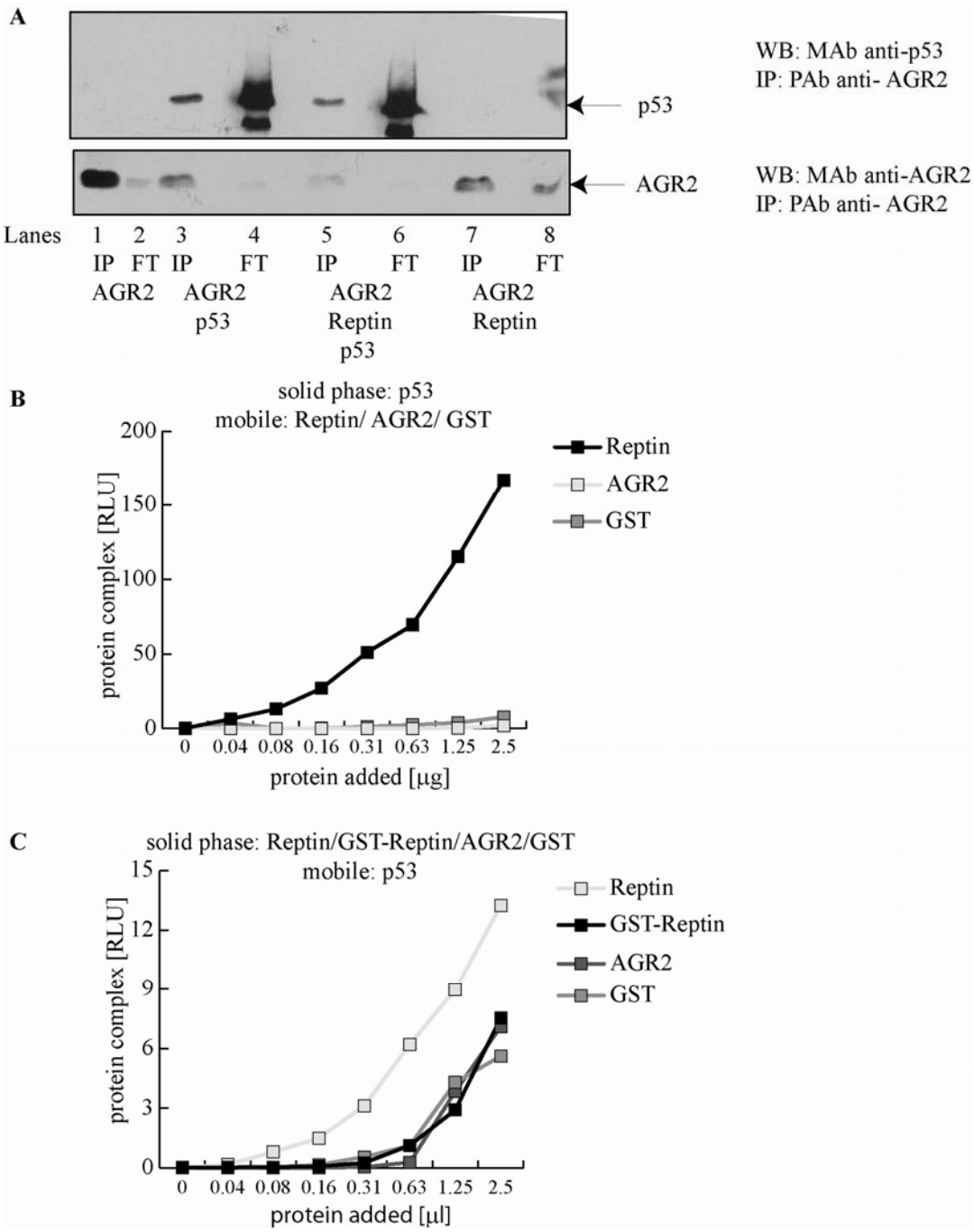
A
WB: MAb anti-p53
IP: PAb anti- AGR2
p53
AGR2
WB: MAb anti-AGR2
IP: PAb anti- AGR2
Lanes 1 2 3 4 5 6 7 8
IP AGR2
FT AGR2
IP AGR2 p53
FT
IP AGR2 Reptin p53
FT
IP AGR2 Reptin
FT
B
solid phase: p53
mobile: Reptin/ AGR2/ GST
protein complex [RLU]
200
150
100
50
0
0 0.04 0.08 0.16 0.31 0.63 1.25 2.5
protein added [µg]
Reptin
AGR2
GST
C
solid phase: Reptin/GST-Reptin/AGR2/GST
mobile: p53
protein complex [RLU]
15
12
9
6
3
0
0 0.04 0.08 0.16 0.31 0.63 1.25 2.5
protein added [µl]
Reptin
GST-Reptin
AGR2
GST

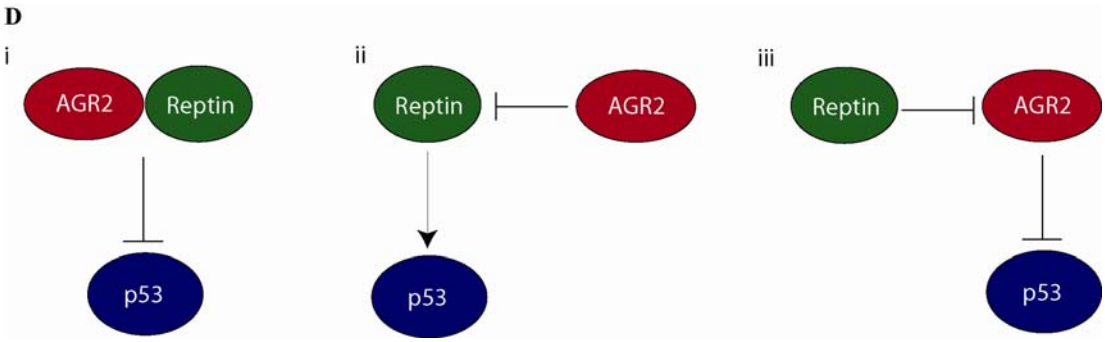

Figure 6.1 Human Reptin and AGR2 form a trimeric complex with p53 protein. (A) Cell lysates from H1299 cells transfected AGR2 (lanes 1 and 2) or with AGR2 and p53 (lanes 3 and 4) or with AGR2, p53 and HA-tagged Reptin (lanes 5 and 6) or with AGR2 and HA-tagged Reptin (lanes 7 and 8) were incubated with anti-AGR2 polyclonal antibody and protein G beads. The AGR2 immune precipitate (IP; lanes 1, 3, 5 and 7) and the unbound fraction (FT, lanes 2, 4, 6 and 8) were loaded onto a 12 % SDS-PAGE gel and analysed by immunoblotting using antibodies to p53 and AGR2. p53 and AGR2 are highlighted. **(B and C)** Either p53 **(B)** or Reptin, GST-tagged Reptin, GST, AGR2 **(C)** was immobilized on the solid phase and a titration of either **(B)** GST-tagged Reptin, GST, AGR2 or **(C)** p53 was added in the mobile phase. The amount of the proteins bound was quantified with antibodies specific for either protein using chemiluminescence. The data are plotted as the extent of protein-protein complex formation (in RLU) as a function of the amount of protein in the mobile phase [μM]. **(D)** Model of the possible roles of the AGR2 and Reptin complex on the p53 pathway.

6.2.2 Reptin and AGR2 exert opposite effects on p53 protein levels and its transcriptional activity

Having proposed the three hypotheses regarding the effect that the AGR2-Reptin complex could exert on the p53 pathway, we first decided to assess the p53 transcriptional activity, upon AGR2 or Reptin overexpression. To this end we used reporter constructs in which the promoters of p53 target genes, namely p21, MDM2 were fused to Firefly luciferase gene. This enabled us to assess p53 transcriptional activity by Dual Luciferase reporter assay.

Firstly, a p53 gene was titrated to determine the amount of DNA required to obtain the maximal activity of p53. To this end, H1299 cell were co-transfected with fixed amounts of p21 reporter plasmid, a renilla luciferase plasmid, as a control for transfection efficiency, and a titration of p53 gene. As little as 5 ng of the p53 gene was sufficient to induce expression of p21-firefly luciferase (Figure 6.2 A). Next, to confirm AGR2-dependent inhibition of p53 transcriptional activity, H1299 cell were co-transfected with fixed amounts of p21 reporter plasmids, a renilla luciferase plasmid and AGR2 protein. As an additional control, MDM2 was transfected, as MDM2 was previously shown to be able to transrepress p53 protein. Both MDM2 and AGR2 attenuated transcription of the p21 reporter gene (Figure 6.2 B). In addition, the effect of AGR2 on MDM2 reporter expression was measured, and a decrease in expression of this promoter was observed, albeit to a lesser extent than in the case of the p21 promoter (Figure 6.2 C). In addition, the effect of AGR2 protein on p53 protein levels was assessed. It was found that overexpression of AGR2 in H1299 AGR2-negative cells resulted in decreased levels or increased ubiquitination of exogenously expressed p53 (Figure 6.2 D). Therefore, we concluded that AGR2 can indeed function as an inhibitor of p53 protein.

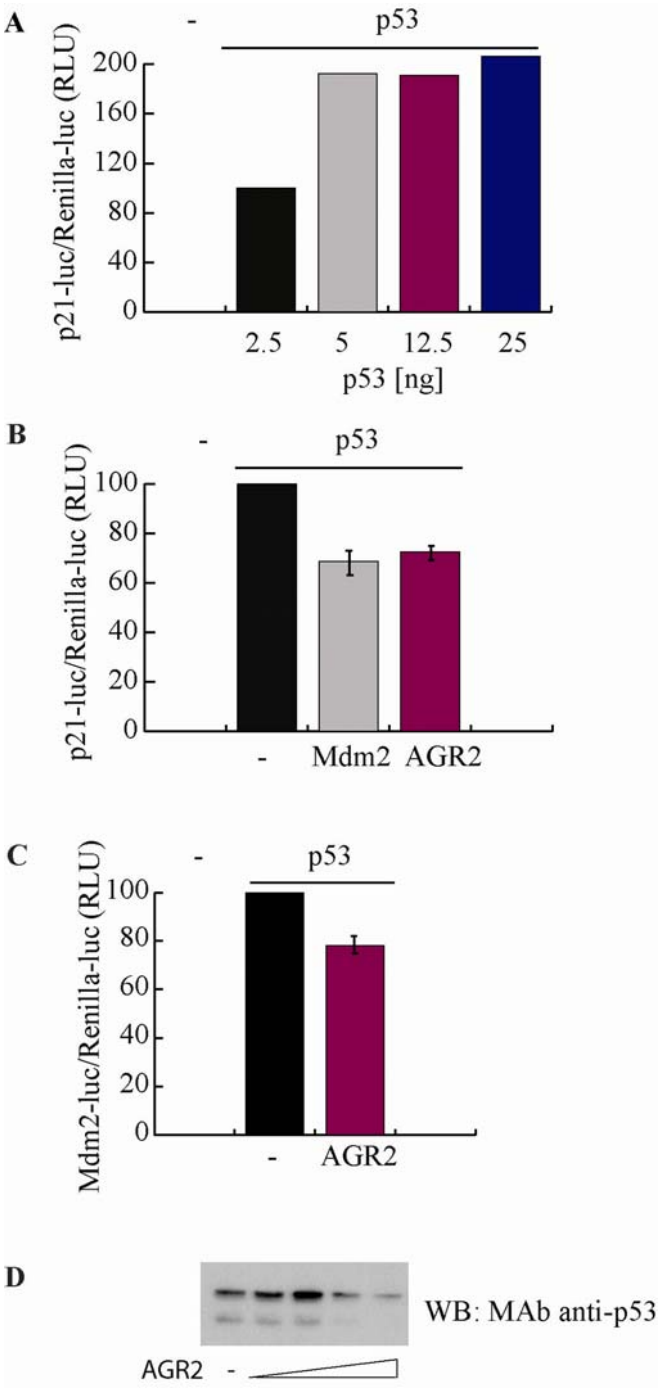

Figure 6.2 Anterior gradient-2 antagonizes p53-dependent transcription. (A) H1299 cells were transfected with increasing amount of the p53 gene (2.5-25 ng), the p21 reporter plasmid and a renilla luciferase plasmid. **(B and C)** H1299 cells were transfected with a fixed amount of the p53 gene, the **(B)** p21 reporter plasmid or **(C)** MDM2 reporter plasmid, a renilla luciferase plasmid and increasing amounts of either MDM2 or AGR2 as indicated in the figure. Twenty four hours post-transfection cells were lysed, dual luciferase reporter assay performed and the readings normalised against Renilla luciferase activity. The results are expressed as the ratio of p21 or MDM2 reporter activity to Renilla reporter activity in [RLU]. Results are representative of at least two independent experiments; error bars represent standard error of replicates. **(D)** H1299 cells were transfected with p53 and without or with the increasing amount of AGR2 for 24 hours. The cells were lysed in the dual luciferase assay lysis buffer and the steady-state levels of p53 measured by immunoblotting using anti-p53 monoclonal antibody (DO-1).

Next, to examine the effect of Reptin on p53 transcriptional activity, H1299 cell were co-transfected with fixed amounts of p21 reporter plasmids, a renilla luciferase plasmid and a titration of Reptin. It was found that Reptin protein could increase expression of p21 gene in a dose-dependent manner, however, only at higher concentrations of the transfected plasmid (Figure 6.3 A). In addition, when the steady-state levels of p53 and p21 were assessed in this experiment, it was found that transfection of the increasing levels of Reptin protein resulted in the stabilisation of p53 protein (Figure 6.3 B). Surprisingly, the effect of Reptin on p21 protein depended on the amount of the transfected Reptin, and at high levels, the amount of p21 protein was not further increased. This contrasted with the results of the luciferase assay, wherein a steady increase in the activity of the p21 reporter was observed with increased levels of Reptin (Figure 6.3 A). However it is worth noting that despite numerous advantages of the luciferase assay, such as high sensitivity and relatively easy methodology, that allows testing multiple conditions in one experiment, there are several drawbacks of this method that could potentially lead to artefacts. The main disadvantage is due to the fact that the transcription of the reporter gene rather than of the endogenous gene is monitored; the former lacks chromatin structure and distal elements in the promoter. As such assessing the steady-state levels of p53 and p21 may be a more reliable method to measure p53 activity. As Reptin overexpression resulted in increased activity of p53, we concluded that either (1) AGR2 could exploit Reptin to inhibit p53 in cells (Figure 6.3 i), or (2) Reptin acts as a shield to neutralize AGR2 inhibtory effect on the p53 pathway (Figure 6.3 ii).

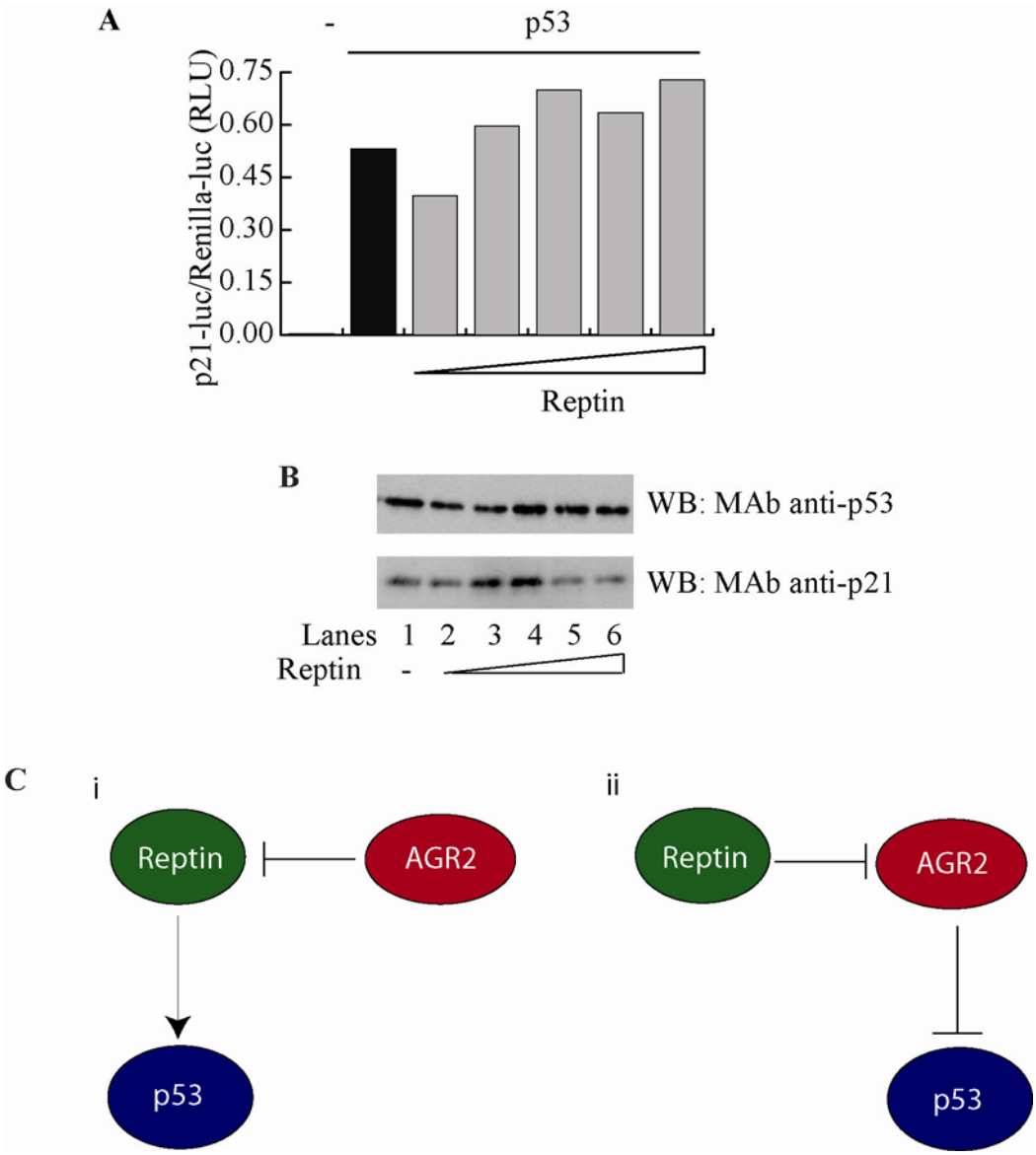

Figure 6.3 Reptin stabilises and activates p53. (A and B) H1299 cells were transfected with a p21 reporter plasmid and a renilla luciferase plasmid, the p53 gene and without or with increasing amount of Reptin. Twenty four hours post- transfection cell were lysed. **(A)** Then dual luciferase reporter assay performed and the readings normalised against Renilla luciferase activity. The results are expressed as the ratio of p21 or MDM2 reporter activity to Renilla reporter activity in [RLU]. Results are representative of at least two independent experiments. **(B)** The steady-state levels of p53 and p21 measured by immunoblotting using specific monoclonal antibodies. **(C)** Model of the possible roles of the AGR2 and Reptin complex on the p53 pathway.

6.2.3 Reptin specifically binds to Box V and Tetramerization domain peptide sequence from p53 protein.

In order to better understand the function of the Reptin-p53 interaction we sought to determine Reptin and p53 binding interface in detail. For this purpose a series of p53 overlapping peptides composed of 15 amino acids and N-terminal biotin tag was used in a peptide pull down assay developed in the lab [577]. In detail, streptavidin agarose beads were coated with p53 peptides (Figure 6.4 A) and incubated with the cell lysates. We found that four peptides were able to specifically pull down ectopically expressed Reptin protein (Figure 6.4 B). Specifically, peptide 26 and 28 that localise to Box V domain of p53, as well as peptide 38 and 39, which reside in tetramerization domain were found (Figure 6.4 B and C).

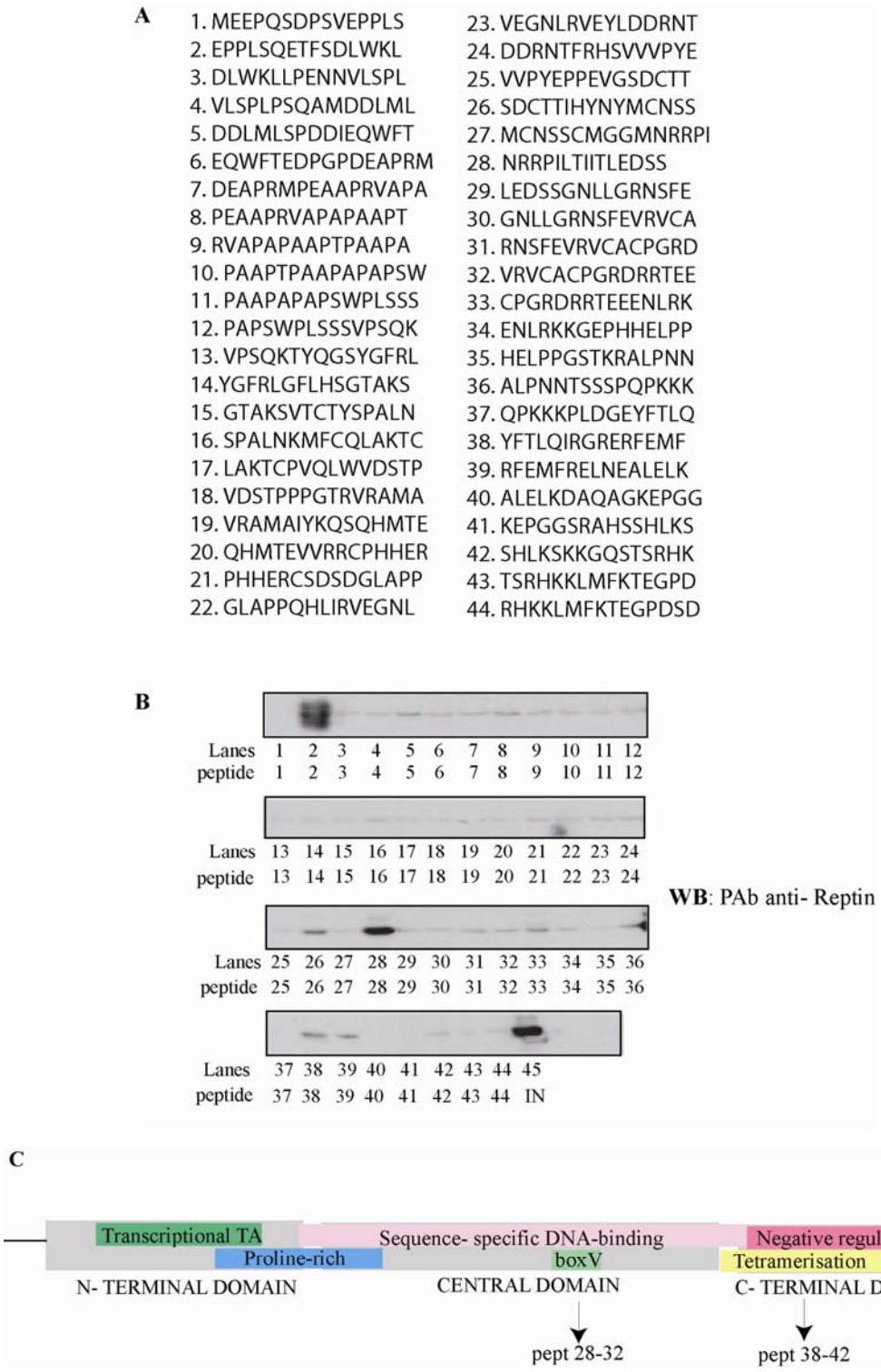

Figure 6.4 Reptin protein binds specifically to Box V and tetramerization domain of p53 protein *in vivo*. (A) A list of p53 overlapping peptides, **(B)** Biotinylated peptides (as in **A**) were coupled to streptavidin beads and incubated with human cell lysate expressing Reptin. The amount of Reptin bound was evaluated by immunoblotting using Reptin- specific antibody; [IN] is an input fraction. **(C)** Schematic representation of the functional domains of p53. Box V (peptides 28-32) and tetramerization domain (peptides 38-42) are highlighted.

Subsequently, we set out to determine whether or not purified Reptin could bind to p53 peptides in an ELISA. Interestingly, we found that Reptin protein expressed in bacteria interacted with two peptides, 31 and 38 (Figure 6.5 A). Peptide 31 did not pull down Reptin in the *in vivo* peptide pull down, however as it is within the same part of the p53 protein as peptides 26 and 28, namely Box V domain, this suggests that this is indeed a valid binding interface. To further test this, we set out to examine if any of the p53 peptides that were shown to bind to Reptin, could disrupt the p53-Reptin complex. To this end p53 was immobilised on the plate and a fixed amount of GST-tagged Reptin protein, pre-incubated with a titration of selected p53 peptides, was added. Interestingly, only peptide 31 was able to efficiently diminish formation of the p53-Reptin complex (Figure 6.5 C). Surprisingly, peptide 38 induced binding of the two proteins, indicating an allosteric mechanism of the regulation of Reptin-p53 protein complex formation (Figure 6.5 B). None of the control peptides, namely peptides 30, 32 or 33 or DMSO caused any significant changes in the stability of p53-Reptin complex (Figure 6.5 B and C). Therefore, we concluded that Reptin specifically binds to two sites on p53, namely the tetramerization domain and Box V domain.

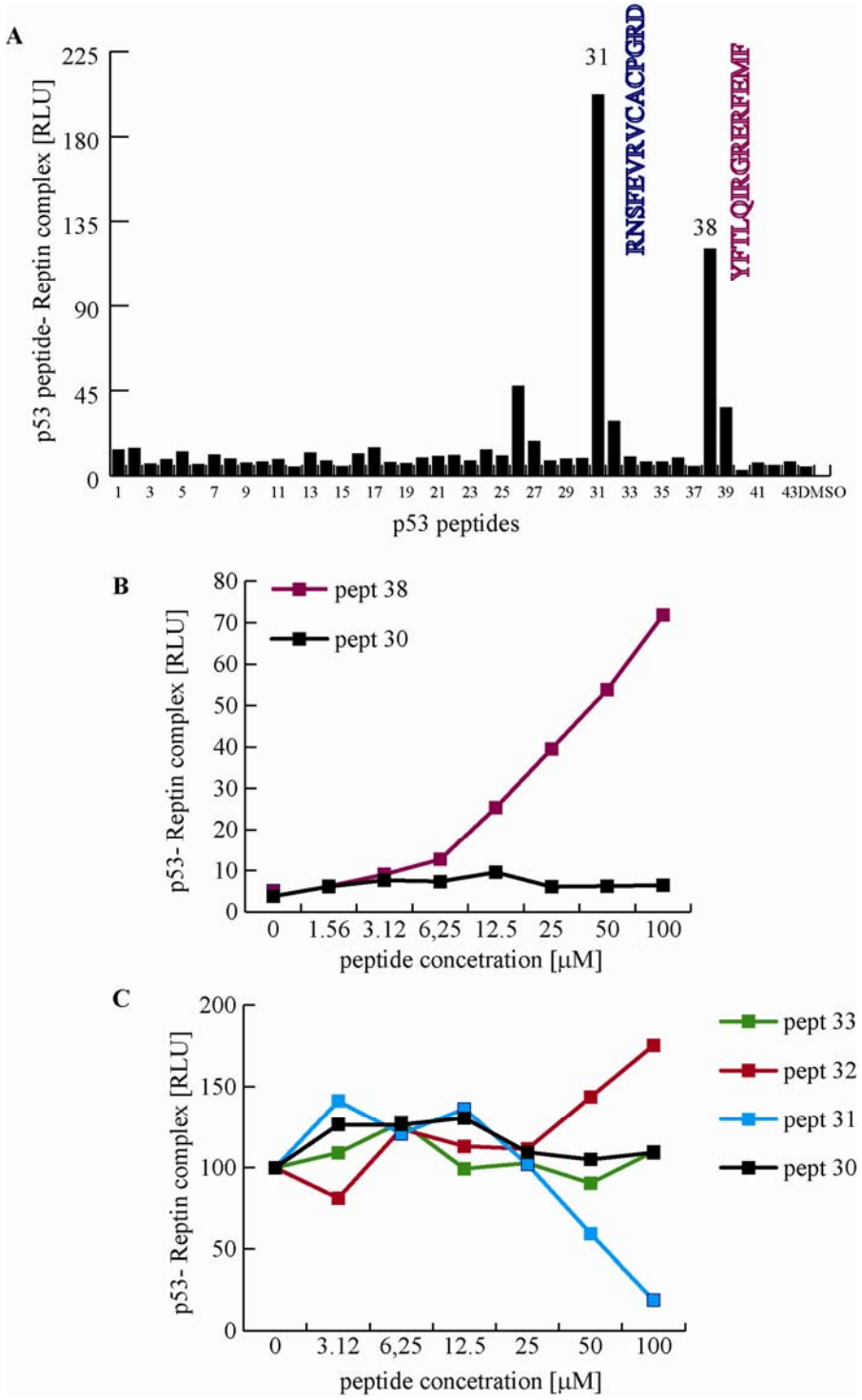

Figure 6.5 Reptin protein binds specifically to box V and tetramerization domain of p53 protein *in vivo*. (A) A fixed amount of the indicated biotinylated peptides (as in **5.3 A**) was added to a microtitre plate coated with streptavidin and incubated with recombinant Reptin. The amount of Reptin bound was quantified with antibodies specific for Reptin using chemiluminescence. The data are plotted as the extent of protein-peptide complex formation [RLU]. **(B and C)** Reptin protein was preincubated with **(B)** a titration of peptides 30 and 38 or **(C)** a titration of peptides 30-33, and added to immobilised p53 protein. The amount of Reptin bound to the full length p53 was quantified with antibodies specific for Reptin using chemiluminescence. The data are plotted as the extent of protein-protein complex formation [RLU].

Having found that Reptin protein binds to Box V site in p53, we were interested to determine whether or not Reptin could also interact with mutant variants of p53 protein, that bear mutations in this domain or in the DNA-binding domain that encompasses the Box V motif. Specifically, we sought to determine if p53 proteins with mutations that result in the unfolded conformation of p53 retained the ability to bind to Reptin protein. Firstly, we decided to establish whether Reptin could form a complex with the well characterised p53 mutants: p53 F270A and p53 R175H. To this effect, we performed co-immunoprecipitation experiments using lysates of H1299 cells transiently expressing AGR2 and HA-tagged Reptin and wild type or mutant variants of p53 protein as indicated in the figure. We found that both wild type and mutant p53 proteins were present in Reptin and AGR2 immunoprecipitates (Figure 6.6 A and B). Interestingly, more p53 proteins was detected in the immunoprecipitates from cell lysates obtained from cells transfected with mutant proteins (Figure 6.6 A and B, lanes 1 vs. 3 and 5).

We explored further Reptin's ability to interact with mutant p53 protein, by assessing whether it could form a complex with p53 S269D or p53 S269A. S269D mutation in p53 has been recently shown to result in an inactive, unfolded form of p53 [164, 674]. Again, it was found that both wild type and mutant p53 were present in the AGR2 immunoprecipitates (Figure 6.6 C). As an additional control, we were interested to see, whether or not Reptin could form a complex with wild type or mutant p53 protein in the absence of AGR2. We confirmed that Reptin protein could bind both wild type and mutant p53 protein independently of AGR2, albeit AGR2 co-transfection increased amount of p53 bound to Reptin (Figure 6.6 E, lanes 1-3 vs. 4-6). In addition, it was found that mutant p53 protein, especially p53 S269D, could bind to Reptin more efficiently than its wild type counterpart (Figure 6.6 C and E). We concluded that Reptin could form a complex with the p53 protein bearing a mutation in the DNA-binding domain. In fact, as mutant p53-Reptin complexes were more abundant than wild type p53-Reptin complex, we could hypothesise that mutant- unfolded conformation of p53, exposes Reptin binding motifs in p53 protein. Alternatively, as mutant p53 proteins are stabilised in the cancer cell lines, it is possible, that the higher amount of p53-Reptin complexes

detected from the cells transiently expressing mutant p53 is a result of the higher total levels of these proteins compared to wild type p53.

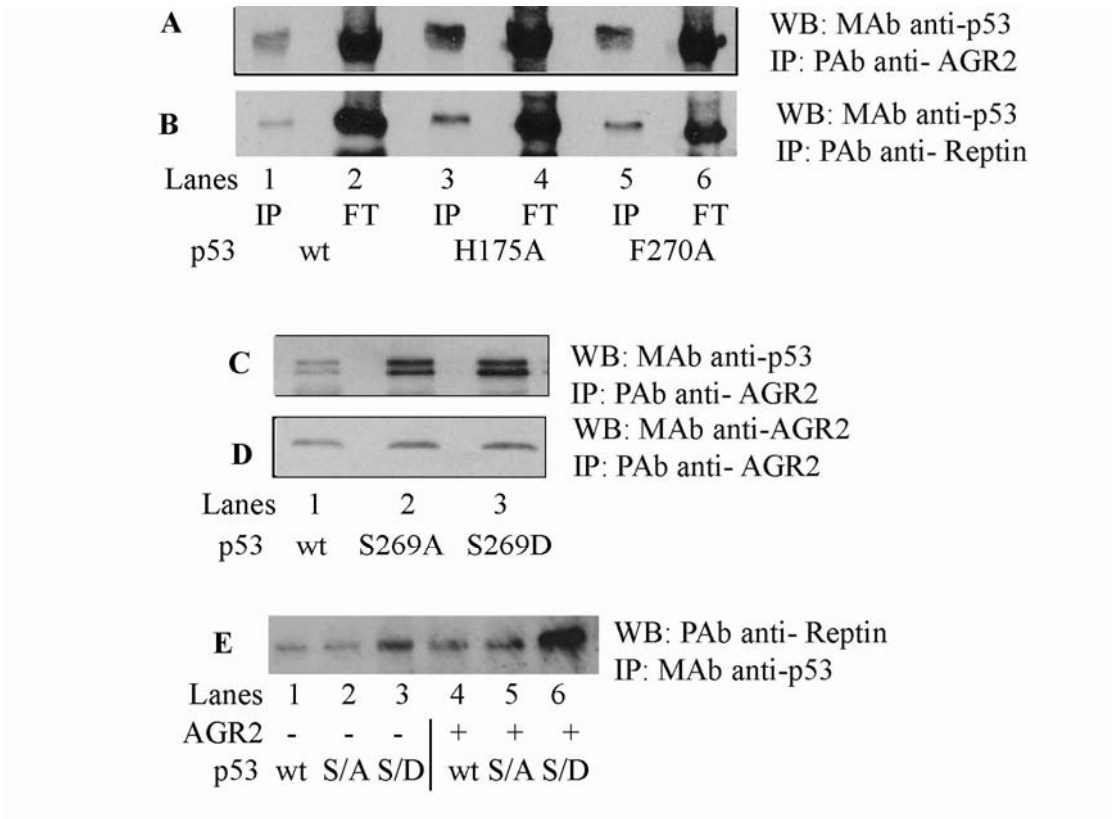

Figure 6.6 Mutant p53 protein forms stable complexes with Reptin in human cell lines. (A and B) Cell lysates from H1299 cells transfected with AGR2 and HA-tagged Reptin, and with either wild type p53 or p53 F270A or p53 R175H were incubated with **(A)** anti-AGR2 polyclonal antibody or **(B)** anti-Reptin polyclonal antibody and protein G beads. The immuneprecipitates were loaded onto a 12 % SDS-PAGE gel and analysed by immunoblotting using antibodies to p53 (DO1). **(C and D)** Cell lysates from H1299 cells transfected with AGR2 and HA-tagged Reptin, and with either wild type p53 or p53 S269D or p53 S269A mutant proteins were incubated with anti-AGR2 polyclonal antibody and protein G beads. The immuno precipitates were loaded onto a 12 % SDS-PAGE gel and analysed by immunoblotting using antibodies to **(C)** p53 (DO1) and **(D)** AGR2. **(E)** Cell lysates from H1299 cells transfected with HA-tagged Reptin, and with either wild type p53 or p53 S269D or p53 S269A mutant proteins and with (lanes 4-6) or without AGR2 (lanes 1-3) were incubated with anti-p53 monoclonal antibody and protein G beads. The immune precipitates were loaded onto a 12 % SDS-PAGE gel and analysed by immunoblotting using antibodies to Reptin.

As Reptin protein was found to bind to peptide 38 from the tetramerization domain in p53, we next decided to investigate this binding interface in more detail. Thus, we created a peptide library that contained deletion variants of peptide 38 and derivatives of peptide 38 in which each amino acid was consecutively replaced with Alanine (Figure 6.7 A). Subsequently to identify peptides that had a reduced or enhanced binding to Reptin, the wild type peptide 38 and variants of peptide 38 were coated onto the microtitre plate and incubated with the respective protein. We found that mutating amino acids 328-331 and 340 to Alanine decreased peptide 38-Reptin binding. Mutation in residues Isoleucine 332, Arginine 333, 335 and 337, Phenylalanine 338 and 341 entirely abolished the interaction. Interestingly, when Glycine 334 and Asparagine 336 were changed into Alanine the binding was in fact enhanced. In addition, deletion of only Tyrosine 327 as well as 1-4 consecutive residues completely prevented the interaction. Interestingly, deletion of only Phenylalanine 341 abolished the interaction, whereas removal of Phenylalanine 341 and adjacent Methionine greatly induced the binding (Figure 6.7 B).

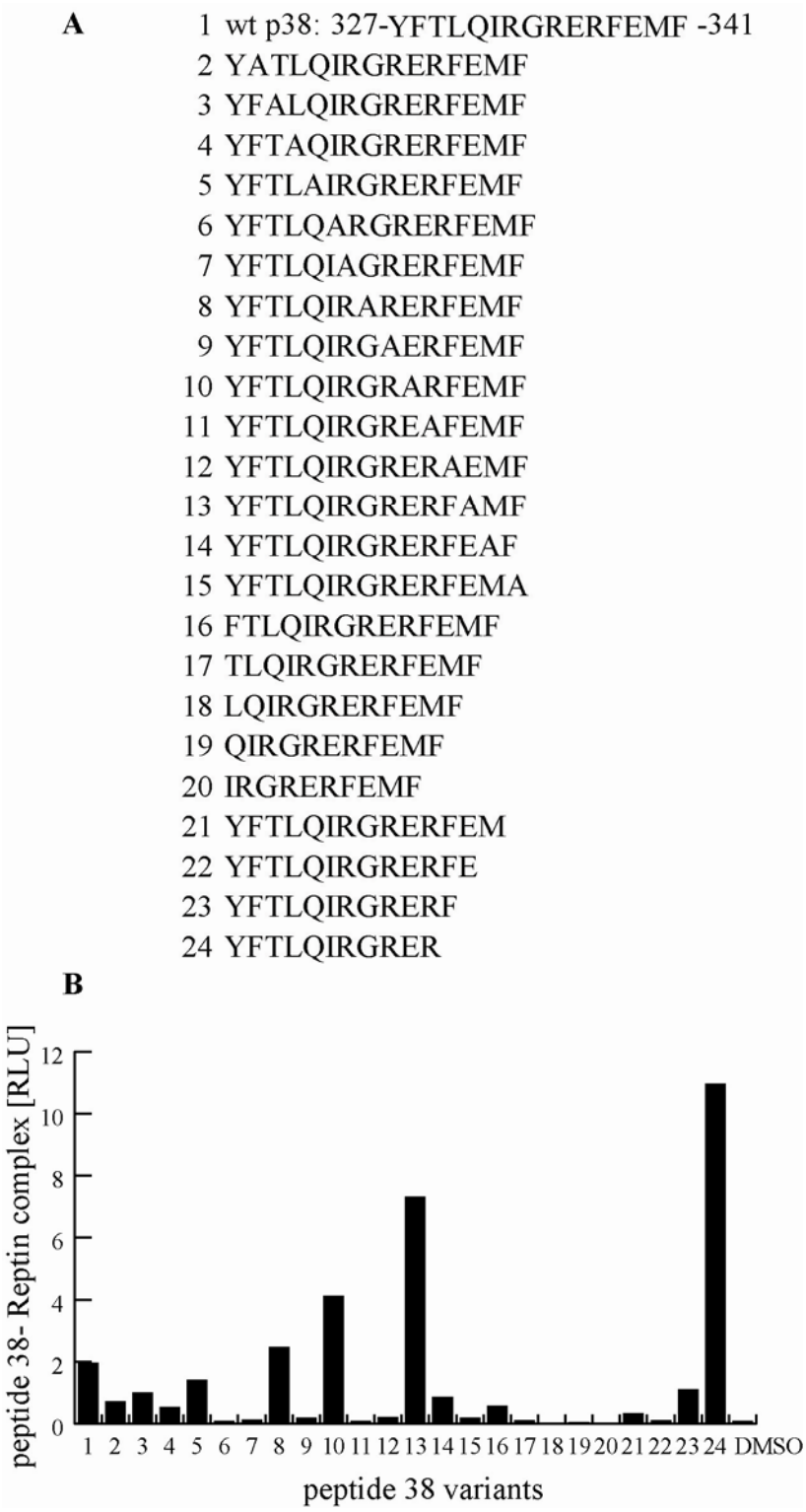

Figure 6.7 Identification of key residues in peptide 38 that stabilize the p53 peptide-Reptin complex. (A) Peptides 2-24 represent modifications in "peptide 38". **(B)** A fixed amount of the indicated biotinylated peptides (as in **A**) was added to a microtitre plate coated with streptavidin and incubated with recombinant Reptin. The amount of Reptin bound was quantified with antibodies specific for Reptin using chemiluminescence. The data are plotted as the extent of protein-peptide complex formation [RLU].

Having defined the residues in peptide 38 that were important for the interaction with Reptin, we set out to generate p53 proteins with mutations of the respective residues. As such following mutant p53 proteins were created: I332V, R333A, R335A, R337A, F338A, E339A.

Firstly we were interested to determine the effect of Reptin overexpression on the wild type and tetramerization domain mutant p53 levels. To this effect H1299 cells were transfected with Reptin and wild type or mutant p53 and the levels of both p53 and p21 proteins were measured. It was found that Reptin stabilised both wild type and mutant p53 proteins. In addition, the levels of p21 increased upon Reptin overexpression (Figure 6.8 A). Interestingly, only p53 R337A displayed a very low activity and it could be only partially rescued upon Reptin overexpression. Subsequently, in order to further investigate Reptin's effect on wild type and mutant p53 steady-state levels and activity, H1299 cells were co-transfected with a titration of Reptin and a fixed amount of wild type or p53 I332V, p53 R337A or p53 F338A. We observed a stimulation of p21 protein with increasing amounts of transfected Reptin in cells transiently expressing wild type p53 protein (Figure 6.8 B). In addition, Reptin overexpression induced p53 F338A in a dose-dependent manner (Figure 6.8 E). Again, it was found that p53 R337A was relatively inactive and Reptin's overexpression could not rescue its activity (Figure 6.8 D). Lastly, p53 I332V protein was active even in the absence of Reptin, and only mild induction of p21 was observed irrespective of the levels of Reptin protein (Figure 6.8 C).

Lastly the effects of AGR2 on Reptin stimulatory role were evaluated. Specifically, H1299 cells were transfected with wild type or p53 I332V, p53 R337A, p53 F338A, p53 R335A, p53 E339A mutant genes and a fixed amount of Reptin and with or without AGR2 gene and the expression levels of both p53 and p21 were determined. We found that co-expressing AGR2 together with Reptin decreased steady-state levels of p53 and p21 proteins compare to cells expressing Reptin only (Figure 6.8 F, lanes 7-12 vs. 1-6).

In addition, in these experiments it was found that Reptin overexpression resulted in the presence of an additional p53 band that is possibly a cleaved product of p53.

Previously Mateo and colleagues performed site directed mutagenesis studies on p53's tetramerization domain and provided insights into which residues and what

mutations affect the stability, folding and oligomerization of p53 protein [174]. Specifically, they reported on two types of mutations including (1) mutations that were affecting dimer/tetramer interface and hence prevented dimer/tetramer formation or (2) mutations of amino acids that were solvent exposed and did not affect p53 oligomerization. These tetramer-disruptive and non-disruptive mutations were I332V, R337A, F338A and R333A, R335A, E336A, E339A, respectively. The mutations made in this study were in the sites found by Mateo to be crucial for the tetramer formation. Therefore, the observed effects of Reptin protein on these mutant proteins can be due to either folding of mutant p53 protein or mutant p53 protein tetramer formation. However in the present study, we could not conclude which mechanism could explain Reptin-dependent stimulation of the activity of p53 protein bearing mutation in tetramerization domain.

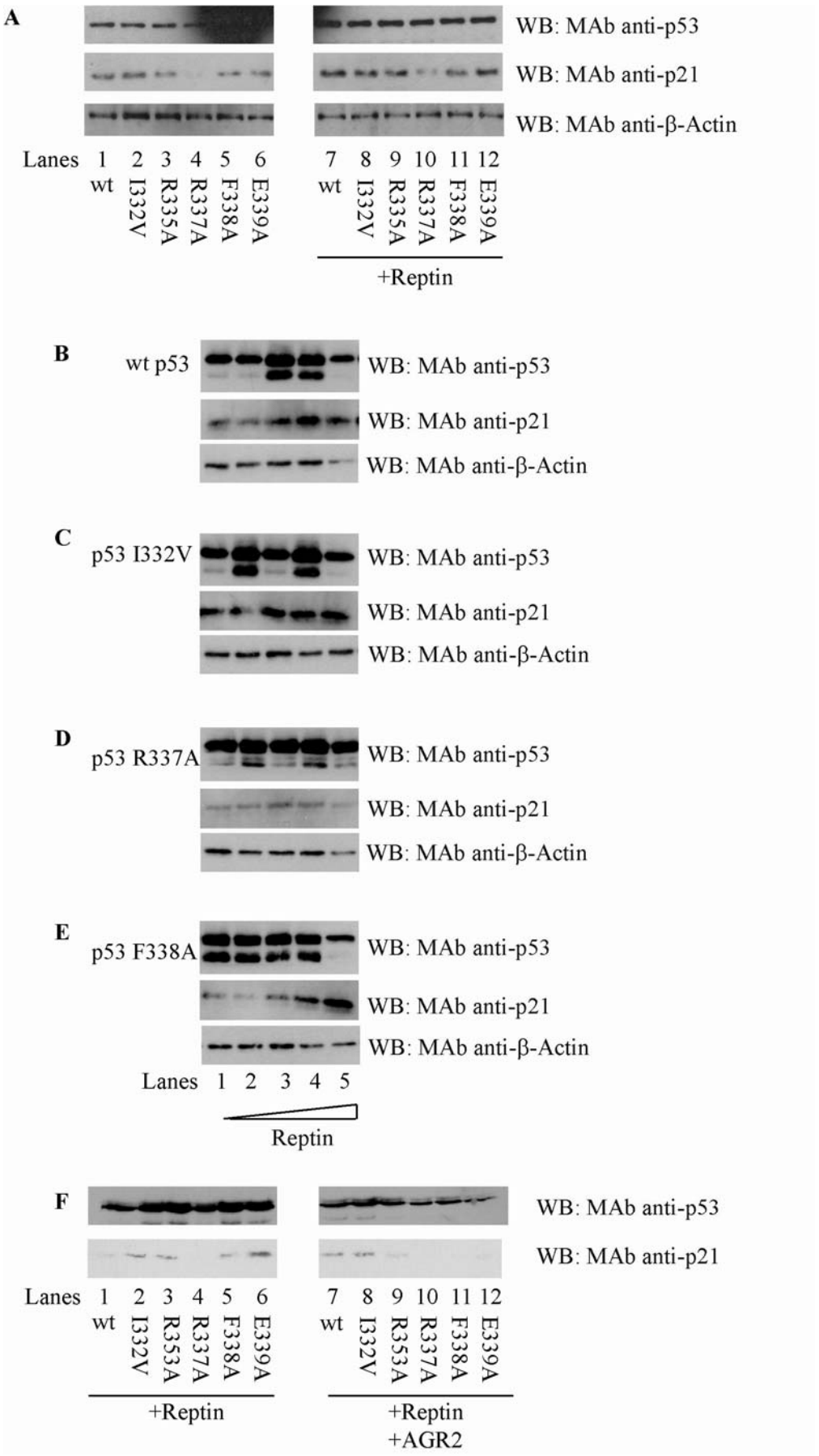
A
WB: MAb anti-p53
WB: MAb anti-p21
WB: MAb anti-β-Actin
Lanes 1 2 3 4 5 6 7 8 9 10 11 12
wt I332V R335A R337A F338A E339A wt I332V R335A R337A F338A E339A
+Reptin
B
wt p53
WB: MAb anti-p53
WB: MAb anti-p21
WB: MAb anti-β-Actin
C
p53 I332V
WB: MAb anti-p53
WB: MAb anti-p21
WB: MAb anti-β-Actin
D
p53 R337A
WB: MAb anti-p53
WB: MAb anti-p21
WB: MAb anti-β-Actin
E
p53 F338A
WB: MAb anti-p53
WB: MAb anti-p21
WB: MAb anti-β-Actin
Lanes 1 2 3 4 5
Reptin
F
WB: MAb anti-p53
WB: MAb anti-p21
Lanes 1 2 3 4 5 6 7 8 9 10 11 12
wt I332V R353A R337A F338A E339A wt I332V R353A R337A F338A E339A
+Reptin
+Reptin
+AGR2

Figure 6.8 Reptin stabilises both wild type and mutant p53 protein. (A) H1299 cells were transfected with the wild type or p53 I332V, p53 R335A p53 R337A, p53 F338A, p53 E339A expression plasmids and with or without HA-tagged Reptin protein expression plasmid. After 24 hours, the cells were harvested and p53 and p21 levels were examined by immunoblotting using specific antibodies. **(B-E)** H1299 cells were transfected with the wild type or p53 I332V, p53 R337A, p53 F338A, expression plasmids and without or with a titration of HA-tagged Reptin. After 24 hours, the cells were harvested and p53 and p21 levels were examined by immunoblotting using specific antibodies. **(F)** H1299 cell were transfected with the wild type or p53 I332V, p53 R335A, p53 R337A, p53 F338A, p53 E339A expression plasmids, with HA-tagged Reptin and without or with AGR2 expression plasmid. After 24 hours, the cells were harvested and p53 and p21 levels were examined by immunoblotting using specific antibodies. β-Actin levels were monitored as a loading control.

As we observed that dose of Reptin gene could change the activity and stability of wild type and mutant p53, we decided to explore further the importance of the Reptin to p53 ratio in regard to the effect Reptin exerts on the p53 pathway. To this effect, H1299 cells were transfected with a titration of p53 protein expression plasmid and a titration of Reptin protein expression plasmid, and the levels of p53 and p21 were examined. We found that Reptin could induce rather than destabilise p53 protein (Figure 6.9 A). Importantly, as the amount of p53 expressed from the same amount of the transfected gene varied between experiments, this also affected the extent of Reptin's mediated stabilisation of p53 protein. In addition, it was found that p21 protein was also induced in response to Reptin overexpression, however, to a different extent depending on the ration of Reptin protein expression plasmid to p53 protein expression plasmid. Furthermore, at the highest levels of both p53 and Reptin, Reptin in fact decreased the levels of p21 protein (Figure 6.9 B).

We concluded that Reptin protein has a dual effect on the p53 protein stability and activity, and that this is dependent upon the ratios of these proteins. At the higher ratios of Reptin to p53 it appears to chaperone p53, as reflected by the increased levels of p53 and p21. However, in cells that already have high levels of active p53, Reptin can in fact inhibit p53 protein. Importantly, the presence of other modulators of p53 protein in H1299 cells, such as MDM2, is likely to add to the complexity of this system and to affect the effect Reptin exerts on the p53 pathway.

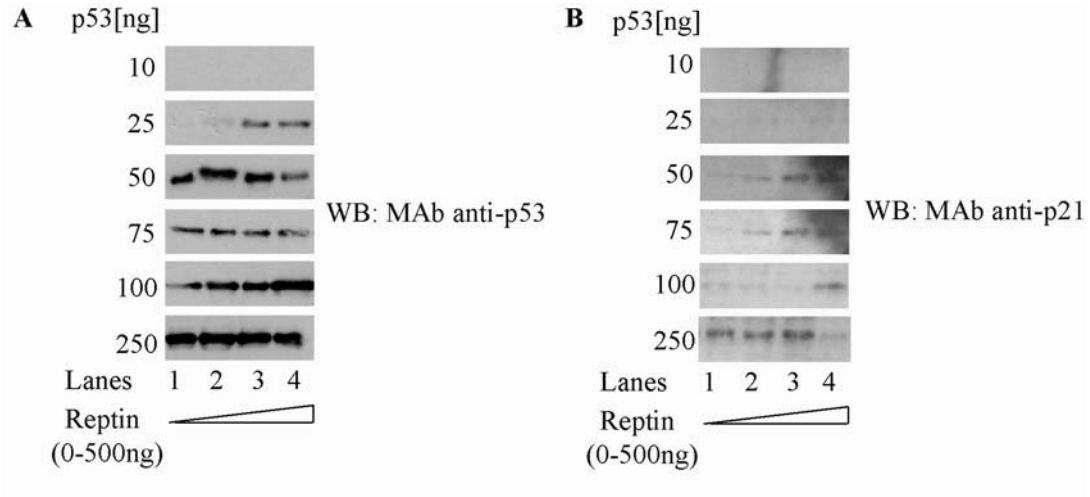

Figure 6.9 Effects of Reptin transfection on p53/p21 protein levels are dependent on the ratio of p53 to Reptin. H1299 cells were transfected with increasing amount of wild type Reptin expression plasmid and a titration of p53 expression plasmid. After 24 hours, the cells were harvested and **(A)** p53 and **(B)** p21 protein levels were examined by immunoblotting using specific antibodies.

While mapping AGR2-Reptin binding interface, it was found that distinctive pools of Reptin protein of different properties existed, depending on whether the protein was purified from *E.coli* or insect Sf9 cells, and whether it was or was not fused to a tag. Therefore, we decided to compare the binding of tagged bacterially expressed Reptin and untagged protein expressed in eukaryotic cells to p53 peptides. It was found that none of the peptides, except for extremely low binding to peptides 17, 18 and peptide 42 from the C-terminal domain, could be bound by Reptin (Figure 6.10 A). This was surprising, as we expected the eukaryotically expressed protein to have similar properties to the protein from human cell lysate. Therefore, we hypothesised that the presence of nucleotide cofactor could mimic the cellular environment better. To test this idea, eukaryotic Reptin was incubated with the p53 peptides in the presence or absence of ADP. Interestingly, we observed that inclusion of nucleotide could greatly increase Reptin's binding to peptide 42 (Figure 6.10 A). Additionally, it revealed additional binding sites for Reptin, such as peptide 41 and 43 that share part of the sequence with peptide 42 (Figure 6.10 A). Further, under these conditions eukaryotically expressed Reptin bound to peptide 38 from the tetramerization domain and to peptide 27 from the Box V domain, which is consistent with the results obtained with bacterially expressed Reptin. This shows that bacterial Reptin, in some respects resembles the nucleotide-bound pool of Reptin. On the other hand if this was true, binding of prokaryotic Reptin to peptides from the C-terminal domain should also have been observed. In fact, we found that upon addition of ATP, bacterially expressed Reptin displayed reduced binding to peptides 26, 31 or 38 (Figure 6.10 B). However surprisingly, Reptin protein expressed in *E.coli* could only bind to peptides 41-43 in the presence of ATP.

As Reptin could differentially bind to the p53 peptides depending on the presence or absence of ATP, we wanted to determine the effect of Walker A or Walker B mutations in Reptin protein on Reptin's ability to stimulate p53 and p21. In addition it has been recently reported for other ATP-binding proteins, such as Hsp90, that ATP binding was important for their p53 modulating activity [264]. Therefore, H1299 cells were transfected with increasing amounts of wild type Reptin or Walker A and Walker B mutant Reptin expression plasmids(Walker A and Walker B mutant Reptin were discussed in Chapter 4 and 5). We did not observe any differences

between wild type and Reptin D299N with respect to p53 stabilisation, as both proteins increased steady-state levels of wild type p53 protein in a dose-dependent manner (Figure 6.10 A). Specifically, it was found that Reptin stabilised p53 protein at ratios of p53 gene to Reptin gene ranging from 1:5 to 1:10 (Figure 6.10 C, lanes 1-3 vs. 4-5). Interestingly, Reptin K83A mutant was not as effective as wild type and Reptin D299N at stabilising p53 under these conditions (Figure 6.10 C). Moreover, although Reptin K83A increased p53 levels to a small extent at the lowest ratio, there was no further stimulation of p53 with increasing amounts of Reptin K83A gene being transfected (Figure 6.10 C). In addition, p21 levels were examined and it was found that wild type Reptin protein overexpression led to the induction of p21 proteins, albeit at a low Reptin to p53 ratio (Figure 6.10 D). Surprisingly, despite the fact that Reptin D299N induced p53 protein levels, decrease rather than an increase in p21 levels was noted. These data again reflects the complexity and many layers of the regulation of p53 protein by Reptin.

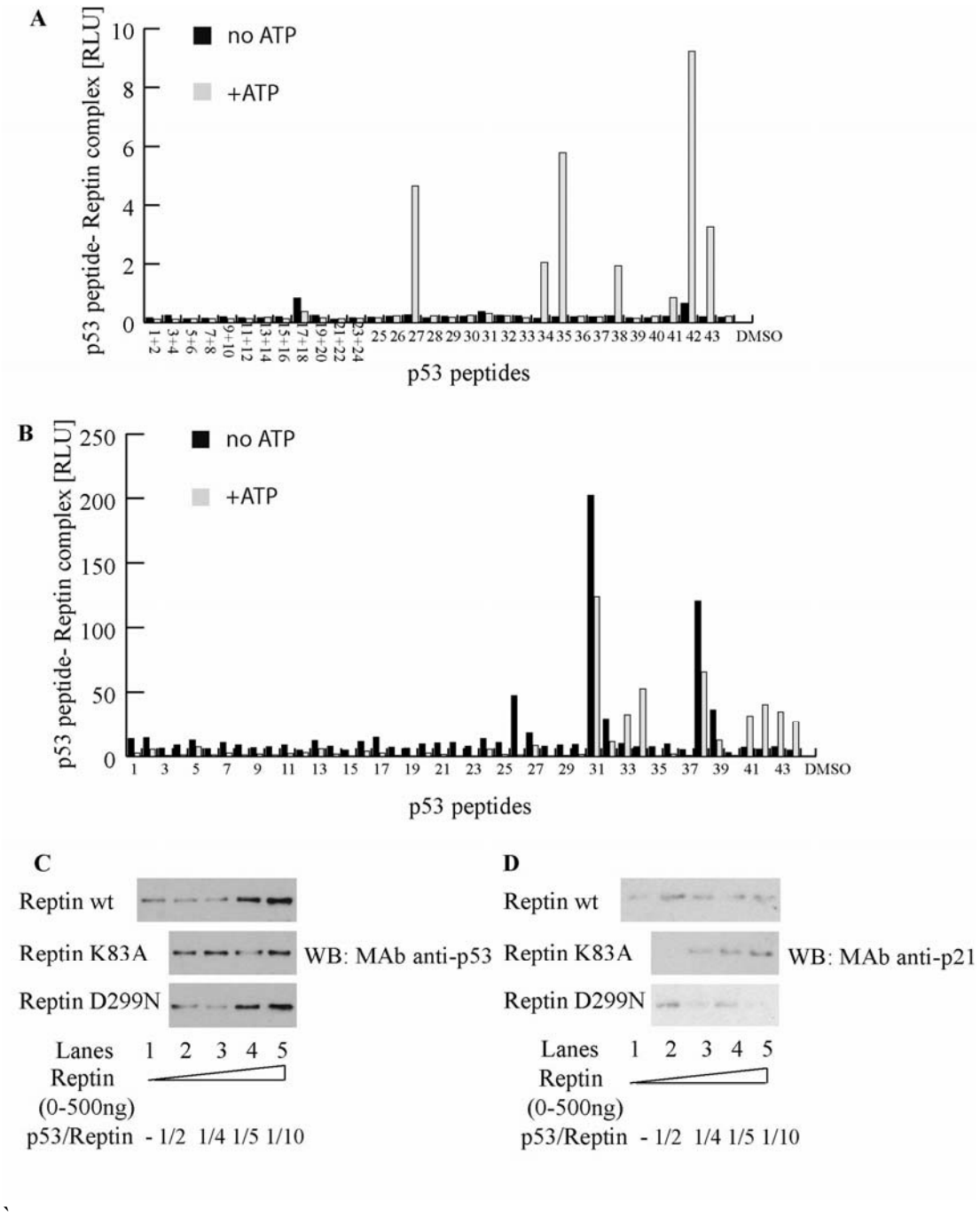

Figure 6.10 Differential binding of recombinant Reptin protein to p53 overlapping peptides. **(A and B)** A fixed amount of the indicated biotinylated peptides (as in **6.4 A**) was added to a microtitre plate coated with streptavidin and incubated with recombinant **(A)** bacterially expressed Reptin with or without ATP or **(B)** Reptin expressed in insect cells with or without ADP. The amount of Reptin bound was quantified with antibodies specific for Reptin using chemiluminescence. The data are plotted as the extent of protein-peptide complex formation [RLU]. **(C and D)** H1299 cells were transfected with increasing amounts of wild type Reptin or Reptin K83A, or Reptin D299N expression plasmids and with constant amount of p53 (50 ng). After 24 hours, the cells were harvested and **(C)** p53 and **(D)** p21 levels were examined by immunoblotting using specific antibodies.

6.2.4 Reptin modulates p53 DNA binding activity

To further dissect Reptin's effect on wild type p53 activity, we set up a direct p53 DNA binding assay. Specifically, an EMSA was performed using a radiolabelled p21 promoter fragments that are known to be recognized by p53 protein. Firstly, the probe was incubated with or without the p53 protein purified from insect cells, to establish whether p53 forms an active, DNA-binding tetramer. Indeed, we observed a shift in the probe incubated with p53 protein and a decrease in the amount of the free probe. Further the titration of p53 protein was performed and a dose dependent increase in the shifted bound probe was observed, indicating p53-specific binding (Figure 6.11 A). As such we examined the effect of Reptin addition on the p53-DNA binding. To this effect, a titration of p53 protein was pre-incubated with a titration of bacterially expressed Reptin and the ability of Reptin protein to activate p53 binding to p53-specific probe was monitored by EMSA. Upon incubation of 0.1 μl or 0.25 μl of purified p53 with the probe we could not detect p53 bound to the probe (Figure 6.11 B, lanes 1 and 2). Interestingly, following pre-incubation of 0.1 μl or 0.25 μl of purified p53 with the increasing amount of Reptin protein, it was found that Reptin could stimulate p53- DNA binding, (Figure 6.11 B, lane 1 vs. 5-8 and lane 2 vs. 9-12). Incubation of 0.25 μl or 0.75 μl of purified p53 with the probe revealed relatively high amount of p53 bound to the probe (Figure 6.11 B, lanes 3 and 4) and this could not be further stimulated with Reptin (Figure 6.11 B, lanes 3 vs. 13-16 and lane 4 vs. 17-20). Further, as we found that prokaryotically and eukaryotically expressed Reptin differed in their p53 binding ability, we tested whether Reptin purified from Sf9 cells could also chaperone p53 for DNA binding. Again, Reptin protein could induce p53's DNA binding (Figure 6.11 C). Given that in Chapter 5 it was found that Reptin protein can shift into different oligomeric species depending on the temperature, we decided to determine how changes in temperature affect its chaperoning activity. To this effect p53 and Reptin were incubated at temperatures ranging from 4ºC to 30ºC and then probe was added. It was found that regardless of the temperature Reptin stimulated p53-DNA binding, but the extent of stimulation at different concentrations of Reptin differed depending on the temperature (Figure

6.11 D). This data indicated that oligomerization of Reptin may have a role in the chaperoning of p53.

Given that ATP and/or ADP affected Reptin-p53 complex formation, we were interested to determine the effect of addition of the nucleotide on Reptin's chaperoning activity. To this effect Reptin was pre-incubated with a titration of either ATP or ADP and the amount of p53 bound to its target DNA was examined. As expected, given that Reptin has two different classes of ATP binding sites, different effects of the addition of nucleotide were observed depending on the concentration of the nucleotide and the type of nucleotide as well as on the amount of Reptin protein. Firstly, when p53 was incubated with a constant amount of Reptin, the addition of increasing amount of ADP enhanced Reptin dependent stimulation of p53-DNA binding (Figure 6.12 A). Contrary to this, ATP inhibited Reptin's effect on p53 binding to its target sequence. Interestingly, when a broader range of concentrations of ADP was incubated with different amounts of Reptin, it was found that the effect of this nucleotide on Reptin's chaperoning activity was largely dependent on the concentration of Reptin and ADP. This is in keeping with chapter 5's results, since it was found that two distinct ATP-binding sites exist in Reptin and in addition Reptin exists as a mixture of different oligomeric species that are likely to have different activities.

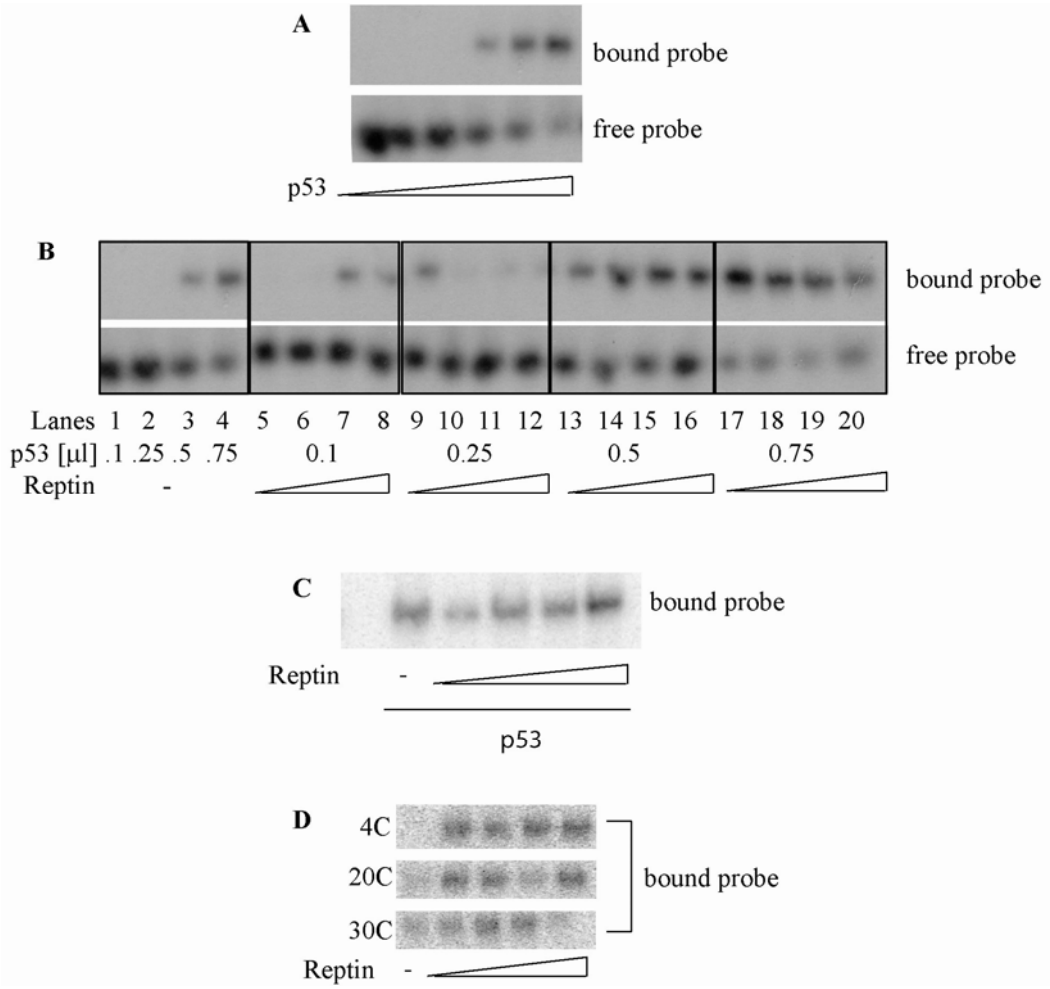

Figure 6.11 Reptin auguments p53-DNA binding function. The DNA binding function of p53 was measured using a radiolabeled p21 DNA sequence and native gel electrophoresis. **(A)** A titration of p53 was incubated with the p21 promoter sequence and the binding activity of p53 was determined **(B)** A titration of p53 protein was incubated without or with a titration of prokaryotically expressed Reptin. **(C)** The p53 protein was incubated without or with eukaryotically expressed Reptin titration. **(D)** The p53 protein was incubated without or with eukaryotically expressed Reptin titration at 4ºC to 30ºC. DNA-p53 complexes were resolved using a native polyacrylamide gel, dried, and detected by storage phosphor screen. Bound and free probe are highlighted. The images of the respective whole gels are in supp figure 6.11.

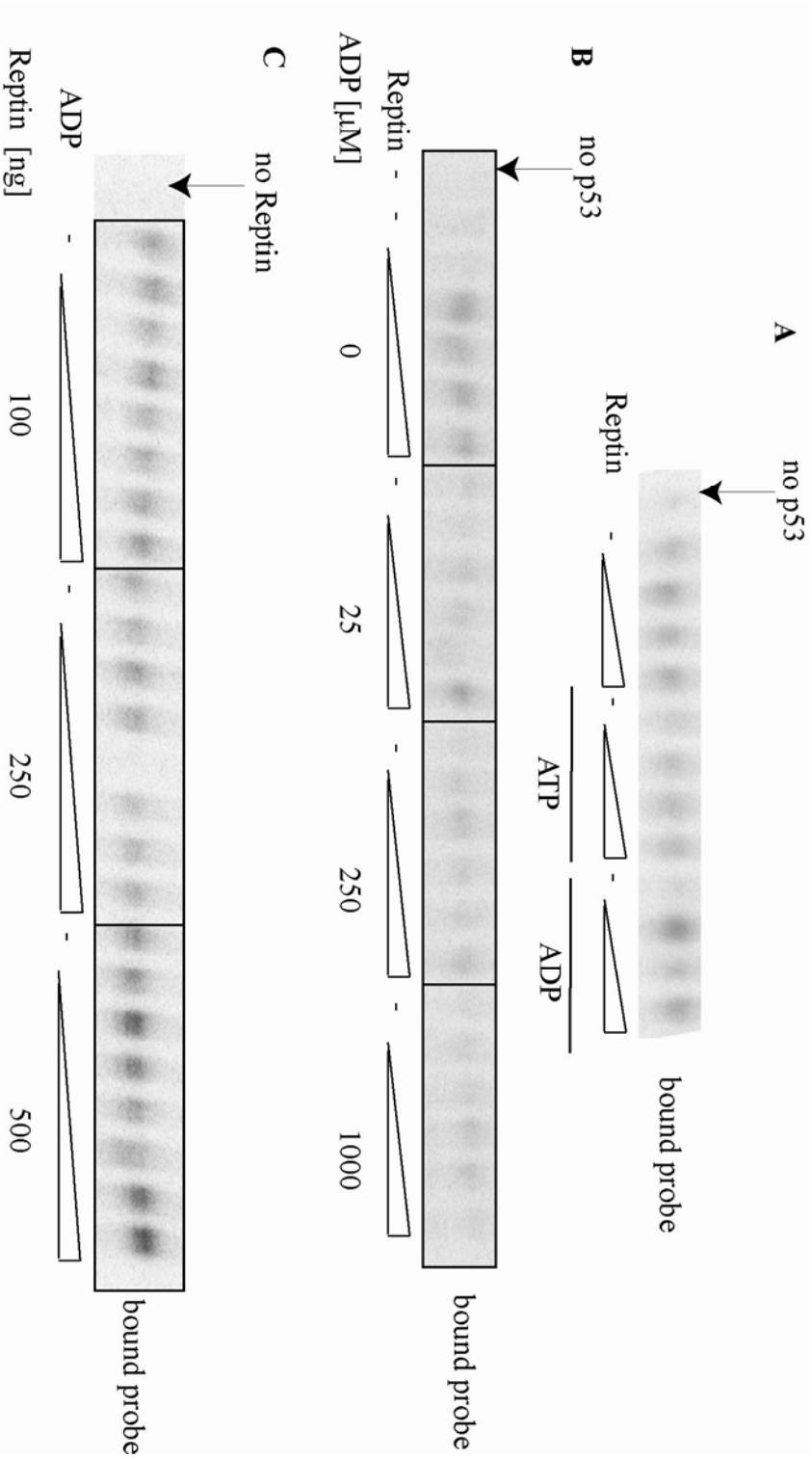

Figure 6.12 Nucleotide effects on Reptin-dependent increase in p53-DNA binding function. The DNA binding function of p53 was measured using a radiolabeled p21 DNA sequence and native gel electrophoresis. p53 was incubated with **(A)** a titration of Reptin pre-incubated without or with ATP or ADP, **(B and C)** a titration of Reptin pre-incubated without or with a titration of ADP, and the binding activity of p53 was determined. The images of the respective whole gels are in supp figure 6.12.

It is worth noting, that we did not observe a supershift of p53 upon addition of Reptin. This implies that despite the direct interaction between Reptin and p53, and the stimulatory effect of the former on the DNA binding activity of the latter, Reptin is not a part of the activated complex. Alternatively, Reptin may be a part of the DNA-p53 complex, but it dissociates from it during electrophoresis. Another possibility is that it could be that Reptin forms a transient ternary assembly that disassembles after p53 is recruited to its putative site. This would be consistent with the chaperoning function of this complex. However to resolve this issue, it could be tested whether or not antibodies specific to Reptin could shift the complex. Interestingly, we found that Reptin could bind to p53 that was bound to its specific sequence. However on the other hand, pre-incubating p53 with increasing amounts of p53-specific sequence, decreased p53 binding to Reptin, when compared to p53 incubated with a non-specific DNA.

6.3 Discussion

The known interactome of wild type p53 protein comprises over 300 proteins however, for many of these interactions the functions of these complexes are not completely understood. The hundreds of proteins that p53 binds to are involved in its folding, degradation, regulating transcription, and other p53-related processes. The mutant p53 interactome is less well-defined than the wild type p53 interactome. Interestingly, a number of studies has recently emerged proving that mutant p53 proteins can bind to some of the components of wild type p53 network and rewire it to gain oncogenic activity.

The p53 protein contains distinct modules that are important for DNA binding, transcription regulation, MDM2 or p300 binding, protein kinase binding, and homo-tetramerization. The great protein binding potential of p53 stems from the fact that it contains disordered regions in its N-terminus and C-terminus and in addition the core domain of p53 is thermodynamically unstable, which adds to the protein's flexibility. These unstructured or labile regions comprise short motifs that allow the binding promiscuity of the protein and therefore allow numerous protein-protein interactions. The multi-binding docking sites in p53 allow fine regulation of this protein, dynamic changes in the interactome at any give time, and consequently affect the cellular outcome of p53 activation.

In this study, we found yet another p53-binding protein, namely Reptin and we showed that Reptin could form a complex with both wild type and mutant p53. Interestingly, three peptide motifs were involved in the interaction with the wild type p53 protein, namely Box V peptide, Arginine-rich region in tetramerization domain and short sequence from the C-terminal regulatory domain. Moreover, differential effect of Reptin protein on the p53 activity was observed, making it a novel protein amongst proteins such as CHIP and MDM2 that depending on as yet not fully understood cellular conditions either downregulate or chaperone p53 protein.

Box V motif is a highly conserved region in the thermodynamically unstable DNA core domain of p53. This region is remarkable for its conformational flexibility [323]. Moreover, this motif has been shown to provide MDM2 ubiquitination signal and form a docking site for multiple protein kinases [160-162, 196]. Interestingly,

mutations in p53 at this interface, or in the core domain of p53, such as R175H or F270A, predispose p53 to MDM2-mediated ubiquitination [160] and it was shown to be due to the increased binding of MDM2 to this mutant protein. Interestingly, we found that Reptin-p53 R175H and Reptin-p53 F270A complexes were more abundant than Reptin-wild type p53 complex, probably due to the higher levels of the mutant protein present in the cell. Indeed, the p53 mutant proteins appear to be inherently stable in cancer cells and were found to be stabilized in some cancers in mice, however not in normal tissues [300, 301, 308]. In addition, Reptin protein formed a stable complex with p53 protein bearing S269D mutation. Ser269 phosphorylation has been recently shown to play a role in inactivating p53 protein following DNA damage. Specifically a model was proposed whereby two distinct pools of wild type p53 could form in response to DNA damage: transcriptionally active one and inactive phospho-Ser269 p53 [164, 674] that could function independently of the classic p53-dependent transcription programme. Indeed, p53 S269D displayed enhanced ubiquitination *in vivo*, was inactive for DNA binding *in vitro* and inactive in respect to p21 and MDM2 induction *in vivo*, however it is stabilised in cells [164, 674]. As Reptin formed a more stable complex with p53 S269D than with the wild type p53 protein, it would be interesting to determine, whether this interaction is involved in the stabilisation of this inactive (at wild type functions) protein, for example by preventing its ubiquitination or degradation. It has not been established yet whether, similar to other mutant proteins, the phospho-mimetic form of p53 protein has independent functions to the wild type protein. However, since Reptin overexpression led to stabilisation of other mutant p53 proteins, we could hypothesise that this is yet another example of mutant p53 protein being able to rewire the wild type p53 protein interacting landscape. Further, these findings could form the basis for developing tools/drugs that disrupt mutant p53 protein-Reptin interactions and lead to degradation of mutant protein in cancer cells.

Some of the mutations that were investigated in this study are know to result in an unfolded or structurally distorted p53 protein. These proteins are commonly found in complexes with molecular chaperones, such as Hsc70 and Hsp90 [164, 308, 674]. In addition, molecular chaperones were found to interact with wild type p53 and assist in its assembly and proper folding [675] and stimulate p53 DNA binding

activity [264]. Similarly to these proteins, Reptin formed a stable complex with the unfolded p53 mutant proteins. In addition, Reptin increased transcriptional activity of wild type and mutant p53 and stabilised wild type p53-DNA binding in EMSA. Based on Reptin's activating role in p53-DNA binding and its increased interaction with unfolded and stabilised mutant p53 protein, we can propose that Reptin is yet another molecular chaperone for p53 protein. As Reptin increased p53 activity even at physiological temperature, it seems that p53-DNA interaction is highly influenced by chaperones even under normal conditions. Indeed, Walerych and colleagues found that Hsp70 and Hsp90 were required for the folding of the wild type p53 protein [263]. In addition, these data also show that a fraction of the p53 is unfolded/misfolded or monomeric and unable to bind DNA *in vitro*. Moreover, the same observation has been made *in vivo* [266]. Although wild type p53 forms a direct interaction with Reptin protein, we could not test whether or not Reptin forms a physical contact with the mutant p53 proteins. In fact, it is possible that the interactions that Reptin forms with mutant p53 proteins are indirect. For example, it was found that Hsp90, another chaperone protein, formed a complex with some p53 structural mutants, such as p53 R175H, however these interaction were not direct and required other chaperone proteins [261].

We found that Reptin-dependent induction of p53 DNA binding was modulated by ATP and ADP. Addition of the nucleotides either stimulated or decreased DNA binding, depending on the concentration and type of the nucleotide. This is in agreement with the findings that Reptin has two distinct ATP binding sites which presumably display diverse affinities to different nucleotides. The presence of ATP or ADP can affect Reptin itself in different ways, depending on various conditions, such as temperature. Moreover, the concentration of the available nucleotide affects the rate of hydrolysis, the occupancy of the ATP binding sites, the conformation and oligomerization. These effects on biochemical properties of Reptin are likely to alter its chaperoning ability and other activities. Reptin, similarly to Hsp90, likely undergoes multiple transient interactions which depending on the presence of nucleotide or co-chaperones can be tuned to performed different tasks. Hence, differences in both *in vitro* and *in vivo* response will be observed, as this is intrinsic and required for the chaperones' activity [332, 588].

In addition, we found that Reptin K83A was less active than wild type Reptin or Reptin D299N at stabilising wild type p53 protein. *In silico* screens, aiming at targeting Reptin ATP-binding pocket could result in the identification of lead molecules that could be used as tools to unravel the mechanism of Reptin-dependent stabilisation and folding of wild type and mutant p53 in cancer cells. Such ideas have already been exploited for another molecular chaperone, namely Hsp90. Natural product geldanamycin and its analogues were found to inhibit Hsp90 and favoured mutant p53 association with the Hsp70-CHIP ubiquitination-degradation proteins [262, 675].

In this study it was found that Reptin stimulated transcription of the p53 target gene p21 *in vivo*. The transcriptional activities of p53 as well as its turnover are tightly regulated by post-translational modifications and PPIs [666]. For example acetylation of p53 is essential for recruitment of transcriptional cofactors whereas phosphorylation alters p53's PPI and consequently modulates p53's activity as a transcription factor. p53 is also targeted for degradation by ubiquitination. Interestingly, Reptin is embedded in the TIP60 complex [360] that has been found previously to participate in p53-acetylation. Specifically, TIP60 acetylates Lys120 in response to DNA damage and this leads to transactivation of apoptotic genes including PUMA [230, 231, 676]. In addition, Tip60 was found to be essential for p21 expression following DNA damage [676, 677]. Moroever, it was found that Tip60 could inhibit MDM2-induced degradation of p53 [676]. As Reptin associates with this acetyltransferase and was found to be critical for the appropriate assembly of Tip60 complex, it is likely that Reptin may modulate p53 activity by affecting p53 or histone acetylation.

In addition, Reptin is also involved in a complex with other p53 modifying enzymes namely SMG-1 and ATM. SMG-1 and ATM kinases control p53 phosphorylation. It appears that SMG-1-dependent phosphorylation initiates p53 phosphorylaiton in response to hypoxia and ATM maintains the phosphorylation of p53 over time [678, 679]. This results in p53-dependent activation of p21 expression. In addition ATM and SMG-1 control p21 stability. Currently, we do not know whether Reptin's regulation of p53 activity involves any of its PPIs and/or p53 PTMs. We did not

observe differences in the phosphorylation or acetylation of common residues in p53 in this study (data not shown).

In addition Reptin overexpression resulted in the stabilisation of p21 protein in cells transiently expressing different types of mutant p53 proteins. p21 was the first discovered cdk inhibitor that, through negative regulation of cell proliferation, is thought to prevent tumourigenesis [680]. Indeed, p21-null mice succumb to cancer development and mice bearing mutant p53, that can activate p21, display later onset of spontaneous tumours [681]. Since Reptin increased p21 expression it could indicate that it acts as tumour suppressor. However, in some cells p21 expression has been associated with pro-survival signals. For example, cells that have lost p21 are more sensitive to anticancer drugs [682]. In addition, p21 was found to be overexpressed in some human cancers [683]. Interestingly, Hsp90 stabilises p21, as Reptin does, and it is thought that it may act as the oncogenic signal in some cancers that depend on p21 for their survival. In this study, Reptin's effect on wild type and mutant p53 activity was only monitored by assessing p53 and p21 levels. However, mutant p53 may exert gain of function on a subset of genes distinct from wild type p53 target genes and their products may promote tumourogenic growth [684, 685]. Therefore it would be interesting to investigate whether Reptin protein, by stabilising mutant p53 protein, increases expression of such genes.

In addition to the core domain, Reptin bound to C-terminal peptide of p53, however, only in the presence of nucleotide. As was already described in chapter 5, the presence of nucleotide affects reptin thermostability and changes its oligomerizations status. This implies that the ATP binding-triggered change in Reptin conformation/oligomerization forms a distinct pool of Reptin that could potentially differentially regulate p53. Interestingly, similar observation of ligand-dependent specificity for target protein was made for MDM2 protein. It was found that MDM2 interaction with RNA caused conformational change that reduced its affinity for its primary binding site in the N-terminus of p53 and switched the specifity for the Box V motif of p53 [160]. This data further underscores the conformational dynamism of Reptin. It is difficult to assess how ATP binding by Reptin regulates the C-terminus of p53-Reptin interaction in cells, as it is hard to establish the amount of Reptin bound to ATP or to ADP or Reptin- nucleotide free

complexes *in vivo*. Determining Reptin's structure and understanding better its oligomerization can give us further insight into p53-Reptin interaction.

The p53 C-terminal regulatory domain contains sites of methylation, acetylation, phosphorylation, ubiquitination, sumoylation, and neddylation that regulate p53 function and protein levels (reviewed in [660, 686]). Reptin interaction with the C-terminal negative regulatory domain could affect the range of modifications that p53 undergoes. For example by binding to this C-terminal domain Reptin may sterically block post-translational modifications. Interestingly, C-terminal domain forms a docking site for a variety of proteins, including proteins acting as transcription cofactors [189, 219, 687], proteins that sequester or inhibit p53 activity by directly binding to the C-terminus [180, 688] and proteins that modify this site [219, 256, 689, 690]. As already mentioned, the large regions of disorder are a key feature of the p53 protein that allows it to have such an extensive interactome [138]. Two implications of this are that this domain can bind various partners, however the mode of binding is different. For example, this domain folds into a helix upon S100B binding [186], it forms β-strand following Sir2 binding [187], β-turn when bound to cAMP response element-binding (CREB) binding protein (CBP) [189] and lastly it lacks any ordered secondary structure in the complex with the cyclin A/cyclin-dependent protein kinase 2 complex [188]. In addition to this, the C-regulatory domain binds DNA non-specifically through the low affinity interactions of several lysine residues and this inhibits binding of a specific DNA sequence by the core domain [691, 692]. This inhibition can be relieved upon C-terminus-specific antibody binding, PTMs, or its deletion [691]. It would be interesting to know whether Reptin's interaction with the C-terminal peptide relieves p53 from the inhibitory effect of binding of this domain to the core domain. At present the structure that CTD adopts upon binding to Reptin is not known. Interestingly, it was found that many of the p53 CTD binding site partners use the hydrophobic binding pocket for the interaction with this motif [693]. As Reptin binds to C-terminal domain only in the presence of ATP (at least in the peptide binding assay), we could speculate that ATP addition generates conformational change that results in the formation, or opening, of the hydrophobic pocket in Reptin. In addition, as the dual effect of Reptin overexpression on p53 stability was observed, it is possible that

depending on whether C-terminus is engaged or not in the p53-Reptin interaction, different responses can be observed.

Interestingly, differential binding to the C-terminus has been shown for the S100 protein family members [180, 694-696]. The S100 protein family comprises over 20 EF-hand calcium-binding proteins with several functions and tissue distributions [697]. S100A4 expression has been associated with metastasis [698, 699]. Interestingly, all of the p53-binding S100 proteins, including S100B and S100A4, S100A1, S100A2, S100A6, and S100A11 bind preferentially to the tetramerization domain [180, 688]. S100 proteins could mostly bind to the p53 monomer, however a subset of S100 proteins could also interact with tetrameric p53 [700]. We do not know at present which oligomerizaiton state of p53 is preferentially bound by Reptin. It is also unclear whether Reptin is directly involved in the regulation of p53's oligomerization state. Interestingly, we found in the peptide binding assay, that Reptin bound with the highest affinity to peptide 38, from the tetramerization domain. In fact, peptide 38 appeared to stabilise Reptin-p53 interaction, indicating that it may be the primary binding site that allosterically modulates Reptin and stimulates binding to other sites on p53.

We found that depending on the p53 to Reptin ratio different effects on p53 activity were observed. In the *in vitro* assays, very high concentration of p53 bound efficiently to DNA without Reptin, and Reptin did not affect it further, or could inhibit the binding, indicating that p53 could form an active tetramer at this concentration. However, at very low levels, p53 was inactive, and only upon incubation with Reptin, p53 binding to its target sequence was observed, suggesting that Reptin could help in folding and assembling of the active p53 tetramer. In the *in vivo* experiments, Reptin could also differentially affect p53 depending on the concentrations of p53. At very low levels of p53 (possibly levels resembling non-stressed situation, when p53 is not active), Reptin activated p53 transcription. However, at the higher levels (reflecting p53 levels in the stressed condition), Reptin could actually downregulate p53 activity. We can hypothesise that under normal conditions p53 is at low levels and remains inactive, and probably a fraction of it exists as a monomer/inactive tetramers. Reptin could bind to monomers and affect the oligomerization equilibrium (help to form tetramer) and activate it for DNA

binding. Conversely, at the high levels of p53, when tetramer is formed on the chromatin, Reptin binds, and may facilitate recruitment of co-factors; for example, Tip60 or other chromatin modelling enzymes and activate p53. In addition in stressed cells, when the concentration of p53 is very high, and all of p53 is tetrameric and active, Reptin could possibly function to dissociate the tetramer or target it for inactivation, or to switch off the response. At the same time, high and low levels of p53 may lead to different amounts of folded and unfolded p53, and switch on different activities of Reptin towards these different pools of p53. Interestingly, S100B has a different effect on p53 activity, depending on its levels, with low to moderate levels having a co-operative effect in the activation of p53 activity [178, 701] and high levels preventing p53 oligomerization and consequently inhibiting its activity [702].

Another relevant observation from the studies on S100 proteins is that despite the high sequence similarities between S100 proteins family members, they bound differentially to p53. Specifically, S100B and S100A2 bind well to both the C-terminal region and the tetramerization domain [180, 688], whereas S100A4 interacts strongly only with the oligomerization module. Similarly, ligand binding by Reptin may bring about different pools of Reptin that either bind, or not, the C-regulatory domain, and exert different effects on p53 activity.

Despite the fact that Reptin chaperoned p53 to bind to its target sequence, we did not find Reptin in the p53-DNA complex, even though Reptin can bind to p53 bound to DNA as suggested by preliminary data (data not shown). However, this is in agreement with the chaperone function of Reptin. Reptin binding to p53 stabilises the latter and induces DNA binding. Once the p53 protein is bound to its target sequence DNA, the chaperone function of Reptin is not required anymore and it dissociates from the complex. Similarly, the mutant p53 stabilising peptide CDB3, which was derived from a p53 binding protein, binds and stabilises p53 DNA-binding domain, however DNA binding to p53 displaces the peptide. Indeed, we found that p21 DNA competed with Reptin for p53 binding in an ELISA and similarly it was found that gadd45 DNA dissociated CDB3 from p53 as well [703].

In this study AGR2 protein decreased wild type p53 protein levels, inhibited its transcriptional activity and decreased p21 protein levels. In addition it was found

that overexpression of AGR2 could overcome Reptin-mediated stabilisation of wild type and mutant p53 indicating that AGR2's inhibition of p53 may be a dominant pathway.

In summary, in this study we found that AGR2-binding protein Reptin interacts with the p53 protein both *in vitro* and *in vivo*. Depending on the ratios of these proteins, Reptin either stabilises p53 protein and increases the transcription of its target gene, or inhibits it and attenuates the expression of p21. In addition, we found that Reptin interacted with and stabilised mutant p53 protein. Given that cancer cells evolved to evade the normal degradation pathways for mutant p53 protein, these findings further our understanding of the mechanisms of mutant p53 stabilisation and manipulating Reptin-mutant p53 interaction may add to the strategies to develop means to degrade mutant p53 protein.

Chapter 7: Conclusions, future work and preliminary data

p53 is a major hub in the cellular network that functions as a tumour suppressor through its role in the regulation of the cell cycle and cell death. The p53 pathway is commonly misregulated in cancers and efforts to reactivate it or to inactivate the oncogenic functions of mutant p53 protein are the main strategies pursued by current drug discovery programmes. In the last decade, AGR2 protein has been found to be overexpressed in a number of different cancers, its expression could predict poor prognosis for ER-positive breast cancer patients and tamoxifen response. In addition, AGR2 has been shown to inhibit p53 activity.

The regulation of AGR2-p53 pathway, as well as the mechanism of AGR2-mediated inhibition was largely undefined before this study. In this work, we have found that TGF-β and ATM kinase pathways downregulate AGR2 protein and that this leads to the stabilisation and activation of p53, and the p53 target gene p21. We have identified novel substrate of ATM kinase, namely SNIP1, and subsequently showed that it is involved in the negative regulation of AGR2 protein. In addition, data obtained using chemical inhibitors of protein degradation suggested that AGR2 is degraded via the lysosomal pathway. However, several questions arose during the course of this study and have not been fully addressed as yet. Firstly, it is not clear what the physiological outcome of TGF-β-ATM-mediated downregulation of AGR2 is. It was hypothesised that removal of AGR2 may be required for the initiation of EMT. However, future work should be directed at determining whether AGR2 loss indeed triggers the EMT and leads to altered migration and invasion. In addition, although it was concluded that AGR2 is degraded in lysosomes, AGR2 protein was predicted to be a secreted protein, and the current report did not rule out the possibility that TGF-β or ATM trigger secretion of AGR2. In the future, the levels of AGR2 in the medium from cells treated with TGF-β will be compared to that of untreated cells. Should AGR2 protein be secreted, this protein could turn out to have an entirely different function in the process of EMT or migration, and, for example, could act as an autocrine pro-migratory factor. Hence, it is crucial to determine

whether AGR2 is indeed targeted for degradation or secreted in response to TGF-β treatment.

In search for the mechanism of AGR2-mediated regulation of p53 pathway, we explored the vaguely understood interactome of AGR2. We found that AGR2 forms a complex with the multifunctional Reptin protein and this interaction is mediated by a short linear motif in the loop sequence of AGR2 protein. In addition, Reptin was found in a complex with p53 protein and could increase its steady-state levels and induced its transcriptional activity. We proposed a model whereby Reptin could chaperone p53 and AGR2 protein could exploit it to inhibit p53, as overexpression of AGR2 could prevent Reptin-mediated stabilisation of p53. Importantly, the stimulatory effect of Reptin was dependent on the ratio of Reptin to p53 protein, and at high p53 to Reptin ratio, Reptin, in fact, downregulated rather than stimulated p53 activity. It is still unclear whether AGR2 indeed blocks Reptin-dependent activation of p53 or whether it is Reptin that actually "shields" p53 from AGR2. Data obtained in this study support the first model, however, the second hypothesis could also be true. Since AGR2 was found in a trimeric complex with p53 and Reptin, it would be interesting to investigate whether AGR2 F104A and AGR2 Y111A (AGR2 loop mutants), that we showed have reduced Reptin binding ability, retain their ability to inhibit p53. The initial observation from H1299 cells transiently expressing either wild type AGR2 or AGR2 loop mutants is that the latter are in fact more potent as inhibitors of p53. These data suggests that AGR2 bound to Reptin looses its p53-inhibitory activity and consequently the mutations in AGR2 sequence that disrupt its binding with Reptin make it a better inhibitor of p53.

The oligomerization properties of Reptin add into the complexity of the AGR2-p53-Reptin pathway. Currently, we do not know whether or not Reptin can interact with either AGR2 or p53 as a hexamer or monomer. Future work could determine this and address the question of whether different oligomeric species of Reptin exert different effects on p53 activity. In this study, it was found that although the Walker A mutant did not affect the levels of p53, it was able to activate p53. On the other hand, Walker B mutant stabilised p53 protein, however, it was less active as a chaperone of p53 transcriptional activity. These differential effects of mutations suggest that indeed depending on the conformation/oligomerization status of Reptin,

different outcomes regarding p53 could be expected. In chapter 5 we found that Walker A mutations sensitises Reptin to ATP-dependent oligomerization, whereas Walker B mutation stabilises the mutant protein in the hexamer form already in the absence of ATP, and addition of ATP can actually disrupt the hexamer. These findings could form a basis for the hypothesis that different pools of Reptin as well as different ratio of Reptin to p53 will result in different cellular responses. Firstly, Reptin is likely to interact with p53 protein both as a hexamer and a monomer, and this could have different effects on p53, as either hexamer or monomer are likely to (1) recruit different co-factors to the complex, (2) have different subcellular localisation, (3) have different ATP-binding and ATPase activities. In addition, the distinct oligomeric forms of Reptin can also differentially affect AGR2 and AGR2's p53-inhibitory function (Figure 7.1).

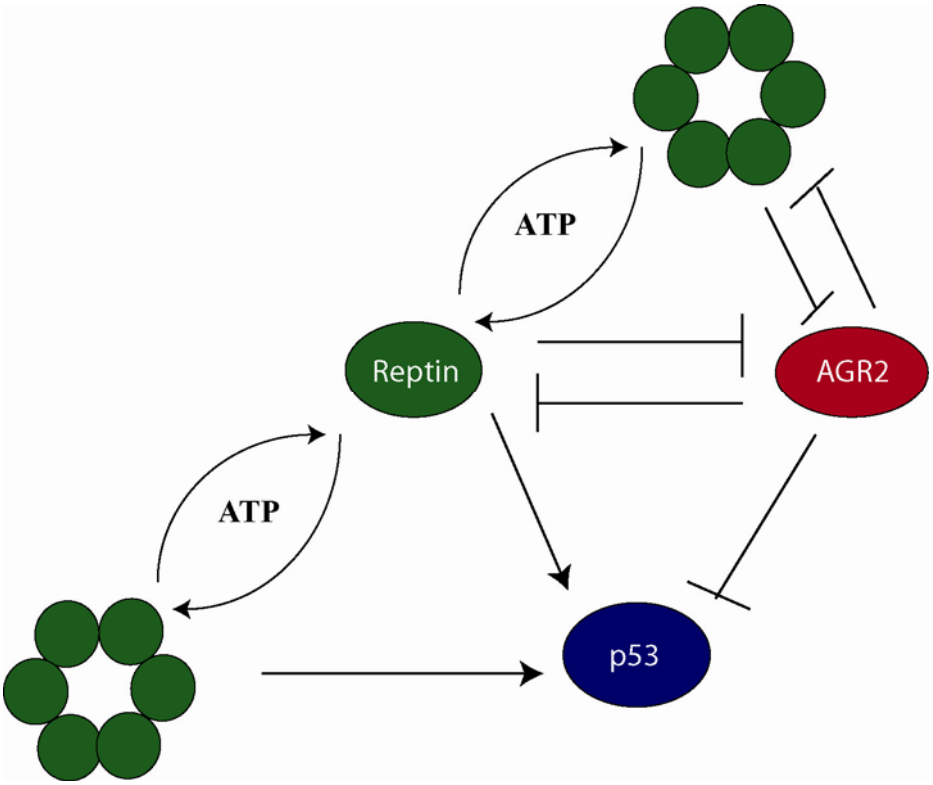

Figure 7.1 Schematic model of hypotheses on the function of Reptin-AGR2-p53 trimeric complex. The nucleotide influences the oligomeric status of Reptin protein. Reptin either as a hexamer or as a monomer interacts with and regulates p53 activity. In addition, AGR2 can regulate either a hexameric or monomeric Reptin and inhibit its chaperoning activity towards p53. Furthermore, Reptin interaction with AGR2, somewhat interferes with the AGR2-mediated inhibition of p53 protein.

This study revealed that ATP or ADP binding to Reptin can allosterically modulate activities of Reptin such as AGR2 binding, p53 peptides binding, and Reptin's p53 chaperoning activity. As such we reasoned that it is important to develop tools that would enable us to investigate the importance of the ATP binding pocket on Reptin's function, including AGR2 binding and chaperoning activity towards p53. Specifically, obtaining small molecules that could target an ATP binding pocket on Reptin could be a useful tool to study Reptin's biochemical properties as well as to modulate AGR2-Reptin, Reptin-p53 complexes, and subsequently establish the function of these assemblies *in vivo*. We have used structure based *in silico* modelling to develop novel modulators of Reptin. As there is no crystal structure solved for Reptin, the screen was performed based on the Pontin structure. The reason for this was that the Reptin and Pontin share high level of homology, especially in the conserved Walker A and B motifs that form the ATP-binding pockets, and thus any hits obtained in modelling could potentially bind to both Reptin and Pontin. In search for Reptin ligands, a database of 5 million compounds was used as an input for a screen looking for compounds that would match Reptin's active site. Subsequently the molecules were docked into the structure using both Vina and Autodock, and compounds that had highest scores were pursued further (unpublished data, Douglas Houston). From the list of thousands of highly scored hits we purchased thirty one compounds (Table 7. 1) and tested them in the ELISA ATP binding assay developed in this study and described in chapter 5. Three groups of compunds were identified: (1) compounds that did not disrupt ATP-Reptin interaction, (2) molecules that competed with ATP for binding to Reptin, and lastly (3) compounds were found that could in fact increase Reptin-ATP interaction (Figure 7.2).

	Mol Name
1	5-(4-methoxyphenyl)-N-(2-thienylmethyl)-7-(trifluoromethyl)pyrazolo[1,5-a]pyrimidine-3-carboxamide
2	4-[3-hydroxy-4-(4-methylbenzoyl)-5-(4-nitrophenyl)-2-oxo-2,5-dihydro-1H-pyrrol-1-yl]butanoic acid
3	5-(4-nitrobenzoyl)-2-(3-pyridinyl)-1H-isoindole-1,3(2H)-dione
4	2-phenylethyl 4-[4-(benzyloxy)phenyl]-6-methyl-2-oxo-1,2,3,4-tetrahydro-5-pyrimidinecarboxylate
5	2-(4-chlorophenyl)-N'-[(5-methyl-2-thienyl)methylene]-4-quinolinecarbohydrazide
6	5-[(2-methyl-1H-indol-3-yl)methylene]-1-(3-methylphenyl)-2,4,6(1H,3H,5H)-pyrimidinetrione
7	4-(2,5-diphenyl-1H-pyrrol-1-yl)benzohydrazide
8	2-chloro-5-(5-{[1-(4-methylphenyl)-2,4,6-trioxotetrahydro-5(2H)-pyrimidinylidene]methyl}-2-furyl)benzoic acid
9	N-[3-(1,3-benzoxazol-2-yl)-4-hydroxyphenyl]-2-oxo-2H-chromene-3-carboxamide
10	4-{[3-(4-fluorophenyl)-2,4-dioxo-1,3-thiazolidin-5-ylidene]methyl}benzoic acid
11	5-(1,3-benzodioxol-5-yl)-N-(tetrahydro-2-furanylmethyl)-7-(trifluoromethyl)pyrazolo[1,5-a]pyrimidine-3-carboxan
12	N-[4-(1-pyrrolidinylsulfonyl)phenyl]-4-biphenylcarboxamide
13	3-(benzyloxy)-N-(6-methyl-2-phenyl-2H-1,2,3-benzotriazol-5-yl)benzamide
14	N-[4-(2-methyl-1,3-thiazol-4-yl)phenyl]-4-biphenylsulfonamide
15	N-(2-chloro-5-[1,3]oxazolo[4,5-b]pyridin-2-ylphenyl)-4-biphenylcarboxamide
16	3-{5-[(2-benzyl-5-imino-7-oxo-5H-[1,3,4]thiadiazolo[3,2-a]pyrimidin-6(7H)-ylidene)methyl]-2-furyl}benzoic acid
17	4-(4-chlorobenzoyl)-1-[3-(dimethylamino)propyl]-3-hydroxy-5-(4-nitrophenyl)-1,5-dihydro-2H-pyrrol-2-one
18	N-[4-(4-morpholinylsulfonyl)phenyl]-4-biphenylcarboxamide
19	4-acetylphenyl 1,3-dioxo-2-phenyl-5-isoindolinecarboxylate
20	3-[(2-thienylcarbonyl)amino]phenyl 4-biphenylcarboxylate
21	methyl N-{[3-(4-methylphenyl)-1-adamantyl]carbonyl}glycinate
22	ethyl N-{[2-(4-ethylphenyl)-4-quinolinyl]carbonyl}glycinate
23	2-(4-fluorophenyl)-4-{3-[3-(4-methylphenoxy)propoxy]benzylidene}-1,3-oxazol-5(4H)-one
24	5-(4-fluorophenyl)-3-[(5-nitro-2-furyl)methylene]-2(3H)-furanone
25	N-(4-methylphenyl)-1-(4-nitrophenyl)cyclopentanecarboxamide
26	N-[2-(4-chlorophenyl)-1-({[3-(trifluoromethyl)phenyl]amino}carbonyl)vinyl]-2-furamide
27	4-[(4-{[4-(1-methyl-1-phenylethyl)phenoxy]methyl}phenyl)sulfonyl]morpholine
28	3,5-dichloro-N-{3-[(2-chlorobenzoyl)amino]phenyl}-2-methoxybenzamide
29	N-(3-chloro-2-methylphenyl)-3-(3-chloro-1H-1,2,4-triazol-1-yl)-1-adamantanecarboxamide
30	4-{[3-(3-nitro-1H-1,2,4-triazol-1-yl)-1-adamantyl]carbonyl}morpholine
31	4'-[(1,3-benzodioxol-5-ylmethylene)amino]-4'-azaspiro[cyclopropane-1,10'-tricyclo[5.2.1.0~2,6~]decane]-8'-ene-

Table 7. 1 List of lead molecules

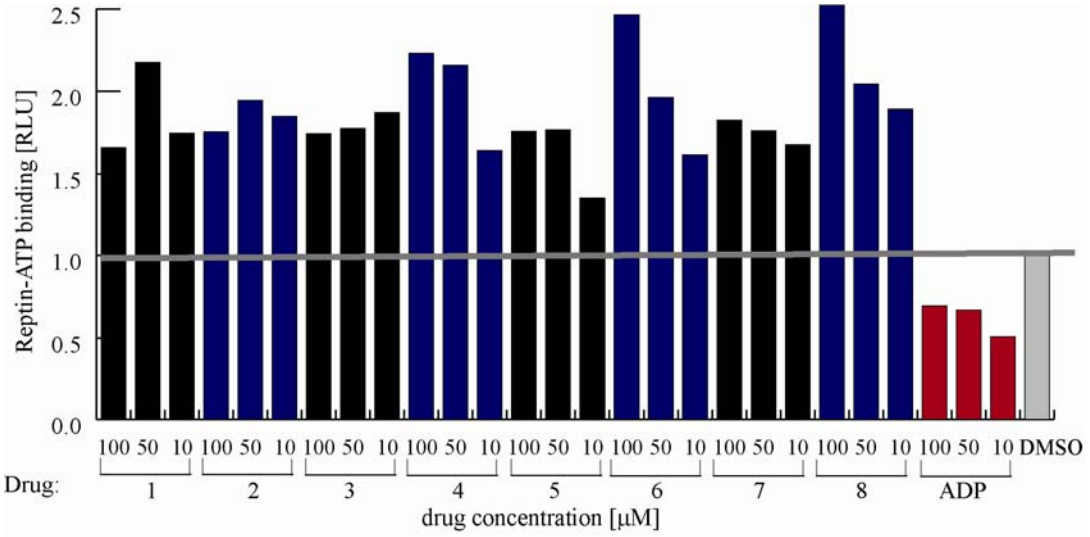
Reptin-ATP binding [RLU]
2.5
2.0
1.5
1.0
0.5
0.0
100 50 10 100 50 10 100 50 10 100 50 10 100 50 10 100 50 10 100 50 10 100 50 10 100 50 10 DMSO
Drug:
1
2
3
4
5
6
7
8
ADP
drug concentration [µM]

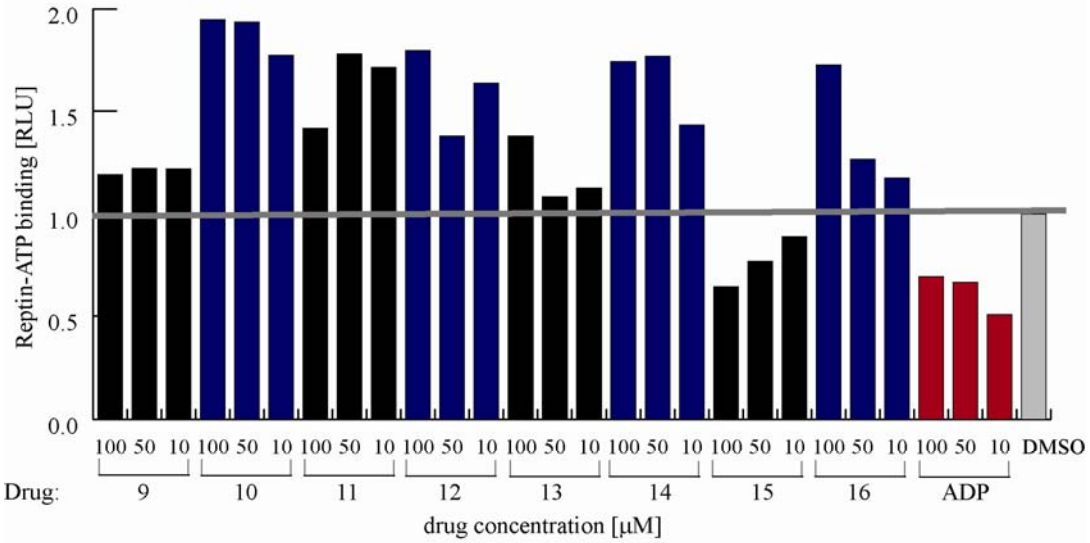
Reptin-ATP binding [RLU]
2.0
1.5
1.0
0.5
0.0
100 50 10 100 50 10 100 50 10 100 50 10 100 50 10 100 50 10 100 50 10 100 50 10 100 50 10 DMSO
Drug:
9
10
11
12
13
14
15
16
ADP
drug concentration [µM]

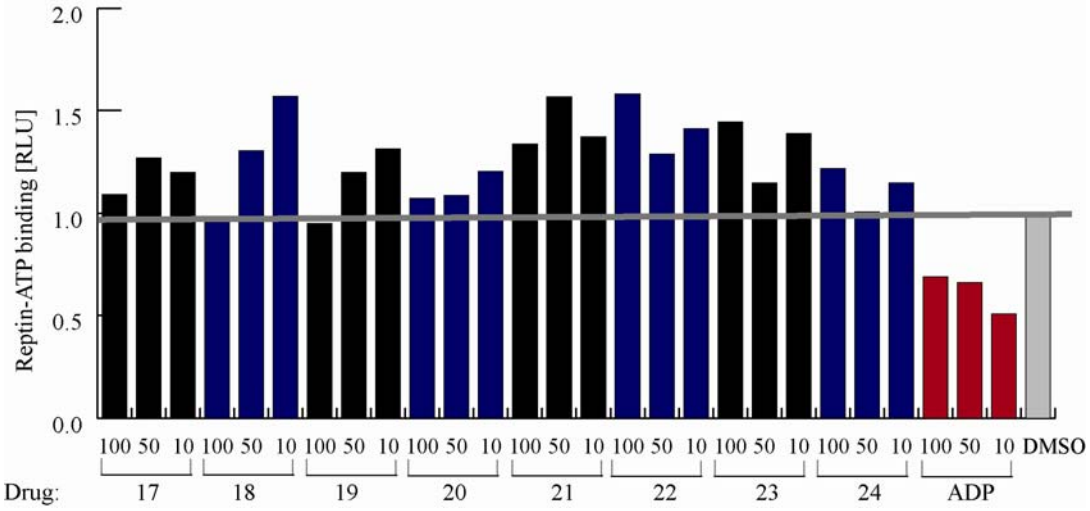
Reptin-ATP binding [RLU]
2.0
1.5
1.0
0.5
0.0
100 50 10 100 50 10 100 50 10 100 50 10 100 50 10 100 50 10 100 50 10 100 50 10 100 50 10 DMSO
Drug:
17
18
19
20
21
22
23
24
ADP

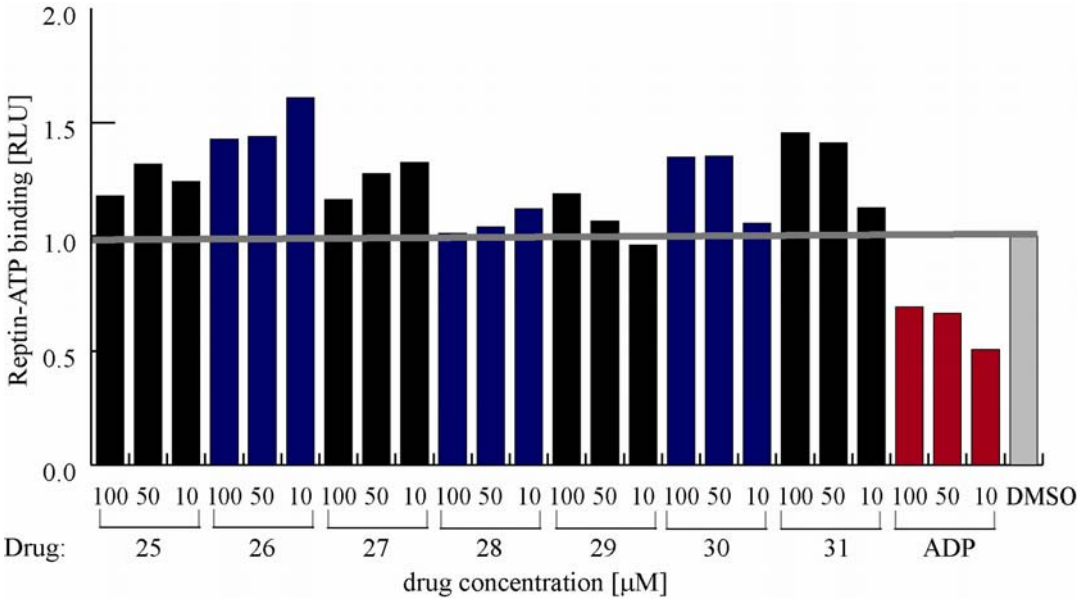

Figure 7.2 Testing the effect of the componds identified in the screen on Reptin-ATP binding. A fixed amount of the indicated biotinylated ATPs (as in **5.7 A**) was added to a microtitre plate coated with streptavidin and incubated with Reptin protein that had been preincubated with a titration of lead molecules (as in **Table 7.1**) or with a titration of ATP. The amount of Reptin bound was quantified with antibodies specific for Reptin using chemiluminescence. The data are plotted as the extent of protein-ATP complex formation [RLU].

Given the complexity of Reptin it is not immediately obvious whether molecules that can stimulate or inhibit ATP binding can prove more useful. In fact, it appears that developing molecules that differentially modulate Reptin's function is important.

Further characterisation of these lead molecules with respect to their effect on Reptin- p53 interaction or Reptin-mediated stimulation of p53-DNA binding is required. Interestingly, the preliminary data suggest, that the binding in the ATP pocket does not have the same effect as ATP binding. For example a selection of compounds has been tested in the assay measuring Reptin-AGR2 binding. It was found that some compounds could enhance whereas others decreased Reptin-AGR2 interaction (Figure 7.3). This means that different compounds cause different allosteric effects on Reptin protein. This could help us defining how particular conformations/oligomerization effects of the given compound affect Reptin function both *in vitro* and *in vivo*. In addition, the compounds will be tested in cross-linking experiments. Identification of molecules that switch equilibrium into a particular oligomeric species could help to unravel their functions in processeses such as chaperoning p53 activity.

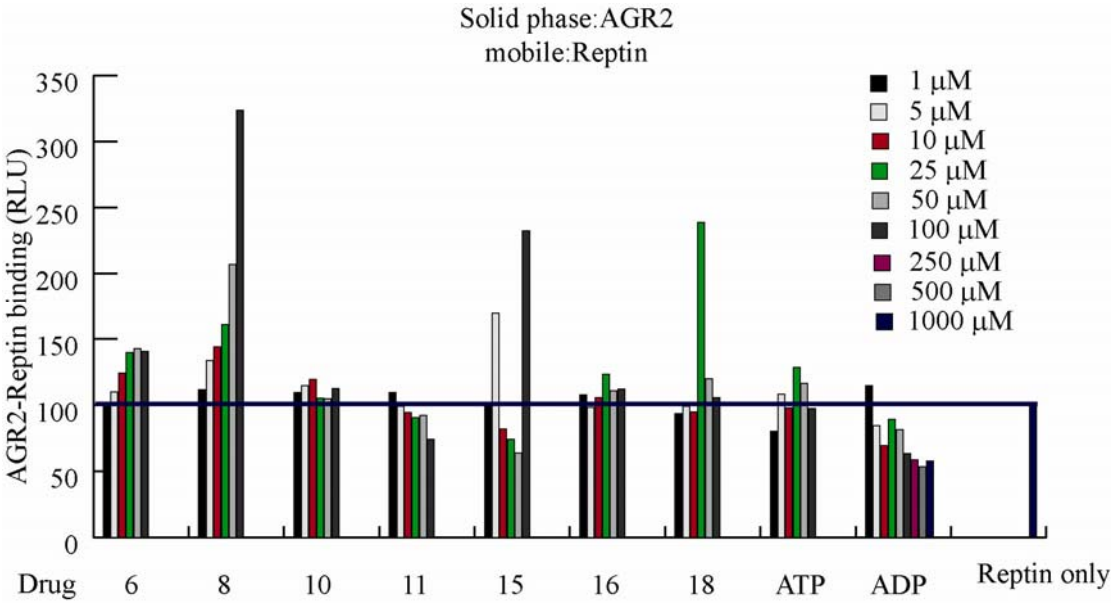

Figure 7.3 Molecules that target ATP-binding pocket of Reptin differentially affect AGR2-Reptin binding. AGR2 was immobilized on the solid phase and Reptin that has been pre-incubated with a titration of compunds or ATP or ADP (as indicated in the figure) was added in the mobile phase. The amount of Reptin bound was quantified with specific antibodies using chemiluminescence. The data are plotted as the extent of protein-protein complex formation (in RLU) as a function of the amount of protein in the mobile phase [μM].

Reptin operates as a part of a different of multi-protein complexes, and our study emphasised that it possesses allosteric sites. Owing to the complexity of this protein, it is not surprising that identified compounds will either stimulate or inhibit different functions of Reptin. Thus, these drugs may form the toolbox to study Reptin-AGR2 complex, Reptin-p53 complex, and other Reptin complexes, such as assemblies with transcriptional machinery, NMD pathway proteins or telomerase complex. In addition they will for a basis to understand Reptin's biochemical properties such as oligomerisation or ATPase activity.

In summary, this study has further defined the mechanism of regulation of AGR2 and p53 pathways. The identification of Reptin protein as the novel AGR2 interacting partner presented in this thesis has formed the basis for unravelling AGR2 function. In addition, biochemical characterisation of Reptin protein has revealed the allosteric properties of this protein. These findings instigated identification of small molecules that modify Reptin's functions and may help to elucidate the mechanism of its function *in vivo*. Finally, this report identified Reptin as a wild type and mutant p53 binding and regulatory protein. The identification of this interaction potentially offers a novel therapeutic strategy for reactivating wild type p53 pathway in cancer cells.

Bibliography

1. Jones, P.A. and S.B. Baylin, *The epigenomics of cancer.* Cell, 2007. **128**(4): p. 683-92.
2. Vogelstein, B. and K.W. Kinzler, *Cancer genes and the pathways they control.* Nat Med, 2004. **10**(8): p. 789-99.
3. Hahn, W.C., et al., *Creation of human tumour cells with defined genetic elements.* Nature, 1999. **400**(6743): p. 464-8.
4. Hanahan, D. and R.A. Weinberg, *The hallmarks of cancer.* Cell, 2000. **100**(1): p. 57-70.
5. Kinzler, K.W. and B. Vogelstein, *Lessons from hereditary colorectal cancer.* Cell, 1996. **87**(2): p. 159-70.
6. Feinberg, A.P. and B. Tycko, *The history of cancer epigenetics.* Nat Rev Cancer, 2004. **4**(2): p. 143-53.
7. Jones, P.A. and P.W. Laird, *Cancer epigenetics comes of age.* Nat Genet, 1999. **21**(2): p. 163-7.
8. Baylin, S.B. and J.G. Herman, *DNA hypermethylation in tumorigenesis: epigenetics joins genetics.* Trends Genet, 2000. **16**(4): p. 168-74.
9. Feinberg, A.P. and B. Vogelstein, *Hypomethylation distinguishes genes of some human cancers from their normal counterparts.* Nature, 1983. **301**(5895): p. 89-92.
10. Seligson, D.B., et al., *Global histone modification patterns predict risk of prostate cancer recurrence.* Nature, 2005. **435**(7046): p. 1262-6.
11. Fraga, M.F., et al., *Loss of acetylation at Lys16 and trimethylation at Lys20 of histone H4 is a common hallmark of human cancer.* Nat Genet, 2005. **37**(4): p. 391-400.
12. Baylin, S.B. and J.E. Ohm, *Epigenetic gene silencing in cancer - a mechanism for early oncogenic pathway addiction?* Nat Rev Cancer, 2006. **6**(2): p. 107-16.
13. Warburg, O., *On the origin of cancer cells.* Science, 1956. **123**(3191): p. 309-14.
14. Zhang, J., P.L. Yang, and N.S. Gray, *Targeting cancer with small molecule kinase inhibitors.* Nat Rev Cancer, 2009. **9**(1): p. 28-39.
15. Futreal, P.A., et al., *A census of human cancer genes.* Nat Rev Cancer, 2004. **4**(3): p. 177-83.
16. Weinstein, I.B., *Cancer. Addiction to oncogenes--the Achilles heal of cancer.* Science, 2002. **297**(5578): p. 63-4.
17. Bachman, K.E., et al., *The PIK3CA gene is mutated with high frequency in human breast cancers.* Cancer Biol Ther, 2004. **3**(8): p. 772-5.
18. Samuels, Y., et al., *High frequency of mutations of the PIK3CA gene in human cancers.* Science, 2004. **304**(5670): p. 554.
19. Sawyers, C.L., *Chronic myeloid leukemia.* N Engl J Med, 1999. **340**(17): p. 1330-40.
20. Rusch, V., et al., *Overexpression of the epidermal growth factor receptor and its ligand transforming growth factor alpha is frequent in resectable non-small cell lung cancer but does not predict tumor progression.* Clin Cancer Res, 1997. **3**(4): p. 515-22.

21. Garrido, M.C. and B.C. Bastian, *KIT as a therapeutic target in melanoma.* J Invest Dermatol. **130**(1): p. 20-7.
22. Davies, H., et al., *Mutations of the BRAF gene in human cancer.* Nature, 2002. **417**(6892): p. 949-54.
23. Druker, B.J., *Inhibition of the Bcr-Abl tyrosine kinase as a therapeutic strategy for CML.* Oncogene, 2002. **21**(56): p. 8541-6.
24. Roberts, P.J. and C.J. Der, *Targeting the Raf-MEK-ERK mitogen-activated protein kinase cascade for the treatment of cancer.* Oncogene, 2007. **26**(22): p. 3291-310.
25. Sharma, S.V. and J. Settleman, *Oncogene addiction: setting the stage for molecularly targeted cancer therapy.* Genes Dev, 2007. **21**(24): p. 3214-31.
26. Gorre, M.E., et al., *Clinical resistance to STI-571 cancer therapy caused by BCR-ABL gene mutation or amplification.* Science, 2001. **293**(5531): p. 876-80.
27. Engelman, J.A., et al., *MET amplification leads to gefitinib resistance in lung cancer by activating ERBB3 signaling.* Science, 2007. **316**(5827): p. 1039-43.
28. Tennant, D.A., R.V. Duran, and E. Gottlieb, *Targeting metabolic transformation for cancer therapy.* Nat Rev Cancer. **10**(4): p. 267-77.
29. DeBerardinis, R.J., et al., *The biology of cancer: metabolic reprogramming fuels cell growth and proliferation.* Cell Metab, 2008. **7**(1): p. 11-20.
30. Altomare, D.A. and J.R. Testa, *Perturbations of the AKT signaling pathway in human cancer.* Oncogene, 2005. **24**(50): p. 7455-64.
31. Plas, D.R. and C.B. Thompson, *Akt-dependent transformation: there is more to growth than just surviving.* Oncogene, 2005. **24**(50): p. 7435-42.
32. Hudes, G., et al., *Temsirolimus, interferon alfa, or both for advanced renal-cell carcinoma.* N Engl J Med, 2007. **356**(22): p. 2271-81.
33. Motzer, R.J., et al., *Efficacy of everolimus in advanced renal cell carcinoma: a double-blind, randomised, placebo-controlled phase III trial.* Lancet, 2008. **372**(9637): p. 449-56.
34. Kobori, M., et al., *Phloretin-induced apoptosis in B16 melanoma 4A5 cells and HL60 human leukemia cells.* Biosci Biotechnol Biochem, 1999. **63**(4): p. 719-25.
35. De Lena, M., et al., *Paclitaxel, cisplatin and lonidamine in advanced ovarian cancer. A phase II study.* Eur J Cancer, 2001. **37**(3): p. 364-8.
36. Di Cosimo, S., et al., *Lonidamine: efficacy and safety in clinical trials for the treatment of solid tumors.* Drugs Today (Barc), 2003. **39**(3): p. 157-74.
37. Goh, K.I., et al., *The human disease network.* Proc Natl Acad Sci U S A, 2007. **104**(21): p. 8685-90.
38. Olivier, M., et al., *The IARC TP53 database: new online mutation analysis and recommendations to users.* Hum Mutat, 2002. **19**(6): p. 607-14.
39. Maslon, M.M. and T.R. Hupp, *Drug discovery and mutant p53.* Trends Cell Biol. **20**(9): p. 542-55.
40. Lambert, J.M., et al., *PRIMA-1 reactivates mutant p53 by covalent binding to the core domain.* Cancer Cell, 2009. **15**(5): p. 376-88.
41. Ellis, R.J., *Molecular chaperones: assisting assembly in addition to folding.* Trends Biochem Sci, 2006. **31**(7): p. 395-401.
42. Whitesell, L. and S.L. Lindquist, *HSP90 and the chaperoning of cancer.* Nat Rev Cancer, 2005. **5**(10): p. 761-72.

43. Bisht, K.S., et al., *Geldanamycin and 17-allylamino-17-demethoxygeldanamycin potentiate the in vitro and in vivo radiation response of cervical tumor cells via the heat shock protein 90-mediated intracellular signaling and cytotoxicity.* Cancer Res, 2003. **63**(24): p. 8984-95.
44. Jones, D.T., et al., *Geldanamycin and herbimycin A induce apoptotic killing of B chronic lymphocytic leukemia cells and augment the cells' sensitivity to cytotoxic drugs.* Blood, 2004. **103**(5): p. 1855-61.
45. Minami, Y., et al., *Selective apoptosis of tandemly duplicated FLT3-transformed leukemia cells by Hsp90 inhibitors.* Leukemia, 2002. **16**(8): p. 1535-40.
46. Albert, R., H. Jeong, and A.L. Barabasi, *Error and attack tolerance of complex networks.* Nature, 2000. **406**(6794): p. 378-82.
47. Barabasi, A.L. and Z.N. Oltvai, *Network biology: understanding the cell's functional organization.* Nat Rev Genet, 2004. **5**(2): p. 101-13.
48. Levine, A.J., J. Momand, and C.A. Finlay, *The p53 tumour suppressor gene.* Nature, 1991. **351**(6326): p. 453-6.
49. Mayo, L.D. and D.B. Donner, *The PTEN, Mdm2, p53 tumor suppressor-oncoprotein network.* Trends Biochem Sci, 2002. **27**(9): p. 462-7.
50. Van Heyningen, V. and P.L. Yeyati, *Mechanisms of non-Mendelian inheritance in genetic disease.* Hum Mol Genet, 2004. **13 Spec No 2**: p. R225-33.
51. Yao, T.P., et al., *Gene dosage-dependent embryonic development and proliferation defects in mice lacking the transcriptional integrator p300.* Cell, 1998. **93**(3): p. 361-72.
52. Olivier, M., M. Hollstein, and P. Hainaut, *TP53 mutations in human cancers: origins, consequences, and clinical use.* Cold Spring Harb Perspect Biol. **2**(1): p. a001008.
53. Toledo, F. and G.M. Wahl, *Regulating the p53 pathway: in vitro hypotheses, in vivo veritas.* Nat Rev Cancer, 2006. **6**(12): p. 909-23.
54. Bensaad, K., et al., *TIGAR, a p53-inducible regulator of glycolysis and apoptosis.* Cell, 2006. **126**(1): p. 107-20.
55. Oda, E., et al., *Noxa, a BH3-only member of the Bcl-2 family and candidate mediator of p53-induced apoptosis.* Science, 2000. **288**(5468): p. 1053-8.
56. Sax, J.K., et al., *BID regulation by p53 contributes to chemosensitivity.* Nat Cell Biol, 2002. **4**(11): p. 842-9.
57. Miyashita, T., et al., *Tumor suppressor p53 is a regulator of bcl-2 and bax gene expression in vitro and in vivo.* Oncogene, 1994. **9**(6): p. 1799-805.
58. Fridman, J.S. and S.W. Lowe, *Control of apoptosis by p53.* Oncogene, 2003. **22**(56): p. 9030-40.
59. Kannan, K., et al., *DNA microarrays identification of primary and secondary target genes regulated by p53.* Oncogene, 2001. **20**(18): p. 2225-34.
60. Maecker, H.L., C. Koumenis, and A.J. Giaccia, *p53 promotes selection for Fas-mediated apoptotic resistance.* Cancer Res, 2000. **60**(16): p. 4638-44.
61. Owen-Schaub, L.B., et al., *Wild-type human p53 and a temperature-sensitive mutant induce Fas/APO-1 expression.* Mol Cell Biol, 1995. **15**(6): p. 3032-40.
62. Robles, A.I., et al., *APAF-1 is a transcriptional target of p53 in DNA damage-induced apoptosis.* Cancer Res, 2001. **61**(18): p. 6660-4.

63. Wu, G.S., et al., *KILLER/DR5 is a DNA damage-inducible p53-regulated death receptor gene.* Nat Genet, 1997. **17**(2): p. 141-3.
64. Jeffers, J.R., et al., *Puma is an essential mediator of p53-dependent and -independent apoptotic pathways.* Cancer Cell, 2003. **4**(4): p. 321-8.
65. Michalak, E.M., et al., *In several cell types tumour suppressor p53 induces apoptosis largely via Puma but Noxa can contribute.* Cell Death Differ, 2008. **15**(6): p. 1019-29.
66. el-Deiry, W.S., *Regulation of p53 downstream genes.* Semin Cancer Biol, 1998. **8**(5): p. 345-57.
67. Halazonetis, T.D., V.G. Gorgoulis, and J. Bartek, *An oncogene-induced DNA damage model for cancer development.* Science, 2008. **319**(5868): p. 1352-5.
68. Kamijo, T., et al., *Tumor suppression at the mouse INK4a locus mediated by the alternative reading frame product p19ARF.* Cell, 1997. **91**(5): p. 649-59.
69. Wright, W.E. and J.W. Shay, *The two-stage mechanism controlling cellular senescence and immortalization.* Exp Gerontol, 1992. **27**(4): p. 383-9.
70. Brown, J.P., W. Wei, and J.M. Sedivy, *Bypass of senescence after disruption of p21CIP1/WAF1 gene in normal diploid human fibroblasts.* Science, 1997. **277**(5327): p. 831-4.
71. Kortlever, R.M., P.J. Higgins, and R. Bernards, *Plasminogen activator inhibitor-1 is a critical downstream target of p53 in the induction of replicative senescence.* Nat Cell Biol, 2006. **8**(8): p. 877-84.
72. Bommer, G.T., et al., *p53-mediated activation of miRNA34 candidate tumor-suppressor genes.* Curr Biol, 2007. **17**(15): p. 1298-307.
73. Braun, C.J., et al., *p53-Responsive micrornas 192 and 215 are capable of inducing cell cycle arrest.* Cancer Res, 2008. **68**(24): p. 10094-104.
74. Chang, T.C., et al., *Transactivation of miR-34a by p53 broadly influences gene expression and promotes apoptosis.* Mol Cell, 2007. **26**(5): p. 745-52.
75. Corney, D.C., et al., *MicroRNA-34b and MicroRNA-34c are targets of p53 and cooperate in control of cell proliferation and adhesion-independent growth.* Cancer Res, 2007. **67**(18): p. 8433-8.
76. He, L., et al., *A microRNA component of the p53 tumour suppressor network.* Nature, 2007. **447**(7148): p. 1130-4.
77. Raver-Shapira, N., et al., *Transcriptional activation of miR-34a contributes to p53-mediated apoptosis.* Mol Cell, 2007. **26**(5): p. 731-43.
78. Tarasov, V., et al., *Differential regulation of microRNAs by p53 revealed by massively parallel sequencing: miR-34a is a p53 target that induces apoptosis and G1-arrest.* Cell Cycle, 2007. **6**(13): p. 1586-93.
79. Deberardinis, R.J., et al., *Brick by brick: metabolism and tumor cell growth.* Curr Opin Genet Dev, 2008. **18**(1): p. 54-61.
80. Aylon, Y. and M. Oren, *New plays in the p53 theater.* Curr Opin Genet Dev. **21**(1): p. 86-92.
81. Sablina, A.A., et al., *The antioxidant function of the p53 tumor suppressor.* Nat Med, 2005. **11**(12): p. 1306-13.
82. Kawauchi, K., et al., *p53 regulates glucose metabolism through an IKK-NF-kappaB pathway and inhibits cell transformation.* Nat Cell Biol, 2008. **10**(5): p. 611-8.
83. Ma, W., et al., *A pivotal role for p53: balancing aerobic respiration and glycolysis.* J Bioenerg Biomembr, 2007. **39**(3): p. 243-6.

84. Jones, R.G., et al., *AMP-activated protein kinase induces a p53-dependent metabolic checkpoint.* Mol Cell, 2005. **18**(3): p. 283-93.
85. Budanov, A.V. and M. Karin, *p53 target genes sestrin1 and sestrin2 connect genotoxic stress and mTOR signaling.* Cell, 2008. **134**(3): p. 451-60.
86. Feng, Z., et al., *The regulation of AMPK beta1, TSC2, and PTEN expression by p53: stress, cell and tissue specificity, and the role of these gene products in modulating the IGF-1-AKT-mTOR pathways.* Cancer Res, 2007. **67**(7): p. 3043-53.
87. Feng, Z. and A.J. Levine, *The regulation of energy metabolism and the IGF-1/mTOR pathways by the p53 protein.* Trends Cell Biol. **20**(7): p. 427-34.
88. Crighton, D., et al., *DRAM, a p53-induced modulator of autophagy, is critical for apoptosis.* Cell, 2006. **126**(1): p. 121-34.
89. Tasdemir, E., et al., *Regulation of autophagy by cytoplasmic p53.* Nat Cell Biol, 2008. **10**(6): p. 676-87.
90. Lane, D.P., et al., *The Mdm2 and p53 genes are conserved in the Arachnids.* Cell Cycle. **9**(4): p. 748-54.
91. Lu, W.J., J.F. Amatruda, and J.M. Abrams, *p53 ancestry: gazing through an evolutionary lens.* Nat Rev Cancer, 2009. **9**(10): p. 758-62.
92. Derry, W.B., A.P. Putzke, and J.H. Rothman, *Caenorhabditis elegans p53: role in apoptosis, meiosis, and stress resistance.* Science, 2001. **294**(5542): p. 591-5.
93. Rogel, A., et al., *p53 cellular tumor antigen: analysis of mRNA levels in normal adult tissues, embryos, and tumors.* Mol Cell Biol, 1985. **5**(10): p. 2851-5.
94. Schmid, P., et al., *Expression of p53 during mouse embryogenesis.* Development, 1991. **113**(3): p. 857-65.
95. MacCallum, D.E., et al., *The p53 response to ionising radiation in adult and developing murine tissues.* Oncogene, 1996. **13**(12): p. 2575-87.
96. Gottlieb, E., et al., *Transgenic mouse model for studying the transcriptional activity of the p53 protein: age- and tissue-dependent changes in radiation-induced activation during embryogenesis.* Embo J, 1997. **16**(6): p. 1381-90.
97. Komarova, E.A., et al., *Transgenic mice with p53-responsive lacZ: p53 activity varies dramatically during normal development and determines radiation and drug sensitivity in vivo.* Embo J, 1997. **16**(6): p. 1391-400.
98. Montes de Oca Luna, R., D.S. Wagner, and G. Lozano, *Rescue of early embryonic lethality in mdm2-deficient mice by deletion of p53.* Nature, 1995. **378**(6553): p. 203-6.
99. Jones, S.N., et al., *Rescue of embryonic lethality in Mdm2-deficient mice by absence of p53.* Nature, 1995. **378**(6553): p. 206-8.
100. Parant, J., et al., *Rescue of embryonic lethality in Mdm4-null mice by loss of Trp53 suggests a nonoverlapping pathway with MDM2 to regulate p53.* Nat Genet, 2001. **29**(1): p. 92-5.
101. Donehower, L.A., et al., *Mice deficient for p53 are developmentally normal but susceptible to spontaneous tumours.* Nature, 1992. **356**(6366): p. 215-21.
102. Armstrong, J.F., et al., *High-frequency developmental abnormalities in p53-deficient mice.* Curr Biol, 1995. **5**(8): p. 931-6.
103. Sah, V.P., et al., *A subset of p53-deficient embryos exhibit exencephaly.* Nat Genet, 1995. **10**(2): p. 175-80.

104. Rotter, V., et al., *Mice with reduced levels of p53 protein exhibit the testicular giant-cell degenerative syndrome.* Proc Natl Acad Sci U S A, 1993. **90**(19): p. 9075-9.
105. Beumer, T.L., et al., *The role of the tumor suppressor p53 in spermatogenesis.* Cell Death Differ, 1998. **5**(8): p. 669-77.
106. Hu, W., et al., *p53 regulates maternal reproduction through LIF.* Nature, 2007. **450**(7170): p. 721-4.
107. Danilova, N., K.M. Sakamoto, and S. Lin, *p53 family in development.* Mech Dev, 2008. **125**(11-12): p. 919-31.
108. Piccolo, S., *p53 regulation orchestrates the TGF-beta response.* Cell, 2008. **133**(5): p. 767-9.
109. Cordenonsi, M., et al., *Links between tumor suppressors: p53 is required for TGF-beta gene responses by cooperating with Smads.* Cell, 2003. **113**(3): p. 301-14.
110. Chen, J., et al., *Loss of function of def selectively up-regulates Delta113p53 expression to arrest expansion growth of digestive organs in zebrafish.* Genes Dev, 2005. **19**(23): p. 2900-11.
111. Campbell, W.A., et al., *Zebrafish lacking Alzheimer presenilin enhancer 2 (Pen-2) demonstrate excessive p53-dependent apoptosis and neuronal loss.* J Neurochem, 2006. **96**(5): p. 1423-40.
112. Villiard, E., et al., *Urodele p53 tolerates amino acid changes found in p53 variants linked to human cancer.* BMC Evol Biol, 2007. **7**: p. 180.
113. Jacobs, W.B., D.R. Kaplan, and F.D. Miller, *The p53 family in nervous system development and disease.* J Neurochem, 2006. **97**(6): p. 1571-84.
114. Tsukada, T., et al., *Enhanced proliferative potential in culture of cells from p53-deficient mice.* Oncogene, 1993. **8**(12): p. 3313-22.
115. Radinsky, R., et al., *Terminal differentiation and apoptosis in experimental lung metastases of human osteogenic sarcoma cells by wild type p53.* Oncogene, 1994. **9**(7): p. 1877-83.
116. Huttinger-Kirchhof, N., et al., *The p53 family inhibitor DeltaNp73 interferes with multiple developmental programs.* Cell Death Differ, 2006. **13**(1): p. 174-7.
117. Molchadsky, A., et al., *p53 plays a role in mesenchymal differentiation programs, in a cell fate dependent manner.* PLoS One, 2008. **3**(11): p. e3707.
118. Halevy, O., *p53 gene is up-regulated during skeletal muscle cell differentiation.* Biochem Biophys Res Commun, 1993. **192**(2): p. 714-9.
119. Cam, H., et al., *p53 family members in myogenic differentiation and rhabdomyosarcoma development.* Cancer Cell, 2006. **10**(4): p. 281-93.
120. Aloni-Grinstein, R., et al., *Wild type p53 functions as a control protein in the differentiation pathway of the B-cell lineage.* Oncogene, 1993. **8**(12): p. 3297-305.
121. Ronen, D., et al., *Induction of HL-60 cells to undergo apoptosis is determined by high levels of wild-type p53 protein whereas differentiation of the cells is mediated by lower p53 levels.* Cell Growth Differ, 1996. **7**(1): p. 21-30.
122. Fuhrken, P.G., et al., *Comparative, genome-scale transcriptional analysis of CHRF-288-11 and primary human megakaryocytic cell cultures provides novel insights into lineage-specific differentiation.* Exp Hematol, 2007. **35**(3): p. 476-489.

123. Fuhrken, P.G., et al., *Tumor suppressor protein p53 regulates megakaryocytic polyploidization and apoptosis.* J Biol Chem, 2008. **283**(23): p. 15589-600.
124. Liu, Y., et al., *p53 regulates hematopoietic stem cell quiescence.* Cell Stem Cell, 2009. **4**(1): p. 37-48.
125. Meletis, K., et al., *p53 suppresses the self-renewal of adult neural stem cells.* Development, 2006. **133**(2): p. 363-9.
126. Lin, T., et al., *p53 induces differentiation of mouse embryonic stem cells by suppressing Nanog expression.* Nat Cell Biol, 2005. **7**(2): p. 165-71.
127. Qin, H., et al., *Regulation of apoptosis and differentiation by p53 in human embryonic stem cells.* J Biol Chem, 2007. **282**(8): p. 5842-52.
128. Pardal, R., M.F. Clarke, and S.J. Morrison, *Applying the principles of stem-cell biology to cancer.* Nat Rev Cancer, 2003. **3**(12): p. 895-902.
129. Gil-Perotin, S., et al., *Loss of p53 induces changes in the behavior of subventricular zone cells: implication for the genesis of glial tumors.* J Neurosci, 2006. **26**(4): p. 1107-16.
130. Lengner, C.J., et al., *Osteoblast differentiation and skeletal development are regulated by Mdm2-p53 signaling.* J Cell Biol, 2006. **172**(6): p. 909-21.
131. Petty, T.J., et al., *An induced fit mechanism regulates p53 DNA binding kinetics to confer sequence specificity.* Embo J. **30**(11): p. 2167-76.
132. Uversky, V.N., *Intrinsically disordered proteins from A to Z.* Int J Biochem Cell Biol.
133. Tompa, P., *Intrinsically unstructured proteins.* Trends Biochem Sci, 2002. **27**(10): p. 527-33.
134. Dunker, A.K., et al., *Flexible nets. The roles of intrinsic disorder in protein interaction networks.* Febs J, 2005. **272**(20): p. 5129-48.
135. Uversky, V.N., C.J. Oldfield, and A.K. Dunker, *Showing your ID: intrinsic disorder as an ID for recognition, regulation and cell signaling.* J Mol Recognit, 2005. **18**(5): p. 343-84.
136. Joerger, A.C. and A.R. Fersht, *Structure-function-rescue: the diverse nature of common p53 cancer mutants.* Oncogene, 2007. **26**(15): p. 2226-42.
137. Vousden, K.H. and C. Prives, *Blinded by the Light: The Growing Complexity of p53.* Cell, 2009. **137**(3): p. 413-31.
138. Bell, S., et al., *p53 contains large unstructured regions in its native state.* J Mol Biol, 2002. **322**(5): p. 917-27.
139. Dawson, R., et al., *The N-terminal domain of p53 is natively unfolded.* J Mol Biol, 2003. **332**(5): p. 1131-41.
140. Lee, H., et al., *Local structural elements in the mostly unstructured transcriptional activation domain of human p53.* J Biol Chem, 2000. **275**(38): p. 29426-32.
141. Dunker, A.K., et al., *Intrinsically disordered protein.* J Mol Graph Model, 2001. **19**(1): p. 26-59.
142. Dunker, A.K. and Z. Obradovic, *The protein trinity--linking function and disorder.* Nat Biotechnol, 2001. **19**(9): p. 805-6.
143. Dyson, H.J. and P.E. Wright, *Coupling of folding and binding for unstructured proteins.* Curr Opin Struct Biol, 2002. **12**(1): p. 54-60.
144. Mohan, A., et al., *Analysis of molecular recognition features (MoRFs).* J Mol Biol, 2006. **362**(5): p. 1043-59.

145. Kussie, P.H., et al., *Structure of the MDM2 oncoprotein bound to the p53 tumor suppressor transactivation domain.* Science, 1996. **274**(5289): p. 948-53.
146. Rosal, R., et al., *NMR solution structure of a peptide from the mdm-2 binding domain of the p53 protein that is selectively cytotoxic to cancer cells.* Biochemistry, 2004. **43**(7): p. 1854-61.
147. Wells, M., et al., *Structure of tumor suppressor p53 and its intrinsically disordered N-terminal transactivation domain.* Proc Natl Acad Sci U S A, 2008. **105**(15): p. 5762-7.
148. Popowicz, G.M., A. Czarna, and T.A. Holak, *Structure of the human Mdmx protein bound to the p53 tumor suppressor transactivation domain.* Cell Cycle, 2008. **7**(15): p. 2441-3.
149. Feng, H., et al., *Structural basis for p300 Taz2-p53 TAD1 binding and modulation by phosphorylation.* Structure, 2009. **17**(2): p. 202-10.
150. Bochkareva, E., et al., *Single-stranded DNA mimicry in the p53 transactivation domain interaction with replication protein A.* Proc Natl Acad Sci U S A, 2005. **102**(43): p. 15412-7.
151. Di Lello, P., et al., *Structure of the Tfb1/p53 complex: Insights into the interaction between the p62/Tfb1 subunit of TFIIH and the activation domain of p53.* Mol Cell, 2006. **22**(6): p. 731-40.
152. Oldfield, C.J., et al., *Flexible nets: disorder and induced fit in the associations of p53 and 14-3-3 with their partners.* BMC Genomics, 2008. **9 Suppl 1**: p. S1.
153. Natan, E., et al., *Interaction of the p53 DNA-Binding Domain with Its N-Terminal Extension Modulates the Stability of the p53 Tetramer.* J Mol Biol. **409**(3): p. 358-68.
154. Avantaggiati, M.L., et al., *Recruitment of p300/CBP in p53-dependent signal pathways.* Cell, 1997. **89**(7): p. 1175-84.
155. Dornan, D., et al., *The proline repeat domain of p53 binds directly to the transcriptional coactivator p300 and allosterically controls DNA-dependent acetylation of p53.* Mol Cell Biol, 2003. **23**(23): p. 8846-61.
156. Picksley, S.M., et al., *Immunochemical analysis of the interaction of p53 with MDM2;--fine mapping of the MDM2 binding site on p53 using synthetic peptides.* Oncogene, 1994. **9**(9): p. 2523-9.
157. Cho, Y., et al., *Crystal structure of a p53 tumor suppressor-DNA complex: understanding tumorigenic mutations.* Science, 1994. **265**(5170): p. 346-55.
158. Hollstein, M., et al., *New approaches to understanding p53 gene tumor mutation spectra.* Mutat Res, 1999. **431**(2): p. 199-209.
159. Soussi, T. and P. May, *Structural aspects of the p53 protein in relation to gene evolution: a second look.* J Mol Biol, 1996. **260**(5): p. 623-37.
160. Shimizu, H., et al., *The conformationally flexible S9-S10 linker region in the core domain of p53 contains a novel MDM2 binding site whose mutation increases ubiquitination of p53 in vivo.* J Biol Chem, 2002. **277**(32): p. 28446-58.
161. Craig, A.L., et al., *The MDM2 ubiquitination signal in the DNA-binding domain of p53 forms a docking site for calcium calmodulin kinase superfamily members.* Mol Cell Biol, 2007. **27**(9): p. 3542-55.

162. Wallace, M., et al., *Dual-site regulation of MDM2 E3-ubiquitin ligase activity.* Mol Cell, 2006. **23**(2): p. 251-63.
163. Shimizu, H., et al., *Destabilizing missense mutations in the tumour suppressor protein p53 enhance its ubiquitination in vitro and in vivo.* Biochem J, 2006. **397**(2): p. 355-67.
164. Fraser, J.A., B. Vojtesek, and T.R. Hupp, *A novel p53 phosphorylation site within the MDM2 ubiquitination signal: I. phosphorylation at SER269 in vivo is linked to inactivation of p53 function.* J Biol Chem. **285**(48): p. 37762-72.
165. Rohaly, G., et al., *A novel human p53 isoform is an essential element of the ATR-intra-S phase checkpoint.* Cell, 2005. **122**(1): p. 21-32.
166. Clore, G.M., et al., *Refined solution structure of the oligomerization domain of the tumour suppressor p53.* Nat Struct Biol, 1995. **2**(4): p. 321-33.
167. Mateu, M.G., M.M. Sanchez Del Pino, and A.R. Fersht, *Mechanism of folding and assembly of a small tetrameric protein domain from tumor suppressor p53.* Nat Struct Biol, 1999. **6**(2): p. 191-8.
168. Wang, P., et al., *p53 domains: structure, oligomerization, and transformation.* Mol Cell Biol, 1994. **14**(8): p. 5182-91.
169. Lee, W., et al., *Solution structure of the tetrameric minimum transforming domain of p53.* Nat Struct Biol, 1994. **1**(12): p. 877-90.
170. Chene, P., *The role of tetramerization in p53 function.* Oncogene, 2001. **20**(21): p. 2611-7.
171. Hupp, T.R., D.P. Lane, and K.L. Ball, *Strategies for manipulating the p53 pathway in the treatment of human cancer.* Biochem J, 2000. **352 Pt 1**: p. 1-17.
172. Chene, P., P. Mittl, and M. Grutter, *In vitro structure-function analysis of the beta-strand 326-333 of human p53.* J Mol Biol, 1997. **273**(4): p. 873-81.
173. Johnson, C.R., et al., *Thermodynamic analysis of the structural stability of the tetrameric oligomerization domain of p53 tumor suppressor.* Biochemistry, 1995. **34**(16): p. 5309-16.
174. Mateu, M.G. and A.R. Fersht, *Nine hydrophobic side chains are key determinants of the thermodynamic stability and oligomerization status of tumour suppressor p53 tetramerization domain.* Embo J, 1998. **17**(10): p. 2748-58.
175. McCoy, M., et al., *Hydrophobic side-chain size is a determinant of the three-dimensional structure of the p53 oligomerization domain.* Embo J, 1997. **16**(20): p. 6230-6.
176. Waterman, J.L., J.L. Shenk, and T.D. Halazonetis, *The dihedral symmetry of the p53 tetramerization domain mandates a conformational switch upon DNA binding.* Embo J, 1995. **14**(3): p. 512-9.
177. Gotz, C., et al., *Protein kinase CK2 interacts with a multi-protein binding domain of p53.* Mol Cell Biochem, 1999. **191**(1-2): p. 111-20.
178. Delphin, C., et al., *The in vitro phosphorylation of p53 by calcium-dependent protein kinase C--characterization of a protein-kinase-C-binding site on p53.* Eur J Biochem, 1997. **245**(3): p. 684-92.
179. Dobner, T., et al., *Blockage by adenovirus E4orf6 of transcriptional activation by the p53 tumor suppressor.* Science, 1996. **272**(5267): p. 1470-3.

180. Fernandez-Fernandez, M.R., D.B. Veprintsev, and A.R. Fersht, *Proteins of the S100 family regulate the oligomerization of p53 tumor suppressor.* Proc Natl Acad Sci U S A, 2005. **102**(13): p. 4735-40.
181. Andrews, P., Y.J. He, and Y. Xiong, *Cytoplasmic localized ubiquitin ligase cullin 7 binds to p53 and promotes cell growth by antagonizing p53 function.* Oncogene, 2006. **25**(33): p. 4534-48.
182. Sheng, Y., et al., *Molecular basis of Pirh2-mediated p53 ubiquitylation.* Nat Struct Mol Biol, 2008. **15**(12): p. 1334-42.
183. Blaydes, J.P., et al., *Stoichiometric phosphorylation of human p53 at Ser315 stimulates p53-dependent transcription.* J Biol Chem, 2001. **276**(7): p. 4699-708.
184. Hupp, T.R. and D.P. Lane, *Regulation of the cryptic sequence-specific DNA-binding function of p53 by protein kinases.* Cold Spring Harb Symp Quant Biol, 1994. **59**: p. 195-206.
185. Sakaguchi, K., et al., *DNA damage activates p53 through a phosphorylation-acetylation cascade.* Genes Dev, 1998. **12**(18): p. 2831-41.
186. Rustandi, R.R., D.M. Baldisseri, and D.J. Weber, *Structure of the negative regulatory domain of p53 bound to S100B(betabeta).* Nat Struct Biol, 2000. **7**(7): p. 570-4.
187. Avalos, J.L., et al., *Structure of a Sir2 enzyme bound to an acetylated p53 peptide.* Mol Cell, 2002. **10**(3): p. 523-35.
188. Lowe, E.D., et al., *Specificity determinants of recruitment peptides bound to phospho-CDK2/cyclin A.* Biochemistry, 2002. **41**(52): p. 15625-34.
189. Mujtaba, S., et al., *Structural mechanism of the bromodomain of the coactivator CBP in p53 transcriptional activation.* Mol Cell, 2004. **13**(2): p. 251-63.
190. Sheng, Y., et al., *Molecular recognition of p53 and MDM2 by USP7/HAUSP.* Nat Struct Mol Biol, 2006. **13**(3): p. 285-91.
191. Chen, J., V. Marechal, and A.J. Levine, *Mapping of the p53 and mdm-2 interaction domains.* Mol Cell Biol, 1993. **13**(7): p. 4107-14.
192. Goodman, R.H. and S. Smolik, *CBP/p300 in cell growth, transformation, and development.* Genes Dev, 2000. **14**(13): p. 1553-77.
193. Dastidar, S.G., D.P. Lane, and C.S. Verma, *Multiple peptide conformations give rise to similar binding affinities: molecular simulations of p53-MDM2.* J Am Chem Soc, 2008. **130**(41): p. 13514-5.
194. Bottger, V., et al., *Identification of novel mdm2 binding peptides by phage display.* Oncogene, 1996. **13**(10): p. 2141-7.
195. Bottger, V., et al., *Comparative study of the p53-mdm2 and p53-MDMX interfaces.* Oncogene, 1999. **18**(1): p. 189-99.
196. MacLaine, N.J., et al., *A central role for CK1 in catalyzing phosphorylation of the p53 transactivation domain at serine 20 after HHV-6B viral infection.* J Biol Chem, 2008. **283**(42): p. 28563-73.
197. Itahana, K., et al., *Targeted inactivation of Mdm2 RING finger E3 ubiquitin ligase activity in the mouse reveals mechanistic insights into p53 regulation.* Cancer Cell, 2007. **12**(4): p. 355-66.
198. Yu, G.W., et al., *The central region of HDM2 provides a second binding site for p53.* Proc Natl Acad Sci U S A, 2006. **103**(5): p. 1227-32.

199. Kostic, M., et al., *Solution structure of the Hdm2 C2H2C4 RING, a domain critical for ubiquitination of p53.* J Mol Biol, 2006. **363**(2): p. 433-50.
200. Worrall, E.G., et al., *The effects of phosphomimetic lid mutation on the thermostability of the N-terminal domain of MDM2.* J Mol Biol. **398**(3): p. 414-28.
201. Kubbutat, M.H., S.N. Jones, and K.H. Vousden, *Regulation of p53 stability by Mdm2.* Nature, 1997. **387**(6630): p. 299-303.
202. Honda, R., H. Tanaka, and H. Yasuda, *Oncoprotein MDM2 is a ubiquitin ligase E3 for tumor suppressor p53.* FEBS Lett, 1997. **420**(1): p. 25-7.
203. Haupt, Y., et al., *Mdm2 promotes the rapid degradation of p53.* Nature, 1997. **387**(6630): p. 296-9.
204. Wu, X., et al., *The p53-mdm-2 autoregulatory feedback loop.* Genes Dev, 1993. **7**(7A): p. 1126-32.
205. Momand, J., et al., *The mdm-2 oncogene product forms a complex with the p53 protein and inhibits p53-mediated transactivation.* Cell, 1992. **69**(7): p. 1237-45.
206. Roth, J., et al., *Nucleo-cytoplasmic shuttling of the hdm2 oncoprotein regulates the levels of the p53 protein via a pathway used by the human immunodeficiency virus rev protein.* Embo J, 1998. **17**(2): p. 554-64.
207. Barak, Y., et al., *mdm2 expression is induced by wild type p53 activity.* Embo J, 1993. **12**(2): p. 461-8.
208. Candeias, M.M., et al., *P53 mRNA controls p53 activity by managing Mdm2 functions.* Nat Cell Biol, 2008. **10**(9): p. 1098-105.
209. Shvarts, A., et al., *MDMX: a novel p53-binding protein with some functional properties of MDM2.* Embo J, 1996. **15**(19): p. 5349-57.
210. Yang, W., et al., *CARPs are ubiquitin ligases that promote MDM2-independent p53 and phospho-p53ser20 degradation.* J Biol Chem, 2007. **282**(5): p. 3273-81.
211. Yamasaki, S., et al., *Cytoplasmic destruction of p53 by the endoplasmic reticulum-resident ubiquitin ligase 'Synoviolin'.* Embo J, 2007. **26**(1): p. 113-22.
212. Leng, R.P., et al., *Pirh2, a p53-induced ubiquitin-protein ligase, promotes p53 degradation.* Cell, 2003. **112**(6): p. 779-91.
213. Esser, C., M. Scheffner, and J. Hohfeld, *The chaperone-associated ubiquitin ligase CHIP is able to target p53 for proteasomal degradation.* J Biol Chem, 2005. **280**(29): p. 27443-8.
214. Dornan, D., et al., *The ubiquitin ligase COP1 is a critical negative regulator of p53.* Nature, 2004. **429**(6987): p. 86-92.
215. Chen, D., et al., *ARF-BP1/Mule is a critical mediator of the ARF tumor suppressor.* Cell, 2005. **121**(7): p. 1071-83.
216. Dyson, H.J. and P.E. Wright, *Intrinsically unstructured proteins and their functions.* Nat Rev Mol Cell Biol, 2005. **6**(3): p. 197-208.
217. Chan, H.M. and N.B. La Thangue, *p300/CBP proteins: HATs for transcriptional bridges and scaffolds.* J Cell Sci, 2001. **114**(Pt 13): p. 2363-73.
218. Schon, O., et al., *Molecular mechanism of the interaction between MDM2 and p53.* J Mol Biol, 2002. **323**(3): p. 491-501.

219. Gu, W. and R.G. Roeder, *Activation of p53 sequence-specific DNA binding by acetylation of the p53 C-terminal domain.* Cell, 1997. **90**(4): p. 595-606.
220. Teufel, D.P., et al., *Four domains of p300 each bind tightly to a sequence spanning both transactivation subdomains of p53.* Proc Natl Acad Sci U S A, 2007. **104**(17): p. 7009-14.
221. Finlan, L. and T.R. Hupp, *The N-terminal interferon-binding domain (IBiD) homology domain of p300 binds to peptides with homology to the p53 transactivation domain.* J Biol Chem, 2004. **279**(47): p. 49395-405.
222. Scolnick, D.M., et al., *CREB-binding protein and p300/CBP-associated factor are transcriptional coactivators of the p53 tumor suppressor protein.* Cancer Res, 1997. **57**(17): p. 3693-6.
223. Lill, N.L., et al., *Binding and modulation of p53 by p300/CBP coactivators.* Nature, 1997. **387**(6635): p. 823-7.
224. Lee, C.W., et al., *Functional interplay between p53 and E2F through co-activator p300.* Oncogene, 1998. **16**(21): p. 2695-710.
225. Tang, Y., et al., *Acetylation is indispensable for p53 activation.* Cell, 2008. **133**(4): p. 612-26.
226. Jin, Y., et al., *MDM2 mediates p300/CREB-binding protein-associated factor ubiquitination and degradation.* J Biol Chem, 2004. **279**(19): p. 20035-43.
227. Shikama, N., et al., *A novel cofactor for p300 that regulates the p53 response.* Mol Cell, 1999. **4**(3): p. 365-76.
228. Demonacos, C., M. Krstic-Demonacos, and N.B. La Thangue, *A TPR motif cofactor contributes to p300 activity in the p53 response.* Mol Cell, 2001. **8**(1): p. 71-84.
229. Jansson, M., et al., *Arginine methylation regulates the p53 response.* Nat Cell Biol, 2008. **10**(12): p. 1431-9.
230. Tang, Y., et al., *Tip60-dependent acetylation of p53 modulates the decision between cell-cycle arrest and apoptosis.* Mol Cell, 2006. **24**(6): p. 827-39.
231. Sykes, S.M., et al., *Acetylation of the p53 DNA-binding domain regulates apoptosis induction.* Mol Cell, 2006. **24**(6): p. 841-51.
232. Liu, L., et al., *p53 sites acetylated in vitro by PCAF and p300 are acetylated in vivo in response to DNA damage.* Mol Cell Biol, 1999. **19**(2): p. 1202-9.
233. Gsponer, J. and M.M. Babu, *The rules of disorder or why disorder rules.* Prog Biophys Mol Biol, 2009. **99**(2-3): p. 94-103.
234. Saito, S., et al., *ATM mediates phosphorylation at multiple p53 sites, including Ser(46), in response to ionizing radiation.* J Biol Chem, 2002. **277**(15): p. 12491-4.
235. Khanna, K.K., et al., *ATM associates with and phosphorylates p53: mapping the region of interaction.* Nat Genet, 1998. **20**(4): p. 398-400.
236. Canman, C.E., et al., *Activation of the ATM kinase by ionizing radiation and phosphorylation of p53.* Science, 1998. **281**(5383): p. 1677-9.
237. Banin, S., et al., *Enhanced phosphorylation of p53 by ATM in response to DNA damage.* Science, 1998. **281**(5383): p. 1674-7.
238. Shieh, S.Y., et al., *The human homologs of checkpoint kinases Chk1 and Cds1 (Chk2) phosphorylate p53 at multiple DNA damage-inducible sites.* Genes Dev, 2000. **14**(3): p. 289-300.
239. Chehab, N.H., et al., *Chk2/hCds1 functions as a DNA damage checkpoint in G(1) by stabilizing p53.* Genes Dev, 2000. **14**(3): p. 278-88.

240. Lambert, P.F., et al., *Phosphorylation of p53 serine 15 increases interaction with CBP.* J Biol Chem, 1998. **273**(49): p. 33048-53.
241. Dornan, D. and T.R. Hupp, *Inhibition of p53-dependent transcription by BOX-I phospho-peptide mimetics that bind to p300.* EMBO Rep, 2001. **2**(2): p. 139-44.
242. Shieh, S.Y., et al., *DNA damage-induced phosphorylation of p53 alleviates inhibition by MDM2.* Cell, 1997. **91**(3): p. 325-34.
243. Craig, A.L., et al., *Novel phosphorylation sites of human tumour suppressor protein p53 at Ser20 and Thr18 that disrupt the binding of mdm2 (mouse double minute 2) protein are modified in human cancers.* Biochem J, 1999. **342 (Pt 1)**: p. 133-41.
244. Brown, C.J., et al., *The electrostatic surface of MDM2 modulates the specificity of its interaction with phosphorylated and unphosphorylated p53 peptides.* Cell Cycle, 2008. **7**(5): p. 608-10.
245. Craig, A., et al., *Allosteric effects mediate CHK2 phosphorylation of the p53 transactivation domain.* EMBO Rep, 2003. **4**(8): p. 787-92.
246. Hofmann, T.G., et al., *Regulation of p53 activity by its interaction with homeodomain-interacting protein kinase-2.* Nat Cell Biol, 2002. **4**(1): p. 1-10.
247. Buschmann, T., et al., *Jun NH2-terminal kinase phosphorylation of p53 on Thr-81 is important for p53 stabilization and transcriptional activities in response to stress.* Mol Cell Biol, 2001. **21**(8): p. 2743-54.
248. Bulavin, D.V., et al., *Phosphorylation of human p53 by p38 kinase coordinates N-terminal phosphorylation and apoptosis in response to UV radiation.* Embo J, 1999. **18**(23): p. 6845-54.
249. Zheng, H., et al., *The prolyl isomerase Pin1 is a regulator of p53 in genotoxic response.* Nature, 2002. **419**(6909): p. 849-53.
250. Zacchi, P., et al., *The prolyl isomerase Pin1 reveals a mechanism to control p53 functions after genotoxic insults.* Nature, 2002. **419**(6909): p. 853-7.
251. Lu, K.P., S.D. Hanes, and T. Hunter, *A human peptidyl-prolyl isomerase essential for regulation of mitosis.* Nature, 1996. **380**(6574): p. 544-7.
252. Berger, M., et al., *Mutations in proline 82 of p53 impair its activation by Pin1 and Chk2 in response to DNA damage.* Mol Cell Biol, 2005. **25**(13): p. 5380-8.
253. Mantovani, F., et al., *The prolyl isomerase Pin1 orchestrates p53 acetylation and dissociation from the apoptosis inhibitor iASPP.* Nat Struct Mol Biol, 2007. **14**(10): p. 912-20.
254. Shi, X., et al., *Modulation of p53 function by SET8-mediated methylation at lysine 382.* Mol Cell, 2007. **27**(4): p. 636-46.
255. Huang, J., et al., *Repression of p53 activity by Smyd2-mediated methylation.* Nature, 2006. **444**(7119): p. 629-32.
256. Chuikov, S., et al., *Regulation of p53 activity through lysine methylation.* Nature, 2004. **432**(7015): p. 353-60.
257. Huang, J., et al., *p53 is regulated by the lysine demethylase LSD1.* Nature, 2007. **449**(7158): p. 105-8.
258. Roy, S., et al., *Structural insight into p53 recognition by the 53BP1 tandem Tudor domain.* J Mol Biol. **398**(4): p. 489-96.

259. Kachirskaia, I., et al., *Role for 53BP1 Tudor domain recognition of p53 dimethylated at lysine 382 in DNA damage signaling.* J Biol Chem, 2008. **283**(50): p. 34660-6.
260. Wegele, H., L. Muller, and J. Buchner, *Hsp70 and Hsp90--a relay team for protein folding.* Rev Physiol Biochem Pharmacol, 2004. **151**: p. 1-44.
261. King, F.W., et al., *Co-chaperones Bag-1, Hop and Hsp40 regulate Hsc70 and Hsp90 interactions with wild-type or mutant p53.* Embo J, 2001. **20**(22): p. 6297-305.
262. Muller, L., et al., *Hsp90 regulates the activity of wild type p53 under physiological and elevated temperatures.* J Biol Chem, 2004. **279**(47): p. 48846-54.
263. Walerych, D., et al., *Hsp70 molecular chaperones are required to support p53 tumor suppressor activity under stress conditions.* Oncogene, 2009. **28**(48): p. 4284-94.
264. Walerych, D., et al., *ATP binding to Hsp90 is sufficient for effective chaperoning of p53 protein.* J Biol Chem. **285**(42): p. 32020-8.
265. Sasaki, M., L. Nie, and C.G. Maki, *MDM2 binding induces a conformational change in p53 that is opposed by heat-shock protein 90 and precedes p53 proteasomal degradation.* J Biol Chem, 2007. **282**(19): p. 14626-34.
266. Butler, J.S. and S.N. Loh, *Folding and misfolding mechanisms of the p53 DNA binding domain at physiological temperature.* Protein Sci, 2006. **15**(11): p. 2457-65.
267. Tripathi, V., et al., *CHIP chaperones wild type p53 tumor suppressor protein.* J Biol Chem, 2007. **282**(39): p. 28441-54.
268. Wawrzynow, B., et al., *MDM2 chaperones the p53 tumor suppressor.* J Biol Chem, 2007. **282**(45): p. 32603-12.
269. Hainaut, P. and M. Hollstein, *p53 and human cancer: the first ten thousand mutations.* Adv Cancer Res, 2000. **77**: p. 81-137.
270. Milner, J., *Flexibility: the key to p53 function?* Trends Biochem Sci, 1995. **20**(2): p. 49-51.
271. Pietenpol, J.A., et al., *Sequence-specific transcriptional activation is essential for growth suppression by p53.* Proc Natl Acad Sci U S A, 1994. **91**(6): p. 1998-2002.
272. Kern, S.E., et al., *Oncogenic forms of p53 inhibit p53-regulated gene expression.* Science, 1992. **256**(5058): p. 827-30.
273. Farmer, G., et al., *Wild-type p53 activates transcription in vitro.* Nature, 1992. **358**(6381): p. 83-6.
274. Godar, S., et al., *Growth-inhibitory and tumor- suppressive functions of p53 depend on its repression of CD44 expression.* Cell, 2008. **134**(1): p. 62-73.
275. Du, L., et al., *CD44 is of functional importance for colorectal cancer stem cells.* Clin Cancer Res, 2008. **14**(21): p. 6751-60.
276. Bourguignon, L.Y., *Hyaluronan-mediated CD44 activation of RhoGTPase signaling and cytoskeleton function promotes tumor progression.* Semin Cancer Biol, 2008. **18**(4): p. 251-9.
277. Morton, J.P., et al., *Mutant p53 drives metastasis and overcomes growth arrest/senescence in pancreatic cancer.* Proc Natl Acad Sci U S A. **107**(1): p. 246-51.

278. Joerger, A.C., H.C. Ang, and A.R. Fersht, *Structural basis for understanding oncogenic p53 mutations and designing rescue drugs.* Proc Natl Acad Sci U S A, 2006. **103**(41): p. 15056-61.
279. Milyavsky, M., et al., *Transcriptional programs following genetic alterations in p53, INK4A, and H-Ras genes along defined stages of malignant transformation.* Cancer Res, 2005. **65**(11): p. 4530-43.
280. Milyavsky, M., et al., *Prolonged culture of telomerase-immortalized human fibroblasts leads to a premalignant phenotype.* Cancer Res, 2003. **63**(21): p. 7147-57.
281. Goldstein, I., et al., *Understanding wild-type and mutant p53 activities in human cancer: new landmarks on the way to targeted therapies.* Cancer Gene Ther. **18**(1): p. 2-11.
282. Buganim, Y., et al., *p53 Regulates the Ras circuit to inhibit the expression of a cancer-related gene signature by various molecular pathways.* Cancer Res. **70**(6): p. 2274-84.
283. Di Agostino, S., et al., *Gain of function of mutant p53: the mutant p53/NF-Y protein complex reveals an aberrant transcriptional mechanism of cell cycle regulation.* Cancer Cell, 2006. **10**(3): p. 191-202.
284. Imbriano, C., et al., *Direct p53 transcriptional repression: in vivo analysis of CCAAT-containing G2/M promoters.* Mol Cell Biol, 2005. **25**(9): p. 3737-51.
285. Yang, A., et al., *On the shoulders of giants: p63, p73 and the rise of p53.* Trends Genet, 2002. **18**(2): p. 90-5.
286. Yang, A., et al., *p63, a p53 homolog at 3q27-29, encodes multiple products with transactivating, death-inducing, and dominant-negative activities.* Mol Cell, 1998. **2**(3): p. 305-16.
287. Wu, G., et al., *DeltaNp63alpha and TAp63alpha regulate transcription of genes with distinct biological functions in cancer and development.* Cancer Res, 2003. **63**(10): p. 2351-7.
288. Osada, M., et al., *Cloning and functional analysis of human p51, which structurally and functionally resembles p53.* Nat Med, 1998. **4**(7): p. 839-43.
289. Lokshin, M., T. Tanaka, and C. Prives, *Transcriptional regulation by p53 and p73.* Cold Spring Harb Symp Quant Biol, 2005. **70**: p. 121-8.
290. Kaghad, M., et al., *Monoallelically expressed gene related to p53 at 1p36, a region frequently deleted in neuroblastoma and other human cancers.* Cell, 1997. **90**(4): p. 809-19.
291. Davison, T.S., et al., *p73 and p63 are homotetramers capable of weak heterotypic interactions with each other but not with p53.* J Biol Chem, 1999. **274**(26): p. 18709-14.
292. Strano, S., et al., *Physical and functional interaction between p53 mutants and different isoforms of p73.* J Biol Chem, 2000. **275**(38): p. 29503-12.
293. Strano, S., et al., *Physical interaction with human tumor-derived p53 mutants inhibits p63 activities.* J Biol Chem, 2002. **277**(21): p. 18817-26.
294. Marin, M.C., et al., *A common polymorphism acts as an intragenic modifier of mutant p53 behaviour.* Nat Genet, 2000. **25**(1): p. 47-54.
295. Irwin, M.S., et al., *Chemosensitivity linked to p73 function.* Cancer Cell, 2003. **3**(4): p. 403-10.

296. Gaiddon, C., et al., *A subset of tumor-derived mutant forms of p53 down-regulate p63 and p73 through a direct interaction with the p53 core domain.* Mol Cell Biol, 2001. **21**(5): p. 1874-87.
297. Di Como, C.J., C. Gaiddon, and C. Prives, *p73 function is inhibited by tumor-derived p53 mutants in mammalian cells.* Mol Cell Biol, 1999. **19**(2): p. 1438-49.
298. Bergamaschi, D., et al., *p53 polymorphism influences response in cancer chemotherapy via modulation of p73-dependent apoptosis.* Cancer Cell, 2003. **3**(4): p. 387-402.
299. Gannon, J.V., et al., *Activating mutations in p53 produce a common conformational effect. A monoclonal antibody specific for the mutant form.* Embo J, 1990. **9**(5): p. 1595-602.
300. Olive, K.P., et al., *Mutant p53 gain of function in two mouse models of Li-Fraumeni syndrome.* Cell, 2004. **119**(6): p. 847-60.
301. Lang, G.A., et al., *Gain of function of a p53 hot spot mutation in a mouse model of Li-Fraumeni syndrome.* Cell, 2004. **119**(6): p. 861-72.
302. Muller, P.A., et al., *Mutant p53 drives invasion by promoting integrin recycling.* Cell, 2009. **139**(7): p. 1327-41.
303. Carroll, D.K., et al., *p63 regulates an adhesion programme and cell survival in epithelial cells.* Nat Cell Biol, 2006. **8**(6): p. 551-61.
304. Derynck, R., R.J. Akhurst, and A. Balmain, *TGF-beta signaling in tumor suppression and cancer progression.* Nat Genet, 2001. **29**(2): p. 117-29.
305. Cordenonsi, M., et al., *Integration of TGF-beta and Ras/MAPK signaling through p53 phosphorylation.* Science, 2007. **315**(5813): p. 840-3.
306. Adorno, M., et al., *A Mutant-p53/Smad complex opposes p63 to empower TGFbeta-induced metastasis.* Cell, 2009. **137**(1): p. 87-98.
307. Kalo, E., et al., *Mutant p53 attenuates the SMAD-dependent transforming growth factor beta1 (TGF-beta1) signaling pathway by repressing the expression of TGF-beta receptor type II.* Mol Cell Biol, 2007. **27**(23): p. 8228-42.
308. Soussi, T. and G. Lozano, *p53 mutation heterogeneity in cancer.* Biochem Biophys Res Commun, 2005. **331**(3): p. 834-42.
309. Samuels-Lev, Y., et al., *ASPP proteins specifically stimulate the apoptotic function of p53.* Mol Cell, 2001. **8**(4): p. 781-94.
310. Mihara, M., et al., *p53 has a direct apoptogenic role at the mitochondria.* Mol Cell, 2003. **11**(3): p. 577-90.
311. Trigiante, G. and X. Lu, *ASPP [corrected] and cancer.* Nat Rev Cancer, 2006. **6**(3): p. 217-26.
312. Gorina, S. and N.P. Pavletich, *Structure of the p53 tumor suppressor bound to the ankyrin and SH3 domains of 53BP2.* Science, 1996. **274**(5289): p. 1001-5.
313. Tidow, H., et al., *Effects of oncogenic mutations and DNA response elements on the binding of p53 to p53-binding protein 2 (53BP2).* J Biol Chem, 2006. **281**(43): p. 32526-33.
314. Dehner, A., et al., *Cooperative binding of p53 to DNA: regulation by protein-protein interactions through a double salt bridge.* Angew Chem Int Ed Engl, 2005. **44**(33): p. 5247-51.

315. Ang, H.C., et al., *Effects of common cancer mutations on stability and DNA binding of full-length p53 compared with isolated core domains.* J Biol Chem, 2006. **281**(31): p. 21934-41.
316. Fontemaggi, G., et al., *The execution of the transcriptional axis mutant p53, E2F1 and ID4 promotes tumor neo-angiogenesis.* Nat Struct Mol Biol, 2009. **16**(10): p. 1086-93.
317. Haupt, S., et al., *Promyelocytic leukemia protein is required for gain of function by mutant p53.* Cancer Res, 2009. **69**(11): p. 4818-26.
318. Lee, J.H. and T.T. Paull, *ATM activation by DNA double-strand breaks through the Mre11-Rad50-Nbs1 complex.* Science, 2005. **308**(5721): p. 551-4.
319. Song, H., M. Hollstein, and Y. Xu, *p53 gain-of-function cancer mutants induce genetic instability by inactivating ATM.* Nat Cell Biol, 2007. **9**(5): p. 573-80.
320. Qin, G., et al., *Cell cycle regulator E2F1 modulates angiogenesis via p53-dependent transcriptional control of VEGF.* Proc Natl Acad Sci U S A, 2006. **103**(29): p. 11015-20.
321. Iggo, R., et al., *Increased expression of mutant forms of p53 oncogene in primary lung cancer.* Lancet, 1990. **335**(8691): p. 675-9.
322. Lavigueur, A., et al., *High incidence of lung, bone, and lymphoid tumors in transgenic mice overexpressing mutant alleles of the p53 oncogene.* Mol Cell Biol, 1989. **9**(9): p. 3982-91.
323. Vojtesek, B., et al., *Conformational changes in p53 analysed using new antibodies to the core DNA binding domain of the protein.* Oncogene, 1995. **10**(2): p. 389-93.
324. Vojtesek, B. and D.P. Lane, *Regulation of p53 protein expression in human breast cancer cell lines.* J Cell Sci, 1993. **105 (Pt 3)**: p. 607-12.
325. Midgley, C.A. and D.P. Lane, *p53 protein stability in tumour cells is not determined by mutation but is dependent on Mdm2 binding.* Oncogene, 1997. **15**(10): p. 1179-89.
326. Selkirk, J.K., et al., *Multiple p53 protein isoforms and formation of oligomeric complexes with heat shock proteins Hsp70 and Hsp90 in the human mammary tumor, T47D, cell line.* Appl Theor Electrophor, 1994. **4**(1): p. 11-8.
327. Hinds, P.W., et al., *Immunological evidence for the association of p53 with a heat shock protein, hsc70, in p53-plus-ras-transformed cell lines.* Mol Cell Biol, 1987. **7**(8): p. 2863-9.
328. Muller, P., et al., *Chaperone-dependent stabilization and degradation of p53 mutants.* Oncogene, 2008. **27**(24): p. 3371-83.
329. Peng, Y., et al., *Inhibition of MDM2 by hsp90 contributes to mutant p53 stabilization.* J Biol Chem, 2001. **276**(44): p. 40583-90.
330. Peng, Y., et al., *Stabilization of the MDM2 oncoprotein by mutant p53.* J Biol Chem, 2001. **276**(9): p. 6874-8.
331. Nagata, Y., et al., *The stabilization mechanism of mutant-type p53 by impaired ubiquitination: the loss of wild-type p53 function and the hsp90 association.* Oncogene, 1999. **18**(44): p. 6037-49.

332. Li, D., et al., *Functional Inactivation of Endogenous MDM2 and CHIP by HSP90 Causes Aberrant Stabilization of Mutant p53 in Human Cancer Cells.* Mol Cancer Res. **9**(5): p. 577-88.
333. Vassilev, L.T., *MDM2 inhibitors for cancer therapy.* Trends Mol Med, 2007. **13**(1): p. 23-31.
334. Chene, P., *Inhibiting the p53-MDM2 interaction: an important target for cancer therapy.* Nat Rev Cancer, 2003. **3**(2): p. 102-9.
335. Vassilev, L.T., et al., *In vivo activation of the p53 pathway by small-molecule antagonists of MDM2.* Science, 2004. **303**(5659): p. 844-8.
336. Tovar, C., et al., *Small-molecule MDM2 antagonists reveal aberrant p53 signaling in cancer: implications for therapy.* Proc Natl Acad Sci U S A, 2006. **103**(6): p. 1888-93.
337. Rivera, M.I., et al., *Selective toxicity of the tricyclic thiophene NSC 652287 in renal carcinoma cell lines: differential accumulation and metabolism.* Biochem Pharmacol, 1999. **57**(11): p. 1283-95.
338. Nieves-Neira, W., et al., *DNA protein cross-links produced by NSC 652287, a novel thiophene derivative active against human renal cancer cells.* Mol Pharmacol, 1999. **56**(3): p. 478-84.
339. Issaeva, N., et al., *Small molecule RITA binds to p53, blocks p53-HDM-2 interaction and activates p53 function in tumors.* Nat Med, 2004. **10**(12): p. 1321-8.
340. Ahmed, A., et al., *Pharmacological activation of a novel p53-dependent S-phase checkpoint involving CHK-1.* Cell Death Dis. **2**: p. e160.
341. Spinnler, C., et al., *Abrogation of Wip1 expression by RITA-activated p53 potentiates apoptosis induction via activation of ATM and inhibition of HdmX.* Cell Death Differ.
342. Wang, S.P., et al., *p53 controls cancer cell invasion by inducing the MDM2-mediated degradation of Slug.* Nat Cell Biol, 2009. **11**(6): p. 694-704.
343. Wawrzynow, B., et al., *A function for the RING finger domain in the allosteric control of MDM2 conformation and activity.* J Biol Chem, 2009. **284**(17): p. 11517-30.
344. Kravchenko, J.E., et al., *Small-molecule RETRA suppresses mutant p53-bearing cancer cells through a p73-dependent salvage pathway.* Proc Natl Acad Sci U S A, 2008. **105**(17): p. 6302-7.
345. Bykov, V.J., et al., *PRIMA-1(MET) synergizes with cisplatin to induce tumor cell apoptosis.* Oncogene, 2005. **24**(21): p. 3484-91.
346. Bykov, V.J., et al., *Restoration of the tumor suppressor function to mutant p53 by a low-molecular-weight compound.* Nat Med, 2002. **8**(3): p. 282-8.
347. Rokaeus, N., et al., *PRIMA-1(MET)/APR-246 targets mutant forms of p53 family members p63 and p73.* Oncogene. **29**(49): p. 6442-51.
348. Zandi, R., et al., *PRIMA-1Met/APR-246 Induces Apoptosis and Tumor Growth Delay in Small Cell Lung Cancer Expressing Mutant p53.* Clin Cancer Res. **17**(9): p. 2830-41.
349. Grinter, S.Z., et al., *An inverse docking approach for identifying new potential anti-cancer targets.* J Mol Graph Model. **29**(6): p. 795-9.
350. Boeckler, F.M., et al., *Targeted rescue of a destabilized mutant of p53 by an in silico screened drug.* Proc Natl Acad Sci U S A, 2008. **105**(30): p. 10360-5.

351. Basse, N., et al., *Toward the rational design of p53-stabilizing drugs: probing the surface of the oncogenic Y220C mutant.* Chem Biol. **17**(1): p. 46-56.
352. Gordo, S., et al., *Stability and structural recovery of the tetramerization domain of p53-R337H mutant induced by a designed templating ligand.* Proc Natl Acad Sci U S A, 2008. **105**(43): p. 16426-31.
353. Teixeira, M.T., B. Dujon, and E. Fabre, *Genome-wide nuclear morphology screen identifies novel genes involved in nuclear architecture and gene-silencing in Saccharomyces cerevisiae.* J Mol Biol, 2002. **321**(4): p. 551-61.
354. Khorasanizadeh, S., *The nucleosome: from genomic organization to genomic regulation.* Cell, 2004. **116**(2): p. 259-72.
355. Conaway, R.C. and J.W. Conaway, *The INO80 chromatin remodeling complex in transcription, replication and repair.* Trends Biochem Sci, 2009. **34**(2): p. 71-7.
356. Shen, X., et al., *A chromatin remodelling complex involved in transcription and DNA processing.* Nature, 2000. **406**(6795): p. 541-4.
357. Jonsson, Z.O., et al., *Rvb1p/Rvb2p recruit Arp5p and assemble a functional Ino80 chromatin remodeling complex.* Mol Cell, 2004. **16**(3): p. 465-77.
358. Jin, J., et al., *A mammalian chromatin remodeling complex with similarities to the yeast INO80 complex.* J Biol Chem, 2005. **280**(50): p. 41207-12.
359. Mizuguchi, G., et al., *ATP-driven exchange of histone H2AZ variant catalyzed by SWR1 chromatin remodeling complex.* Science, 2004. **303**(5656): p. 343-8.
360. Ikura, T., et al., *Involvement of the TIP60 histone acetylase complex in DNA repair and apoptosis.* Cell, 2000. **102**(4): p. 463-73.
361. Gaughan, L., et al., *Tip60 and histone deacetylase 1 regulate androgen receptor activity through changes to the acetylation status of the receptor.* J Biol Chem, 2002. **277**(29): p. 25904-13.
362. Taubert, S., et al., *E2F-dependent histone acetylation and recruitment of the Tip60 acetyltransferase complex to chromatin in late G1.* Mol Cell Biol, 2004. **24**(10): p. 4546-56.
363. Frank, S.R., et al., *MYC recruits the TIP60 histone acetyltransferase complex to chromatin.* EMBO Rep, 2003. **4**(6): p. 575-80.
364. Etard, C., et al., *Pontin and Reptin regulate cell proliferation in early Xenopus embryos in collaboration with c-Myc and Miz-1.* Mech Dev, 2005. **122**(4): p. 545-56.
365. Bauer, A., et al., *Pontin52 and reptin52 function as antagonistic regulators of beta-catenin signalling activity.* Embo J, 2000. **19**(22): p. 6121-30.
366. Diop, S.B., et al., *Reptin and Pontin function antagonistically with PcG and TrxG complexes to mediate Hox gene control.* EMBO Rep, 2008. **9**(3): p. 260-6.
367. Kim, J.H., et al., *Transcriptional regulation of a metastasis suppressor gene by Tip60 and beta-catenin complexes.* Nature, 2005. **434**(7035): p. 921-6.
368. Kanemaki, M., et al., *TIP49b, a new RuvB-like DNA helicase, is included in a complex together with another RuvB-like DNA helicase, TIP49a.* J Biol Chem, 1999. **274**(32): p. 22437-44.
369. Ohdate, H., et al., *Impairment of the DNA binding activity of the TATA-binding protein renders the transcriptional function of Rvb2p/Tih2p, the yeast*

RuvB-like protein, essential for cell growth. J Biol Chem, 2003. **278**(17): p. 14647-56.
370. Wood, M.A., S.B. McMahon, and M.D. Cole, *An ATPase/helicase complex is an essential cofactor for oncogenic transformation by c-Myc.* Mol Cell, 2000. **5**(2): p. 321-30.
371. Cho, S.G., et al., *TIP49b, a regulator of activating transcription factor 2 response to stress and DNA damage.* Mol Cell Biol, 2001. **21**(24): p. 8398-413.
372. de La Coste, A., et al., *Somatic mutations of the beta-catenin gene are frequent in mouse and human hepatocellular carcinomas.* Proc Natl Acad Sci U S A, 1998. **95**(15): p. 8847-51.
373. Fodde, R., R. Smits, and H. Clevers, *APC, signal transduction and genetic instability in colorectal cancer.* Nat Rev Cancer, 2001. **1**(1): p. 55-67.
374. Polakis, P., *Wnt signaling and cancer.* Genes Dev, 2000. **14**(15): p. 1837-51.
375. Olson, L.E., et al., *Homeodomain-mediated beta-catenin-dependent switching events dictate cell-lineage determination.* Cell, 2006. **125**(3): p. 593-605.
376. Kim, J.H., et al., *Roles of sumoylation of a reptin chromatin-remodelling complex in cancer metastasis.* Nat Cell Biol, 2006. **8**(6): p. 631-9.
377. Weiske, J. and O. Huber, *The histidine triad protein Hint1 interacts with Pontin and Reptin and inhibits TCF-beta-catenin-mediated transcription.* J Cell Sci, 2005. **118**(Pt 14): p. 3117-29.
378. Rashid, S., et al., *Endosomal adaptor proteins APPL1 and APPL2 are novel activators of beta-catenin/TCF-mediated transcription.* J Biol Chem, 2009. **284**(27): p. 18115-28.
379. Sancar, A., et al., *Molecular mechanisms of mammalian DNA repair and the DNA damage checkpoints.* Annu Rev Biochem, 2004. **73**: p. 39-85.
380. Bakkenist, C.J. and M.B. Kastan, *DNA damage activates ATM through intermolecular autophosphorylation and dimer dissociation.* Nature, 2003. **421**(6922): p. 499-506.
381. Morrison, A.J., et al., *INO80 and gamma-H2AX interaction links ATP-dependent chromatin remodeling to DNA damage repair.* Cell, 2004. **119**(6): p. 767-75.
382. van Attikum, H., O. Fritsch, and S.M. Gasser, *Distinct roles for SWR1 and INO80 chromatin remodeling complexes at chromosomal double-strand breaks.* Embo J, 2007. **26**(18): p. 4113-25.
383. van Attikum, H., et al., *Recruitment of the INO80 complex by H2A phosphorylation links ATP-dependent chromatin remodeling with DNA double-strand break repair.* Cell, 2004. **119**(6): p. 777-88.
384. Wu, S., et al., *A YY1-INO80 complex regulates genomic stability through homologous recombination-based repair.* Nat Struct Mol Biol, 2007. **14**(12): p. 1165-72.
385. Sun, Y., et al., *A role for the Tip60 histone acetyltransferase in the acetylation and activation of ATM.* Proc Natl Acad Sci U S A, 2005. **102**(37): p. 13182-7.
386. Sun, Y., et al., *DNA damage-induced acetylation of lysine 3016 of ATM activates ATM kinase activity.* Mol Cell Biol, 2007. **27**(24): p. 8502-9.

387. Murr, R., et al., *Histone acetylation by Trrap-Tip60 modulates loading of repair proteins and repair of DNA double-strand breaks.* Nat Cell Biol, 2006. **8**(1): p. 91-9.
388. Jha, S., E. Shibata, and A. Dutta, *Human Rvb1/Tip49 is required for the histone acetyltransferase activity of Tip60/NuA4 and for the downregulation of phosphorylation on H2AX after DNA damage.* Mol Cell Biol, 2008. **28**(8): p. 2690-700.
389. Ni, L., et al., *RPAP3 interacts with Reptin to regulate UV-induced phosphorylation of H2AX and DNA damage.* J Cell Biochem, 2009. **106**(5): p. 920-8.
390. Izumi, N., et al., *AAA+ proteins RUVBL1 and RUVBL2 coordinate PIKK activity and function in nonsense-mediated mRNA decay.* Sci Signal. **3**(116): p. ra27.
391. Kiss, T., *Small nucleolar RNAs: an abundant group of noncoding RNAs with diverse cellular functions.* Cell, 2002. **109**(2): p. 145-8.
392. King, T.H., et al., *A well-connected and conserved nucleoplasmic helicase is required for production of box C/D and H/ACA snoRNAs and localization of snoRNP proteins.* Mol Cell Biol, 2001. **21**(22): p. 7731-46.
393. Newman, D.R., et al., *Box C/D snoRNA-associated proteins: two pairs of evolutionarily ancient proteins and possible links to replication and transcription.* Rna, 2000. **6**(6): p. 861-79.
394. Watkins, N.J., A. Dickmanns, and R. Luhrmann, *Conserved stem II of the box C/D motif is essential for nucleolar localization and is required, along with the 15.5K protein, for the hierarchical assembly of the box C/D snoRNP.* Mol Cell Biol, 2002. **22**(23): p. 8342-52.
395. Watkins, N.J., et al., *Assembly and maturation of the U3 snoRNP in the nucleoplasm in a large dynamic multiprotein complex.* Mol Cell, 2004. **16**(5): p. 789-98.
396. Zhao, R., et al., *Molecular chaperone Hsp90 stabilizes Pih1/Nop17 to maintain R2TP complex activity that regulates snoRNA accumulation.* J Cell Biol, 2008. **180**(3): p. 563-78.
397. Venteicher, A.S., et al., *Identification of ATPases pontin and reptin as telomerase components essential for holoenzyme assembly.* Cell, 2008. **132**(6): p. 945-57.
398. Blackburn, E.H., *Switching and signaling at the telomere.* Cell, 2001. **106**(6): p. 661-73.
399. Gartner, W., et al., *The ATP-dependent helicase RUVBL1/TIP49a associates with tubulin during mitosis.* Cell Motil Cytoskeleton, 2003. **56**(2): p. 79-93.
400. Sigala, B., et al., *Relocalization of human chromatin remodeling cofactor TIP48 in mitosis.* Exp Cell Res, 2005. **310**(2): p. 357-69.
401. Ducat, D., et al., *Regulation of microtubule assembly and organization in mitosis by the AAA+ ATPase Pontin.* Mol Biol Cell, 2008. **19**(7): p. 3097-110.
402. Aberger, F., et al., *Anterior specification of embryonic ectoderm: the role of the Xenopus cement gland-specific gene XAG-2.* Mech Dev, 1998. **72**(1-2): p. 115-30.

403. Bouwmeester, T., et al., *Cerberus is a head-inducing secreted factor expressed in the anterior endoderm of Spemann's organizer.* Nature, 1996. **382**(6592): p. 595-601.
404. Hemmati-Brivanlou, A., O.G. Kelly, and D.A. Melton, *Follistatin, an antagonist of activin, is expressed in the Spemann organizer and displays direct neuralizing activity.* Cell, 1994. **77**(2): p. 283-95.
405. Lamb, T.M., et al., *Neural induction by the secreted polypeptide noggin.* Science, 1993. **262**(5134): p. 713-8.
406. Sasai, Y., et al., *Regulation of neural induction by the Chd and Bmp-4 antagonistic patterning signals in Xenopus.* Nature, 1995. **376**(6538): p. 333-6.
407. Thompson, D.A. and R.J. Weigel, *hAG-2, the human homologue of the Xenopus laevis cement gland gene XAG-2, is coexpressed with estrogen receptor in breast cancer cell lines.* Biochem Biophys Res Commun, 1998. **251**(1): p. 111-6.
408. Brychtova, V., B. Vojtesek, and R. Hrstka, *Anterior gradient 2: a novel player in tumor cell biology.* Cancer Lett. **304**(1): p. 1-7.
409. Fritzsche, F.R., et al., *Prognostic relevance of AGR2 expression in breast cancer.* Clin Cancer Res, 2006. **12**(6): p. 1728-34.
410. Zhang, J.S., et al., *AGR2, an androgen-inducible secretory protein overexpressed in prostate cancer.* Genes Chromosomes Cancer, 2005. **43**(3): p. 249-59.
411. Wang, Z., Y. Hao, and A.W. Lowe, *The adenocarcinoma-associated antigen, AGR2, promotes tumor growth, cell migration, and cellular transformation.* Cancer Res, 2008. **68**(2): p. 492-7.
412. Persson, S., et al., *Diversity of the protein disulfide isomerase family: identification of breast tumor induced Hag2 and Hag3 as novel members of the protein family.* Mol Phylogenet Evol, 2005. **36**(3): p. 734-40.
413. Sevier, C.S. and C.A. Kaiser, *Formation and transfer of disulphide bonds in living cells.* Nat Rev Mol Cell Biol, 2002. **3**(11): p. 836-47.
414. Anelli, T., et al., *ERp44, a novel endoplasmic reticulum folding assistant of the thioredoxin family.* Embo J, 2002. **21**(4): p. 835-44.
415. Ferrari, D.M. and H.D. Soling, *The protein disulphide-isomerase family: unravelling a string of folds.* Biochem J, 1999. **339 (Pt 1)**: p. 1-10.
416. Freedman, R.B., T.R. Hirst, and M.F. Tuite, *Protein disulphide isomerase: building bridges in protein folding.* Trends Biochem Sci, 1994. **19**(8): p. 331-6.
417. Tachibana, C. and T.H. Stevens, *The yeast EUG1 gene encodes an endoplasmic reticulum protein that is functionally related to protein disulfide isomerase.* Mol Cell Biol, 1992. **12**(10): p. 4601-11.
418. Norgaard, P., et al., *Functional differences in yeast protein disulfide isomerases.* J Cell Biol, 2001. **152**(3): p. 553-62.
419. Wunderlich, M., et al., *Efficient catalysis of disulfide formation during protein folding with a single active-site cysteine.* J Mol Biol, 1995. **247**(1): p. 28-33.
420. Fourtouna, A., et al., *The Anterior Gradient-2 Pathway as a Model for Developing Peptide-Aptamer Anti-Cancer Drug Leads that Stimulate p53 Function.* Current Chemical Biology, 2009. **3**(2): p. 124-137.

421. Park, S.W., et al., *The protein disulfide isomerase AGR2 is essential for production of intestinal mucus.* Proc Natl Acad Sci U S A, 2009. **106**(17): p. 6950-5.
422. Zhao, F., et al., *Disruption of Paneth and goblet cell homeostasis and increased endoplasmic reticulum stress in Agr2-/- mice.* Dev Biol. **338**(2): p. 270-9.
423. Fletcher, G.C., et al., *hAG-2 and hAG-3, human homologues of genes involved in differentiation, are associated with oestrogen receptor-positive breast tumours and interact with metastasis gene C4.4a and dystroglycan.* Br J Cancer, 2003. **88**(4): p. 579-85.
424. Murray, E., et al., *Microarray-formatted clinical biomarker assay development using peptide aptamers to anterior gradient-2.* Biochemistry, 2007. **46**(48): p. 13742-51.
425. Nicholson, J., *(manuscript in preparation).*
426. Innes, H.E., et al., *Significance of the metastasis-inducing protein AGR2 for outcome in hormonally treated breast cancer patients.* Br J Cancer, 2006. **94**(7): p. 1057-65.
427. Liu, D., et al., *Human homologue of cement gland protein, a novel metastasis inducer associated with breast carcinomas.* Cancer Res, 2005. **65**(9): p. 3796-805.
428. Shen, D., et al., *Loss of annexin A1 expression in human breast cancer detected by multiple high-throughput analyses.* Biochem Biophys Res Commun, 2005. **326**(1): p. 218-27.
429. Zhang, Y., et al., *Increased expression of anterior gradient-2 is significantly associated with poor survival of prostate cancer patients.* Prostate Cancer Prostatic Dis, 2007. **10**(3): p. 293-300.
430. Vivekanandan, P., S.T. Micchelli, and M. Torbenson, *Anterior gradient-2 is overexpressed by fibrolamellar carcinomas.* Hum Pathol, 2009. **40**(3): p. 293-9.
431. Iacobuzio-Donahue, C.A., et al., *Highly expressed genes in pancreatic ductal adenocarcinomas: a comprehensive characterization and comparison of the transcription profiles obtained from three major technologies.* Cancer Res, 2003. **63**(24): p. 8614-22.
432. Missiaglia, E., et al., *Analysis of gene expression in cancer cell lines identifies candidate markers for pancreatic tumorigenesis and metastasis.* Int J Cancer, 2004. **112**(1): p. 100-12.
433. Lee, S., et al., *Differential expression in normal-adenoma-carcinoma sequence suggests complex molecular carcinogenesis in colon.* Oncol Rep, 2006. **16**(4): p. 747-54.
434. Park, K., et al., *AGR2, a mucinous ovarian cancer marker, promotes cell proliferation and migration.* Exp Mol Med. **43**(2): p. 91-100.
435. Smirnov, D.A., et al., *Global gene expression profiling of circulating tumor cells.* Cancer Res, 2005. **65**(12): p. 4993-7.
436. Hrstka, R., et al., *The pro-metastatic protein anterior gradient-2 predicts poor prognosis in tamoxifen-treated breast cancers.* Oncogene. **29**(34): p. 4838-47.

437. Pohler, E., et al., *The Barrett's antigen anterior gradient-2 silences the p53 transcriptional response to DNA damage.* Mol Cell Proteomics, 2004. **3**(6): p. 534-47.
438. Kaiser, J., *Toxicology. Just how bad is dioxin?* Science, 2000. **288**(5473): p. 1941-4.
439. Paajarvi, G., et al., *TCDD activates Mdm2 and attenuates the p53 response to DNA damaging agents.* Carcinogenesis, 2005. **26**(1): p. 201-8.
440. Ray, S.S. and H.I. Swanson, *Dioxin-induced immortalization of normal human keratinocytes and silencing of p53 and p16INK4a.* J Biol Chem, 2004. **279**(26): p. 27187-93.
441. Ambolet-Camoit, A., et al., *2,3,7,8-tetrachlorodibenzo-p-dioxin counteracts the p53 response to a genotoxicant by upregulating expression of the metastasis marker agr2 in the hepatocarcinoma cell line HepG2.* Toxicol Sci. **115**(2): p. 501-12.
442. Ramachandran, V., et al., *Anterior gradient 2 is expressed and secreted during the development of pancreatic cancer and promotes cancer cell survival.* Cancer Res, 2008. **68**(19): p. 7811-8.
443. Lee, D.H., et al., *Identification of proteins differentially expressed in gastric cancer cells with high metastatic potential for invasion to lymph nodes.* Mol Cells.
444. Zweitzig, D.R., et al., *Physiological stress induces the metastasis marker AGR2 in breast cancer cells.* Mol Cell Biochem, 2007. **306**(1-2): p. 255-60.
445. Sive, H. and L. Bradley, *A sticky problem: the Xenopus cement gland as a paradigm for anteroposterior patterning.* Dev Dyn, 1996. **205**(3): p. 265-80.
446. Kumar, A., et al., *Molecular basis for the nerve dependence of limb regeneration in an adult vertebrate.* Science, 2007. **318**(5851): p. 772-7.
447. Cheng, H. and C.P. Leblond, *Origin, differentiation and renewal of the four main epithelial cell types in the mouse small intestine. V. Unitarian Theory of the origin of the four epithelial cell types.* Am J Anat, 1974. **141**(4): p. 537-61.
448. Andreu, P., et al., *A genetic study of the role of the Wnt/beta-catenin signalling in Paneth cell differentiation.* Dev Biol, 2008. **324**(2): p. 288-96.
449. Batlle, E., et al., *Beta-catenin and TCF mediate cell positioning in the intestinal epithelium by controlling the expression of EphB/ephrinB.* Cell, 2002. **111**(2): p. 251-63.
450. van Es, J.H., et al., *Wnt signalling induces maturation of Paneth cells in intestinal crypts.* Nat Cell Biol, 2005. **7**(4): p. 381-6.
451. Zheng, W., et al., *Evaluation of AGR2 and AGR3 as candidate genes for inflammatory bowel disease.* Genes Immun, 2006. **7**(1): p. 11-8.
452. Chang, J., et al., *Proteomic changes during intestinal cell maturation in vivo.* J Proteomics, 2008. **71**(5): p. 530-46.
453. Lepreux, S., P. Bioulac-Sage, and E. Chevet, *Differential expression of the anterior gradient protein-2 is a conserved feature during morphogenesis and carcinogenesis of the biliary tree.* Liver Int, 2011. **31**(3): p. 322-8.
454. Fearon, E.R. and B. Vogelstein, *A genetic model for colorectal tumorigenesis.* Cell, 1990. **61**(5): p. 759-67.
455. Neshat, K., et al., *Barrett's esophagus: a model of human neoplastic progression.* Cold Spring Harb Symp Quant Biol, 1994. **59**: p. 577-83.

456. Lamlum, H., et al., *The type of somatic mutation at APC in familial adenomatous polyposis is determined by the site of the germline mutation: a new facet to Knudson's 'two-hit' hypothesis.* Nat Med, 1999. **5**(9): p. 1071-5.
457. Miyaki, M., et al., *Familial polyposis: recent advances.* Crit Rev Oncol Hematol, 1995. **19**(1): p. 1-31.
458. Hollstein, M., et al., *p53 mutations in human cancers.* Science, 1991. **253**(5015): p. 49-53.
459. Xing, E.P., et al., *Aberrant methylation of p16INK4a and deletion of p15INK4b are frequent events in human esophageal cancer in Linxian, China.* Carcinogenesis, 1999. **20**(1): p. 77-84.
460. Mandard, A.M., P. Hainaut, and M. Hollstein, *Genetic steps in the development of squamous cell carcinoma of the esophagus.* Mutat Res, 2000. **462**(2-3): p. 335-42.
461. Falck, J., et al., *Functional impact of concomitant versus alternative defects in the Chk2-p53 tumour suppressor pathway.* Oncogene, 2001. **20**(39): p. 5503-10.
462. Hopwood, D., et al., *Biochemical analysis of the stress protein response in human oesophageal epithelium.* Gut, 1997. **41**(2): p. 156-63.
463. Yagui-Beltran, A., et al., *The human oesophageal squamous epithelium exhibits a novel type of heat shock protein response.* Eur J Biochem, 2001. **268**(20): p. 5343-55.
464. Massague, J., *TGFbeta in Cancer.* Cell, 2008. **134**(2): p. 215-30.
465. Macias-Silva, M., et al., *MADR2 is a substrate of the TGFbeta receptor and its phosphorylation is required for nuclear accumulation and signaling.* Cell, 1996. **87**(7): p. 1215-24.
466. Lin, H.Y., et al., *Expression cloning of the TGF-beta type II receptor, a functional transmembrane serine/threonine kinase.* Cell, 1992. **68**(4): p. 775-85.
467. Lagna, G., et al., *Partnership between DPC4 and SMAD proteins in TGF-beta signalling pathways.* Nature, 1996. **383**(6603): p. 832-6.
468. Nakao, A., et al., *TGF-beta receptor-mediated signalling through Smad2, Smad3 and Smad4.* Embo J, 1997. **16**(17): p. 5353-62.
469. Zhang, Y., et al., *Receptor-associated Mad homologues synergize as effectors of the TGF-beta response.* Nature, 1996. **383**(6596): p. 168-72.
470. Shi, Y., et al., *Crystal structure of a Smad MH1 domain bound to DNA: insights on DNA binding in TGF-beta signaling.* Cell, 1998. **94**(5): p. 585-94.
471. Chen, X., et al., *Smad4 and FAST-1 in the assembly of activin-responsive factor.* Nature, 1997. **389**(6646): p. 85-9.
472. Feng, X.H. and R. Derynck, *Specificity and versatility in tgf-beta signaling through Smads.* Annu Rev Cell Dev Biol, 2005. **21**: p. 659-93.
473. Feng, X.H., et al., *The tumor suppressor Smad4/DPC4 and transcriptional adaptor CBP/p300 are coactivators for smad3 in TGF-beta-induced transcriptional activation.* Genes Dev, 1998. **12**(14): p. 2153-63.
474. Itoh, F., et al., *Synergy and antagonism between Notch and BMP receptor signaling pathways in endothelial cells.* Embo J, 2004. **23**(3): p. 541-51.
475. Janknecht, R., N.J. Wells, and T. Hunter, *TGF-beta-stimulated cooperation of smad proteins with the coactivators CBP/p300.* Genes Dev, 1998. **12**(14): p. 2114-9.

476. Leong, G.M., et al., *Ski-interacting protein interacts with Smad proteins to augment transforming growth factor-beta-dependent transcription.* J Biol Chem, 2001. **276**(21): p. 18243-8.
477. Pouponnot, C., L. Jayaraman, and J. Massague, *Physical and functional interaction of SMADs and p300/CBP.* J Biol Chem, 1998. **273**(36): p. 22865-8.
478. Shioda, T., et al., *Transcriptional activating activity of Smad4: roles of SMAD hetero-oligomerization and enhancement by an associating transactivator.* Proc Natl Acad Sci U S A, 1998. **95**(17): p. 9785-90.
479. Topper, J.N., et al., *CREB binding protein is a required coactivator for Smad-dependent, transforming growth factor beta transcriptional responses in endothelial cells.* Proc Natl Acad Sci U S A, 1998. **95**(16): p. 9506-11.
480. Kim, R.H., et al., *A novel smad nuclear interacting protein, SNIP1, suppresses p300-dependent TGF-beta signal transduction.* Genes Dev, 2000. **14**(13): p. 1605-16.
481. Luo, K., et al., *The Ski oncoprotein interacts with the Smad proteins to repress TGFbeta signaling.* Genes Dev, 1999. **13**(17): p. 2196-206.
482. Wang, W., et al., *Ski represses bone morphogenic protein signaling in Xenopus and mammalian cells.* Proc Natl Acad Sci U S A, 2000. **97**(26): p. 14394-9.
483. Wu, J.W., et al., *Structural mechanism of Smad4 recognition by the nuclear oncoprotein Ski: insights on Ski-mediated repression of TGF-beta signaling.* Cell, 2002. **111**(3): p. 357-67.
484. Meulmeester, E. and P. Ten Dijke, *The dynamic roles of TGF-beta in cancer.* J Pathol. **223**(2): p. 205-18.
485. Ohkawara, B., et al., *Role of the TAK1-NLK-STAT3 pathway in TGF-beta-mediated mesoderm induction.* Genes Dev, 2004. **18**(4): p. 381-6.
486. Yamashita, M., et al., *TRAF6 mediates Smad-independent activation of JNK and p38 by TGF-beta.* Mol Cell, 2008. **31**(6): p. 918-24.
487. Mulder, K.M., *Role of Ras and Mapks in TGFbeta signaling.* Cytokine Growth Factor Rev, 2000. **11**(1-2): p. 23-35.
488. Massague, J., *How cells read TGF-beta signals.* Nat Rev Mol Cell Biol, 2000. **1**(3): p. 169-78.
489. Takebayashi-Suzuki, K., et al., *Interplay between the tumor suppressor p53 and TGF beta signaling shapes embryonic body axes in Xenopus.* Development, 2003. **130**(17): p. 3929-39.
490. Wilkinson, D.S., et al., *A direct intersection between p53 and transforming growth factor beta pathways targets chromatin modification and transcription repression of the alpha-fetoprotein gene.* Mol Cell Biol, 2005. **25**(3): p. 1200-12.
491. Wilkinson, D.S., et al., *Chromatin-bound p53 anchors activated Smads and the mSin3A corepressor to confer transforming-growth-factor-beta-mediated transcription repression.* Mol Cell Biol, 2008. **28**(6): p. 1988-98.
492. Saito, S., et al., *Phosphorylation site interdependence of human p53 post-translational modifications in response to stress.* J Biol Chem, 2003. **278**(39): p. 37536-44.

493. Matsuoka, S., et al., *ATM and ATR substrate analysis reveals extensive protein networks responsive to DNA damage.* Science, 2007. **316**(5828): p. 1160-6.
494. Craig, A.L., et al., *Signaling to p53: the use of phospho-specific antibodies to probe for in vivo kinase activation.* Methods Mol Biol, 2003. **234**: p. 171-202.
495. Roche, K.C., et al., *Regulation of ATR-dependent pathways by the FHA domain containing protein SNIP1.* Oncogene, 2007. **26**(31): p. 4523-30.
496. Cuervo, A.M. and J.F. Dice, *Lysosomes, a meeting point of proteins, chaperones, and proteases.* J Mol Med, 1998. **76**(1): p. 6-12.
497. Glickman, M.H. and A. Ciechanover, *The ubiquitin-proteasome proteolytic pathway: destruction for the sake of construction.* Physiol Rev, 2002. **82**(2): p. 373-428.
498. Ciechanover, A., *Intracellular protein degradation: from a vague idea through the lysosome and the ubiquitin-proteasome system and onto human diseases and drug targeting.* Medicina (B Aires). **70**(2): p. 105-19.
499. Lane, D.P., *Cancer. p53, guardian of the genome.* Nature, 1992. **358**(6381): p. 15-6.
500. Kastan, M.B., et al., *Participation of p53 protein in the cellular response to DNA damage.* Cancer Res, 1991. **51**(23 Pt 1): p. 6304-11.
501. Maltzman, W. and L. Czyzyk, *UV irradiation stimulates levels of p53 cellular tumor antigen in nontransformed mouse cells.* Mol Cell Biol, 1984. **4**(9): p. 1689-94.
502. Nelson, W.G. and M.B. Kastan, *DNA strand breaks: the DNA template alterations that trigger p53-dependent DNA damage response pathways.* Mol Cell Biol, 1994. **14**(3): p. 1815-23.
503. Graeber, T.G., et al., *Hypoxia induces accumulation of p53 protein, but activation of a G1-phase checkpoint by low-oxygen conditions is independent of p53 status.* Mol Cell Biol, 1994. **14**(9): p. 6264-77.
504. Wynford-Thomas, D., *Telomeres, p53 and cellular senescence.* Oncol Res, 1996. **8**(10-11): p. 387-98.
505. Takaoka, A., et al., *Integration of interferon-alpha/beta signalling to p53 responses in tumour suppression and antiviral defence.* Nature, 2003. **424**(6948): p. 516-23.
506. Boutell, C. and R.D. Everett, *Herpes simplex virus type 1 infection induces the stabilization of p53 in a USP7- and ATM-independent manner.* J Virol, 2004. **78**(15): p. 8068-77.
507. Lee, S.M., et al., *A nucleocytoplasmic malate dehydrogenase regulates p53 transcriptional activity in response to metabolic stress.* Cell Death Differ, 2009. **16**(5): p. 738-48.
508. Linke, S.P., et al., *A reversible, p53-dependent G0/G1 cell cycle arrest induced by ribonucleotide depletion in the absence of detectable DNA damage.* Genes Dev, 1996. **10**(8): p. 934-47.
509. Vousden, K.H. and D.P. Lane, *p53 in health and disease.* Nat Rev Mol Cell Biol, 2007. **8**(4): p. 275-83.
510. Wiman, K.G., *Strategies for therapeutic targeting of the p53 pathway in cancer.* Cell Death Differ, 2006. **13**(6): p. 921-6.
511. Massague, J. and D. Wotton, *Transcriptional control by the TGF-beta/Smad signaling system.* Embo J, 2000. **19**(8): p. 1745-54.

512. Ding, W., et al., *Sprouty2 downregulation plays a pivotal role in mediating crosstalk between TGF-beta1 signaling and EGF as well as FGF receptor tyrosine kinase-ERK pathways in mesenchymal cells.* J Cell Physiol, 2007. **212**(3): p. 796-806.
513. Kang, J.S., et al., *Repression of Runx2 function by TGF-beta through recruitment of class II histone deacetylases by Smad3.* Embo J, 2005. **24**(14): p. 2543-55.
514. Huber, M., et al., *Comparison of proteomic and genomic analyses of the human breast cancer cell line T47D and the antiestrogen-resistant derivative T47D-r.* Mol Cell Proteomics, 2004. **3**(1): p. 43-55.
515. Ren, Y., et al., *Dual effects of TGF-beta on ERalpha-mediated estrogenic transcriptional activity in breast cancer.* Mol Cancer, 2009. **8**: p. 111.
516. Wu, L., et al., *Smad4 as a transcription corepressor for estrogen receptor alpha.* J Biol Chem, 2003. **278**(17): p. 15192-200.
517. Matsuda, T., et al., *Cross-talk between transforming growth factor-beta and estrogen receptor signaling through Smad3.* J Biol Chem, 2001. **276**(46): p. 42908-14.
518. Bleeker, F.E., et al., *Mutational profiling of cancer candidate genes in glioblastoma, melanoma and pancreatic carcinoma reveals a snapshot of their genomic landscapes.* Hum Mutat, 2009. **30**(2): p. E451-9.
519. Miyaki, M. and T. Kuroki, *Role of Smad4 (DPC4) inactivation in human cancer.* Biochem Biophys Res Commun, 2003. **306**(4): p. 799-804.
520. Seshimo, I., et al., *Expression and mutation of SMAD4 in poorly differentiated carcinoma and signet-ring cell carcinoma of the colorectum.* J Exp Clin Cancer Res, 2006. **25**(3): p. 433-42.
521. Jakob, J., et al., *Two somatic biallelic lesions within and near SMAD4 in a human breast cancer cell line.* Genes Chromosomes Cancer, 2005. **42**(4): p. 372-83.
522. Zhong, D., et al., *Homozygous deletion of SMAD4 in breast cancer cell lines and invasive ductal carcinomas.* Cancer Biol Ther, 2006. **5**(6): p. 601-7.
523. Onwuegbusi, B.A., et al., *Impaired transforming growth factor beta signalling in Barrett's carcinogenesis due to frequent SMAD4 inactivation.* Gut, 2006. **55**(6): p. 764-74.
524. Lim, S.K. and F.M. Hoffmann, *Smad4 cooperates with lymphoid enhancer-binding factor 1/T cell-specific factor to increase c-myc expression in the absence of TGF-beta signaling.* Proc Natl Acad Sci U S A, 2006. **103**(49): p. 18580-5.
525. de Caestecker, M.P., E. Piek, and A.B. Roberts, *Role of transforming growth factor-beta signaling in cancer.* J Natl Cancer Inst, 2000. **92**(17): p. 1388-402.
526. Torquati, A., et al., *RUNX3 inhibits cell proliferation and induces apoptosis by reinstating transforming growth factor beta responsiveness in esophageal adenocarcinoma cells.* Surgery, 2004. **136**(2): p. 310-6.
527. von Rahden, B.H., et al., *Overexpression of TGF-beta1 in esophageal (Barrett's) adenocarcinoma is associated with advanced stage of disease and poor prognosis.* Mol Carcinog, 2006. **45**(10): p. 786-94.
528. Thiery, J.P., et al., *Epithelial-mesenchymal transitions in development and disease.* Cell, 2009. **139**(5): p. 871-90.

529. Yang, J. and R.A. Weinberg, *Epithelial-mesenchymal transition: at the crossroads of development and tumor metastasis.* Dev Cell, 2008. **14**(6): p. 818-29.
530. Burdsal, C.A., C.H. Damsky, and R.A. Pedersen, *The role of E-cadherin and integrins in mesoderm differentiation and migration at the mammalian primitive streak.* Development, 1993. **118**(3): p. 829-44.
531. Kasai, H., et al., *TGF-beta1 induces human alveolar epithelial to mesenchymal cell transition (EMT).* Respir Res, 2005. **6**: p. 56.
532. Wells, A., *Tumor invasion: role of growth factor-induced cell motility.* Adv Cancer Res, 2000. **78**: p. 31-101.
533. Wells, A., C. Yates, and C.R. Shepard, *E-cadherin as an indicator of mesenchymal to epithelial reverting transitions during the metastatic seeding of disseminated carcinomas.* Clin Exp Metastasis, 2008. **25**(6): p. 621-8.
534. Kowalski, P.J., M.A. Rubin, and C.G. Kleer, *E-cadherin expression in primary carcinomas of the breast and its distant metastases.* Breast Cancer Res, 2003. **5**(6): p. R217-22.
535. Yates, C.C., et al., *Co-culturing human prostate carcinoma cells with hepatocytes leads to increased expression of E-cadherin.* Br J Cancer, 2007. **96**(8): p. 1246-52.
536. Janda, E., et al., *Raf plus TGFbeta-dependent EMT is initiated by endocytosis and lysosomal degradation of E-cadherin.* Oncogene, 2006. **25**(54): p. 7117-30.
537. Vince, J.E., et al., *TWEAK-FN14 signaling induces lysosomal degradation of a cIAP1-TRAF2 complex to sensitize tumor cells to TNFalpha.* J Cell Biol, 2008. **182**(1): p. 171-84.
538. Wileman, T., C. Pettey, and C. Terhorst, *Recognition for degradation in the endoplasmic reticulum and lysosomes prevents the transport of single TCR beta and CD3 delta subunits of the T-cell antigen receptor to the surface of cells.* Int Immunol, 1990. **2**(8): p. 743-54.
539. Mizushima, N., *Autophagy: process and function.* Genes Dev, 2007. **21**(22): p. 2861-73.
540. Gajewska, M., B. Gajkowska, and T. Motyl, *Apoptosis and autophagy induced by TGF-B1 in bovine mammary epithelial BME-UV1 cells.* J Physiol Pharmacol, 2005. **56 Suppl 3**: p. 143-57.
541. Kiyono, K., et al., *Autophagy is activated by TGF-beta and potentiates TGF-beta-mediated growth inhibition in human hepatocellular carcinoma cells.* Cancer Res, 2009. **69**(23): p. 8844-52.
542. Seglen, P.O. and P.B. Gordon, *3-Methyladenine: specific inhibitor of autophagic/lysosomal protein degradation in isolated rat hepatocytes.* Proc Natl Acad Sci U S A, 1982. **79**(6): p. 1889-92.
543. Wijnhoven, B.P., W.N. Dinjens, and M. Pignatelli, *E-cadherin-catenin cell-cell adhesion complex and human cancer.* Br J Surg, 2000. **87**(8): p. 992-1005.
544. Hu, P.P., et al., *The MEK pathway is required for stimulation of p21(WAF1/CIP1) by transforming growth factor-beta.* J Biol Chem, 1999. **274**(50): p. 35381-7.
545. Attisano, L. and J.L. Wrana, *Signal transduction by the TGF-beta superfamily.* Science, 2002. **296**(5573): p. 1646-7.

546. Derynck, R. and Y.E. Zhang, *Smad-dependent and Smad-independent pathways in TGF-beta family signalling.* Nature, 2003. **425**(6958): p. 577-84.
547. Kirshner, J., et al., *Inhibition of transforming growth factor-beta1 signaling attenuates ataxia telangiectasia mutated activity in response to genotoxic stress.* Cancer Res, 2006. **66**(22): p. 10861-9.
548. Chen, L.H., et al., *Autophagy inhibition enhances apoptosis triggered by BO-1051, an N-mustard derivative, and involves the ATM signaling pathway.* Biochem Pharmacol. **81**(5): p. 594-605.
549. Alexander, A., et al., *ATM signals to TSC2 in the cytoplasm to regulate mTORC1 in response to ROS.* Proc Natl Acad Sci U S A. **107**(9): p. 4153-8.
550. Kim, E.L., et al., *Chloroquine activates the p53 pathway and induces apoptosis in human glioma cells.* Neuro Oncol. **12**(4): p. 389-400.
551. Loehberg, C.R., et al., *Ataxia telangiectasia-mutated and p53 are potential mediators of chloroquine-induced resistance to mammary carcinogenesis.* Cancer Res, 2007. **67**(24): p. 12026-33.
552. Maclean, K.H., et al., *Targeting lysosomal degradation induces p53-dependent cell death and prevents cancer in mouse models of lymphomagenesis.* J Clin Invest, 2008. **118**(1): p. 79-88.
553. Schneider, J.G., et al., *ATM-dependent suppression of stress signaling reduces vascular disease in metabolic syndrome.* Cell Metab, 2006. **4**(5): p. 377-89.
554. Kim, R.H., et al., *SNIP1 inhibits NF-kappa B signaling by competing for its binding to the C/H1 domain of CBP/p300 transcriptional co-activators.* J Biol Chem, 2001. **276**(49): p. 46297-304.
555. Roche, K.C., et al., *The FHA domain protein SNIP1 is a regulator of the cell cycle and cyclin D1 expression.* Oncogene, 2004. **23**(50): p. 8185-95.
556. Fujii, M., et al., *SNIP1 is a candidate modifier of the transcriptional activity of c-Myc on E box-dependent target genes.* Mol Cell, 2006. **24**(5): p. 771-83.
557. Vanderlaag, K.E., et al., *Anterior gradient-2 plays a critical role in breast cancer cell growth and survival by modulating cyclin D1, estrogen receptor-alpha and survivin.* Breast Cancer Res. **12**(3): p. R32.
558. Cusick, M.E., et al., *Interactome: gateway into systems biology.* Hum Mol Genet, 2005. **14 Spec No. 2**: p. R171-81.
559. Bonetta, L., *Protein-protein interactions: Interactome under construction.* Nature. **468**(7325): p. 851-4.
560. Oliver, S., *Guilt-by-association goes global.* Nature, 2000. **403**(6770): p. 601-3.
561. Valencia, A. and F. Pazos, *Computational methods for the prediction of protein interactions.* Curr Opin Struct Biol, 2002. **12**(3): p. 368-73.
562. Fields, S. and O. Song, *A novel genetic system to detect protein-protein interactions.* Nature, 1989. **340**(6230): p. 245-6.
563. Uetz, P., et al., *A comprehensive analysis of protein-protein interactions in Saccharomyces cerevisiae.* Nature, 2000. **403**(6770): p. 623-7.
564. Ito, T., et al., *A comprehensive two-hybrid analysis to explore the yeast protein interactome.* Proc Natl Acad Sci U S A, 2001. **98**(8): p. 4569-74.
565. Figeys, D., *Combining different 'omics' technologies to map and validate protein-protein interactions in humans.* Brief Funct Genomic Proteomic, 2004. **2**(4): p. 357-65.

566. Giot, L., et al., *A protein interaction map of Drosophila melanogaster.* Science, 2003. **302**(5651): p. 1727-36.
567. Stelzl, U., et al., *A human protein-protein interaction network: a resource for annotating the proteome.* Cell, 2005. **122**(6): p. 957-68.
568. Chen, C.H., et al., *Bidirectional signals transduced by DAPK-ERK interaction promote the apoptotic effect of DAPK.* Embo J, 2005. **24**(2): p. 294-304.
569. Ponting, C.P. and R.R. Russell, *The natural history of protein domains.* Annu Rev Biophys Biomol Struct, 2002. **31**: p. 45-71.
570. Semenza, J.C., et al., *ERD2, a yeast gene required for the receptor-mediated retrieval of luminal ER proteins from the secretory pathway.* Cell, 1990. **61**(7): p. 1349-57.
571. Neduva, V. and R.B. Russell, *Linear motifs: evolutionary interaction switches.* FEBS Lett, 2005. **579**(15): p. 3342-5.
572. Lee, C., et al., *Structural basis for the recognition of the E2F transactivation domain by the retinoblastoma tumor suppressor.* Genes Dev, 2002. **16**(24): p. 3199-212.
573. Stomski, F.C., et al., *Identification of a 14-3-3 binding sequence in the common beta chain of the granulocyte-macrophage colony-stimulating factor (GM-CSF), interleukin-3 (IL-3), and IL-5 receptors that is serine-phosphorylated by GM-CSF.* Blood, 1999. **94**(6): p. 1933-42.
574. Stevens, C. and T.R. Hupp, *Novel insights into DAPK autophagic signalling using peptide aptamer combinatorial protein-interaction screens.* Autophagy, 2008. **4**(4): p. 531-3.
575. Stevens, C., et al., *Peptide combinatorial libraries identify TSC2 as a death-associated protein kinase (DAPK) death domain-binding protein and reveal a stimulatory role for DAPK in mTORC1 signaling.* J Biol Chem, 2009. **284**(1): p. 334-44.
576. Murray, E., *manuscript in preparation.* 2011.
577. Narayan, V., et al., *A multiprotein binding interface in an intrinsically disordered region of the tumor suppressor protein interferon regulatory factor-1.* J Biol Chem. **286**(16): p. 14291-303.
578. Rowe, M.L., et al., *Solution structure and dynamics of ERp18, a small endoplasmic reticulum resident oxidoreductase.* Biochemistry, 2009. **48**(21): p. 4596-606.
579. Jessop, C.E., et al., *Protein disulphide isomerase family members show distinct substrate specificity: P5 is targeted to BiP client proteins.* J Cell Sci, 2009. **122**(Pt 23): p. 4287-95.
580. Cheung, K.L., et al., *Alternative oligomeric states of the yeast Rvb1/Rvb2 complex induced by histidine tags.* J Mol Biol. **404**(3): p. 478-92.
581. Gorynia, S., et al., *Cloning, expression, purification, crystallization and preliminary X-ray analysis of the human RuvBL1-RuvBL2 complex.* Acta Crystallogr Sect F Struct Biol Cryst Commun, 2008. **64**(Pt 9): p. 840-6.
582. Koegl, M. and P. Uetz, *Improving yeast two-hybrid screening systems.* Brief Funct Genomic Proteomic, 2007. **6**(4): p. 302-12.
583. Acevedo, L.G., et al., *Analysis of the mechanisms mediating tumor-specific changes in gene expression in human liver tumors.* Cancer Res, 2008. **68**(8): p. 2641-51.

584. Blanc, J.F., et al., *Proteomic analysis of differentially expressed proteins in hepatocellular carcinoma developed in patients with chronic viral hepatitis C.* Proteomics, 2005. **5**(14): p. 3778-89.
585. Haurie, V., et al., *Adenosine triphosphatase pontin is overexpressed in hepatocellular carcinoma and coregulated with reptin through a new posttranslational mechanism.* Hepatology, 2009. **50**(6): p. 1871-83.
586. Iizuka, N., et al., *Involvement of c-myc-regulated genes in hepatocellular carcinoma related to genotype-C hepatitis B virus.* J Cancer Res Clin Oncol, 2006. **132**(7): p. 473-81.
587. Rousseau, B., et al., *Overexpression and role of the ATPase and putative DNA helicase RuvB-like 2 in human hepatocellular carcinoma.* Hepatology, 2007. **46**(4): p. 1108-18.
588. Li, W., et al., *Reptin is required for the transcription of telomerase reverse transcriptase and over-expressed in gastric cancer.* Mol Cancer. **9**: p. 132.
589. Dyrskjot, L., et al., *Gene expression in the urinary bladder: a common carcinoma in situ gene expression signature exists disregarding histopathological classification.* Cancer Res, 2004. **64**(11): p. 4040-8.
590. Sanchez-Carbayo, M., et al., *Defining molecular profiles of poor outcome in patients with invasive bladder cancer using oligonucleotide microarrays.* J Clin Oncol, 2006. **24**(5): p. 778-89.
591. Basso, K., et al., *Reverse engineering of regulatory networks in human B cells.* Nat Genet, 2005. **37**(4): p. 382-90.
592. Xie, X., et al., *RUVBL2, a novel AS160-binding protein, regulates insulin-stimulated GLUT4 translocation.* Cell Res, 2009. **19**(9): p. 1090-7.
593. Diella, F., et al., *Understanding eukaryotic linear motifs and their role in cell signaling and regulation.* Front Biosci, 2008. **13**: p. 6580-603.
594. Gould, C.M., et al., *ELM: the status of the 2010 eukaryotic linear motif resource.* Nucleic Acids Res. **38**(Database issue): p. D167-80.
595. Dosztanyi, Z., B. Meszaros, and I. Simon, *ANCHOR: web server for predicting protein binding regions in disordered proteins.* Bioinformatics, 2009. **25**(20): p. 2745-6.
596. Fornerod, M., et al., *CRM1 is an export receptor for leucine-rich nuclear export signals.* Cell, 1997. **90**(6): p. 1051-60.
597. la Cour, T., et al., *Analysis and prediction of leucine-rich nuclear export signals.* Protein Eng Des Sel, 2004. **17**(6): p. 527-36.
598. Wen, W., et al., *Identification of a signal for rapid export of proteins from the nucleus.* Cell, 1995. **82**(3): p. 463-73.
599. Holbrook, J.A., et al., *Nonsense-mediated decay approaches the clinic.* Nat Genet, 2004. **36**(8): p. 801-8.
600. Wiese, C., et al., *Disparate requirements for the Walker A and B ATPase motifs of human RAD51D in homologous recombination.* Nucleic Acids Res, 2006. **34**(9): p. 2833-43.
601. Kurash, J.K., et al., *Methylation of p53 by Set7/9 mediates p53 acetylation and activity in vivo.* Mol Cell, 2008. **29**(3): p. 392-400.
602. Baek, S.H., et al., *Exchange of N-CoR corepressor and Tip60 coactivator complexes links gene expression by NF-kappaB and beta-amyloid precursor protein.* Cell, 2002. **110**(1): p. 55-67.

603. Saraste, M., P.R. Sibbald, and A. Wittinghofer, *The P-loop--a common motif in ATP- and GTP-binding proteins.* Trends Biochem Sci, 1990. **15**(11): p. 430-4.
604. Vetter, I.R. and A. Wittinghofer, *Nucleoside triphosphate-binding proteins: different scaffolds to achieve phosphoryl transfer.* Q Rev Biophys, 1999. **32**(1): p. 1-56.
605. Walker, J.E., et al., *Distantly related sequences in the alpha- and beta-subunits of ATP synthase, myosin, kinases and other ATP-requiring enzymes and a common nucleotide binding fold.* Embo J, 1982. **1**(8): p. 945-51.
606. Leipe, D.D., E.V. Koonin, and L. Aravind, *Evolution and classification of P-loop kinases and related proteins.* J Mol Biol, 2003. **333**(4): p. 781-815.
607. Iyer, L.M., et al., *Evolutionary history and higher order classification of AAA+ ATPases.* J Struct Biol, 2004. **146**(1-2): p. 11-31.
608. Neuwald, A.F., et al., *AAA+: A class of chaperone-like ATPases associated with the assembly, operation, and disassembly of protein complexes.* Genome Res, 1999. **9**(1): p. 27-43.
609. Ogura, T. and A.J. Wilkinson, *AAA+ superfamily ATPases: common structure--diverse function.* Genes Cells, 2001. **6**(7): p. 575-97.
610. Babst, M., et al., *The Vps4p AAA ATPase regulates membrane association of a Vps protein complex required for normal endosome function.* Embo J, 1998. **17**(11): p. 2982-93.
611. Matveeva, E.A., P. He, and S.W. Whiteheart, *N-Ethylmaleimide-sensitive fusion protein contains high and low affinity ATP-binding sites that are functionally distinct.* J Biol Chem, 1997. **272**(42): p. 26413-8.
612. Story, R.M. and T.A. Steitz, *Structure of the recA protein-ADP complex.* Nature, 1992. **355**(6358): p. 374-6.
613. Weibezahn, J., et al., *Characterization of a trap mutant of the AAA+ chaperone ClpB.* J Biol Chem, 2003. **278**(35): p. 32608-17.
614. Guenther, B., et al., *Crystal structure of the delta' subunit of the clamp-loader complex of E. coli DNA polymerase III.* Cell, 1997. **91**(3): p. 335-45.
615. Karata, K., et al., *Dissecting the role of a conserved motif (the second region of homology) in the AAA family of ATPases. Site-directed mutagenesis of the ATP-dependent protease FtsH.* J Biol Chem, 1999. **274**(37): p. 26225-32.
616. Ogura, T., S.W. Whiteheart, and A.J. Wilkinson, *Conserved arginine residues implicated in ATP hydrolysis, nucleotide-sensing, and inter-subunit interactions in AAA and AAA+ ATPases.* J Struct Biol, 2004. **146**(1-2): p. 106-12.
617. Maegley, K.A., S.J. Admiraal, and D. Herschlag, *Ras-catalyzed hydrolysis of GTP: a new perspective from model studies.* Proc Natl Acad Sci U S A, 1996. **93**(16): p. 8160-6.
618. Tucker, P.A. and L. Sallai, *The AAA+ superfamily--a myriad of motions.* Curr Opin Struct Biol, 2007. **17**(6): p. 641-52.
619. Muller, B., I.R. Tsaneva, and S.C. West, *Branch migration of Holliday junctions promoted by the Escherichia coli RuvA and RuvB proteins. II. Interaction of RuvB with DNA.* J Biol Chem, 1993. **268**(23): p. 17185-9.
620. Muller, B., I.R. Tsaneva, and S.C. West, *Branch migration of Holliday junctions promoted by the Escherichia coli RuvA and RuvB proteins. I.*

Comparison of RuvAB- and RuvB-mediated reactions. J Biol Chem, 1993. **268**(23): p. 17179-84.
621. Tsaneva, I.R., B. Muller, and S.C. West, *RuvA and RuvB proteins of Escherichia coli exhibit DNA helicase activity in vitro.* Proc Natl Acad Sci U S A, 1993. **90**(4): p. 1315-9.
622. Qiu, X.B., et al., *An eukaryotic RuvB-like protein (RUVBL1) essential for growth.* J Biol Chem, 1998. **273**(43): p. 27786-93.
623. Matias, P.M., et al., *Crystal structure of the human AAA+ protein RuvBL1.* J Biol Chem, 2006. **281**(50): p. 38918-29.
624. Rottbauer, W., et al., *Reptin and pontin antagonistically regulate heart growth in zebrafish embryos.* Cell, 2002. **111**(5): p. 661-72.
625. Makino, Y., et al., *A rat RuvB-like protein, TIP49a, is a germ cell-enriched novel DNA helicase.* J Biol Chem, 1999. **274**(22): p. 15329-35.
626. Papin, C., et al., *3'- to 5' DNA unwinding by TIP49b proteins.* Febs J. **277**(12): p. 2705-14.
627. Gribun, A., et al., *Yeast Rvb1 and Rvb2 are ATP-dependent DNA helicases that form a heterohexameric complex.* J Mol Biol, 2008. **376**(5): p. 1320-33.
628. Choi, J., K. Heo, and W. An, *Cooperative action of TIP48 and TIP49 in H2A.Z exchange catalyzed by acetylation of nucleosomal H2A.* Nucleic Acids Res, 2009. **37**(18): p. 5993-6007.
629. Puri, T., et al., *Dodecameric structure and ATPase activity of the human TIP48/TIP49 complex.* J Mol Biol, 2007. **366**(1): p. 179-92.
630. Lim, C.R., et al., *The Saccharomyces cerevisiae RuvB-like protein, Tih2p, is required for cell cycle progression and RNA polymerase II-directed transcription.* J Biol Chem, 2000. **275**(29): p. 22409-17.
631. Kakugawa, S., et al., *RuvB-like protein 2 is a suppressor of influenza A virus polymerases.* J Virol, 2009. **83**(13): p. 6429-34.
632. Hanson, P.I. and S.W. Whiteheart, *AAA+ proteins: have engine, will work.* Nat Rev Mol Cell Biol, 2005. **6**(7): p. 519-29.
633. Makino, Y., et al., *TIP49, homologous to the bacterial DNA helicase RuvB, acts as an autoantigen in human.* Biochem Biophys Res Commun, 1998. **245**(3): p. 819-23.
634. Gohshi, T., et al., *Molecular cloning of mouse p47, a second group mammalian RuvB DNA helicase-like protein: homology with those from human and Saccharomyces cerevisiae.* J Biochem, 1999. **125**(5): p. 939-46.
635. Kikuchi, N., et al., *Molecular shape and ATP binding activity of rat p50, a putative mammalian homologue of RuvB DNA helicase.* J Biochem, 1999. **125**(3): p. 487-94.
636. Boulon, S., et al., *HSP90 and its R2TP/Prefoldin-like cochaperone are involved in the cytoplasmic assembly of RNA polymerase II.* Mol Cell. **39**(6): p. 912-24.
637. Torreira, E., et al., *Architecture of the pontin/reptin complex, essential in the assembly of several macromolecular complexes.* Structure, 2008. **16**(10): p. 1511-20.
638. Niewiarowski, A., et al., *Oligomeric assembly and interactions within the human RuvB-like RuvBL1 and RuvBL2 complexes.* Biochem J. **429**(1): p. 113-25.

639. Soderman, K. and P. Reichard, *A nitrocellulose filter binding assay for ribonucleotide reductase.* Anal Biochem, 1986. **152**(1): p. 89-93.
640. Sauer, R.T., et al., *Sculpting the proteome with AAA(+) proteases and disassembly machines.* Cell, 2004. **119**(1): p. 9-18.
641. Vale, R.D., *AAA proteins. Lords of the ring.* J Cell Biol, 2000. **150**(1): p. F13-9.
642. Martin, A., T.A. Baker, and R.T. Sauer, *Rebuilt AAA + motors reveal operating principles for ATP-fuelled machines.* Nature, 2005. **437**(7062): p. 1115-20.
643. Garnier, C., et al., *Binding of ATP to heat shock protein 90: evidence for an ATP-binding site in the C-terminal domain.* J Biol Chem, 2002. **277**(14): p. 12208-14.
644. Horwitz, A.A., et al., *ATP-induced structural transitions in PAN, the proteasome-regulatory ATPase complex in Archaea.* J Biol Chem, 2007. **282**(31): p. 22921-9.
645. Smith, D.M., et al., *ATP binds to proteasomal ATPases in pairs with distinct functional effects, implying an ordered reaction cycle.* Cell. **144**(4): p. 526-38.
646. Hersch, G.L., et al., *Asymmetric interactions of ATP with the AAA+ ClpX6 unfoldase: allosteric control of a protein machine.* Cell, 2005. **121**(7): p. 1017-27.
647. Singleton, M.R., et al., *Crystal structure of T7 gene 4 ring helicase indicates a mechanism for sequential hydrolysis of nucleotides.* Cell, 2000. **101**(6): p. 589-600.
648. Marrione, P.E. and M.M. Cox, *Allosteric effects of RuvA protein, ATP, and DNA on RuvB protein-mediated ATP hydrolysis.* Biochemistry, 1996. **35**(34): p. 11228-38.
649. Jeruzalmi, D., et al., *Mechanism of processivity clamp opening by the delta subunit wrench of the clamp loader complex of E. coli DNA polymerase III.* Cell, 2001. **106**(4): p. 417-28.
650. Schwacha, A. and S.P. Bell, *Interactions between two catalytically distinct MCM subgroups are essential for coordinated ATP hydrolysis and DNA replication.* Mol Cell, 2001. **8**(5): p. 1093-104.
651. Bujalowski, W. and M.M. Klonowska, *Negative cooperativity in the binding of nucleotides to Escherichia coli replicative helicase DnaB protein. Interactions with fluorescent nucleotide analogs.* Biochemistry, 1993. **32**(22): p. 5888-900.
652. Dong, F., E.P. Gogol, and P.H. von Hippel, *The phage T4-coded DNA replication helicase (gp41) forms a hexamer upon activation by nucleoside triphosphate.* J Biol Chem, 1995. **270**(13): p. 7462-73.
653. Geiselmann, J. and P.H. von Hippel, *Functional interactions of ligand cofactors with Escherichia coli transcription termination factor rho. I. Binding of ATP.* Protein Sci, 1992. **1**(7): p. 850-60.
654. Hishida, T., et al., *Direct evidence that a conserved arginine in RuvB AAA+ ATPase acts as an allosteric effector for the ATPase activity of the adjacent subunit in a hexamer.* Proc Natl Acad Sci U S A, 2004. **101**(26): p. 9573-7.
655. Putnam, C.D., et al., *Structure and mechanism of the RuvB Holliday junction branch migration motor.* J Mol Biol, 2001. **311**(2): p. 297-310.

656. Yamada, K., et al., *Crystal structure of the RuvA-RuvB complex: a structural basis for the Holliday junction migrating motor machinery.* Mol Cell, 2002. **10**(3): p. 671-81.
657. Orelle, C., et al., *The conserved glutamate residue adjacent to the Walker-B motif is the catalytic base for ATP hydrolysis in the ATP-binding cassette transporter BmrA.* J Biol Chem, 2003. **278**(47): p. 47002-8.
658. Schmidt, M., et al., *Nucleotide binding activity of SecA homodimer is conformationally regulated by temperature and altered by prlD and azi mutations.* J Biol Chem, 2000. **275**(20): p. 15440-8.
659. Mogk, A., et al., *Roles of individual domains and conserved motifs of the AAA+ chaperone ClpB in oligomerization, ATP hydrolysis, and chaperone activity.* J Biol Chem, 2003. **278**(20): p. 17615-24.
660. Lavin, M.F. and N. Gueven, *The complexity of p53 stabilization and activation.* Cell Death Differ, 2006. **13**(6): p. 941-50.
661. el-Deiry, W.S., et al., *Definition of a consensus binding site for p53.* Nat Genet, 1992. **1**(1): p. 45-9.
662. Harms, K., S. Nozell, and X. Chen, *The common and distinct target genes of the p53 family transcription factors.* Cell Mol Life Sci, 2004. **61**(7-8): p. 822-42.
663. Miyashita, T. and J.C. Reed, *Tumor suppressor p53 is a direct transcriptional activator of the human bax gene.* Cell, 1995. **80**(2): p. 293-9.
664. Petitjean, A., et al., *TP53 mutations in human cancers: functional selection and impact on cancer prognosis and outcomes.* Oncogene, 2007. **26**(15): p. 2157-65.
665. Kamada, R., et al., *Cancer-associated p53 tetramerization domain mutants: quantitative analysis reveals a low threshold for tumor suppressor inactivation.* J Biol Chem. **286**(1): p. 252-8.
666. Kruse, J.P. and W. Gu, *Modes of p53 regulation.* Cell, 2009. **137**(4): p. 609-22.
667. Canadillas, J.M., et al., *Solution structure of p53 core domain: structural basis for its instability.* Proc Natl Acad Sci U S A, 2006. **103**(7): p. 2109-14.
668. Bullock, A.N., et al., *Thermodynamic stability of wild-type and mutant p53 core domain.* Proc Natl Acad Sci U S A, 1997. **94**(26): p. 14338-42.
669. Friedler, A., et al., *Kinetic instability of p53 core domain mutants: implications for rescue by small molecules.* J Biol Chem, 2003. **278**(26): p. 24108-12.
670. Hansen, S., T.R. Hupp, and D.P. Lane, *Allosteric regulation of the thermostability and DNA binding activity of human p53 by specific interacting proteins. CRC Cell Transformation Group.* J Biol Chem, 1996. **271**(7): p. 3917-24.
671. Delphin, C. and J. Baudier, *The protein kinase C activator, phorbol ester, cooperates with the wild-type p53 species of Ras-transformed embryo fibroblasts growth arrest.* J Biol Chem, 1994. **269**(47): p. 29579-87.
672. Hupp, T.R., et al., *Regulation of the specific DNA binding function of p53.* Cell, 1992. **71**(5): p. 875-86.
673. Chan, H.M., et al., *The p400 E1A-associated protein is a novel component of the p53 --> p21 senescence pathway.* Genes Dev, 2005. **19**(2): p. 196-201.

674. Fraser, J.A., et al., *A novel p53 phosphorylation site within the MDM2 ubiquitination signal: II. a model in which phosphorylation at SER269 induces a mutant conformation to p53.* J Biol Chem. **285**(48): p. 37773-86.
675. Walerych, D., et al., *Hsp90 chaperones wild-type p53 tumor suppressor protein.* J Biol Chem, 2004. **279**(47): p. 48836-45.
676. Legube, G., et al., *Role of the histone acetyl transferase Tip60 in the p53 pathway.* J Biol Chem, 2004. **279**(43): p. 44825-33.
677. Berns, K., et al., *A large-scale RNAi screen in human cells identifies new components of the p53 pathway.* Nature, 2004. **428**(6981): p. 431-7.
678. Gehen, S.C., et al., *hSMG-1 and ATM sequentially and independently regulate the G1 checkpoint during oxidative stress.* Oncogene, 2008. **27**(29): p. 4065-74.
679. Brumbaugh, K.M., et al., *The mRNA surveillance protein hSMG-1 functions in genotoxic stress response pathways in mammalian cells.* Mol Cell, 2004. **14**(5): p. 585-98.
680. Harper, J.W., et al., *The p21 Cdk-interacting protein Cip1 is a potent inhibitor of G1 cyclin-dependent kinases.* Cell, 1993. **75**(4): p. 805-16.
681. Lozano, G. and G.P. Zambetti, *What have animal models taught us about the p53 pathway?* J Pathol, 2005. **205**(2): p. 206-20.
682. Waldman, T., et al., *Uncoupling of S phase and mitosis induced by anticancer agents in cells lacking p21.* Nature, 1996. **381**(6584): p. 713-6.
683. Seoane, J., H.V. Le, and J. Massague, *Myc suppression of the p21(Cip1) Cdk inhibitor influences the outcome of the p53 response to DNA damage.* Nature, 2002. **419**(6908): p. 729-34.
684. Kim, E. and W. Deppert, *Transcriptional activities of mutant p53: when mutations are more than a loss.* J Cell Biochem, 2004. **93**(5): p. 878-86.
685. Brosh, R. and V. Rotter, *When mutants gain new powers: news from the mutant p53 field.* Nat Rev Cancer, 2009. **9**(10): p. 701-13.
686. Bode, A.M. and Z. Dong, *Post-translational modification of p53 in tumorigenesis.* Nat Rev Cancer, 2004. **4**(10): p. 793-805.
687. Espinosa, J.M. and B.M. Emerson, *Transcriptional regulation by p53 through intrinsic DNA/chromatin binding and site-directed cofactor recruitment.* Mol Cell, 2001. **8**(1): p. 57-69.
688. Fernandez-Fernandez, M.R., T.J. Rutherford, and A.R. Fersht, *Members of the S100 family bind p53 in two distinct ways.* Protein Sci, 2008. **17**(10): p. 1663-70.
689. Chernov, M.V., et al., *Regulation of ubiquitination and degradation of p53 in unstressed cells through C-terminal phosphorylation.* J Biol Chem, 2001. **276**(34): p. 31819-24.
690. Feng, L., et al., *Functional analysis of the roles of posttranslational modifications at the p53 C terminus in regulating p53 stability and activity.* Mol Cell Biol, 2005. **25**(13): p. 5389-95.
691. Weinberg, R.L., et al., *Regulation of DNA binding of p53 by its C-terminal domain.* J Mol Biol, 2004. **342**(3): p. 801-11.
692. Bayle, J.H., B. Elenbaas, and A.J. Levine, *The carboxyl-terminal domain of the p53 protein regulates sequence-specific DNA binding through its nonspecific nucleic acid-binding activity.* Proc Natl Acad Sci U S A, 1995. **92**(12): p. 5729-33.

693. Allen, W.J., et al., *Modeling the relationship between the p53 C-terminal domain and its binding partners using molecular dynamics.* J Phys Chem B. **114**(41): p. 13201-13.
694. Baudier, J., et al., *Characterization of the tumor suppressor protein p53 as a protein kinase C substrate and a S100b-binding protein.* Proc Natl Acad Sci U S A, 1992. **89**(23): p. 11627-31.
695. Chen, H., et al., *Binding to intracellular targets of the metastasis-inducing protein, S100A4 (p9Ka).* Biochem Biophys Res Commun, 2001. **286**(5): p. 1212-7.
696. Grigorian, M., et al., *Tumor suppressor p53 protein is a new target for the metastasis-associated Mts1/S100A4 protein: functional consequences of their interaction.* J Biol Chem, 2001. **276**(25): p. 22699-708.
697. Schafer, B.W. and C.W. Heizmann, *The S100 family of EF-hand calcium-binding proteins: functions and pathology.* Trends Biochem Sci, 1996. **21**(4): p. 134-40.
698. Lloyd, B.H., et al., *Human S100A4 (p9Ka) induces the metastatic phenotype upon benign tumour cells.* Oncogene, 1998. **17**(4): p. 465-73.
699. Ebralidze, A., et al., *Isolation and characterization of a gene specifically expressed in different metastatic cells and whose deduced gene product has a high degree of homology to a Ca2+-binding protein family.* Genes Dev, 1989. **3**(7): p. 1086-93.
700. van Dieck, J., et al., *Modulation of the oligomerization state of p53 by differential binding of proteins of the S100 family to p53 monomers and tetramers.* J Biol Chem, 2009. **284**(20): p. 13804-11.
701. Scotto, C., et al., *Calcium and S100B regulation of p53-dependent cell growth arrest and apoptosis.* Mol Cell Biol, 1998. **18**(7): p. 4272-81.
702. Lin, J., et al., *Inhibition of p53 transcriptional activity by the S100B calcium-binding protein.* J Biol Chem, 2001. **276**(37): p. 35037-41.
703. Friedler, A., et al., *A peptide that binds and stabilizes p53 core domain: chaperone strategy for rescue of oncogenic mutants.* Proc Natl Acad Sci U S A, 2002. **99**(2): p. 937-42.

Appendix 1

p53 interactome and bibliography (date of discovery in brackets)

5.8S RNA (1991-1992) [13-14]
14-3-3 (1998) [74-75]
Abl1 (2000) [104]
AIMP2 (2008) [288]
ANKRD2 (2004) [204]
ANKRD11 (2008) [295]
ANXA3 (2005) *[224]*
Apak (2009) [314]
APTX (2004) [203]
ARA54-associated AR inhibitor (2010) [345]
ARF (1998) [73]
ARIH2 (2005) *[224]*
ARL3 (2005) *[224]*
ASCOM (2009) [310]
ASSP1 (2001) [139]
ASSP2 (2001) [139]
ATF3 (2002) [154]
ATM (1998) [80]
AURKA (2002) [167]
AXIN1 (2004) [213]
BACH1 (2008) [296]
BAF53 (2007) [273]
Bak1 (2004) [202]
BARD1 (2001) [146]
BCL-2 (2005) [214]
BCL-XL (2005) [214]
BCR (2005) *[224]*
BID (2009) [335]
BLM (2001) [134-135]
BRCA1 [69-70]
BRCA2 (1998) [76]
BRD7 (2010) [346]
BTBD2 (2005) *[224]*
ß-TrCP1 (2009) [305]
BZLF1 (1994) [31]
CABIN1 (2009) [328]
CABLES2 (2003) [197]
CARM1 (2004) [207]
CARPs (2007) [254]
Casein kinase II (1992) [17]
CCDC106 (2005) *[224]*, [227]
CCL18 (2005) *[224]*
CCNG1 (2003) [178]

CCT5 (2005) *[224]*
Cdc14 (2000) [103]
CDC42 (2005) *[224]*
CDK5 (2007) [266]
CDK7 (1998) [77]
CDK9 (2006) [237]
CDKN2AIP (2007) [258]
CDKN2C (2005) *[224]*
C/EBPß (2006) [232]
CEBPZ (2003) [184]
CHD8 (2008) [298]
CHEK1 (2002) [158]
CHIP (2007) [269]
COP1 (2004) [205]
COPS5 (2001) [128]
COX-2 (2005) [217-218]
COX17 (2005) *[224]*
CREBB (1997) [58]
CREBBP (2000) [106]
CRYAB (2007) [256]
CSE1L (2007) [268]
CSNK1A (2008) [294]
CUL4A (2006) [240]
CUL7 (2006) [239]
CUL9 (2003) [177]
Cyclin A (2000) [107]
DAPK-1 (2007) [261]
DAXX (2004) [212]
DCTN2 (2000) [110]
DLEU1 (2005) *[224]*
DMC1 (2004) [206]
DNA (1991) [15]
DNA helicase (1994) [36]
DNA-PK (2001) [145]
DNMT3A (2005) [227]
DP1 (1995) [43]
DTL (2006) [240]
DVL2 (2005) *[226]*
DYNC1 (2000) [110]
E1B (1982) [1]
E2F1(1995) [43]
E4F1 (2000) [102]
E6 protein of HPV-16 and -18 (1990) [11]
EBNA-5 (1993) [28]
EBNA3C (2009) [316]
EBV/C3d receptor (CR2) (1989) [18]
ECD (2006) [238]
EEF2 (2003) [191]

EGR1 (2001) [125]
EIF2S2 (2005) *[224]*
ELL (1999) [92]
EP300 (1997) [57]
EP400 (1997) [51]
EPHA3 (2004) [211]
ERα (1997) [64]
ERCC3 (1995) [41]
ERCC2 (1995) [41]
ERH (2005) *[224]*
ERK1/2 (2000) [114]
ETHE1 (2007) [257]
ETS-1 (2001) [141-142]
EWS-Fli1 (2010) [343]
F-actin (1999) [84-85]
FBXO11 (2007) [251]
FBXO42 (2009) [319]
Ferritin (2009) [331]
FGF1 (2009) [333]
FLIP (2008) [286]
FOXO3A (2009) [325]
FXYD6 (2005) *[224]*
G3BP2 (2007) [262]
GATA-1 (2009) [318]
GCN5 (2008) [280]
GNL3 (2002) [173]
GPS2 (2001) [137]
GRP 78 (2009) [339]
GSK3 (2002) [163]
GSTM4 (2005) *[224]*
GTSE1 (2003) [189]
HABP4 (2006) [234]
HAUSP (2002) [159]
hBub1 (2009) [307]
HBx antigen (1993) [26, 38]
HDAC2 (2010) [348]
HECW1 (2008) [285]
hHR23 (2003) [198]
HHV-6 (1997) [53]
HHV-6 U14 (2005) [230]
HIF-1α (1998) [71]
HIPK1 (2003) [185]
HIPK2 (2002) [149-150]
HIV-1 Tat protein (1995) [37]
HLA-A2.1 (1994) [32]
HMGA1 (2006) [243]
HMGB1 (2001) [124]
HNF4a (2002) [152]

hnRNP K (2008) [283]
HNRNPUL1 (2005) [219]
Hsc70 (1984) [4-6]
HSF1 (2009) [311]
HSF3 (2001) [126]
HSPA9 (2006) [241-242]
Hsp40 (1986) [6]
Hsp68 (1987) [7]
Hsp70 (1987) [7]
Hsp72/73 (1988) [8-9]
HSPB1 (2005) *[224]*
hTEP1 (1999) [101]
httex1p (2000) [105]
iASPP (2003) [175]
ICP0 (2003) [192]
IFI 16 [116]
IκBα (2002) [155]
IKBm (2003) [196]
ING1b (2002) [168]
ING4 (2003) [187]
ING5 (2003) [187]
K-bZIP (2000) [118]
KDM1 (2007) [270]
KLF5 (2006) [235]
LAMA4 (2005) *[224]*
LANA2 (2001) [119]
LMO3 (2010) [341]
MAD2L1BP (2005) *[224]*
MAGEB18 (2005) *[226]*
MAGED2 (2007) [274]
MAP1B (2008) [289]
MAP3K8 (2009) [308]
MAPK8 (1997) [65]
MAPK9 (1997) [65]
MAPK10 (1997) [65]
MAPKAPK-2 (2002) [153]
MBP1 (1999) [90]
MDC1 (2003) [194, 267]
MDH1 (2009) [312]
MDM2 (1992) [16]
MDMX (1996) [49]
MED1 (1997) [66-67]
MKRN1 (2009) [317]
MNAT1 (1997) [62-63]
Mot-2 (1998) [78]
MPHOSPH6 (2005) *[224]*
MSL2 (2009) [303]
MSX1 (2005) [215]

MT (2006) [233]
MTA1 (2003) [193, 337]
MTA2 [115]
mtDNA polymerase gamma (2005) [228]
MUC1 (2005) [216]
MYC (2005) [229]
MYST2 (2008) [276]
MYST3 (2009) [302]
NCL (2002) [165]
Necdin (1999) [93]
Nef (2002) [156]
NF-Y (2006) [244]
NIR (2005) [231]
NOL3 (2007) [275]
Notch1 (2007) [259]
NP (2005) *[224]*
NPM (2002) [164]
NQO1 (2003) [182]
NQO2 (2007) [264]
NR3C1 (2000) [113]
NR4A1 (2006) [249]
NR4A2 (2009) [326]
NS3 (1998) [79]
NS5A (2001) [120]
NTHL1 (2004) [210]
NUB1 (2010) [340]
NUMB (2008) [277]
NUPR1 (2008) [290]
OTUD5 (2009) [324]
P33ING1 (1998) [68]
p34cdc2 kinase/cyclin B1(1990) [12]
P40 (2001) [123]
P42 and p38 (hot spot mt p53) (1994) [34]
p53 (1988) [10]
PAD4 (2010) [348]
PADI4 (2008) [291]
PAFAH1B3 (2005) *[224]*
PARK7 (2008) [278]
PARP-1(1997) [60]
PAX6 (2010) [344]
PBK (2007) [263]
PCAF (1999) [81]
PCDHA4 (2005) *[224]*
PCNA (2006) [240]
peptidyl-prolyl cis/trans isomerase cyclophilin 18 [332]
PHB (2003) [195]
PIAS1 (2001) [91]
PIAS2 (2002) [157]

PIASy (2001) [130]
Pin1 (2002) [169-170]
Pirh2 (2003) [183]
PKC (1997) [54]
PKR (1999) [86]
PLAGL1 (2001) [127]
PLK1 (2004) [208]
PLK3 (2001) [143]
PML (2000) [111-112]
POLA1 (2002) [160]
POU4F1 (1999) [88-89]
POU4F2 (2006) [248]
PPA1 (2005) *[224]*
PPID (1998) [48] (mutant p53)
PPP2R5C (2007) [253]
PRPK (2001) [147]
PRKRIR (2002) [174]
PRMT1 (2004) [207]
PRMT5 (2008) [297]
Pseudomonas aeruginosa azurin (2005) [221]
PSMD11 (2005) *[224]*
PSME3 (2008) [279]
PTEN (2003) [180]
PTGS2 [138]
PTK2 (2005) [222]
PTK2B (2010) [334]
PTTG1 (2002) [171]
RAB4A (2005) [224] (yeast two hybrid)
RAD9 (2007) [260]
Rad51 (1996) [44-45]
RAD54 (2003) [46]
RBBP6 (1997) [52]
Ref-1 (1999) [98]
Rep78 (1999) [95]
RFC1 (2003) [176]
RFWD3 (2010) [347]
RPA (1993) [29-30]
RPS3 (2009) [329]
RRM2 (2003) [181]
RRM2B (2003) [181]
S100A1 (2009) [299]
S100A2 (2005) [223]
S100A4 (2001) [136]
S100A6 (2008) [300-301]
S100A11 (2008) [300]
S100b (1992) [19]
SAT1 (2005) *[224]*
SERPINB9 (2005) *[224]*

SETD2 (2008) [293]
Sin3a (1999) [97]
SIRT1 (2001) [140]
SIVA1 (2009) [330-331]
SMA3 (2005) *[224]*
SMAD2 (2009) mutant p53) [309]
SMAR1 (2003) [179]
SMARCA4 (2002) [162]
SMARCB1 (2002) [162]
SMARCD1 (2008) [282]
SMN1 (2001) [148]
SNAI2 (2009) [313]
SNRPN (2005) *[224]*
SOCS1 (2009) [338]
SOX4 (2009) [306]
SPI1 (2008) [281]
SSBP1 (2009) [304]
STAT1 (2004) [199]
STIP1 (1986) [6]
STK11 (2001) [129]
Striamin (1999) [87]
STX5 (2005) *[224]*
Spot-1 (1995) [42]
SUB1 (2004) [200]
SULT1E1 (2005) *[224]*
SUMO-1 (1999) [99-100]
SUMO-2 (2006) [245]
SUMO-3 (2006) [245]
SVH-B (2007) [272]
SYVN1 (2007) [252]
TADA2b (2008) [280]
TADA3L (2001) [144]
TAF1 (2004) [201]
TAF1B (2000) [108]
TAF3 (2008) [287]
TAF9 (2008) [280]
TAFII31 (1995) [40]
TAFII40 (1995) [39]
TAFII60 (1995) [39]
T-antigen (1979) [2, 3]
TBP (1992) [20]
TFAM (2003) [188]
TFAP2A (2002) [172]
TFIIH (1994) [35]
TFIIIB (1996) [50]
THAP8 (2005) *[224]*
THRB (1996) [46]
TIP60 (2006) [250]

TK1 (2005) *[224]*
Tmsb4x (2005) *[224]*
TOE1 (2009) [322]
Topoisomerase I (1996) [47]
Topoisomerase II (1997) [55-56]
TOPORS (1999) [94] two-hybrid assay
TP53BP1 (1994) [33]
TP53BP2 (1994) [33]
TP53INP1 (2003) [190]
Transcription factor Sp1 (SP1) (1993) [22-25] (mt p53 [25])
Transcription factor Sp3 (2005) [220]
TRIM24 (2009) [323]
TRAP80 (1999) [82]
TRRAP (2002) [166]
trkA (1997) [61]
TSG101 (2001) [122]
TTK (2009) [315]
Tubulin alpha (2000) [110]
Tubulin beta (2000) [110]
TWIST1 (2008) [284]
TXN (2009) [327]
UBE2A (2003) [186]
UBE2I (1996) [48]
UBE2N (2006) [247]
UBE3A (1993) [21]
UCHL1 (2008) [292]
UIMC1 (2009) [320]
USP10 (2010) [342]
USP11 (2009) [324]
USP39 (2009) [324]
VHL (2006) [236]
VIM (2005) [225]
vIRF (2001) [132-133]
WDR33 (2005) *[224]*
WDR48 (2009) [324]
WRN (1999) [96]
WT1 (1993) [27]
WWOX1 (2001) [121]
WWP1 (2007) [255]
WWP2 (2007) [255]
XPO1 (1999) [83]
YBX1 (2000) [117]
YY1 (2004) [209]
ZBTB2 (2009) [321]
ZBTB17 (2010) [336]
ZMIZ1 (2007) [265]
ZMIZ2 (2007) [265]
ZMYND11 (2007) [271]

ZNF24 (2005) *[224]*
ZNF148 (2001) [131]
ZNF346 (2006) [246]

1. Sarnow, P., et al., *Adenovirus E1b-58kd tumor antigen and SV40 large tumor antigen are physically associated with the same 54 kd cellular protein in transformed cells.* Cell, 1982. **28**(2): p. 387-94.
2. Lane, D.P. and L.V. Crawford, *T antigen is bound to a host protein in SV40-transformed cells.* Nature, 1979. **278**(5701): p. 261-3.
3. Linzer, D.I. and A.J. Levine, *Characterization of a 54K dalton cellular SV40 tumor antigen present in SV40-transformed cells and uninfected embryonal carcinoma cells.* Cell, 1979. **17**(1): p. 43-52.
4. Pinhasi, O. and M. Oren, *Expression of the mouse p53 cellular tumor antigen in monkey cells.* Mol Cell Biol, 1984. **4**(10): p. 2180-6.
5. Hinds, P.W., et al., *Immunological evidence for the association of p53 with a heat shock protein, hsc70, in p53-plus-ras-transformed cell lines.* Mol Cell Biol, 1987. **7**(8): p. 2863-9.
6. Pinhasi-Kimhi, O., et al., *Specific interaction between the p53 cellular tumour antigen and major heat shock proteins.* Nature, 1986. **320**(6058): p. 182-4.
7. Sturzbecher, H.W., et al., *Mutant p53 proteins bind hsp 72/73 cellular heat shock-related proteins in SV40-transformed monkey cells.* Oncogene, 1987. **1**(2): p. 201-11.
8. Ehrhart, J.C., et al., *Specific interaction between a subset of the p53 protein family and heat shock proteins hsp72/hsc73 in a human osteosarcoma cell line.* Oncogene, 1988. **3**(5): p. 595-603.
9. Matsumoto, H., et al., *p53 proteins accumulated by heat stress associate with heat shock proteins HSP72/HSC73 in human glioblastoma cell lines.* Cancer Lett, 1994. **87**(1): p. 39-46.
10. Kraiss, S., et al., *Oligomerization of oncoprotein p53.* J Virol, 1988. **62**(12): p. 4737-44.
11. Werness, B.A., A.J. Levine, and P.M. Howley, *Association of human papillomavirus types 16 and 18 E6 proteins with p53.* Science, 1990. **248**(4951): p. 76-9.
12. Sturzbecher, H.W., et al., *p53 interacts with p34cdc2 in mammalian cells: implications for cell cycle control and oncogenesis.* Oncogene, 1990. **5**(6): p. 795-81.
13. Samad, A. and R.B. Carroll, *The tumor suppressor p53 is bound to RNA by a stable covalent linkage.* Mol Cell Biol, 1991. **11**(3): p. 1598-606.
14. Fontoura, B.M., et al., *p53 is covalently linked to 5.8S rRNA.* Mol Cell Biol, 1992. **12**(11): p. 5145-51.
15. Kern, S.E., et al., *Identification of p53 as a sequence-specific DNA-binding protein.* Science, 1991. **252**(5013): p. 1708-11.

16. Momand, J., et al., *The mdm-2 oncogene product forms a complex with the p53 protein and inhibits p53-mediated transactivation.* Cell, 1992. **69**(7): p. 1237-45.
17. Filhol, O., et al., *Casein kinase II and the tumor suppressor protein P53 associate in a molecular complex that is negatively regulated upon P53 phosphorylation.* J Biol Chem, 1992. **267**(29): p. 20577-83.
18. Barel, M., et al., *Epstein-Barr virus/complement fragment C3d receptor (CR2) reacts with p53, a cellular antioncogene-encoded membrane phosphoprotein: detection by polyclonal anti-idiotypic anti-CR2 antibodies.* Proc Natl Acad Sci U S A, 1989. **86**(24): p. 10054-8.
19. Baudier, J., et al., *Characterization of the tumor suppressor protein p53 as a protein kinase C substrate and a S100b-binding protein.* Proc Natl Acad Sci U S A, 1992. **89**(23): p. 11627-31.
20. Seto, E., et al., *Wild-type p53 binds to the TATA-binding protein and represses transcription.* Proc Natl Acad Sci U S A, 1992. **89**(24): p. 12028-32.
21. Huibregtse, J.M., M. Scheffner, and P.M. Howley, *Cloning and expression of the cDNA for E6-AP, a protein that mediates the interaction of the human papillomavirus E6 oncoprotein with p53.* Mol Cell Biol, 1993. **13**(2): p. 775-84.
22. Borellini, F. and R.I. Glazer, *Induction of Sp1-p53 DNA-binding heterocomplexes during granulocyte/macrophage colony-stimulating factor-dependent proliferation in human erythroleukemia cell line TF-1.* J Biol Chem, 1993. **268**(11): p. 7923-8.
23. Torgeman, A., et al., *Sp1-p53 heterocomplex mediates activation of HTLV-I long terminal repeat by 12-O-tetradecanoylphorbol-13-acetate that is antagonized by protein kinase C.* Virology, 2001. **281**(1): p. 10-20.
24. Koutsodontis, G., et al., *Sp1 plays a critical role in the transcriptional activation of the human cyclin-dependent kinase inhibitor p21(WAF1/Cip1) gene by the p53 tumor suppressor protein.* J Biol Chem, 2001. **276**(31): p. 29116-25.
25. Chicas, A., P. Molina, and J. Bargonetti, *Mutant p53 forms a complex with Sp1 on HIV-LTR DNA.* Biochem Biophys Res Commun, 2000. **279**(2): p. 383-90.
26. Feitelson, M.A., et al., *Hepatitis B x antigen and p53 are associated in vitro and in liver tissues from patients with primary hepatocellular carcinoma.* Oncogene, 1993. **8**(5): p. 1109-17.
27. Maheswaran, S., et al., *Physical and functional interaction between WT1 and p53 proteins.* Proc Natl Acad Sci U S A, 1993. **90**(11): p. 5100-4.
28. Szekely, L., et al., *EBNA-5, an Epstein-Barr virus-encoded nuclear antigen, binds to the retinoblastoma and p53 proteins.* Proc Natl Acad Sci U S A, 1993. **90**(12): p. 5455-9.
29. Li, R. and M.R. Botchan, *The acidic transcriptional activation domains of VP16 and p53 bind the cellular replication protein A and stimulate in vitro BPV-1 DNA replication.* Cell, 1993. **73**(6): p. 1207-21.
30. Dutta, A., et al., *Inhibition of DNA replication factor RPA by p53.* Nature, 1993. **365**(6441): p. 79-82.

31. Zhang, Q., D. Gutsch, and S. Kenney, *Functional and physical interaction between p53 and BZLF1: implications for Epstein-Barr virus latency.* Mol Cell Biol, 1994. **14**(3): p. 1929-38.
32. Stuber, G., et al., *Identification of wild-type and mutant p53 peptides binding to HLA-A2 assessed by a peptide loading-deficient cell line assay and a novel major histocompatibility complex class I peptide binding assay.* Eur J Immunol, 1994. **24**(3): p. 765-8.
33. Iwabuchi, K., et al., *Two cellular proteins that bind to wild-type but not mutant p53.* Proc Natl Acad Sci U S A, 1994. **91**(13): p. 6098-102.
34. Chen, Y., P.L. Chen, and W.H. Lee, *Hot-spot p53 mutants interact specifically with two cellular proteins during progression of the cell cycle.* Mol Cell Biol, 1994. **14**(10): p. 6764-72.
35. Xiao, H., et al., *Binding of basal transcription factor TFIIH to the acidic activation domains of VP16 and p53.* Mol Cell Biol, 1994. **14**(10): p. 7013-24.
36. Sakurai, T., et al., *Anti-oncogene product p53 binds DNA helicase.* Exp Cell Res, 1994. **215**(1): p. 57-62.
37. Longo, F., et al., *A novel approach to protein-protein interaction: complex formation between the p53 tumor suppressor and the HIV Tat proteins.* Biochem Biophys Res Commun, 1995. **206**(1): p. 326-34.
38. Truant, R., et al., *Direct interaction of the hepatitis B virus HBx protein with p53 leads to inhibition by HBx of p53 response element-directed transactivation.* J Virol, 1995. **69**(3): p. 1851-9.
39. Thut, C.J., et al., *p53 transcriptional activation mediated by coactivators TAFII40 and TAFII60.* Science, 1995. **267**(5194): p. 100-4.
40. Lu, H. and A.J. Levine, *Human TAFII31 protein is a transcriptional coactivator of the p53 protein.* Proc Natl Acad Sci U S A, 1995. **92**(11): p. 5154-8.
41. Wang, X.W., et al., *p53 modulation of TFIIH-associated nucleotide excision repair activity.* Nat Genet, 1995. **10**(2): p. 188-95.
42. Elkind, N.B., N. Goldfinger, and V. Rotter, *Spot-1, a novel NLS-binding protein that interacts with p53 through a domain encoded by p(CA)n repeats.* Oncogene, 1995. **11**(5): p. 841-51.
43. O'Connor, D.J., et al., *Physical and functional interactions between p53 and cell cycle co-operating transcription factors, E2F1 and DP1.* Embo J, 1995. **14**(24): p. 6184-92.
44. Sturzbecher, H.W., et al., *p53 is linked directly to homologous recombination processes via RAD51/RecA protein interaction.* Embo J, 1996. **15**(8): p. 1992-2002.
45. Linke, S.P., et al., *p53 interacts with hRAD51 and hRAD54, and directly modulates homologous recombination.* Cancer Res, 2003. **63**(10): p. 2596-605.
46. Yap, N., C.L. Yu, and S.Y. Cheng, *Modulation of the transcriptional activity of thyroid hormone receptors by the tumor suppressor p53.* Proc Natl Acad Sci U S A, 1996. **93**(9): p. 4273-7.
47. Gobert, C., et al., *Modulation of DNA topoisomerase I activity by p53.* Biochemistry, 1996. **35**(18): p. 5778-86.

48. Shen, Z., et al., *Associations of UBE2I with RAD52, UBL1, p53, and RAD51 proteins in a yeast two-hybrid system.* Genomics, 1996. **37**(2): p. 183-6.
49. Shvarts, A., et al., *MDMX: a novel p53-binding protein with some functional properties of MDM2.* Embo J, 1996. **15**(19): p. 5349-57.
50. Chesnokov, I., et al., *p53 inhibits RNA polymerase III-directed transcription in a promoter-dependent manner.* Mol Cell Biol, 1996. **16**(12): p. 7084-8.
51. Lill, N.L., et al., *p300 family members associate with the carboxyl terminus of simian virus 40 large tumor antigen.* J Virol, 1997. **71**(1): p. 129-37.
52. Simons, A., et al., *PACT: cloning and characterization of a cellular p53 binding protein that interacts with Rb.* Oncogene, 1997. **14**(2): p. 145-55.
53. Kashanchi, F., et al., *Human herpesvirus 6 (HHV-6) ORF-1 transactivating gene exhibits malignant transforming activity and its protein binds to p53.* Oncogene, 1997. **14**(3): p. 359-67.
54. Delphin, C., et al., *The in vitro phosphorylation of p53 by calcium-dependent protein kinase C--characterization of a protein-kinase-C-binding site on p53.* Eur J Biochem, 1997. **245**(3): p. 684-92.
55. Yuwen, H., et al., *Binding of wild-type p53 by topoisomerase II and overexpression of topoisomerase II in human hepatocellular carcinoma.* Biochem Biophys Res Commun, 1997. **234**(1): p. 194-7.
56. Cowell, I.G., et al., *Human topoisomerase IIalpha and IIbeta interact with the C-terminal region of p53.* Exp Cell Res, 2000. **255**(1): p. 86-94.
57. Avantaggiati, M.L., et al., *Recruitment of p300/CBP in p53-dependent signal pathways.* Cell, 1997. **89**(7): p. 1175-84.
58. Gu, W., X.L. Shi, and R.G. Roeder, *Synergistic activation of transcription by CBP and p53.* Nature, 1997. **387**(6635): p. 819-23.
59. Lill, N.L., et al., *Binding and modulation of p53 by p300/CBP coactivators.* Nature, 1997. **387**(6635): p. 823-7.
60. Vaziri, H., et al., *ATM-dependent telomere loss in aging human diploid fibroblasts and DNA damage lead to the post-translational activation of p53 protein involving poly(ADP-ribose) polymerase.* Embo J, 1997. **16**(19): p. 6018-33.
61. Montano, X., *P53 associates with trk tyrosine kinase.* Oncogene, 1997. **15**(3): p. 245-56.
62. Lu, H., et al., *The CDK7-cycH-p36 complex of transcription factor IIH phosphorylates p53, enhancing its sequence-specific DNA binding activity in vitro.* Mol Cell Biol, 1997. **17**(10): p. 5923-34.
63. Ko, L.J., et al., *p53 is phosphorylated by CDK7-cyclin H in a p36MAT1-dependent manner.* Mol Cell Biol, 1997. **17**(12): p. 7220-9.
64. Yu, C.L., et al., *The tumor suppressor p53 is a negative regulator of estrogen receptor signaling pathways.* Biochem Biophys Res Commun, 1997. **239**(2): p. 617-20.
65. Hu, M.C., W.R. Qiu, and Y.P. Wang, *JNK1, JNK2 and JNK3 are p53 N-terminal serine 34 kinases.* Oncogene, 1997. **15**(19): p. 2277-87.
66. Drane, P., et al., *Identification of RB18A, a 205 kDa new p53 regulatory protein which shares antigenic and functional properties with p53.* Oncogene, 1997. **15**(25): p. 3013-24.

67. Frade, R., M. Balbo, and M. Barel, *RB18A, whose gene is localized on chromosome 17q12-q21.1, regulates in vivo p53 transactivating activity.* Cancer Res, 2000. **60**(23): p. 6585-9.
68. Garkavtsev, I., et al., *The candidate tumour suppressor p33ING1 cooperates with p53 in cell growth control.* Nature, 1998. **391**(6664): p. 295-8.
69. Ouchi, T., et al., *BRCA1 regulates p53-dependent gene expression.* Proc Natl Acad Sci U S A, 1998. **95**(5): p. 2302-6.
70. Zhang, H., et al., *BRCA1 physically associates with p53 and stimulates its transcriptional activity.* Oncogene, 1998. **16**(13): p. 1713-21.
71. An, W.G., et al., *Stabilization of wild-type p53 by hypoxia-inducible factor 1alpha.* Nature, 1998. **392**(6674): p. 405-8.
72. Whitesell, L., et al., *The physical association of multiple molecular chaperone proteins with mutant p53 is altered by geldanamycin, an hsp90-binding agent.* Mol Cell Biol, 1998. **18**(3): p. 1517-24.
73. Kamijo, T., et al., *Functional and physical interactions of the ARF tumor suppressor with p53 and Mdm2.* Proc Natl Acad Sci U S A, 1998. **95**(14): p. 8292-7.
74. Waterman, M.J., et al., *ATM-dependent activation of p53 involves dephosphorylation and association with 14-3-3 proteins.* Nat Genet, 1998. **19**(2): p. 175-8.
75. Stavridi, E.S., et al., *Substitutions that compromise the ionizing radiation-induced association of p53 with 14-3-3 proteins also compromise the ability of p53 to induce cell cycle arrest.* Cancer Res, 2001. **61**(19): p. 7030-3.
76. Marmorstein, L.Y., T. Ouchi, and S.A. Aaronson, *The BRCA2 gene product functionally interacts with p53 and RAD51.* Proc Natl Acad Sci U S A, 1998. **95**(23): p. 13869-74.
77. Schneider, E., M. Montenarh, and P. Wagner, *Regulation of CAK kinase activity by p53.* Oncogene, 1998. **17**(21): p. 2733-41.
78. Wadhwa, R., et al., *Inactivation of tumor suppressor p53 by mot-2, a hsp70 family member.* J Biol Chem, 1998. **273**(45): p. 29586-91.
79. Ishido, S. and H. Hotta, *Complex formation of the nonstructural protein 3 of hepatitis C virus with the p53 tumor suppressor.* FEBS Lett, 1998. **438**(3): p. 258-62.
80. Khanna, K.K., et al., *ATM associates with and phosphorylates p53: mapping the region of interaction.* Nat Genet, 1998. **20**(4): p. 398-400.
81. Liu, L., et al., *p53 sites acetylated in vitro by PCAF and p300 are acetylated in vivo in response to DNA damage.* Mol Cell Biol, 1999. **19**(2): p. 1202-9.
82. Ito, M., et al., *Identity between TRAP and SMCC complexes indicates novel pathways for the function of nuclear receptors and diverse mammalian activators.* Mol Cell, 1999. **3**(3): p. 361-70.
83. Stommel, J.M., et al., *A leucine-rich nuclear export signal in the p53 tetramerization domain: regulation of subcellular localization and p53 activity by NES masking.* Embo J, 1999. **18**(6): p. 1660-72.
84. Metcalfe, S., et al., *Wild-type p53 protein shows calcium-dependent binding to F-actin.* Oncogene, 1999. **18**(14): p. 2351-5.
85. Okorokov, A.L., et al., *The interaction of p53 with the nuclear matrix is mediated by F-actin and modulated by DNA damage.* Oncogene, 2002. **21**(3): p. 356-67.

86. Cuddihy, A.R., et al., *The double-stranded RNA activated protein kinase PKR physically associates with the tumor suppressor p53 protein and phosphorylates human p53 on serine 392 in vitro.* Oncogene, 1999. **18**(17): p. 2690-702.
87. Wadhwa, R., et al., *Cloning and characterization of a novel gene, striamin, that interacts with the tumor suppressor protein p53.* J Biol Chem, 1999. **274**(21): p. 14948-55.
88. Budhram-Mahadeo, V., et al., *p53 suppresses the activation of the Bcl-2 promoter by the Brn-3a POU family transcription factor.* J Biol Chem, 1999. **274**(21): p. 15237-44.
89. Hudson, C.D., et al., *Brn-3a transcription factor blocks p53-mediated activation of proapoptotic target genes Noxa and Bax in vitro and in vivo to determine cell fate.* J Biol Chem, 2005. **280**(12): p. 11851-8.
90. Gallagher, W.M., et al., *MBP1: a novel mutant p53-specific protein partner with oncogenic properties.* Oncogene, 1999. **18**(24): p. 3608-16.
91. Kahyo, T., T. Nishida, and H. Yasuda, *Involvement of PIAS1 in the sumoylation of tumor suppressor p53.* Mol Cell, 2001. **8**(3): p. 713-8.
92. Shinobu, N., et al., *Physical interaction and functional antagonism between the RNA polymerase II elongation factor ELL and p53.* J Biol Chem, 1999. **274**(24): p. 17003-10.
93. Taniura, H., K. Matsumoto, and K. Yoshikawa, *Physical and functional interactions of neuronal growth suppressor necdin with p53.* J Biol Chem, 1999. **274**(23): p. 16242-8.
94. Zhou, R., H. Wen, and S.Z. Ao, *Identification of a novel gene encoding a p53-associated protein.* Gene, 1999. **235**(1-2): p. 93-101.
95. Batchu, R.B., et al., *Interaction of adeno-associated virus Rep78 with p53: implications in growth inhibition.* Cancer Res, 1999. **59**(15): p. 3592-5.
96. Blander, G., et al., *Physical and functional interaction between p53 and the Werner's syndrome protein.* J Biol Chem, 1999. **274**(41): p. 29463-9.
97. Murphy, M., et al., *Transcriptional repression by wild-type p53 utilizes histone deacetylases, mediated by interaction with mSin3a.* Genes Dev, 1999. **13**(19): p. 2490-501.
98. Gaiddon, C., N.C. Moorthy, and C. Prives, *Ref-1 regulates the transactivation and pro-apoptotic functions of p53 in vivo.* Embo J, 1999. **18**(20): p. 5609-21.
99. Rodriguez, M.S., et al., *SUMO-1 modification activates the transcriptional response of p53.* Embo J, 1999. **18**(22): p. 6455-61.
100. Gostissa, M., et al., *Activation of p53 by conjugation to the ubiquitin-like protein SUMO-1.* Embo J, 1999. **18**(22): p. 6462-71.
101. Li, H., et al., *Molecular interactions between telomerase and the tumor suppressor protein p53 in vitro.* Oncogene, 1999. **18**(48): p. 6785-94.
102. Sandy, P., et al., *p53 is involved in the p120E4F-mediated growth arrest.* Oncogene, 2000. **19**(2): p. 188-99.
103. Li, L., M. Ljungman, and J.E. Dixon, *The human Cdc14 phosphatases interact with and dephosphorylate the tumor suppressor protein p53.* J Biol Chem, 2000. **275**(4): p. 2410-4.
104. Nie, Y., et al., *Stimulation of p53 DNA binding by c-Abl requires the p53 C terminus and tetramerization.* Mol Cell Biol, 2000. **20**(3): p. 741-8.

105. Steffan, J.S., et al., *The Huntington's disease protein interacts with p53 and CREB-binding protein and represses transcription.* Proc Natl Acad Sci U S A, 2000. **97**(12): p. 6763-8.
106. Giebler, H.A., I. Lemasson, and J.K. Nyborg, *p53 recruitment of CREB binding protein mediated through phosphorylated CREB: a novel pathway of tumor suppressor regulation.* Mol Cell Biol, 2000. **20**(13): p. 4849-58.
107. Luciani, M.G., et al., *The C-terminal regulatory domain of p53 contains a functional docking site for cyclin A.* J Mol Biol, 2000. **300**(3): p. 503-18.
108. Zhai, W. and L. Comai, *Repression of RNA polymerase I transcription by the tumor suppressor p53.* Mol Cell Biol, 2000. **20**(16): p. 5930-8.
109. Strano, S., et al., *Physical and functional interaction between p53 mutants and different isoforms of p73.* J Biol Chem, 2000. **275**(38): p. 29503-12.
110. Giannakakou, P., et al., *p53 is associated with cellular microtubules and is transported to the nucleus by dynein.* Nat Cell Biol, 2000. **2**(10): p. 709-17.
111. Guo, A., et al., *The function of PML in p53-dependent apoptosis.* Nat Cell Biol, 2000. **2**(10): p. 730-6.
112. Fogal, V., et al., *Regulation of p53 activity in nuclear bodies by a specific PML isoform.* Embo J, 2000. **19**(22): p. 6185-95.
113. Sengupta, S., et al., *Negative cross-talk between p53 and the glucocorticoid receptor and its role in neuroblastoma cells.* Embo J, 2000. **19**(22): p. 6051-64.
114. Persons, D.L., E.M. Yazlovitskaya, and J.C. Pelling, *Effect of extracellular signal-regulated kinase on p53 accumulation in response to cisplatin.* J Biol Chem, 2000. **275**(46): p. 35778-85.
115. Luo, J., et al., *Deacetylation of p53 modulates its effect on cell growth and apoptosis.* Nature, 2000. **408**(6810): p. 377-81.
116. Johnstone, R.W., et al., *Functional interaction between p53 and the interferon-inducible nucleoprotein IFI 16.* Oncogene, 2000. **19**(52): p. 6033-42.
117. Okamoto, T., et al., *Direct interaction of p53 with the Y-box binding protein, YB-1: a mechanism for regulation of human gene expression.* Oncogene, 2000. **19**(54): p. 6194-202.
118. Park, J., et al., *The K-bZIP protein from Kaposi's sarcoma-associated herpesvirus interacts with p53 and represses its transcriptional activity.* J Virol, 2000. **74**(24): p. 11977-82.
119. Rivas, C., et al., *Kaposi's sarcoma-associated herpesvirus LANA2 is a B-cell-specific latent viral protein that inhibits p53.* J Virol, 2001. **75**(1): p. 429-38.
120. Majumder, M., et al., *Hepatitis C virus NS5A physically associates with p53 and regulates p21/waf1 gene expression in a p53-dependent manner.* J Virol, 2001. **75**(3): p. 1401-7.
121. Chang, N.S., et al., *Hyaluronidase induction of a WW domain-containing oxidoreductase that enhances tumor necrosis factor cytotoxicity.* J Biol Chem, 2001. **276**(5): p. 3361-70.
122. Li, L., et al., *A TSG101/MDM2 regulatory loop modulates MDM2 degradation and MDM2/p53 feedback control.* Proc Natl Acad Sci U S A, 2001. **98**(4): p. 1619-24.

123. Ratovitski, E.A., et al., *p53 associates with and targets Delta Np63 into a protein degradation pathway.* Proc Natl Acad Sci U S A, 2001. **98**(4): p. 1817-22.
124. Imamura, T., et al., *Interaction with p53 enhances binding of cisplatin-modified DNA by high mobility group 1 protein.* J Biol Chem, 2001. **276**(10): p. 7534-40.
125. Liu, J., et al., *Physical interaction between p53 and primary response gene Egr-1.* Int J Oncol, 2001. **18**(4): p. 863-70.
126. Tanikawa, J., et al., *Regulation of c-Myb activity by tumor suppressor p53.* Blood Cells Mol Dis, 2001. **27**(2): p. 479-82.
127. Huang, S.M., A.H. Schonthal, and M.R. Stallcup, *Enhancement of p53-dependent gene activation by the transcriptional coactivator Zac1.* Oncogene, 2001. **20**(17): p. 2134-43.
128. Bech-Otschir, D., et al., *COP9 signalosome-specific phosphorylation targets p53 to degradation by the ubiquitin system.* Embo J, 2001. **20**(7): p. 1630-9.
129. Karuman, P., et al., *The Peutz-Jegher gene product LKB1 is a mediator of p53-dependent cell death.* Mol Cell, 2001. **7**(6): p. 1307-19.
130. Nelson, V., G.E. Davis, and S.A. Maxwell, *A putative protein inhibitor of activated STAT (PIASy) interacts with p53 and inhibits p53-mediated transactivation but not apoptosis.* Apoptosis, 2001. **6**(3): p. 221-34.
131. Bai, L. and J.L. Merchant, *ZBP-89 promotes growth arrest through stabilization of p53.* Mol Cell Biol, 2001. **21**(14): p. 4670-83.
132. Seo, T., et al., *Viral interferon regulatory factor 1 of Kaposi's sarcoma-associated herpesvirus binds to p53 and represses p53-dependent transcription and apoptosis.* J Virol, 2001. **75**(13): p. 6193-8.
133. Nakamura, H., et al., *Inhibition of p53 tumor suppressor by viral interferon regulatory factor.* J Virol, 2001. **75**(16): p. 7572-82.
134. Wang, X.W., et al., *Functional interaction of p53 and BLM DNA helicase in apoptosis.* J Biol Chem, 2001. **276**(35): p. 32948-55.
135. Garkavtsev, I.V., et al., *The Bloom syndrome protein interacts and cooperates with p53 in regulation of transcription and cell growth control.* Oncogene, 2001. **20**(57): p. 8276-80.
136. Chen, H., et al., *Binding to intracellular targets of the metastasis-inducing protein, S100A4 (p9Ka).* Biochem Biophys Res Commun, 2001. **286**(5): p. 1212-7.
137. Peng, Y.C., et al., *AMF1 (GPS2) modulates p53 transactivation.* Mol Cell Biol, 2001. **21**(17): p. 5913-24.
138. King, J.G., Jr. and K. Khalili, *Inhibition of human brain tumor cell growth by the anti-inflammatory drug, flurbiprofen.* Oncogene, 2001. **20**(47): p. 6864-70.
139. Samuels-Lev, Y., et al., *ASPP proteins specifically stimulate the apoptotic function of p53.* Mol Cell, 2001. **8**(4): p. 781-94.
140. Vaziri, H., et al., *hSIR2(SIRT1) functions as an NAD-dependent p53 deacetylase.* Cell, 2001. **107**(2): p. 149-59.
141. Sampath, J., et al., *Mutant p53 cooperates with ETS and selectively up-regulates human MDR1 not MRP1.* J Biol Chem, 2001. **276**(42): p. 39359-67.

142. Kim, E., et al., *Tumor suppressor p53 inhibits transcriptional activation of invasion gene thromboxane synthase mediated by the proto-oncogenic factor ets-1.* Oncogene, 2003. **22**(49): p. 7716-27.
143. Xie, S., et al., *Plk3 functionally links DNA damage to cell cycle arrest and apoptosis at least in part via the p53 pathway.* J Biol Chem, 2001. **276**(46): p. 43305-12.
144. Wang, T., et al., *hADA3 is required for p53 activity.* Embo J, 2001. **20**(22): p. 6404-13.
145. Achanta, G., et al., *Interaction of p53 and DNA-PK in response to nucleoside analogues: potential role as a sensor complex for DNA damage.* Cancer Res, 2001. **61**(24): p. 8723-9.
146. Irminger-Finger, I., et al., *Identification of BARD1 as mediator between proapoptotic stress and p53-dependent apoptosis.* Mol Cell, 2001. **8**(6): p. 1255-66.
147. Abe, Y., et al., *Cloning and characterization of a p53-related protein kinase expressed in interleukin-2-activated cytotoxic T-cells, epithelial tumor cell lines, and the testes.* J Biol Chem, 2001. **276**(47): p. 44003-11.
148. Young, P.J., et al., *A direct interaction between the survival motor neuron protein and p53 and its relationship to spinal muscular atrophy.* J Biol Chem, 2002. **277**(4): p. 2852-9.
149. D'Orazi, G., et al., *Homeodomain-interacting protein kinase-2 phosphorylates p53 at Ser 46 and mediates apoptosis.* Nat Cell Biol, 2002. **4**(1): p. 11-9.
150. Hofmann, T.G., et al., *Regulation of p53 activity by its interaction with homeodomain-interacting protein kinase-2.* Nat Cell Biol, 2002. **4**(1): p. 1-10.
151. Kim, E.J., J.S. Park, and S.J. Um, *Identification and characterization of HIPK2 interacting with p73 and modulating functions of the p53 family in vivo.* J Biol Chem, 2002. **277**(35): p. 32020-8.
152. Maeda, Y., et al., *Repression of hepatocyte nuclear factor 4alpha tumor suppressor p53: involvement of the ligand-binding domain and histone deacetylase activity.* Mol Endocrinol, 2002. **16**(2): p. 402-10.
153. She, Q.B., W.Y. Ma, and Z. Dong, *Role of MAP kinases in UVB-induced phosphorylation of p53 at serine 20.* Oncogene, 2002. **21**(10): p. 1580-9.
154. Yan, C., H. Wang, and D.D. Boyd, *ATF3 represses 72-kDa type IV collagenase (MMP-2) expression by antagonizing p53-dependent trans-activation of the collagenase promoter.* J Biol Chem, 2002. **277**(13): p. 10804-12.
155. Chang, N.S., *The non-ankyrin C terminus of Ikappa Balpha physically interacts with p53 in vivo and dissociates in response to apoptotic stress, hypoxia, DNA damage, and transforming growth factor-beta 1-mediated growth suppression.* J Biol Chem, 2002. **277**(12): p. 10323-31.
156. Greenway, A.L., et al., *Human immunodeficiency virus type 1 Nef binds to tumor suppressor p53 and protects cells against p53-mediated apoptosis.* J Virol, 2002. **76**(6): p. 2692-702.
157. Schmidt, D. and S. Muller, *Members of the PIAS family act as SUMO ligases for c-Jun and p53 and repress p53 activity.* Proc Natl Acad Sci U S A, 2002. **99**(5): p. 2872-7.

158. Tian, H., et al., *Radiation-induced phosphorylation of Chk1 at S345 is associated with p53-dependent cell cycle arrest pathways.* Neoplasia, 2002. **4**(2): p. 171-80.
159. Li, M., et al., *Deubiquitination of p53 by HAUSP is an important pathway for p53 stabilization.* Nature, 2002. **416**(6881): p. 648-53.
160. Melle, C. and H.P. Nasheuer, *Physical and functional interactions of the tumor suppressor protein p53 and DNA polymerase alpha-primase.* Nucleic Acids Res, 2002. **30**(7): p. 1493-9.
161. Strano, S., et al., *Physical interaction with human tumor-derived p53 mutants inhibits p63 activities.* J Biol Chem, 2002. **277**(21): p. 18817-26.
162. Lee, D., et al., *SWI/SNF complex interacts with tumor suppressor p53 and is necessary for the activation of p53-mediated transcription.* J Biol Chem, 2002. **277**(25): p. 22330-7.
163. Watcharasit, P., et al., *Direct, activating interaction between glycogen synthase kinase-3beta and p53 after DNA damage.* Proc Natl Acad Sci U S A, 2002. **99**(12): p. 7951-5.
164. Colombo, E., et al., *Nucleophosmin regulates the stability and transcriptional activity of p53.* Nat Cell Biol, 2002. **4**(7): p. 529-33.
165. Daniely, Y., D.D. Dimitrova, and J.A. Borowiec, *Stress-dependent nucleolin mobilization mediated by p53-nucleolin complex formation.* Mol Cell Biol, 2002. **22**(16): p. 6014-22.
166. Ard, P.G., et al., *Transcriptional regulation of the mdm2 oncogene by p53 requires TRRAP acetyltransferase complexes.* Mol Cell Biol, 2002. **22**(16): p. 5650-61.
167. Chen, S.S., et al., *Suppression of the STK15 oncogenic activity requires a transactivation-independent p53 function.* Embo J, 2002. **21**(17): p. 4491-9.
168. Leung, K.M., et al., *The candidate tumor suppressor ING1b can stabilize p53 by disrupting the regulation of p53 by MDM2.* Cancer Res, 2002. **62**(17): p. 4890-3.
169. Zacchi, P., et al., *The prolyl isomerase Pin1 reveals a mechanism to control p53 functions after genotoxic insults.* Nature, 2002. **419**(6909): p. 853-7.
170. Wulf, G.M., et al., *Role of Pin1 in the regulation of p53 stability and p21 transactivation, and cell cycle checkpoints in response to DNA damage.* J Biol Chem, 2002. **277**(50): p. 47976-9.
171. Bernal, J.A., et al., *Human securin interacts with p53 and modulates p53-mediated transcriptional activity and apoptosis.* Nat Genet, 2002. **32**(2): p. 306-11.
172. McPherson, L.A., A.V. Loktev, and R.J. Weigel, *Tumor suppressor activity of AP2alpha mediated through a direct interaction with p53.* J Biol Chem, 2002. **277**(47): p. 45028-33.
173. Tsai, R.Y. and R.D. McKay, *A nucleolar mechanism controlling cell proliferation in stem cells and cancer cells.* Genes Dev, 2002. **16**(23): p. 2991-3003.
174. Lin, Y., et al., *Death-associated protein 4 binds MST1 and augments MST1-induced apoptosis.* J Biol Chem, 2002. **277**(50): p. 47991-8001.
175. Bergamaschi, D., et al., *iASPP oncoprotein is a key inhibitor of p53 conserved from worm to human.* Nat Genet, 2003. **33**(2): p. 162-7.

176. Anderson, L.A. and N.D. Perkins, *Regulation of RelA (p65) function by the large subunit of replication factor C.* Mol Cell Biol, 2003. **23**(2): p. 721-32.
177. Nikolaev, A.Y., et al., *Parc: a cytoplasmic anchor for p53.* Cell, 2003. **112**(1): p. 29-40.
178. Zhao, L., et al., *Cyclin G1 has growth inhibitory activity linked to the ARF-Mdm2-p53 and pRb tumor suppressor pathways.* Mol Cancer Res, 2003. **1**(3): p. 195-206.
179. Kaul, R., et al., *Direct interaction with and activation of p53 by SMAR1 retards cell-cycle progression at G2/M phase and delays tumor growth in mice.* Int J Cancer, 2003. **103**(5): p. 606-15.
180. Freeman, D.J., et al., *PTEN tumor suppressor regulates p53 protein levels and activity through phosphatase-dependent and -independent mechanisms.* Cancer Cell, 2003. **3**(2): p. 117-30.
181. Xue, L., et al., *Wild-type p53 regulates human ribonucleotide reductase by protein-protein interaction with p53R2 as well as hRRM2 subunits.* Cancer Res, 2003. **63**(5): p. 980-6.
182. Anwar, A., et al., *Interaction of human NAD(P)H:quinone oxidoreductase 1 (NQO1) with the tumor suppressor protein p53 in cells and cell-free systems.* J Biol Chem, 2003. **278**(12): p. 10368-73.
183. Leng, R.P., et al., *Pirh2, a p53-induced ubiquitin-protein ligase, promotes p53 degradation.* Cell, 2003. **112**(6): p. 779-91.
184. Uramoto, H., et al., *Physical interaction of tumour suppressor p53/p73 with CCAAT-binding transcription factor 2 (CTF2) and differential regulation of human high-mobility group 1 (HMG1) gene expression.* Biochem J, 2003. **371**(Pt 2): p. 301-10.
185. Kondo, S., et al., *Characterization of cells and gene-targeted mice deficient for the p53-binding kinase homeodomain-interacting protein kinase 1 (HIPK1).* Proc Natl Acad Sci U S A, 2003. **100**(9): p. 5431-6.
186. Lyakhovich, A. and M.P. Shekhar, *Supramolecular complex formation between Rad6 and proteins of the p53 pathway during DNA damage-induced response.* Mol Cell Biol, 2003. **23**(7): p. 2463-75.
187. Shiseki, M., et al., *p29ING4 and p28ING5 bind to p53 and p300, and enhance p53 activity.* Cancer Res, 2003. **63**(10): p. 2373-8.
188. Yoshida, Y., et al., *P53 physically interacts with mitochondrial transcription factor A and differentially regulates binding to damaged DNA.* Cancer Res, 2003. **63**(13): p. 3729-34.
189. Monte, M., et al., *The cell cycle-regulated protein human GTSE-1 controls DNA damage-induced apoptosis by affecting p53 function.* J Biol Chem, 2003. **278**(32): p. 30356-64.
190. Tomasini, R., et al., *TP53INP1s and homeodomain-interacting protein kinase-2 (HIPK2) are partners in regulating p53 activity.* J Biol Chem, 2003. **278**(39): p. 37722-9.
191. Yin, X., et al., *Cytoplasmic complex of p53 and eEF2.* J Cell Physiol, 2003. **196**(3): p. 474-82.
192. Boutell, C. and R.D. Everett, *The herpes simplex virus type 1 (HSV-1) regulatory protein ICP0 interacts with and Ubiquitinates p53.* J Biol Chem, 2003. **278**(38): p. 36596-602.

193. Yao, Y.L. and W.M. Yang, *The metastasis-associated proteins 1 and 2 form distinct protein complexes with histone deacetylase activity.* J Biol Chem, 2003. **278**(43): p. 42560-8.
194. Xu, X. and D.F. Stern, *NFBD1/MDC1 regulates ionizing radiation-induced focus formation by DNA checkpoint signaling and repair factors.* Faseb J, 2003. **17**(13): p. 1842-8.
195. Fusaro, G., et al., *Prohibitin induces the transcriptional activity of p53 and is exported from the nucleus upon apoptotic signaling.* J Biol Chem, 2003. **278**(48): p. 47853-61.
196. Zhou, M., et al., *Transfection of a dominant-negative mutant NF-kB inhibitor (IkBm) represses p53-dependent apoptosis in acute lymphoblastic leukemia cells: interaction of IkBm and p53.* Oncogene, 2003. **22**(50): p. 8137-44.
197. Matsuoka, M., et al., *ik3-2, a relative to ik3-1/Cables, is involved in both p53-mediated and p53-independent apoptotic pathways.* Biochem Biophys Res Commun, 2003. **312**(2): p. 520-9.
198. Glockzin, S., et al., *Involvement of the DNA repair protein hHR23 in p53 degradation.* Mol Cell Biol, 2003. **23**(24): p. 8960-9.
199. Townsend, P.A., et al., *STAT-1 interacts with p53 to enhance DNA damage-induced apoptosis.* J Biol Chem, 2004. **279**(7): p. 5811-20.
200. Banerjee, S., B.R. Kumar, and T.K. Kundu, *General transcriptional coactivator PC4 activates p53 function.* Mol Cell Biol, 2004. **24**(5): p. 2052-62.
201. Li, H.H., et al., *Phosphorylation on Thr-55 by TAF1 mediates degradation of p53: a role for TAF1 in cell G1 progression.* Mol Cell, 2004. **13**(6): p. 867-78.
202. Leu, J.I., et al., *Mitochondrial p53 activates Bak and causes disruption of a Bak-Mcl1 complex.* Nat Cell Biol, 2004. **6**(5): p. 443-50.
203. Gueven, N., et al., *Aprataxin, a novel protein that protects against genotoxic stress.* Hum Mol Genet, 2004. **13**(10): p. 1081-93.
204. Kojic, S., et al., *The Ankrd2 protein, a link between the sarcomere and the nucleus in skeletal muscle.* J Mol Biol, 2004. **339**(2): p. 313-25.
205. Dornan, D., et al., *The ubiquitin ligase COP1 is a critical negative regulator of p53.* Nature, 2004. **429**(6987): p. 86-92.
206. Habu, T., et al., *p53 Protein interacts specifically with the meiosis-specific mammalian RecA-like protein DMC1 in meiosis.* Carcinogenesis, 2004. **25**(6): p. 889-93.
207. An, W., J. Kim, and R.G. Roeder, *Ordered cooperative functions of PRMT1, p300, and CARM1 in transcriptional activation by p53.* Cell, 2004. **117**(6): p. 735-48.
208. Ando, K., et al., *Polo-like kinase 1 (Plk1) inhibits p53 function by physical interaction and phosphorylation.* J Biol Chem, 2004. **279**(24): p. 25549-61.
209. Sui, G., et al., *Yin Yang 1 is a negative regulator of p53.* Cell, 2004. **117**(7): p. 859-72.
210. Oyama, M., et al., *Human NTH1 physically interacts with p53 and proliferating cell nuclear antigen.* Biochem Biophys Res Commun, 2004. **321**(1): p. 183-91.

211. Jiang, T., et al., *Bi-directional regulation between tyrosine kinase Etk/BMX and tumor suppressor p53 in response to DNA damage.* J Biol Chem, 2004. **279**(48): p. 50181-9.
212. Gostissa, M., et al., *The transcriptional repressor hDaxx potentiates p53-dependent apoptosis.* J Biol Chem, 2004. **279**(46): p. 48013-23.
213. Rui, Y., et al., *Axin stimulates p53 functions by activation of HIPK2 kinase through multimeric complex formation.* Embo J, 2004. **23**(23): p. 4583-94.
214. Park, B.S., et al., *Phospho-ser 15-p53 translocates into mitochondria and interacts with Bcl-2 and Bcl-xL in eugenol-induced apoptosis.* Apoptosis, 2005. **10**(1): p. 193-200.
215. Park, K., et al., *Homeobox Msx1 interacts with p53 tumor suppressor and inhibits tumor growth by inducing apoptosis.* Cancer Res, 2005. **65**(3): p. 749-57.
216. Wei, X., H. Xu, and D. Kufe, *Human MUC1 oncoprotein regulates p53-responsive gene transcription in the genotoxic stress response.* Cancer Cell, 2005. **7**(2): p. 167-78.
217. Choi, E.M., et al., *COX-2 regulates p53 activity and inhibits DNA damage-induced apoptosis.* Biochem Biophys Res Commun, 2005. **328**(4): p. 1107-12.
218. Corcoran, C.A., et al., *Cyclooxygenase-2 interacts with p53 and interferes with p53-dependent transcription and apoptosis.* Oncogene, 2005. **24**(9): p. 1634-40.
219. Barral, P.M., et al., *The interaction of the hnRNP family member E1B-AP5 with p53.* FEBS Lett, 2005. **579**(13): p. 2752-8.
220. Koutsodontis, G., et al., *Physical and functional interactions between members of the tumour suppressor p53 and the Sp families of transcription factors: importance for the regulation of genes involved in cell-cycle arrest and apoptosis.* Biochem J, 2005. **389**(Pt 2): p. 443-55.
221. Apiyo, D. and P. Wittung-Stafshede, *Unique complex between bacterial azurin and tumor-suppressor protein p53.* Biochem Biophys Res Commun, 2005. **332**(4): p. 965-8.
222. Golubovskaya, V.M., R. Finch, and W.G. Cance, *Direct interaction of the N-terminal domain of focal adhesion kinase with the N-terminal transactivation domain of p53.* J Biol Chem, 2005. **280**(26): p. 25008-21.
223. Mueller, A., et al., *The calcium-binding protein S100A2 interacts with p53 and modulates its transcriptional activity.* J Biol Chem, 2005. **280**(32): p. 29186-93.
224. Stelzl, U., et al., *A human protein-protein interaction network: a resource for annotating the proteome.* Cell, 2005. **122**(6): p. 957-68.
225. Yang, X., et al., *Cleavage of p53-vimentin complex enhances tumor necrosis factor-related apoptosis-inducing ligand-mediated apoptosis of rheumatoid arthritis synovial fibroblasts.* Am J Pathol, 2005. **167**(3): p. 705-19.
226. Rual, J.F., et al., *Towards a proteome-scale map of the human protein-protein interaction network.* Nature, 2005. **437**(7062): p. 1173-8.
227. Wang, Y.A., et al., *DNA methyltransferase-3a interacts with p53 and represses p53-mediated gene expression.* Cancer Biol Ther, 2005. **4**(10): p. 1138-43.

228. Achanta, G., et al., *Novel role of p53 in maintaining mitochondrial genetic stability through interaction with DNA Pol gamma.* Embo J, 2005. **24**(19): p. 3482-92.
229. Zhu, N., et al., *Transcriptional repression of the eukaryotic initiation factor 4E gene by wild type p53.* Biochem Biophys Res Commun, 2005. **335**(4): p. 1272-9.
230. Takemoto, M., et al., *Human herpesvirus 6 open reading frame U14 protein and cellular p53 interact with each other and are contained in the virion.* J Virol, 2005. **79**(20): p. 13037-46.
231. Hublitz, P., et al., *NIR is a novel INHAT repressor that modulates the transcriptional activity of p53.* Genes Dev, 2005. **19**(23): p. 2912-24.
232. Schneider-Merck, T., et al., *Physical interaction and mutual transrepression between CCAAT/enhancer-binding protein beta and the p53 tumor suppressor.* J Biol Chem, 2006. **281**(1): p. 269-78.
233. Ostrakhovitch, E.A., et al., *Interaction of metallothionein with tumor suppressor p53 protein.* FEBS Lett, 2006. **580**(5): p. 1235-8.
234. Nery, F.C., et al., *Evidence for the interaction of the regulatory protein Ki-1/57 with p53 and its interacting proteins.* Biochem Biophys Res Commun, 2006. **341**(3): p. 847-55.
235. Zhu, N., et al., *KLF5 Interacts with p53 in regulating survivin expression in acute lymphoblastic leukemia.* J Biol Chem, 2006. **281**(21): p. 14711-8.
236. Roe, J.S., et al., *p53 stabilization and transactivation by a von Hippel-Lindau protein.* Mol Cell, 2006. **22**(3): p. 395-405.
237. Claudio, P.P., et al., *Cdk9 phosphorylates p53 on serine 392 independently of CKII.* J Cell Physiol, 2006. **208**(3): p. 602-12.
238. Zhang, Y., et al., *The human orthologue of Drosophila ecdysoneless protein interacts with p53 and regulates its function.* Cancer Res, 2006. **66**(14): p. 7167-75.
239. Andrews, P., Y.J. He, and Y. Xiong, *Cytoplasmic localized ubiquitin ligase cullin 7 binds to p53 and promotes cell growth by antagonizing p53 function.* Oncogene, 2006. **25**(33): p. 4534-48.
240. Banks, D., et al., *L2DTL/CDT2 and PCNA interact with p53 and regulate p53 polyubiquitination and protein stability through MDM2 and CUL4A/DDB1 complexes.* Cell Cycle, 2006. **5**(15): p. 1719-29.
241. Ma, Z., et al., *Mortalin controls centrosome duplication via modulating centrosomal localization of p53.* Oncogene, 2006. **25**(39): p. 5377-90.
242. Walker, C., S. Bottger, and B. Low, *Mortalin-based cytoplasmic sequestration of p53 in a nonmammalian cancer model.* Am J Pathol, 2006. **168**(5): p. 1526-30.
243. Pierantoni, G.M., et al., *High Mobility Group A1 (HMGA1) proteins interact with p53 and inhibit its apoptotic activity.* Cell Death Differ, 2006. **13**(9): p. 1554-63.
244. Di Agostino, S., et al., *Gain of function of mutant p53: the mutant p53/NF-Y protein complex reveals an aberrant transcriptional mechanism of cell cycle regulation.* Cancer Cell, 2006. **10**(3): p. 191-202.
245. Li, T., et al., *Expression of SUMO-2/3 induced senescence through p53- and pRB-mediated pathways.* J Biol Chem, 2006. **281**(47): p. 36221-7.

246. Yang, M., et al., *JAZ mediates G1 cell-cycle arrest and apoptosis by positively regulating p53 transcriptional activity.* Blood, 2006. **108**(13): p. 4136-45.
247. Laine, A., et al., *Regulation of p53 localization and activity by Ubc13.* Mol Cell Biol, 2006. **26**(23): p. 8901-13.
248. Budhram-Mahadeo, V.S., et al., *Brn-3b enhances the pro-apoptotic effects of p53 but not its induction of cell cycle arrest by cooperating in trans-activation of bax expression.* Nucleic Acids Res, 2006. **34**(22): p. 6640-52.
249. Zhao, B.X., et al., *p53 mediates the negative regulation of MDM2 by orphan receptor TR3.* Embo J, 2006. **25**(24): p. 5703-15.
250. Tang, Y., et al., *Tip60-dependent acetylation of p53 modulates the decision between cell-cycle arrest and apoptosis.* Mol Cell, 2006. **24**(6): p. 827-39.
251. Abida, W.M., et al., *FBXO11 promotes the Neddylation of p53 and inhibits its transcriptional activity.* J Biol Chem, 2007. **282**(3): p. 1797-804.
252. Yamasaki, S., et al., *Cytoplasmic destruction of p53 by the endoplasmic reticulum-resident ubiquitin ligase 'Synoviolin'.* Embo J, 2007. **26**(1): p. 113-22.
253. Li, H.H., et al., *A specific PP2A regulatory subunit, B56gamma, mediates DNA damage-induced dephosphorylation of p53 at Thr55.* Embo J, 2007. **26**(2): p. 402-11.
254. Yang, W., et al., *CARPs are ubiquitin ligases that promote MDM2-independent p53 and phospho-p53ser20 degradation.* J Biol Chem, 2007. **282**(5): p. 3273-81.
255. Laine, A. and Z. Ronai, *Regulation of p53 localization and transcription by the HECT domain E3 ligase WWP1.* Oncogene, 2007. **26**(10): p. 1477-83.
256. Liu, S., et al., *Small heat shock protein alphaB-crystallin binds to p53 to sequester its translocation to mitochondria during hydrogen peroxide-induced apoptosis.* Biochem Biophys Res Commun, 2007. **354**(1): p. 109-14.
257. Higashitsuji, H., et al., *Enhanced deacetylation of p53 by the anti-apoptotic protein HSCO in association with histone deacetylase 1.* J Biol Chem, 2007. **282**(18): p. 13716-25.
258. Kamrul, H.M., R. Wadhwa, and S.C. Kaul, *CARF binds to three members (ARF, p53, and HDM2) of the p53 tumor-suppressor pathway.* Ann N Y Acad Sci, 2007. **1100**: p. 312-5.
259. Kim, S.B., et al., *Activated Notch1 interacts with p53 to inhibit its phosphorylation and transactivation.* Cell Death Differ, 2007. **14**(5): p. 982-91.
260. Ishikawa, K., et al., *Rad9 modulates the P21WAF1 pathway by direct association with p53.* BMC Mol Biol, 2007. **8**: p. 37.
261. Craig, A.L., et al., *The MDM2 ubiquitination signal in the DNA-binding domain of p53 forms a docking site for calcium calmodulin kinase superfamily members.* Mol Cell Biol, 2007. **27**(9): p. 3542-55.
262. Kim, M.M., et al., *Modulation of p53 and MDM2 activity by novel interaction with Ras-GAP binding proteins (G3BP).* Oncogene, 2007. **26**(29): p. 4209-15.
263. Nandi, A.K., et al., *Attenuation of DNA damage checkpoint by PBK, a novel mitotic kinase, involves protein-protein interaction with tumor suppressor p53.* Biochem Biophys Res Commun, 2007. **358**(1): p. 181-8.

264. Gong, X., et al., *NRH:quinone oxidoreductase 2 and NAD(P)H:quinone oxidoreductase 1 protect tumor suppressor p53 against 20s proteasomal degradation leading to stabilization and activation of p53.* Cancer Res, 2007. **67**(11): p. 5380-8.
265. Lee, J., J. Beliakoff, and Z. Sun, *The novel PIAS-like protein hZimp10 is a transcriptional co-activator of the p53 tumor suppressor.* Nucleic Acids Res, 2007. **35**(13): p. 4523-34.
266. Lee, J.H., et al., *Stabilization and activation of p53 induced by Cdk5 contributes to neuronal cell death.* J Cell Sci, 2007. **120**(Pt 13): p. 2259-71.
267. Nakanishi, M., et al., *NFBD1/MDC1 associates with p53 and regulates its function at the crossroad between cell survival and death in response to DNA damage.* J Biol Chem, 2007. **282**(31): p. 22993-3004.
268. Tanaka, T., et al., *hCAS/CSE1L associates with chromatin and regulates expression of select p53 target genes.* Cell, 2007. **130**(4): p. 638-50.
269. Tripathi, V., et al., *CHIP chaperones wild type p53 tumor suppressor protein.* J Biol Chem, 2007. **282**(39): p. 28441-54.
270. Huang, J., et al., *p53 is regulated by the lysine demethylase LSD1.* Nature, 2007. **449**(7158): p. 105-8.
271. Zhang, W., et al., *BS69 is involved in cellular senescence through the p53-p21Cip1 pathway.* EMBO Rep, 2007. **8**(10): p. 952-8.
272. Zhou, X., et al., *SVH-B interacts directly with p53 and suppresses the transcriptional activity of p53.* FEBS Lett, 2007. **581**(25): p. 4943-8.
273. Wang, M., et al., *BAF53 interacts with p53 and functions in p53-mediated p21-gene transcription.* J Biochem, 2007. **142**(5): p. 613-20.
274. Papageorgio, C., et al., *MAGED2: a novel p53-dissociator.* Int J Oncol, 2007. **31**(5): p. 1205-11.
275. Foo, R.S., et al., *Regulation of p53 tetramerization and nuclear export by ARC.* Proc Natl Acad Sci U S A, 2007. **104**(52): p. 20826-31.
276. Iizuka, M., et al., *Hbo1 Links p53-dependent stress signaling to DNA replication licensing.* Mol Cell Biol, 2008. **28**(1): p. 140-53.
277. Colaluca, I.N., et al., *NUMB controls p53 tumour suppressor activity.* Nature, 2008. **451**(7174): p. 76-80.
278. Fan, J., et al., *DJ-1 decreases Bax expression through repressing p53 transcriptional activity.* J Biol Chem, 2008. **283**(7): p. 4022-30.
279. Zhang, Z. and R. Zhang, *Proteasome activator PA28 gamma regulates p53 by enhancing its MDM2-mediated degradation.* Embo J, 2008. **27**(6): p. 852-64.
280. Gamper, A.M. and R.G. Roeder, *Multivalent binding of p53 to the STAGA complex mediates coactivator recruitment after UV damage.* Mol Cell Biol, 2008. **28**(8): p. 2517-27.
281. Tschan, M.P., et al., *PU.1 binding to the p53 family of tumor suppressors impairs their transcriptional activity.* Oncogene, 2008. **27**(24): p. 3489-93.
282. Oh, J., et al., *BAF60a interacts with p53 to recruit the SWI/SNF complex.* J Biol Chem, 2008. **283**(18): p. 11924-34.
283. Chen, Y., et al., *Arginine methylation of hnRNP K enhances p53 transcriptional activity.* FEBS Lett, 2008. **582**(12): p. 1761-5.
284. Shiota, M., et al., *Twist and p53 reciprocally regulate target genes via direct interaction.* Oncogene, 2008.

285. Li, Y., et al., *A novel HECT-type E3 ubiquitin protein ligase NEDL1 enhances the p53-mediated apoptotic cell death in its catalytic activity-independent manner.* Oncogene, 2008. **27**(26): p. 3700-9.
286. Abedini, M.R., et al., *Cisplatin induces p53-dependent FLICE-like inhibitory protein ubiquitination in ovarian cancer cells.* Cancer Res, 2008. **68**(12): p. 4511-7.
287. Bereczki, O., et al., *TATA binding protein associated factor 3 (TAF3) interacts with p53 and inhibits its function.* BMC Mol Biol, 2008. **9**: p. 57.
288. Han, J.M., et al., *AIMP2/p38, the scaffold for the multi-tRNA synthetase complex, responds to genotoxic stresses via p53.* Proc Natl Acad Sci U S A, 2008. **105**(32): p. 11206-11.
289. Lee, S.Y., et al., *Microtubule-associated protein 1B light chain (MAP1B-LC1) negatively regulates the activity of tumor suppressor p53 in neuroblastoma cells.* FEBS Lett, 2008. **582**(19): p. 2826-32.
290. Clark, D.W., et al., *NUPR1 interacts with p53, transcriptionally regulates p21 and rescues breast epithelial cells from doxorubicin-induced genotoxic stress.* Curr Cancer Drug Targets, 2008. **8**(5): p. 421-30.
291. Li, P., et al., *Regulation of p53 target gene expression by peptidylarginine deiminase 4.* Mol Cell Biol, 2008. **28**(15): p. 4745-58.
292. Yu, J., et al., *Epigenetic identification of ubiquitin carboxyl-terminal hydrolase L1 as a functional tumor suppressor and biomarker for hepatocellular carcinoma and other digestive tumors.* Hepatology, 2008. **48**(2): p. 508-18.
293. Xie, P., et al., *Histone methyltransferase protein SETD2 interacts with p53 and selectively regulates its downstream genes.* Cell Signal, 2008. **20**(9): p. 1671-8.
294. Alsheich-Bartok, O., et al., *PML enhances the regulation of p53 by CK1 in response to DNA damage.* Oncogene, 2008. **27**(26): p. 3653-61.
295. MacLaine, N.J., et al., *A central role for CK1 in catalyzing phosphorylation of the p53 transactivation domain at serine 20 after HHV-6B viral infection.* J Biol Chem, 2008. **283**(42): p. 28563-73.
296. Neilsen, P.M., et al., *Identification of ANKRD11 as a p53 coactivator.* J Cell Sci, 2008. **121**(Pt 21): p. 3541-52.
297. Dohi, Y., et al., *Bach1 inhibits oxidative stress-induced cellular senescence by impeding p53 function on chromatin.* Nat Struct Mol Biol, 2008. **15**(12): p. 1246-54.
298. Jansson, M., et al., *Arginine methylation regulates the p53 response.* Nat Cell Biol, 2008. **10**(12): p. 1431-9.
299. Nishiyama, M., et al., *CHD8 suppresses p53-mediated apoptosis through histone H1 recruitment during early embryogenesis.* Nat Cell Biol, 2009. **11**(2): p. 172-82.
300. Fernandez-Fernandez, M.R., T.J. Rutherford, and A.R. Fersht, *Members of the S100 family bind p53 in two distinct ways.* Protein Sci, 2008. **17**(10): p. 1663-70.
301. Slomnicki, L.P., B. Nawrot, and W. Lesniak, *S100A6 binds p53 and affects its activity.* Int J Biochem Cell Biol, 2009. **41**(4): p. 784-90.

302. Rokudai, S., et al., *Monocytic leukemia zinc finger (MOZ) interacts with p53 to induce p21 expression and cell-cycle arrest.* J Biol Chem, 2009. **284**(1): p. 237-44.
303. Kruse, J.P. and W. Gu, *MSL2 promotes Mdm2-independent cytoplasmic localization of p53.* J Biol Chem, 2009. **284**(5): p. 3250-63.
304. Wong, T.S., et al., *Physical and functional interactions between human mitochondrial single-stranded DNA-binding protein and tumour suppressor p53.* Nucleic Acids Res, 2009. **37**(2): p. 568-81.
305. Xia, Y., et al., *Phosphorylation of p53 by IkappaB kinase 2 promotes its degradation by beta-TrCP.* Proc Natl Acad Sci U S A, 2009. **106**(8): p. 2629-34.
306. Pan, X., et al., *Induction of SOX4 by DNA damage is critical for p53 stabilization and function.* Proc Natl Acad Sci U S A, 2009. **106**(10): p. 3788-93.
307. Gao, F., et al., *hBub1 negatively regulates p53 mediated early cell death upon mitotic checkpoint activation.* Cancer Biol Ther, 2009. **8**(7): p. 548-56.
308. Khanal, P., et al., *Tpl-2 kinase downregulates the activity of p53 and enhances signaling pathways leading to activation of activator protein 1 induced by EGF.* Carcinogenesis, 2009. **30**(4): p. 682-9.
309. Adorno, M., et al., *A Mutant-p53/Smad complex opposes p63 to empower TGFbeta-induced metastasis.* Cell, 2009. **137**(1): p. 87-98.
310. Lee, J., et al., *A tumor suppressive coactivator complex of p53 containing ASC-2 and histone H3-lysine-4 methyltransferase MLL3 or its paralogue MLL4.* Proc Natl Acad Sci U S A, 2009. **106**(21): p. 8513-8.
311. Dai, C., et al., *Heat shock factor 1 is a powerful multifaceted modifier of carcinogenesis.* Cell, 2007. **130**(6): p. 1005-18.
312. Lee, S.M., et al., *A nucleocytoplasmic malate dehydrogenase regulates p53 transcriptional activity in response to metabolic stress.* Cell Death Differ, 2009. **16**(5): p. 738-48.
313. Wang, S.P., et al., *p53 controls cancer cell invasion by inducing the MDM2-mediated degradation of Slug.* Nat Cell Biol, 2009. **11**(6): p. 694-704.
314. Tian, C., et al., *KRAB-type zinc-finger protein Apak specifically regulates p53-dependent apoptosis.* Nat Cell Biol, 2009. **11**(5): p. 580-91.
315. Huang, Y.F., M.D. Chang, and S.Y. Shieh, *TTK/hMps1 mediates the p53-dependent postmitotic checkpoint by phosphorylating p53 at Thr18.* Mol Cell Biol, 2009. **29**(11): p. 2935-44.
316. Yi, F., et al., *Epstein-Barr virus nuclear antigen 3C targets p53 and modulates its transcriptional and apoptotic activities.* Virology, 2009. **388**(2): p. 236-47.
317. Lee, E.W., et al., *Differential regulation of p53 and p21 by MKRN1 E3 ligase controls cell cycle arrest and apoptosis.* Embo J, 2009. **28**(14): p. 2100-13.
318. Trainor, C.D., et al., *GATA-1 associates with and inhibits p53.* Blood, 2009. **114**(1): p. 165-73.
319. Sun, L., et al., *JFK, a Kelch domain-containing F-box protein, links the SCF complex to p53 regulation.* Proc Natl Acad Sci U S A, 2009. **106**(25): p. 10195-200.

320. Yan, J., et al., *A regulatory loop composed of RAP80-HDM2-p53 provides RAP80-enhanced p53 degradation by HDM2 in response to DNA damage.* J Biol Chem, 2009. **284**(29): p. 19280-9.
321. Jeon, B.N., et al., *ZBTB2, a novel master regulator of the p53 pathway.* J Biol Chem, 2009. **284**(27): p. 17935-46.
322. Sperandio, S., et al., *TOE1 interacts with p53 to modulate its transactivation potential.* FEBS Lett, 2009. **583**(13): p. 2165-70.
323. Allton, K., et al., *Trim24 targets endogenous p53 for degradation.* Proc Natl Acad Sci U S A, 2009. **106**(28): p. 11612-6.
324. Sowa, M.E., et al., *Defining the human deubiquitinating enzyme interaction landscape.* Cell, 2009. **138**(2): p. 389-403.
325. Miyaguchi, Y., K. Tsuchiya, and K. Sakamoto, *P53 negatively regulates the transcriptional activity of FOXO3a under oxidative stress.* Cell Biol Int, 2009. **33**(8): p. 853-60.
326. Zhang, T., et al., *NGFI-B nuclear orphan receptor Nurr1 interacts with p53 and suppresses its transcriptional activity.* Mol Cancer Res, 2009. **7**(8): p. 1408-15.
327. Stoner, C.S., et al., *Effect of thioredoxin deletion and p53 cysteine replacement on human p53 activity in wild-type and thioredoxin reductase null yeast.* Biochemistry, 2009. **48**(38): p. 9156-69.
328. Jang, H., et al., *Cabin1 restrains p53 activity on chromatin.* Nat Struct Mol Biol, 2009. **16**(9): p. 910-5.
329. Yadavilli, S., et al., *Ribosomal protein S3: A multi-functional protein that interacts with both p53 and MDM2 through its KH domain.* DNA Repair (Amst), 2009. **8**(10): p. 1215-24.
330. Du, W., et al., *Suppression of p53 activity by Siva1.* Cell Death Differ, 2009. **16**(11): p. 1493-504.
331. Lee, J.H., et al., *Ferritin binds and activates p53 under oxidative stress.* Biochem Biophys Res Commun, 2009. **389**(3): p. 399-404.
332. Baum, N., et al., *The prolyl cis/trans isomerase cyclophilin 18 interacts with the tumor suppressor p53 and modifies its functions in cell cycle regulation and apoptosis.* Oncogene, 2009. **28**(44): p. 3915-25.
333. Rodriguez-Enfedaque, A., et al., *FGF1 nuclear translocation is required for both its neurotrophic activity and its p53-dependent apoptosis protection.* Biochim Biophys Acta, 2009. **1793**(11): p. 1719-27.
334. Lim, S.T., et al., *Pyk2 inhibition of p53 as an adaptive and intrinsic mechanism facilitating cell proliferation and survival.* J Biol Chem. 2010 **285**(3): p. 1743-53.
335. Song, G., et al., *Association of p53 with Bid induces cell death in response to etoposide treatment in hepatocellular carcinoma.* Curr Cancer Drug Targets, 2009. **9**(7): p. 871-80.
336. Miao, L., et al., *ARF antagonizes the ability of Miz-1 to inhibit p53-mediated transactivation.* Oncogene. 2010 **29**(5): p. 711-22.
337. Li, D.Q., et al., *MTA1 coregulator regulates p53 stability and function.* J Biol Chem, 2009. **284**(50): p. 34545-52.
338. Calabrese, V., et al., *SOCS1 links cytokine signaling to p53 and senescence.* Mol Cell, 2009. **36**(5): p. 754-67.

339. Arnaudeau, S., et al., *Glucose-regulated protein 78: a new partner of p53 in trophoblast.* Proteomics, 2009. **9**(23): p. 5316-27.
340. Liu, G. and D.P. Xirodimas, *NUB1 promotes cytoplasmic localization of p53 through cooperation of the NEDD8 and ubiquitin pathways.* Oncogene 2010 **29**: p. 2252-2261.
341. Larsen, S., et al., *LMO3 interacts with p53 and inhibits its transcriptional activity.* Biochem Biophys Res Commun. 2010 **392**(3): p. 252-7.
342. Yuan, J., et al., *USP10 regulates p53 localization and stability by deubiquitinating p53.* Cell. 2010 **140**(3): p. 384-96.
343. Li, Y., et al., *Inhibition of the transcriptional function of p53 by EWS-Fli1 chimeric protein in Ewing Family Tumors.* Cancer Lett. 2010. **294**(1): p. 57-65
344. Tripathi, R. and R. Mishra, *Interaction of Pax6 with SPARC and p53 in Brain of Mice Indicates Smad3 Dependent Auto-regulation.* J Mol Neurosci. 2010. **41**(3): p. 397-403
345. Zhang, Z.W., et al., *Transgelin induces apoptosis of human prostate LNCaP cells through its interaction with p53.* Asian J Androl. 2010 **12**(2): p. 186-95.
346. Drost, J., et al., *BRD7 is a candidate tumour suppressor gene required for p53 function.* Nat Cell Biol. 2010 **12**: p. 380-389
347. Fu, X., et al., *RFWD3-Mdm2 ubiquitin ligase complex positively regulates p53 stability in response to DNA damage.* Proc Natl Acad Sci U S A. 2010 **107**(10): p. 4579-84.
348. Li, P., et al., *Coordination of PAD4 and HDAC2 in the regulation of p53-target gene expression.* Oncogene. 2010 **29**: p. 3153-3162

Appendix 2

Supplementary figures

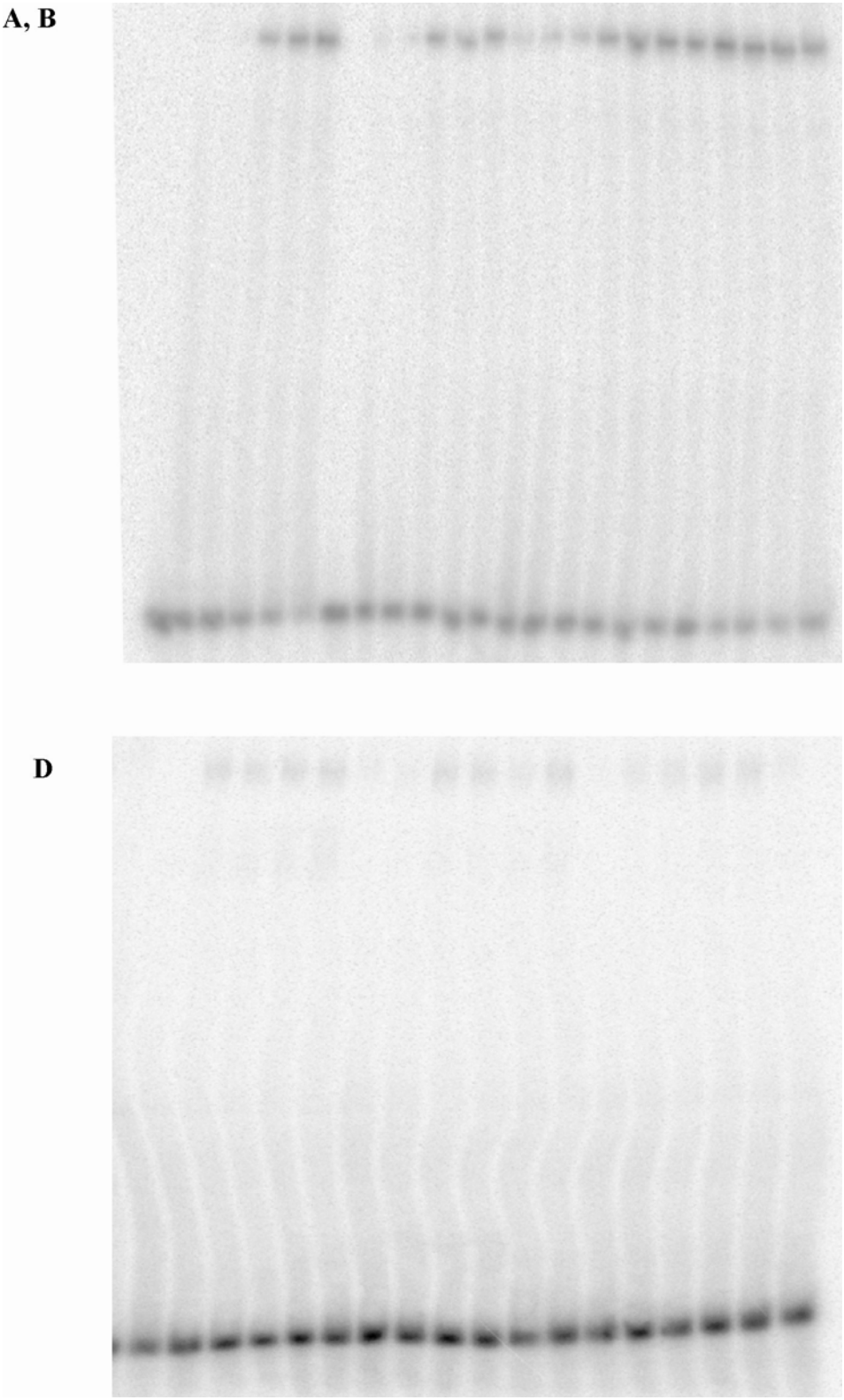

Supp Fig. 1 Images of the whole gel as in figure 6.11

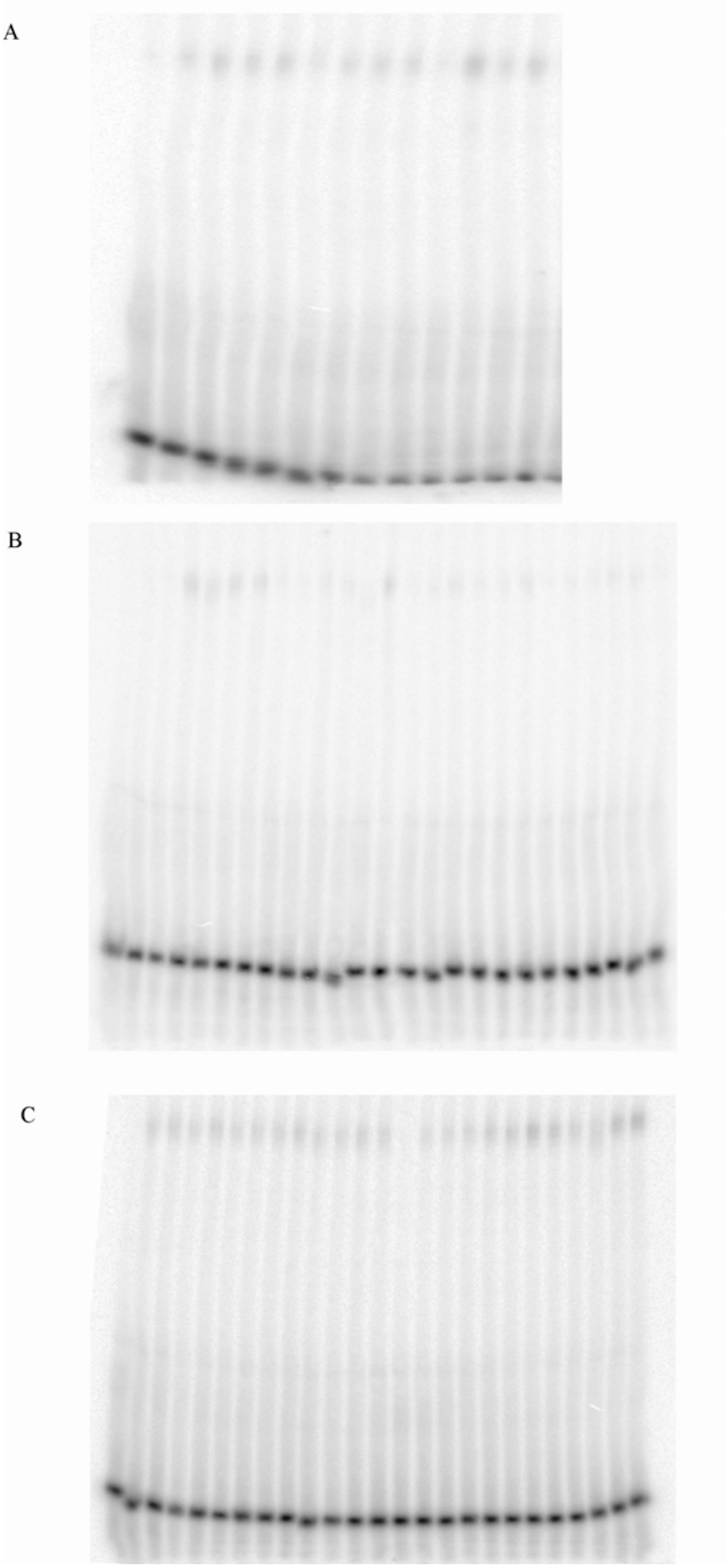

Supp Fig. 2 Images of the whole gel as in figure 6.12

Appendix 3

Papers

doi:10.1016/j.jmb.2010.09.035 J. Mol. Biol. (2010) 404, 418–438

Contents lists available at www.sciencedirect.com

Journal of Molecular Biology

journal homepage: http://ees.elsevier.com.jmb

A Divergent Substrate-Binding Loop within the Pro-oncogenic Protein Anterior Gradient-2 Forms a Docking Site for Reptin

Magdalena M. Maslon[1], Roman Hrstka[2], Borek Vojtesek[2] and Ted R. Hupp[1]*

[1]*Cancer Research UK p53 Signal Transduction Laboratories, Cell Signalling Unit, Institute of Genetics and Molecular Medicine, University of Edinburgh, Edinburgh EX4 2XR, Scotland, UK*
[2]*Masaryk Memorial Cancer Institute, Brno 656 53, Czech Republic*

Received 15 June 2010; received in revised form 15 September 2010; accepted 15 September 2010
Available online 1 October 2010

Edited by M. Yaniv

Keywords:
p53;
Reptin;
AGR2;
cancer;
ATP

Anterior gradient-2 (AGR2) functions in a range of biological systems, including goblet cell formation, limb regeneration, inhibition of p53, and metastasis. There are no well-validated binding proteins for AGR2 protein despite the wealth of data implicating an important cellular function in vertebrates. The yeast two-hybrid system was used to isolate the ATP binding protein Reptin as an AGR2-interacting protein. AGR2 formed a stable complex in human cell lysates with Reptin, thus validating Reptin as an AGR2 binding protein in cells. Reptin was also shown to be overproduced in a panel of primary breast cancer biopsy specimens, relative to normal adjacent tissue from the same patient, suggesting a role in cancer growth *in vivo*. Mutations were made at the two ATP binding motifs in Reptin to evaluate the effects of ATP on Reptin–AGR2 complex stability. Loss-of-ATP binding mutations at the Walker A motif (K83A) or gain-of-ATP binding mutations at the Walker B motif (D299N) resulted in Reptin mutants with altered oligomerization, thermostability, and AGR2 binding properties. These data indicate that the two ATP binding motifs of Reptin play a role in regulating the stability of the AGR2–Reptin complex. The minimal region of AGR2 interacting with Reptin was localized using overlapping peptide libraries derived from the AGR2 protein sequence. The Reptin docking site was mapped to a divergent octapeptide loop in the AGR2 superfamily between amino acids 104 and 111. Mutations at codon Y104 or F111 in full-length AGR2 destabilized the binding of Reptin. These data highlight the existence of a protein docking motif on AGR2 and an ATP-regulated peptide-binding activity for Reptin. This knowledge has implications for isolating other AGR2-interacting proteins, for developing assays to isolate small molecules that target the Reptin ATP binding site, and for measuring the effects of the Reptin–AGR2 complex in cancer cell growth.

*Corresponding author. E-mail address: ted.hupp@ed.ac.uk.

Abbreviations used: AGR2, anterior gradient-2; PDI, protein disulfide isomerase; ER, endoplasmic reticulum; HA, hemagglutinin; GST, glutathione *S*-transferase; DLS, dynamic light scattering; WT, wild type; PCR, polymerase chain reaction; PBS, phosphate-buffered saline; HUBMA/B/C, His-ubiquitin modification buffer A/B/C.

Introduction

Anterior gradient-2 (AGR2) is a protein whose function is proving to play an increasingly critical role in a diverse range of biological systems, including vertebrate tissue development, inflammatory tissue injury responses, and cancer progression. AGR2 was identified initially as a secretory factor expressed in the anterior region of the dorsal ectoderm in *Xenopus laevis* embryos, where it was postulated to mediate the specification of dorsoanterior ectodermal fate, particularly in the formation of the cement gland.[1,2] AGR2 was subsequently cloned as a gene whose expression is induced by the estrogen receptor α,[3] and subsequent studies in primary breast carcinomas have also shown significant associations between AGR2 expression and estrogen receptor-α positivity or tamoxifen resistance.[4,5] Clinical studies have shown that the AGR2 protein is overexpressed in a wide range of human cancers, including carcinomas of the esophagus, pancreas, breast, prostate, and lung.[4,6–9] More biological studies in cell lines have shown a significant role for AGR2 in tumor-associated pathways, including tumor growth, cellular transformation, cell migration, limb regeneration, and metastasis.[8,10–12]

AGR2 protein was also identified as part of a clinical proteomics screen aimed at discovering novel inhibitors of the tumor suppressor p53, and it was subsequently validated as a potent inhibitor of p53 activity and of the p53-dependent response to DNA damage.[11] The latter data provide a specific oncogenic pathway into which AGR2 integrates; however, the signaling mechanisms that drive AGR2 to inhibit p53 are not defined. Although there are no well-validated binding proteins in human cells that can explain how AGR2 can act as a pro-oncogenic protein, peptide aptamer screens have identified a specific peptide-binding activity for the AGR2 protein for peptides containing an (S/T)xIΦΦ consensus motif, suggesting that the AGR2 protein might prove to have a peptide groove able to interact with cellular proteins containing such a consensus motif.[13] Furthermore, penetratin peptides linked to this AGR2-binding (S/T)xIΦΦ motif or EGFP fusions to the (S/T) xIΦΦ motif can stabilize AGR2 in cells and stimulate p53 activity, indicating that the AGR2 protein can interact with this peptide consensus motif *in vivo*.[14] A yeast two-hybrid screen has also been used to previously identify the prometastatic proteins C4.4 and DYS1 as interactors of AGR2[15]; however, there was no biological validation of C4.4 and DYS1 as a bona fide protein–protein interaction in human cells. However, potential extracellular receptor functions for AGR2 in human cells remain possible, because an interaction between the newt extracellular receptor PROD1 and newt AGR2 was identified using a yeast two-hybrid screen and validated to demonstrate a direct signaling role for AGR2 in amphibian limb regeneration.[10]

Although the general biochemical functions of AGR2 in human cells remain undefined, *AGR2* is part of the protein disulfide isomerase (PDI) superfamily that contains core thioredoxin folds (CxxC or CxxS motif), which have the potential to act as molecular chaperones that regulate protein folding via regulation of disulfide-bond formation.[16] There are five protein members of this family: TRX1 (thought to be predominantly the nuclear thioredoxin), TRX2 (thought to be predominantly the mitochondrial thioredoxin), endoplasmic reticulum (ER) protein 18 (ERP18; the ancestral protein in the AGR2/AGR3 group that has potent reducing potential),[17] AGR2, and the AGR2 ortholog AGR3. AGR2 and AGR3 are confined to vertebrates, and both have the CxxS core motif instead of the CxxC motif of TRX1, TRX2, and ERP18.[18] The majority of PDIs/ERPs harbor a typical H/KDEL ER retrieval signal. A putative ER retention sequence that has been shown to regulate the intracellular localization of AGR2 in human cells has been identified at the C-terminus of AGR2.[14] It is therefore possible that at least one function of the AGR2 is to act as a PDI and hence as a protein molecular chaperone. A recent study has confirmed that AGR2 is essential for the production of the intestinal mucin MUC2, a cysteine-rich glycoprotein that forms the protective mucus gel lining the intestine. The cysteine residue within the AGR2 thioredoxin-like domain was shown to form a mixed disulfide bond with a cysteine in the N-terminus or C-terminus of MUC2 as it is being processed.[19] However, there are currently no established biochemical mechanisms to explain the function or the regulation of AGR2 protein.

In this report, a yeast two-hybrid screen was used to identify a potentially novel interacting protein for the AGR2 protein from a human breast cancer library. A protein named Reptin was identified by the yeast two-hybrid screen and validated as an interacting protein of AGR2 in human cells. Reptin is a highly conserved member of the AAA+ family that can be found in numerous multiprotein complexes linked to transcription, DNA damage response, and nonsense-mediated RNA decay.[20–25] This protein is a member of the highly conserved RuvBl1/2 superfamily containing ATP binding motifs and DNA binding and helicase functions and an ability to form biologically relevant protein–protein interactions with proteins implicated in cancer, including Myc, Tip60, APPL1, Pontin, and telomerase holoenzyme complexes.[20,23,26–29] The validation of Reptin as an AGR2 binding protein gives rise to a potentially novel signaling complex involved in prometastatic cancer development. Our mapping of the determinants that mediate a specific

Reptin–AGR2 protein–protein complex *in vitro* provides biochemical insights for understanding how the Reptin–AGR2 complex can be regulated in cells. These data also provide ideas for development of *in vitro* enzyme assays for the screening of small molecules that might be used to disrupt the AGR2–Reptin complex in cancer cells as potential therapeutic leads.

Results

Reptin is overexpressed in primary human cancers and forms a stable protein–protein complex with AGR2 protein in cancer cells

In our search for proteins interacting with human AGR2 protein, we used a yeast two-hybrid assay with LexA fused to AGR2 as bait screened against a cDNA library derived from breast cancer cells (Fig. 1a). These hits appear relatively specific for the AGR2 bait because a parallel yeast two-hybrid screen performed on the AGR2 ortholog AGR3 (sharing approximately 75% homology) yielded a completely distinct set of interacting proteins (data not shown).

Two extracellular prometastatic receptors identified (Fig. 1a; C4.4A and DAG1) were previously published to be AGR2-interacting proteins based on a yeast two-hybrid screen,[15] but these interactors were not validated as AGR2 binding proteins. Yeast two-hybrid approaches for identifying interacting proteins can be prone to the generation of false-positives[30]; for example, we have been unable to validate despite numerous approaches in human cell systems or *in vitro* using purified proteins a direct interaction between the HECTD1 ubiquitin ligase (Fig. 1a) and AGR2 protein (unpublished data). Furthermore, as the interactions proposed between AGR2 and C4.4A or DAG1 based on the yeast two-hybrid screen require an extracellular localization of AGR2, we did not further validate C4.4A and DAG1 as potential interactors of AGR2. The reason for excluding these potential interactors is that our laboratory cannot observe AGR2 secreted and/or localized at the plasma membrane, as has been suggested by others.[15] Rather, we have published data showing the localization of endogenous or red fluorescent protein-tagged AGR2 to the ER, perinucleus, and nucleus.[14] Peptide aptamers generated to AGR2[13] also shift AGR2 out of nuclear fraction into cytosolic compartments.[14] As such, we focused our efforts at validating nuclear proteins from the yeast two-hybrid screen as potential AGR2 interactors—particularly one protein of specific relevance within the AAA+++ superfamily named Reptin.

Reptin can be a nuclear protein involved in range of functions, including DNA repair, transcription regulation, and chromatin structural control.[24] Similar to AGR2, Reptin is also involved in prometastatic signaling using cell lines *in vitro*, but this involves, in part, interactions of Reptin with the transcription regulator Myc or Tip60.[31] Furthermore, there is some evidence that Reptin is

(a)

Name	Accession	Function
Reptin	CAG38538	Interacts with Tip60 and Myc transcription factors, contains intrinsic ATPase and helicase functions
Rip140	NP_003480	Nuclear de-acetylase that interacts with hormone receptor activation domains
LGN	AAN01266	Modulation of G protein activation
HECTD1	AAW65983	HECT-homology domain containing Ubiquitin ligase superfamily
CKAP2	AAH10901	Regulates cyclin- kinase functions
TMEM123	AL050161	Cell-membrane mediated cell death
C4.4A	AF082889	Metastasis linked activity, previously published, unvalidated AGR2-Y2H interactor
DAG1	L19711	Metastasis linked activity, previously published, unvalidated AGR2-Y2H interactor

(b)

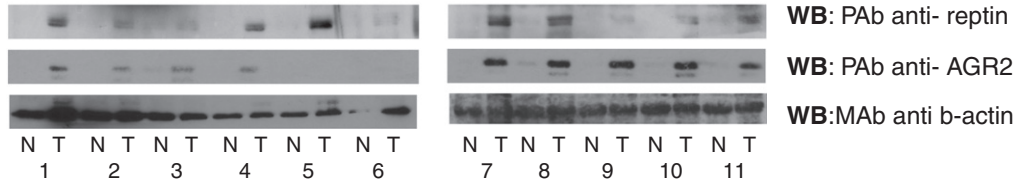

Fig. 1. Reptin and AGR2 are both overproduced in primary human cancers. (a) Summary of AGR2 yeast two-hybrid interactors. Yeast two-hybrid analysis was performed by Hybrigenics using the bait vector consisting of pB27 containing a LexA C-terminal fusion to human AGR2 (21–175) and screened against human breast tumor epithelial cell RP1. Only highly significant overlapping hits are depicted including name, accession number, and functions. (b) Immunoblotting of lysates derived from breast cancers and normal adjacent tissue from the same patient. Sample biopsy specimens [from T (tumor) and N (normal)] were prepared in lysis buffer as described previously,[5,44] separated by electrophoresis, and immunoblotted using antibodies to Reptin, AGR2, and actin, as indicated.

overproduced in primary cancers, hepatocellular carcinoma,[32] and gastric cancer.[33] However, there are no data on whether Reptin and AGR2 can be coexpressed in primary human cancers. If there were, then this would form an important rationale for continued evaluation of Reptin–AGR2 interactions. A panel of primary human breast cancers and normal adjacent tissue from the same patient were lysed to examine whether Reptin is in fact overexpressed in primary cancers. These human cancers were previously used to demonstrate that AGR2 overproduction predicts poor prognosis in tamoxifen-resistant breast cancers.[5] The immunoblotting of lysates from this panel of breast cancer biopsy specimens or normal adjacent tissue from the same patient demonstrated the overproduction of AGR2 in the cancers in the majority of patients (Fig. 1b, samples 1, 2, 3, 4, and 7–11), as expected from previous immunohistochemical evaluations.[5] Similarly, Reptin was also overproduced in the

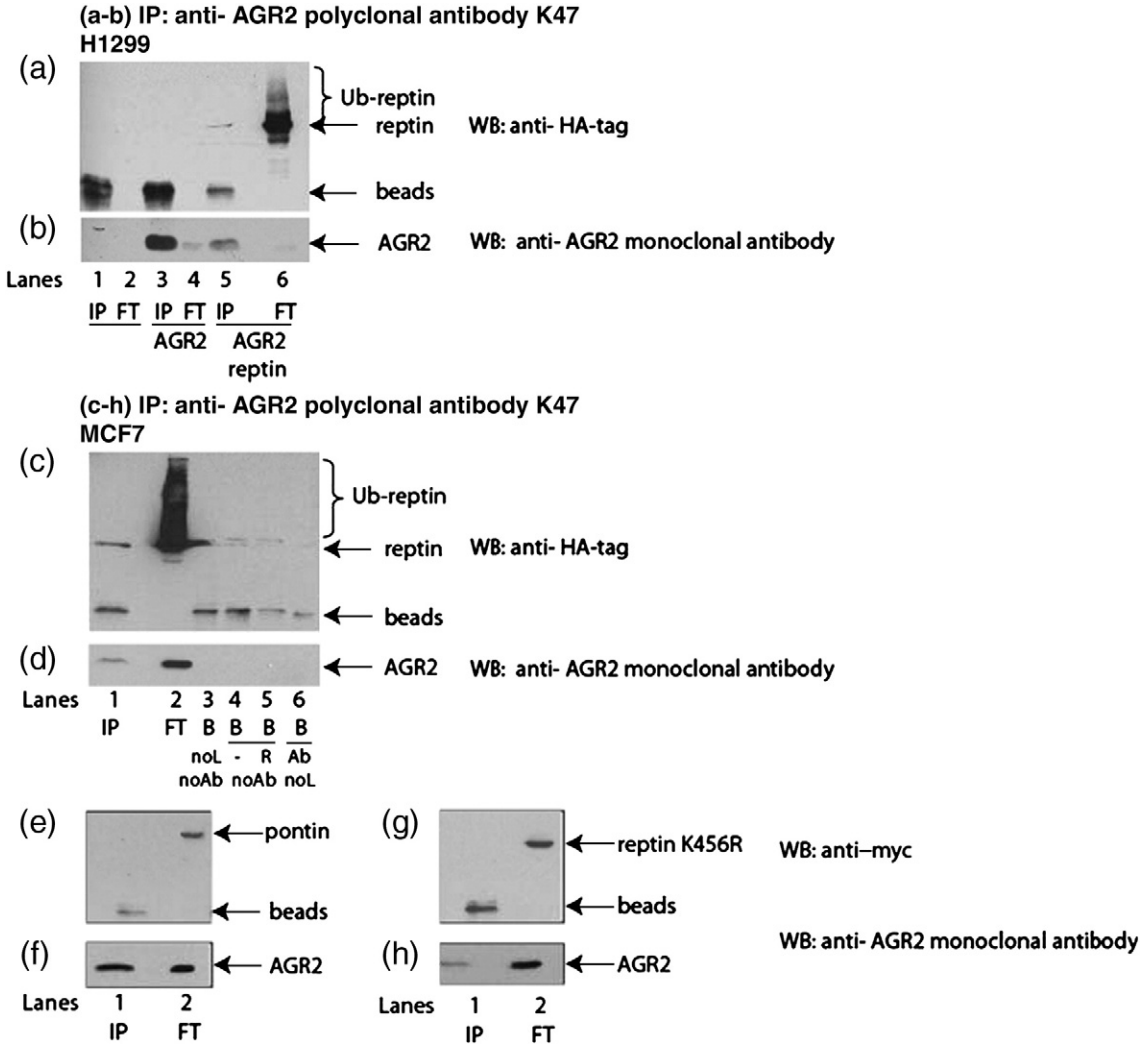

Fig. 2. Co-immunoprecipitation of human Reptin and AGR2 protein in human cancer cells. (a and b) Reptin and AGR2 form a complex in cells. Cell lysates from H1299 human breast cancer cells (no AGR2) transfected with vector control (lanes 1 and 2), with the AGR2 vector (lanes 3 and 4), or with AGR2 and HA-tagged Reptin (lanes 5 and 6) were incubated with the anti-AGR2 rabbit polyclonal antibody (K47) and protein G beads. The AGR2 immunoprecipitate [IP] (lanes 1, 3, and 5) or the unbound, flow-through fraction [FT] (lanes 2, 4, and 6) was immunoblotted to quantify the extent of (a) HA-tagged Reptin or (b) AGR2 in each fraction. Reptin, ubiquitinated Reptin, and AGR2 are highlighted. (c–h) Neither mutant Reptin nor Pontin forms a complex with AGR2 in cells. Cell lysates from MCF7 cells expressing endogenous AGR2 transfected with (c and d) WT Reptin, (e and f) Myc-tagged Pontin, and (g and h) Myc-tagged Reptin^{K456R} were immunoprecipitated with the anti-AGR2 polyclonal antibody K47. The bound [IP] and unbound [FT] fractions were immunoblotted to quantify the extent of Reptin, Pontin, or Reptin^{K456} proteins bound to AGR2. The immunoblots were exposed for the same times, and Reptin, ubiquitinated Reptin, protein G beads, Pontin, and AGR2 are highlighted.

majority of these cancer biopsy specimens (Fig. 1b, samples 1–11). Thus, the combined overexpression of AGR2 and Reptin in primary human breast cancer makes Reptin a more compelling and physiologically relevant AGR2-interacting protein.

To evaluate whether the association between Reptin and AGR2 is physiological in human cells, we performed co-immunoprecipitation experiments using lysates of H1299 lung carcinoma cells transiently expressing hemagglutinin (HA)-tagged Reptin and AGR2. The transfection of AGR2 alone into cells demonstrated that the transfected AGR2 protein could be immunoprecipitated with a polyclonal antibody (K47) specific for AGR2 (Fig. 2b, lane 3), with a small proportion in the unbound, flow-through fraction (Fig. 2b, lane 4). As a control, AGR2 is not detectable in cells that were not transfected with AGR2 (Fig. 2b, lanes 1 and 2). The transfection of HA-tagged Reptin into cells resulted in the immunoprecipitation of the Reptin protein with AGR2 (Fig. 2a, lane 5).

A pool of Reptin protein in the unbound fraction was composed of high-molecular-mass adducts (Fig. 2a, lane 6), presumably due to ubiquitin-like modification. A control was performed to determine whether the high-molecular-mass ladder of ubiquitin-like adducts was ubiquitin, NEDD8, or SUMO-1. His-tagged versions of the latter ubiquitin/ubiquitin-like genes were co-transfected into cells with HA-tagged Reptin, and following purification of the *in vivo* His-tagged proteins on a nickel affinity column, the pellets were analyzed by immunoblotting for Reptin. The data demonstrate that the dominant adduct on Reptin is ubiquitin, not NEDD8 or SUMO-1 (Fig. 3b, lane 2). This is distinct from a prior report that suggested a dominant modification on Reptin is SUMO-1.[21] This might reflect a cell-specific difference in the type of ubiquitin-like modification that is catalyzed on Reptin. As an additional control, basal p53 modification by ubiquitin and SUMO-1 could be detected (Fig. 3b, lanes 2 and 4), whereas MDM2 could drive enhanced ubiquitination or NEDDylation of p53 (Fig. 3b, lanes 6 and 7). These latter data indicate that integrity of the His-tagged NEDD8 and SUMO-1 genes is adequate and that the low amount of NEDDylation or SUMOylation of Reptin presumably highlights the specificity of ubiquitination on Reptin.

In order to define determinants that mediate the specificity of the co-immunoprecipitation of Reptin with AGR2, we also evaluated the ability of the Reptin ortholog and partner protein Pontin/RuvBl1 to interact with endogenous AGR2 in MCF7 cells. Pontin is thought to form a hetero-oligomer with Reptin,[34] although it has also been published that Reptin has biochemical functions that are Pontin independent.[21] Although transfected Reptin was able to form an immune complex with endogenous

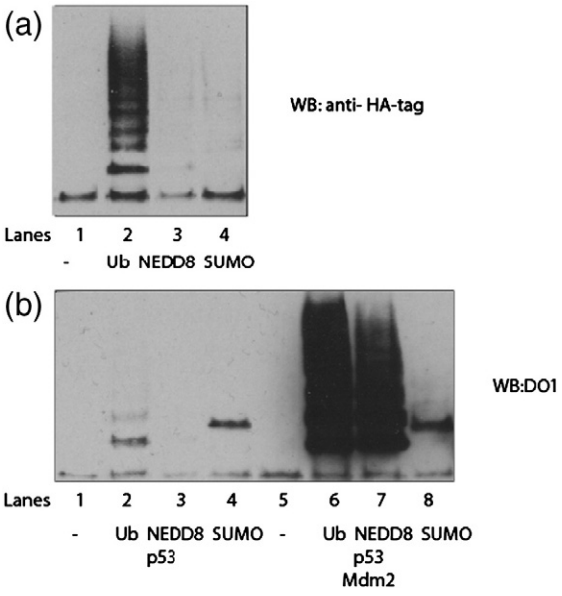

Fig. 3. Reptin is selectively ubiquitinated in cells. (a) Evaluation of Reptin ubiquitin-like modification in cells. The HA-tagged vector expressing Reptin was co-transfected with His-ubiquitin, His-NEDD8, and His-SUMO-1 expression vectors. After the nickel affinity purification stage, the expressed Reptin was examined for changes in the amount of posttranslational modification by immunoblotting with an anti-HA-tag antibody. (b) Evaluation of p53 ubiquitin-like modification in cells. A vector expressing WT p53 was co-transfected with vectors expressing His-ubiquitin, His-NEDD8, and His-SUMO-1 without (lanes 1–4) or with (lanes 5–8) the co-transfection of MDM2. The expressed p53 was examined for changes in the amount of posttranslational modification by immunoblotting with an anti-p53 antibody (DO-1) after the nickel affinity chromatography stage.

AGR2 (Fig. 2c and d, lane 1), Pontin did not form any detectable complex with Reptin (Fig. 2e and f, lane 1 *versus* lane 2). Furthermore, the Reptin mutant K456R, which cannot form ubiquitin-like adducts,[21] was not able to form a stable complex with AGR2 (Fig. 2g and h, lane 1 *versus* lane 2). Together, these results confirm that the yeast two-hybrid system did in fact reveal a specific protein–protein interaction between AGR2 and Reptin that can be detected in human cell lines. As such, we developed biochemical approaches in order to validate the determinants that define the specific binding between Reptin and AGR2.

ATP regulates the stability of the Reptin–AGR2 protein complex

In order to determine whether Reptin binding to AGR2 is direct and not due to a bridging factor *in vivo* (in the yeast or human cell systems), we

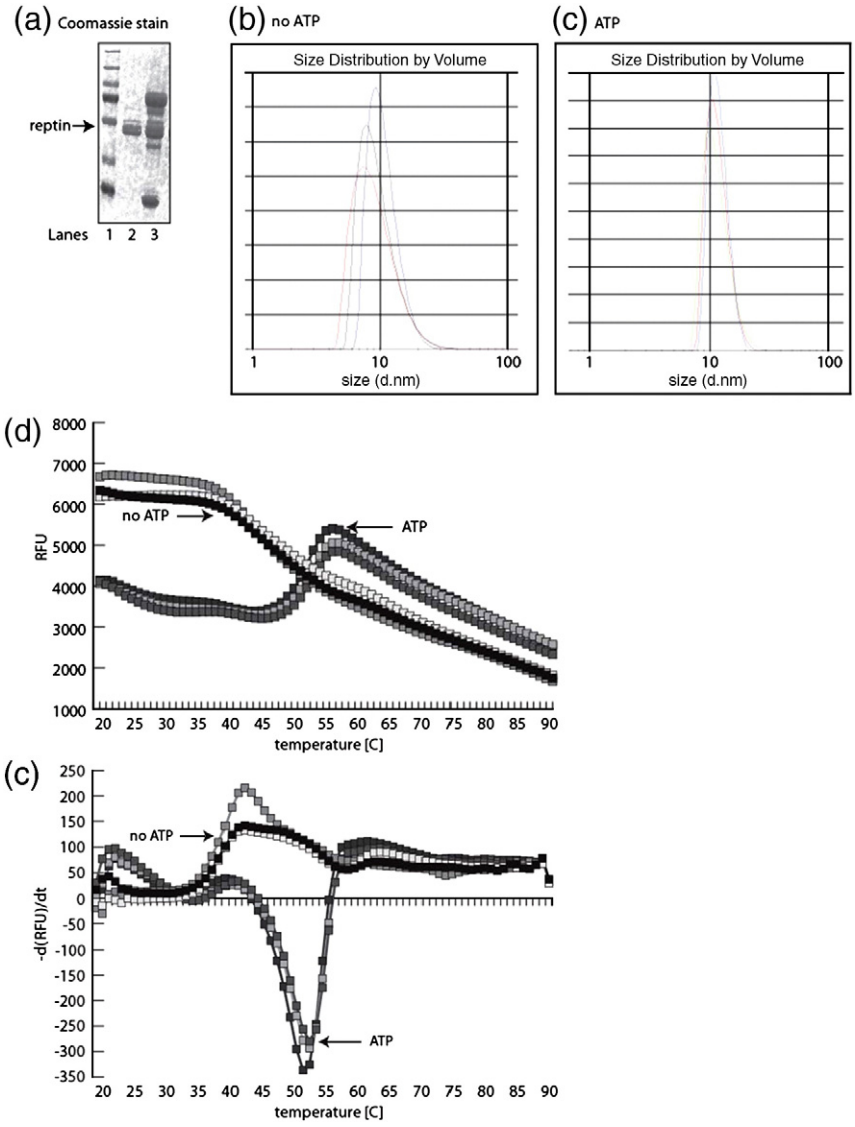

Fig. 4. Purification and ATP binding properties of untagged human Reptin protein. (a) Purification of recombinant Reptin. Reptin was cloned into a vector producing a GST fusion protein containing a PreScission protease cleavage site after adsorption of GST-Reptin onto the glutathione beads, followed by rigorous washing and elution of Reptin protein in purified form and then by dialysis into buffer as indicated in Methods. Lane 1, markers; lane 2, full-length untagged Reptin; lane 3, GST-tagged Reptin. (b and c) Reptin (50 μM) was subjected to analysis by light scattering in the absence and in the presence of ligand ATP, as indicated in Materials and Methods. (d) Reptin unfolding as a function of temperature change in the absence and in the presence of ligand. SYPRO Orange fluorescence was used to measure the thermal unfolding events between 20 °C and 89 °C, and experiments were done in triplicate in the absence or presence of ATP. (e) Phase transitions in the Reptin thermal melt profile. The gradient of protein unfolding was plotted against the temperature gradient to obtain the midpoint temperature of transition (T_m) in the absence and in the presence of ATP.

first purified and characterized Reptin protein biochemically to ensure that the integrity of the protein was adequate for biochemical analyses. Recombinant human Reptin protein was over-produced as a recombinant glutathione *S*-transferase (GST)-tagged fusion protein expressed in *Escherichia coli* and purified after protease cleavage from the GST tag (Fig. 4a, lane 3 *versus* lane 2). The use of dynamic light scattering (DLS) to characterize the oligomeric state of highly purified Reptin revealed a protein fraction with a relatively homogenous nature (Fig. 4b) that was shifted in apparent mass as defined by changes in DLS after the inclusion of ATP (Fig. 4c). The latter data are consistent with previous reports that Reptin can bind ATP, although one previous report indicated that His-tagged Reptin does not increase its oligomeric nature in the presence of ATP.[34]

Lastly, we analyzed the ATP binding potential of Reptin using thermal-shift assay. Increase in protein denaturation or unfolding as a function of temperature can be measured by the interaction with SYPRO Orange, a dye that binds to hydrophobic regions exposed or unfolded regions of proteins and results in fluorescence.[35] Ligand binding can alter the thermostability of a target protein and cause a change in the rate of unfolding as a function of increasing temperature. In the absence of ligand, there is a high basal fluorescence of Reptin (~6400 RFU) that reduces gradually as a function of increasing temperature (Fig. 4d). When the data are plotted as rate of change in fluorescence at each temperature, Reptin does not undergo a classic unfolding transition (Fig. 4e). These data suggest that hydrophobic regions on ATP-free Reptin are being concealed rather than exposed upon heating. However, in the presence of ATP, a classic ligand-dependent thermal unfolding transition was observed as defined by increases in the rate of SYPRO Orange dye binding as a function of increasing temperature (Fig. 4d and e). Also, in the presence of ATP, there is a reduction in the basal fluorescence at 20 °C (~4100 RFU; Fig. 4d). These data suggest that the higher fluorescence seen at 20 °C in the absence of ATP is due to the SYPRO Orange dye binding to the hydrophobic ATP binding motifs and ATP conceals the pocket from dye binding. Together, these data suggest that the biochemical integrity of the Reptin protein we have purified by this method is sufficient and that the protein is active as an ATP binding protein. This form of Reptin was used to determine if it indeed binds directly to AGR2 and if so to define the determinants in Reptin that drive specific binding to AGR2 protein.

Nitrocellulose filter-based ATP binding assays were utilized to define the apparent stoichiometry of the Reptin–ATP complex. A titration of Reptin protein (from 0.25–1.0 pmol) using α-^{32}P-labeled ATP as a ligand revealed that approximately 0.5 pmol of ATP can be bound per picomole of Reptin (Fig. 5a). With the use of the nonhydrolyzable ATP analog γ-S-labeled ATP, up to approximately 0.18 pmol of ATP binding activity could be detected per picomole of Reptin (Fig. 5a). Because Reptin has two ATP binding sites and can become more oligomeric in the presence of ATP (Fig. 4), these data suggest that the hydrolysis of ATP might stimulate or stabilize ATP binding allosterically or that the nonhydrolyzable ATP analog does not functionally mimic ATP in these ATP binding pockets. In addition, as we were unable to detect 2 mol ATP bound per mole of Reptin, these data suggest a negative cooperativity between the two ATP binding pockets on the protein (see Discussion). Using this ATP-binding active form of Reptin, we determined whether Reptin bound to AGR2 protein directly using an ELISA to measure protein–protein interactions. When AGR2 was adsorbed onto the solid phase (96-well microtiter plate) and subjected to a Reptin titration in the mobile phase, a

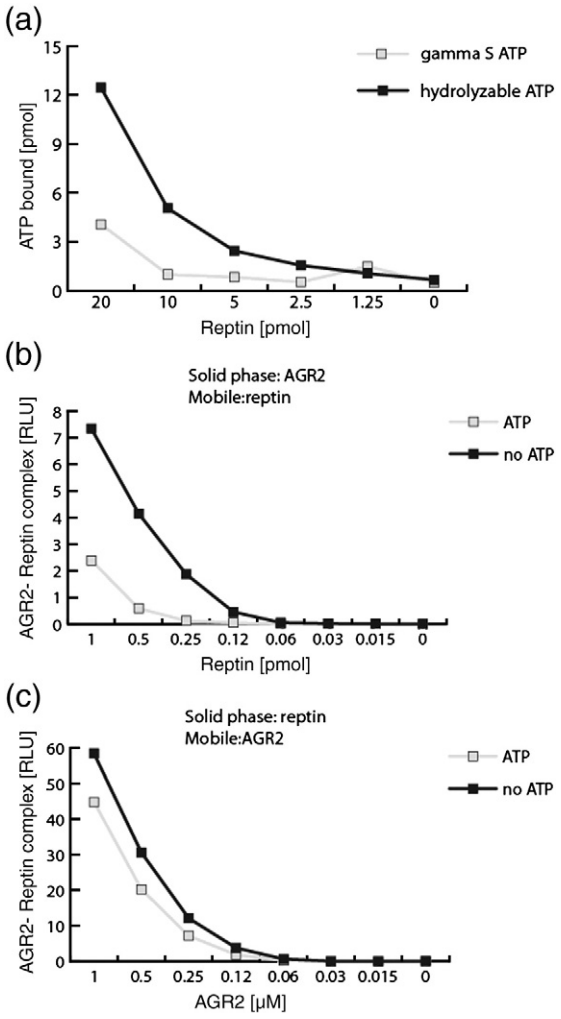

Fig. 5. The effects of ATP on the stability of the Reptin–AGR2 protein complex. (a) ATP binding activity of Reptin. ATP binding was measured by quantifying the amount of radioactive ATP bound to a nitrocellulose filter as a function of increasing Reptin protein levels. The black line represents binding to ATP, and the light line represents binding to nonhydrolyzable ATP. The data are plotted as picomoles of ATP bound as a function of increasing Reptin protein levels (in picomoles). (b and c) ATP destabilizes the Reptin–AGR2 protein complex. Either AGR2 (b) or Reptin (c) was immobilized in the solid phase, and in the mobile phase either Reptin (b) or AGR2 (c) was titrated in the absence or presence of ATP. The amount of Reptin or AGR2 bound was quantified with antibodies specific for either protein using chemiluminescence. The data are plotted as the extent of protein–protein complex formation (in relative luminescence units) as a function of increasing protein in the mobile phase (in micromolar concentrations).

stable complex can be detected between the two proteins (Fig. 5b). This confirms that the immunoprecipitation and yeast two-hybrid observed between AGR2 and Reptin *in vivo* (Fig. 2) can be due to a direct protein–protein interaction between the two proteins. A titration of Reptin in the presence of ATP reveals that ATP can reduce the stability of the Reptin–AGR2 complex by approximately threefold (Fig. 5b). Corroborating this assay, when Reptin is adsorbed to the solid phase, with AGR2 titrated in the mobile phase, a stable complex can be detected between AGR2 and Reptin that is also attenuated by the inclusion of ATP, but by approximately 20% (Fig. 5c). The difference in the extent of ATP-dependent reductions in AGR2 binding to Reptin might be due to the conformation of the respective protein (AGR2 in Fig. 5b and Reptin in Fig. 5c) when adsorbed to the solid phase. These data confirm that Reptin and AGR2 can form a direct complex and that the conformation of Reptin in its ATP-bound state can affect the stability of the complex.

Mutation of either of the two ATP binding sites on Reptin destabilizes the AGR2–Reptin complex

Reptin has a number of conserved sequence motifs. Notably, it has two motifs critical for nucleotide binding and hydrolysis, namely the P-loop NTP binding motif (also known as the Walker A box) and the DEAD motif (also known as the Walker B box),[31] respectively. In order to further evaluate the effects of the two ATP binding domains of Reptin (Fig. 6ai) on the stability of the AGR2–

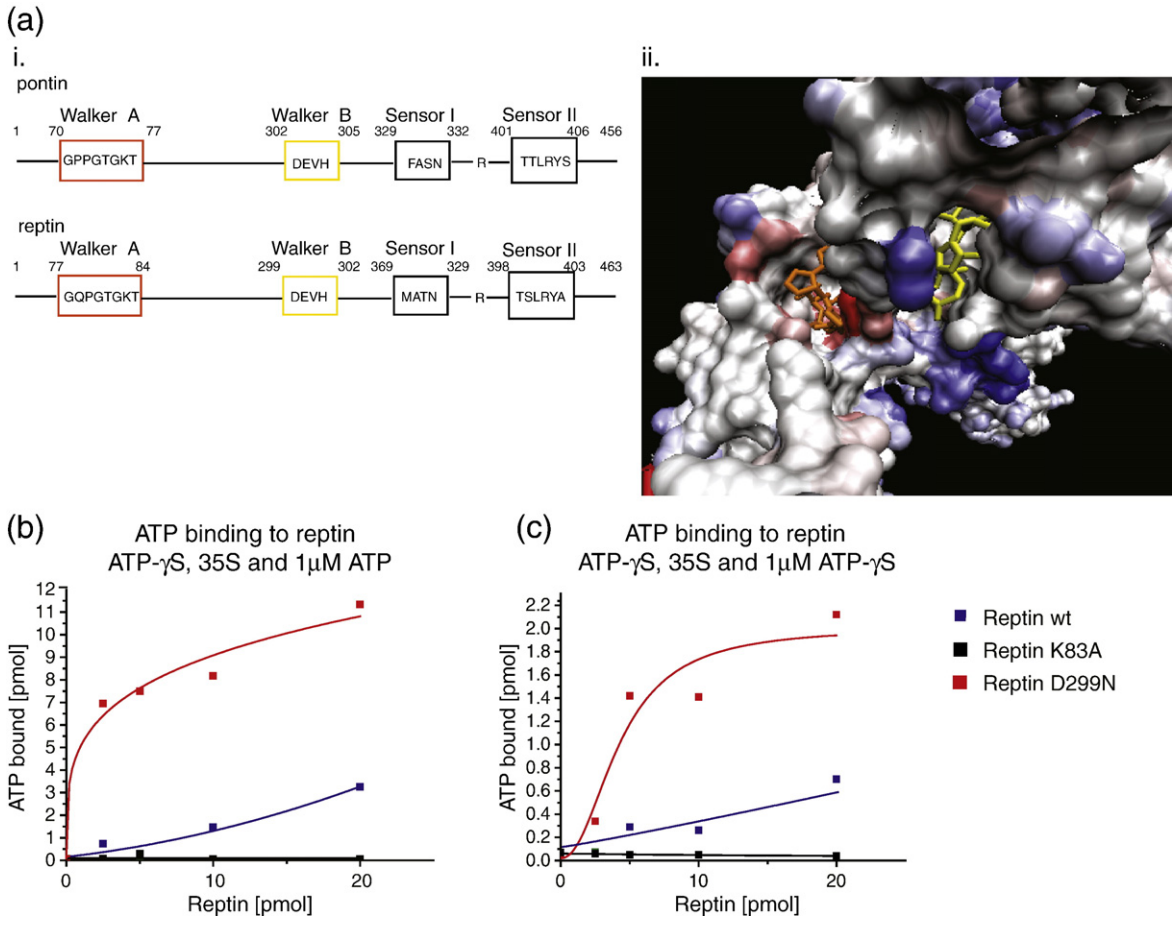

Fig. 6. The effects of Reptin ATP binding site mutations on binding to ATP. (a) (Left panel i) The key functional domains of Reptin and its ortholog Pontin are shown, including the Walker A and Walker B ATP binding motifs and the sensor motifs. (Right panel ii) Diagram of the structure of human Pontin with the Walker A and B ATP binding sites highlighted in blue and red, respectively; the Protein Data Bank code for Pontin is 2C9O. (b and c) ATP binding activity of Reptin ATP site mutants. Radioactive ATP binding was measured by quantifying the amount of (b) ATP (spiked with radioactive γ-^{35}S-labeled ATP or (c) γ-S-labeled ATP (spiked with radioactive γ-^{35}S-labeled ATP) bound to a nitrocellulose filter as a function of increasing WT and mutant Reptin protein levels. The data are plotted as picomoles of ATP bound as a function of increasing Reptin protein levels (in picomoles).

Reptin complex, we generated the single point mutants in the ATP binding sites, K83A and D299N. The Walker A mutation (K to A) is thought to induce a loss-of-function mutation, whereas the Walker B mutation (D to N) is thought to reduce ATP hydrolysis, but it actually increases ATP binding.[36] As expected, Reptin^{D299N} exhibited a higher affinity for the radioactive nonhydrolyzable ATP analog γ-^{35}S-labeled ATP (in the presence of nonradioactive ATP) than the wild-type (WT) Reptin, whereas the mutant Reptin^{K83A} exhibited a reduced binding affinity for γ-^{35}S-labeled ATP (Fig. 6b). Similar results were observed using radioactive γ-S-labeled ATP in the presence of nonradioactive γ-S-labeled ATP (Fig. 6c). The data also suggest that mutation of codon 83 Walker A motif attenuates ATP binding allosterically by the remaining WT Walker B motif. However, the inactivity of Reptin^{K83A} in this assay is complicated by the observation that this mutant appears to interact with ATP using three assays (described below). This suggests that the nitrocellulose binding assay underestimates the specific activity of Reptin^{K83A} as an ATP binding protein, possibly due to the remaining WT Walker B motif.

Chemical cross-linking was performed to determine if changes in the ATP-dependent oligomeric structure of Reptin (Fig. 4c) correlate with differences in the ATP binding functions of the Reptin^{K83A} and Reptin^{D299N} mutant proteins. Increasing the concentration of cross-linker into reactions with WT Reptin yielded an oligomeric ladder (Fig. 7a, lane 6 *versus* lanes 1–5) that was partially resistant to cross-linking as defined by the resilience of a pool of monomeric protein to cross-linking at the highest concentration of 0.2% (Fig. 7a, lane 1 *versus* lane 6). In the presence of ATP, there was a marginal difference in the oligomerization of Reptin (Fig. 7a, lanes 7–12), indicating that the cross-linking assay is not revealing dramatic changes in the conformation of the WT Reptin. Nevertheless, the Reptin^{K83A} and Reptin^{D299N} mutant proteins exhibited striking and opposing behavior in the cross-linking assay to each other and to WT Reptin. The Reptin^{K83A} mutant protein was sensitive to loss of monomeric subunit as a function of increasing concentration of cross-linker in the presence of ATP (Fig. 7b, lane 12 *versus* lanes 7–11), whereas this mutant appeared similar to WT Reptin in the absence of ATP (Fig. 7b, lanes 1–6, *versus* Fig. 7a, lanes 1–6). These data indicate that the Reptin^{K83A} mutant protein can in fact interact with ATP in this assay format, contrasting with its inactivity in the nitrocellulose filter ATP binding assay. By contrast, Reptin^{D299N} exhibited a loss in monomeric Reptin as a function of increasing cross-linking in the absence of ATP (Fig. 7c, lanes 1–6) but was resistant to cross-linking of its monomer in the presence of ATP (Fig. 7c, lanes 7–12). These data indicate that the Reptin^{K83A} and Reptin^{D299N} have different conformational responses to ATP binding between each other (summarized in Fig. 7d and e) and compared with WT Reptin. The oscillating response of WT Reptin might be due to a dynamic equilibrium between monomeric and oligomeric states at the temperature used in these assays (21 °C), as we have data (unpublished results) showing that the oligomeric nature of Reptin can be dramatically influenced by temperatures ranging from the extreme of 0 °C to 37 °C.

In conclusion, characterization of Reptin^{K83A} and Reptin^{D299N} ATP binding site mutant proteins indicated that they both respond differently from WT Reptin and opposing each other in terms of ATP-dependent changes in oligomeric cross-linking and in ATP binding. The proximity of the ATP binding motifs containing the K83 and D299 codons based on the homology of Reptin to the structure of its ortholog Pontin (Fig. 6ai) suggests a potential allosteric shift of one ATP binding motif might locally affect the affinity of the other ATP binding motif for its ligand. The data also suggest that mutating the individual Walker B ATP binding site in Reptin creates a gain-of-function activity due to reduction in ATP hydrolysis and thus increases in binding affinity for ATP.

Using the WT Reptin and these Reptin ATP binding site mutants, we evaluated whether the mutant proteins exhibited differences in stable binding to AGR2 protein. When AGR2 was incubated in the solid phase with WT Reptin in the mobile phase, the typical ATP-dependent reduction in AGR2 binding (as in Fig. 4c) could be observed (Fig. 8a). With the use of the loss-of-ATP binding function mutant (Walker A motif, K83A), significant reduction in AGR2 binding could be observed (Fig. 8a), highlighting an important role for the Walker A motif in regulating the AGR2 binding activity of Reptin.

The gain-of-function mutant in the Walker B motif (D299N) was analyzed alone and in combination with the double mutation D299N and K83A to also evaluate how these mutations affected Reptin binding to AGR2. As with WT Reptin, we first evaluated whether the D299N mutant protein had an altered thermostability using the thermal-shift assay. Interestingly, Reptin^{D299N} exhibited an intrinsically more thermoresistant property as a function of increasing temperature (Fig. 8b) that was further stabilized approximately 15 °C by the inclusion of ATP (Fig. 8b). These data are further consistent with a gain-of-function conformational effect on the Reptin structure, with respect to ATP binding. Although the Reptin^{D299N} mutant protein bound well to AGR2 (Fig. 8c) and was partially destabilized from AGR2 binding by ATP (Fig. 8c), the double Reptin mutant was significantly reduced in AGR2 binding activity in the absence or presence of ATP (Fig. 8c). These data indicate that the loss-of-ATP

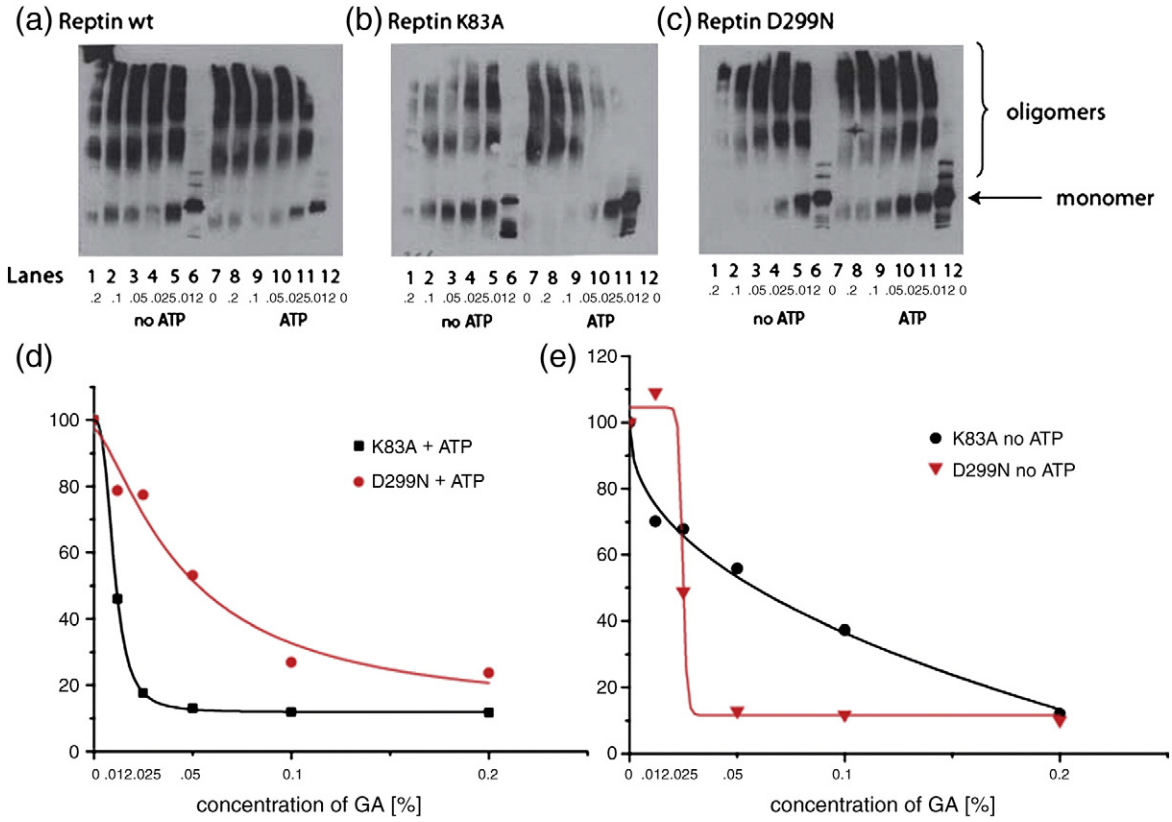

Fig. 7. Reptin mutants display distinct changes in ATP-dependent oligomerization as defined using a cross-linking assay. (a–c) Oligomerization of Reptin. Reactions were set up using (a) WT Reptin, (b) Reptin^{K83A}, and (c) Reptin^{D299N} mutant proteins. A titration of glutaraldehyde (from 0.012% to 0.2%) in the absence or presence of ATP was followed by immunoblotting for changes in the extent of oligomerization of Reptin from the monomeric state (arrow). (d and e) Quantitation in the changes in the extent of monomeric oligomerization of Reptin^{K83A} and Reptin^{D299N} mutant proteins in the absence or presence of ATP.

binding K83A mutation is dominant over the gain-of-ATP binding D299N mutation, with respect to AGR2 binding. Together, these data establish that Reptin can bind directly to AGR2 and that this interaction is likely to be specific since the ATP binding domains and in turn the conformation of Reptin play a role in driving the stability of the AGR–Reptin complex. Having validated one regulatory determinant in Reptin that regulates its stable binding to AGR2, we next evaluated whether we could identify determinants in AGR2 that mediate its stable binding to Reptin.

The divergent substrate-binding loop in the AGR2 superfamily forms the dominant Reptin binding interface

A significant proportion of the human proteome is composed of intrinsically disordered peptides and linear domains that form docking sites for protein–protein interactions.[37] As such, we used an overlapping peptide library derived from the AGR2 open reading frame to determine whether any linear domain/peptide docking sites exist for Reptin within the AGR2 protein sequence. The overlapping peptide library was composed of 15 amino acids with 10 amino acid overlaps, and each peptide contained an N-terminal biotin-SGSG spacer (Fig. 9a). The incubation of the biotinylated peptides derived from AGR2 with human cell lysates containing endogenous Reptin resulted in the specific binding of Reptin to one peptide motif, named peptide 10 (Fig. 9b). Intriguingly, this peptide motif overlaps with the previously identified unique surface loop in the AGR2 gene family (Fig. 9cii). This family is composed of the founder gene Erp18 and the AGR2 ortholog AGR3, which have both appeared in the vertebrate lineage and have not undergone gene expansion since their appearance in vertebrates.[18] The position in the three-dimensional structure of the divergent loop extension containing the sequence from AGR2 was modeled into the Erp18 crystal structure[38] (Fig. 9ci, red), and it has been proposed that this divergent surface loop could form a substrate docking site for distinct interacting proteins in this Erp18/AGR2/AGR3 family.[39] The sequence

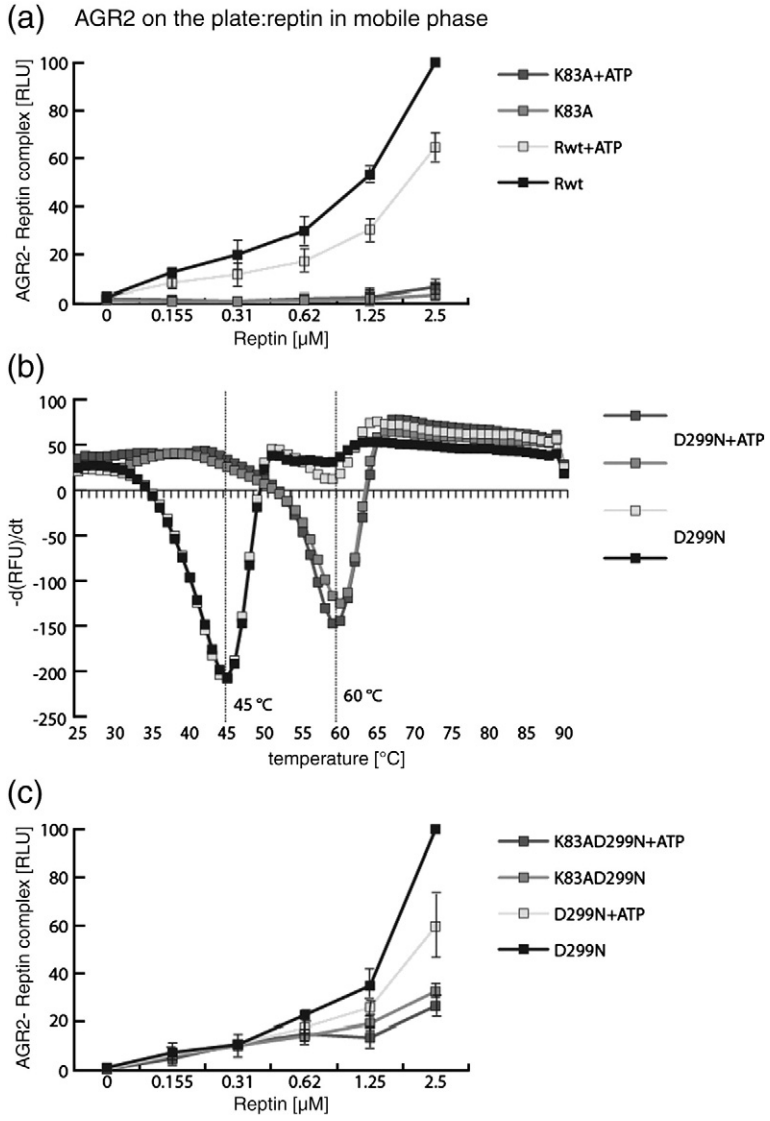

Fig. 8. The effects of ATP binding site mutations in Reptin on binding to AGR2. (a). The effects of the Walker A site mutation on the Reptin–AGR2 protein complex. Reactions were set up using (i) WT Reptin or (ii) Reptin^{K83A} in which AGR2 is in the solid phase and Reptin is in the mobile phase. The amount of Reptin bound was quantified with antibodies specific for Reptin protein titrated in the mobile phase using chemiluminescence. The data are plotted as the extent of protein–protein complex formation (in relative luminescence units) as a function of increasing protein in the mobile phase (in micromolar concentrations). (b). Reptin^{D299N} unfolding as a function of temperature change in the absence and in the presence of ligand. SYPRO Orange fluorescence was used to measure the thermal unfolding events between 20 °C and 89 °C, and experiments were done in triplicate in the absence or presence of ATP. The raw data were plotted as the gradient of protein unfolding was plotted against the temperature gradient to obtain the midpoint temperature of transition (T_m) in the absence and in the presence of ATP. (c) The effects of the Walker B site mutation and double ATP site mutations on the Reptin–AGR2 protein complex. Reactions were set up using (i) Reptin^{D299N} or (ii) Reptin$^{D299N/K83A}$ mutant proteins in which AGR2 is in the solid phase and the amount of Reptin or bound was quantified with antibodies specific for Reptin titrated in the mobile phase using chemiluminescence. The data are plotted as the extent of protein–protein complex formation (in relative luminescence units) as a function of increasing protein in the mobile phase (in micromolar concentrations).

of amino acids in this divergent loop in the Erp18/AGR2/AGR3 protein family is shown in Fig. 9cii.

Alanine scan and truncation mutagenesis were performed on peptides containing the surface loop (Fig. 10a). The data reveal that most amino acid residues from 104-FVLLNLVY-111 play a rate-limiting role in binding to Reptin, as their mutation to alanine attenuates Reptin binding to AGR2 (Fig.

(a) AGR2 spanning peptides

1. llvalsytlardttv
2. rdttvkpgakkdtkd
3. kdtkdsrpklpqtls
4. pqtlsrgwgdqliwt
5. qliwtqtyeealyks
6. alyksktsnkplmii
7. plmiihhldecphsq
8. cphsqalkkvfaenk
9. faenkeiqklaeqfv
10. aeqfvllnlvyettd
11. yettdkhlspdgqyv
12. dgqyvprimfvdpsl
13. vdpsltvraditgry
14. itgrysnrlyayepa
15. ayepadtallldnmk
16. ldnmkkalkllktel

(b)

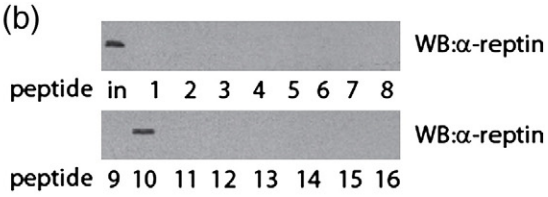

(c)

i.

ii.

```
AGR2            -MEKIPVSAFLLLVALSYTLARDTTVKPGAKKDTKDSRPKLPQTLSRGWGDQLIWTQTYE 59
AGR3            MMLHSALGLCLLLVTVSSNLA--IAIK-------KEKRP--PQTLSRGWGDDITWVQTYE 49
ERP18           -METRPRLGATCLLGFSFLLLVISSDG--------------HNGLGKGFGDHIHWR-TLE 44
                 *   .      *: .*  *    :                 : *.:*:**.: *  * *

AGR2            EALYKSKTSNKPLMIIHHLDECPHSQALKKVFAENKEIQKLAE-QFVLLNLVYET--TDK 116
AGR3            EGLFYAQKSKKPLMVIHHLEDCQYSQALKKVFAQNEEIQEMAQNKFIMLNLMHET--TDK 107
ERP18           DGKKEAAASGLPLMVIIHKSWCGACKALKPKFAESTEISELSH-NFVMVNLEDEEEPKDE 103
                :.   :  *  ***:* * . *  .:***  **:. **.:::. :*:::**  *   .*:

AGR2            HLSPDGQYVPRIMFVDPSLTVRADITGRYSNRLYAYEPADTALLLDNMKKALKLLKTEL- 175
AGR3            NLSPDGQYVPRIMFVDPSLTVRADIAGRYSNRLYTYEPRDLPLLIENMKKALRLIQSEL- 166
ERP18           DFSPDGGYIPRILFLDPSGKVHPEIINENGNPSYKYFYVSAEQVVQGMKEAQERLTGDAF 163
                .:**** *:***:*:*** .*:.:* .. .*  * *   .   :::.**:* . :  :

AGR2            ---------
AGR3            ---------
ERP18           RKKHLEDEL 172
```

Fig. 9. Identification of a specific binding site for Reptin on AGR2. (a) Human cell lysates expressing Reptin were incubated in a buffer containing the indicated biotinylated peptides (peptides 1–16 of human AGR2) coupled to streptavidin beads. The amount of Reptin bound was evaluated by immunoblotting the bound fractions as indicated in panel (b): "in" indicates input fraction, and the numbers 1–16 represent the peptide sequences in part (a). (c) [i] Homology model of the position of the divergent peptide loop from AGR2 that has the Reptin binding site based on the structure of the AGR2 ortholog Erp18 (Protein Data Bank code 2K8V). [ii]. Sequences in the divergent loop between AGR2, AGR3, and ERP18 proteins.

10b, lanes 4–7 and 9–11); the exceptional amino acid is N108 (lane 8). Alanine substitution of residues outwith this region does not attenuate Reptin binding to the peptides (Fig. 10b, lanes 1–3 and 12–15). Truncation mutagenesis also confirmed that this loop motif forms the specific interface for Reptin. C-terminal truncations from E111 to D114 do not reduce Reptin binding (Fig. 10b, lanes 16–19). However, the removal of Y111 reduces Reptin binding (Fig. 10b, lanes 20–22). This defines the C-terminal end of the Reptin binding site on the AGR2 peptide. Similarly, the N-terminal regions in the loop peptide were also truncated to define the N-terminal residues in the peptide that are important for binding to Reptin. The deletion of A101 to Q103 did not reduce Reptin binding (Fig. 10b, lanes 23–25). However, deletion of F104 reduced Reptin binding (Fig. 10b, lanes 26–39), highlighting the N-terminal residue required for binding to Reptin. The minimal peptide that exhibited binding to Reptin was 8 amino acids long (104-FVLLNLVY-111; Fig. 10b, lane 34), and the peptide displayed reduced binding to Reptin when the F104A or Y111A mutation was introduced (Fig. 10b, lanes 35 and 36 *versus* lane 34).

This divergent loop in AGR2 from 104–111 (Fig. 9c) might mediate specificity in its interactions with potential partner proteins. We examined this by evaluating whether the peptide derived from this loop in AGR3 (Fig. 9cii) bound with higher or lower affinity to Reptin. The peptide used from AGR3 had the sequence QNKFIMLNLMHETTD, and it did not bind Reptin (Fig. 10b, lane 37), compared with the AGR2 sequence AEQFVLLNLVYETTD, which did bind Reptin (Fig. 10b, lane 1 or lane 41). Mutating the KF in AGR3 to the QF present in AGR2 did not restore AGR3 peptide binding to Reptin (Fig. 10b, lane 38). However, introducing the H-to-Y mutation in the C-terminal region of the AGR3 peptide restored its binding to Reptin (Fig. 10b, lane 39 *versus* lane 37).

We finally evaluated whether inactivating mutation of full-length AGR2 protein in this divergent loop (based on the peptide screens in Fig. 10) reduced the interaction between Reptin and AGR2. We did not delete this loop as this might make gross mutations that alter the structure of the AGR2 protein. The peptide mapping data indicated that mutation of seven of eight residues could attenuate the binding of Reptin to AGR2 peptides, suggesting that the entire peptide contains side chains making important contacts with a potential peptide-binding groove in Reptin protein. As such, it might not be possible to make single point mutations on the full-length AGR2 protein if the structure of the constrained loop would require multiple mutations in the loop to attenuate the stability of the full-length Reptin–AGR2 protein complex. Nevertheless, we first focused on making two single point mutations in residues F104 and Y111, because these two residues form the N-terminal and C-terminal ends of the peptide binding between Reptin and the AGR2 peptide and these are bulky hydrophobic residues that might contribute significantly to the stability of the full-length AGR2–Reptin protein complex.

With the use of ELISA binding assays where AGR2 is immobilized in the solid phase, mutation of full-length AGR2 at codon 111 (Y to A) did not reduce the stability of the Reptin–AGR2 complex (Fig. 11b) and the $AGR2^{Y111A}$ mutant protein still retained destabilization in the presence of ATP similar to WT AGR2 (Fig. 11b). However, the $AGR2^{F104A}$ mutant protein was substantially destabilized in its binding to Reptin (Fig. 11b), indicating that the F104 residue forms an important contact point for Reptin in the context of the full-length protein complex. When Reptin was first immobilized in the solid phase, the $AGR2^{Y111A}$ mutant protein was reduced in Reptin binding and the $AGR2^{F104A}$ mutant protein was substantially destabilized in its binding to Reptin (Fig. 11a).

Discussion

Defining regulatory motifs in Reptin that regulate binding to AGR2

AGR2 is a prometastatic and p53 inhibitory protein involved in a range of oncogenic pathways, such as tamoxifen resistance and cell migration, as well as additional biological functions in limb regeneration and inflammatory responses.[5,10,12,19] Despite the wealth of data accumulating on AGR2, there are no validated interacting proteins for the AGR2 protein in human cells, with only the newt receptor PROD1 identified as an AGR2-interacting protein in yeast two-hybrid that functions in newt limb regeneration.[10] In this current work, we report on yeast two-hybrid interactors for AGR2 from a human cDNA library, one of which (Reptin) was evaluated using biochemical approaches for whether it formed a bona fide interaction with the AGR2 protein. In order to validate the interaction between the two proteins, we set out to determine whether we could identify limiting determinants in both AGR2 and Reptin proteins, whose characteristics would allow us to measure the validity of the potential protein–protein interaction. In the case of Reptin, we exploited its major functional motif; its two ATP binding sites. In the case of AGR2, because there is no identified ligand binding domain, we exploited the likelihood that small linear domains/unstructured motifs might mediate a specific interaction between AGR2 and Reptin. Our data indeed demonstrate that the ATP binding motifs of Reptin and the proposed substrate-binding loop of AGR2

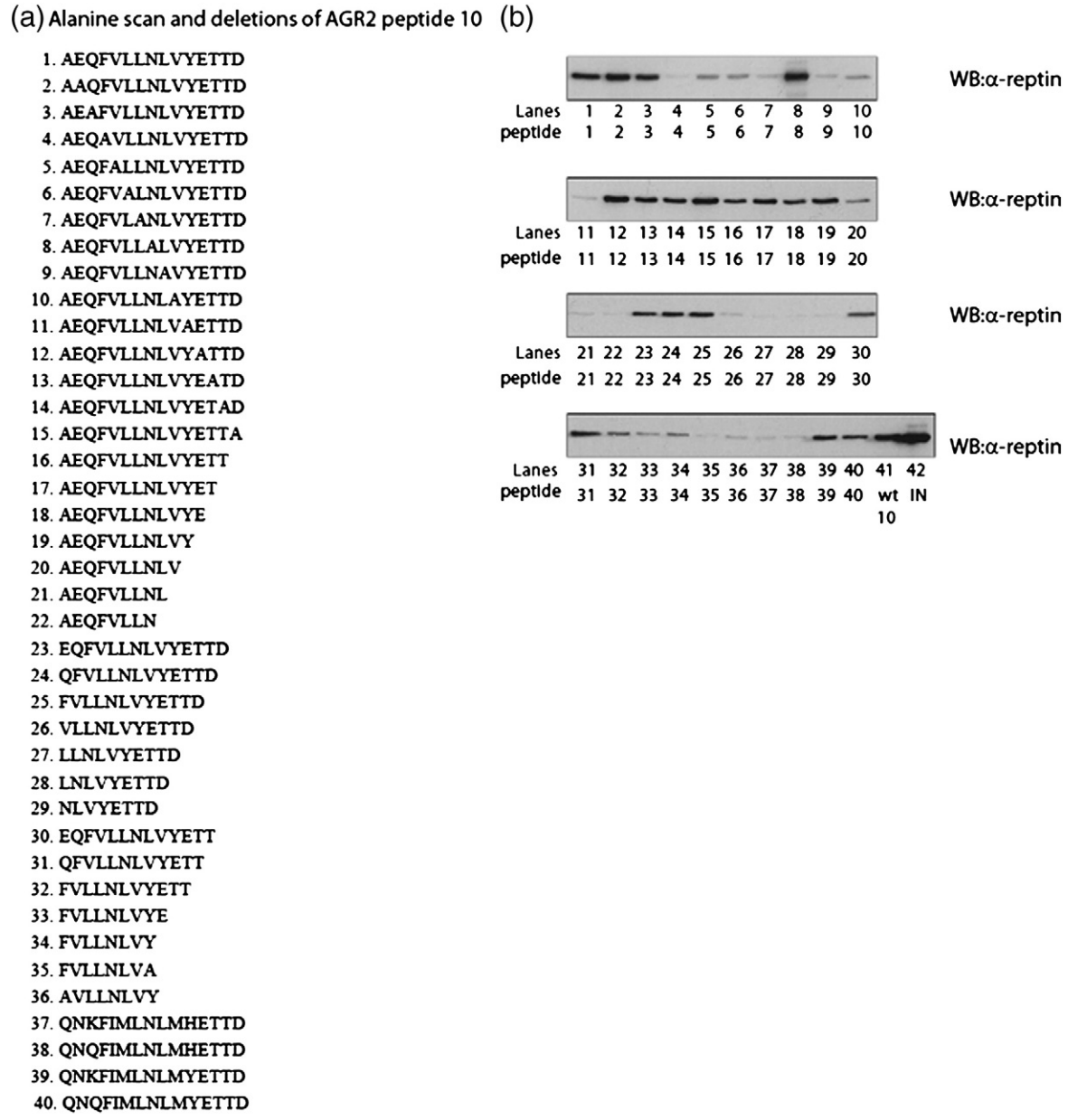

Fig. 10. Identification of key residues that stabilize the AGR2 peptide–Reptin complex. (a) Peptides 1–36 represent modifications in peptide 10 (Fig. 9), including C-terminal and N-terminal truncations and alanine-substituted mutants. Peptides 37–40 represent the divergent loop in the AGR2 ortholog AGR3 (peptide 37 is the AGR3 sequence and 38–40 mutations in this sequence). (b) Human cell lysates expressing Reptin were incubated in a buffer containing the indicated biotinylated peptides [as in panel (a); peptides 1–40 of human AGR2 or AGR3] coupled to streptavidin beads. The amount of Reptin bound was evaluated by immunoblotting the bound fractions as indicated in lanes 1–40. Lane 41 contains the positive control peptide 41, and lane 42 is the input lysate [IN].

are determinants that drive a specific complex between AGR2 and Reptin proteins.

The biochemical integrity of Reptin was measured with respect to its ATP binding activity using WT and ATP binding site mutants of the protein and included the following: (i) increases in mass as defined by light scattering in the presence of ATP; (ii) classic thermal unfolding transition in the presence of ATP; (iii) ATP binding activity using nitrocellulose filter binding assays; (iv) ATP binding quantified as defined by changes in oligomerization potential using chemical cross-linkers; and (v) ATP-dependent changes in binding to AGR2. In these cases, there was only one experimental discrepancy: the Reptin^{K83A} mutant protein was completely defective in ATP binding as defined using the filter binding assay. However, this

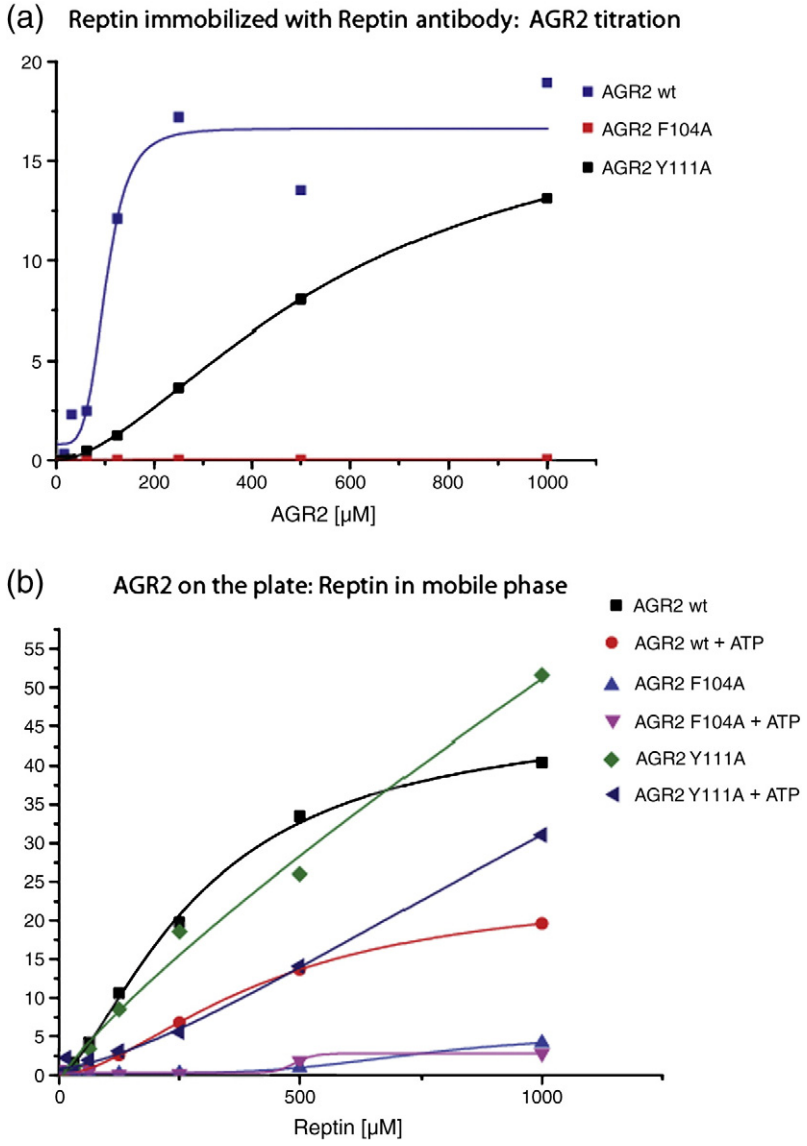

Fig. 11. The effects of AGR2 loop mutations on the stability of the Reptin–AGR2 complex. (a and b) Reactions were set up using WT AGR2, AGR2^{Y111A}, and theAGR2^{F104A} mutant proteins in which (a) Reptin is in the solid phase or (b) AGR2 is in the solid phase in the absence and in the presence of ATP. The amount of Reptin or AGR2 bound was quantified with antibodies specific for either protein titrated in the mobile phase using chemiluminescence. The data are plotted as the extent of protein–protein complex formation (in relative luminescence units) as a function of increasing protein in the mobile phase (in micromolar concentrations).

Reptin^{K83A} mutant protein was more responsive in ATP-mediated oligomerization than WT Reptin using the chemical cross-linking assay. This discrepancy in the ATP nitrocellulose filter binding assay might involve a potential inactivation of Reptin^{K83A} mutant protein ATP binding activity when it is adsorbed to the nitrocellulose filter and washed at 0 °C. The protein binding assays, thermal shifts, and the oligomerization assay are evaluated in solution at room temperature or higher. The ATP filter binding assay is very sensitive to temperature as this assay involves exploiting the difference between ATP and target protein in their hydrophobic interactions with the nitrocellulose filter at low temperatures.[40] Thus, the lower temperatures required for wash buffer in this assay might alter the affinity of ATP for the Reptin^{K83A} mutant protein. Indeed, our continuing characterization indicates that the oligomerization of WT Reptin is dependent on temperature, especially at very low temperatures, and this might also underestimate the ATP binding function of the Reptin^{K83A} mutant protein.

In contrast to the Walker A K83A mutant that essentially acts as a loss-of-function mutation with

respect to ATP binding, the Walker B mutant Reptin^{D299N} mutant protein was more active than WT Reptin in ATP binding using the nitrocellulose filter binding assay, more responsive to ATP in the oligomerization cross-linking assay, and more intrinsically thermoresistant in the thermal-shift assays even without ATP inclusion. Because there are two ATP binding sites for Reptin, it can be implied that the ATP binding function for both Reptin^{K83A} and Reptin^{D299N} mutant proteins could be regulated through an allosteric effect of one site on the other remaining active motif. Indeed, with the use of the double ATP binding site mutant, it is established that the K83A mutation is dominant over the D299N mutation with respect to AGR2 binding (Fig. 8c), suggesting that an allosteric effect between the two sites does exist. Although there is no high-resolution structure available for Reptin, a fragment of its ortholog Pontin has been crystallized[41] and is summarized in Fig. 6a. The ATP binding motifs are proximal, being poised by two structural lobes, and the proximity of the ATP binding motifs to each other might alter allosterically the ATP binding function of Reptin.

Prior to the current work, there have been minimal studies on potential allostery in the ATP binding properties of Reptin. One study reported that mutating the Reptin ATP binding site (D299N) did not inhibit the ATP binding function of the mixed Pontin–Reptin oligomer[34] and that ATP did not change the oligomeric state of WT Reptin.[34] This are in contrast with our data showing that the WT Reptin increases in apparent mass defined using light scattering and that our preparations of Reptin^{D299N} mutant protein display elevated intrinsic thermostability, elevated ATP binding, and a different response to ATP-dependent oligomerization as defined by cross-linking. These might be due to differences in the protein concentration or temperatures we have used in light scattering or cross-linking experiments compared with the gel-filtration method used in the prior report. In addition, our purified recombinant Reptin preparations are untagged, whereas the prior report utilized His-tagged protein.[34] Although a tag is often thought to be neutral, it can sometimes have an effect on a protein; indeed, this is specifically the case for Reptin. When we initially used a GST-tagged Reptin protein in our biochemical characterizations, it displayed an activated rather than an attenuated binding affinity for AGR2 protein in the presence of ATP (unpublished data). As a result, we only used untagged recombinant Reptin in this current work. Together, these data provide a proof of concept that a protein–protein interaction between Reptin and a target protein can be modified allosterically by the ATP binding motifs of the protein. How these affect other Reptin–protein interactions, including Pontin, APPL1/2, telomerase, or Tip60, as well as helicase activities, remains to be determined.

Defining amino acid motifs in AGR2 that form a docking site for Reptin

Having identified determinants in Reptin that contribute to its stable binding of AGR2, we next determined whether determinants in AGR2 that mediate its binding to Reptin could be identified. AGR2 is a member of the PDI superfamily that contains thioredoxin/PDI homology folds (CxxC or CxxS motif). These proteins can function similar to molecular chaperones to regulate protein folding via regulation of disulfide-bond formation.[18] Proteins with a CxxC motif, such as Erp57, have been shown to have their interactome trapped by using the CxxS artificial mutant that apparently traps normal *in vivo* interactors with the mutant Erp57 protein.[39] This PDI motif within AGR2 is the CxxS motif characteristic of a PDI subclass of molecular chaperones that use this motif as a redox catalyst able to form a covalent complex with other target proteins, similar to how Mucin has been reported to with AGR2.[19] In our evaluations, the AGR2^{C81A} mutant protein is able to form a Reptin complex and WT AGR2 (data not shown), indicating that the PDI thioredoxin fold of AGR2 is not directly involved as a rate-limiting determinant in binding stably to Reptin. As such, we set out to evaluate how other determinants in AGR2 protein sequence might be exploited to determine whether Reptin has a specific docking site on the protein.

One of the recent paradigm shifts in the field of protein science is the realization that a large percentage of the protein sequence information is not only in stable globular domains but also in small linear motifs, linear domains, or intrinsically unstructured domains that form small docking sites for a protein with a peptide-binding groove.[37] Proteins that have a large percentage of the protein sequence information in an unstructured landscape include regulatory proteins, such as p53, that sit in signaling hubs that form a scaffold for the formation of large numbers of diverse, low-affinity, and transient but specific protein–protein interactions.[42] These linear motifs can also be embedded within structural domains themselves. In the case of AGR2, we utilized an overlapping peptide library that represents the primary linear amino acid sequence information of the protein with the aim of determining whether or not there are any linear motifs that can form a stable complex with full-length Reptin. Using this approach, we were in fact able to detect a linear domain that can bind stably to Reptin, and this was localized by mutagenesis with amino acids 104–111 on the AGR2 primary sequence. This region is notable in that it represents a divergent loop in the Erp18/AGR2/AGR3 family of proteins that has been proposed to represent substrate binding sites for the molecular chaperone function of the protein.[39] That amino acids 104–111 from AGR2 form the minimal docking site

peptide that can bind to Reptin and that the AGR2 mutant protein Y104A completely loses the ability to bind stably to Reptin are consistent with this substrate docking model. What this model proposes, however, is that perhaps AGR2 can bind to Reptin at this loop and in turn regulate Reptin's many functions by chaperoning: ATPase activity, ATP binding, helicase functions, telomerase/Pontin binding, APPL1/2 binding, TIP60 interactions, and other related protein signaling functions. As we can convert the AGR3 peptide loop to Reptin binding protein by generating an H111–Y111 conversion (Fig. 10), we are currently generating an AGR3 protein with a WT AGR2 loop to determine if we can switch AGR3 to a Reptin binding protein *in vitro* and in cells. As AGR3 has a distinct subcellular localization from AGR2 (unpublished data; with AGR3 being more mitochondrial and of the plasma membrane), we are also evaluating whether a change in this loop on AGR3 changes its intracellular localization.

In summary, we report on the first well-validated protein–protein interaction for the pro-oncogenic protein AGR2. Reptin was identified as an AGR2 binding protein in a yeast two-hybrid screen and validated as an AGR2 binding protein in human cells. Limiting determinants for both AGR2 and Reptin were identified using *in vitro* protein enzymological approaches; AGR2 uses a divergent peptide substrate-binding loop to bind to Reptin, and Reptin in turn uses two allosterically interacting ATP binding motifs to control its binding activity toward AGR2. Because Reptin can also function as a prometastatic transcription protein and we show for the first time that Reptin can be overproduced in human breast cancers (Fig. 1b), future research in cell-based studies will inform whether AGR2 uses its substrate-binding loop to chaperone Reptin into inactive and activated transcriptional states and/or whether the allosteric ATP binding motifs of Reptin regulate AGR2 function as a prometastatic factor in cancer. The sets of AGR2 and Reptin mutants that were generated will be useful for such cellular assays. In addition, as both Reptin and AGR2 can be thought of as potential anticancer drug targets due to their prometastatic functions, biochemically based screening assays that utilize the substrate-binding loop of AGR2 or ATP binding motifs of Reptin might form biochemical assays for the development of small molecules that regulate this protein–protein complex *in vivo*.

Materials and Methods

Reagents

Fetal bovine serum was from Autogen Bioclear. Dulbecco's modified Eagle's medium and RPMI were provided by Gibco. Trypsin/EDTA solution and penicillin–streptomycin were supplied by Invitrogen. Attractene was from Qiagen. Hybond-C nylon membrane for immunoblotting was supplied by Amersham Pharmacia Biotech. ATP-γS [adenosine 5′-*O*-(3-thiotriphosphate)] and ATP (adenosine 5′ thiotriphosphate) were from Calbiochem. The following antibodies were used: anti-HA tag monoclonal antibody and anti-Myc tag rabbit polyclonal antibody (Sigma), anti-His tag monoclonal antibody (Novagen), anti-AGR2 monoclonal antibody (Abnova), anti-AGR2 polyclonal antibody (Moravian Biotechnologies), and anti-Reptin rabbit polyclonal antibody (Abnova). Secondary antibodies were from Dako Cytomation. All peptides were synthesized with a biotin tag and an SGSG spacer at the N-terminus and were from Mimotopes.

Plasmids

The human HA-tagged Reptin and AGR2 for mammalian and bacterial expression were cloned into Gateway Entry clones (Invitrogen) for subsequent use. The human Reptin sequence for cloning into a new *E. coli* expression system was amplified using the following primers: forward primer 5′-GGGGACAAGTTTGTACAAAAAAG-CAGGCTTCCTGGAAGTTCTGTTCCAGGGGCCC ATGGCAACCGTTACAGCCACAACC-3′ and reverse primer 5′-GGGGACCACTTTGTACAAGAAAGCTGGGTC-CAGGAGGTGTCCATGGTCTCG-3′. The forward primer had a PreScission protease cleavage site inserted. Following amplification, the polymerase chain reaction (PCR) product was first inserted into pDONR201 and then into pDEST-15 using Gateway technology (Invitrogen) to generate GST-tagged Reptin. Myc-tagged Reptin and Pontin for mammalian expression were a kind gift from Dr Marta Miaczynska (International Institute of Molecular and Cell Biology, Warsaw, Poland). Point mutations in the abovementioned plasmids were introduced using the following primers: for the Reptin D299N mutant, forward primer 5′-GAGTGCTGTTCATCAACGAGGTCCA-CATGC-3′ and reverse primer 5′-GCATGTGGACCTCGTT-GATGAACAGCACTC-3′; for the Reptin K83A mutant, forward primer 5′-GCACGGGGGCGACGGCCATCG-3′ and reverse primer 5′-CGATGGCCGTCGCCCCCGTGC-3′; for generating the AGR2 F104A mutant, forward primer 5′-TGGCAGAGCAGGCTGTCCTCCTC-3′ and reverse primer 5′-GAGGAGGACAGCCTGCTCTGCCA-3′; and for generating the AGR2 Y111A mutant, forward primer 5′-CCTCAATCTGGTTGCTGAAACAACTGAC-3′ and reverse primer 5′-GTCAGTTGTTTCAGCAACCAGATT-GAGG-3′.

Cell culture and transfection

H1299 and MCF7 cell lines were grown in RPMI or Dulbecco's modified Eagle's medium supplemented with 10% (v/v) fetal bovine serum and 1% (v/v) penicillin–streptomycin mix. Both cell lines were maintained at 5% CO_2. Cells were seeded 24 h prior to transfection, and DNA was transfected using Attractene, following standard protocol. Cells were lysed in immunoprecipitation

lysis buffer as described below. Clarified cell lysates were normalized for the protein concentration using the Bradford method.[43]

Western blotting

Samples were resolved by SDS-PAGE through 12% (w/v) Tris-glycine gels. Gels were transferred onto nitrocellulose membranes in transfer buffer [0.192 M glycine, 25 mM Tris, and 20% (v/v) methanol] at 300 mA for 90 min. Following transfer, the membrane was stained with black Indian ink to confirm even protein transfer and loading. Membranes were blocked for 1 h in 5% milk-PBST [5% (w/v) dried skimmed milk and 0.1% (v/v) Tween 20 in phosphate-buffered saline]. Membranes were then incubated with primary antibodies overnight, followed by secondary antibodies conjugated to horseradish peroxidase for 1 h. Bound antibody was detected by enhanced chemiluminescence, and immunoblots were quantified using ImageJ. When indicated, gels were stained with Coomassie blue R-450 (Sigma; 5% Coomassie blue in 40% methanol and 10% acetic acid). Lysates and preparation from primary breast cancer and normal tissue samples have been previously described.[5,44]

Expression and purification of WT and mutant Reptin

GST-Reptin WT and mutants were expressed in BL21-AI (Invitrogen) and purified from soluble lysates using glutathione beads (GE Healthcare) according to the manufacturer's instructions. In detail, cells were lysed with 10% sucrose, 50 mM Tris, pH 8.0, 400 mM NaCl, 0.5% Triton X-100, 1 mM DTT, 1 mM benzamidine, 0.5 mg/ml lysozyme, and protease inhibitors for 30 min on ice and then sonicated. Lysate was incubated with glutathione beads for 90 min at 4 °C with rotation, followed by thorough washes with 20 mM Hepes, pH 7.5, 1 M NaCl, 1 mM DTT, and 1 mM benzamidine; thorough washes with 20 mM Hepes, pH 7.5, 0.05 mM NaCl, 1 mM DTT, and 1 mM benzamidine; and a final wash with 50 mM Tris–HCl, pH 8.0, 1 mM EDTA, 120 mM NaCl, and 1 mM DTT. The rigorous washes were required to remove nonspecifically bound proteins. Reptin protein was cleaved off the column using PreScission protease (GE Healthcare) into 50 mM Tris–HCl, pH 8.0, 1 mM EDTA, 120 mM NaCl, and 1 mM DTT and stored frozen in liquid nitrogen at 6–9 mg/ml.

Expression and purification of WT and mutant AGR2

His-tagged AGR2 was expressed in BL21-AI and purified using Ni^{2+}-nitrilotriacetic acid-agarose (Qiagen) according to the manufacturer's instructions. In detail, cells were lysed in a buffer containing 20 mM Tris–HCl, pH 8.0, 150 mM NaCl, 10 mM $MgCl_2$, 0.05% Tween 20, 10% glycerol, 20 mM imidazole, pH 8.0, and 0.1 mg/ml on ice for 30 min and then sonicated. Lysate was incubated with Ni-agarose (on rotary shaker at 4 °C for 1 h) and washed two times in lysis buffer and three times in lysis buffer with 40 mM imidazole, and then protein was eluted with lysis buffer containing 150 mM imidazole.

Thermal protein unfolding assay and light scattering

Thermal shifts

Extent of protein unfolding was measured using fluorescent SYPRO Orange dye (Invitrogen). Purified Reptin (5 μM) with or that without ATP was added in buffer containing 50 mM Tris–HCl, pH 8.0, 1 mM EDTA, 120 mM NaCl, and 1 mM DTT before the addition of SYPRO Orange. Samples were aliquoted onto a 96-well PCR plate and sealed with optical-quality sealing film (Bio-Rad). The rate of protein unfolding was measured using an iCycler iQ Real-Time PCR system (Bio-Rad) by heating samples from 20 °C to 90 °C at increments of 1 °C and with a 30-s incubation at each increment. Fluorescence intensity was measured using excitation/emission wavelengths of 485 nm/575 nm in relative light units, and thermal denaturation graphs were plotted as a function of the gradient of protein unfolding against the temperature gradient [d(RFU)/dT].

Light scattering

Light scattering was measured in a temperature-controlled Zetasizer Auto Plate Sampler. Buffer (50 mM Tris–HCL, pH 8.0, 1 mM EDTA, 120 mM NaCl, and 1 mM DTT) was filtered using 0.2 μM as a background control. The mean hydrodynamic radius, R_h, of Reptin was measured by DLS with a Zetasizer APS (Malvern Instruments, UK) equipped with a 50-mW laser light source of wavelength 830 nm. Scattering data were collected at a scattering angle of 90 ° for 10 s, repeated at least 12 times, and averaged. The experiments were repeated in triplicate. Autocorrelation data were fit to a model of a multiple-exponential form suitable for polydisperse solutions using the protein-specific software supplied with the instrument. This generated a distribution of particles by size. DLS is very sensitive to aggregation as scattering is a function of R_h to the sixth power. Size analysis was carried out on 50 μM Reptin in 50 mM Tris–HCl, pH 8.0, 1 mM EDTA, 120 mM NaCl, and 1 mM DTT at 10 °C. Samples were passed through a 0. 22-μm filter (Ultrafree-MC, Millipore, UK), centrifuged at 4 °C, 12*g*, prior to analysis.

Protein–protein interaction assays (ELISA)

Purified recombinant His-AGR2 (100 ng), Reptin (100 ng), anti-AGR2 monoclonal antibody (100 ng), anti-His monoclonal antibody (100 ng), and anti-Reptin antibody (100 ng) were immobilized on a microtiter plate 0.1 M $NaHCO_3$ buffer, pH 8.6, at 4 °C overnight. Excess protein was washed away in PBS containing 0.1% (v/v) Tween 20. Nonreactive sites were blocked using PBS containing 3% bovine serum albumin. A titration of the protein of interest (in the solid phase or mobile phase, as highlighted in each figure) with or that without ATP or ATP-γ-S as indicated in the legend to the figures was added in 1× reaction buffer [25 mM Hepes, pH 7.5, 50 mM KCl, 10 mM $MgCl_2$, 5% (v/v) glycerol, 0.1% (v/v) Tween 20, and 2 mg/ml bovine serum albumin] for 1 h at room temperature. After washing in PBS containing 0.1% (v/v) Tween 20, anti-His tag monoclonal, anti-Reptin polyclonal, and anti-AGR2 polyclonal antibodies were

added. The unbound primary antibody was washed away, and then the appropriate secondary antibody was added. After washing, electrochemical luminescence was quantified using a luminometer (Fluoroskan Ascent FL, Labsystems).

ATP filter binding assay

Reptin was incubated with 0.57 μCi γ-^{35}S-labeled ATP at 4 °C for 15 min in 20 μl of ATP binding assay buffer (20 mM Tris–HCl, pH 7.5, 70 mm KCl, and 1 mM $MgCl_2$). In some experiments, Reptin was further incubated with DNA fragments at 30 °C for 5 min in the same buffer. Samples were passed through nitrocellulose membranes (Millipore HA, 0.45 μm) at room temperature and washed rapidly with 20 volumes of ice-cold buffer T using a vacuum suction. The radioactivity remaining on the filter was monitored with a liquid scintillation counter (Perkin Elmer).

Peptide binding assays

H1299 cells were lysed in 0.1% Triton X-100 lysis buffer (50 mM Hepes, 0.1 mM EDTA, 150 mM NaCl, 10 mM NaF, 2 mM DTT, 0.1% Triton X-100, and 1× protease inhibitor mixture). Lysates were incubated with 40 μg/ml avidin for 30 min on ice. Then, lysates were precleared by incubation with streptavidin-agarose (Sigma) beads for 1 h. In the meantime, 0.4 μl of peptide was incubated with streptavidin-agarose (Sigma) beads in buffer W (100 mM Tris, pH 8.0, 150 mM NaCl, and 1 mM EDTA) for 1 h at room temperature with gentle rotation and then washed three times with the same buffer. Cleared lysate (0.2 mg) was then added to the peptide-coated beads in a final volume of 200 μl and rotated at room temperature. After 1 h, beads were washed once with buffer W, four times with PBS + 0.2% Triton X-100, and once more with buffer W. Sample buffer was then added to the beads, and bound protein was eluted by boiling for 3×5 min and immunoblotted to quantitate the amount of Reptin bound.

Immunoprecipitation of protein complexes from cell lysates

The cells were harvested and lysed in co-immunoprecipitation buffer (25 mM Tris, pH 7.2, 0.4 M KCl, 1% NP-40, and 1 × protease inhibitor mixture). The lysates were precleared by incubation with Sepharose CL 4B (Sigma-Aldrich) and protein G-Sepharose™ 4 FastFlow (GE Healthcare) at 4 °C with rotation for 40 min. Subsequently, 1 μg of primary antibody (K47 polyclonal specific for AGR2) was incubated with 600 μg of protein in the precleared lysate in a final volume of 200 μl for 2 h at 4 °C with gentle rotation. A total of 15 μl of protein G-Sepharose was then added to the abovementioned samples and incubated for 1 h at 4 °C with gentle rotation. Supernatant (flow-through) was collected, and the beads were washed four times with 500 μl of co-immunoprecipitation buffer. Samples were eluted by adding 50 μl of 4 × SDS sample buffer containing 0.2 M DTT and incubating at 95 °C for 5 min. The eluate was then collected and analyzed by Western blotting.

His-ubiquitin conjugate pull-down assay

Cells co-transfected with HA-tagged Reptin or p53 and/or human MDM2 along with pCMV-His-ubiquitin, NEDD8, or SUMO plasmids for 24 h were incubated with 10 μM MG132 for 4 h and then harvested and washed in PBS before the addition of 6 ml of HUBMA (His-ubiquitin modification buffer A; 6 M guanidinium chloride, 0.1 M Na_2HPO_4/NaH_2PO_4, pH 8.0,10 mM Tris–HCl, and 10 mM 2-mercaptoethanol) and 5 mM imidazole. The lysate was homogenized using a 24-G syringe needle before adding 75 μl of Ni^{2+}-nitrilotriacetic acid-agarose beads and rotating at room temperature (21 °C) for 4 h. The beads were centrifuged at 2000 *g* for 5 min, and the supernatant was discarded before washing sequentially with 750 μl of HUBMA, HUBMB (8 M urea, 0.1 M Na_2HPO_4/NaH_2PO_4, pH 8.0, 10 mM Tris–HCl, and 10 mM 2-mercaptoethanol), HUBMC (8 M urea, 0.1 M Na_2HPO_4/NaH_2PO_4, pH 6.3, 10 mM Tris–HCl, and 10 mM 2-mercaptoethanol), HUBMC with 0.2% (v/v) Triton X-100, and finally HUBMC and 0.1% (v/v) Triton X-100. To the washed beads, 75 μl of His-ubiquitin elution buffer [0.2 M imidazole, 5% (w/v) SDS, 0.15 M Tris–HCl, pH 6.7, 10% (v/v) glycerol, and 0.72 M 2-mercaptoethanol] was added and incubated for 20 min at room temperature. A total of 75 μl of 2XSDS sample buffer was added to the eluted ubiquitin conjugates and subjected to Western blot analysis as indicated in the legend to Fig. 3.

Oligomerization assay using cross-linker

Recombinant WT or mutant Reptin protein (2 μg) with or without 1 mM ATP was mixed with serial twofold dilutions of glutaraldehyde, from 0.2% to 0%, in a total volume of 20 μl and incubated for 1 h at room temperature. The reaction was stopped with 10 μl of 1 M Tris, pH 8.0, sample buffer was added, and samples were boiled, separated using 8% SDS-polyacrylamide gel, and immunoblotted to detect monomeric and oligomeric Reptin.

Acknowledgements

B.V. was supported by the European Regional Development Fund through IGA MZCR NS/9812-4 and RECAMO CZ.1.05/2.1.00/03.0101. R.H. was supported with GACR P301/10/1615. This work was funded by Cancer Research UK Program Grant C483/A6354 (T.R.H.) and a Cancer Research UK PhD Studentship to M.M.M. (C483/A8033). We acknowledge our use of the Edinburgh Biophysical Characterization Facility (supported by the Scottish University Life Sciences Alliance and the Biotechnology and Biological Sciences Research Council).

References

1. Bradley, L., Wainstock, D. & Sive, H. (1996). Positive and negative signals modulate formation of the Xenopus cement gland. *Development*, **122**, 2739–2750.

2. Sive, H. & Bradley, L. (1996). A sticky problem: the Xenopus cement gland as a paradigm for anteroposterior patterning. *Dev. Dyn.* **205**, 265–280.
3. Thompson, D. A. & Weigel, R. J. (1998). hAG-2, the human homologue of the *Xenopus laevis* cement gland gene XAG-2, is coexpressed with estrogen receptor in breast cancer cell lines. *Biochem. Biophys. Res. Commun.* **251**, 111–116.
4. Fritzsche, F. R., Dahl, E., Pahl, S., Burkhardt, M., Luo, J., Mayordomo, E. *et al.* (2006). Prognostic relevance of AGR2 expression in breast cancer. *Clin. Cancer Res.* **12**, 1728–1734.
5. Hrstka, R., Nenutil, R., Fourtouna, I., Maslon, M. M., Naughton, C., Langdon, S. *et al.* (2010). The prometastatic protein anterior gradient-2 predicts poor prognosis in tamoxifen-treated breast cancers. *Oncogene*, **29**, 4838–4847.
6. Riener, M. O., Pilarsky, C., Gerhardt, J., Grutzmann, R., Fritzsche, F. R., Bahra, M. *et al.* (2009). Prognostic significance of AGR2 in pancreatic ductal adenocarcinoma. *Histol. Histopathol.* **24**, 1121–1128.
7. Fritzsche, F. R., Dahl, E., Dankof, A., Burkhardt, M., Pahl, S., Petersen, I. *et al.* (2007). Expression of AGR2 in non small cell lung cancer. *Histol. Histopathol.* **22**, 703–708.
8. Zhang, J. S., Gong, A., Cheville, J. C., Smith, D. I. & Young, C. Y. (2005). AGR2, an androgen-inducible secretory protein overexpressed in prostate cancer. *Genes Chromosomes Cancer*, **43**, 249–259.
9. Liu, D., Rudland, P. S., Sibson, D. R., Platt-Higgins, A. & Barraclough, R. (2005). Human homologue of cement gland protein, a novel metastasis inducer associated with breast carcinomas. *Cancer Res.* **65**, 3796–3805.
10. Kumar, A., Godwin, J. W., Gates, P. B., Garza-Garcia, A. A. & Brockes, J. P. (2007). Molecular basis for the nerve dependence of limb regeneration in an adult vertebrate. *Science*, **318**, 772–777.
11. Pohler, E., Craig, A. L., Cotton, J., Lawrie, L., Dillon, J. F., Ross, P. *et al.* (2004). The Barrett's antigen anterior gradient-2 silences the p53 transcriptional response to DNA damage. *Mol. Cell. Proteomics*, **3**, 534–547.
12. Wang, Z., Hao, Y. & Lowe, A. W. (2008). The adenocarcinoma-associated antigen, AGR2, promotes tumor growth, cell migration, and cellular transformation. *Cancer Res.* **68**, 492–497.
13. Murray, E., McKenna, E. O., Burch, L. R., Dillon, J., Langridge-Smith, P., Kolch, W. *et al.* (2007). Microarray-formatted clinical biomarker assay development using peptide aptamers to anterior gradient-2. *Biochemistry*, **46**, 13742–13751.
14. Fourtouna, I., Murray, E., Nicholson, J., Maslon, M. M., Pang, L., Dryden, D. & Hupp, T. R. (2009). The anterior gradient-2 pathway as a model for developing peptide-aptamer anti-cancer drug leads that stimulate p53 function. *Curr. Chem. Biol.* **3**, 124–137.
15. Fletcher, G. C., Patel, S., Tyson, K., Adam, P. J., Schenker, M., Loader, J. A. *et al.* (2003). hAG-2 and hAG-3, human homologues of genes involved in differentiation, are associated with oestrogen receptor-positive breast tumours and interact with metastasis gene C4.4a and dystroglycan. *Br. J. Cancer*, **88**, 579–585.
16. Liepinsh, E., Baryshev, M., Sharipo, A., Ingelman-Sundberg, M., Otting, G. & Mkrtchian, S. (2001). Thioredoxin fold as homodimerization module in the putative chaperone ERp29: NMR structures of the domains and experimental model of the 51 kDa dimer. *Structure (Camb.)*, **9**, 457–471.
17. Alanen, H. I., Williamson, R. A., Howard, M. J., Lappi, A. K., Jantti, H. P., Rautio, S. M. *et al.* (2003). Functional characterization of ERp18, a new endoplasmic reticulum-located thioredoxin superfamily member. *J. Biol. Chem.* **278**, 28912–28920.
18. Persson, S., Rosenquist, M., Knoblach, B., Khosravi-Far, R., Sommarin, M. & Michalak, M. (2005). Diversity of the protein disulfide isomerase family: identification of breast tumor induced Hag2 and Hag3 as novel members of the protein family. *Mol. Phylogenet. Evol.* **36**, 734–740.
19. Park, S. W., Zhen, G., Verhaeghe, C., Nakagami, Y., Nguyenvu, L. T., Barczak, A. J. *et al.* (2009). The protein disulfide isomerase AGR2 is essential for production of intestinal mucus. *Proc. Natl Acad. Sci. USA*, **106**, 6950–6955.
20. Kim, J. H., Kim, B., Cai, L., Choi, H. J., Ohgi, K. A., Tran, C. *et al.* (2005). Transcriptional regulation of a metastasis suppressor gene by Tip60 and beta-catenin complexes. *Nature*, **434**, 921–926.
21. Kim, J. H., Choi, H. J., Kim, B., Kim, M. H., Lee, J. M., Kim, I. S. *et al.* (2006). Roles of sumoylation of a reptin chromatin-remodelling complex in cancer metastasis. *Nat. Cell Biol.* **8**, 631–639.
22. Gallant, P. (2007). Control of transcription by Pontin and Reptin. *Trends Cell Biol.* **17**, 187–192.
23. Rashid, S., Pilecka, I., Torun, A., Olchowik, M., Bielinska, B. & Miaczynska, M. (2009). Endosomal adaptor proteins APPL1 and APPL2 are novel activators of beta-catenin/TCF-mediated transcription. *J. Biol. Chem.* **284**, 18115–18128.
24. Jha, S. & Dutta, A. (2009). RVB1/RVB2: running rings around molecular biology. *Mol. Cell*, **34**, 521–533.
25. Izumi, N., Yamashita, A., Iwamatsu, A., Kurata, R., Nakamura, H., Saari, B. *et al.* (2010). AAA+ proteins RUVBL1 and RUVBL2 coordinate PIKK activity and function in nonsense-mediated mRNA decay. *Sci. Signal.* **3**, ra27.
26. Venteicher, A. S., Meng, Z., Mason, P. J., Veenstra, T. D. & Artandi, S. E. (2008). Identification of ATPases pontin and reptin as telomerase components essential for holoenzyme assembly. *Cell*, **132**, 945–957.
27. Qi, D., Jin, H., Lilja, T. & Mannervik, M. (2006). *Drosophila* Reptin and other TIP60 complex components promote generation of silent chromatin. *Genetics*, **174**, 241–251.
28. Bellosta, P., Hulf, T., Balla Diop, S., Usseglio, F., Pradel, J., Aragnol, D. & Gallant, P. (2005). Myc interacts genetically with Tip48/Reptin and Tip49/Pontin to control growth and proliferation during *Drosophila* development. *Proc. Natl Acad. Sci. USA*, **102**, 11799–11804.
29. Bauer, A., Chauvet, S., Huber, O., Usseglio, F., Rothbacher, U., Aragnol, D. *et al.* (2000). Pontin52 and reptin52 function as antagonistic regulators of beta-catenin signalling activity. *EMBO J.* **19**, 6121–6130.
30. Ito, T., Chiba, T., Ozawa, R., Yoshida, M., Hattori, M. & Sakaki, Y. (2001). A comprehensive two-hybrid analysis to explore the yeast protein interactome. *Proc. Natl Acad. Sci. USA*, **98**, 4569–4574.

31. Huber, O., Menard, L., Haurie, V., Nicou, A., Taras, D. & Rosenbaum, J. (2008). Pontin and reptin, two related ATPases with multiple roles in cancer. *Cancer Res.* **68**, 6873–6876.
32. Rousseau, B., Menard, L., Haurie, V., Taras, D., Blanc, J. F., Moreau-Gaudry, F. *et al.* (2007). Overexpression and role of the ATPase and putative DNA helicase RuvB-like 2 in human hepatocellular carcinoma. *Hepatology*, **46**, 1108–1118.
33. Li, W., Zeng, J., Li, Q., Zhao, L., Liu, T., Bjorkholm, M. *et al.* (2010). Reptin is required for the transcription of telomerase reverse transcriptase and over-expressed in gastric cancer. *Mol. Cancer*, **9**, 132–142.
34. Puri, T., Wendler, P., Sigala, B., Saibil, H. & Tsaneva, I. R. (2007). Dodecameric structure and ATPase activity of the human TIP48/TIP49 complex. *J. Mol. Biol.* **366**, 179–192.
35. Lo, M. C., Aulabaugh, A., Jin, G., Cowling, R., Bard, J., Malamas, M. & Ellestad, G. (2004). Evaluation of fluorescence-based thermal shift assays for hit identification in drug discovery. *Anal. Biochem.* **332**, 153–159.
36. Hanson, P. & Whiteheart, S. (2005). AAA+ proteins: have engine, will work. *Nat. Rev. Mol. Cell Biol.* **6**, 519–529.
37. Uversky, V. N., Oldfield, C. J. & Dunker, A. K. (2008). Intrinsically disordered proteins in human diseases: introducing the D2 concept. *Annu. Rev. Biophys.* **37**, 215–246.
38. Rowe, M. L., Ruddock, L. W., Kelly, G., Schmidt, J. M., Williamson, R. A. & Howard, M. J. (2009). Solution structure and dynamics of ERp18, a small endoplasmic reticulum resident oxidoreductase. *Biochemistry*, **48**, 4596–4606.
39. Jessop, C. E., Watkins, R. H., Simmons, J. J., Tasab, M. & Bulleid, N. J. (2009). Protein disulphide isomerase family members show distinct substrate specificity: P5 is targeted to BiP client proteins. *J. Cell Sci.* **122**, 4287–4295.
40. Oehler, S., Alex, R. & Barker, A. (1999). Is nitrocellulose filter binding really a universal assay for protein–DNA interactions? *Anal. Biochem.* **268**, 330–336.
41. Torreira, E., Jha, S., Lopez-Blanco, J. R., Arias-Palomo, E., Chacon, P., Canas, C. *et al.* (2008). Architecture of the pontin/reptin complex, essential in the assembly of several macromolecular complexes. *Structure*, **16**, 1511–1520.
42. Nicholson, J. & Hupp, T. R. (2010). The molecular dynamics of MDM2. *Cell Cycle*, **9**, 1878–1881.
43. Loffler, B. M. & Kunze, H. (1989). Refinement of the Coomassie brilliant blue G assay for quantitative protein determination. *Anal. Biochem.* **177**, 100–102.
44. Craig, A. L., Burch, L., Vojtesek, B., Mikutowska, J., Thompson, A. & Hupp, T. R. (1999). Novel phosphorylation sites of human tumour suppressor protein p53 at Ser20 and Thr18 that disrupt the binding of mdm2 (mouse double minute 2) protein are modified in human cancers. *Biochem. J.* **342**, 133–141.

Review

Cell PRESS

Article Series: Thirty years of p53

Drug discovery and mutant p53

Magda M. Maslon and Ted R. Hupp

University of Edinburgh, Institute of Genetics and Molecular Medicine, Cell Signalling Unit, Cancer Research UK p53 Signal Transduction Group, Edinburgh EH4 2XR, UK

Missense mutations in the p53 gene are commonly selected for in developing human cancer cells. These diverse mutations in p53 can inactivate its normal sequence-specific DNA-binding and transactivation function, but these mutations can also stabilize a mutant form of p53 with pro-oncogenic potential. Recent multidisciplinary advances have demonstrated exciting and unexpected potential in therapeutically targeting the mutant p53 pathway, including: the development of biophysical models to explain how mutations inactivate p53 and strategies for refolding and reactivation of mutant p53, the ability of mutant p53 protein to escape MDM2-mediated degradation in human cancers, and the growing 'interactome' of mutant p53 that begins to explain how the mutant p53 protein can contribute to diverse oncogenic and pro-metastatic signaling. Our rapidly accumulating knowledge on mutant p53-signaling pathways will facilitate drug discovery programmes in the challenging area of protein–protein interactions and mutant protein conformational control.

Introduction

Thirty years following the discovery of the oncoprotein p53 we learn that the p53 gene and its major regulatory effector MDM2 (transformed mouse 3T3 cell double minute 2), the p53 binding protein homolog, both appeared surprisingly early in eukaryotic evolution [1]. This striking discovery has given the p53–MDM2 axis significant time to evolve and imbed itself as a major signaling hub involving at present hundreds of dynamic protein–protein interactions (PPIs) (Figure 1A and Table S1 in the supplementary material online). p53 protein itself also binds to a vast number of DNA promoter regions [2]. One implication of this ancient MDM2–p53 PPI network (i.e. interactome) is that it controls a huge range of molecular pathways in humans, ranging from autophagy and DNA damage responses to differentiation, senescence, cell–cell interactions, and apoptosis, as well as fundamental energy generation pathways including ATP generation by oxidative phosphorylation. It is perhaps not surprising, then, that p53 regulates diverse aspects of animal life including ageing, fitness, virus infection, reproduction, and cancer.

Silencing the function of wild-type p53 (wt-p53) or mutation of the gene encoding p53 (*TP53*) are the most common genetic alterations in human cancer [3]. Thus, the second implication of this large p53 interactome is that the 'transcriptionally inactive' mutant p53 selected for in human cancers might contribute to carcinogenesis by significantly rewiring the normal PPI landscape (Figure 1A). The magnitude of the PPI landscape of some proteins such as ataxia telangiectasia mutated (ATM) [4], eukaryotic translation initiation factor 3 (eIF3) [5], or ephrin receptor B2 (EPHB2/ERK) [6] is just beginning to be understood. However, we do not precisely know yet what the mutant p53 PPI landscape might look like, but it can lead to disease phenotypes that increase as a function of increasing age, such as cancer and infection. Genetic and biochemical studies have shown that targeting the p53 pathway could offer therapeutic advances in cancer treatment [7]. The characterization of mutant *TP53* alleles has generated key paradigms in the field including (i) unfolded, mutant p53 protein accumulates in the nucleus of cancer cells *in vivo* [8], (ii) mutant p53 acts in a dominant-negative fashion forming mixed tetramers that unfold the wt-p53 protein [9], (iii) mutations usually attenuate the sequence-specific DNA-binding function of p53 [10], and (iv) mutant p53 can induce distinct changes in gene expression by establishing novel PPIs with transcriptional components. This can in turn be linked to the oncogenic activity of gain-of-function p53 mutations [11,12].

The effects of stabilized mutant p53 protein are far-reaching. These effects include enhanced genome instability by inactivating the ATM pathway [13] as well as an altered transcriptome by selected PPIs with transcription components that can lead to invasion, stimulation of angiogenesis, drug-resistance, and differentiation blocks. There are many, excellent comprehensive reviews on mutant p53 [14]. This review will discuss the most recent advances and approaches used to study the pro-oncogenic functions of mutant p53 *in vitro* and *in vivo*, the regulation of mutant p53 degradation by the ubiquitin–proteasome system (and the rationale for targeting mutant p53 degradation to attenuate pro-migratory functions of cancer cells), and the perhaps more challenging approach of using chemical biology strategies that aim to refold mutant p53 protein into the wild-type tumor suppressor conformation. Continued research in these three areas will probably produce exciting new prospects for manipulating specifically the conformation and function of mutant p53. Such research using mutant p53 as a model also will allow the development of more generalized concepts and proof-of-principle studies for tackling a very difficult area in the drug discovery field: manipulating mutant protein conformations and inhibiting PPIs in human disease.

Corresponding author: Hupp, T.R. (ted.hupp@ed.ac.uk)

0962-8924/$ – see front matter © 2010 Published by Elsevier Ltd. doi:10.1016/j.tcb.2010.06.005 Trends in Cell Biology 20 (2010) 542–555

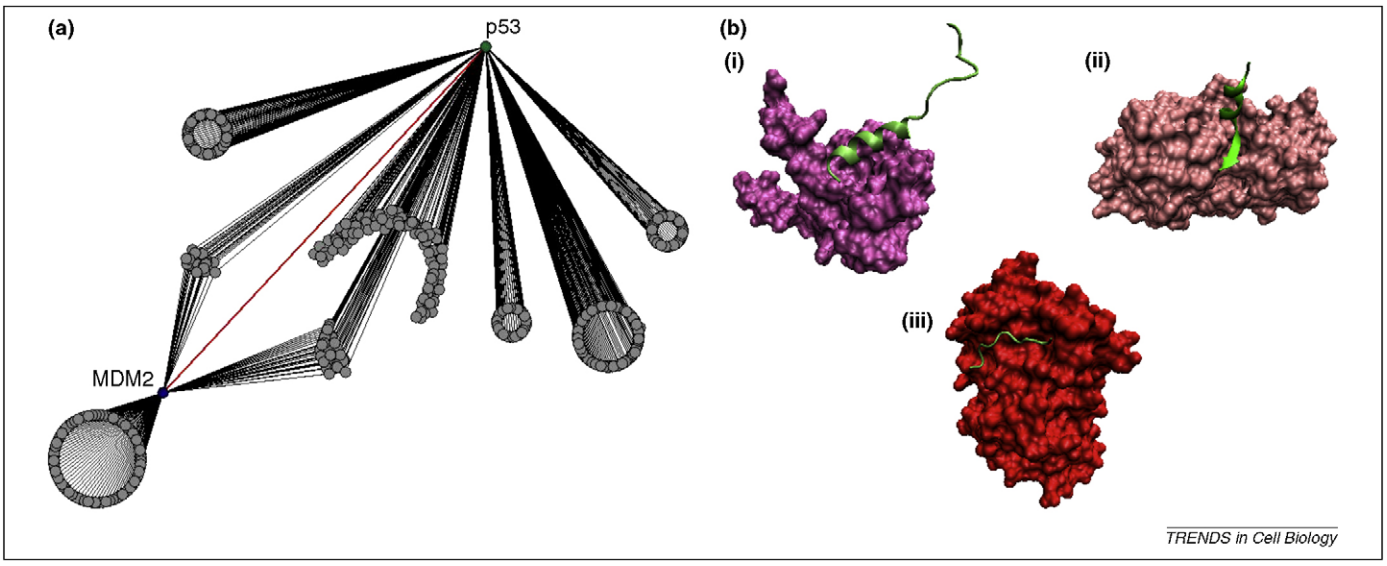

Figure 1. **(a)** The interactomes of p53 and MDM2. Annotation of the hundreds of published binding proteins that have been reported for p53 or MDM2 (using the Human Genome Navigator, http://www.hugenavigator.net/; and acquired from PubMed, http://www.ncbi.nlm.nih.gov/pubmed) are highlighted with some classes of molecules sharing interactions with both MDM2 or p53 and others with no direct overlap (Tables S1 and S2 in supplementary material online; updated at www.ecrc.ed.ac.uk/groups/studys.asp?studyID=4). It is not known yet how many of these p53-interactors are actually specific for mutant or wt-p53; some of these interactors have not been subjected to rigorous validation using the tools of protein science. **(b)** A mechanism to explain the interconnectivity of p53. Example of combinatorial diversity driving the interaction of one small intrinsically disordered p53 peptide motif with three different class of binding proteins. The p53 C-terminal peptide (GQSTSRHKKLMFKTE) (purple) adopting three different conformations in complex with the peptide binding grooves of **(i)** S100β, **(ii)** sirtuin, or **(iii)** cyclin A2 [protein data bank (PDB) codes 1DT7, 2H2D and 1H26 respectively; http://www.pdb.org]. The implications of these data are that many of the intrinsically disordered peptide motifs of the p53 tetramer could provide docking sites for a range of PPIs and help to explain in part the vast interactome of p53.

Why we need to target mutant p53 protein in human cancer: the pro-oncogenic functions of mutant p53

Transcription functions of mutant p53

Tumor-associated mutations in the *TP53* gene cover a large proportion of the region encoding the p53 DNA-binding domain [3]. These mutations result in a p53 protein with reduced sequence-specific DNA-binding activity and thereby produce a 'transcriptionally inactive' p53. Common *TP53* mutations in human cancers, such as R175H or R273H, determine a p53 that is essentially inactive as a sequence-specific DNA-binding protein and transcription factor for genes that normally are induced by wt-p53 to maintain tissue integrity. These data have formed a central p53 paradigm that links tumor suppression to its activity as a DNA-binding protein and transcription factor [15].

Loss-of-function mutations in p53 destabilize thermodynamically the DNA-binding domain [16], thereby not only reducing the expression of genes that are transactivated by p53 but also derepressing genes that are normally suppressed by p53 [17]. The most striking derepression published recently was the enhanced expression of the CD44 receptor in the absence of functional p53 [18] (Figure 2A). There can also be a staged evolution to the mutant *TP53* (*Trp53* in mouse) gene status of a cancer cell. First, there can be selection for mutation in p53 that produces a mutant protein with the ability to oligomerize with wt-p53, distort the wt-p53 conformation, inhibit its function, and promote aggressive cancer growth *in vivo* [12,19]. An additional event can occur that selects for deletion of the remaining wt-p53 allele. The selection pressures that drive the survival of cancer cells that maintain both wt-p53 alleles or that select for inactivating or gain-of-function mutant alleles are not defined. Significant challenges in future will involve understanding the mechanisms that regulate these evolutionary p53 crossroads in developing cancer cells. A recent milestone in this area was the analysis of p53 mutations in microdissected crypts within oesophageal metaplastic and dysplastic biopsies [20]. It is striking that distinct and multiple independent p53 mutant clones are selected for in this tissue type. The oesophageal cancer progression sequence provides a unique physiological model for studying the types of p53 mutations that are selected for *in vivo*. Such selection pressures might relate to the interactions of the developing cancer cell with normal tissue matrix [21] and to other genetic changes that take place in these pre-cancerous cells such as mutation or deletion of the gene encoding p16.

Despite the obvious fact that mutant p53 proteins can be inactive as sequence-specific DNA-binding proteins, these p53 mutants are not necessarily wholly 'inactive'. Selection pressures in cancer cells drive the stabilization of mutant p53 protein in the nucleus *in vivo* leading to a significant change in the PPI network of the p53 interactome. These mutant p53 proteins that are inert for DNA binding can stimulate gene expression through PPIs with transcription factors rather than through sequence-specific DNA-binding to wild-type consensus sites. Such p53 mutants can drive expression of genes involved in repair or anti-apoptotic pathways such as the molecular chaperone network and growth-stimulatory genes including cyclins. The mutant p53 proteins can be considered to have a gain-of-function because they are not actually functionally inactive and they do not act like *TP53*-null alleles [12]. This latter concept was supported by recent transgenic data showing that some mutant *TP53* alleles can actually support metastatic cancer development *in vivo*, unlike the *TP53*-null controls [22]. Not all *TP53* alleles with mutations within

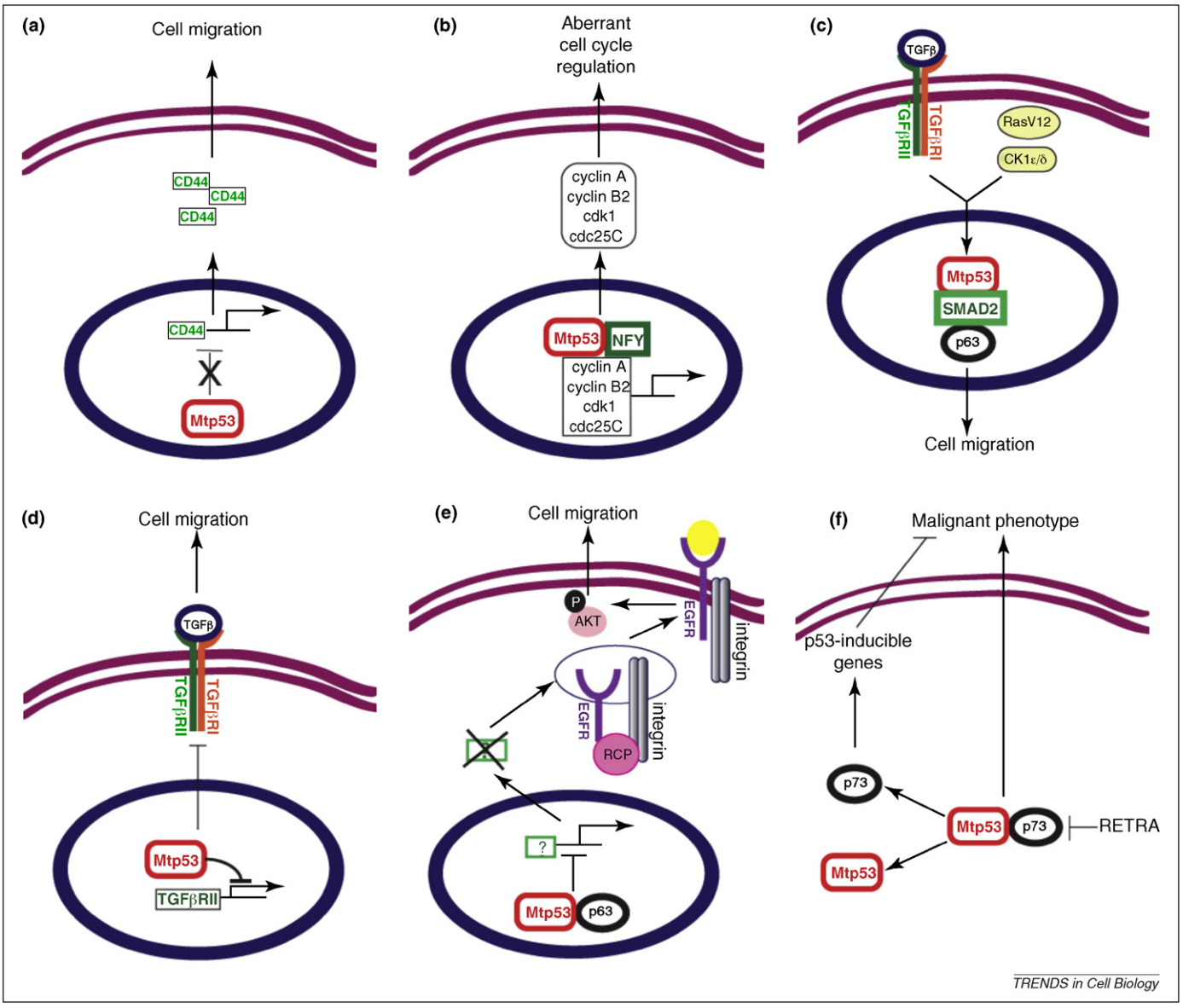

Figure 2. Signaling pathways mediating the pro-oncogenic functions of mutant p53. **(a)** Loss of function of p53 derepresses proteins such as the CD44 receptor [18]. **(b)** Mutant p53 protein interactions with transcription factors such as NF-Y drive pro-oncogenic changes in the transcriptome [25]. **(c)** TGF-β and RAS-CK1 signaling drive mutant p53 interactions with SMAD2 and suppress p63 signaling [30]. **(d)** Mutant p53 can suppress a range of TGF-β-responsive genes including that encoding TGFBR2, thereby reducing wound healing and cell migration [32]. **(e)** Mutant p53 interactions with p63 suppress anti-migration genes and stimulate integrin recycling and cell migration [33]. **(f)** Mutant p53 suppression of p73 can be attenuated by molecules such as RETRA that was identified by screening cancer cells containing mutant p53 for restimulation of p53-family responsive promoters [34].

the DNA-binding domain have been shown to be pro-metastatic and there are thought to be degrees of 'aggressiveness' linked to the potential for the mutant p53 to be in an unfolded conformation. Some alleles such as R175H are one of the most pro-oncogenic and unfolded or destabilized [16]. Other allelic forms such as R273H are not as unfolded, are not as aggressive in transformation assays, and are sometimes considered to be only DNA-contact mutants. However, p53 encoded by the R273H allele also shows allosteric or conformational defects in some assays [23,24] thus complicating a full understanding of what determinants in p53 drive gain-of-function pro-oncogenic signaling.

Such concepts can be used to develop two distinct therapeutic strategies that target mutant p53. First, reactivation of mutant p53 into a wt-p53 conformation could repress pro-oncogenic signaling proteins such as CD44, as well as stimulate the normal wt-p53 tumor suppressor network. Second, direct or indirect inhibition of 'active' mutant p53, thereby promoting more aggressive pro-metastatic cancers *in vivo* [12,19,22], would obviously form an attractive drug target. Among the first mechanistic evidence that mutant p53 has a novel biochemical function was the identification of an interaction between mutant p53 and NF-Y (Figure 2B) that led to a change in pro-oncogenic gene expression [25]. Multiple transcription targets of mutant p53 are now known that are involved in anti-apoptotic signaling, inflammation, invasion, and cell growth [14].

These effects of mutant p53 involve, in part, PPIs (as in Figure 1A) that are likely to identify an ever-growing list of 'druggable' targets in the future. Developing small

molecules that disrupt PPIs is thought to be very difficult, but we are now developing diverse rules for how to target PPIs. An example of 'drugging' a p53 PPI was highlighted by a recent study that identified a small molecule that blocked SNAIL-mediated degradation of wt-p53 [26]. The small molecule (GN25) was not toxic to normal cells and did not affect mutant p53, thus displaying a degree of specificity. Such concepts are likely to be applicable to mutant p53 PPIs, with success limited to the diversity of the chemical library used. Understanding in detail how the many mutant p53 protein signaling events occur will facilitate such developments. Understanding how many distinct types of mutant p53 exist, in terms of the specific PPIs they embrace, will also be a major aim of p53 research. Below we review a recently defined mutant p53 PPI that regulates pro-metastatic signaling.

The function and regulation of p53 in pro-metastatic pathways

The 30th anniversary of the discovery of p53 has led to an excellent review series explaining the detailed functions of mutant p53 [27]. Here we focus on three recent mechanistic advances regarding the pro-metastatic function of mutant p53: (i) mutant p53 induces aggressive pro-metastatic cancers in animals models that are not seen in p53-null animals [22], (ii) mutant p53 changes the transcriptome of the cancer cell towards pro-metastatic signaling [18], and (iii) mutant p53 can promote its gain-of-function effects through a broad set of PPIs that stimulate diverse pro-metastatic signaling pathways. Defining the diversity of the PPIs that are driven by mutant p53 proteins and the diversity of allele-specificity in the mutant p53 interactome will remain a major challenge. Highlighted below are studies describing the ability of mutant p53 to stimulate invasion, migration and colonization of cancer growth *in vivo*. This pro-metastatic property of mutant p53 makes a strong argument for targeting mutant p53 with new therapeutic strategies, as described in the next sections (degrading mutant p53 and switching mutant p53 to the wild-type conformation).

Mutant p53 cooperates with TGF-β-induced cell migration

The transforming growth factor beta (TGF-β) pathway is known to cross-talk with the wt-p53 pathway, adding to the multiple physiological signaling inputs that can trigger p53 activation [28]. Understanding fully the cross-talk between TGF-β and mutant p53 is complicated by the fact that TGF-β can act both as a tumor suppressor at early stages in carcinogenesis and as a pro-metastatic signal at advanced stages [29]. The latter property of TGF-β emphasizes the need for a mechanistic understanding of its interactions with mutant p53. A recent study has shown that gain-of-function mutant p53 can bind to SMAD2 and cooperate with TGF-β to suppress p63 growth-suppressor signal (Figure 2C). This signal attenuates metastasis suppressor gene expression and induces pro-migratory events in a range of cell lines, xenograft models and skin cancer models, but also provides a key PPI driving a signal that could nucleate drug-discovery assays at this hub [30]. Indeed, the signaling events that inhibit p63 function in turn include a RAS-CK1 cascade that can stabilize the mutant p53 PPI with SMAD2. However, these data cannot yet be reconciled due to the fact that transgenic pro-oncogenic p53s encoded by the mouse equivalent of the R175H allele do not have developmental defects similar to those seen in p63-null animals [31]. These data suggest that mutant p53 inhibition of p63 might be confined to selected cancer cells and is not necessarily fundamental to mutant p53 function. Nevertheless, these data elegantly define the multiple components of one signal transduction pathway that offers a therapeutic strategy for attenuating the metastatic functions of the pro-oncogenic class of mutant p53; for example, at least by inhibiting the upstream signal induced by CK1ε and RAS [30].

Mutant p53 suppresses the TGF-β pathway

Despite the data demonstrating a novel signaling pathway that induces mutant p53 to cooperate with TGF-β (Figure 2C), studies demonstrating the opposite have also been reported – mutant p53 can attenuate TGF-β induced migration through the suppression of a range of TGF-β-dependent genes including that encoding the receptor protein TGFBR2 [32] (Figure 2D). These apparently contradictory data make defining the signaling pathways that activate mutant p53 relatively difficult and demonstrate that the pro-invasion potential of mutant p53 is not a universal property of mutant p53 alleles and depends on the cell type. Such data also indicate that drug leads which degrade mutant p53 (as discussed in the second section of this review) could actually stimulate TGF-β-mediated cell migration in some cell types. The choice to degrade mutant p53 or to inhibit mutant p53 will depend on the context of the specific cancer cell type.

In the latter study showing that mutant p53 inhibits cell migration [32], using head and neck cancer models, an association was indeed found between p53 mutation status, expression of NF-κB-related genes, and suppression of TGFBR2. Depletion of mutant p53 using siRNA resulted in restoration of TGFBR2 expression, increased expression of TGF-β-responsive genes, and suppression of proinflammatory NF-κB signaling. Using *Tgfbr2* knockout mice, the authors also demonstrated that abrogation of TGF-β signaling led to sustained induction of the NF-κB pathway. The fact that these studies [30,32] demonstrated opposing effects of mutant p53 on TGF-β-dependent signaling and cell migration might reflect the cell-specific nature of TGF-β function as both a metastatic promoter and a tumor suppressor. The development of additional physiologically relevant models with emphasis on the cancer cell types used would facilitate prioritizing concepts on the role of mutant p53 in cell migration.

Mutant p53 promotes integrin recycling

Another recent study demonstrated that specific mutant p53 alleles can drive cell escape from mutant Ras-induced senescence in pancreatic adenocarcinoma and promote metastasis in animal models [22]. A correlation between p53 accumulation in human pancreatic cancer and the number of lymph node metastases was also noted [22]. In a complementary study evaluating the effects of mutant p53 on cell migration it was confirmed that two common

p53 alleles (R175H and R273H) could drive enhanced random cell motility and loss of polarity *in vitro* [33]. However, it is difficult to generalize such results because the same mutant p53 allelic forms were shown to suppress TGF-β-mediated cell migration in the same cancer cell type [32]. In addition, because the R273H form is generally thought to be a DNA-contact mutant, this mutant does not necessarily have the same pro-migratory gain-of-function phenotype as the conformational mutant encoded by the R175H allele. However, whether the R273H form acts as a DNA-binding contact mutant or not is controversial. There are data showing that the R273H form can act as a conformation mutant – it can be activated for DNA binding and shows allosteric defects in its inactivity as a DNA-binding protein and transcription factor [23,24]. Thus, the data showing that R273H can stimulate migration indicate that, under these conditions, the mutant might behave as a conformational mutant and not merely as a loss-of-function DNA-binding mutant.

Supporting the data demonstrating that mutant p53 can promote cell migration *in vitro*, an intestinal tumor model driven from the adenomatous polyposis coli (*Apc*) gene was utilized in which tumorigenesis can be initiated by loss of the wild-type *Apc* gene in transgenic mice containing a single conditional inactivatable ('floxed') $Apc^{fl/+}$ allele [33]. When these mice were crossed to animals carrying an inducible knock-out *Trp53* (p53) allele or an inducible dominant-negative *Trp53* knock-in allele, both sets developed intestinal tumors with a similar frequency and timeframe, but the mutant p53 animals had significantly more invasive tumors containing stabilized mutant p53 protein. The mutant p53 protein was stabilized in the nucleus of the cancer cells in these mouse models, a classic signature of many mutant human p53 proteins in cancers *in vivo* [8].

In these models, mutant p53 can drive invasion through silencing of the p63 pathway and recycling of the integrin/EGFR signaling pathway [33], but this outcome was TGF-β independent and AKT-dependent (Figure 2E). In these studies two distinct signals account for migration (Figure 2C and E), and we can propose a mechanism to explain these differences. When TGF-β cooperates with mutant p53 to drive migration, an intrinsically disordered motif in the N-terminus of mutant p53 is implicated in binding to SMAD-2 to form a trimeric complex with p63 [30]. In the other study (in the absence of the TGF-β signal), the C-terminus of p53 is implicated in attenuating p63-dependent transcription under conditions where integrin/EGFR recycling occurs [33]. Thus, the apparent contradiction that mutant p53 can either suppress or drive cell invasion and/or aggressive cancer growth *in vivo* might be better reconciled if the 'interactome' of the mutant p53 proteins (if not the 'proteome' of the cancer cell) could be identified, annotated and distinguished experimentally.

A novel screening approach for 'inhibiting' mutant p53

The extensive amount of intrinsic disorder in the human proteome that drive combinatorial diversity in signal transduction adds another, but at present obscure, layer into understanding of PPI network rewiring in diseases such as cancer. In addition, the unexpectedly large and growing size of the p53 protein interactome (Figure 1A) raises fundamentally new questions normally confined to the systems biology field. How do we generate experimental strategies to understand the vast and dynamic PPI landscape of a normal and diseased cell? How can these approaches facilitate anti-cancer drug development? One approach would be to develop systematic cell-based subscreens to annotate the mutant p53 interactome into functional subsets. For example, to begin to 'inhibit' the mutant p53 interactome in cancer cells, assays need to be generated that can provide an indirect read-out of the functions of a relatively specific PPI group.

An elegant and thoughtful study identifying the small molecule RETRA forms a roadmap for such specific screens [34]. One of the binding proteins for mutant p53 is the p53-family member and transcription factor p73 (Table S1). p73 can transactivate some of the same target genes as wt-p53. Mutant p53 protein can directly inhibit such functions of p73 by forming mixed inactivating complexes (Figure 2F). Assays were therefore established in cells containing mutant p53 and a p53-/p73-responsive transcriptional reporter. Small molecule libraries were screened that activate the p53-/p73-responsive promoter in such cells; molecules that directly activated wt-p53 were removed in secondary screens, and leads that specifically allowed 'stimulation' of p73 function in the mutant p53 background were identified. Such leads were shown to function strictly in cells containing mutant p53 and could function in xenograft systems. This approach goes beyond normal cell-based screens that measure a biochemical activity because it takes into account the interactome of mutant p53. A proof-of-concept for annotating the mutant p53 interactome that is relevant for drug discovery in cancer was demonstrated by this study, further highlighting the exciting possibility of targeting the mutant p53 pathway as an anti-cancer strategy.

Mutant p53 protein ubiquitination and degradation

Proteins of the ubiquitin–chaperone system interacting with mutant p53

The studies summarized in the previous section highlight recent evidence that mutant p53 can often, but not always, play a dominant role in cell migration or invasion. Therefore, in cancers where mutant p53 does show pro-oncogenic functions, another therapeutic strategy to inhibit its function would be to exploit intracellular pathways that can promote mutant p53 degradation. The synthesis, folding, and degradation of wt-p53 is a well-documented area that provides strategic support for this approach [35]. The numbers of interacting proteins for a 'hub' protein such as wt-p53 or mutant p53 are in the hundreds, and the mechanistic basis for this extensive interactome involves the large regions of intrinsically disordered peptide docking sites that exist within the p53 protein tetramer (Figure 1B). The p53 interactome (Figure 1A) is not 'stable' but is dynamic and changes over time, reflecting the properties of weak, transient but highly specific peptide–protein interactions. The wt-p53 interactome is more well-defined than the mutant p53 interactome. Although the mutant p53 interactome is just emerging as a distinct entity, some proteins that regulate or misregulate mutant p53 protein degradation in cancers are already proving to

be relevant for strategies that mediate degradation of pro-oncogenic mutant p53 protein in cancer cells.

Two of the first sets of p53-interacting proteins were the heat shock protein (HSP, molecular chaperone) family and MDM2 [36–38]. Most striking was the stable complex that formed between what is now known to be mutant p53 protein and the chaperone system in Ha-Ras transformed cells [39–41]. These molecular chaperone interactions with mutant p53 are still proving to be fundamental to cancer and we now know that mutant p53, HSP90 and various chaperones, along with specific ubiquitin ligases such as CHIP and MDM2, can even exist in a functional complex [42–47]. The interactions between p53 and the molecular chaperones relates to the balance between the degradation and synthesis of p53. Wt-p53 and mutant p53 protein stability can be regulated in distinct ways. Wt-p53 can be a very short-lived protein under both negative control [48,49] and positive control [50] by MDM2, whereas mutant p53 protein can be stable in a range of cell systems. This forms a central paradigm in our understanding of p53, and defining how this degradation of wt-p53 and/or stabilization of mutant p53 takes place is a fundamental and still unresolved area. A framework now exists that will allow us to begin to describe the molecular mechanisms underlying the synthesis of p53 protein, balanced against the factors that promote the degradation of p53 protein (Figure 3). In the case of wt-p53 there are now many E3 ubiquitin ligases that regulate its degradation [51], including the most recently identified RING-domain-containing protein TRIM24 [52]. SNAIL was also reported recently to bind to and stimulate the degradation of wt-p53, and small molecule inhibitors were also identified that block this pathway and reactivate the wt-p53 response [26].

Progress in understanding how these pathways of synthesis and degradation are linked to mutant p53 protein has been relatively slow. For example, although MDM2 binding to the p53 mRNA stimulates the synthesis of p53 as a fundamental part of the p53–MDM2 feedback loop [50], how mutant p53 synthesis is controlled is not fully understood (Figure 3). The difficulty is mainly due to the absence of p53–MDM2 in genetically tractable organisms such as yeast, flies, or worms that would normally provide a rapid and elegant approach for discovering the degradation and synthesis pathways of mutant p53 (Figure 3). The primitive four-celled eukaryote *Trichoplax adhaerens*, that contains the ancient p53–MDM2 axis [1], might someday provide such a genetic model. In the absence of such classic genetic screens the cancer cell biology field has exploited the small molecule natural product geldanamycin (and analogs) that bind to HSP90 to shed light on both wt-p53 assembly and mutant p53 protein degradation control [43]. HSP90 is a molecular chaperone that can generally promote the assembly and folding of native proteins including wt-p53 [53] whereas geldanamycin inhibits HSP90 resulting in substrate transfer for degradation by the HSP70–CHIP ubiquitination–degradation system. In some cancer cell types the inhibition of HSP90 with drug leads such as geldanamycin can destabilize mutant p53 protein and drive p53 association towards a complex containing HSP70 and the ubiquitin ligase CHIP, thereby promoting mutant p53 degradation [54]. HSP90 inhibition might therefore form an attractive strategy for degrading mutant p53 protein. Because the chaperone-linked quality-control ubiquitin ligase CHIP [55] is also involved in regulating mutant p53 conformation and ubiquitination [45,54,56], strategies that target mutant p53 protein degradation by manipulation of the CHIP–chaperone ubiquitination–degradation system will probably provide a further opportunity to develop new therapeutic approaches (Figure 3). This will require a much better characterization and understanding of the CHIP interactome than we have at present. Recent research begins to explain how the well-studied ubiquitin ligase MDM2 functions enzymatically; this will allow better targeting of MDM2 with drug leads and the development of improved assays for identifying and targeting additional E3 ligases and chaperone components that might degrade mutant p53. The tools and approaches developed to study the dynamics of the multi-protein ubiquitin complex including MDM2 will also

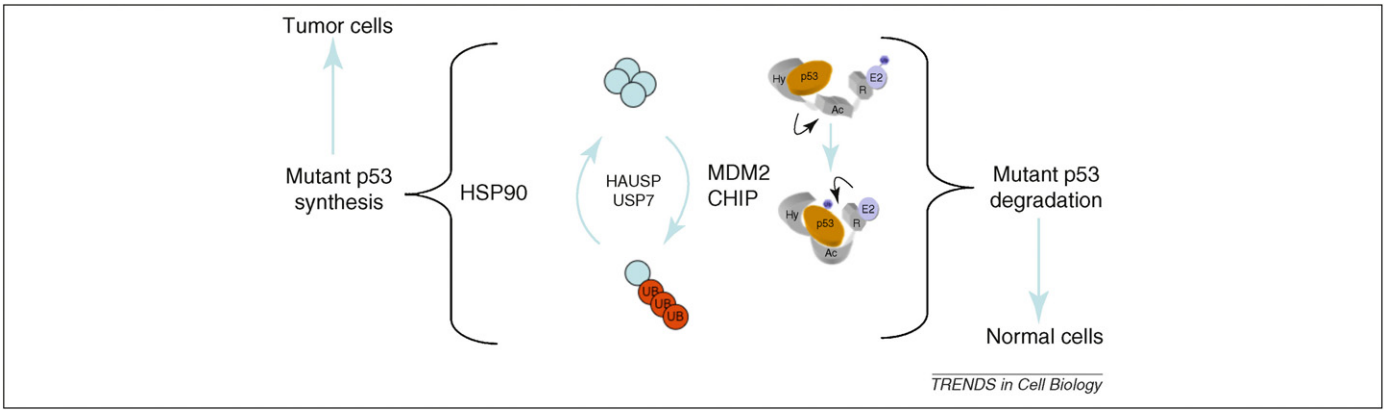

Figure 3. Regulating mutant p53 protein levels in cells. Wt-p53 is ubiquitinated and degraded by the MDM2 feedback loop (Figure 4 for molecular details). Mutant p53 is similarly linked to MDM2 function but in more complicated manner. Mutant p53 protein in cancer cells can be stabilized in the nucleus by the HSP90-dependent synthesis and chaperonin protein-folding pathway; these assembly pathways can be blocked by HSP90 inhibition, leading to mutant p53 degradation through an HSP70–CHIP-dependent pathway [54]. This offers novel therapeutic opportunities for degrading mutant p53 by targeting the 'HSP90-pathway', although more fundamental details are required for specific assay design. Conversely, although mutant p53 can be degraded in normal murine tissues by an MDM2-dependent pathway [77] involving unfolding of its intrinsic ubiquitination signal in the DNA-binding domain [67,73], the mutant p53 in murine or human cancer tissue *in vivo* evades the normal CHIP and MDM2 ubiquitination and degradation system [54,56], presumably through the HSP90 signaling pathway and the HAUSP/USP7 signaling pathway whose control of p53 ubiquitination is relatively complex [114]. It has also been established that the HSP90 core chaperone complex is 'rearranged' in cancer compared to normal cells [113]; this could provide a mechanistic rationale for this effect and provide an opportunity for therapeutic modification of cancer-specific PPIs.

hopefully be transferred to the dissection of other E3 ubiquitin ligases such as CHIP.

How MDM2 operates as an E3 ubiquitin ligase

The interactome of MDM2 protein is growing with an intriguing set of partner proteins that begin to explain its diverse functions (Figure 1A and Table S2). MDM2 function as a p53 inhibitor takes place at the level of transcriptional suppression and ubiquitin-mediated degradation [37,48,49]. MDM2 can also play a positive or stimulatory role in wt-p53 pathways including protein folding/chaperone functions [57], protein translation [35], and ubiquitination after certain types of irradiation [58]. In fact, a recent report has shown that wt-p53 induction of MDM2 can in turn degrade SLUG and attenuate cell migration [59], providing a situation where MDM2 can act as a positive mediator of p53-dependent metastasis suppression. Precisely how these negative and positive functions of MDM2 are linked to the p53 pathway and/or are affected by mutant p53 control are so far undefined.

Understanding the mechanisms whereby MDM2 functions as a p53 inhibitor or stimulator will be crucial for making effective choices on ways to regulate the negative or positive control that MDM2 exerts over wild-type or mutant p53. For example, MDM2-binding ligands (such as Nutlin) might actually stimulate metastasis according to the MDM2-mediated SLUG degradation model. In addition, although there is ample evidence that the hydrophobic pocket of MDM2 can function as a druggable target capable of inhibiting MDM2 function and activating p53 [60–62], there was no mechanistic evidence that such drugs would actually block the ubiquitination function of MDM2. Indeed, recent work has shown that the hydrophobic pocket acts as an agonist–acceptor for MDM2-mediated ubiquitination and its occupation by ligand stimulates MDM2-mediated ubiquitination of p53 [63,64] (Figure 4). This allosteric reaction is highlighted further by the conformational interactions revealed biophysically between the RING domain and the acidic domain [65], as well as the MDM2 lid and the acidic domain [64,66], both of which drive MDM2 binding to the ubiquitination signal in the p53 DNA-binding domain. This 'ubiquitination signal' forms the second identified MDM2 binding site on p53 [63,67,68].

MDM2 not only functions as an E3 ubiquitin ligase but also as a chromatin-associated factor that suppresses p53 activity in the nucleus [69]. Small molecules that block the E3 ubiquitin ligase function of MDM2 might be different from those that release p53 from MDM2 suppression as a transcription factor. Such drug leads that block E3 ubiquitin ligase function of MDM2 could bind the acidic domain, the RING domain, the E2–E3 interface, or the MDM2–MDMX interface (Figure 4). Stimulation of MDM2 E3 ubiquitin ligase function is also possible given that the MDM2 lid can act in a gain-of-function manner [64] and that mutations in the RING domain of MDM2 open the MDM2 N-terminal hydrophobic pocket, thereby stimulating MDM2 function as a p53 inhibitor [65]. It will be interesting to see how manipulating these domains of MDM2 alters mutant p53 ubiquitination, synthesis, stability, and oncogenic transcription functions. Such fundamental knowledge of how MDM2 can function allos-

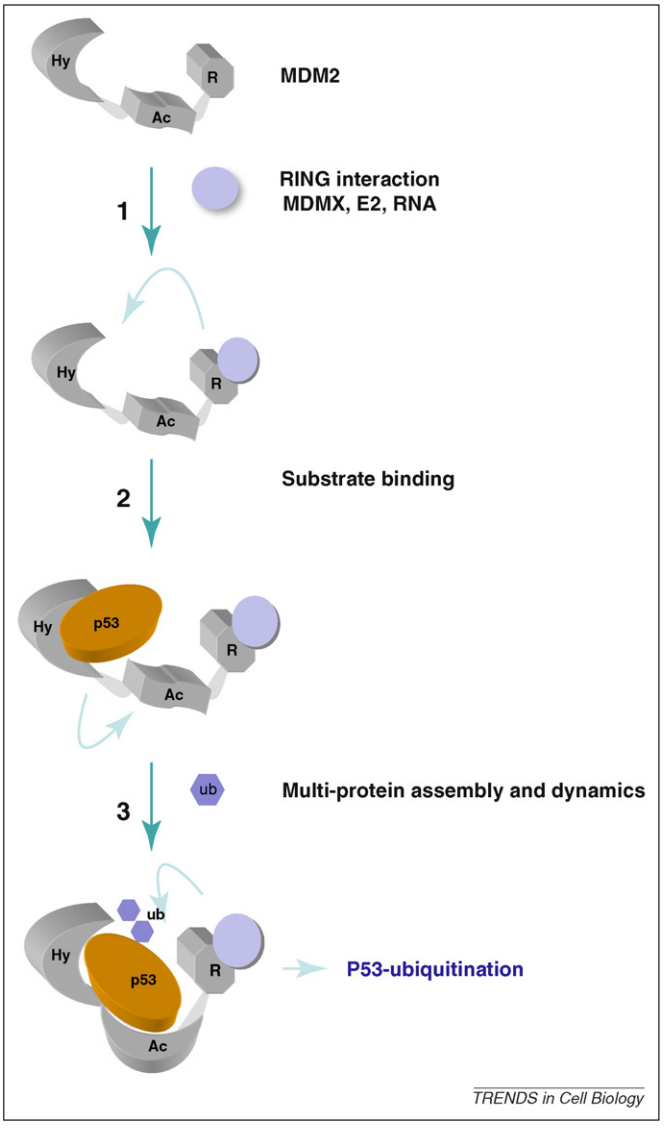

Figure 4. The dynamic multi-protein MDM2 pre-ubiquitin complex. Characterization of MDM2-mediated ubiquitination of p53 has demonstrated that ubiquitination of p53 is driven by allosteric interactions between the hydrophobic pocket (Hy) in the N-terminus of MDM2, the acidic domain of MDM2 that interacts with the ubiquitination signal in the DNA-binding domain of p53, and the multi-functional RING domain (R). **(1)** RING-domain interactions with the E2-ubiquitin intermediate, heterodimers with MDMX, and/or RNA interactions have all been reported to regulate the rates of ubiquitination. Mutations in the RING domain increase intrinsic tryptophan fluorescence of the acidic domain and also increase ligand binding to the hydrophobic pocket, further highlighting the central role of the RING scaffold in regulating MDM2 specific activity. **(2)** Substrate binding (i.e. p53) to the hydrophobic pocket results in conformation changes (arrow) that stabilize the **(3)** MDM2 acidic-domain interactions with the ubiquitination signal in the DNA-binding domain of p53. This ubiquitination signal in p53 is at the site of mutant p53 'unfolding', and such unfolding sensitizes ectopically expressed mutant p53 to ubiquitination in cell lines and to degradation in normal tissue *in vivo*. This model provides a framework for understanding why small molecules such as Nutlin do not inhibit p53 ubiquitination by MDM2 and highlights other protein–protein interfaces that might form the basis for assays to evaluate stimulation or inhibition of the E3 ubiquitin ligase function of MDM2. Additional, dynamic, transient, but specific PPIs that might form druggable interfaces include the acidic domain-docking interfaces, RING-E2, the N-terminal MDM2 lid (not shown), the zinc finger (not shown), and additional MDM2 interaction sites that regulate the dynamics of ubiquitin transfer, as reported previously [82] and including the new pyridoacridine alkaloids [115] as well as MDMX-binding ligands [116] that might disrupt the stability of the MDM2–MDMX heterodimer. Similar characterization of the mutant p53 E3 ubiquitin ligases such as CHIP would similarly begin to provide novel assays for small molecule lead discovery aimed at manipulating the ubiquitination of mutant p53.

terically as a ubiquitin ligase will also help transfer generic assays that can be used to identify CHIP small molecule regulators.

Mutant p53 ubiquitination and degradation in cancers

One of the key paradigms in p53 cancer biology is the accumulation of unfolded mutant p53 in the nucleus of cancer cells [8,70]. The intriguing feature of the second MDM2 binding site for MDM2 on p53 [67] is that this forms the precise conformationally flexible epitope within the thermodynamically unstable DNA-binding domain that is exposed on mutant p53 in human cancers [71]. This flexible site within p53 reflects the now established intrinsic thermodynamic instability of p53 [72] and in turn builds on one of the original paradigms in the p53 field – that p53 can exist in either a wild-type or a 'denatured' and unfolded conformation [9,70]. Mutations in p53 at this second interface increase MDM2 interactions and increase p53 ubiquitination [73]. *In vitro* studies have shown that a trimeric complex of MDM2–CHIP–HSP90 can unfold p53 [45], although we still do not know whether *in vivo* unfolding of the p53 protein plays a role in its ubiquitination. There is only a correlation between mutations that unfold p53 protein, such as R175H or F270A, and the sensitization of these mutant p53 proteins to MDM2-dependent ubiquitination [73]. There are other E3 ubiquitin ligases that also play a role in mutant p53 ubiquitination and degradation including CHIP [43,54,56]. Further, the ubiquitin-specific protease USP7 (HAUSP) was identified originally as a mutant p53 (R175H)-binding protein [74], but how this ubiquitin-modifying protein integrates into the wt-p53 and/or mutant p53 MDM2/CHIP/HSP90 degradation control is largely undefined (Figure 3).

The enhanced sensitivity of mutant p53 protein to MDM2-mediated ubiquitination and degradation is complex. Despite the fact that 'unfolding' mutations in p53 expose the second MDM2 binding site and sensitize mutant p53 to ubiquitination in cancer cell lines *in vitro* [67,73], the human mutant p53 protein is stabilized in the nucleus of cancer cells *in vivo* [8,75,76]. A recent transgenic study has resolved this discrepancy. Mouse transgenes containing the R175H equivalent murine allele sensitize the murine mutant p53 protein to enhanced MDM2-dependent degradation in normal tissues *in vivo* [77], but cancers derived from such mice show stabilization of the mutant p53 protein *in vivo* [77]. These data indicate that, under normal conditions, the destabilizing mutation can indeed sensitize mutant p53 to ubiquitination and degradation by MDM2, but cancer cells evade this effect – resulting in mutant p53 stabilization. Thus, there are a growing number of biochemical strategies that can be used to affect mutant p53 levels, and the more we know mechanistically about the factors that regulate mutant p53 ubiquitination and degradation, including the ubiquitin ligases CHIP and MDM2, HSP90, and HAUSP, the better choice we will have for developing effective drug targets.

Reactivation of mutant p53 Protein

The reactivatable nature of the p53 pathway

Inhibiting mutant p53 by either disrupting its PPIs (first section; Figures 1A,2) or by targeting the signaling pathways through which mutant p53 protein escapes degradation (second section; Figure 3), present very difficult challenges in the drug discovery field. Reactivating mutant p53 protein into the wild-type conformation with small molecules is even more ambitious. The concept that wt-p53 protein is 'activatable' using biologics (e.g. monoclonal antibodies/peptide aptamers) provided unexpected evidence that rational strategies could be developed to stimulate p53 function post-translationally [78–80]. The propensity of wt-p53 to be stimulated by artificial agents is due to its intrinsic instability at physiological temperatures. The newly established 'ensemble' model of allostery can explain in part how an intrinsically unstable protein can be stabilized allosterically by specific 'ligands' into a more active conformational landscape [81]. Subsequent research has led to the realization that the wt-p53 pathway itself (including upstream effectors or downstream mediators of p53) is activatable by a range of strategies including blocking p53-inhibitors such as MDM2 [60,61,82] or replacement of p53-mediators (e.g. p21-peptide mimetics) [83–85]. Because approximately half of human cancers maintain wt-p53 alleles, the hope for novel therapeutics that reactivate wt-p53 pathways has led to cell-based small molecule screens that measure increases in p53 activity. This approach has identified a range of small molecules such as RITA, that still lacks a known target [86], and Tenovins that inhibit deacetylases [87]. These p53 stimulatory leads have been reviewed previously [7].

In contrast to stimulating wt-p53 function, reactivation of a mutant and inactive protein as a therapeutic strategy might appear insurmountable if not naive. However, a pioneering concept for allosteric protein control – using hemoglobin as a model for identifying small molecule modifiers of oxygen binding [88,89] – provided early hope for rational strategies aimed at manipulating protein conformation. Indeed, mutant p53 protein can be stimulated using biologics such as antibodies and specific peptides that interact with p53 [23,80,90–92]. The p53 activating peptide can also stimulate p53 activity in animal models, providing an important proof-of-concept for the utility of biologics approaches in regulating PPIs *in vivo* [80]. Elegant cell-based screens have also identified small molecules such as PRIMA-1 that can reactivate mutant p53 functions [93].

The thermodynamically unstable and intrinsically disordered p53 protein

Insights into how mutant p53 protein can be reactivated stem from two recent advances in the protein science field, one of which is essentially a paradigm shift. Since the advent of protein crystallographic approaches a half-century ago, a crucial aim of biological research has been to 'solve protein structure' in order to explain protein function. This pioneering discipline in 20th century science – the structure–function paradigm – has formulated thousands of structures that reveal the ordered and stable nature of particular functional domains on proteins. It was quite surprising to realize at the beginning of the 21st century that a vast number of proteins are thermodynamically unstable and/or are composed of a large degree of intrinsic disorder. The degree of intrinsic disorder in any given

proteome is linked to increasing complexity of multicellular life, and the paradigm shift is the realization that more than half the proteome of higher eukaryotes is 'disordered' or 'unstable' (termed intrinsically disordered proteins or intrinsically unfolded proteins; IDP's or IUP's) [94]. Because less than 5% of a prokaryotic proteome is thought to be disordered, whereas 50% of the protein sequence in humans is estimated to be disordered, it appears that the evolution of more complex life required this unstable but dynamic proteome.

This realization has led to the concept of regulatory proteins with a large degree of intrinsic disorder or thermodynamic instability sitting at 'hubs' and signaling through a large network of weak, transient, but highly specific PPIs [94]. These proteins, including p53, use such instability to permit the formation of dynamic, transient, weak, but specific PPIs with now hundreds of interactors (Figure 1A). For example, just one disordered 12 amino-acid motif in the C-terminal tail of p53 can adopt distinct conformations because it interacts with peptide-binding grooves of several different proteins (Figure 1B). The intrinsically unstructured tail of p53 presumably docks onto a large number of target proteins. These concepts highlight the combinatorial and functional diversity of the disordered linear domain.

Other emerging examples of proteins with their dynamic interactomes measured into the hundreds include ATM [4], eIF3 [5], and ERK [6]. Another recent example of conformational diversity in a regulatory protein was the observation that a member of the small HSP family can exist in hundreds of different stoichiometries with client proteins, and this explains in part how these chaperones regulate the assembly of diverse proteins [95]. Such built-in flexibility and plasticity, intractable to structural biology, highlights how intrinsic disorder is used by biological systems to regulate dynamic processes. Of course it is not known how many of these conformations are functional *in vivo*, but this insight will help to develop experimental approaches to understanding how proteins such as p53 can have such an unexpectedly large number of interacting proteins. Such plasticity permits p53 to bind to hundreds of proteins, and it is not difficult to envisage how the 'stabilized' mutant p53 protein in cancer can change the proteomic landscape of a cancer cell.

With half the sequence space in the human proteome disordered, and globular domains sometimes showing intrinsic thermodynamic instability, new experimental approaches will be required to understand and define this protein sequence space. The second advance in the protein science field highlights the approach of building such space models – this primarily comes from Alan Fersht's lab where the shape and structure of the p53 tetramer were analyzed using a combination of techniques including nuclear magnetic resonance (NMR), small angle X-ray scattering, and imprinting onto this shape the smaller structural domains that are amenable to crystallization [96]. The shape of the p53 tetramer and orientation of the disordered C and N-terminal 'arms' generate an intriguing view of p53 [97]. In the absence of DNA the p53 tetramer is largely extended with the N- and C-termini 'open' for interactions with a host of proteins [72,96,98], as in the example in Figure 1A,B. The interaction of the N-termini of p53 with the core DNA-binding domain of p53, recently identified using fluorescence resonance energy transfer (FRET) analysis [97], can be explained by the flexibility of the N-terminus; this could provide a mechanism to account for intradomain allostery such as the ability of mutant temperature-sensitive p53 function to be rescued by deletion of 4 amino acids in the N-terminal domain [99].

Interdomain allostery within p53 is also possible considering that translation of wt-p53 with mutant p53 can drive the wild-type polypeptide into the mutant conformation. This alternative translation product of the p53 message, dubbed 'p47', can also form homo-oligomers [100], suggesting that there are determinants that prevent it from forming mixed complexes with full-length p53 protein encoded by the same mRNA. Because mutations in p53 will affect the dynamic range of these multiple disordered conformations, including self-oligomerization, mutant p53 could be considered to spend more time in an 'extended' and 'inactive' state than wt-p53 protein. Such a view of p53 also explains how peptides or antibodies that bind to the protein can 'activate' the mutant protein [92] because these effector molecules do not change the conformation of the mutant protein. These activating molecules shift the mutant from a dynamic and unstable conformational landscape into a more stable landscape suitable for DNA-binding.

Three new leads for reactivating mutant p53

The enhanced intrinsic thermodynamic or kinetic instability of mutant p53 can be exploited to design ligands that can interact with and stabilize the mutant protein in a conformation compatible with DNA-binding. However, not all p53 mutants can have their dynamic equilibrium shifted to the wt-p53 state. Mutations attenuating DNA binding of p53 can also reside (i) outside the active site, resulting in destabilization of the core DNA-binding domain, (ii) within the active site, and precluding stable protein-DNA contacts, or (iii) within the oligomerization domain, resulting in reduced tetramer stability. Recent advances in protein science, structural biology, chemical biology, and *in silico* screening have made it possible to develop specific molecules that can interact with mutant p53 and shift the dynamic equilibrium, as demonstrated using a peptide mimetic [91].

(i) Reactivation of unfolded mutant p53. There are mutations in p53 (such as R175H) that significantly destabilize its structure. A recent report suggests that covalent modification of thiols by the small molecule PRIMA-1 is capable of stabilizing mutant p53 in an active conformation [101]. PRIMA-1 was originally identified from a functional cell-based screen for mutant p53 reactivation and forms an exciting approach to mutant p53 reactivation by covalent adduct formation. How distinct classes of p53 mutants respond to PRIMA-1 will also be important to understand to further define its mechanisms of action. For example, can tetramerization-domain p53 mutants or DNA-contact mutants be stimulated by PRIMA-1?

It is surprising that a cell-based screen could identify a small molecule that covalently binds directly and specifically to p53 *in vivo*. Indeed, it is possible that this molecule

is highly reactive *in vivo* to many proteins through binding to thiol groups, and might act in part as an anti-oxidant. It cannot be ruled out that PRIMA-1 reactivates mutant p53 by altering the protein folding pathways in the cell that respond to thiol-modifying agents. The incubation of the PRIMA-1 molecule with cells and examination of the protein adducts recovered using mass spectrometry would define its specificity and therefore mode of action.

(ii) Stabilization of mutant p53. Mutations in p53 (such as Y220C or F270L) do not grossly unfold the mutant p53 and these mutations can create predicted cavities or grooves on the surface (Figure 5). Using *in silico* modeling, lead molecules have been identified that can stabilize such mutant p53 conformations *in vitro* [102,103], providing another proof-of-concept that the core DNA-binding domain of mutant p53 can be the target for rational drug design. This approach might be confined to mutant p53 proteins which present such cavities or grooves exposed to solvent, but it also is evident that this could require many distinct types of small molecules that fit into the specific cavities generated by mutation.

Nevertheless, recent concepts that p53 protein exists in a dynamic range of conformations – the new allostery [81] – are important to consider. The fact that mutations in p53 do not 'change' the conformation of p53, but rather shift its dynamic equilibrium towards different conformational states, suggests that the concept of stabilizing mutant p53 protein will probably be successful in some situations. Further, the fact that PRIMA-1 (above) can reactivate mutant p53 also indicates that, whether predominantly direct or indirect, the cell possesses the enzymes capable of refolding a mutant protein. We need to learn how to exploit this folding machinery for drug discovery purposes.

(iii) Stabilization of mutant p53 tetramers. Mutations can occur in p53 outwith the core DNA-binding domain; the most notable sites are those within the tetramerization domain that mediates dimer–dimer interactions [104]. A recent report of small molecules that stabilize the equilibrium of the mutant tetramerization domain demonstrates the power of *in silico* modeling to isolate lead molecules that regulate the stability of PPIs and polypeptide conformational equilibrium [105]. The selection of small molecules that fit into grooves of allosteric sites on proteins is reminiscent of prior work on hemoglobin [89] but exemplifies the growing realization of the dynamic nature of protein–ligand binding grooves [106].

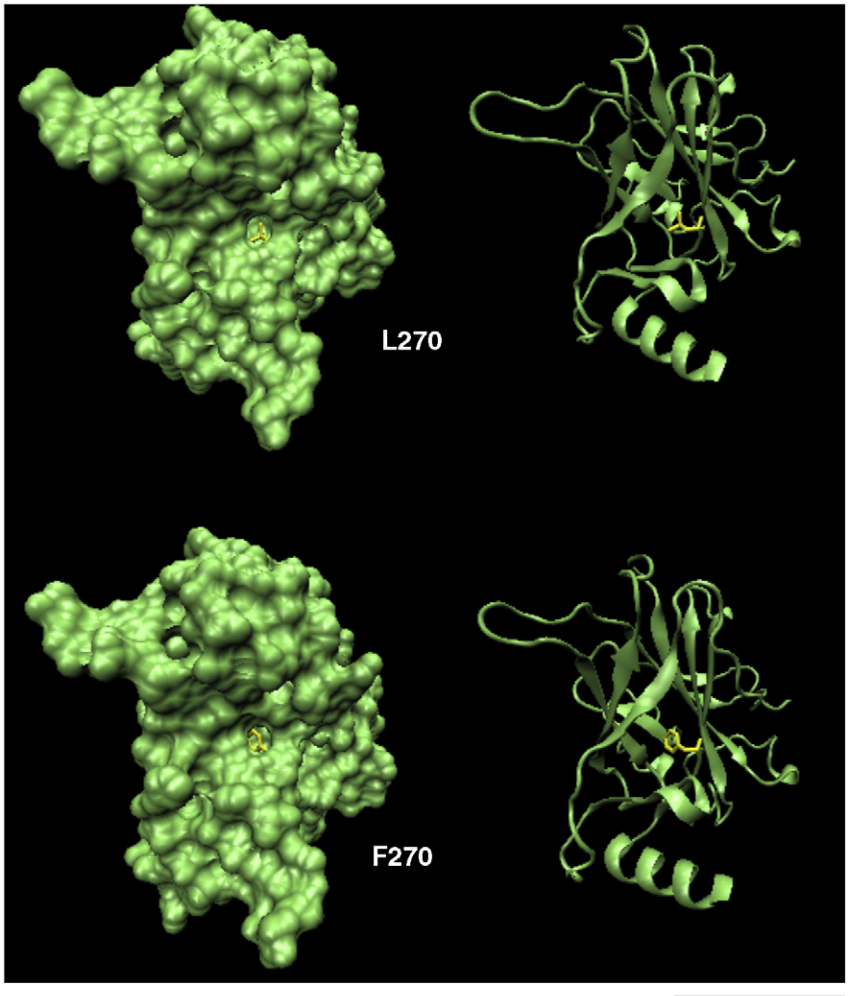

Figure 5. Druggable cavities on mutant p53. The crystal structure of p53 allows *in silico* modeling and molecular dynamics to drive new insights into rational drug discovery. The example shown below highlights the F270 position (PDB code 2J1Z) at which mutation to amino acids such as leucine in human cancers provides a potential pocket for the isolation of small molecules that stabilize this class of mutant p53 [103].

In summary, some class of mutant p53 proteins exhibit a shift in the dynamic range of conformational landscapes and it is possible to develop ligands that stabilize these mutants in the wt-p53 or active conformational state. However, some p53 mutants have a completely destabilized structural landscape that might be more difficult to target with small molecules. It could be more logical to inhibit such p53 mutants or stimulate their degradation (as in the second section), especially considering that they can promote aggressive cancer growth *in vivo*.

Perspectives and future directions

Mutant p53 can sometimes function as a dominant-negative pro-oncogenic protein that promotes aggressive cancer growth *in vivo*, and this provides a rationale for developing novel therapeutic strategies targeting the mutant p53 pathway. The classes of p53 mutants are diverse and would require distinct strategies for therapeutic targeting. We would also need to take into account the cell type and microenvironment of the cancer cell and not just the *TP53* allele type. A landmark study reporting that multiple independent and distinct p53 mutations can be selected in dysplastic crypts from the same patient [20] – and that in the cancer tissue itself only one mutant *TP53* allele spreads and dominates – highlights the need to understand which *TP53* allele and which microenvironment contributes to and/or drives such a selection. Approaches reviewed here that might target mutant p53 include (i) directly reactivating mutant p53 protein, (ii) stimulating the degradation of mutant p53 protein and/or inhibiting mutant p53 protein synthesis, and (iii) disrupting the mutant p53 interactome landscape or inhibiting specific mutant p53 PPIs. Because mutant p53 protein is structurally disordered and its dominant function is mediated by PPIs, therapeutic strategies will need to be developed that take such PPIs into account.

Discovering PPIs is one of the central aims of research in life sciences. Such information not only adds to our fundamental knowledge of life processes but also deepens our understanding of disease mechanisms and provides logical approaches for developing novel therapeutic leads for regulating a PPI. We can speculate on key advances in the near future relating to mutant p53 interaction and regulation that will facilitate drug discovery in the mutant p53 pathway (Box 1). One of the surprising facts that cancer research has taught us is that a large proportion of the 'cancer proteome' is not only driven by classically 'druggable' enzymes such as protein kinases and proteases, but instead involves vast networks of dynamic and weakly interacting protein–protein networks (Figure 1A). In parallel, a paradigm shift developed in the protein science field over the past 15 years now recognizes that half the human proteome is comprised, not only of stable and ordered globular domains, but of intrinsically disordered regions that provide relatively weak, transient but highly specific peptide-signaling scaffolds. Such a view provides new insight into how drugging oncoprotein complexes works – for example, through targeting peptide-binding grooves in proteins such as MDM2, HSP90 [107], CyclinA [108], BCL6 [109], LMO2 [110], and IAPs [111]. In addition, the rearrangement of multi-protein–protein complexes can be observed in cancer cells [112,113]. Thus, perturbations in PPI networks drive the vast cancer landscape and this provides a rationale for specifically targeting PPIs.

Ultimately, therefore, one key advance in cancer drug development over the next 30 years will be to learn how to target PPIs. Learning what to expect and how to accept unconventional outcomes of drugging PPIs will also be important. For example, we already have unconventional outcomes in the p53 field: the relatively low-affinity 'p53 activating peptide' [81] can surprisingly work in animal models to selectively kill cancer cells [80]. The thiol-modifying drug lead PRIMA-1 that refolds mutant p53 *in vivo* [93,101] might also target a large number of proteins, but its 'non-specific' function might not be as important as the fact that it can actually reactivate mutant p53. At present, these types of PPI regulators do not easily fit into the standard view of a high-affinity and highly specific drug lead for clinical evaluations. Over the coming decades we will need to understand better how to study and manipulate the 'disordered' proteome, such as that of mutant p53, and to learn what to accept in a drug lead that targets a PPI. This is an enormous challenge that we cannot ignore and that we need to take on if we are to exploit fully our knowledge of the cancer proteome to develop better classes of anti-cancer drugs.

Box 1. Drug discovery and mutant p53

Key areas for understanding how to develop new therapeutics that target the mutant p53 pathway.

- **Degrading mutant p53**: defining the molecular mechanisms that explain how mutant p53 protein evades the mutant-protein degradation machinery in cancer and developing drug leads that stimulate mutant p53 protein degradation.
- **Activating mutant p53**: developing panels of novel small molecules that stabilize the conformation of specific allelic forms of mutant p53 protein and defining how many such forms are likely to respond to this approach.
- **Inhibiting mutant p53**: exploiting the dynamic depth of the growing mutant p53 interactome to drive drug development screens that inhibit mutant p53 PPIs.
- **Regulating mutant p53**: determining how the distinct classes of mutant p53 proteins are actually regulated by signaling pathways, what unique interactomes these mutant p53's might possess, and how the tissue microenvironment effects these mutants p53 PPIs.

Acknowledgements

M.M.M. is supported by a Cancer Research UK PhD studentship (C483/A8033). Research in the T.R.H. lab is supported by a Programme Grant (C483/A6354) from Cancer Research UK. We thank Jude Nicholson for enthusiastic discussions on proteostasis and MDM2 dynamics.

Appendix A. Supplementary data

Supplementary data associated with this article can be found, in the online version, at doi:10.1016/j.tcb.2010.06.005.

References

1 Lane, D.P. *et al.* (2010) Mdm2 and p53 are highly conserved from placozoans to man. *Cell Cycle* 9, 540–547

2 Wei, C.L. *et al.* (2006) A global map of p53 transcription-factor binding sites in the human genome. *Cell* 124, 207–219

3 Olivier, M. *et al.* (2002) The IARC TP53 database: new online mutation analysis and recommendations to users. *Hum. Mutat.* 19, 607–614

4 Matsuoka, S. *et al.* (2007) ATM and ATR substrate analysis reveals extensive protein networks responsive to DNA damage. *Science* 316, 1160–1166
5 Sha, Z. *et al.* (2009) The eIF3 interactome reveals the translasome, a supercomplex linking protein synthesis and degradation machineries. *Mol. Cell* 36, 141–152
6 von Kriegsheim, A. *et al.* (2009) Cell fate decisions are specified by the dynamic ERK interactome. *Nat. Cell Biol.* 11, 1458–1464
7 Brown, C.J. *et al.* (2009) Awakening guardian angels: drugging the p53 pathway. *Nat. Rev. Cancer* 9, 862–873
8 Rodrigues, N.R. *et al.* (1990) p53 mutations in colorectal cancer. *Proc. Natl. Acad. Sci. U. S. A.* 87, 7555–7559
9 Milner, J. and Medcalf, E.A. (1991) Cotranslation of activated mutant p53 with wild type drives the wild-type p53 protein into the mutant conformation. *Cell* 65, 765–774
10 Kern, S.E. *et al.* (1991) Identification of p53 as a sequence-specific DNA-binding protein. *Science* 252, 1708–1711
11 Wolf, D. *et al.* (1984) Reconstitution of p53 expression in a nonproducer Ab-MuLV-transformed cell line by transfection of a functional p53 gene. *Cell* 38, 119–126
12 Dittmer, D. *et al.* (1993) Gain of function mutations in p53. *Nat. Genet.* 4, 42–46
13 Song, H. *et al.* (2007) p53 gain-of-function cancer mutants induce genetic instability by inactivating ATM. *Nat. Cell Biol.* 9, 573–580
14 Brosh, R. and Rotter, V. (2009) When mutants gain new powers: news from the mutant p53 field. *Nat. Rev. Cancer* 9, 701–713
15 Pietenpol, J.A. *et al.* (1994) Sequence-specific transcriptional activation is essential for growth suppression by p53. *Proc. Natl. Acad. Sci. U. S. A.* 91, 1998–2002
16 Bullock, A.N. *et al.* (1997) Thermodynamic stability of wild-type and mutant p53 core domain. *Proc. Natl. Acad. Sci. U. S. A.* 94, 14338–14342
17 Levine, A.J. *et al.* (2006) The P53 pathway: what questions remain to be explored? *Cell Death Differ.* 13, 1027–1036
18 Godar, S. *et al.* (2008) Growth-inhibitory and tumor- suppressive functions of p53 depend on its repression of CD44 expression. *Cell* 134, 62–73
19 Lang, G.A. *et al.* (2004) Gain of function of a p53 hot spot mutation in a mouse model of Li-Fraumeni syndrome. *Cell* 119, 861–872
20 Leedham, S.J. *et al.* (2008) Individual crypt genetic heterogeneity and the origin of metaplastic glandular epithelium in human Barrett's oesophagus. *Gut* 57, 1041–1048
21 Saadi, A. *et al.* (2010) Stromal genes discriminate preinvasive from invasive disease, predict outcome, and highlight inflammatory pathways in digestive cancers. *Proc. Natl. Acad. Sci. U. S. A.* 107, 2177–2182
22 Morton, J.P. *et al.* (2010) Mutant p53 drives metastasis and overcomes growth arrest/senescence in pancreatic cancer. *Proc. Natl. Acad. Sci. U. S. A.* 107, 246–251
23 Hupp, T.R. *et al.* (1993) Activation of the cryptic DNA binding function of mutant forms of p53. *Nucl. Acids Res.* 21, 3167–3174
24 Fields, S. and Jang, S.K. (1990) Presence of a potent transcription activating sequence in the p53 protein. *Science* 249 (4972), 1046–1049
25 Di Agostino, S. *et al.* (2006) Gain of function of mutant p53: the mutant p53/NF-Y protein complex reveals an aberrant transcriptional mechanism of cell cycle regulation. *Cancer Cell* 10, 191–202
26 Lee, S.H. *et al.* (2010) Antitumor effect of novel small chemical inhibitors of Snail-p53 binding in K-Ras-mutated cancer cells. *Oncogene* advance online publication 7 June 2010; DOI:10.1038/onc.2010.208
27 Shalgi, R. *et al.* (2009) Coupling transcriptional and post-transcriptional miRNA regulation in the control of cell fate. *Aging (Albany)* 1, 762–770
28 Cordenonsi, M. *et al.* (2007) Integration of TGF-beta and Ras/MAPK signaling through p53 phosphorylation. *Science* 315, 840–843
29 Massague, J. (2008) TGFbeta in Cancer. *Cell* 134, 215–2130
30 Adorno, M. *et al.* (2009) A mutant-p53/Smad complex opposes p63 to empower TGFbeta-induced metastasis. *Cell* 137, 87–98
31 Finlan, L.E. and Hupp, T.R. (2006) Epidermal stem cells and cancer stem cells: insights into cancer and potential therapeutic strategies. *Eur. J. Cancer* 42, 1283–12892
32 Kalo, E. *et al.* (2007) Mutant p53 attenuates the SMAD-dependent transforming growth factor beta1 (TGF-beta1) signaling pathway by repressing the expression of TGF-beta receptor type II. *Mol. Cell Biol.* 27, 8228–8242
33 Muller, P.A. *et al.* (2009) Mutant p53 drives invasion by promoting integrin recycling. *Cell* 139, 1327–1341
34 Kravchenko, J.E. *et al.* (2008) Small-molecule RETRA suppresses mutant p53-bearing cancer cells through a p73-dependent salvage pathway. *Proc. Natl. Acad. Sci. U. S. A.* 105, 6302–6307
35 Candeias, M.M. *et al.* (2008) P53 mRNA controls p53 activity by managing Mdm2 functions. *Nat. Cell Biol.* 10, 1098–1105
36 Pinhasi-Kimhi, O. *et al.* (1986) Specific interaction between the p53 cellular tumour antigen and major heat shock proteins. *Nature* 320, 182–184
37 Momand, J. *et al.* (1992) The mdm-2 oncogene product forms a complex with the p53 protein and inhibits p53-mediated transactivation. *Cell* 69 (7), 1237–1245
38 Barak, Y. and Oren, M. (1992) Enhanced binding of a 95 kDa protein to p53 in cells undergoing p53-mediated growth arrest. *EMBO J.* 11, 2115–2121
39 Clarke, C.F. *et al.* (1988) Purification of complexes of nuclear oncogene p53 with rat and Escherichia coli heat shock proteins: *in vitro* dissociation of hsc70 and dnaK from murine p53 by ATP. *Mol. Cell Biol.* 8, 1206–1215
40 Hinds, P.W. *et al.* (1987) Immunological evidence for the association of p53 with a heat shock protein, hsc70, in p53-plus-ras-transformed cell lines. *Mol. Cell Biol.* 7, 2863–2869
41 Finlay, C.A. *et al.* (1988) Activating mutations for transformation by p53 produce a gene product that forms an hsc70-p53 complex with an altered half-life. *Mol. Cell Biol.* 8, 531–539
42 Blagosklonny, M.V. *et al.* (1996) Mutant conformation of p53 translated *in vitro* or *in vivo* requires functional HSP90. *Proc. Natl. Acad. Sci. U. S. A.* 93, 8379–8383
43 Blagosklonny, M.V. *et al.* (1995) Geldanamycin selectively destabilizes and conformationally alters mutated p53. *Oncogene* 11, 933–939
44 Muller, P. *et al.* (2005) Hsp90 is essential for restoring cellular functions of temperature-sensitive p53 mutant protein but not for stabilization and activation of wild-type p53: implications for cancer therapy. *J. Biol. Chem.* 280, 6682–6691
45 Burch, L. *et al.* (2004) Expansion of protein interaction maps by phage peptide display using MDM2 as a prototypical conformationally flexible target protein. *J. Mol. Biol.* 337, 129–1245
46 Walerych, D. *et al.* (2009) Hsp70 molecular chaperones are required to support p53 tumor suppressor activity under stress conditions. *Oncogene* 28, 4284–4294
47 Peng, Y. *et al.* (2001) Inhibition of MDM2 by hsp90 contributes to mutant p53 stabilization. *J. Biol. Chem.* 276, 40583–40590
48 Kubbutat, M.H. *et al.* (1997) Regulation of p53 stability by Mdm2. *Nature* 387, 299–303
49 Haupt, Y. *et al.* (1997) Mdm2 promotes the rapid degradation of p53. *Nature* 387, 296–299
50 Candeias, M.M. *et al.* (2008) p53 mRNA controls p53 activity by managing Mdm2 functions. *Nat. Cell Biol.* 10, 1098–1105
51 Corcoran, C.A. *et al.* (2004) The p53 paddy wagon: COP1, Pirh2 and MDM2 are found resisting apoptosis and growth arrest. *Cancer Biol. Ther.* 3, 721–725
52 Allton, K. *et al.* (2009) Trim24 targets endogenous p53 for degradation. *Proc. Natl. Acad. Sci. U. S. A.* 106, 11612–11616
53 Walerych, D. *et al.* (2004) Hsp90 chaperones wild-type p53 tumor suppressor protein. *J. Biol. Chem.* 279, 48836–48845
54 Muller, P. *et al.* (2008) Chaperone-dependent stabilization and degradation of p53 mutants. *Oncogene* 27, 3371–3383
55 McDonough, H. and Patterson, C. (2003) CHIP: a link between the chaperone and proteasome systems. *Cell Stress Chaperones* 8, 303–308
56 Lukashchuk, N. and Vousden, K.H. (2007) Ubiquitination and degradation of mutant p53. *Mol. Cell Biol.* 27, 8284–8295
57 Wawrzynow, B. *et al.* (2007) MDM2 chaperones the p53 tumor suppressor. *J. Biol. Chem.* 282, 32603–32612
58 Fu, X. *et al.* (2010) RFWD3-Mdm2 ubiquitin ligase complex positively regulates p53 stability in response to DNA damage. *Proc. Natl. Acad. Sci. U. S. A.* 107, 4579–4584
59 Wang, S.P. *et al.* (2009) p53 controls cancer cell invasion by inducing the MDM2-mediated degradation of Slug. *Nat. Cell Biol.* 11, 694–704

60 Bottger, A. *et al.* (1997) Design of a synthetic Mdm2-binding mini protein that activates the p53 response *in vivo*. *Curr. Biol.* 7, 860–869
61 Blaydes, J.P. and Wynford-Thomas, D. (1998) The proliferation of normal human fibroblasts is dependent upon negative regulation of p53 function by mdm2. *Oncogene* 16, 3317–3322
62 Vassilev, L.T. *et al.* (2004) *In vivo* activation of the p53 pathway by small-molecule antagonists of MDM2. *Science* 303, 844–848
63 Wallace, M. *et al.* (2006) Dual-site regulation of MDM2 E3-ubiquitin ligase activity. *Mol. Cell* 23, 251–263
64 Worrall, E.G. *et al.* (2009) Regulation of the E3 ubiquitin ligase activity of MDM2 by an N-terminal pseudo-substrate motif. *J. Chem. Biol.* 2, 113–129
65 Wawrzynow, B. *et al.* (2009) A function for the RING finger domain in the allosteric control of MDM2 conformation and activity. *J. Biol. Chem.* 284, 11517–11530
66 Worrall, E.G. *et al.* (2010) The effects of phosphomimetic lid mutation on the thermostability of the N-terminal domain of MDM2. *J. Mol. Biol.* 398, 414–428
67 Shimizu, H. *et al.* (2002) The conformationally flexible S9-S10 linker region in the core domain of p53 contains a novel MDM2 binding site whose mutation increases ubiquitination of p53 *in vivo*. *J. Biol. Chem.* 277, 28446–28458
68 Yu, G.W. *et al.* (2006) The central region of HDM2 provides a second binding site for p53. *Proc. Natl. Acad. Sci. U. S. A.* 103, 1227–1232
69 Arva, N.C. *et al.* (2005) A chromatin-associated and transcriptionally inactive p53-Mdm2 complex occurs in mdm2 SNP309 homozygous cells. *J. Biol. Chem.* 280, 26776–26787
70 Gannon, J.V. *et al.* (1990) Activating mutations in p53 produce a common conformational effect. A monoclonal antibody specific for the mutant form. *EMBO J.* 9, 1595–1602
71 Vojtesek, B. *et al.* (1995) Conformational changes in p53 analysed using new antibodies to the core DNA binding domain of the protein. *Oncogene* 10, 389–393
72 Joerger, A.C. and Fersht, A.R. (2008) Structural biology of the tumor suppressor p53. *Annu. Rev. Biochem.* 77, 557–582
73 Shimizu, H. *et al.* (2006) Destabilizing missense mutations in the tumour suppressor protein p53 enhance its ubiquitination *in vitro* and *in vivo*. *Biochem. J.* 397, 355–367
74 Li, M. *et al.* (2002) Deubiquitination of p53 by HAUSP is an important pathway for p53 stabilization. *Nature* 416, 648–653
75 Vojtesek, B. and Lane, D.P. (1993) Regulation of p53 protein expression in human breast cancer cell lines. *J. Cell Sci.* 105, 607–612
76 Midgley, C.A. and Lane, D.P. (1997) p53 protein stability in tumour cells is not determined by mutation but is dependent on Mdm2 binding. *Oncogene* 15, 1179–1189
77 Terzian, T. *et al.* (2008) The inherent instability of mutant p53 is alleviated by Mdm2 or p16INK4a loss. *Genes Dev.* 22, 1337–1344
78 Mercer, W.E. *et al.* (1984) Role of the p53 protein in cell proliferation as studied by microinjection of monoclonal antibodies. *Mol. Cell Biol.* 4, 276–281
79 Hupp, T.R. *et al.* (1995) Small peptides activate the latent sequence-specific DNA binding function of p53. *Cell* 83, 237–245
80 Snyder, E.L. *et al.* (2004) Treatment of terminal peritoneal carcinomatosis by a transducible p53-activating peptide. *PLoS Biol.* 2, E36
81 Hilser, V.J. (2010) Biochemistry. An ensemble view of allostery. *Science* 327, 653–654
82 Yang, Y. *et al.* (2005) Small molecule inhibitors of HDM2 ubiquitin ligase activity stabilize and activate p53 in cells. *Cancer Cell* 7, 547–559
83 Ball, K.L. *et al.* (1997) Cell-cycle arrest and inhibition of Cdk4 activity by small peptides based on the carboxy-terminal domain of p21WAF1. *Curr. Biol.* 7, 71–80
84 Mutoh, M. *et al.* (1999) A p21(Waf1/Cip1) carboxyl-terminal peptide exhibited cyclin-dependent kinase-inhibitory activity and cytotoxicity when introduced into human cells. *Cancer Res.* 59, 3480–3488
85 Kontopidis, G. *et al.* (2005) Structural and biochemical studies of human proliferating cell nuclear antigen complexes provide a rationale for cyclin association and inhibitor design. *Proc. Natl. Acad. Sci. U. S. A.* 102, 1871–1876
86 Issaeva, N. *et al.* (2004) Small molecule RITA binds to p53, blocks p53-HDM-2 interaction and activates p53 function in tumors. *Nat. Med.* 10, 1321–1328
87 Lain, S. *et al.* (2008) Discovery, *in vivo* activity, and mechanism of action of a small-molecule p53 activator. *Cancer Cell* 13, 454–463
88 Lalezari, I. *et al.* (1990) New effectors of human hemoglobin: structure and function. *Biochemistry* 29, 1515–1523
89 Lalezari, I. *et al.* (1988) LR16, a compound with potent effects on the oxygen affinity of hemoglobin, on blood cholesterol, and on low density lipoprotein. *Proc. Natl. Acad. Sci. U. S. A.* 85, 6117–6121
90 Selivanova, G. *et al.* (1997) Restoration of the growth suppression function of mutant p53 by a synthetic peptide derived from the p53 C-terminal domain. *Nat. Med.* 3, 632–638
91 Issaeva, N. *et al.* (2003) Rescue of mutants of the tumor suppressor p53 in cancer cells by a designed peptide. *Proc. Natl. Acad. Sci. U. S. A.* 100, 13303–71330
92 Friedler, A. *et al.* (2002) A peptide that binds and stabilizes p53 core domain: chaperone strategy for rescue of oncogenic mutants. *Proc. Natl. Acad. Sci. U. S. A.* 99, 937–942
93 Bykov, V.J. *et al.* (2002) Restoration of the tumor suppressor function to mutant p53 by a low-molecular-weight compound. *Nat. Med.* 8, 282–288
94 Uversky, V.N. *et al.* (2008) Intrinsically disordered proteins in human diseases: introducing the D2 concept. *Annu. Rev. Biophys.* 37, 215–246
95 Stengel, F. *et al.* (2010) Quaternary dynamics and plasticity underlie small heat shock protein chaperone function. *Proc. Natl. Acad. Sci. U. S. A.* 107, 2007–2012
96 Wells, M. *et al.* (2008) Structure of tumor suppressor p53 and its intrinsically disordered N-terminal transactivation domain. *Proc. Natl. Acad. Sci. U. S. A.* 105, 5762–5767
97 Huang, F. *et al.* (2009) Multiple conformations of full-length p53 detected with single-molecule fluorescence resonance energy transfer. *Proc. Natl. Acad. Sci. U. S. A.* 106 (49), 20758–20763
98 Canadillas, J.M. *et al.* (2006) Solution structure of p53 core domain: structural basis for its instability. *Proc. Natl. Acad. Sci. U. S. A.* 103, 2109–2114
99 Liu, W.L. *et al.* (2001) Biological significance of a small highly conserved region in the N terminus of the p53 tumour suppressor protein. *J. Mol. Biol.* 313, 711–731
100 Bourougaa, K. *et al.* (2010) Endoplasmic reticulum stress induces G2 cell-cycle arrest via mRNA translation of the p53 isoform p53/47. *Mol. Cell* 38, 78–88
101 Lambert, J.M. *et al.* (2009) PRIMA-1 reactivates mutant p53 by covalent binding to the core domain. *Cancer Cell* 15, 376–388
102 Basse, N. *et al.* (2010) Toward the rational design of p53-stabilizing drugs: probing the surface of the oncogenic Y220C mutant. *Chem. Biol.* 17, 46–56
103 Boeckler, F.M. *et al.* (2008) Targeted rescue of a destabilized mutant of p53 by an in silico screened drug. *Proc. Natl. Acad. Sci. U. S. A.* 105, 10360–10365
104 Jeffrey, P.D. *et al.* (1995) Crystal structure of the tetramerization domain of the p53 tumor suppressor at 1.7 angstroms. *Science* 267, 1498–1502
105 Gordo, S. *et al.* (2008) Stability and structural recovery of the tetramerization domain of p53-R337H mutant induced by a designed templating ligand. *Proc. Natl. Acad. Sci. U. S. A.* 105, 16426–16431
106 Boehr, D.D. *et al.* (2009) The role of dynamic conformational ensembles in biomolecular recognition. *Nat. Chem. Biol.* 5, 789–796
107 Plescia, J. *et al.* (2005) Rational design of shepherdin, a novel anticancer agent. *Cancer Cell* 7, 457–468
108 Kontopidis, G. *et al.* (2003) Insights into cyclin groove recognition: complex crystal structures and inhibitor design through ligand exchange. *Structure* 11 (12), 1537–1546
109 Cerchietti, L.C. *et al.* (2010) A small-molecule inhibitor of BCL6 kills DLBCL cells *in vitro* and *in vivo*. *Cancer Cell* 17, 400–411
110 Appert, A. *et al.* (2009) Targeting LMO2 with a peptide aptamer establishes a necessary function in overt T-cell neoplasia. *Cancer Res.* 69, 4784–4790
111 Wang, L. *et al.* (2008) TNF-alpha induces two distinct caspase-8 activation pathways. *Cell* 133, 693–703

112 Xiong, Y. *et al.* (1993) Subunit rearrangement of the cyclin-dependent kinases is associated with cellular transformation. *Genes Dev.* 7, 1572–1583
113 Kamal, A. *et al.* (2003) A high-affinity conformation of Hsp90 confers tumour selectivity on Hsp90 inhibitors. *Nature* 425, 407–410
114 Cummins, J.M. *et al.* (2004) Tumour suppression: disruption of HAUSP gene stabilizes p53. *Nature* 428, 1 p following 486
115 Clement, J.A. *et al.* (2008) Discovery of new pyridoacridine alkaloids from Lissoclinum cf. badium that inhibit the ubiquitin ligase activity of Hdm2 and stabilize p53. *Bioorg. Med. Chem.* 16, 10022–10028
116 Reed, D. *et al.* (2010) Identification and characterization of the first small molecule inhibitor of MDMX. *J. Biol. Chem.* 285, 10786–10796